SID 66-408

OF THE EFFECTS OF POTENTIAL STRUCTURES AND MATERIALS DEVELOPMENTS ON LAUNCH VEHICLE PERFORMANCE AND COST - Phast 1 Report

# DEVELOPMENT OF PROGRAMMED ASSISTANCE IN DIRECTING STRUCTURES RESEARCH

## - INTERIM REPORT -

(PHASE I)

By J.A. Boddy and J.C. Mitchell

June 1966

Distribution of this report is provided in the interest of information exchange. Responsibility for the contents resides in the authors and organization that prepared it.

Prepared Under Contract NAS7-368 by
NORTH AMERICAN AVIATION, INC.,
SPACE AND INFORMATION SYSTEMS DIVISION
Downey, California

for

Headquarters, Office of Advanced Research and Technology
NATIONAL AERONAUTICS AND SPACE ADMINISTRATION

Hard copy (HC) 7.00
Microfiche (MF) 1.75
ff 653 July 65

FACILITY FORM 602
N67 10876 (ACCESSION NUMBER)
365 (PAGES)
CR-79720 (NASA CR OR TMX OR AD NUMBER)
(THRU)
(CODE)
31 (CATEGORY)

# FOREWORD

This report documents Phase I study effort completed under Contract NAS7-368, Development of Programmed Assistance in Directing Structures Research. The report covers the contract period from 25 May 1965 through 25 May 1966.

Phase I of this program involved modifying and utilizing existing automated analytical techniques to determine significant structures/materials research areas in current and predicted expendable launch vehicle systems. The Phase I study covers the parametric synthesis of expendable launch vehicles and a more detailed design synthesis of some of the structural components of these vehicle systems.

Study effort was accomplished at the Space and Information Systems Division of North American Aviation, Inc., Downey, by the Structures and Dynamics Department, Research and Engineering Division, under the direction of Dr. L. A. Harris. Principal investigators included Messrs. J. C. Mitchell, L. A. Moss, and C. W. Martindale, with additional contributions by Messrs. D. Jones (Propulsion), C. H. Savage (Materials), L. B. Norwood (Manufacturing), and R. W. Johnson (Structural Systems). All work was under the direct supervision of Mr. W. D. McKaig, Program Manager, and J. A. Boddy, Project Engineer.

# SUMMARY

The North American Aviation, Inc., S&ID launch vehicle synthesis programs were modified to suit the specific requirements of this study so that they could be used to synthesize families of vertically launched, tandem staged booster vehicles. The vehicle sizing programs used two operational modes (1) to achieve minimum vehicle lift-off weight for new vehicle systems, and (2) to achieve maximum vehicle payload weight for modified existing vehicle systems.

Based upon predicted improvements in propulsion and propellant characteristics, base point vehicles were synthesized considering structure/materials advances through three periods; i.e., the current year to 1970, 1970 to 1980, and the post-1980 period. For each of the periods the equivalent 100-n.mi earth orbital payloads were classified into the following ranges:

1. 30,000 to 100,000 pounds—medium range payload class
2. 225,000 to 500,000 pounds—Saturn payload class
3. 1,000,000 to 2,000,000 pounds—post-Saturn payload class

These payload ranges were assumed to encompass anticipated future missions for the periods under consideration and resulted in the identification and definition, in sufficient detail, of typical vehicle systems on which to operate in order to assess the effects of structures/materials advances and to identify areas where research in structures and materials will be most effective from a technological and systems aspect.

Structural analysis was conducted on a spectrum of stage diameters (260 to 540 inches) and a range of loading intensities (2000 to 20,000 pounds per inch), and included structural shell analyses to obtain minimum weight for monocoque, integral skin-stringer, top hat section skin-stringer, bonded honeycomb sandwich, and waffle constructions. Materials investigated for the three periods included steel, aluminum, titanium, and beryllium. Manufacturing limitations and improvements and various methods of analysis were considered in the structural investigation. These ranges and types of parameters were assumed to cover the three payload classes.



PRECEDING PAGE BLANK NOT FILMED.

The method of evaluation involved a component-by-component substitution in the base point vehicle systems. Estimated manufacturing complexity factors, material costs with year, and manhour requirements were included in the cost assessment. Cost assessment was accomplished by isolating each structural component and performing a comparative evaluation of the new component to the base point component, which was considered to be aluminum integral skin-stringer construction. Final assessment is made in terms of component weight reduction, equivalent payload gained from this reduction, and cost ratio for the new component which is identified as additional dollars cost per pound of payload gained. The three merit functions are then organized in arrays to order their importance.

This report covers Phase I of a proposed three-phase program. Phase I was involved in developing and demonstrating the programmed assistance approach. Numerous tradeoffs were conducted to demonstrate the approach feasibility and to indicate the varied capability that has been built into the various programs. Test case results are presented to illustrate this approach and to indicate, within the restricted test spectrum considered, areas and corridors wherein research is most likely to result in the greatest benefit. The study programs developed were exercised with a representative spectrum of projected vehicle systems and anticipated types of research and development. When other research ideas are conceived in the future they can be exercised through the various programs to determine their relative merits and regions of applications. The various base points vehicles that were considered can be later modified to reflect any future changes in predictions and mission requirements.

# CONTENTS


| | Page |
|---|---|
| NTRODUCTION | 1 |
| TUDY APPROACH | 5 |
| VEHICLE SYNTHESIS | 9 |
| EVALUATION OF STRUCTURAL COMPONENTS | 11 |
| ARAMETRIC SYNTHESIS | 13 |
| MISSION DEFINITION | 13 |
| TECHNOLOGICAL PREDICTIONS | 17 |
| Materials | 17 |
| Manufacturing | 27 |
| Propulsion | 36 |
| VEHICLE ANALYSIS | 43 |
| Initial Stage Proportioning | 43 |
| Vehicle Size—Payload Range Variations | 60 |
| Stage Mass Fractions | 60 |
| Selection of Specific Test Cases | 63 |
| Maximum Payload Mode Proportioning | 63 |
| Payload Variations with Specific Impulse | 67 |
| Test Case Geometries and Weights | 69 |
| Payload Exchange Ratios | 91 |
| Loading Environments | 91 |
| STRUCTURAL DESIGN SYNTHESIS | 103 |
| EFFECTS OF IMPROVEMENTS IN MATERIAL PROPERTIES | 115 |
| EFFECT OF CHOICE OF BASIC CONSTRUCTION | 125 |
| EFFECTS OF DIFFERENT TYPES OF CONSTRUCTION | 131 |
| EFFECT OF MANUFACTURING RESTRICTIONS | 143 |
| ASSESSMENT | 155 |
| WEIGHT MERIT FUNCTION | 157 |
| PAYLOAD WEIGHT CHANGES | 167 |
| COST MERIT FUNCTION | 169 |
| CONCLUSIONS | 201 |

Page

APPENDIXES . . . . . 205
A. STAGE PROPORTIONING . . . . . 205
Velocity Losses . . . . . 206
Velocity Loss - Altitude Time . . . . . 211
Velocity Loss - Performance Characteristics . . . . . 211
Minimum Liftoff Mode . . . . . 221
Maximum Payload Mode . . . . . 230
Generalized Payload Exchange Ratio . . . . . 242
Empirical Evaluation of Maximum Dynamic Pressure Conditions. . . . . 247
B. STAGE MASS FRACTION SUBROUTINE . . . . . 253
Operational Modes . . . . . 254
Subroutine Logic . . . . . 255
Coefficients . . . . . 261
Test Cases . . . . . 267
Preliminary Design Synthesis Loads Check . . . . . 268
Subroutine Nomenclature . . . . . 301
C. STRESS ANALYSIS . . . . . 303
Optimization Procedure . . . . . 303
Structural Analysis Criteria . . . . . 305
Skin-Stringer . . . . . 311
Waffle . . . . . 316
Sandwich Cylinders . . . . . 323
Computer Program . . . . . 328
Program Options . . . . . 336

REFERENCES . . . . . 345

# ILLUSTRATIONS


| Figure | | Page |
|---|---|---|
| 1 | Evaluation Logic | 10 |
| 2 | Design Synthesis | 12 |
| 3 | Future Strength Properties of a High-Strength Aluminum Alloy | 19 |
| 4 | Future Strength Properties of a Titanium Alloy for Service to -423 F | 20 |
| 5 | Future Strength Properties of a Heat-Treated Titanium Alloy | 21 |
| 6 | Future Strength Properties of a Magnesium Alloy | 22 |
| 7 | Future Strength Properties of Beryllium | 23 |
| 8 | Future Strength Properties of a High-Strength Steel | 24 |
| 9 | Liquid Propellant Rocket Engine Thrust Trends | 37 |
| 10 | Estimated Future Performance Trends for First-Stage Liquid Propellant Rocket Engines | 38 |
| 11 | Estimated Future Performance Trends for Upper-Stage Liquid Propellant Rocket Engines | 39 |
| 12 | Current and Predicted Future Engine Thrust-to-Weight Ratio Trends | 41 |
| 13 | Liquid Propellant Engine Thrust-to-Weight Ratio - Regenerative Cooled | 42 |
| 14 | Parametric Proportioning Logic | 46 |
| 15 | Stage Mass Fractions for Initial Proportioning | 47 |
| 16 | Effect of Stage Proportioning on Liftoff Weight for Future Medium Range Payload Class | 55 |
| 17 | Effect of Stage Proportioning on Liftoff Weight for Future Saturn Payload Class Vehicle | 56 |
| 18 | Effect of Stage Proportioning on Liftoff Weight for Post-Saturn Payload Class Advanced Two-Stage Vehicle | 57 |
| 19 | Effect of Stage Proportioning on Liftoff Weight for Post-Saturn Payload Class Advanced Three-Stage Vehicle | 59 |
| 20 | Vehicle Size - Payload Range Variation Two-Stage Vehicles - Current and Advanced Propellant Characteristics | 61 |
| 21 | Vehicle Size - Payload Range Variation Three-Stage Vehicles - Current and Advanced Propellant Characteristics | 61 |
| 22 | Stage Mass Fraction Logic | 62 |
| 23 | Mass Fraction Variation With Propellant Weight | 64 |

| Figure | | Page |
|---|---|---|
| 24 | Mass Fraction Variation With Propellant Weight - Two Stage Future Saturn Payload Class Vehicle | 65 |
| 25 | Maximum Payload Proportioning Logic | 66 |
| 26 | Variation of Vehicle Payload With Specific Impulse | 67 |
| 27 | Variation of Vehicle Payload With Specific Impulse - Medium Range Payload Class Vehicle and Post-Saturn Payload Class Vehicle | 68 |
| 28 | Inboard Profile Saturn Class Vehicle Two-Stage Current ISP 240,000-Pound Orbital Payload | 70 |
| 29 | Inboard Profile Saturn Class Vehicle Two-Stage 1985 ISP 445,000-Pound Orbital Payload | 73 |
| 30 | Inboard Profile Saturn Class Vehicle Two-Stage 1975 ISP 330,000-Pound Orbital Payload | 76 |
| 31 | Inboard Profile Medium Range Payload Class Vehicle Two-Stage Current ISP 30,000-Pound Orbital Payload | 79 |
| 32 | Inboard Profile - Post-Saturn Class Vehicle Two-Stage Current ISP 1,000,000-Pound Orbital Payload | 80 |
| 33 | Inboard Profile - Medium Payload Range Vehicle Two-Stage 1985 ISP 100,000-Pound Orbital Payload | 85 |
| 34 | Inboard Profile - Post-Saturn Payload Class Vehicle Two-Stage 1985 ISP 2,000,000-Pound Orbital Payload | 86 |
| 35 | Generalized Payload Exchange Ratios | 92 |
| 36 | Limit Loads - Max. $q\alpha$ condition - Current Saturn Class Vehicle 240,000-Pound Payload | 97 |
| 37 | Ultimate Applied Loads—Saturn Payload Class Vehicles | 98 |
| 38 | Ultimate Applied Load Medium Payload Range Vehicles | 99 |
| 39 | Ultimate Applied Loads Post-Saturn Class Vehicles | 100 |
| 40 | Minimum Weight Construction Comparisons | 102 |
| 41 | CRT Printout-Unit Weight Versus Loading Index | 110 |
| 42 | Unit Weight Reductions Resulting From Material Improvements - Honeycomb Sandwich | 116 |
| 43 | Unit Weights Resulting From Material Improvements - Skin-Stringer (Top Hat Section - Beryllium) | 119 |
| 44 | Effect of Compression Yield Improvement on Unit Weight - "Z" Section Skin-Stringer (Beryllium) | 120 |
| 45 | Effect of Material Improvements - Beryllium Constructions | 122 |
| 46 | Effect of Material Improvements in Pressure Tanks | 123 |
| 47 | Material Improvements Applied to Waffle Construction | 124 |
| 48 | Effect of Material Change on Honeycomb Sandwich Construction | 126 |
| 49 | Material Substitution - Unit Weight (Skin-Stringer) | 127 |
| 50 | Effect of Material Change on Waffle | 128 |

| Figure | | Page |
|---|---|---|
| 51 | Unit Weight for Different Types of Construction (Aluminum) | 132 |
| 52 | Unit Weights for Different Types of Construction (Titanium) | 133 |
| 53 | Unit Weights for Different Types of Construction (Beryllium) | 134 |
| 54 | Effect of Change of Stringer Geometry | 136 |
| 55 | Effect of Analytical Methods | 138 |
| 56 | Effect of Analytical Methods (Aluminum - 198 in. Radius) | 139 |
| 57 | Effect of Analytical Methods - Honeycomb Sandwich | 140 |
| 58 | Effect of Analytical Methods - Honeycomb Sandwich - Beryllium | 141 |
| 59 | Effect of Tank Pressure on Minimum Weight Design | 142 |
| 60 | Effect of Radius and Internal Pressure on Minimum Weight Design | 142 |
| 61 | Effect of Sandwich Height Restriction | 144 |
| 62 | Radius and Height Restriction | 145 |
| 63 | Honeycomb Sandwich - Effect of Material With Height Restriction (Radius 270 in.) | 146 |
| 64 | Various Materials With Height Restrictions (Radius 198 in.) | 147 |
| 65 | Various Materials With Height Restrictions (Radius 130 in.) | 148 |
| 66 | Effect of Pitch Restriction on Unit Weight | 149 |
| 67 | Unit Weight Variation for Buckled and Unbuckled Design | 153 |
| 68 | Component Cost Variation With Weight | 172 |
| 69 | Estimated Material Cost With Year | 173 |
| 70 | Comparison of Construction Complexity Factors | 174 |
| 71 | Engineering Logic Assessment Subroutine | 177 |
| 72 | Cost Ratios for 1985 Saturn Payload Class Two-Stage Vehicle | 199 |
| A-1 | Payload Variation With Constant Velocity Losses | 208 |
| A-2 | Payload Variation With Velocity Loss Estimation | 208 |
| A-3 | Payload Variation - Velocity Loss Size Dependent | 209 |
| A-4 | Payload Variation - Velocity Loss Performance Dependent | 209 |
| A-5 | Payload Variation With Burnout Angle | 210 |
| A-6 | Velocity Loss - Altitude, Time Dependent | 212 |
| A-7 | Change in First-Stage Losses Due to Altitude Variation of Gravity | 215 |
| A-8 | First-Stage Gravity-Loss Constant | 216 |
| A-9 | First-Stage Mass Ratio Correction Factor | 217 |
| A-10 | First-Stage Drag-Loss Constant | 219 |

| Figure | | Page |
|---|---|---|
| A-11 | First-Stage Thrust Atmospheric Losses | 220 |
| A-12 | Average Upper-Stage Flight-Path Angle | 222 |
| A-13 | First-Stage Burnout Angle Nomograph | 223 |
| A-14 | Flow Logic for Top Stage Evaluation | 228 |
| A-15 | Flow Logic of Other Stage Evaluation | 231 |
| A-16 | Flow Logic for Second and First Stages | 232 |
| A-17 | Minimum Liftoff Proportioning Logic | 233 |
| A-18 | Maximum Payload Stage Proportioning Logic | 237 |
| A-19 | Generalized Payload Exchange Ratio Program Logic | 248 |
| A-20 | Axial Acceleration During Stage Operation | 251 |
| A-21 | Time at Maximum Dynamic Pressure | 252 |
| B-1 | Tandem Tankage Multistage Vehicle | 256 |
| B-2 | Stage Geometry-Indicator = 0 | 257 |
| B-3 | Stage Geometry-Indicator = 1 | 258 |
| B-4 | Bulkhead Volume Coefficients | 262 |
| B-5 | Bulkhead Area Coefficients | 262 |
| B-6 | Bulkhead Weight Coefficients | 264 |
| B-7 | Engineering Flow Diagram | 269 |
| B-8 | Case 9, Inboard Profile - Three-Stage Vehicle | 273 |
| B-9 | Case 9, Stage Mass Fractions and Partials - Three-Stage Vehicle | 275 |
| B-10 | Case 12, Inboard Profile 225,000-Pound Payload Two-Stage Vehicle Current Isp | 279 |
| B-11 | Case 12, Stage Mass Fractions and Partials | 280 |
| B-12 | Case 15, Inboard Profile 300,000-Pound Payload Two-Stage Vehicle 1975 Isp | 281 |
| B-13 | Case 15, Stage Mass Fractions and Partials | 282 |
| B-14 | Case 18, Inboard Profile 400,000-Pound Payload Two-Stage Vehicle 1985 Isp | 283 |
| B-15 | Case 18, Stage Mass Fractions and Partials | 284 |
| B-16 | Case 20, Inboard Profile 240,000-Pound Payload Two-Stage Vehicle Current Isp | 285 |
| B-17 | Case 21, Inboard Profile 330,000-Pound Payload Two-Stage Vehicle 1975 Isp | 286 |
| B-18 | Case 22, Inboard Profile 445,000-Pound Payload Two-Stage Vehicle 1985 Isp | 287 |
| B-19 | Preliminary Design Synthesis Load Stations | 292 |
| C-1 | Monocoque Cylinder | 307 |
| C-2 | Buckling Stress Coefficients, $C_c$ for Unstiffened Pressurized Circular Cylinders in Axial Compression | 309 |
| C-3 | Increase in Axial Compressive Buckling Stress Coefficients of Cylinders Due to Pressure | 310 |

| Figure | | Page |
|---|---|---|
| C-4 | Skin-Stringer | 312 |
| C-5 | Waffle Cylinder | 317 |
| C-6 | Sandwich Cylinder | 324 |
| C-7 | Monocoque Program Logic | 332 |

# TABLES


| Table | | Page |
|---|---|---|
| 1 | Mission Payload Equivalence | 14 |
| 2 | Manufacturing Complexity of Integral Skin-Stringer | 29 |
| 3 | Manufacturing Complexity of Attached Skin-Stringer | 30 |
| 4 | Manufacturing Complexity of Honeycomb Sandwich | 31 |
| 5 | Manufacturing Complexity of Corrugated Sandwich | 32 |
| 6 | Manufacturing Complexity of Multilayer Corrugation | 33 |
| 7 | Generic Families - Two-Stage Launch Vehicles, Minimum Liftoff Mode Proportioned Vehicles | 44 |
| 8 | Generic Families - Three-Stage Launch Vehicles, Minimum Liftoff Mode Proportioned Vehicles | 45 |
| 9 | Minimum Liftoff Stage Proportioning Computer Printout - Medium Range Payload, Two-Stage Vehicle | 51 |
| 10 | Minimum Liftoff Stage Proportioning Computer Printout - Future Saturn Class Two-Stage Vehicle | 52 |
| 11 | Minimum Liftoff Stage Proportioning Computer Printout - Post-Saturn Class Two-Stage Vehicle | 53 |
| 12 | Minimum Liftoff Stage Proportioning Computer Printout - Post-Saturn Class Three-Stage Vehicle | 54 |
| 13 | Stage Definition for Selected Test Case Vehicles (Maximum Payload Stage Proportioning) Two Stage Vehicles | 58 |
| 14 | Computer Weight Statement - Saturn Class Vehicle Two-Stage Current ISP (240,000-Pound Orbital Payload) | 71 |
| 15 | Computer Weight Performance Data Saturn Class Vehicle Two-Stage Current ISP (240,000-Pound Orbital Payload). | 72 |
| 16 | Computer Weight Statement - Saturn Class Vehicle Two-Stage 1985 ISP (445,000-Pound Orbital Payload) | 74 |
| 17 | Computer Weight Performance Data Saturn Class Vehicle Two-Stage 1985 ISP (445,000-Pound Orbital Payload) | 75 |
| 18 | Computer Weight Statement - Saturn Class Vehicle Two-Stage 1975 ISP (330,000-Pound Orbital Payload). | 77 |
| 19 | Computer Weight Performance Data Saturn Class Vehicle Two-Stage 1975 ISP (330,000-Pound Orbital Payload) | 78 |
| 20 | Computer Weight Statement—Medium Range Payload Vehicle Two-Stage Current ISP (30,000-Pound Orbital Payload) | 81 |
| 21 | Computer Weight Performance Data—Medium Range Payload Vehicle Two-Stage Current ISP (30,000-Pound Orbital Payload) | 82 |




...G PAGE BLANK NOT FILMED.

| Table | | Page |
|---|---|---|
| 22 | Computer Weight Statement - Post-Saturn Class Vehicle Two-Stage Current ISP (1,000,000-Pound Orbital Payload) | 83 |
| 23 | Computer Weight Performance Data Post-Saturn Class Vehicle Two-Stage Current ISP (1,000,000-Pound Orbital Payload). | 84 |
| 24 | Computer Weight Statement - Medium Range Payload Vehicles Two-Stage 1985 ISP (100,000-Pound Orbital Payload). | 87 |
| 25 | Computer Weight Performance Data—Medium Range Payload Vehicle Two-Stage 1985 ISP (100,000-Pound Orbital Payload). | 88 |
| 26 | Computer Weight Statement - Post-Saturn Vehicle Two-Stage 1985 ISP (2,000,000-Pound Orbital Payload) | 89 |
| 27 | Computer Weight Performance Data—Post-Saturn Class Vehicle Two-Stage 1985 ISP (2,000,000-Pound Orbital Payload) | 90 |
| 28 | Generalized Payload Exchange Ratios Medium Range Payload Vehicles | 93 |
| 29 | Generalized Payload Exchange Ratios Saturn Class Vehicles | 94 |
| 30 | Generalized Payload Exchange Ratios Post-Saturn Class Vehicles | 95 |
| 31 | Structural Components and Their Design Applied Load ($N_x$ in Pounds per Inch) | 101 |
| 32 | Monocoque and Waffle Printouts | 108 |
| 33 | Skin-Stringer and Honeycomb Sandwich Printouts | 109 |
| 34 | Current Material Properties - Aluminum, Titanium and Beryllium | 111 |
| 35 | Representative Material Properties and Advancements | 112 |
| 36 | Effect of Pitch Restriction on Unit Weight | 151 |
| 37 | Component Weight Changes With Material/Construction Type Current Saturn Payload Class Two-Stage Vehicle | 158 |
| 38 | Component Weight Changes With Material Types Current Saturn Payload Class Two-Stage Vehicle | 159 |
| 39 | Component Weight Changes With Material/Construction Types 1985 Saturn Payload Class Two-Stage Vehicle | 160 |
| 40 | Component Weight Changes With Material Types 1985 Saturn Payload Class Two-Stage Vehicle | 161 |
| 41 | Component Weight Changes With Material/Construction Types Medium Range Payload Class Vehicles | 162 |
| 42 | Component Weight Changes With Material/Construction Types Post-Saturn Payload Class Vehicles | 163 |
| 43 | Payload Merit Functions for Two-Stage Current Saturn Class Vehicles | 168 |

| Table | | Page |
|---|---|---|
| 44 | Manufacturing Complexity Factors - S&ID and Lockheed | 171 |
| 45 | Component Weights and Costs - Current Saturn Payload Class Vehicle | 180 |
| 46 | Component Weights and Costs - 1985 Saturn Payload Class Vehicle | 181 |
| 47 | Component Weights and Costs - Current Medium Range Payload Vehicle | 182 |
| 48 | Component Weights and Costs - 1985 Medium Range Payload Vehicle | 183 |
| 49 | Component Weights and Costs - Current Post Saturn Payload Class Vehicle | 184 |
| 50 | Component Weights and Costs - 1985 Post Saturn Payload Class Vehicle | 185 |
| 51 | Study Merit Functions - Current Saturn Payload Class Vehicle | 187 |
| 52 | Study Merit Functions - 1985 Saturn Payload Class Vehicle | 189 |
| 53 | Study Merit Functions - Current Medium Range Payload Vehicle | 191 |
| 54 | Study Merit Functions - 1985 Medium Range Payload Vehicle | 193 |
| 55 | Study Merit Functions - Current Post Saturn Payload Class Vehicle | 195 |
| 56 | Study Merit Functions - 1985 Post Saturn Payload Class Vehicle | 197 |
| A-1 | Minimum Liftoff Input Nomenclature | 229 |
| A-2 | Maximum Payload Input Nomenclature | 239 |
| A-3 | Two-Stage Vehicle - Maximum Payload Printout | 241 |
| A-4 | Input Nomenclature for Generalized Payload Exchange Ratio | 246 |
| B-1 | Subroutine Input Nomenclature | 265 |
| B-2 | Weight Performance Printout Summary Three-Stage Vehicles - Minimum Liftoff Mode | 271 |
| B-3 | Weight Performance Printout Summary Two-Stage Vehicles - Minimum Liftoff Mode | 272 |
| B-4 | Case 9 Vehicle Geometry - Three-Stage Vehicle | 274 |
| B-5 | Case 9 Parametric Loads - Three-Stage Vehicle | 276 |
| B-6 | Case 9 Parametric Applied and Design Loads Three-Stage Vehicle | 277 |
| B-7 | Case 9 Parametric Weight Statement - Three-Stage Vehicle | 278 |
| B-8 | Case 20 Vehicle Geometry | 288 |
| B-9 | Case 20 Parametric Loads | 289 |
| B-10 | Case 20 Parametric Applied and Design Loads Stage Partials | 290 |

| Table | | Page |
|---|---|---|
| B-11 | Case 20 Parametric Weight Statement | 291 |
| B-12 | Case 20 Preliminary Design Synthesis - Weight and Balance Summary | 293 |
| B-13 | Case 20 Preliminary Design Synthesis Loads Check | 294 |
| C-1 | Input-Output Nomenclature | 329 |
| C-2 | Monocoque Printout | 331 |
| C-3 | Skin Stringer Printout | 334 |
| C-4 | Waffle Printout | 334 |
| C-5 | Honeycomb Sandwich Printout | 337 |
| C-6 | Influence of Face Sheet Buckling on Unit Shell Weight | 339 |
| C-7 | Influence of Stringer Shape on Optimum Configuration | 340 |
| C-8 | Influence of Stringer Pitch | 341 |
| C-9 | Influence of Core Depth and Density on Unit Shell Weight | 342 |
| C-10 | Influence of Analytical Methods on Honeycomb Sandwich Construction | 343 |

# INTRODUCTION

This study contract stems from the need for a technique to economically determine and evaluate areas in which research and development in the structural/material sciences can lead to significant improvements in future launch vehicle systems, whether these systems are uprated modifications to existing systems or entirely new. The problem in planning for and allocating research and development funds efficiently is a very complex one, requiring detailed direction for an overall research plan involving research directed towards specific useful application in future vehicle systems. Any research and development in the field of structures/material is both costly and time-consuming. Therefore, the primary decisions that must be made are (1) where best to allocate funds, and (2) when will be the most opportune time to fund the research study to ensure sufficient development lead time for its inclusion in a specific vehicle system.

In order that decisions be sensible and timely the spectrum of future vehicle systems, which result from predicted advances in all the other technological disciplines, must be understood. Any program or technique that is developed to help provide the necessary data for research and development planning must have the ability to synthesize these future launch vehicle systems and to measure the interaction of the basic launch vehicle parameters with the structural system as they affect vehicle performance and cost. Any techniques that are developed to assist in defining the required research direction must be capable of starting from basic mission requirements. With a minimum of input data, the program must synthesize realistic vehicle systems to meet these requirements, evaluate the effects of suggested structures/material advancements on the various components of the synthesized vehicle, and identify the most useful type of research and its best application. This application should be identified by specific vehicle systems and type of components.

To produce data that fully represents the overall effects of any type of research in structures and material, the analytical approach must consider basic performance improvements in terms of weight reductions and payload gained, together with the monetary aspect of fabricating the end product and determining the relative economics when applied to specific vehicle systems. Therefore, it is an inadequate argument to say, for example, that investing a great deal of money in the development of beryllium is justified because beryllium has a high strength-to-weight ratio that will result in lighter

structures. While it is true that this ratio furnishes the basic ingredients to design a lighter structure in which compression stability is the critical design failure mode, a fundamental question must be answered before a long-range, costly R&D effort can be justified—"What performance payoff can be expected in future vehicle systems and how much will it cost?" Answering such a question requires a knowledge of what the advanced launch vehicle system might resemble, whether the system consists of up-rated components of existing vehicles or radical new designs.

Due to the vast array of vehicle system parameters that have to be considered, together with the numerous suggested types of applicable structures/material research and development, the synthesis must be parametric for vehicle descriptions and at least preliminary design when the structural details are described.[1] Therefore, the use of high-speed digital computers is mandatory, and the sophisticated synthesis programs that are required must be carefully managed to control the computational time within acceptable limits. It should be understood that original ideas, new design concepts, vehicle system arrangements, etc., can be conceived only by the human mind; this capability is presently entirely beyond digital computers. However, these computers can assess the value and performance of these concepts for a large array of vehicle systems to indicate the most beneficial area of application. The great advantage of the automated approach of programmed assistance is its ability to quickly and efficiently translate these ideas into realistic applications and present data displays from which research direction can be logically deduced.

Sizing a realistic vehicle has to consider the development period in order to include not only predicted advancements in material and structures, but also those advancements that would probably occur in the other disciplines that primarily influence the vehicle design. For example, the vehicle propulsion system must be representative of the period considered—items such as changes in thrust, specific impulse, propellant density, and the basic engine accessories must be unique to that particular period. The complicated interplay of these parameters is difficult to measure manually and, therefore, requires this automated procedure to make these interactions fully understood.

---

[1] Parametric Synthesis - An automated technique in which numerous vehicle systems are synthesized using limited input parameters and resulting in lumped-mass definitions of vehicle stages and their primary subsystems, stage performance ratios, and gross size characteristics.

[illegible] Synthesis - An automated technique in which a few vehicle systems are subjected to [illegible] preliminary design analysis considering component design constraints and resulting in identification of [illegible] design within the limits of the input constraints—in this study considering only the [illegible].

The automated technique must be flexible enough that parameter inputs can be readily altered. Efficient running time and readily discernible displays must be used to output the large quantities of data in order that important parameters can be selected. This technique must also be flexible enough that it can easily be used to analyze other vehicle configurations and structural arrangements at some future date without requiring a completely new program approach or extensive modification.

From a structural standpoint, the size, design loading, and thermal environment of a structural component have considerable influence upon the choice of materials, type of constructions, and fabrication method employed. In order to realistically determine what these advanced launch vehicles and their structural design environments might represent, it is necessary to begin with mission definitions and to establish payload, vehicle size, and performance characteristics. Vehicle system parameters strongly interplay with each other, and the vehicle structural system is strongly influenced by each of them. With its strong dependency on other subsystems, structural sciences research cannot be evolved in a vacuum. It must reflect the basic mission requirement and its interaction between the structural system and the other functional systems. Economic measurements must also be included to determine the worth of conducting research in a particular structural area.

The effort documented in this report utilizes the North American Aviation, Inc., Space and Information Systems Division (S&ID) background in launch vehicle synthesis and computer-aided design by modifying existing subroutines from these in-house computer programs. This study draws heavily upon previous S&ID launch vehicle synthesis work (References 1, 2, 3, and 4) and the parametric synthesis and preliminary design synthesis phases of S&ID computer-aided design (Reference 2).

This report covers the first phase of a planned three-phase program, each phase lasting one year. Phase I involves utilizing modified automated synthesis analytical techniques to determine significant structures/materials research areas in current and predicted expendable launch vehicle systems. It covers the parametric synthesis of expendable launch vehicles, followed by a more detailed design synthesis of the cylindrical shell structural components of these vehicle systems. The vehicle systems included vertical launched multistage tandem arrangements with RP-1/LOX and $LH_2$/LOX propellant combinations and structural shell systems of monocoque, skin-stringer, honeycomb sandwich, and waffle constructions for aluminum, titanium, beryllium and steel materials. Planned effort during Phase II includes (1) design synthesis of additional components (interstages, frustums, thrust structures, and bulkheads) and additional structures/materials shell concepts; (2) extending the vehicle parametric synthesis method to include recoverable first-stage booster systems to measure the influence of developments in structures and materials technology on the general configuration of advanced vertically launched, horizontally recovered, powered flyback, winged vehicles; and (3) defining methods for turning computer programs over to the NASA.

Phase III of the program will complete the parametric synthesis of recoverable launch vehicles, including upper stages and include design synthesis of basic structural systems to predict weight savings attainable on specific structural components through advances in the structural sciences.

## STUDY APPROACH

To accomplish study objectives, modified programs were utilized to synthesize vehicle systems, perform preliminary structural design analysis, and conduct trade-off studies to accomplish the following:

1. Identify systems-oriented functional research that will result in maximum performance dividends

2. Isolate structures/materials areas requiring future research

3. Evaluate the weight, performance, and cost benefits of conducting research in the indicated structures/materials areas

The two basic tasks considered in this phase of the study were vehicle parametric synthesis and preliminary design synthesis. For Task I, launch vehicle parametric synthesis, the S&ID launch vehicle program was modified to the particular study requirements and was used to evaluate the influence of various developments in structures and materials technology on the general configuration of advanced, vertical-launched, expendable vehicle systems. The program was used to synthesize, parametrically, basepoint vehicle structural-system unit weight requirements from limited and preliminary definitions of payload, mission requirements, propulsion system type, general vehicle configuration, and various structural concepts and materials. Computer test cases were obtained to identify the effects of likely forecast trends in structural development, fabrication technology, materials properties, environmental factors, and systems requirements on structural system weight and cost.

Task II initiated the launch vehicle preliminary design synthesis portion of the study. This involved the structural preliminary design subroutines of the S&ID launch vehicle program which were modified and then used to define, in detail, the weight reductions that can be realized in specific structural components through advances in structural research and development. These subroutines analyzed the structural system component by component, considering realistic design loads and thermal environmental conditions, types of construction, and materials properties. During this phase, the preliminary design synthesis trade-off studies were restricted to pressurized and unpressurized shells with monocoque, skin-stringer, honeycomb sandwich and waffle constructions. Because of S&ID's computer synthesis experience the programs for TASK I and II were kept separate and executed separately or in combination with each other.

The basic study approach can be differentiated into five steps, which re performed systematically for the various basepoint designs and the pectra of structural developments:

1. Predict the future vehicle and mission requirements

2. Synthesize vehicle generic families from their mission requirements

3. Evaluate weight reductions of components for structural/material improvements in these vehicle families

4. Assess the effectiveness of all predicted improvements

5. Identify significant research areas by an ordering of beneficial effectiveness

## PREDICTION

For example, the periods covered in the prediction task are from the present through 1970, from 1970 to 1980, and post-1980. The investigation covers tandem boost systems, and predictions to identify future payload weights and sizes for specific missions, the number of vehicles required, and the mission velocity requirements for these missions. System characteristics were identified for future periods by type and number of propulsion systems, type of propellant that might be used, number of stages, design criteria (e.g., would there be any change in manned-unmanned criteria), type of material and construction elements available and, finally unit cost predictions. The cost assessment was based upon present-day dollars, and material price predictions were derived by extrapolating historical information. Material cost predictions as a function of year were estimated for study inputs and can be considered the best estimates presently obtainable.

## SYNTHESIS

The synthesis task involved defining basepoint vehicles for the considered payload spectrum, parametrically proportioning the stages for these vehicle systems, and providing sensitivity measurements for both a maximum payload weight mode and a minimum liftoff weight mode.[2] The program must derive realistic stage mass fractions for each stage of these vehicles.

Maximum Payload Weight Mode - Vehicle sizing from a given lift-off weight to achieve maximum payload weight.

Minimum Lift-off Weight Mode - Vehicle sizing from a given payload weight to achieve minimum vehicle lift-off weight.

weight reduction program might clearly define a requirement for removing so many pounds from a stage. The weight reduction arrays may be quickly scanned to select component constructions that aid in meeting the target weight. If vehicle performance is part of the selection criteria, the same array indicates the component that will achieve a maximum payload improvement. Cost assessment ratio ordering is flexible; for example, this may be measured as minimum dollars per pound of payload in orbit or additional dollars per pound of payload improvement. Each cost ratio is meaningful if ordered in ascending or descending magnitudes. The important measure of their effectiveness is obtained by their relative ordering. Since only the basic cost is involved in the design and fabrication of these structural components, the resulting magnitude of the cost ratio's will be rather low when considered in terms of dollars per pound of payload from those obtained from a cost effectiveness study of an overall vehicle system. Structural cost comprises only one element of a total systems cost effectiveness study which must include design, testing, launching, tracking, ground equipment, etc. This study does not attempt to investigate cost effectiveness. It does present a preliminary method for assessing costs for a particular exchange of structural components, although this method has not been completely verified and requires further investigation.

# VEHICLE SYNTHESIS

The phase of the study covered in this report was limited to the synthesis of vertical-launched, tandem-staged bipropellant vehicles. Test cases were conducted on two- and three-stage vehicles. Construction/material design synthesis measurements were made for pressurized and unpressurized cylindrical shells using aluminum, titanium, steel, and beryllium materials in monocoque, skin-stringer, bonded honeycomb sandwich, and waffle shell constructions.

Figure 1 differentiates the parametric synthesis task from the preliminary design synthesis task and illustrates how the flow of information between program elements is affected. Vehicle synthesis is initiated by defining mission requirements (payload weight and velocity) and the propulsion characteristics for the mission (thrust levels, specific impulse, mixture ratio, propellant type and density). A general configuration indicator for the vehicle is defined for the digital program. This permits identifying the proper stage sizing model to identify tankage arrangements, fineness ratios, diameters, bulkhead aspect ratios, etc.

Preliminary basepoint shell construction data are provided by the stress analysis subroutines and stored in terms of generalized unit weight/radius versus applied load/radius curves. The minimum liftoff mode of the stage proportioning subroutine (Appendix A) is used to initiate stage-wise performance characteristics for the stage mass fraction subroutine (Appendix B) which sizes basepoint vehicles and identifies mass fraction partials about the basepoints. The generalized shell weight curves are used to weigh vehicles in the mass fraction operation. The resulting mass fraction curves are then recycled through the maximum payload mode proportioning subroutine. When the vehicle has been proportioned satisfactorily, the generalized payload exchange ratios are produced for the basepoint vehicles. Printouts from the mass fraction operation are obtained to define vehicle geometry, weight statements, mechanical loading environment, and mass properties.

Enough data are then available to check the trajectory with a larger external program (such as S&ID's Flight Science Trajectory Program AP-188). However, data indicate that this option may not be necessary due to the parametric approach and the parametric related accuracy of the proportioning operation. A more thorough check of the vehicle mechanical loadings can also be obtained from a preliminary design loads program, such as the sizing-loads subroutines of S&ID's Launch Vehicle Preliminary

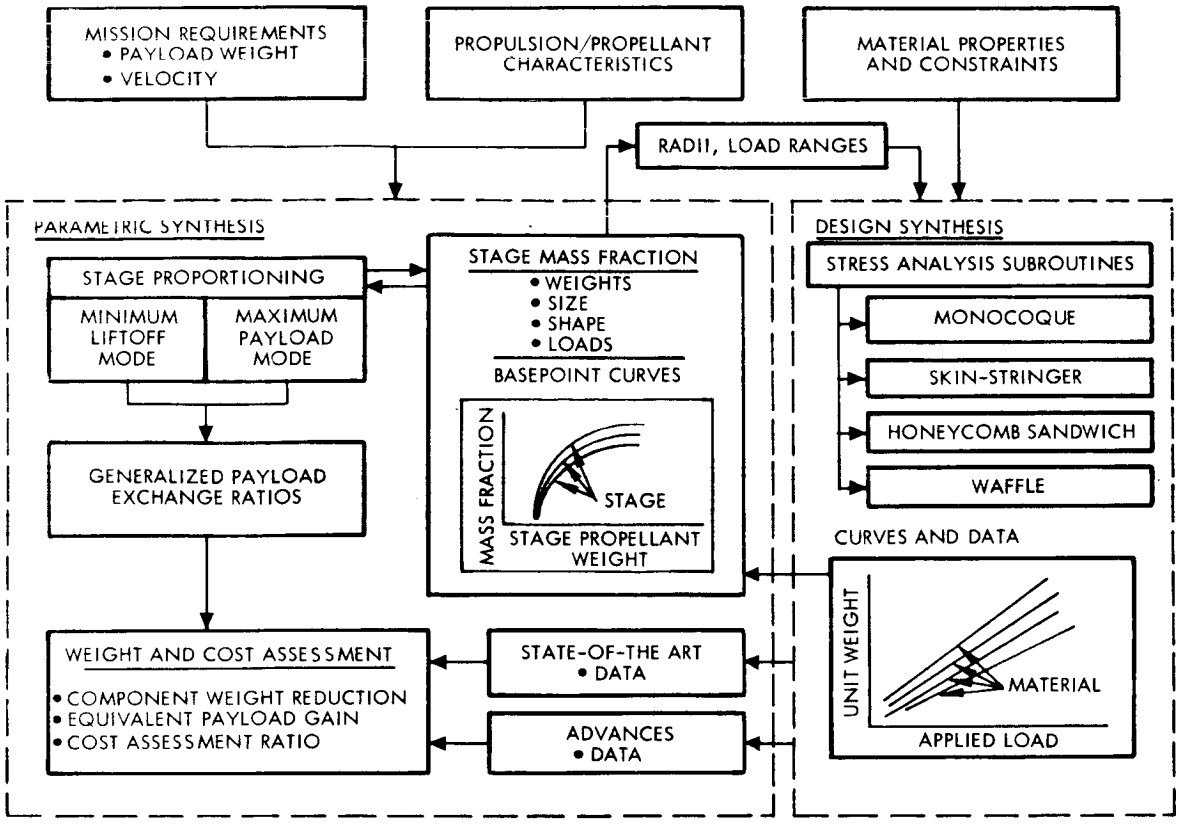



Figure 1. Evaluation Logic

Design Synthesis Program 6J-400 (Reference 2). If an adjustment of the parametric loads is desired, coefficients can be supplied to the mass fraction subroutine and the operation recycled. These large programs are not part of this study but are merely used as check points.

When basepoint vehicles have been properly established, a range of loading intensities is considered for the design synthesis stress analysis operation to provide design data covering all pertinent construction types and materials. These data, in terms of applied load, unit weight, radius, and pressure can be fed directly to the assessment model to determine the direct effect upon component weight, equivalent payload, and cost assessment ratio when one material-construction structural component is substituted for another. If desired, the generalized weight-load curves for these alternate designs can be used by the stage mass fraction subroutine and the proportioning operation to resize the entire vehicle.

The [illegible] subroutine independency in the program logic provides [illegible] flexibility that is demonstrated in later sections of this report. For example, each basic subroutine illustrated in Figure 1 (stage proportioning, stage mass [illegible] exchange ratios, cost assessment model, and stress analyses) can be executed by itself or with others in the program. The particular subroutine linkage illustrated in Figure 1 is unique and provides a simplified means of solving the basic problem identified in this report.

# EVALUATION OF STRUCTURAL COMPONENTS

The structural components generated in the design synthesis subroutine are based on a range of vehicle diameters, loading intensities, and thermal environments representative of the medium, Saturn, and post-Saturn class vehicles. The design requirements associated with these vehicle classes are combined with manufacturing constraints, such as minimum skin gauges, to form the design criteria for the structural component.

Various design parameters (skin and stringer thicknesses, stringer and frame pitches, stringer shapes and sizes, etc.) are considered as orthonormal vectors ($e_i$) forming a (n) dimensional topology to represent all design variations. The unit weight of each design is the magnitude of the radius vector from the origin to the point in design space. Design synthesis is involved with the problem of minimizing this radius vector with imposed boundary conditions requiring the resultant structure to obey a constraint hyposphere of design load environments, manufacturing restrictions, limitations, etc. The design weight is formulated by

$$W = \text{Minimum} \left[ \sum_{i-1}^{n} f\ (a_i e_i) \cdot f\ (a_i e_i) \right]^{1/2}$$

where

$a_i$ = weighting coefficients assigned to the various design parameters

$f\ (\ )$ = function transforming design parameters into shell unit weight.

The design criteria and material properties representative of current or anticipated future materials are used to formulate an initial configuration or point in design space. Then, the principal parameters or dimensions of the initial configuration are varied until the minimum weight design consistent with the design requirements and manufacturing constraints is located, as illustrated in Figure 2.

In this study phase, the structural components were restricted to cylindrical shells with monocoque, skin-stringer, sandwich, or waffle cross-sections. The primary failure modes considered for these constructions are material failure, local instability, and general instability, and are discussed in detail in Appendix C.

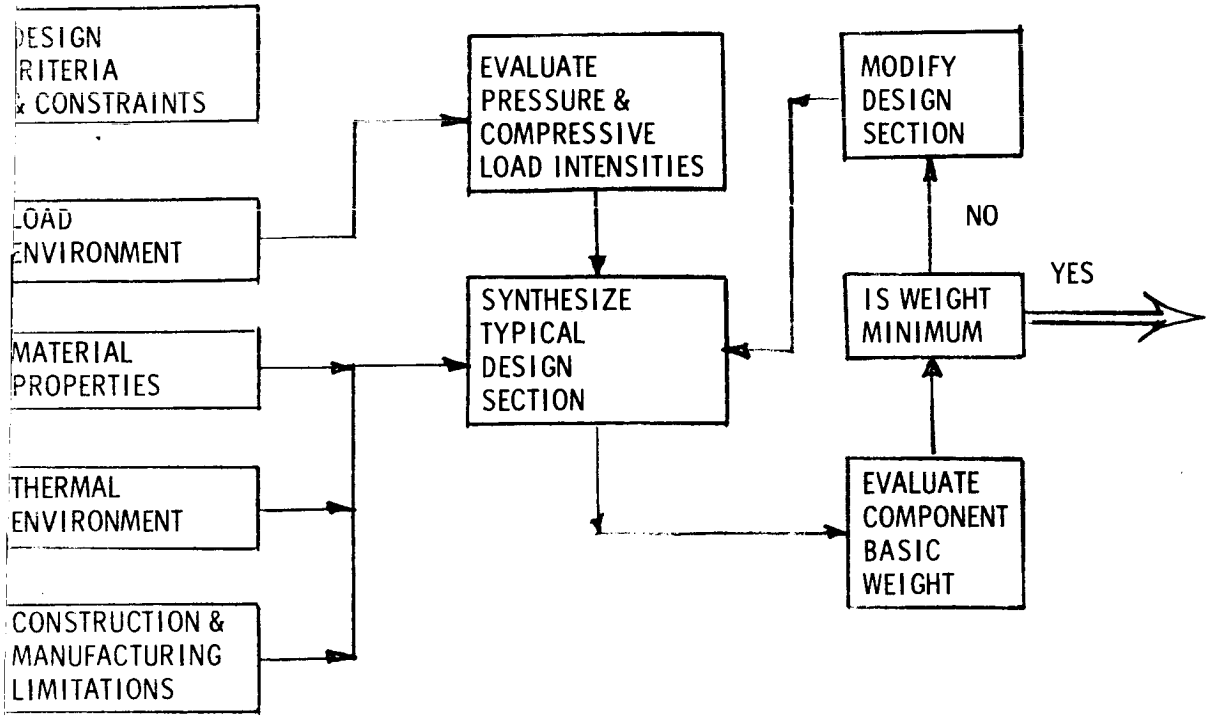



Figure 2. Design Synthesis

The potential benefits of predicted advances in materials/structures are demonstrated and compared in the three basic study merit functions: component weight, equivalent payload weight, and cost assessment ratio. The payload exchange ratios (Figure 1) are defined for changing a single component in each stage of the basepoint vehicle. The basepoint design load for each component is used to define structural shell designs for alternate structures/materials configurations. A parametric weight assessment for each component is included to account for close-outs, joining, end-rings, and manufacturing tolerances.

The alternate material/construction type was substituted component by component to display merit functions for all vehicle stages. The resulting tables list the component name, weight, change in weight in the particular component from the basepoint, change in equivalent payload weight due to substitution, and cost assessment ratio for the component in terms of a comparison with the basepoint component. Since the delta changes from the basepoint vehicle are illustrated in this table for each component, assessment tables can be compared for all alternate material/construction types investigated.

The effectiveness of using a particular alternate material/construction types can be determined for a particular component by comparing the merit functions in the various tables. These merit functions can then be organized [illegible] minimizes component weight, maximizes equivalent payload gain, and minimizes the cost assessment ratio. A further discussion of this effectiveness technique along with test results is covered in the assessment section of this report.

## PARAMETRIC SYNTHESIS

Initiation of the parametric synthesis task is dependent upon a definition of the missions to be investigated and technological predictions concerning the advances that might be expected in material properties, manufacturing techniques, and propulsion/propellant systems. For this phase of the study, three basic periods were selected for investigation:

1. Current period: 1966 to 1970
2. Near-term period: 1970 to 1980 (1975)
3. Future 1980 + (1985)

For the material property predictions used in the test cases included in this report, Material A is associated with the current period; Material B is associated with the near-term period; and Material C is associated with the future 1980 + period.

The test cases in this report cover two- and three-stage launch vehicles capable of injecting payloads into near-earth orbit. Therefore, for purposes of this report, the equivalent payload is the payload in a 100-n.mi. near-earth orbit. However, the program and technique can be used to operate on various equivalent payload concepts, such as escape payload from earth orbit by including velocity calculations for injection, ejection, and transfer modes.

## MISSION DEFINITION

A survey of current and past studies was conducted to identify a reasonable spectrum of equivalent payloads in earth orbit (References 7 and 8).

Table 1 presents a summary of earth orbital payload weights for various missions that have performance windows at particular points within the three time periods under investigation. These missions included lunar, Martian, planetary, and near-earth space station operations. The equivalent payload in earth orbit represented in the right-hand column shows that three basic ranges of payload weights will probably satisfy most of the missions.

| MISSION DESCRIPTION | DURATION DAYS | CREW | DATE | LAUNCHES | PAYLOAD WEIGHT 1000 lb. |
|---|---|---|---|---|---|
| LUNAR | | | | | |
| APOLLO APPLICATIONS | 34 | 2-3 | 1970+ | | 96-100 |
| APOLLO LOGISTICS SUPPORT | 14-20 | 2-3 | 1972+ | 4/YEAR | 184-190 |
| EXPLORATION SYSTEM FOR APOLLO | 90-600 | 6 | 1975-80 | 3/YEAR | 260-350 |
| EXPLORATION SYSTEMS | | | 1980+ | 3/YEAR | 300-500 |
| MARS | | | | | |
| MANNED FLYBY | 640 | 4 | 1972 | | 335 |
| MANNED FLYBY | 440 | 4 | 1973 | | 450 |
| MANNED FLYBY | 350 | 4 | 1972 | | 940 |
| MANNED ORBITER, VENUS FLYBY | 550 | 4 | 1975 | | 1080 |
| MANNED ORBITER, VENUS FLYBY | 700 | 4 | 1977 | | 1150 |
| MANNED LANDER, VENUS FLYBY | 670 | 4 | 1979 | | 1280 |
| MANNED LANDER | | 4 | 1984 | | 1280 |
| MANNED LANDER | | 4 | 1984 | | 1120 |
| VENUS | | | | | |
| MANNED FLYBY | 360 | 4 | 1972 | | 178 |
| SPACE STATIONS | | | | | |
| MORL | | | 1972 | 4-5/YEAR | 100-200 |
| MANNED SURVEILLANCE RECON & CONTROL | | | 1980 | 3/YEAR | 43 |
| MANNED REQUEST/POST ATTACK RECON | | | 1975 | 4/YEAR | 50 |
| MANNED INSPECTION (RENDEZVOUS) | | | 1975 | 12/YEAR | 45-50 |

The significant payload range (Table 1) appears to be from 225,000 to 00,000 pounds. A modified two-stage Saturn V-type launch vehicle would ossess a similar payload capability of approximately 225,000 pounds; herefore, this vehicle payload combination is identified in this report as the aturn payload class. Table 1 also indicates that a smaller payload spectrum s required for space station operations. This payload class ranges from 0,000 to 100,000 pounds in near-earth orbit and is identified in this report s a medium range payload class, or small payload class. For the manned Mars missions shown in Table 1, a new range of payloads is required in the million-pound class. These requirements could probably be achieved by endezvous of several Saturn V-type payloads. However, if and when a new ayload class vehicle is developed it would probably satisfy the requirement f injecting a payload of from one to two million pounds into earth orbit. Whether this latter vehicle (post Saturn payload class) is likely or worthwhile s not considered part of this study. However, in the future, advanced upper stage technology in nuclear and electric propulsion systems would bring all planets within range of the one- to two-million-pound payload class. This payload range is included as a future vehicle class upon which to base material/construction tradeoffs. The payload ranges can then be differentiated into three distinct classes: (1) from 30,000 to 100,000 pounds; (2) from 225,000 to 500,000 pounds; and (3) from one to two million pounds.

The launch rates indicated in Table 1 resulted in various launch rate measurements in the cost assessment operation. The primary launch rate for this study was established at six launches per year. Using a time period of approximately 10 years, it appears that the minimum number of vehicles to be investigated would be on the order of 60. In the test case results illustrated later in this report, this parameter was perturbated from 60 to 240 for the cost sensitivity studies.

The payload weight classes, time periods, and launch rates discussed herein are postulations based on past studies and current literature, and are not intended as an indication of what should or should not be achieved. These estimates were made only to provide basepoint vehicle systems for the test cases presented herein.

# TECHNOLOGICAL PREDICTIONS

## MATERIALS

To a large extent, the design of future space vehicle systems will depend upon the properties of the structural materials available at the time the design is conceived and implemented. Proper direction of useful structures research in the future is predicated upon the recognition of the significant role of materials and of the possible changes expected in materials characteristics within the next two decades. Sufficient consideration should be given to predicted changes in strength, stiffness, density, availability, fabricability, weldability, and compatibility with relation to future space vehicle system designs. The following predictions are based upon S&ID experience and general trends identified in References 9 through 15.

Efficient design of future vehicles will incorporate numerous materials selected specifically to withstand the varied and often complex environmental conditions peculiar not only to the outer structure, but also to the inner structural components, tankage, and life support systems. Present alloy systems that have performed well in space structures are expected to continue in use for the next 15 years or more with some improvements in properties. These alloy systems include those of aluminum, titanium, magnesium, beryllium, and iron. The refractory alloys and superalloys are not included since the high-temperature regimes, where they exhibit outstanding strength properties, will not be encountered by the structures considered in this phase of the study.

It is anticipated that the improvements in material properties and availability in a wider range of sizes and forms will be achieved by continuous cooperative research and development efforts conducted by industry and governmental agencies. Such efforts will be extensive and time consuming and will be directed toward accomplishing the following objectives:

1. Increased strength
2. Increased stiffness
3. Decreased density
4. Increased ductility
5. Increased toughness



PRECEDING PAGE BLANK NOT FILMED.

6. Increased fabricability

7. Increased weldability

8. Increased availability in size and form

The preceding objectives will be realized from progress in the following specific areas of materials and fabrication technology:

1. Alloy development

2. Heat treatment

3. Joining

4. Rolling

5. Forging

6. High-energy-rate forming

It is expected that alloy development programs will focus on systematic investigation of the present leading alloy systems. In conjunction with the alloy development programs, it is anticipated that efforts will be expended to develop heat-treating procedures that will result in the highest strength compatible with adequate ductility and toughness. Concurrently, research will be implemented to develop equipment and processes to produce high-efficiency joints. This attainment will permit the use of lighter-gage sheets in some structural areas and will eliminate the necessity of leaving weld lands in other areas to compensate for loss of strength in the weld zone affected by the heat. Thus, structural weight will be reduced considerably. Future demands of advanced vehicle designs for lighter-gage and wider sheets combined with closer control of thickness will promote development of improved rolling equipment and processes. The need for highly reliable and more complex components will accelerate future development of high-energy-rate processes, such as pneumatic (Dynapak), magnetic, electric discharge, and explosive forming processes.

Based on current concepts and research trends and on the rate of improvement in the past 15 years, predictions of strength properties changes in the leading alloy systems are presented in Figures 3 through 8 for a period extending beyond 1980. Figure 3 shows the expected improvements in a high-strength aluminum alloy system. A small increase in both ultimate and yield strengths is indicated with no change in stiffness within the time period under consideration. At present, aluminum alloys are generally considered to possess good fabricability. However, some of the higher strength alloys

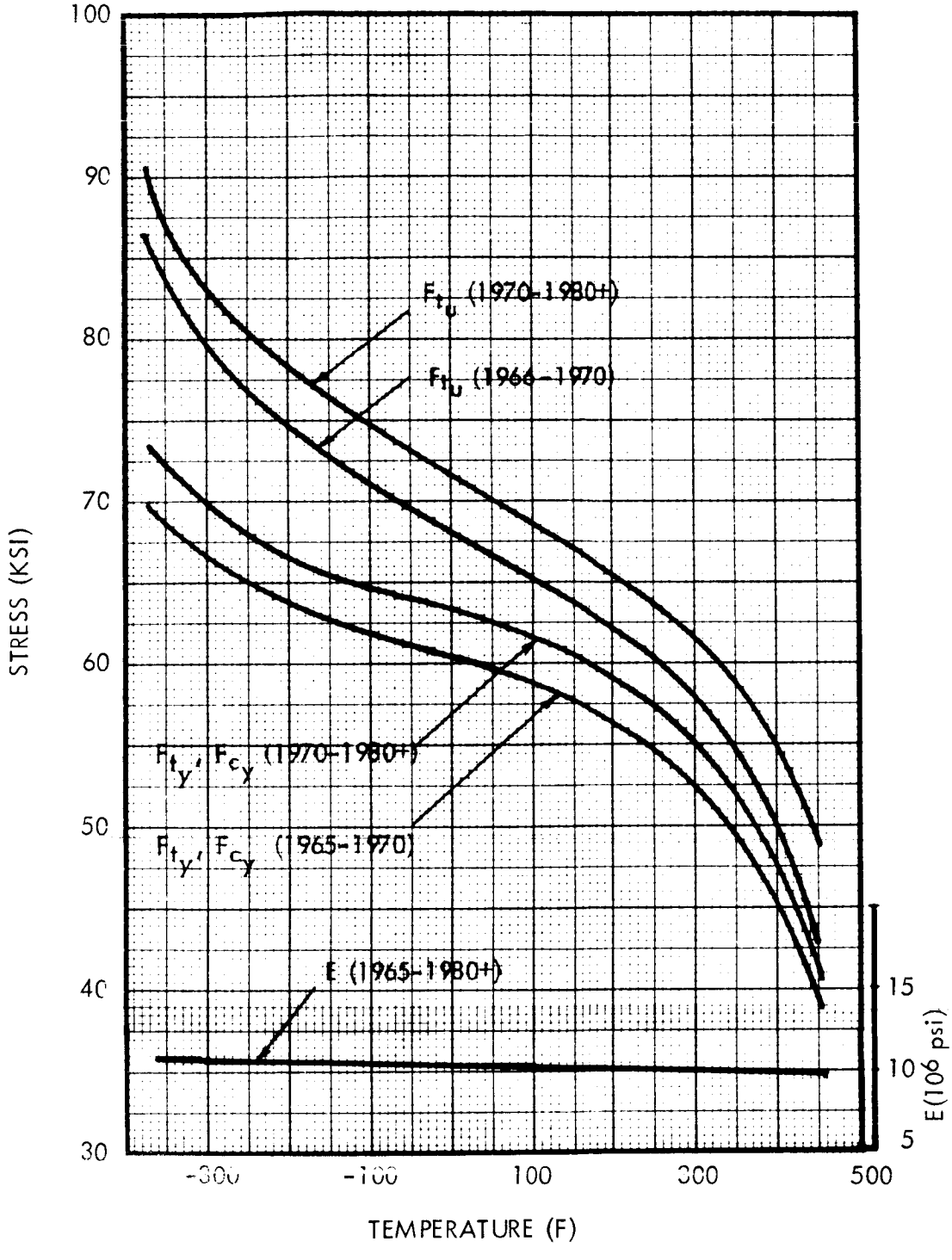



Figure 3. Future Strength Properties of a High-Strength Aluminum Alloy

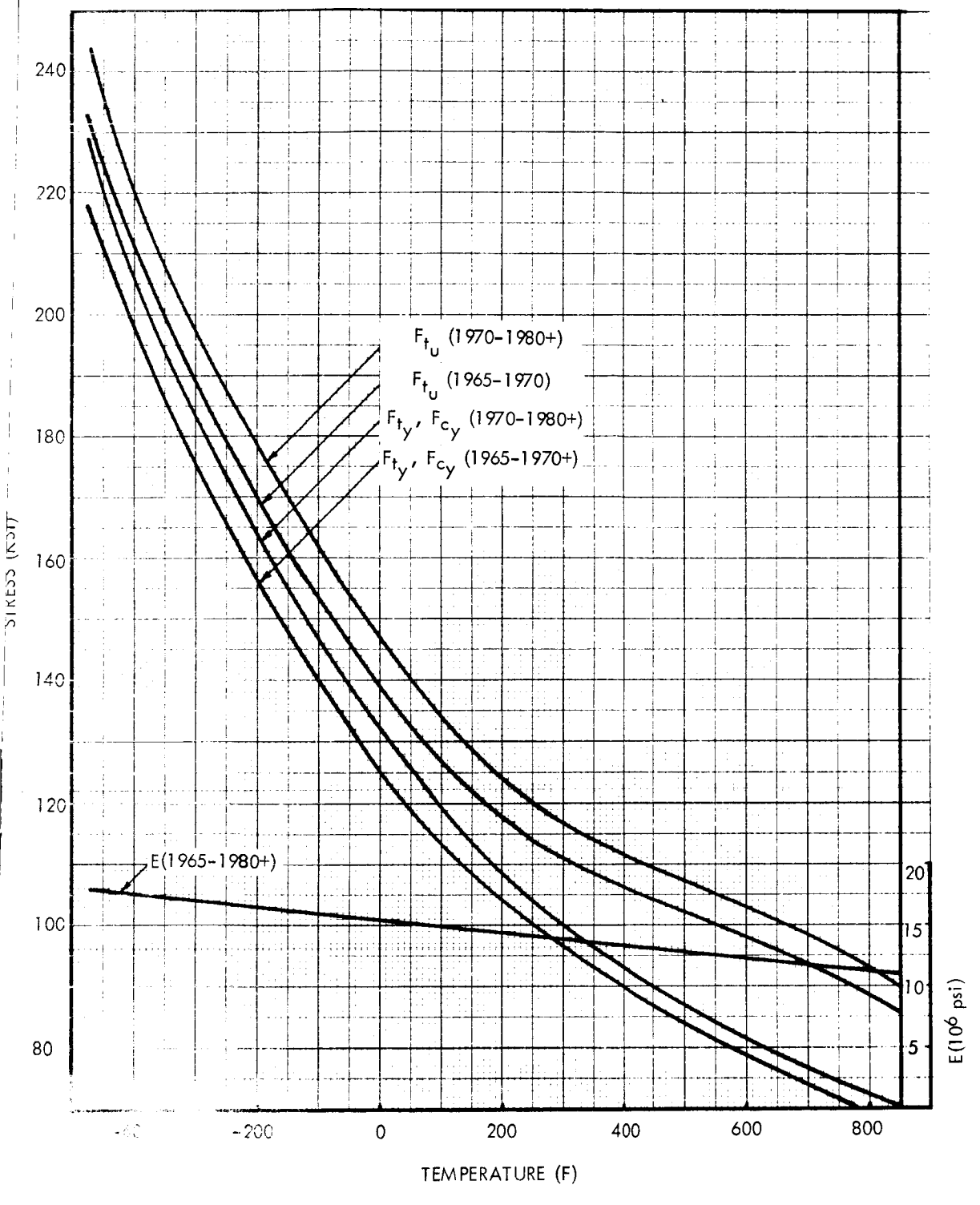



Figure 4. Future Strength Properties of a Titanium Alloy for Service to -423F

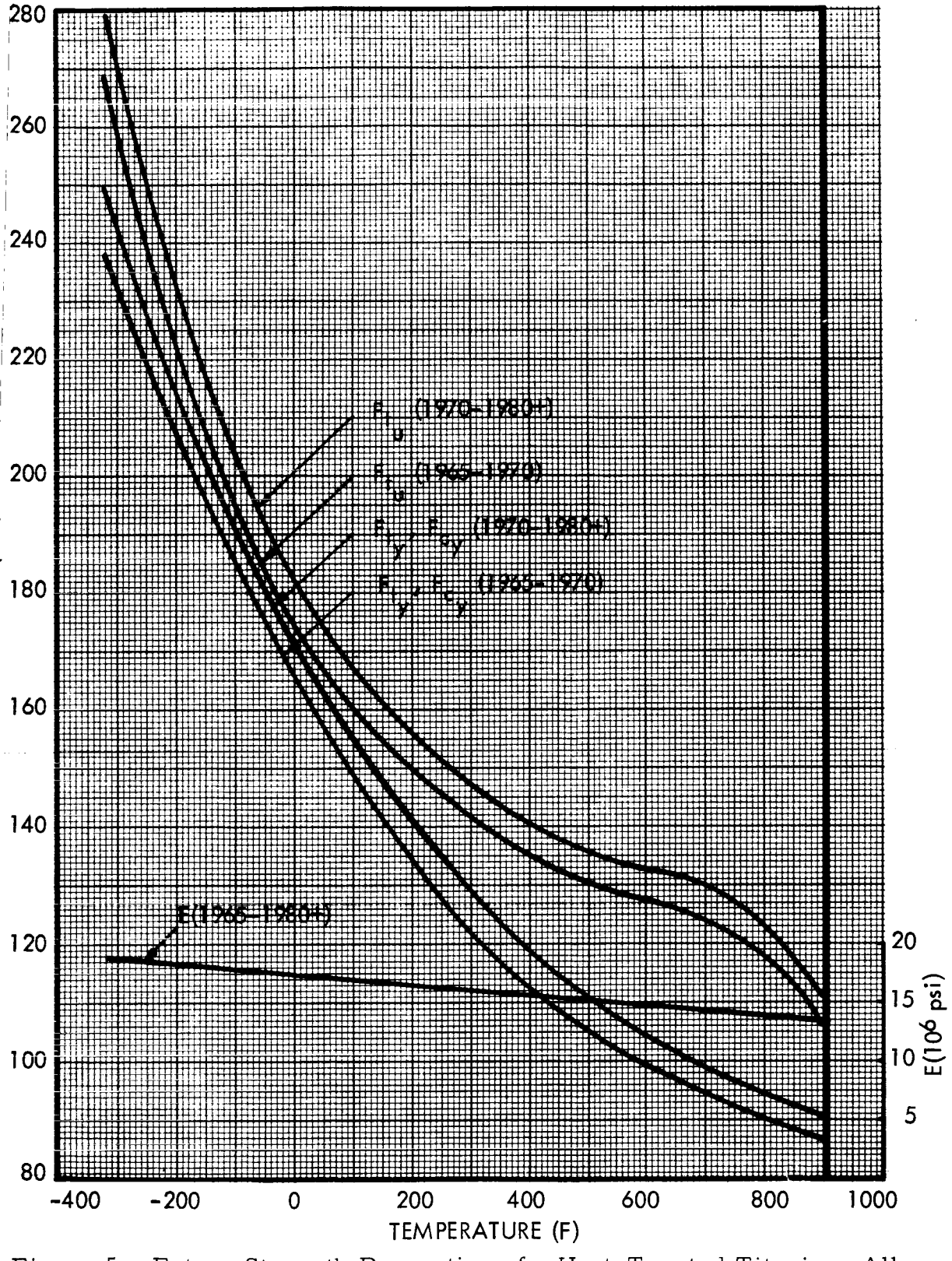



Figure 5. Future Strength Properties of a Heat-Treated Titanium Alloy

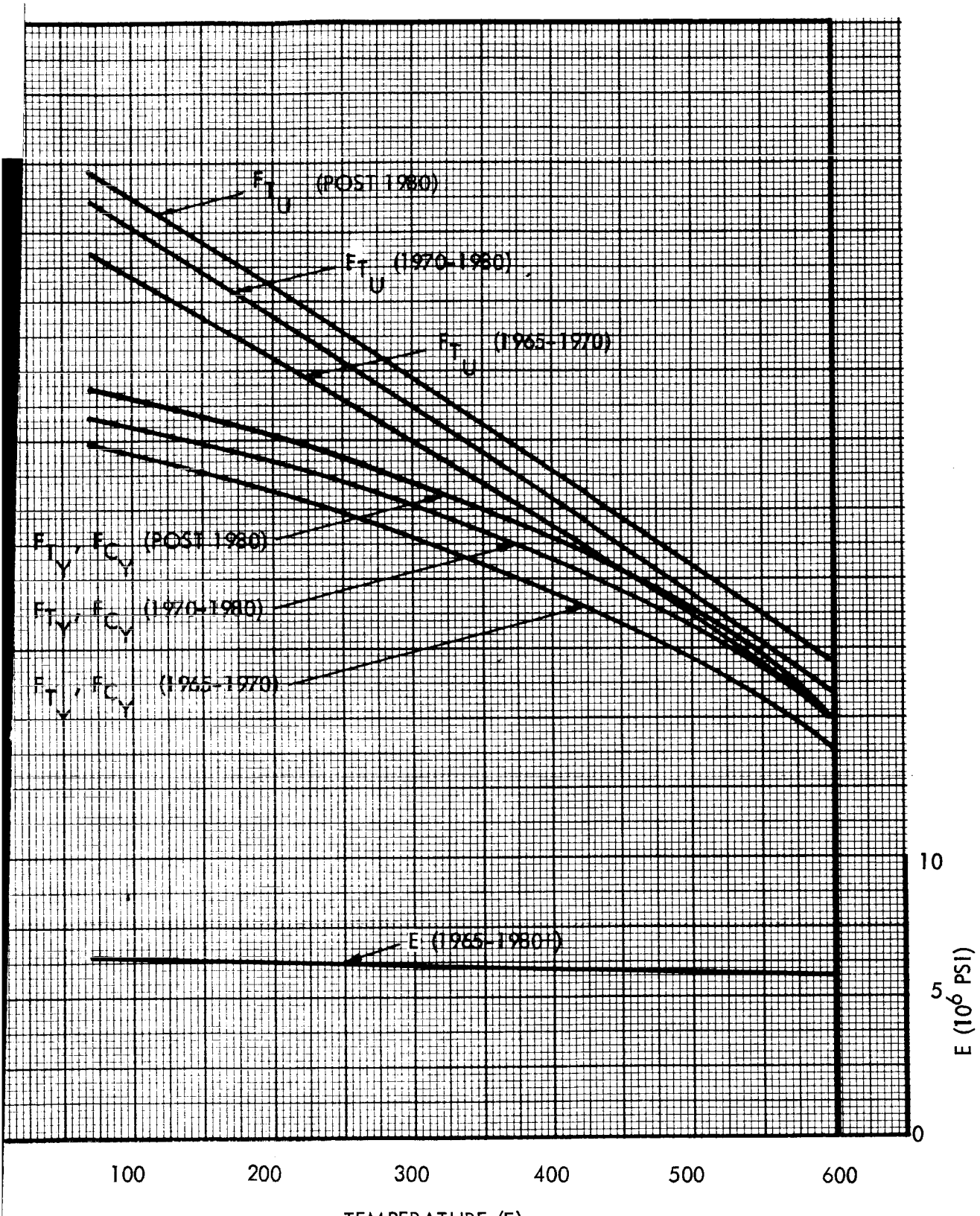



Figure 6. Future Strength Properties of a Magnesium Alloy

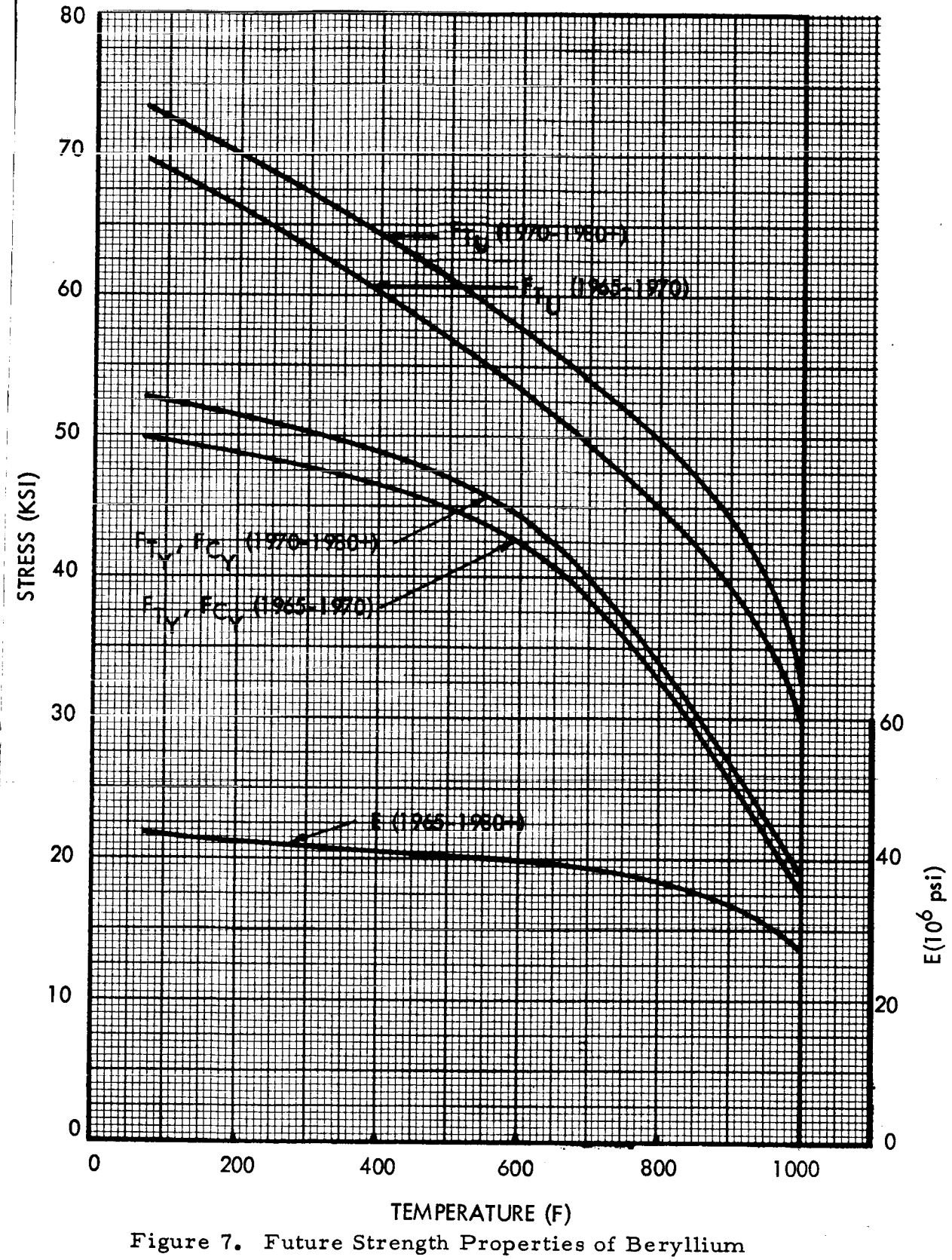



Figure 7. Future Strength Properties of Beryllium

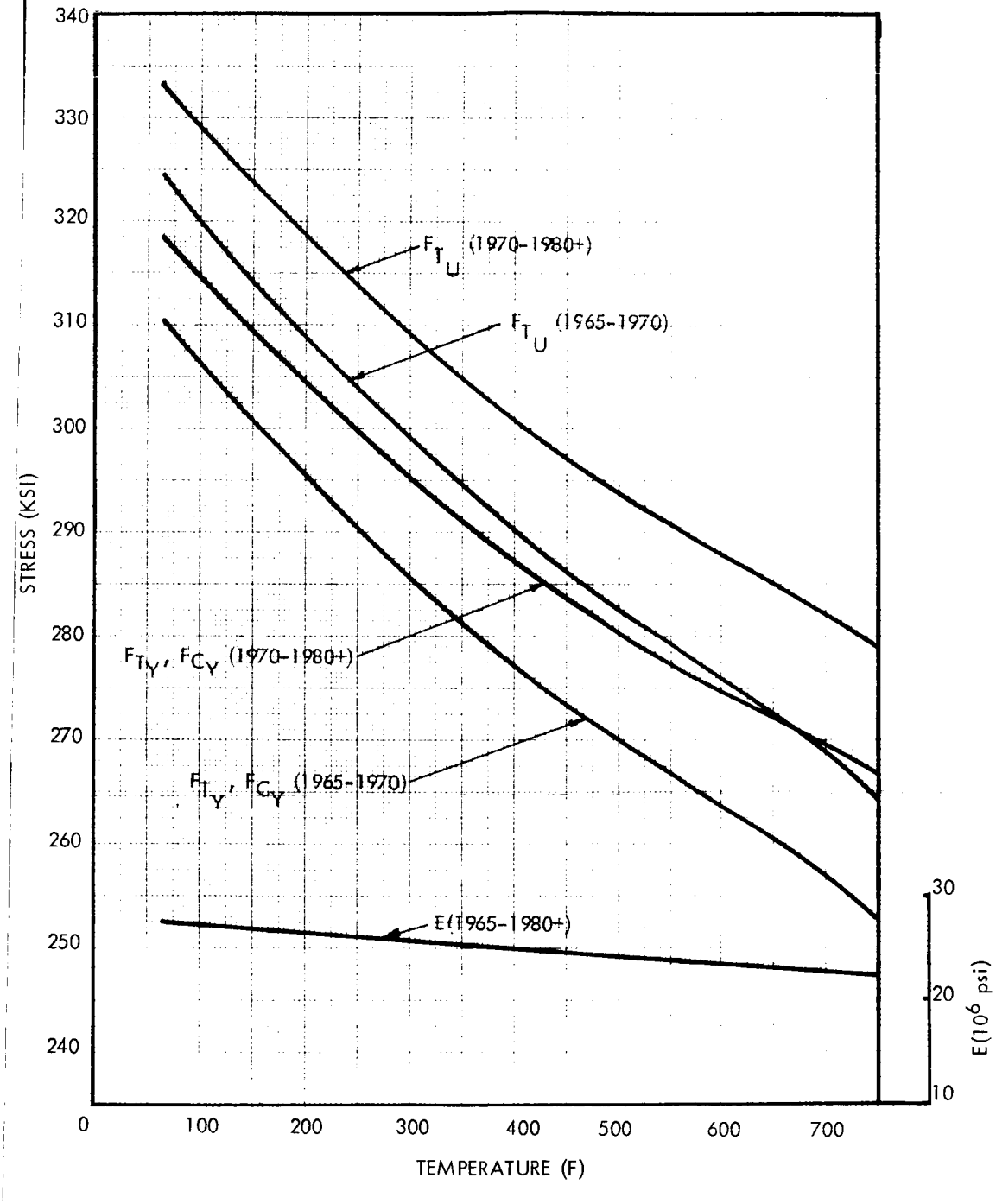



Figure 8. Future Strength Properties of a High-Strength Steel

re not fusion-weldable and are subject to microcracking during machining perations. Research efforts in recent years have resulted in development f weldable, high-strength alloys. It is projected that the property values hown in Figure 3 will be achieved as this alloy development trend is continued, with emphasis on improved weldability and increased strength.

The use of aluminum alloys has proven acceptable for $LH_2$ and LOX ankage as well as for $LF_2$, 50/50 $N_2H_4$ - UDMH blend, and MMH. The pplicability of aluminum alloys for $N_2O_4$, which may contain water and xygen difluoride, is dependent on the alloy content, It appears that the ower the alloy content of the aluminum, the higher is the corrosion resistnce to $N_2O_4$ contaminated with water. Most high-strength aluminum alloys re now available in a standard minimum gage of 0.014 inch. It is expected hat a high-strength alloy will be available in this thickness to 1970. Between 970 and 1980 it is anticipated that the standard minimum gage for this material will be 0.005 inch on a production basis. Typical increases of 0 percent in both the tensile ultimate and compressive yield are considered ikely before 1985.

Titanium alloys are readily formable and weldable when the proper echniques and processing precautions are used. As a direct result of alloy development and improvements in processing, it is predicted that the properties presented in Figures 4 and 5 will be achieved. The alloy of Figure 4 will be usable to -423 F for $LH_2$ tankage since it will possess adequate oughness to this temperature. Continuation of research concerning the effects of interstitial elements on the properties of titanium alloys will contribute to the development of such an alloy. Figure 5 presents strength properties for a higher-strength alloy which will exhibit insufficient toughness below -320 F. The impact sensitivity of titanium alloys in contact with strong oxidizers limits their use in tankage. In LOX, ignition of titanium propagates catastrophically when impacted. Titanium alloys must be carefully evaluated prior to use with strong oxidizers, especially as new oxidizers are developed in the future. The present standard minimum sheet thickness for titanium alloys is 0.020 inch. Thinner gages can be obtained by chem-milling the sheet. Further reduction in standard minimum thickness is not expected before 1970. By 1980 it is expected that rolling equipment and processing will be developed to produce a minimum gage of 0.010 inch, which will remain as a minimum for the post-1980 period.

Magnesium alloys possess low density and low strength and, as a result, do not exhibit as high a strength-to-density ratio as the aluminum or titanium alloys. Anticipated increases in strength properties in a magnesium alloy are presented in Figure 6. These increases could conceivably result from alloy modification, improved processing, and refined heat-treating procedures. These improvements are not large, but will probably be continuous from 1965 to 1980 and beyond. The modulus of elasticity of

magnesium alloys is low. It is projected that no appreciable improvement will result in this property over this period since alloy additions made to accomplish this improvement would impair the already low toughness.

The magnesium alloys require special forming and welding procedures. Forming must be done at slightly elevated temperatures with special tooling; welding must be accomplished under a protective atmosphere. These characteristics are not expected to be altered over the next two decades. Magnesium alloys are susceptible to corrosion from the chemicals proposed as propellants for advanced propulsion systems. At present, magnesium alloys exhibit low corrosion resistance to 50/50 hydrazine - UDMH blend and fair corrosion resistance to dry $N_2O_4$. The standard minimum-gage sheet available for magnesium alloys is 0.016 inch unless purchased by special order. In the case of a special order, the minimum sheet thickness is 0.006 inch. It is expected that this will be the case for future higher-strength alloys.

Beryllium is an outstanding structural metal because of its high strength-to-weight and stiffness-to-weight ratios. However, this material has the disadvantage of possessing very low ductility and, as a result, must be used with certain precautions. Special design procedures have been developed and should be followed which capitalize on the advantageous properties of beryllium and which avoid stress conditions conducive to brittle failure. Research and development programs have been conducted over the past several years to improve the ductility of beryllium and some progress has been made to achieve this objective through special ingot casting and rolling techniques. Alloy development programs have resulted in the formulation of a beryllium-aluminum alloy which exhibits greater ductility, but lower strength and stiffness characteristics. It is expected that future research and development during the next 15 years or so will continue to exploit these approaches with emphasis on ductility improvement rather than strength and stiffness. The curves shown in Figure 7 indicate this trend with no increase in strength to 1970 and a small increase in the period between 1970 and post-1980. No change in modulus of elasticity is indicated within the time period considered.

Beryllium sheet can be successfully formed with special tooling and techniques at elevated temperatures. Conventional welding processes do not produce efficient and reproducible welds in beryllium. Brazing, diffusion bonding, adhesive bonding and mechanical joining have been used effectively, and development of these processes will continue in the future for the fabrication of advanced vehicle components. Light-gage sheet stock of beryllium is presently available to 0.020 inch on special order. Successful production of foil thicknesses has been accomplished in narrow strips. It is expected that as the demand for this material increases, the minimum sheet thickness for wide sheets will be decreased to 0.015 inch by 1970-1975.

Alloy steels must exhibit very high strength to compensate for their elatively high density to compete on a strength-to-weight basis with the ghter alloys previously discussed. The development of the high-strength araging steels in recent years has placed them in such a competitive posi- on for some structural applications. These new steels not only possess very igh strength and toughness, but are readily fabricated, welded and heat- reated. Parts can be easily formed from this type of steel in the annealed ondition and then heat-treated by a simple reheating which has the advantage f minimizing distortion. Considerable research effort is being concentrated n this class of steel to further improve the strength properties. Alloy and rocessing developments are expected to be effective over the next 15 years nd beyond to the extent indicated in Figure 8. Sheets of maraging steels are eing produced to a minimum gage of 0.015 inch in wide sheets. Thinner ages can be produced in narrow strips. It is not expected that any appreci- ble decrease in thickness will be achieved before 1980 due to the major apital investment required to replace rolling mill and associated equipment. lthough maraging steels are shown, very little evaluation was attempted luring this phase of the study in the design synthesis area for its application o the various structural components. Initial studies indicated that steels ould not be competitive, weight-wise, with other alloys.

For the six alloy systems discussed, it is forecast that any future hanges in density will be negligible.

## MANUFACTURING

The effect of manufacturing complexity upon selection of a particular ype of material or type of construction for a vehicle component can be rbitrary. These complexities can be more accurately predicted if a good historical manufacturing base is used to relate material/construction types. For this study, the Saturn S-II manufacturing program was selected as a basis for comparison. The following discussion presents a comparison of the estimated manufacturing cost for fabrication, tooling, and equipment of the current S-II concept with four other fabrication concepts and for three specific time periods (1965 to 1970, 1970 to 1980, and post-1980), assuming alloy modifications for each of the time periods mentioned.

The materials considered during this period are aluminum, titanium, magnesium, beryllium, and maraging steel. It is anticipated that some alloy changes may take place within this time period; however, these changes will be minor and manufacturing will be able to keep abreast of them with routine development effort. Although material sheet sizes and gages may change, thinner and larger-sized sheets will present no particular manu- facturing problems but may require more elaborate handling fixtures and facilities. Also, precautions must be observed in handling parts to prevent damage to any protection coating system that may be necessary for the materials studied. This is especially true for closed or entrapped areas.

Tables 2 through 6 present comparison of the estimated complexity factors of the current S-II fabrication, tooling, and equipment to other materials and constructions.

Manufacturing complexity factors, which are variable input to this study, are subjected to the personal prejudice and industrial experience of the company involved; comparison of factors from two separate sources (NAA and Lockheed) are included in the assessment section of this report. A brief discussion of anticipated complexity is presented in the following paragraphs.

Integral Stiffener Concept (Table 2)

This concept is currently in use and no unusual problems are anticipated. However, some development effort will be required for welding, bonding, and brazing methods required to join these materials. Processes for aluminum, except for a possible increase in welding time due to alloy change, will be the same as at present. Titanium machining will present some problems but the major effort will be in developing hot sizing processes to eliminate the distortion caused by machining. Magnesium, due to its corrosive nature, will require establishment of adequate protective coatings. Additionally, development will be necessary in the area of welding and bonding. Beryllium, in addition to its general fabrication problems, will require specific development for brazing and bonding. Special handling fixtures will be required to protect parts and, of course, equipment facilities are more complex because of the rigid safety requirements made mandatory for manufacturing parts of this material. Maraging steel, though more difficult to machine, would present no particular problems.

Attached Stringer Concept (Table 3)

It is assumed these will be joined by mechanical attachment, resistance welding, brazing, or bonding. The aluminum approach is straightforward, requiring no new techniques or development. However, in the titanium approach, because of the forming and hot sizing processes, some development will be necessary. Although this material is currently being welded and bonded, problems have been experienced that indicate that additional development effort is required. This is especially true if an alloy change has been made. Again, protecting magnesium from corrosion will be a major problem, particularly in the joining areas. Also development will be required in the welding and bonding areas. No additional problems are anticipated for beryllium other than the usual fabrication, joining, and handling problems already discussed. In the maraging steel approach, it is assumed that lighter gages will be used which will necessitate more elaborate handling fixtures to protect the material.

Table 2. Manufacturing Complexity of Integral Skin Stringer*

| Concept | Complexity | | | Remarks |
|---|---|---|---|---|
| | Fabrication | Tooling | Equipment ** | |
|  Integral stiffener (machined) | | | | |
| Aluminum | 1.05X | X | X | Minor alloy changes may require some weld development. |
| Titanium | 1.75X | 1.70X | 1.50X | Minor alloy changes will necessitate extensive weld and adhesive bonding development. Special hot sizing die will have to be developed. |
| Magnesium | 1.25X | 1.50X | 1.25X | Major welding and adhesive bonding development will be required. Also corrosion protection methods must be developed. |
| Beryllium | 3.50X | 2.50X | 3.50X | Development is required in brazing-welding, bonding, and to reduce material handling problems and general fabrication problems. |
| Maraging steel | 1.20X | X | X | No particular problems are anticipated. |

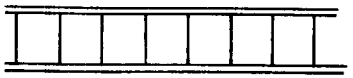
*Based on current S-II fabrication complexity (X) to other concepts and materials currently available or with minor alloy modification.

**Tooling includes manufacturing jigs, welding, hold-down fixtures, etc. Equipment consists of welding, riveting, cutting, machining equipment, and measurement and control devices, etc.

| Concept | Complexity | | | Remarks |
|---|---|---|---|---|
| | Fabrication | Tooling | Equipment | |
|  Attached stiffeners (rivet, spot, bond) | | | | |
| Aluminum | 0.90X | 0.95X | 0.85X | No particular problems are anticipated. |
| Titanium | 1.40X | 1.20X | 1.20X | Hot forming and sizing problems. Development is required for welding and adhesive bonding. |
| Magnesium | 1.25X | 1.20X | 1.20X | Hot forming and sizing problems. Corrosion protection, welding, and bonding development required. |
| Beryllium | 3.50X | 2.50X | 3.50X | Development required as noted in Table 2. |
| Maraging steel | 0.95X | X | 0.95X | Lighter gage may necessitate development of material handling methods. |

*Based on current S-II fabrication complexity (X) to other concepts and materials currently available or with minor alloy modification.

Table 4. Manufacturing Complexity of Honeycomb Sandwich*

| Concept | Complexity | | | Remarks |
|---|---|---|---|---|
| | Fabrication | Tooling | Equipment | |
|  Honeycomb sandwich (bonded) | | | | |
| Aluminum | 1.50X | 1.50X | 1.20X | Suggest minimum gauge 0.20 in. for welding. |
| Titanium | 1.80X | 1.70X | 1.50X | Suggest minimum gauge 0.20 in. for welding. |
| Magnesium | 1.75X | 1.50X | 1.30X | Corrosion protection, welding, and bonding development are required. |
| Beryllium | 4.00X | 2.50X | 3.50X | Development is required as noted in Table 2. |
| Maraging steel | 1.60X | 1.50X | 1.20X | No particular problems are anticipated. |

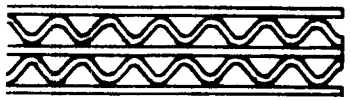
*Based on current S-II fabrication complexity (X) to other concepts and materials currently available or with minor alloy modification.

Table 5. Manufacturing [illegible]

| Concept | Complexity | | | Remarks |
|---|---|---|---|---|
| | Fabrication | Tooling | Equipment | |
|  Corrugated sand. (Adhesive or diffusion bonding) | | | | |
| Aluminum | | | | Diffusion bonding will require development. |
| Adhesive | 1.60X | 1.50X | 1.20X | |
| Diffusion | 2.00X | 1.60X | 1.30X | |
| Titanium | | | | Major development is necessary for welding and adhesive bonding. |
| Adhesive | 1.80X | 1.50X | 1.20X | |
| Diffusion | 2.20X | 1.60X | 1.30X | |
| Magnesium | | | | Development is necessary for diffusion and adhesive bonding as well as corrosion protective methods. |
| Adhesive | 1.80X | 1.50X | 1.20X | |
| Diffusion | 2.40X | 1.60X | 1.30X | |
| Beryllium | | | | Development is required as noted in Table 2. Also, development is required in diffusion bonding using an interleaf material. |
| Adhesive | 4.50X | 2.50X | 3.50X | |
| Diffusion | 5.00X | 3.00X | 3.50X | |
| Maraging steel | | | | No particular problems are anticipated. Diffusion bonding may require some development. |
| Adhesive | 1.60X | 1.50X | 1.20X | |
| Diffusion | 2.00X | 1.60X | 1.30X | |

*Based on current S-II fabrication complexity (X) to other concepts and materials currently available or with minor alloy modification.

Table 6. Manufacturing Complexity of Multilayer Corrugation

| Concept | Complexity | | | Remarks |
|---|---|---|---|---|
| | Fabrication | Tooling | Equipment | |
|  Multilayer corrugated (bonded) | | | | |
| Aluminum | 1.80X | 1.60X | 1.20X | No particular problems are anticipated. Some tooling development may be necessary for maintaining corrugated node alignment. |
| Titanium | 2.00X | 1.60X | 1.20X | Development is necessary in the welding and bonding area. Also tool development is necessary for node alignment. |
| Magnesium | 2.00X | 1.60X | 1.20X | Development is required for corrosion protection, welding and bonding. Also tool development is required for node alignment. |
| Beryllium | 5.00X | 3.00X | 3.50X | Development is required as noted in Table 2. Also tool development is required for node alignment. |
| Maraging steel | 1.80X | 1.60X | 1.20X | No particular problems are anticipated, except tool development for node alignment. |

*Based on current S-II fabrication complexity (X) to other concepts and materials currently available or with minor alloy modification.

Bonded Honeycomb Concept (Table 4)

No problems are anticipated on the aluminum bonded honeycomb concept. However, a minimum gage of 0.020 inch would be recommended for practicability in welding. In the titanium approach, welding and bonding development will be required. Again, a minimum gage of 0.020 inch is recommended for welding. The magnesium approach seems impractical since it is believed that adequate protection cannot be provided within the honeycomb for corrosion resistance. However, if a process could be developed to assure adequate corrosion protection, bonding and welding development would still be required. No particular problems are anticipated with maraging steel for this concept.

Corrugated Sandwich Concept (Table 5)

It is assumed that the joints will be made by either an adhesive or diffusion bonding process of some type. Adhesive bonding of aluminum will present no problem. However, it is anticipated that some development may be required to establish a diffusion bonding process. Panel joining will require design study and technique development. Diffusion or roll bonding processes for titanium have been well developed by Battelle Institute and NAA. However, a major development effort will be necessary to establish adequate adhesive bonding and weld joining techniques. In addition to the corrosion problems associated with magnesium, considerable development effort will be required in the diffusion and adhesive bonding areas. For the beryllium approach, adhesive bonding appears to be practical, however, some development would be necessary. Roll diffusion bonding of beryllium requires development effort. Although there is little experience recorded in diffusion bonding of maraging steel, no particular problems would be anticipated.

Multilayer Corrugated Sandwich Concept (Table 6)

No particular problems, other than those already indicated, are anticipated for this concept. Minor complications in the tooling area, due to the necessity of maintaining corrugation node alignment of the multiple layers, will require some development but no other major tooling problem areas are envisioned. Weld joining the multilayered panels will necessitate coordinated design-manufacturing effort to determine a practical approach for joining the three individual skins.

Manufacturing Period—1970 to 1980

It is anticipated that the alloys previously discussed under the earlier time period will be modified to improve their physical properties. Normally, such changes increase the fabrication problems. However, it can be assumed

hat routine development programs, during this same period, will permit hanufacturing to keep abreast of the changes and develop adequate technique mprovements. Specific development programs will be necessary for some reas, as indicated for the earlier time period. Additionally, as the alloys re modified, forming methods and techniques may require further upgrading nd development. It is logical to assume that specific methods may have to e developed for each type alloy because of the inherent properties of the naterial.

The comparison tables list various complexity factors based on hanges from the current S-II fabrication and material concept to those ioted on the chart with the expected material and alloy modifications. The complexity factors for this period (1970-1980) will be approximately 25 percent less in the areas of fabrication and tooling but the same for equipment as that shown on Tables 2 through 6, assuming the changes of 1965-1970 had been effected previously. However, if the interim modifications had not been incorporated, and the change from current S-II to 1970-1980 modifications was made in one step, the complexity factors as shown on the chart would also apply to this period.

Manufacturing Period—Post-1980

In the period following 1980, it is assumed that the five alloys under study will have been extended their fullest; therefore, additional improvements would be considered as new alloys rather than modifications. Again, it can be assumed that development effort will parallel the alloy changes, although some specific development programs will be necessary, particularly in the area of welding and bonding. It is anticipated that sheets will be larger and thinner, possibly requiring additional development in the field of handling. If weld land thicknesses are reduced to below 0.020, development in the technique and tooling approaches used may be necessary. Also, forming operations for the larger and thinner sheets may necessitate development of larger equipment such as stretch presses, wrap formers, etc.

The complexity factor for this period (post-1980) will be based on the previously mentioned comparison tables. Assuming that the changes expected in the 1970-1980 are incorporated and that experience in the use of the modified materials is gained, the complexity factor for the fabrication and tooling approaches will be approximately 15 percent less than is indicated on the chart, and the equipment will be approximately 5 percent more, due to the larger equipment needs. If it is assumed that the interim modifications will not have been incorporated and the change from current S-II to the improvements of this period (post-1980) will have been made in one step, the complexity factors would increase approximately 5 percent over those shown on the chart.

These values were compared with a series of complexity factors eveloped by Lockheed Aircraft (Reference 16) and are in fairly close agree- ient. Similar NAA-S&ID complexity factors were used in the Advanced itanium Tankage Study (per Reference 1) to determine the relative merits f the various types of construction and materials when compared with bonded oneycomb sandwich structure with titanium facing sheets and aluminum ore.

## PROPULSION

To provide propulsion and propellant trend predictions, liquid propel- ant rocket engines have been investigated on the basis of past developments, cheduled future developments, and projected rocket engine capabilities uring the 1965 to 1980 period.

Figure 9 presents the trend of rocket engine thrust as a function of the ear of initial flight. These data are the result of the current investigation s well as numerous past S&ID investigations aimed at projecting rocket ngine developments. These investigations have indicated that the prime overnor on rocket engine thrust level is the national goal, whether it be pace exploration or the result of military requirements. Past developments ave tended to conform to the following pattern: a liquid oxygen/RP-1 engine s developed first at a given thrust level. After the development and suc- essful operation of such engines, there follows the development of a new igher performance engine employing high-energy (or storable) propellants. This engine development format has occurred on several occasions in the past and is expected to continue in the future, due to the desire for high con- fidence in engine development programs. In Figure 9, it can be seen that it requires approximately 10 years to achieve an order of magnitude increase in engine thrust level. It can also be seen that, approximately five years following the basic engine development at a given thrust level, a high-energy engine is produced. Typically, each step requires a substantial increase in the then current technology.

Engine performance predictions during the desired time period are shown in Figures 10 and 11. These data are based on past and current rocket engines performance, with the addition of the performance predicted for advanced engines now in the early stages of development. The extrap- olation of this data into the post-1975 period has been made by considering advanced propellant combinations that are now undergoing basic performance feasibility tests. Figure 10 presents predicted performance of first-stage engines in which, in most cases, it is desired to utilize the dense propellant combinations, thereby minimizing first-stage volume and cost. Such pro- pellants are liquid oxygen/RP-1, and the storable combination of nitrogen/ tetroxide and Aerozine-50, and advanced storable formulations containing light metals. The upper stage rocket engine performance predictions shown

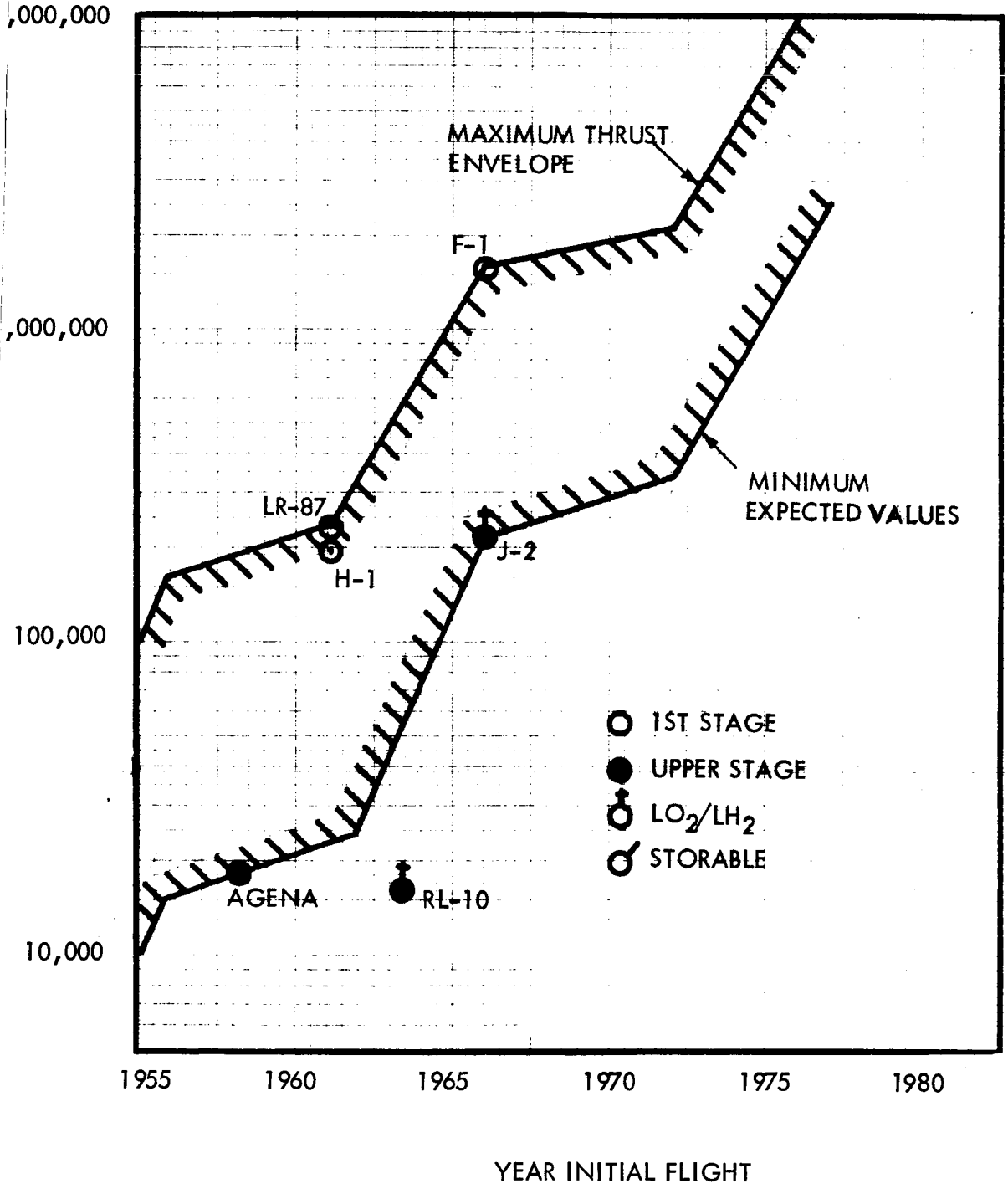



Figure 9. Liquid Propellant Rocket Engine Thrust Trends

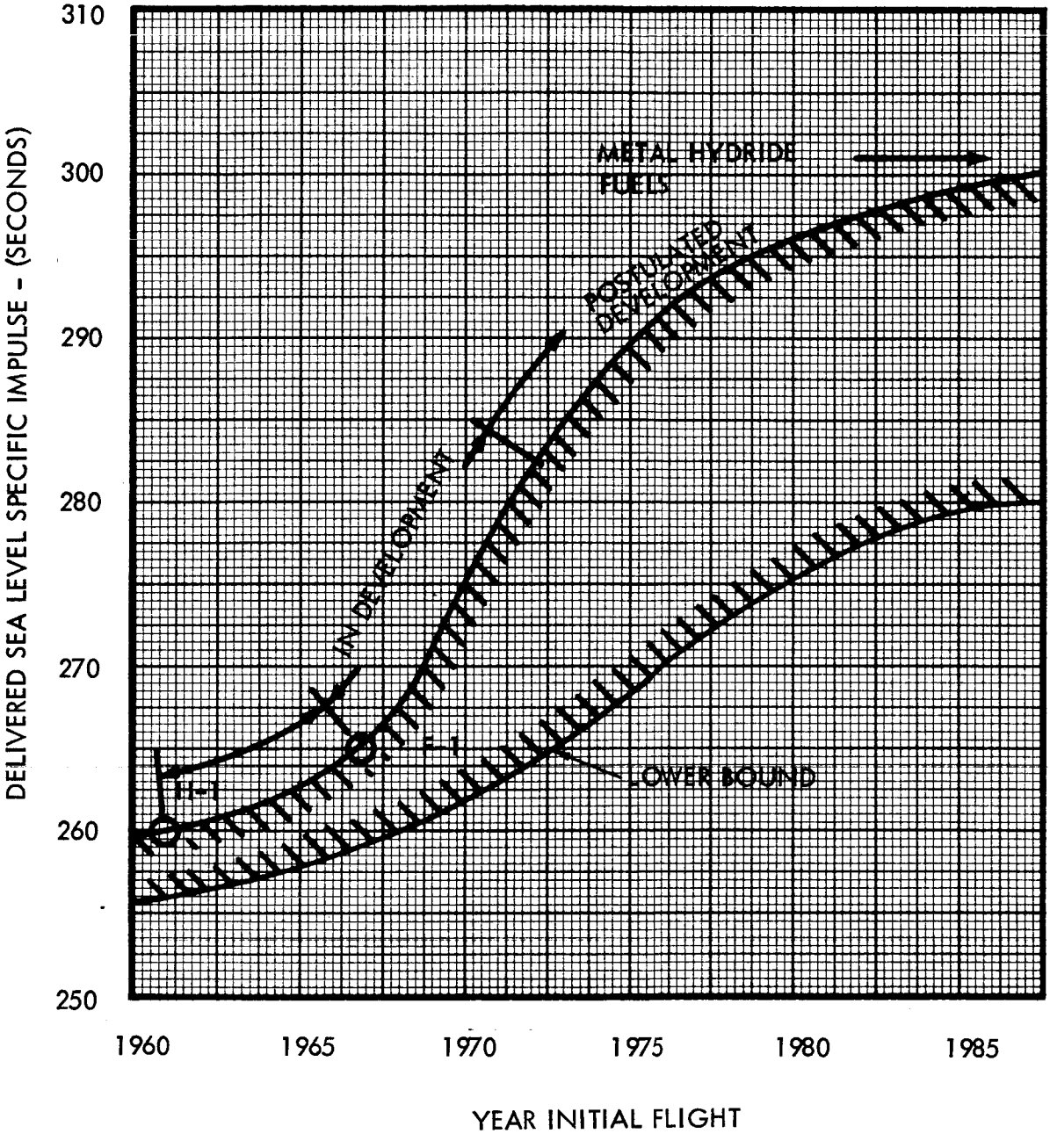



Figure 10. Estimated Future Performance Trends for First Stage Liquid Propellant Rocket Engines

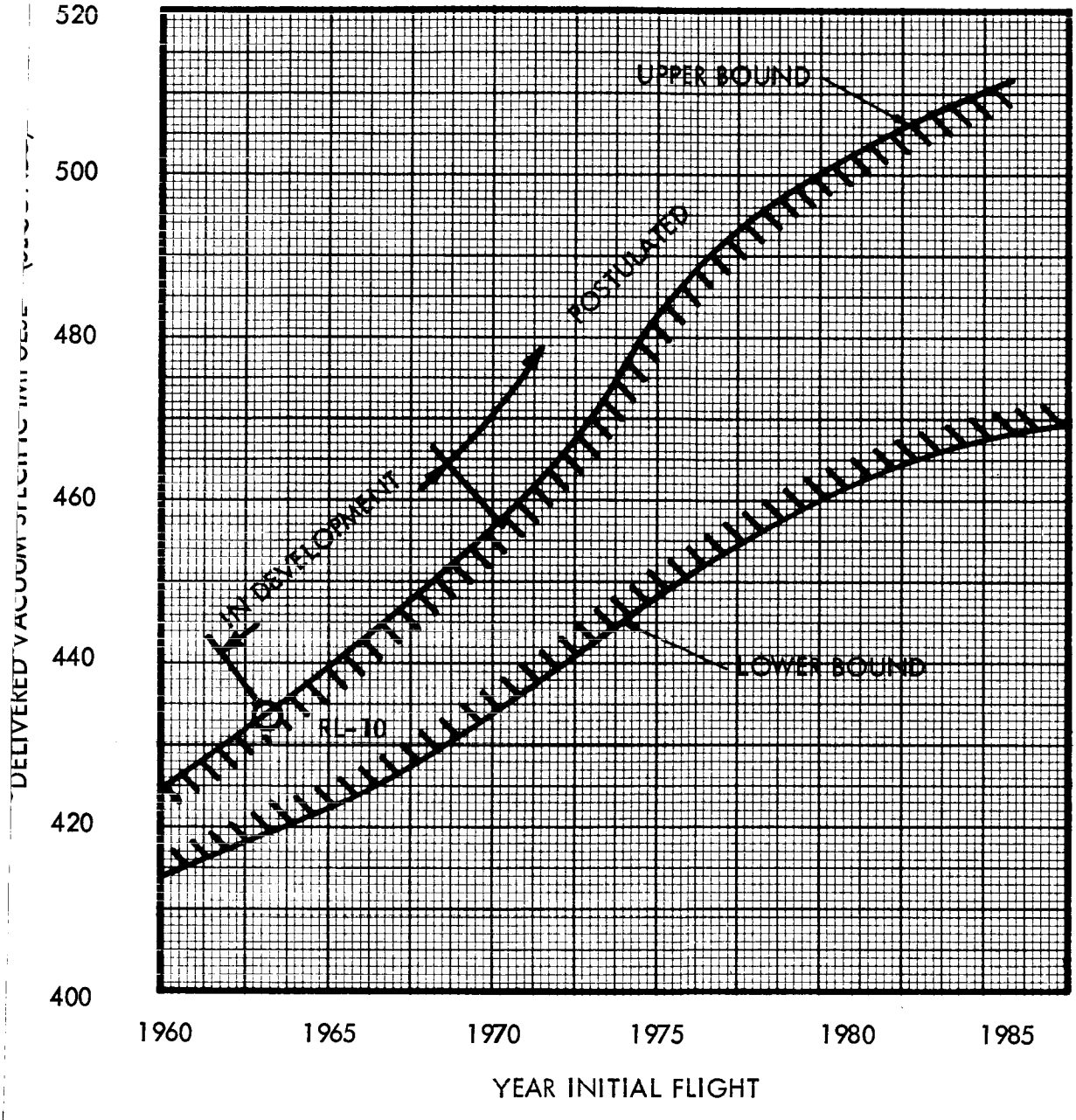



Figure 11. Estimated Future Performance Trends for Upper Stage Liquid Propellant Rocket Engines

n Figure 11 are based on the utilization of high-energy propellant combinations typified by liquid oxygen/hydrogen, fluorine/hydrogen, and later additions of the light metals and light metal hydrides.

Figure 12 presents engine thrust-to-engine-weight ratio trends. These data are also based on past and planned developments. It will be noted that here is a distinct difference in engine weight between engines employing cryogenic propellants and those employing the storable propellants. This is due to the relatively high density exhibited by the storable propellants and the resulting reduction in turbomachinery and thrust chamber weight. Figure 13 presents 1965 engine thrust-to-engine-weight ratio as a function of thrust level for various engines ranging in size from 15 thousand to 1.5 million pounds of thrust. These data may be modified to reflect weight characteristics during any year by ratioing according to the trends presented in Figure 12.

As previously noted, predictions of rocket engine characteristics beyond 1972 period can be fairly arbitrary, due to the lack of a definition of national goals and, hence, vehicle requirements in the succeeding years; such developments must lie within the realm of technical feasibility and development program practicality, however. Thus, such predictions must be based on the assumption that these goals will tend to progress at roughly the same rate as they have in the past 15 years.

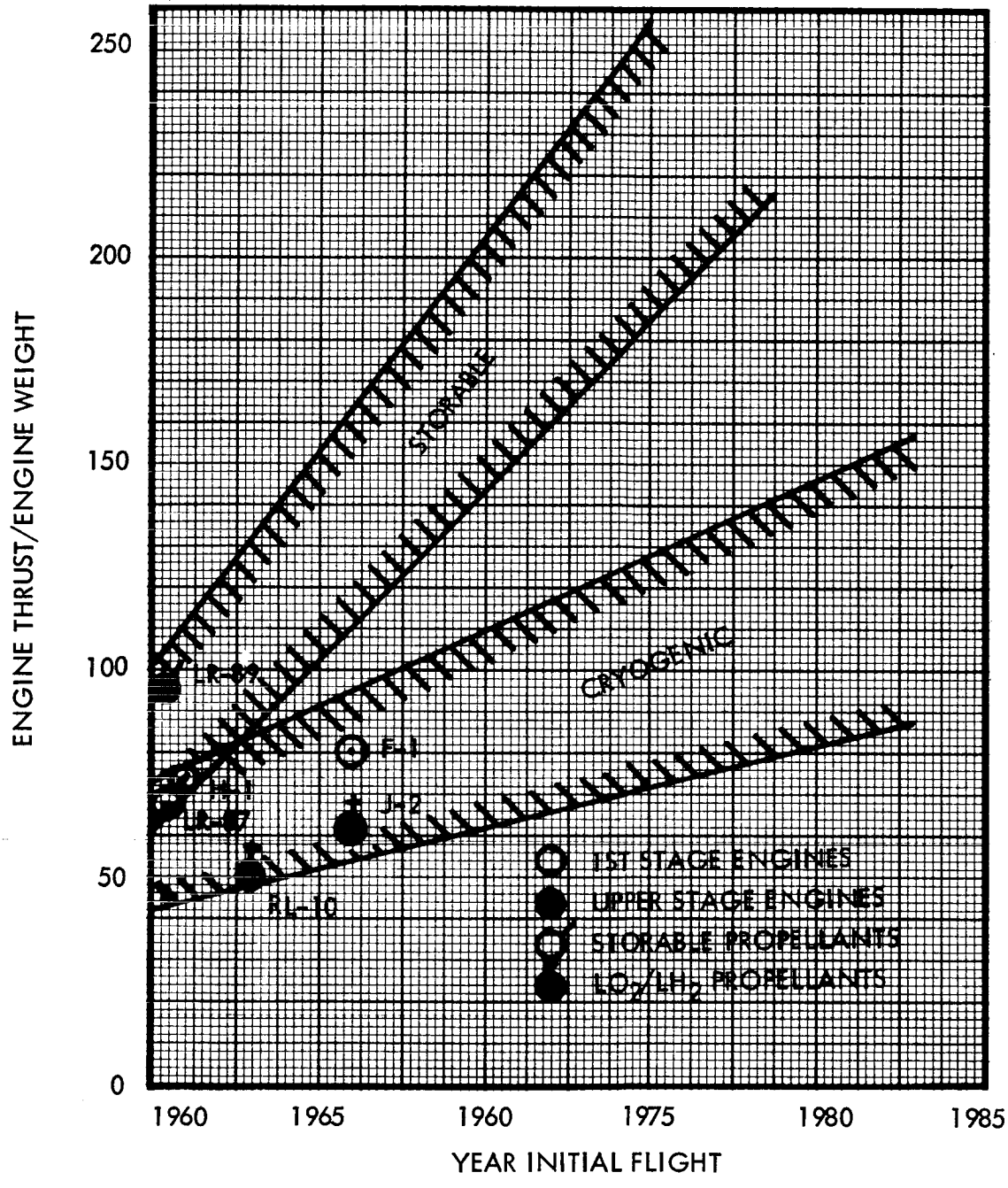



Figure 12. Current and Predicted Future Engine Thrust-To-Weight Ratio Trends

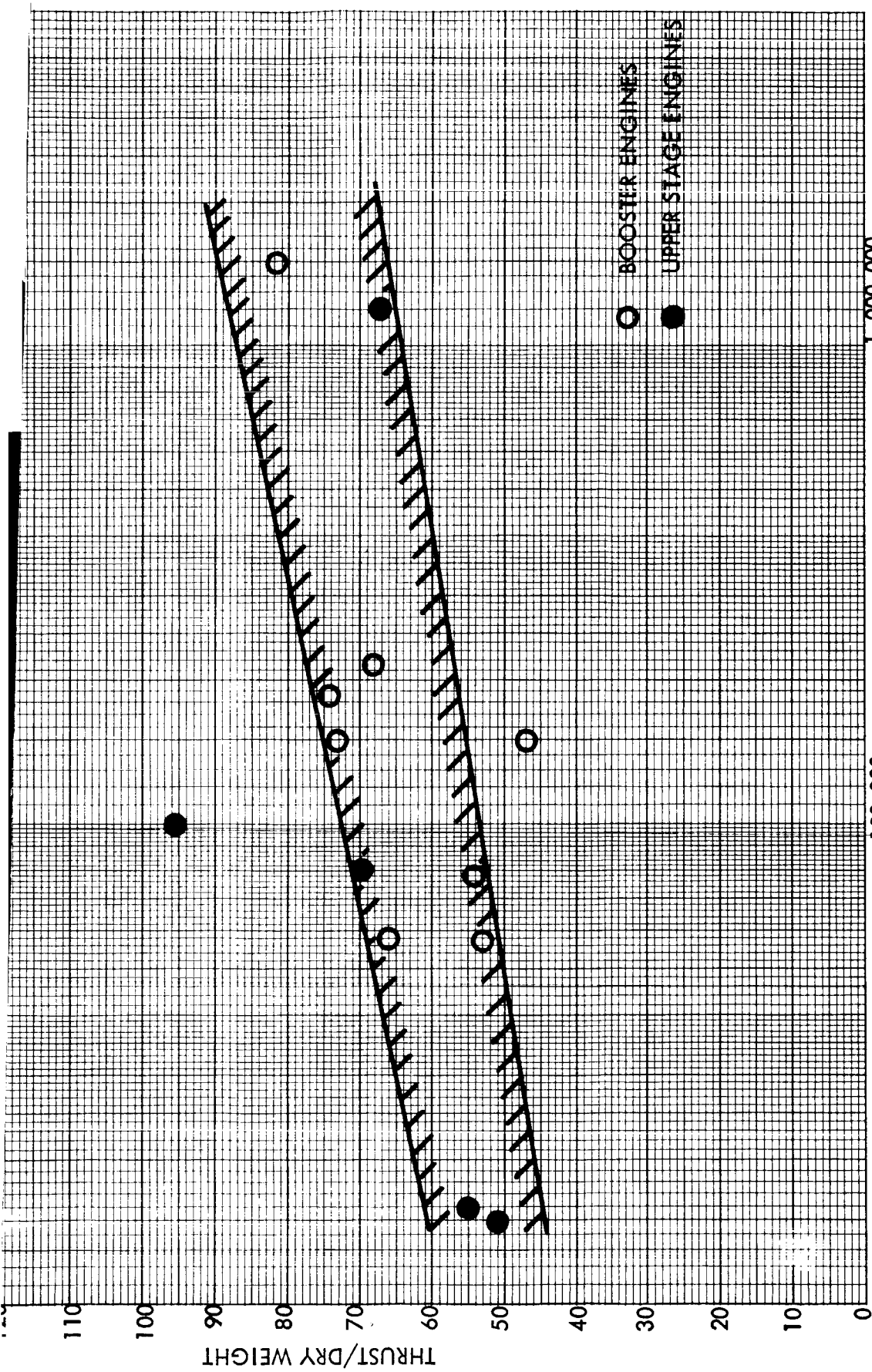



Figure 13. Liquid Propellant Engine Thrust to Weight Ratio - Regenerative Cooled

# VEHICLE ANALYSIS

Vehicle analysis primarily consists of the parametric synthesis operation as previously illustrated (Figure 1), and includes stage proportioning, mass fraction derivations, payload exchange ratio derivation, and incorporation of structural design synthesis data in the weight and cost assessment operation. Test cases subjected to these steps are shown in Tables 7 and 8.

An automated program such as that used for this study can efficiently cycle through a great many cases. These cases are most easily evaluated by examining the digital output data and curves. However, to present all these data in one report would result in a tremendous volume and would not aid in demonstrating the tool developed or the type of results that can be achieved: therefore, initial computer runs were made through the large spectrum of vehicles and specific test cases were selected for presentation in this report to demonstrate the approach. Some data are summarized and illustrated in this section of the report with more detailed analytical data presented in the Appendixes of this report.

## INITIAL STAGE PROPORTIONING

The vehicles illustrated in Tables 7 and 8 were subjected to a minimum liftoff weight proportioning as illustrated in Figure 14 and discussed further in Appendix A. These "first-cut" proportions were obtained using the generalized stage mass fraction curves illustrated in Figure 15. These first-order mass fraction curves were calculated using typical Saturn V structural shell unit weights, subsystems, and characteristic stage velocities. The mass fraction subroutine was exercised through various stage velocity combinations using a total velocity which is typical for the Saturn V trajectory. The initial exercise at proportioning used this curve and resulted in various vehicle sizes for which better mass fractions could be obtained. These mass fractions were then iterated through the proportioning subroutine to define the mass properties of the candidate vehicles, and finally the load environments, vehicle geometries, and vehicle payload weight. The stage proportioning-dynamic programming approach is discussed in References 17, 18 and 19.

Stage mass fraction, in this report, is the principal stage efficiency ratio and is defined as the stage usable propellant weight divided by the sum of the stage usable propellant weight and the stage burnout weight. Stage weight proportioning is greatly influenced by the stage mass fraction, stage

Table 7. Generic Families - Two-Stage Liquid Proportioned Vehicles

| Computer Case Number | Payload Class (lb) | Time Period | Stage Performance | | | |
|---|---|---|---|---|---|---|
| | | | 1 | | 2 | |
| | | | ΔV | Isp AV | ΔV | Isp VAC |
| 11 | 30,000 | Current | 10,402 | 289.8 | 20,600 | 424 |
| 12 | 225,000 | Current | 10,861 | 289.8 | 19,800 | 424 |
| 13 | 1,000,000 | Current | 11,123 | 289.8 | 19,400 | 424 |
| 14 | 60,000 | 1975 | 10,523 | 308.0 | 20,800 | 460 |
| 15 | 300,000 | 1975 | 11,236 | 308.0 | 19,800 | 460 |
| 16 | 1,500,000 | 1975 | 11,150 | 308.0 | 19,800 | 460 |
| 17 | 100,000 | 1985 | 11,123 | 333.0 | 20,600 | 500 |
| 18 | 400,000 | 1985 | 11,535 | 333.0 | 20,000 | 500 |
| 19 | 2,000,000 | 1985 | 11,630 | 333.0 | 19,800 | 500 |

ΔV = Stage characteristic velocity in feet per second
Isp = Specific impulse in seconds

Table 8. Generic Families - Three-Stage Launch Vehicles, Minimum Earth Mode
Proportioned Vehicles

| Computer Case Number | Payload Class (lb) | Time Period | Stage Performance | | | | | |
|---|---|---|---|---|---|---|---|---|
| | | | 1 | | 2 | | 3 | |
| | | | ΔV | Isp AV | ΔV | Isp VAC | ΔV | Isp VAC |
| 2 | 30,000 | Current | 9,565 | 289.8 | 7,000 | 424 | 15,200 | 424 |
| 3 | 225,000 | Current | 9,945 | 289.8 | 12,200 | 424 | 9,200 | 424 |
| 4 | 1,000,000 | Current | 9,730 | 289.8 | 12,600 | 424 | 9,000 | 424 |
| 5 | 60,000 | 1975 | 10,175 | 308.0 | 6,800 | 460 | 15,000 | 460 |
| 6 | 300,000 | 1975 | 10,350 | 308.0 | 13,000 | 460 | 8,400 | 460 |
| 7 | 1,500,000 | 1975 | 10,285 | 308.0 | 13,000 | 460 | 8,400 | 460 |
| 8 | 100,000 | 1985 | 10,925 | 333.0 | 7,200 | 500 | 14,200 | 500 |
| 9 | 400,000 | 1985 | 10,995 | 333.0 | 12,500 | 500 | 8,400 | 500 |
| 10 | 2,000,000 | 1985 | 10,935 | 333.0 | 12,800 | 500 | 8,400 | 500 |

ΔV = Stage characteristic velocity in feet per second
Isp = Specific impulse in seconds

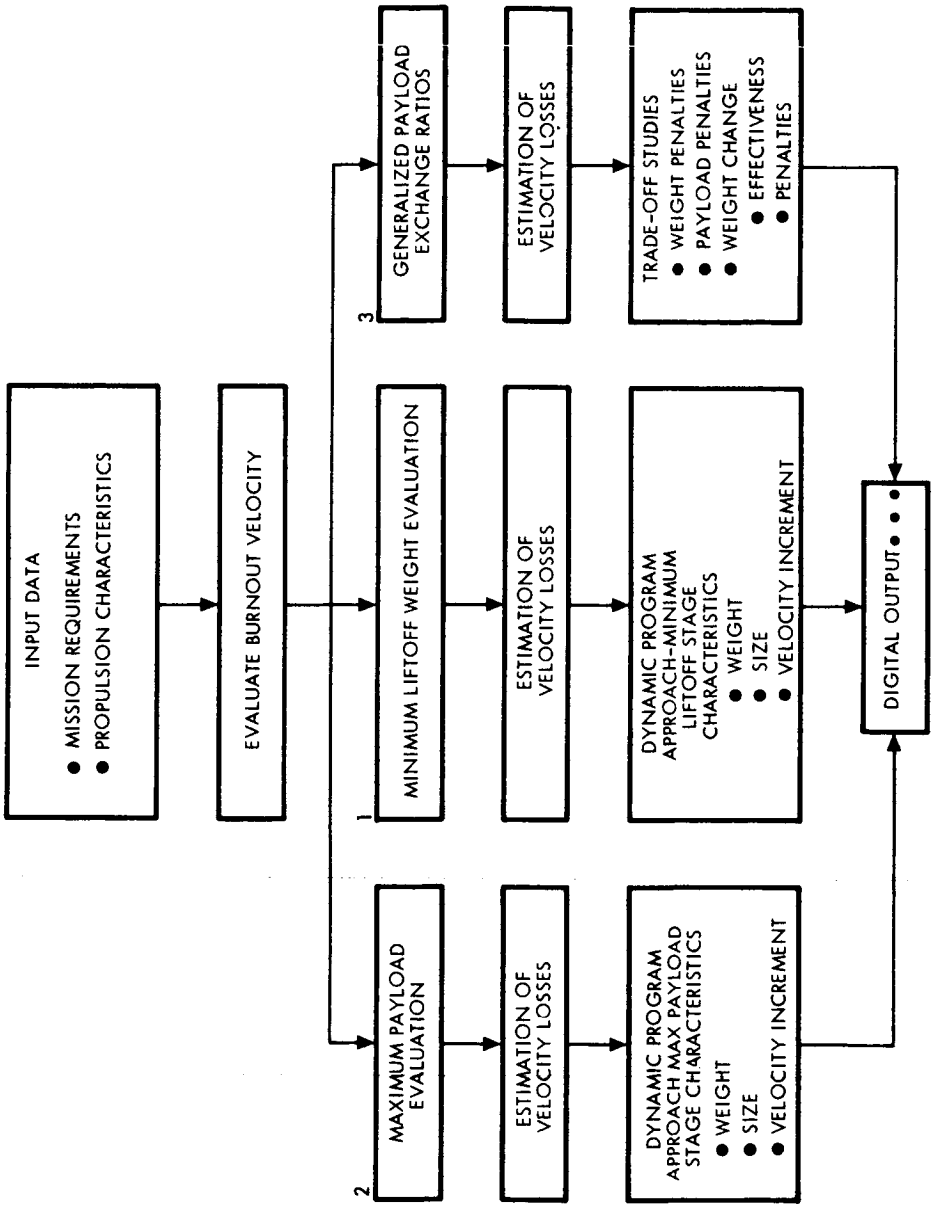



Figure 14. Parametric Proportioning Logic

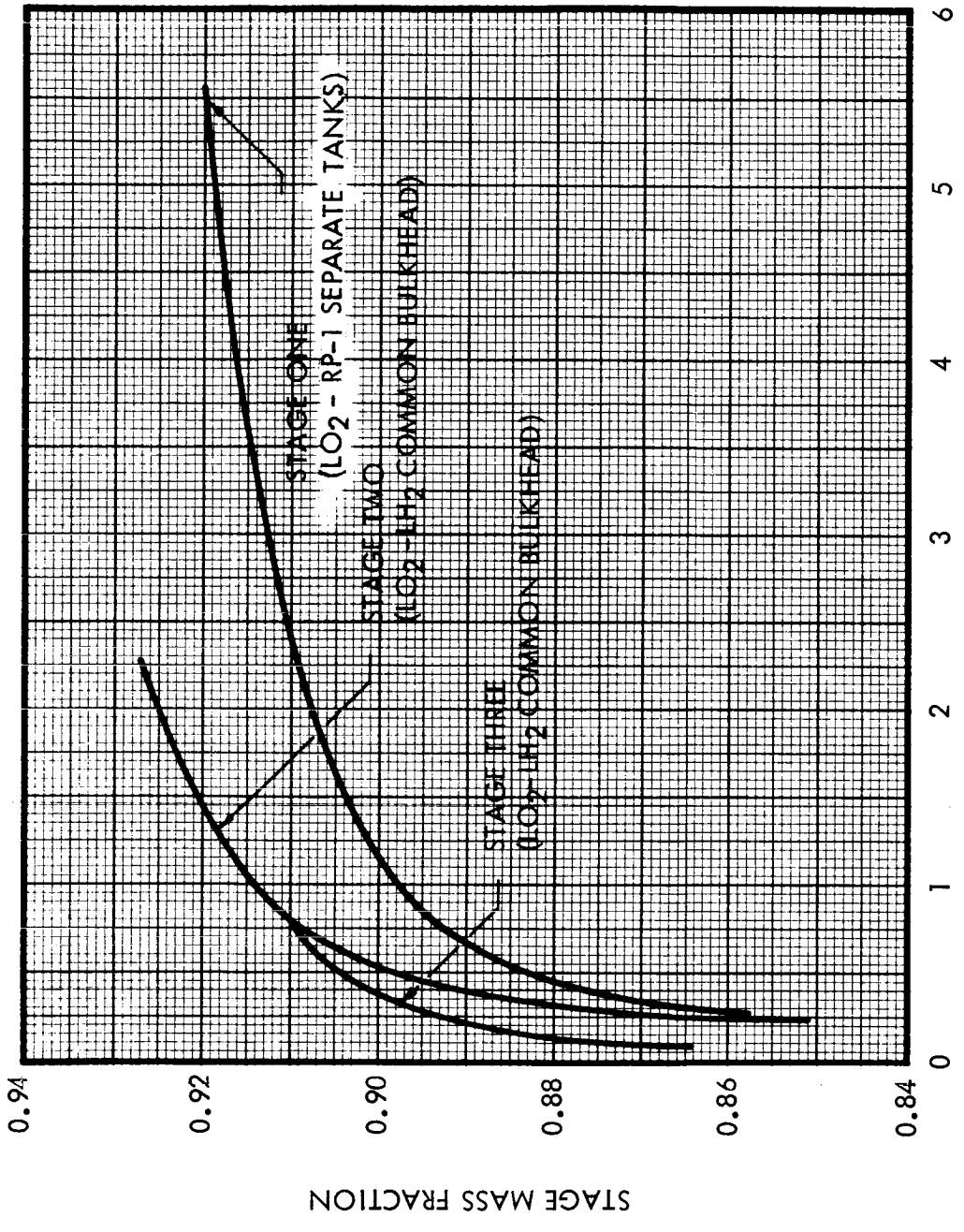



Figure 15. Stage Mass Fractions For Initial Proportioning

racteristic velocity, stage velocity losses, and stage performance cific impulse. This multistage proportioning is most simply expressed he following stage weight relationship:

$$W_{o_i} = \frac{W_{PL_i}}{1 - \dfrac{\left[1 - \dfrac{1}{\exp\left(\dfrac{\Delta V_i + \Delta V_{L_i}}{I_i g}\right)}\right]}{\nu_{B_i}}}$$

ere

$W_{o_i}$ = Vehicle Gross Weight

$W_{PL_i}$ = Stage Payload Weight ($W_{PL_{i-1}} = W_{o_i}$)

$\nu_{B_i}$ = Stage Mass Fraction

$\Delta V_i$ = Stage Performance Velocity

$\Delta V_{L_i}$ = Stage Velocity Losses

$I_i$ = Stage Specific Impulse

$g$ = Gravity Constant

$i$ = stage $i = 1, n$ $n$ = total number of stages

In the stage proportioning accomplished for this study the stage per- rmance velocity ($\Delta V_i$) included a performance "pad" of three-fourths of one ercent to account for performance contingencies and weight growth factors. he relationship of stage payload weight to vehicle gross weight is deter- ined from the previous stage payload and becomes more complex as the umber of stages increase. For this reason, the dynamic programming pproach (Appendix A) was developed and used in this study to evaluate these ultistage vehicles.

Stage mass fraction is influenced by the stage size, construction type, ystem type and the loading environment induced by the stage immediately elow the stage in question and the payload above the stage. The mass raction curves used in the initial proportioning (Figure 15), were repre- entative values and served merely to initialize the synthesis.

These mass fractions are typical for a three-stage Saturn-type vehicle sing aluminum integral skin-stringer construction for the pressurized and npressurized shells. The particular aluminum material reported herein is eferred to as "Aluminum A" and is typical for current material technology

ving a modulus of elasticity of 10,000,000 psi and a yield strength of ,000 psi at 300 F. These values are similar to those of 2014-T6 and 75-T6 aluminums. The same material was used to parametrically deter- ne weights of the pressure-designed membrane bulkheads. The initializing ass fraction curves reflect state-of-the-art propulsion and propellant chnology and include known equipment weight trends.

For this particular study all basepoint lower stages used RP-1/$LO_2$ opellants with mixture ratios of 2.25:1. The first stage oxidizer was cated in the upper first stage tank. All upper stages used $LO_2/LH_2$ pro- llant with a mixture ratio of 5:1 and with the oxidizer located in the aft nk. Typical ullage factors used to size propellant tankages were similar those established for the Saturn V vehicle (6 percent in RP-1 and $LO_2$ tanks d 8 percent in $LH_2$ tanks). Engines were sized to expansion ratios of 25 on e first stages and 35 on the upper stages with chamber pressures of 1000 psi the first stages and 632 psi on the upper stages. The first and second ages all are multi-engined with the third stage using one engine. Thrust to eight ratios were limited to typical manned values to reduce the maximum celeration experienced at end boost.

Figure 14 identifies the three basic stage proportioning procedural eps followed for investigating the study test cases. The procedure was as llows:

1. Starting with known payload weights for specific missions and a generalized mass fraction curve, proportion vehicles to minimum liftoff weight.

2. Investigate mass fraction variations for the minimum liftoff mode proportioned vehicles, and, using these data and the minimum liftoff weights and thrust levels, recycle the vehicles to achieve maximum payload.

3. Check final mass fractions of maximized payload vehicles and cycle selected maximized payload vehicles through the generalized payload exchange ratio subroutine.

This phase of the study was concerned with developing the programmed ssistance method and testing the method on reasonable vehicles. The stage roportioning operation was evolved to permit rapid investigation of a large pectrum of vehicles and, since the problem is unique, many approaches were nvestigated. The final logic used represents the best approach identified of hose investigated. A more complete discussion of these methods and the articular method adopted may be found in Appendix A.

Tables 9, 10, and 11 present computer printouts for the three payload class two-stage vehicles and illustrate how the minimum weight vehicle combination is dynamically selected. The headings indicated in Tables 9, 10, 11, and 12 are defined as follows:

| | |
|---|---|
| I | The number of the stage |
| J | The number of velocity steps above the minimum velocity for the ith stage |
| K | The $j^{*}$th step from the i + 1 stage (minimum liftoff mode) or i - 1 stage (maximum payload mode) that is combined with the jth step of the ith stage for an optimal policy |
| WTOTAL | Total vehicle weight (lb) |
| WPROP | Stage propellant weight (lb) |
| WEMPTY | Stage burnout weight (lb) |
| WSTAGE | Stage gross weight (lb) |
| DVEL | Actual velocity increment of stage (fps) |
| VLOSS | Velocity loss for the stage (fps) |
| TIME | Stage burning time (sec) |
| ABO | Burnout angle at end boost Stage 1 (deg) |

The combination of all stages represents an optimally proportioned vehicle to obtain minimum liftoff weight. The minimum selected values are indicated in the tables. The data from Tables 9, 10, and 11 are plotted in Figures 16, 17, and 18. In these curves, total vehicle weight and first stage weight are shown as a function of second stage weight. The area of efficient stage proportioning is indicated on these curves and their accompanying data printouts (Tables 9, 10, 11). A large number of combinations were investigated to isolate the efficient staging regimes. Tables 9, 10, and 11 and Figures 16, 17, and 18 represent results for the two-stage vehicles. Table 13 and Figure 19 present similar minimum liftoff proportioning results for a three-stage post-Saturn payload class vehicle with a payload capability of 1,500,000 pounds. Specific impulses, thrust levels and structure are typical of 1975 predictions.

A wide range of latitude in second stage size variation is allowable in the medium range and Saturn payload class vehicles without significantly increasing the vehicle liftoff weight (Figures 16 and 17). The post-Saturn payload class two-stage vehicle which has a 1-1/2-million-pound payload

## Table 9. Minimum Liftoff Stage Proportioning Computer Printout Medium Range Payload - Two Stage Vehicle

| | | Stage 1 | | | | | | | | Stage 2 | | | | | | |
|---|---|---|---|---|---|---|---|---|---|---|---|---|---|---|---|---|
| J | K | WTOTAL | WPROP | WEMPTY | WSTAGE | DVEL | VLOSS | TIME | ABO | WTOTAL | WPROP | WEMPTY | WSTAGE | DVEL | VLOSS | TIME |
| 1 | 1 | 6868105. | 5193212. | 457353. | 5650565. | 15904. | 5070. | 212. | 81. | 1217540. | 741302. | 76238. | 817540. | 15000. | 333. | 304. |
| 2 | 1 | 6823122. | 5133120. | 452495. | 5585616. | 15728. | 5077. | 211. | 80. | 1237507. | 759479. | 78028. | 837507. | 15200. | 351. | 307. |
| 3 | 1 | 6780530. | 5074813. | 447838. | 5522651. | 15553. | 5083. | 210. | 80. | 1257878. | 778025. | 79953. | 857878. | 15400. | 370. | 309. |
| 4 | 1 | 6739673. | 5017726. | 443282. | 5461007. | 15379. | 5089. | 208. | 79. | 1278666. | 796950. | 81716. | 878666. | 15600. | 389. | 312. |
| 5 | 1 | 6700498. | 4961800. | 438818. | 5400618. | 15204. | 5094. | 207. | 79. | 1299881. | 816263. | 83617. | 899881. | 15800. | 409. | 314. |
| 6 | 1 | 6662510. | 4906567. | 434409. | 5340976. | 15028. | 5099. | 206. | 79. | 1321534. | 835976. | 85558. | 921534. | 16000. | 430. | 316. |
| 7 | 1 | 6627036. | 4853245. | 430153. | 5283398. | 14854. | 5103. | 205. | 78. | 1343638. | 856099. | 87539. | 943638. | 16200. | 452. | 319. |
| 8 | 1 | 6592228. | 4800112. | 425912. | 5226023. | 14679. | 5106. | 204. | 78. | 1366205. | 876644. | 89561. | 966205. | 16400. | 474. | 321. |
| 9 | 1 | 6559851. | 4749788. | 421815. | 5170603. | 14505. | 5109. | 203. | 77. | 1389248. | 897622. | 91626. | 989248. | 16600. | 494. | 323. |
| 10 | 1 | 6528004. | 4697521. | 417722. | 5115243. | 14330. | 5111. | 201. | 77. | 1412761. | 919028. | 93733. | 1012761. | 16800. | 520. | 325. |
| 11 | 1 | 6498590. | 4648024. | 413772. | 5061796. | 14156. | 5112. | 200. | 77. | 1436794. | 940908. | 95887. | 1036794. | 17000. | 544. | 327. |
| 12 | 1 | 6469750. | 4598581. | 409825. | 5008406. | 13981. | 5113. | 199. | 76. | 1461345. | 963258. | 98087. | 1061345. | 17200. | 569. | 330. |
| 13 | 1 | 6443199. | 4550763. | 406008. | 4956771. | 13808. | 5113. | 198. | 76. | 1486428. | 986093. | 100334. | 1086428. | 17400. | 595. | 332. |
| 14 | 1 | 6417181. | 4502933. | 402190. | 4905123. | 13633. | 5112. | 196. | 75. | 1512058. | 1009427. | 102631. | 1112058. | 17600. | 621. | 334. |
| 15 | 1 | 6393395. | 4456647. | 398495. | 4855142. | 13459. | 5111. | 195. | 75. | 1538253. | 1033274. | 104979. | 1138253. | 17800. | 649. | 336. |
| 16 | 1 | 6370109. | 4410287. | 394794. | 4805081. | 13285. | 5108. | 194. | 74. | 1565028. | 1057650. | 107378. | 1165028. | 18000. | 677. | 338. |
| 17 | 1 | 6349004. | 4365393. | 391211. | 4756604. | 13111. | 5105. | 193. | 74. | 1592400. | 1082569. | 109831. | 1192400. | 18200. | 706. | 340. |
| 18 | 1 | 6328371. | 4320366. | 387616. | 4707982. | 12937. | 5102. | 191. | 73. | 1620389. | 1108050. | 112339. | 1220389. | 18400. | 736. | 342. |
| 19 | 1 | 6309452. | 4276338. | 384101. | 4660440. | 12763. | 5097. | 190. | 73. | 1649013. | 1134109. | 114904. | 1249013. | 18600. | 767. | 344. |
| 20 | 1 | 6291826. | 4232901. | 380634. | 4613535. | 12589. | 5092. | 188. | 72. | 1678291. | 1160763. | 117528. | 1278291. | 18800. | 798. | 346. |
| 21 | 1 | 6275471. | 4190018. | 377210. | 4567228. | 12416. | 5085. | 187. | 72. | 1708243. | 1188031. | 120212. | 1308243. | 19000. | 831. | 348. |
| 22 | 1 | 6260377. | 4147657. | 373829. | 4521485. | 12242. | 5078. | 186. | 71. | 1738892. | 1215933. | 122958. | 1338892. | 19200. | 865. | 350. |
| 23 | 1 | 6246533. | 4105789. | 370486. | 4476276. | 12069. | 5070. | 184. | 71. | 1770258. | 1244489. | 125769. | 1370258. | 19400. | 899. | 351. |
| 24 | 1 | 6233933. | 4064387. | 367181. | 4431568. | 11895. | 5061. | 183. | 70. | 1802365. | 1273719. | 128646. | 1402365. | 19600. | 935. | 353. |
| 25 | 1 | 6222568. | 4023420. | 363911. | 4387331. | 11722. | 5051. | 181. | 70. | 1835237. | 1303645. | 131592. | 1435237. | 19800. | 972. | 355. |
| 26 | 1 | 6212635. | 3982991. | 360745. | 4343736. | 11549. | 5040. | 180. | 69. | 1868900. | 1334291. | 134609. | 1468900. | 20000. | 1010. | 357. |
| 27 | 1 | 6204058. | 3943021. | 357699. | 4300719. | 11376. | 5028. | 178. | 69. | 1903338. | 1365643. | 137695. | 1503338. | 20200. | 1049. | 359. |
| 28 | 1 | 6196801. | 3903461. | 354686. | 4258147. | 11203. | 5015. | 176. | 68. | 1938654. | 1397794. | 140860. | 1538654. | 20400. | 1089. | 361. |
| 29 | 1 | 6190750. | 3864212. | 351696. | 4215908. | 11030. | 5000. | 175. | 67. | 1974842. | 1430739. | 144103. | 1574842. | 20600. | 1130. | 362. |
| 30 | 1 | 6185908. | 3825250. | 348729. | 4173978. | 10857. | 4985. | 173. | 67. | 2011930. | 1464504. | 147426. | 1611930. | 20800. | 1172. | 364. |
| 31 | 1 | 6182280. | 3786549. | 345781. | 4132330. | 10684. | 4968. | 171. | 66. | 2049950. | 1499117. | 150833. | 1649950. | 21000. | 1216. | 366. |
| 32 | 1 | 6179873. | 3748087. | 342851. | 4090938. | 10511. | 4951. | 170. | 66. | 2088935. | 1534608. | 154327. | 1688935. | 21200. | 1261. | 367. |
| *33 | 1 | 6179101. | 3710215. | 339967. | 4050182. | 10339. | 4932. | 168. | 65. | 2128919. | 1571009. | 157910. | 1728919. | 21400. | 1307. | 369. |
| 34 | 1 | 6180088. | 3673018. | 337133. | 4010151. | 10168. | 4913. | 166. | 64. | 2169937. | 1608351. | 161586. | 1769937. | 21600. | 1355. | 371. |

*Minimum Configuration

Table 10. Minimum Liftoff Stage Proportioning Computer Printout Future Saturn Class - Two Stage Vehicle

| | | Stage 1 | | | | | | | Stage 2 | | | | | | |
|---|---|---|---|---|---|---|---|---|---|---|---|---|---|---|---|
| J | K | WTOTAL | WPROP | WEMPTY | WSTAGE | DVEL | VLOSS | TIME | ABO | WTOTAL | WPROP | WEMPTY | WSTAGE | DVEL | VLOSS | TIME |
| 1 | 1 | 1655951. | 1294174. | 140606. | 1434781. | 15820. | 4969. | 202. | 80. | 221171. | 141432. | 19739. | 161171. | 15000. | 351. | 294. |
| 2 | 1 | 1629259. | 1266403. | 137820. | 1404223. | 15620. | 4963. | 201. | 80. | 225037. | 145000. | 20037. | 165037. | 15200. | 357. | 296. |
| 3 | 1 | 1605723. | 1241165. | 135573. | 1376737. | 15420. | 4957. | 200. | 80. | 228985. | 148644. | 20341. | 168985. | 15400. | 363. | 299. |
| 4 | 1 | 1583396. | 1216927. | 133367. | 1350294. | 15220. | 4951. | 199. | 80. | 233102. | 152418. | 20684. | 173102. | 15600. | 371. | 301. |
| 5 | 1 | 1562695. | 1193995. | 131275. | 1325270. | 15020. | 4945. | 197. | 79. | 237425. | 156365. | 21059. | 177425. | 15800. | 379. | 303. |
| 6 | 1 | 1543948. | 1172802. | 129343. | 1302144. | 14826. | 4939. | 196. | 79. | 241804. | 160364. | 21439. | 181804. | 16000. | 387. | 305. |
| 7 | 1 | 1524736. | 1151091. | 127359. | 1278450. | 14626. | 4933. | 195. | 79. | 246285. | 164457. | 21828. | 186285. | 16200. | 397. | 307. |
| 8 | 1 | 1507927. | 1131563. | 125492. | 1257055. | 14435. | 4928. | 194. | 79. | 250872. | 168646. | 22226. | 190872. | 16400. | 407. | 309. |
| 9 | 1 | 1492100. | 1112683. | 123849. | 1236532. | 14242. | 4922. | 193. | 79. | 255568. | 172934. | 22633. | 195568. | 16600. | 419. | 311. |
| 10 | 1 | 1476453. | 1094012. | 122066. | 1216078. | 14049. | 4917. | 191. | 79. | 260375. | 177324. | 23051. | 200375. | 16800. | 432. | 313. |
| 11 | 1 | 1462538. | 1076677. | 120563. | 1197240. | 13858. | 4912. | 190. | 78. | 265298. | 181820. | 23478. | 205298. | 17000. | 445. | 315. |
| 12 | 1 | 1448811. | 1059544. | 118927. | 1178471. | 13669. | 4908. | 189. | 78. | 270340. | 186425. | 23915. | 210340. | 17200. | 460. | 317. |
| 13 | 1 | 1436239. | 1043302. | 117431. | 1160734. | 13481. | 4903. | 188. | 78. | 275506. | 191142. | 24363. | 215506. | 17400. | 476. | 319. |
| 14 | 1 | 1424622. | 1027806. | 116017. | 1143823. | 13294. | 4899. | 186. | 77. | 280799. | 195976. | 24823. | 220799. | 17600. | 494. | 321. |
| 15 | 1 | 1413860. | 1012970. | 114667. | 1127636. | 13109. | 4895. | 185. | 77. | 286223. | 200930. | 25293. | 226223. | 17800. | 513. | 323. |
| 16 | 1 | 1403896. | 998746. | 113366. | 1112112. | 12925. | 4891. | 184. | 77. | 291784. | 206008. | 25776. | 231784. | 18000. | 533. | 325. |
| 17 | 1 | 1394614. | 985047. | 112082. | 1097129. | 12744. | 4887. | 183. | 76. | 297485. | 211215. | 26270. | 237485. | 18200. | 555. | 327. |
| 18 | 1 | 1386082. | 971907. | 110843. | 1082750. | 12563. | 4883. | 181. | 76. | 303332. | 216554. | 26778. | 243332. | 18400. | 578. | 328. |
| 19 | 1 | 1378329. | 959344. | 109656. | 1068999. | 12385. | 4879. | 180. | 75. | 309329. | 222031. | 27298. | 249329. | 18600. | 603. | 330. |
| 20 | 1 | 1371344. | 947340. | 108522. | 1055862. | 12208. | 4875. | 179. | 75. | 315483. | 227651. | 27832. | 255483. | 18800. | 630. | 332. |
| 21 | 1 | 1365117. | 935881. | 107439. | 1043320. | 12033. | 4871. | 177. | 74. | 321798. | 233418. | 28380. | 261798. | 19000. | 658. | 334. |
| 22 | 1 | 1359636. | 924950. | 106406. | 1031356. | 11860. | 4867. | 176. | 74. | 328280. | 239338. | 28942. | 268280. | 19200. | 688. | 335. |
| 23 | 1 | 1354892. | 914534. | 105421. | 1019956. | 11689. | 4863. | 174. | 73. | 334937. | 245417. | 29520. | 274937. | 19400. | 721. | 337. |
| 24 | 1 | 1349761. | 903615. | 104385. | 1008000. | 11514. | 4859. | 173. | 73. | 341761. | 251651. | 30109. | 281761. | 19600. | 756. | 339. |
| 25 | 1 | 1346099. | 893902. | 103469. | 997371. | 11345. | 4855. | 172. | 72. | 348728. | 258024. | 30704. | 288728. | 19800. | 793. | 340. |
| 26 | 1 | 1343161. | 884679. | 102598. | 987277. | 11179. | 4850. | 170. | 72. | 355884. | 264569. | 31315. | 295884. | 20000. | 832. | 342. |
| 27 | 1 | 1340916. | 875910. | 101769. | 977679. | 11015. | 4845. | 169. | 71. | 363237. | 271295. | 31942. | 303237. | 20200. | 873. | 344. |
| 28 | 1 | 1339363. | 867585. | 100982. | 968567. | 10852. | 4839. | 167. | 70. | 370796. | 278209. | 32587. | 310796. | 20400. | 916. | 345. |
| 29 | 1 | 1338498. | 859694. | 100236. | 959930. | 10692. | 4834. | 166. | 69. | 378568. | 285317. | 33251. | 318568. | 20600. | 962. | 347. |
| * 30 | 1 | 1338321. | 852230. | 99531. | 951761. | 10533. | 4828. | 165. | 69. | 386560. | 292628. | 33933. | 326560. | 20800. | 1010. | 348. |
| 31 | 1 | 1338833. | 845185. | 98865. | 944049. | 10377. | 4821. | 163. | 68. | 394784. | 300149. | 34634. | 334784. | 21000. | 1062. | 350. |

*Minimum Configuration

## Table 11. Minimum Liftoff Stage Proportioning Computer Printout Post-Saturn Class - Two Stage Vehicle

| | | | Stage 1 | | | | | | | | Stage 2 | | | | | | |
|---|---|---|---|---|---|---|---|---|---|---|---|---|---|---|---|---|---|
| | J | K | WTOTAL | WPROP | WEMPTY | WSTAGE | DVEL | VLOSS | TIME | ABO | WTOTAL | WPROP | WEMPTY | WSTAGE | DVEL | VLOSS | TIME |
| | 1 | 1 | 32589357. | 25331999. | 2204575. | 27536574. | 15621. | 4766. | 201. | 80. | 5052783. | 3231431. | 321352. | 3552783. | 15000. | 354. | 294. |
| | 2 | 1 | 32210023. | 24897873. | 2166794. | 27064667. | 15421. | 4757. | 200. | 80. | 5145356. | 3315708. | 329648. | 3645356. | 15200. | 361. | 296. |
| | 3 | 1 | 31821326. | 24453166. | 2128093. | 26581258. | 15216. | 4748. | 199. | 80. | 5240068. | 3401933. | 338135. | 3740068. | 15400. | 368. | 299. |
| | 4 | 1 | 31475764. | 24046113. | 2092668. | 26138781. | 15016. | 4739. | 197. | 79. | 5336983. | 3490163. | 346820. | 3836983. | 15600. | 376. | 301. |
| | 5 | 1 | 31145656. | 23651186. | 2058298. | 25709484. | 14816. | 4731. | 196. | 79. | 5436172. | 3580463. | 355709. | 3936172. | 15800. | 385. | 303. |
| | 6 | 1 | 30830319. | 23267690. | 2024924. | 25292613. | 14616. | 4723. | 195. | 79. | 5537706. | 3672898. | 364808. | 4037706. | 16000. | 395. | 305. |
| | 7 | 1 | 30529124. | 22894978. | 1992487. | 24887465. | 14416. | 4715. | 194. | 79. | 5641659. | 3767536. | 374123. | 4141659. | 16200. | 406. | 307. |
| | 8 | 1 | 30277134. | 22566040. | 1963861. | 24529900. | 14225. | 4708. | 193. | 79. | 5747234. | 3863650. | 383584. | 4247234. | 16400. | 417. | 309. |
| | 9 | 1 | 30026143. | 22234933. | 1935045. | 24169978. | 14031. | 4701. | 191. | 78. | 5856165. | 3962820. | 393346. | 4356165. | 16600. | 430. | 311. |
| | 10 | 1 | 29793505. | 21918269. | 1907487. | 23825755. | 13839. | 4695. | 190. | 78. | 5967749. | 4064404. | 403345. | 4467749. | 16800. | 444. | 313. |
| | 11 | 1 | 29578353. | 21615169. | 1881109. | 23496278. | 13648. | 4689. | 189. | 78. | 6082075. | 4168485. | 413590. | 4582075. | 17000. | 459. | 315. |
| | 12 | 1 | 29380276. | 21325171. | 1855871. | 23181042. | 13459. | 4683. | 188. | 78. | 6199234. | 4275145. | 424089. | 4699234. | 17200. | 475. | 317. |
| | 13 | 1 | 29198887. | 21047831. | 1831735. | 22879566. | 13271. | 4677. | 186. | 77. | 6319322. | 4384471. | 434851. | 4819322. | 17400. | 493. | 319. |
| | 14 | 1 | 29033833. | 20782731. | 1808664. | 22591395. | 13085. | 4672. | 185. | 77. | 6442438. | 4496555. | 445883. | 4942438. | 17600. | 512. | 321. |
| | 15 | 1 | 28884799. | 20529486. | 1786625. | 22316110. | 12901. | 4667. | 184. | 77. | 6568689. | 4611492. | 457197. | 5068689. | 17800. | 532. | 323. |
| | 16 | 1 | 28751497. | 20287730. | 1765585. | 22053315. | 12719. | 4663. | 182. | 76. | 6698182. | 4729381. | 468801. | 5198182. | 18000. | 554. | 325. |
| | 17 | 1 | 28633678. | 20057128. | 1745516. | 21802644. | 12538. | 4659. | 181. | 76. | 6831034. | 4850327. | 480707. | 5331034. | 18200. | 578. | 327. |
| | 18 | 1 | 28531123. | 19837368. | 1726391. | 21563760. | 12360. | 4655. | 180. | 75. | 6967363. | 4974440. | 492924. | 5467363. | 18400. | 603. | 328. |
| | 19 | 1 | 28443641. | 19628160. | 1708184. | 21336344. | 12183. | 4651. | 178. | 75. | 7107297. | 5101834. | 505463. | 5607297. | 18600. | 630. | 330. |
| | 20 | 1 | 28371080. | 19429240. | 1690873. | 21120113. | 12009. | 4647. | 177. | 74. | 7250967. | 5232629. | 518338. | 5750967. | 18800. | 658. | 332. |
| | 21 | 1 | 28313317. | 19240368. | 1674436. | 20914804. | 11836. | 4643. | 176. | 74. | 7398513. | 5366953. | 531560. | 5898513. | 19000. | 689. | 334. |
| | 22 | 1 | 28270254. | 19061322. | 1658854. | 20720176. | 11666. | 4640. | 174. | 73. | 7550079. | 5504936. | 545142. | 6050079. | 19200. | 721. | 335. |
| | 23 | 1 | 28222045. | 18873701. | 1642526. | 20516226. | 11492. | 4636. | 173. | 73. | 7705819. | 5646720. | 559099. | 6205819. | 19400. | 757. | 337. |
| | 24 | 1 | 28204671. | 18710458. | 1628319. | 20338777. | 11324. | 4632. | 171. | 72. | 7865894. | 5792451. | 573444. | 6365894. | 19600. | 793. | 339. |
| * | 25 | 1 | 28202084. | 18556674. | 1614935. | 20171610. | 11159. | 4629. | 170. | 71. | 8030474. | 5942282. | 588192. | 6530474. | 19800. | 832. | 340. |
| | 26 | 1 | 28213803. | 18411743. | 1602322. | 20014065. | 10996. | 4625. | 169. | 71. | 8199738. | 6096377. | 603360. | 6699738. | 20000. | 873. | 342. |

*Minimum Configuration

## Table 12. Minimum Liftoff Stage Proportioning Computer Printout Post-Saturn Class - Three Stage Vehicle

### FIRST AND SECOND STAGES

| | Stage 1 | | | | | | | | Stage 2 | | | | | | |
|---|---|---|---|---|---|---|---|---|---|---|---|---|---|---|---|
| | K | WTOTAL | WPROP | WEMPTY | WSTAGE | DVEL | VLOSS | TIME | ABO | WTOTAL | WPROP | WEMPTY | WSTAGE | DVEL | VLOSS | TIME |
| | 1 | 28917968. | 21927003. | 1907588. | 23834591. | 14767. | 4733. | 196. | 79. | 5083377. | 2133387. | 173137. | 2306525. | 8000. | 534. | 193. |
| | 1 | 28562470. | 21528277. | 1872900. | 23401177. | 14574. | 4726. | 195. | 79. | 5161294. | 2206566. | 177875. | 2384441. | 8200. | 549. | 197. |
| | 1 | 28223926. | 21144066. | 1839474. | 22983540. | 14383. | 4718. | 194. | 79. | 5240386. | 2280849. | 182684. | 2463533. | 8400. | 564. | 200. |
| | 1 | 27904105. | 20775720. | 1807429. | 22583149. | 14194. | 4712. | 192. | 79. | 5320957. | 2356521. | 187583. | 2544104. | 8600. | 581. | 204. |
| | 1 | 27601654. | 20422086. | 1776664. | 22198750. | 14006. | 4705. | 191. | 78. | 5402904. | 2433486. | 192566. | 2626051. | 8800. | 600. | 207. |
| | 1 | 27316813. | 20083208. | 1747182. | 21830390. | 13820. | 4699. | 190. | 78. | 5486423. | 2511848. | 197722. | 2709570. | 9000. | 620. | 211. |
| | 1 | 27052749. | 19761249. | 1719173. | 21480422. | 13636. | 4694. | 189. | 78. | 5572328. | 2592000. | 203475. | 2795475. | 9200. | 641. | 214. |
| | 1 | 26804390. | 19452342. | 1692299. | 21144641. | 13454. | 4688. | 188. | 78. | 5659750. | 2673568. | 209329. | 2882897. | 9400. | 664. | 217. |
| | 2 | 26570863. | 19155732. | 1666494. | 20822227. | 13274. | 4683. | 186. | 77. | 5748637. | 2715537. | 212342. | 2927878. | 9400. | 690. | 217. |
| | 2 | 26351642. | 18870924. | 1641717. | 20512641. | 13096. | 4679. | 185. | 77. | 5839001. | 2799849. | 218393. | 3018242. | 9600. | 717. | 221. |
| | 2 | 26146749. | 18597820. | 1617958. | 20215778. | 12921. | 4674. | 184. | 77. | 5930971. | 2885661. | 224552. | 3110213. | 9800. | 745. | 224. |
| | 2 | 25955094. | 18335530. | 1595139. | 19930669. | 12747. | 4670. | 183. | 76. | 6024425. | 2972856. | 230810. | 3203666. | 10000. | 776. | 227. |
| | 4 | 25776582. | 18083876. | 1573246. | 19657122. | 12576. | 4666. | 181. | 76. | 6119460. | 2977313. | 231130. | 3208443. | 9800. | 811. | 224. |
| | 5 | 25613661. | 17844464. | 1552418. | 19396882. | 12407. | 4662. | 180. | 75. | 6216780. | 3024727. | 234677. | 3259404. | 9800. | 847. | 224. |
| | 3 | 25450351. | 17601611. | 1531290. | 19132901. | 12235. | 4659. | 179. | 75. | 6317450. | 3203425. | 248542. | 3451966. | 10400. | 882. | 233. |
| | 2 | 25319008. | 17385831. | 1512518. | 18898349. | 12070. | 4655. | 177. | 75. | 6420659. | 3340709. | 259193. | 3599901. | 10800. | 918. | 239. |
| | 2 | 25193654. | 17175088. | 1494184. | 18669271. | 11907. | 4652. | 176. | 74. | 6524383. | 3436964. | 266661. | 3703625. | 11000. | 959. | 242. |
| | 2 | 25080249. | 16973556. | 1476651. | 18450206. | 11746. | 4649. | 175. | 74. | 6630043. | 3535016. | 274268. | 3809285. | 11200. | 1002. | 245. |
| | 1 | 24990275. | 16788783. | 1460576. | 18249359. | 11588. | 4645. | 174. | 73. | 6740917. | 3678652. | 285413. | 3964064. | 11600. | 1045. | 251. |
| | 1 | 24899945. | 16604468. | 1444541. | 18049009. | 11432. | 4642. | 172. | 72. | 6850937. | 3780750. | 293334. | 4074084. | 11800. | 1093. | 254. |
| | 1 | 24821092. | 16428786. | 1429257. | 17858043. | 11278. | 4639. | 171. | 72. | 6963049. | 3884790. | 301406. | 4186196. | 12000. | 1143. | 257. |
| | 1 | 24752976. | 16261013. | 1414662. | 17675674. | 11127. | 4636. | 170. | 71. | 7077302. | 3990817. | 309632. | 4300449. | 12200. | 1196. | 259. |
| | 3 | 24685395. | 16099675. | 1400625. | 17500300. | 10984. | 4633. | 169. | 71. | 7185095. | 4008599. | 311012. | 4319611. | 12000. | 1257. | 257. |
| | 3 | 24639118. | 15948663. | 1387488. | 17336151. | 10839. | 4629. | 167. | 70. | 7302968. | 4117985. | 319499. | 4437484. | 12200. | 1315. | 259. |
| | 3 | 24604041. | 15805876. | 1375066. | 17180942. | 10696. | 4525. | 166. | 69. | 7423099. | 4229467. | 328148. | 4557615. | 12400. | 1376. | 262. |
| | 3 | 24579558. | 15670708. | 1363306. | 17034014. | 10555. | 4622. | 165. | 69. | 7545544. | 4343096. | 336964. | 4680060. | 12600. | 1439. | 265. |
| | 3 | 24565590. | 15543034. | 1352199. | 16895233. | 10417. | 4618. | 163. | 68. | 7670358. | 4458923. | 345951. | 4804874. | 12800. | 1505. | 267. |
| * | 3 | 24562082. | 15422750. | 1341735. | 16764485. | 10282. | 4613. | 162. | 67. | 7797598. | 4577002. | 355112. | 4932114. | 13000. | 1573. | 270. |
| | 1 | 24590607. | 15316568. | 1332497. | 16649065. | 10142. | 4608. | 161. | 67. | 7941542. | 4792832. | 371858. | 5164690. | 13600. | 1637. | 278. |

### THIRD STAGE

| | I | J | WTOTAL | WPROP | WEMPTY | WSTAGE | DVEL | TIME |
|---|---|---|---|---|---|---|---|---|
| | 3 | 1 | 2776853. | 1165382. | 111471. | 1276853. | 8000. | 226. |
| | 3 | 2 | 2820758. | 1205911. | 114847. | 1320758. | 8200. | 230. |
| * | 3 | 3 | 2865484. | 1247198. | 118286. | 1365484. | 8400. | 234. |
| | 3 | 4 | 2911017. | 1289230. | 121787. | 1411017. | 8600. | 238. |
| | 3 | 5 | 2957376. | 1332024. | 125352. | 1457376. | 8800. | 242. |
| | 3 | 6 | 3004577. | 1375596. | 128982. | 1504577. | 9000. | 246. |
| | 3 | 7 | 3052641. | 1419964. | 132677. | 1552641. | 9200. | 250. |
| | 3 | 8 | 3101587. | 1465146. | 136441. | 1601587. | 9400. | 254. |
| | 3 | 9 | 3151415. | 1511151. | 140264. | 1651415. | 9600. | 258. |
| | 3 | 10 | 3202105. | 1557979. | 144127. | 1702105. | 9800. | 262. |
| | 3 | 11 | 3253731. | 1605671. | 148061. | 1753731. | 10000. | 266. |
| | 3 | 12 | 3306318. | 1654250. | 152068. | 1806318. | 10200. | 269. |
| | 3 | 13 | 3359885. | 1703736. | 156149. | 1859886. | 10400. | 273. |
| | 3 | 14 | 3414458. | 1754150. | 160308. | 1914458. | 10600. | 277. |
| | 3 | 15 | 3470059. | 1805514. | 164545. | 1970059. | 10800. | 280. |

*Minimum Configuration

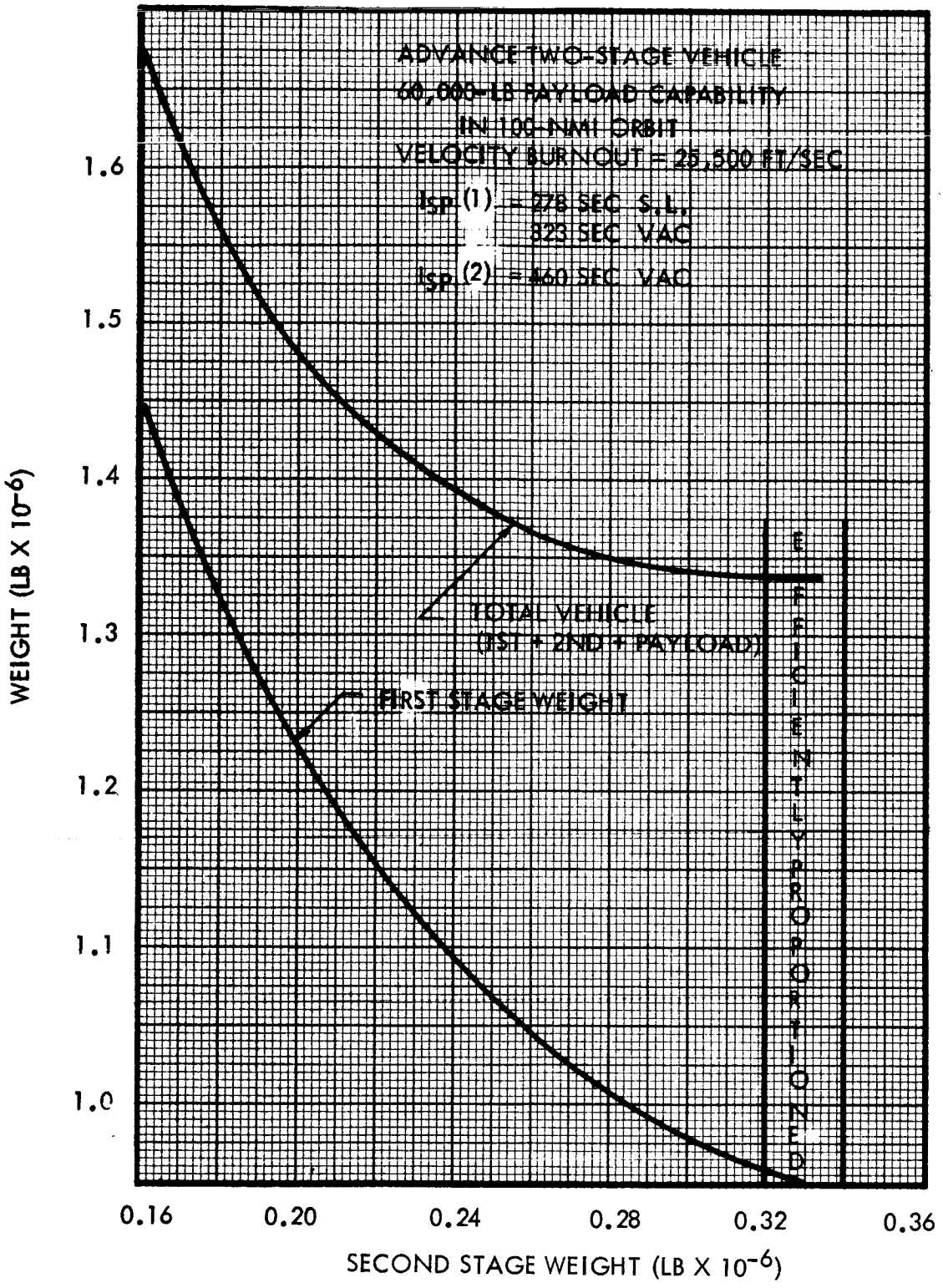



**Figure 16.** Effect of Stage Proportioning of Liftoff Weight for Future Medium Range Payload Class

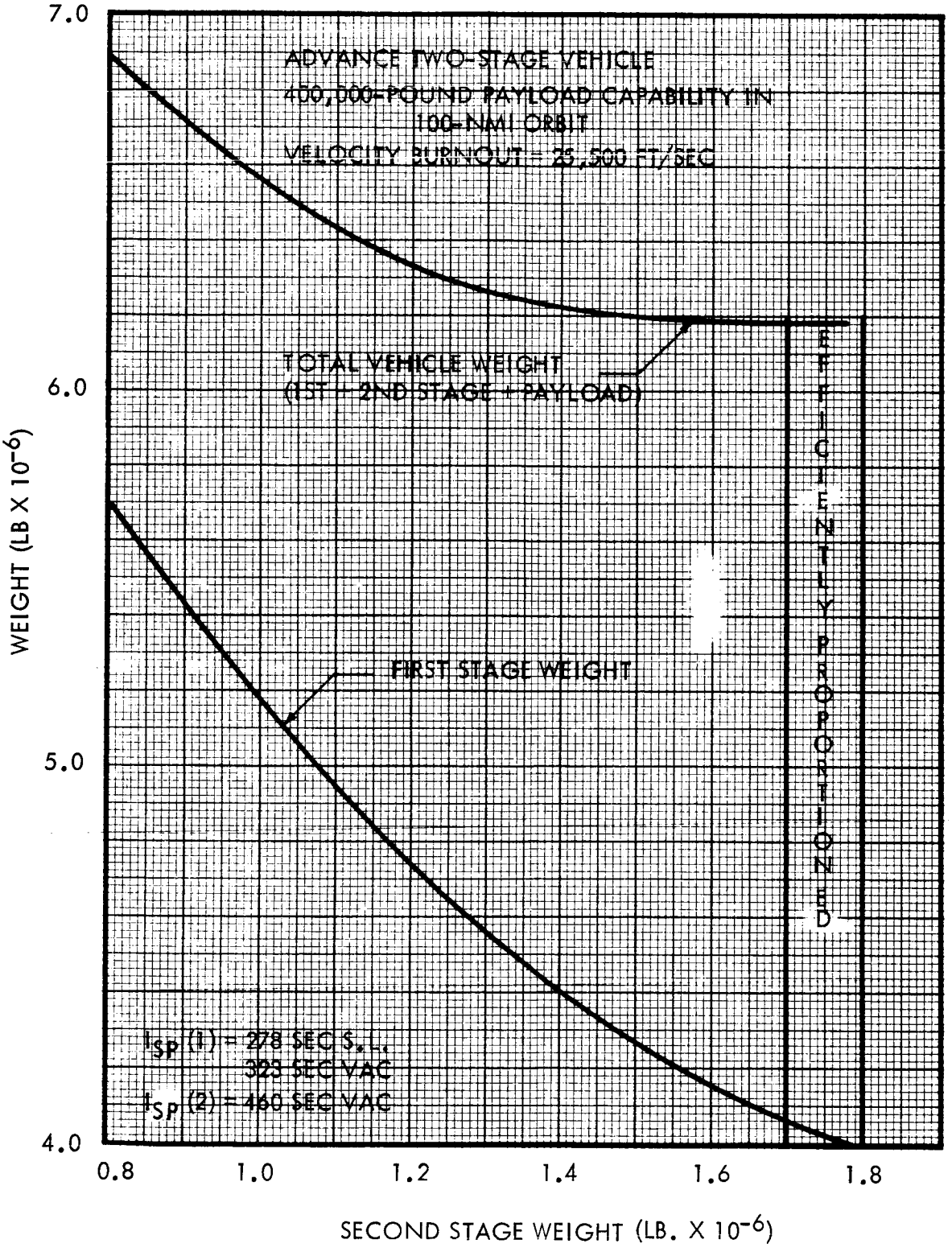



Figure 17. Effect of Stage Proportioning on Liftoff Weight for Future Saturn Payload Class Vehicle

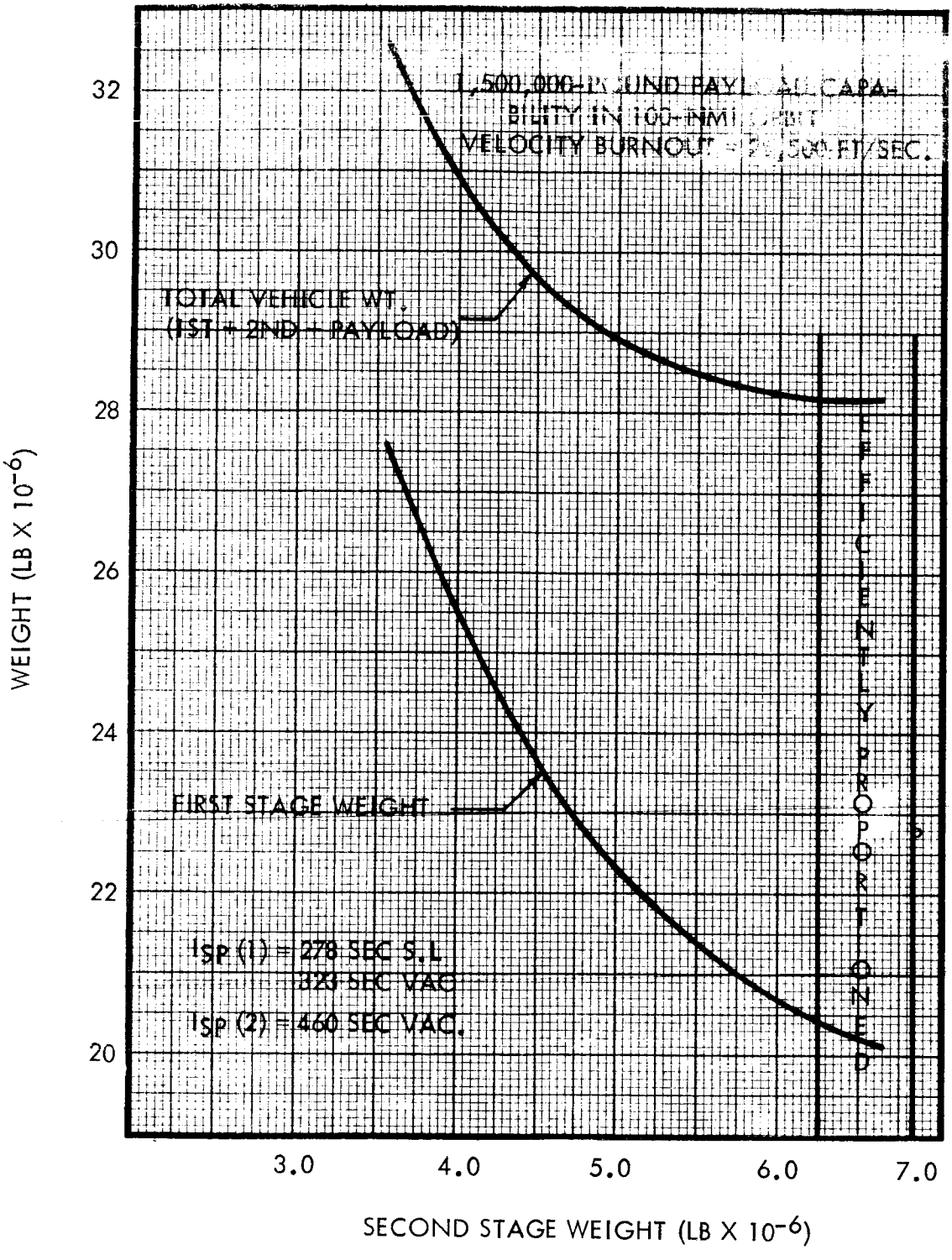



Figure 18. Effect of Stage Proportioning of Liftoff Weight for Post-Saturn Payload Class - Advanced Two-Stage Vehicle

## Table 13. Stage Definition for Selected Test Case Vehicles (Maximum Payload Stage Proportioning) Two-Stage Vehicles

| Stage | | Medium Payload Range | | | Saturn Class Range | | | Post-Saturn Range | | |
|---|---|---|---|---|---|---|---|---|---|---|
| | | Current | 1975 | 1985 | Current | 1975 | 1985 | Current | 1975 | 1985 |
| 1 | Lift Off Weight $W_{TO} \times 10^{-6}$ lb | 0.960 | 1.0560 | 1.152 | 6.0 | 6.6 | 7.2 | 24.0 | 26.4 | 28.8 |
| | Stage Weight $W_{ST}$ (1) $\times 10^{-6}$ lb | 0.7192 | 0.7696 | 0.8301 | 4.4893 | 4.8176 | 5.2184 | 17.5846 | 19.2258 | 20.4772 |
| | Propellant Weight $W_{PROP}$ (1) $\times 10^{-6}$ lb | 0.6539 | 0.6952 | 0.7454 | 4.1540 | 4.4596 | 4.8322 | 16.2888 | 1.7774 | 18.9095 |
| | Stage Burn Out Weight $W_{BO}$ (1) $\times 10^{-6}$ lb | 0.06540 | 0.07438 | 0.08463 | 0.3353 | 0.3579 | 0.3861 | 1.2957 | 1.4517 | 1.5676 |
| | Specific Impulse | 263 SL<br>302 VAC | 278 SL<br>323 VAC | 300 SL<br>350 VAC | 263 SL<br>302 VAC | 278 SL<br>323 VAC | 300 SL<br>350 VAC | 263 SL<br>302 VAC | 278 SL<br>323 VAC | 300 SL<br>350 VAC |
| | Burn Out Velocity $V_{BO}$ ft/sec | 5,600 | 5,700 | 6,200 | 7,000 | 7,100 | 7,700 | 6,700 | 7,100 | 7,300 |
| | Stage Velocity Loss $V_{LOSS}$ ft/sec | 5,472 | 5,427 | 5,491 | 4,410 | 4,559 | 4,776 | 4,291 | 4,481 | 4,691 |
| | Stage Burning Time $t_{BO}$ sec | 143 | 148 | 157 | 145 | 152 | 163 | 143 | 152 | 160 |
| | Burn Out Angle $\alpha_{BO}$ day | 73.99 | 71.47 | 70.06 | 75.07 | 73.43 | 72.94 | 73.75 | 73.17 | 71.26 |
| 2 | Gross Weight $W_o$ (2) $\times 10^{-6}$ lb | 0.2407 | 0.2864 | 0.3219 | 1.5106 | 1.7824 | 1.9816 | 6.4154 | 7.1742 | 8.3228 |
| | Stage Weight $W_{ST}$ (2) $\times 10^{-6}$ lb | 0.2095 | 0.2422 | 0.2609 | 1.2488 | 1.4206 | 1.4942 | 5.2728 | 5.6464 | 6.3014 |
| | Propellant Weight $W_{PROP}$ (2) | 0.1885 | 0.2172 | 0.2331 | 1.1552 | 1.3110 | 1.3801 | 4.9221 | 5.2631 | 5.8707 |
| | Stage Burn Out Weight $W_{BO}$ (2) | 0.02097 | 0.02495 | 0.02774 | 0.0993 | 0.1096 | 0.1141 | 0.3507 | 0.3832 | 0.4307 |
| | Specific Impulse Isp (2) | 424 | 460 | 500 | 424 | 460 | 500 | 424 | 460 | 500 |
| | Stage Velocity Loss $V_{LOSS}$ (2) | 784 | 1,099 | 1,292 | 912 | 1,161 | 1,262 | 960 | 1,656 | 1,338 |
| | Stage Burning Time $t_{BO}$ (sec) | 393 | 453 | 484 | 486 | 546 | 573 | 462 | 487 | 542 |
| | Payload Weight $W_{PL}$ (lbs) | 31,276 | 44,212 | 61,062 | 261,885 | 361,848 | 487,441 | 1,142,700 | 1,527,800 | 2,021,375 |
| | Burn Out Velocity $V_{BO}$ (fps) | 25,500 | 25,500 | 25,500 | 25,500 | 25,500 | 25,500 | 25,500 | 25,500 | 25,500 |

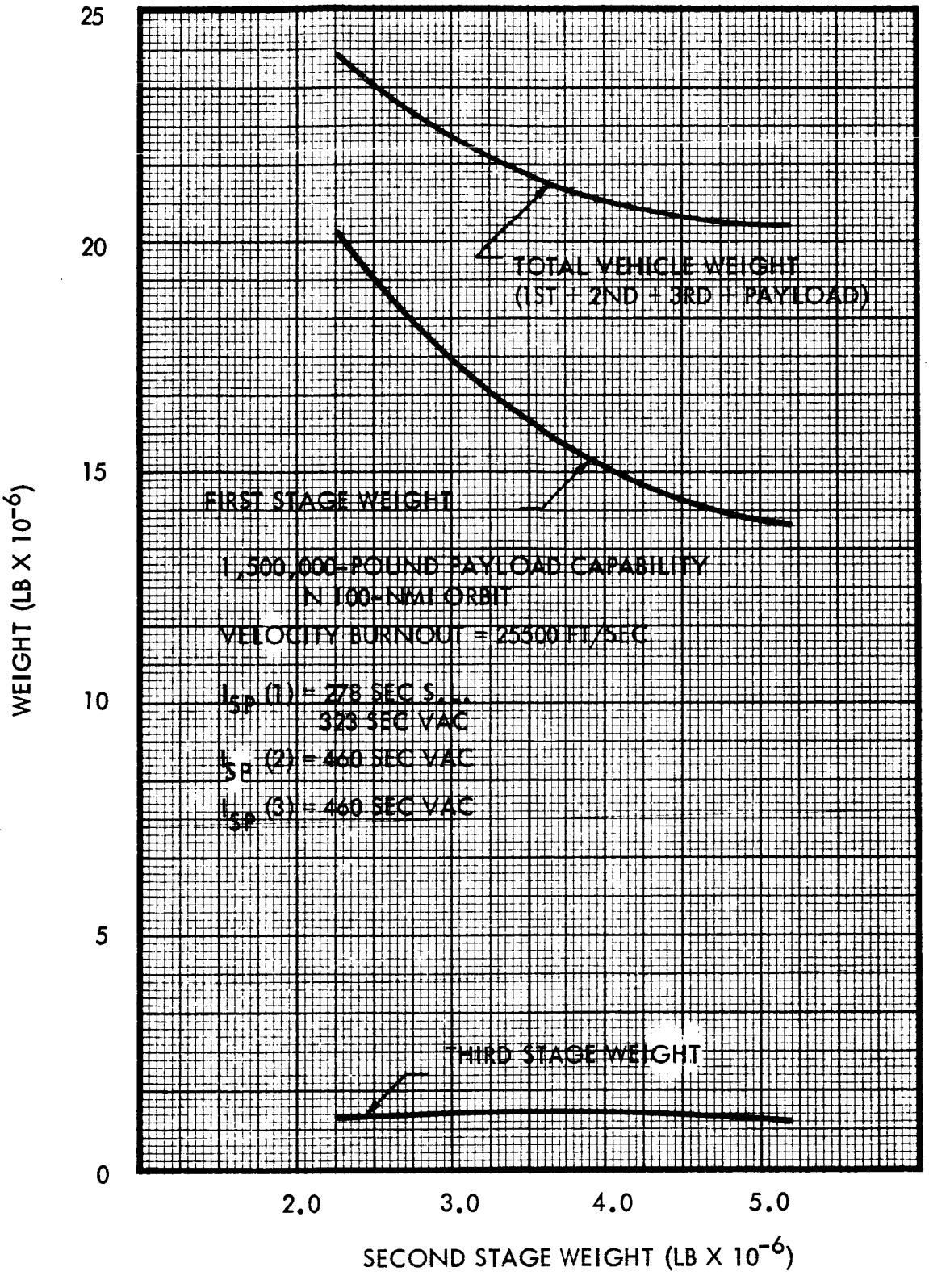



Figure 19. Effect of Stage Proportioning on Liftoff Weight for Post-Saturn Payload Class Advanced Three-Stage Vehicle

(Figure 18) demonstrates the additional vehicle liftoff weight (about 10 percent) that can be incurred with poorly proportioned stages. The three-stage vehicle indicates a less severe weight penalty and also optimizes at a smaller liftoff weight.

## VEHICLE SIZE - PAYLOAD RANGE VARIATIONS

The optimum proportioned vehicles and their associated liftoff weights were obtained from a large number of computer runs through the complete payload spectrum. Similar data could be generated to determine effects of thrust-to-weight changes.

Figures 20 and 21 present comparisons of vehicle liftoff weight to payload for the two-stage vehicles (Figure 20) and the three-stage vehicles (Figure 21). Figure 20 also includes a plot of the post-Saturn payload class three-stage vehicle which indicates that the payload/gross parameter is not too greatly affected by using a three-stage vehicle in place of a two-stage vehicle. These curves were generated using propellant and thrust characteristics identified for the three basic periods.

For a fixed payload weight requirement, Figures 20 and 21 indicate the liftoff weight variation as a function of change in specific impulse. Also, for a constant liftoff weight, they provide an indication of the anticipated payload improvement which is verified later in this study using the maximum payload subroutine.

Subjecting the minimum liftoff proportioned vehicles to a critical analysis produced results which indicated that specific reasonable test cases should be selected from the vehicle spectrum and used as base points for the structures/materials tradeoff study.

## STAGE MASS FRACTIONS

The second step in the proportioning process, maximum payload evaluation per Figure 14, required derivations of mass fractions for each vehicle and vehicle stage in the study to isolate values which reflect the number of stages, the unique propulsion/propellant characteristics, and the more exacting payload influence. Here again, the basic structural shells were considered as Aluminum A integral skin-stringer constructions. The stage mass fraction subroutine was used to provide better estimates for the base point vehicles to define allowable limits to which stage propellant could be varied without altering the loading environment beyond input criteria, and to produce stage mass fraction trends as a function of stage propellant weight within the defined limits.

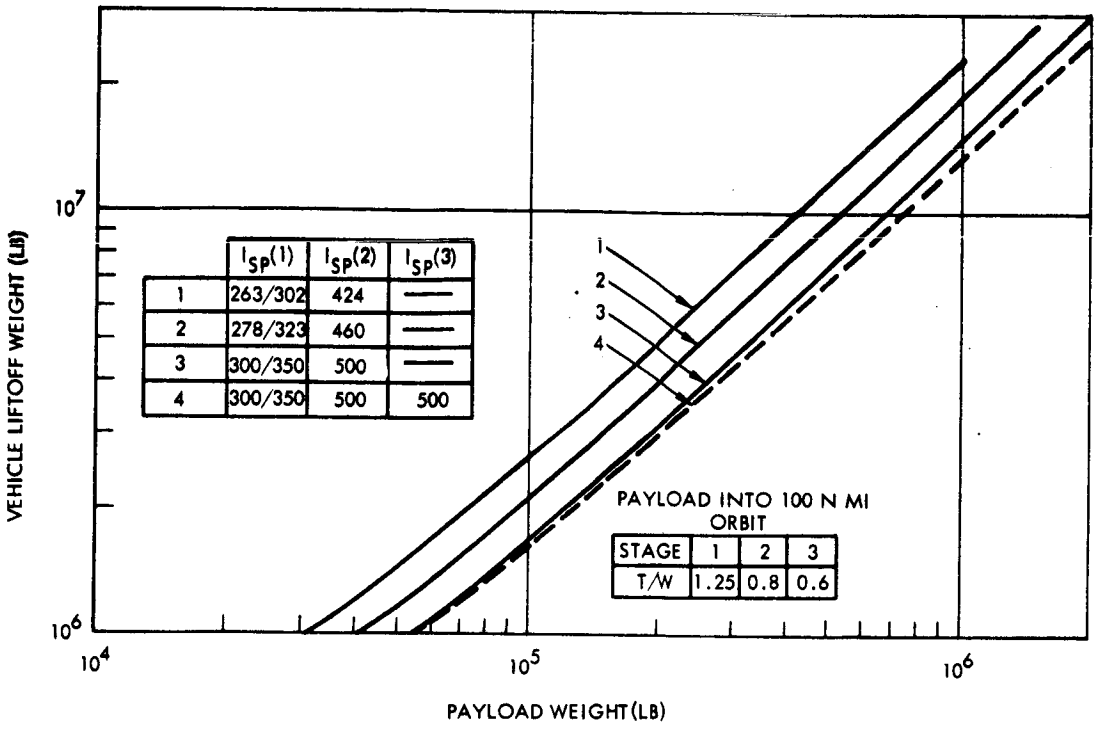



Figure 20. Vehicle Size—Payload Range Variation Two - Stage Vehicles—Current and Advanced Propellant Characteristics

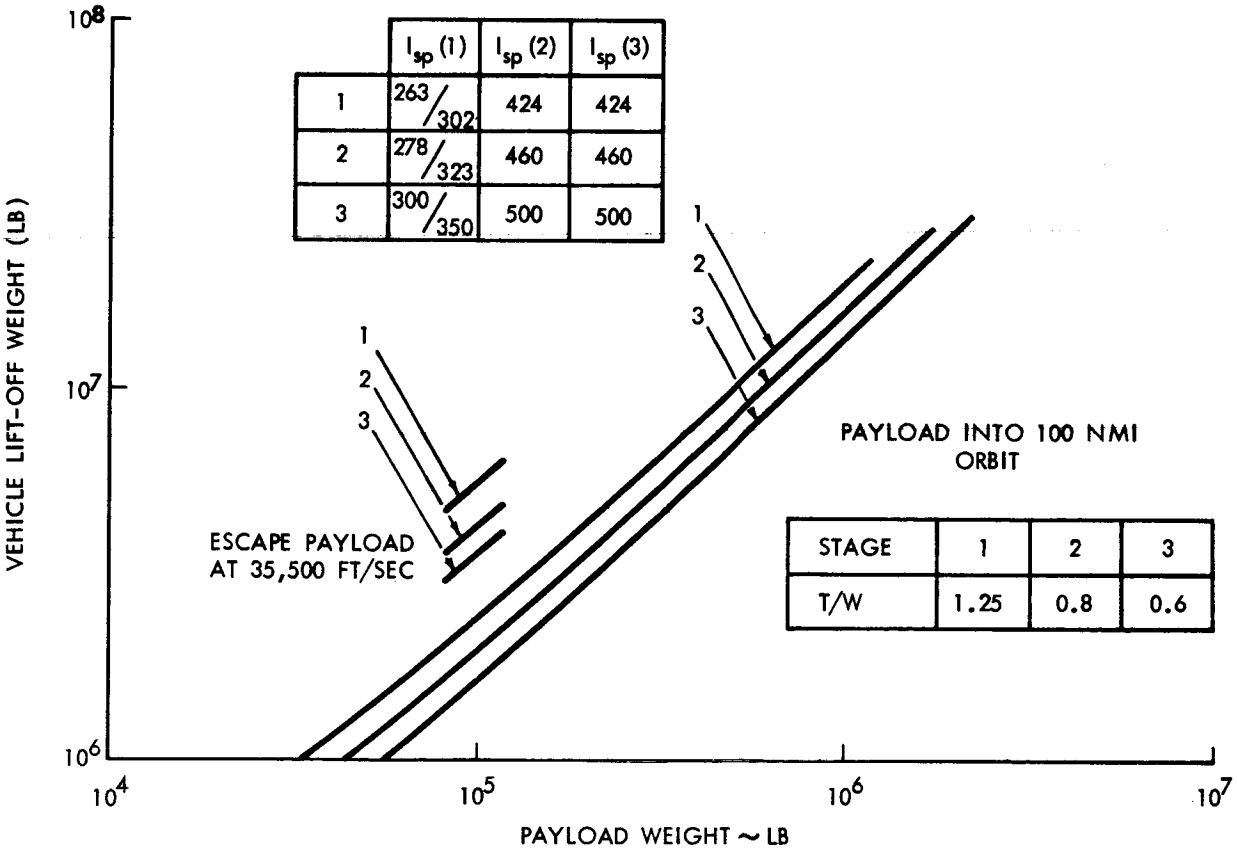



Figure 21. Vehicle Size—Payload Range Variation Three - Stage Vehicles—Current and Advanced Propellant Characteristics

Figure 22 is a diagram of the basic stage mass fraction logic which is discussed in more detail in Appendix B. Two types of inputs are used in this subroutine: (1) those fed directly from the stage proportioning logic, and (2) those input to control the mathematical model, operational mode, and output. The second type of input also includes construction unit weight versus applied load curves for pressurized and unpressurized shells derived from the design synthesis subroutines. The subroutine includes a parametric assessment of loads and internal pressures and uses internally computed mass properties and flight loads criteria from the proportioning output. An average design load value is used for each of the various flight conditions and the critical loading condition for each basic component is identified. Engine geometry sizing and subsystems estimating techniques are parametric and provide output data which has been successfully correlated with existing hardware designs.

In this study, S&ID Computer Aided Design automated inboard profile drawing and mass fraction curve subroutines were used in addition to the mass fraction operation to output automated inboard sketches of the vehicles investigated and mass fraction trends. (These subroutines are not essential to the approach and are not a part of this study but were used to provide economic automated displays of some pertinent data.)

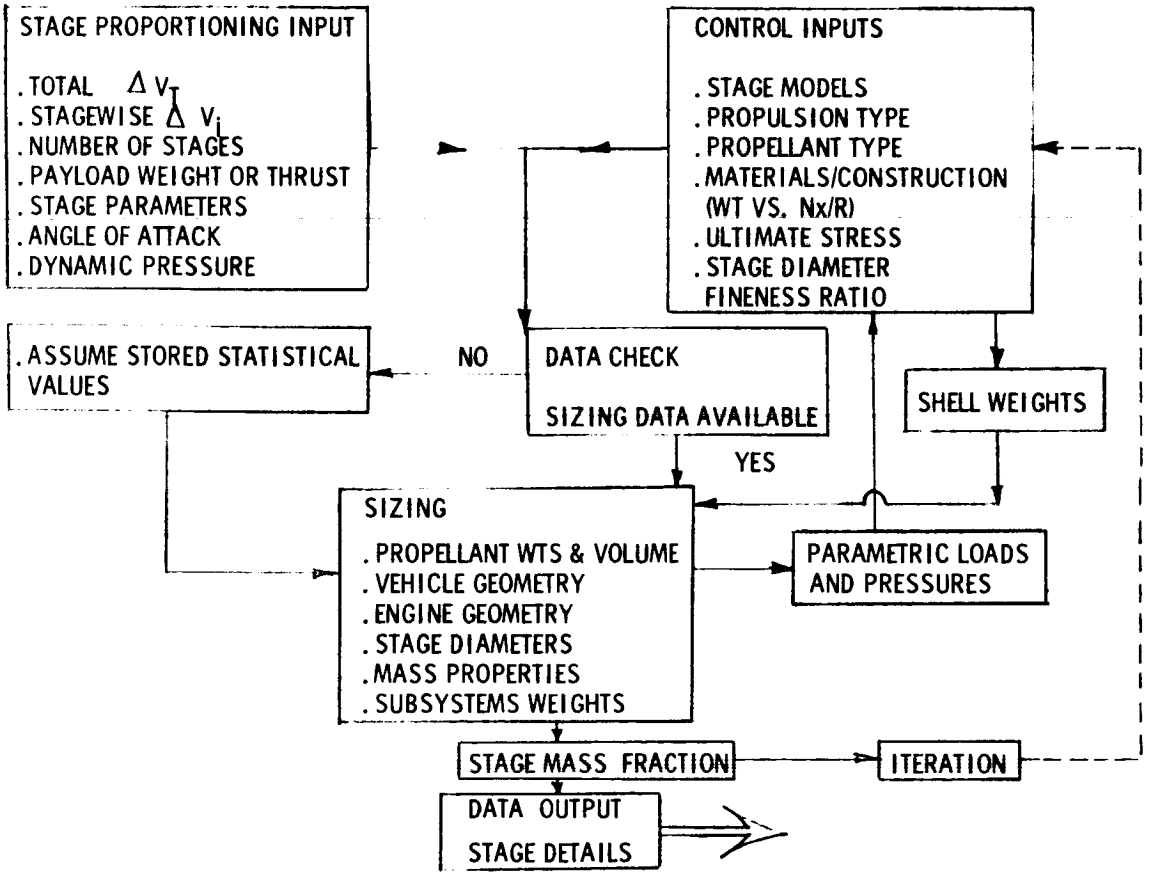



Figure 22. Stage Mass Fraction Logic

Figures 23 and 24 present summary curves of the mass fraction trends or the two-stage vehicles identified in the vehicle spectrum in Table 7. Each tagewise curve is related to its companion stage and considers the effects of ayload above the stage, thrust levels imposed on the stage, and the specific mpulse of the stage. CRT curves for these cases may be found in Appendix B.

## SELECTION OF SPECIFIC TEST CASES

A large amount of data was produced in synthesizing the two and three stage vehicles, and this spectrum of vehicles was narrowed to a few specific test cases which demonstrate the influence of structures and materials on a vehicle typical of one that might be part of the NASA stable. For injecting payloads into a 100 nmi earth orbit, the two-stage vehicle appears to be the most likely candidate. In addition, the vehicle which more closely approximates the first two stages of the Saturn V vehicle is the most interesting; therefore, the prime test cases selected for this study were the Saturn class payload two-stage vehicles. Alternative comparisons are described herein for the medium payload class and post-Saturn payload class two-stage vehicles.

The prime objective in synthesizing these current and future vehicle systems is to obtain a complete design description (size, shape, loading environment) of the individual structural components. These design descriptions provide realistic bases for conducting design synthesis studies on individual structural components and for measuring the effects of material and structural improvements.

## MAXIMUM PAYLOAD MODE PROPORTIONING

Results of the minimum liftoff proportioning were based upon preliminary estimates of stage mass fractions. The maximum payload proportioning mode (discussed in more detail in Appendix A) used refined mass fraction data and the previously identified liftoff weight to derive more exact maximum payload weight. Figure 25 briefly illustrates the technique used in maximizing vehicle payload. In the process employed, the previously established liftoff weights are used to initialize first stage propellant requirements for a range of burnout velocities. The refined mass fraction curves, for the case in question, are then used to assess weight change due to propellant requirements. Using proportioned first stages, the upper stages are then dynamically proportioned to maximize payload. Table 13 presents a summary of the data obtained from the maximum payload mode proportioning for the two-stage test case vehicles and their alternatives.

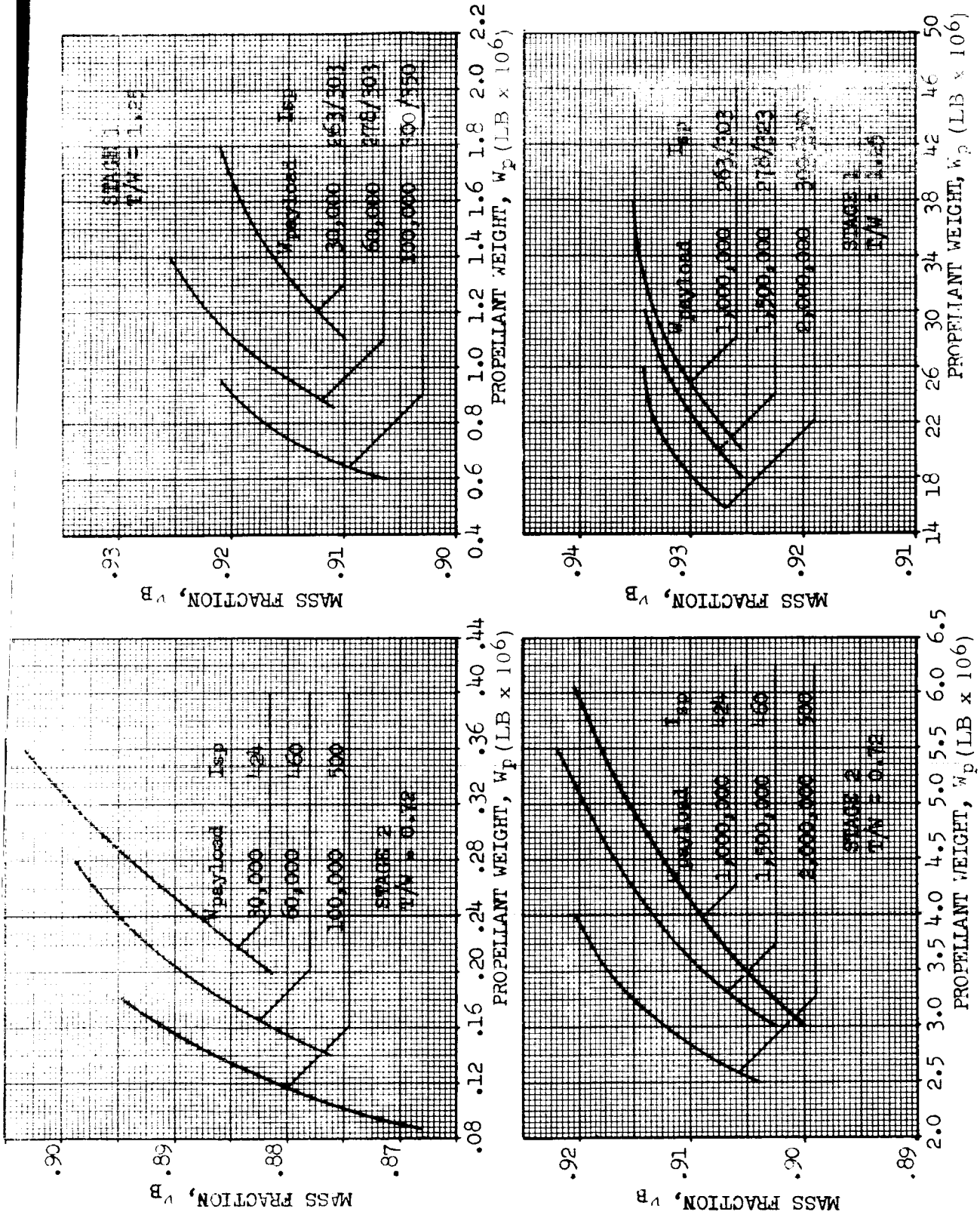



Figure 23. Mass Fraction Variation With Propellant Weight

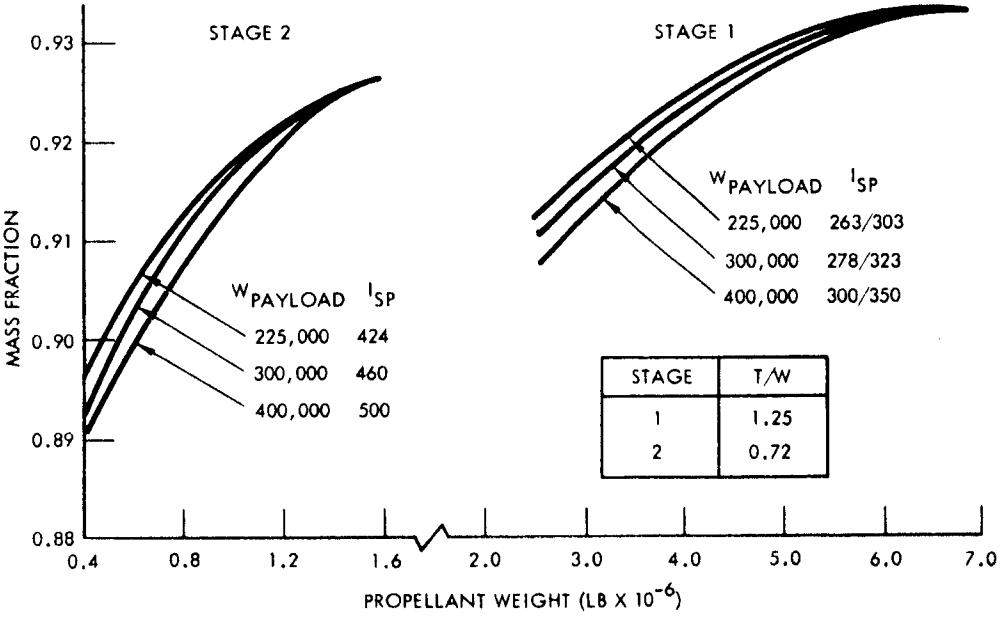



Figure 24. Mass Fraction Variation with Propellant Weight—Two Stage Future Saturn Payload Class Vehicle

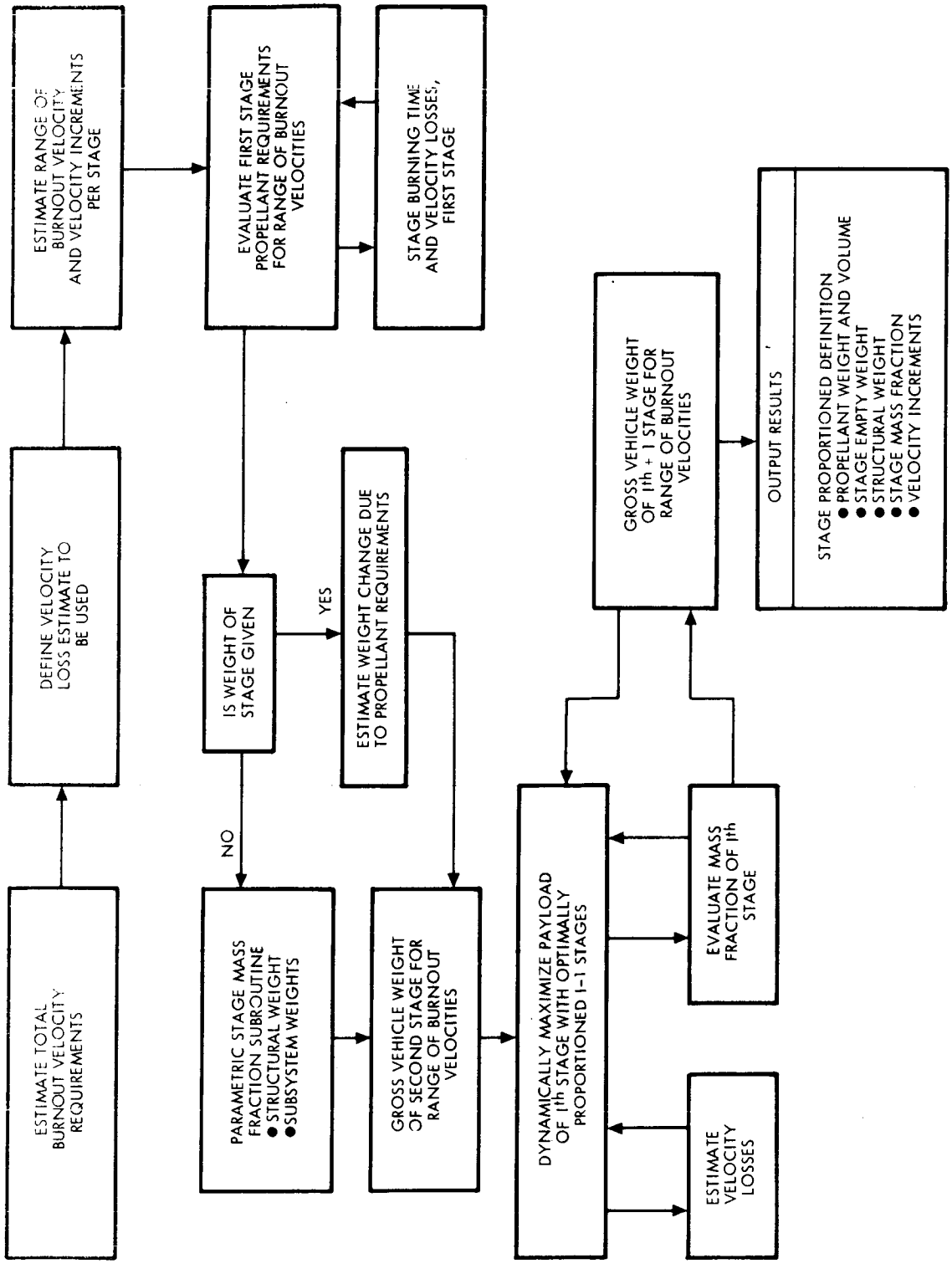



Figure 25. Maximum Payload Proportioning Logic

The payload values obtained using the maximum payload mode in Table 13 are slightly different from previous values (Figures 23 and 24). This difference is due to a better stage mass fraction estimate. The step-wise proportioning approach permits convergence to the realistic vehicle performance capability which is consistent with the weight definition of the individual stages.

## PAYLOAD VARIATIONS WITH SPECIFIC IMPULSE

Figure 26 illustrates payload weight variations for the Saturn class vehicles with changes in specific impulse and thrust level. There are numerous methods of uprating vehicle systems, two of which are illustrated in Figure 26. The first changes specific impulse in the first and/or second stages with the vehicle gross weight and liftoff thrust remaining constant. The second method measures the effects of improvements in both specific impulse and increase thrust levels. Initial thrust-to-weight ratio was kept constant by changing vehicle gross weight to match the thrust levels. The data from Table 13 is also used in Figure 27 to illustrate the variation of vehicle payload with specific impulse for the alternative medium payload range vehicles and the post-Saturn class vehicles.

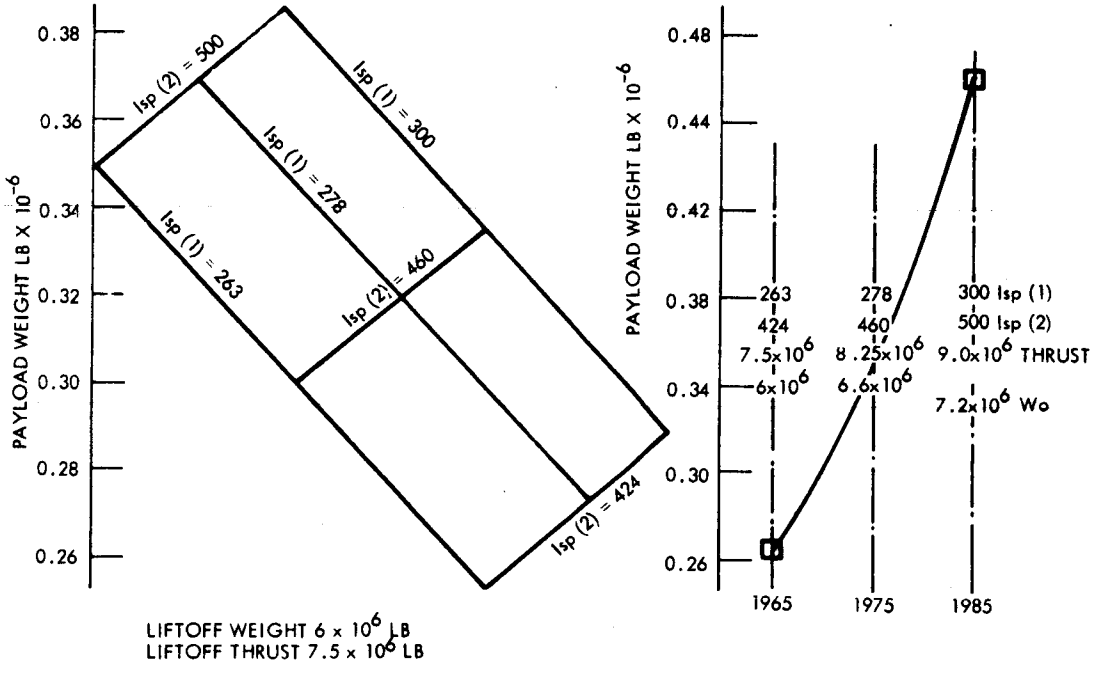



Figure 26. Variation of Vehicle Payload with Specific Impulse

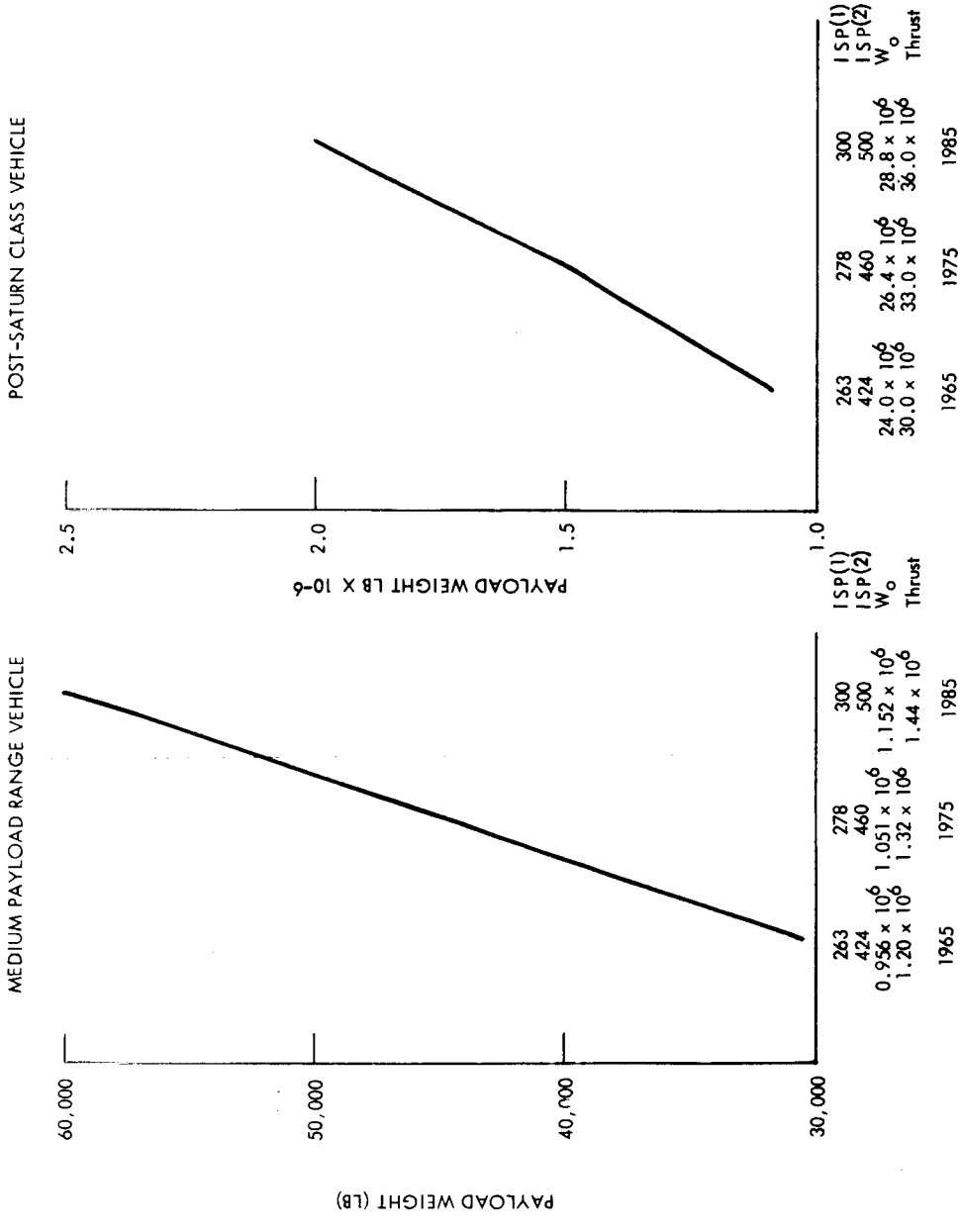



Figure 27. Variation of Vehicle Payload With Specific Impulse - Medium Range Payload Class Vehicle and Post-Saturn Payload Class Vehicle

## TEST CASE GEOMETRIES AND WEIGHTS

As previously discussed, a large spectrum of two- and three-stage vehicles was initially parametrically assessed to identify stage sizes and stage mass fractions. The two-stage vehicles were selected for prime consideration and among these vehicles the Saturn class payload vehicles appeared to be of special interest when considering the postulated earth orbital payload requirements and the present and future Saturn V vehicle. To reduce the number of cases subjected to weight and cost assessments, two specific vehicles were selected for basic comparisons. The two Saturn class vehicles — (1) current Isp with 240,000-pound payload and, (2) 1985 Isp with 445,000-pound payload — and their respective weights and performance definitions are shown in Figure 28 and Tables 14 and 15, and Figure 29 and Tables 16 and 17. Figure 30 and Tables 18 and 19 present similar data for the 1975 Isp configuration with a 330,000-pound payload. The payloads shown in Figures 28, 29, and 30 resulted from a final recycling through the stage mass fraction subroutine after maximizing the payload and represent the most refined estimates in this study.

The two vehicles per Tables 14 and 16 were selected as base points for design synthesis tradeoffs. The four alternative vehicles for the medium range payload class and the post-Saturn payload class are illustrated in Figures 31 and 32 and Tables 20 through 23 for the current Isp sizing and in Figures 33 and 34 and Tables 24 through 27 for the 1985 Isp sizing. The two base points and the four alternative vehicles were subjected to further analysis as covered in later sections of this report.

The stage fineness ratios in Figures 28 through 34 are not necessarily optimum. In the Saturn type vehicles (Figures 28, 29, and 30), controls were put into the program to approximate the current stage geometries of the Saturn V lower stages. In the medium payload range vehicles (Figures 31 and 33) the program was instructed to approximate a 260-inch diameter and make the first stage aft tankage with tangent $\sqrt{2}$ bulkheads. In the post-Saturn payload vehicles the program was first run limiting stage diameters to 540 inches. The program indicated that this could not be accomplished on either first stage; therefore a larger diameter was permitted (640 to 648 inches) and the vehicle sized. The 2,000,000 pound payload vehicle (Figure 34) illustrates a large fineness ratio, and it appears that a much larger diameter or a change in the basic propulsion system parameters might be required. However, this vehicle does present large diameters and loading intensities and therefore is valid for comparison. The payloads indicated on the CRT drawings (Figures 28 through 34) were low density, which could conceivably be a $LOX/LH_2$ orbital escape stage, and contribute to the large fineness ratio.

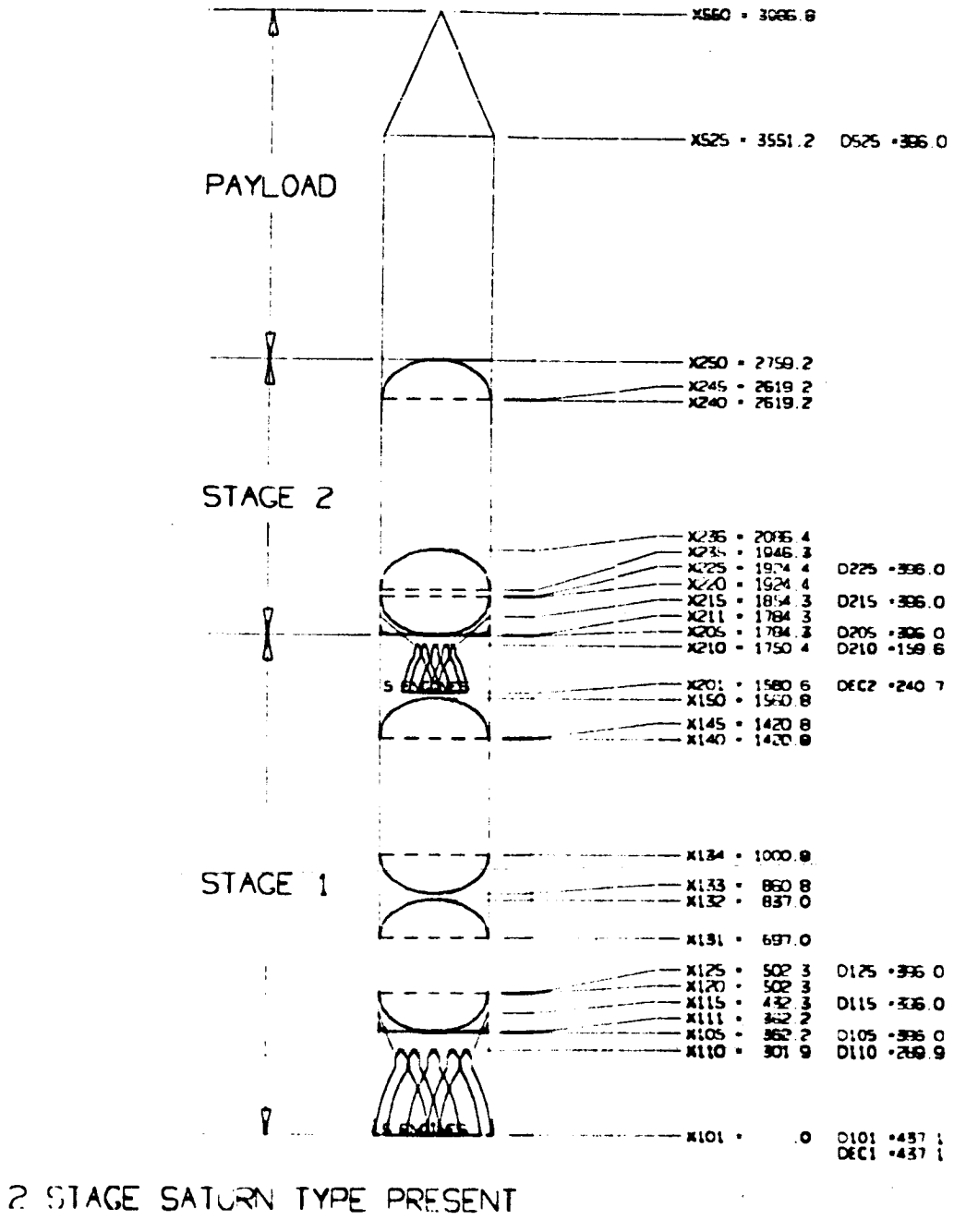



Figure 28. Inboard Profile Saturn Class Vehicle Two-Stage Current Isp 240,000 lb Orbital Payload

Table 14. Computer Weight Statement - Saturn Class Vehicle Two-Stage Current Isp
(240,000 lb Orbital Payload)

WEIGHT STATEMENT

| ITEM | | STAGE 1 WEIGHT (LB) | STAGE 2 WEIGHT (LB) |
|---|---|---|---|
| STRUCTURE | | | |
| INTERSTAGE | | 10688. | 0. |
| FWD SKIRT | | 6638. | 5017. |
| FWD BULKHEAD | | 2474. | 2474. |
| FWD TANKWALL | | 19625. | 24041. |
| INT BULKHEAD | | 7473. | 4453. |
| CENTER SHELL SECTION | | 14384. | 0. |
| INT AFT BULKHEAD | | 2474. | 0. |
| AFT TANKWALL | | 9029. | 874. |
| AFT BULKHEAD | | 7355. | 10887. |
| AFT SKIRT | | 6668. | 5703. |
| THRUST STRUCTURE | | 46952. | 6330. |
| ENGINES | | 94509. | 16587. |
| PROP SYS | | 30863. | 7202. |
| ULLAGE SYS | | 0. | 0. |
| SEP SYS | | 2709. | 84. |
| TVC SYS | | 9458. | 1095. |
| FIXED EQPT | | 5568. | 5046. |
| RES PROP | | 62613. | 11119. |
| CONT | | 0. | 3192. |
| | BURNOUT | 340481. | 104103. |
| PROPELLANT | | 4233452. | 1081997. |
| | GROSS | 4573934. | 1186100. |
| PAYLOAD | | 1426066. | 239966. |
| | VEHICLE | 6000000. | 1426066. |

Table 15. Computer Weight Performance Data Saturn Class Vehicle Two Stage Current Isp (240,000 lb Orbital Payload)

PERFORMANCE DATA

| | |
|---|---|
| STAGE | 1 |
| VEHICLE GROSS | 6000000. |
| STAGE GROSS | 4573934. |
| PROPELLANT | 4233452. |
| PAYLOAD | 1426066. |
| STAGE MASS FRACTION | 0.9256 |
| PERFORMANCE RATIO | 0.7056 |
| WEIGHT PARTIAL | 0.00731002 |
| MASS FRACTION PARTIAL | 0.00000022 |
| STAGE VELOCITY | 11410.00 |
| VEL. INCREMENT | 100.00 |
| ALLOWABLE VEL. | 1400.00 |

| | |
|---|---|
| STAGE | 2 |
| VEHICLE GROSS | 1426066. |
| STAGE GROSS | 1186100. |
| PROPELLANT | 1081997. |
| PAYLOAD | 239966. |
| STAGE MASS FRACTION | 0.9122 |
| PERFORMANCE RATIO | 0.7587 |
| WEIGHT PARTIAL | 0.02486917 |
| MASS FRACTION PARTIAL | 0.00000084 |
| STAGE VELOCITY | 19412.00 |
| VEL. INCREMENT | 100.00 |
| ALLOWABLE VEL. | 1500.00 |

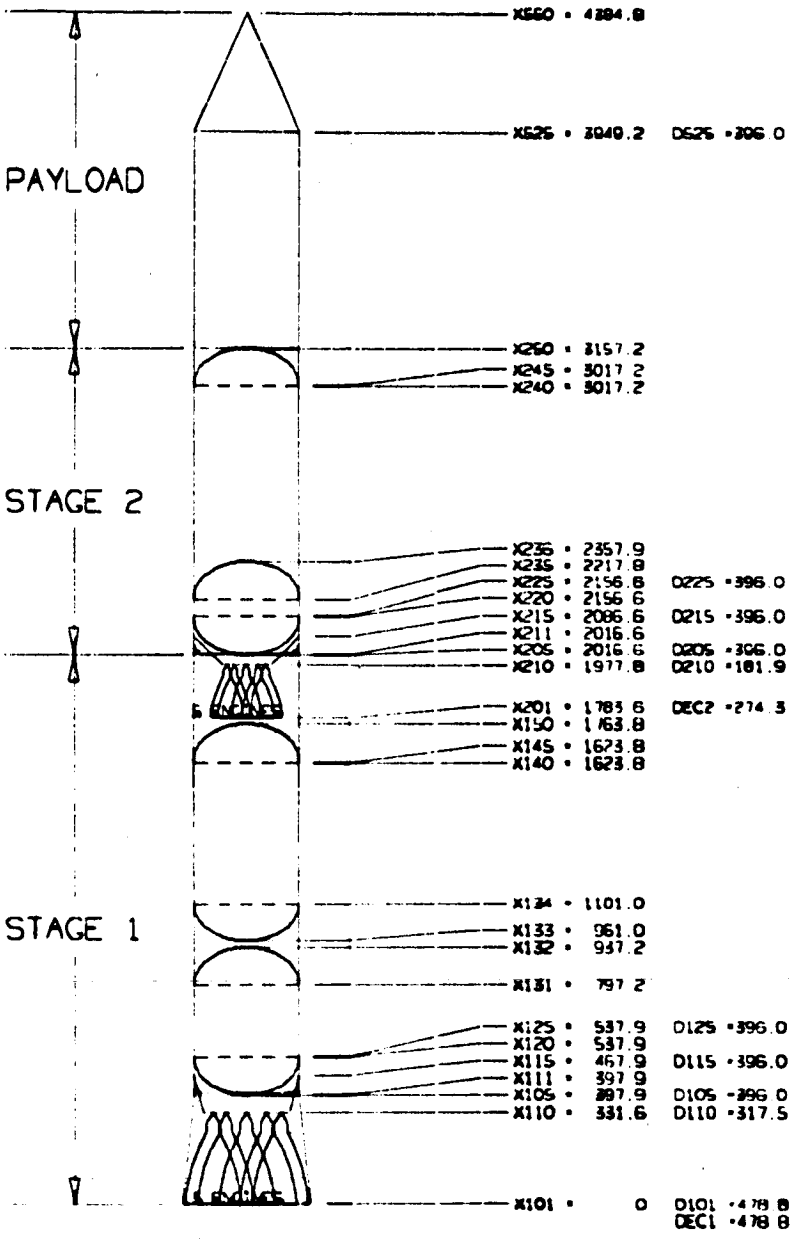



Figure 29. Inboard Profile Saturn Class Vehicle Two-Stage 1985 Isp 445,000 lb Orbital Payload

Table 16. Computer Weight Statement - Saturn Class Vehicle Two-Stage 1985 Isp
(445,000 lb Orbital Payload)

WEIGHT STATEMENT

| ITEM | | STAGE 1 WEIGHT (LB) | STAGE 2 WEIGHT (LB) |
|---|---|---|---|
| STRUCTURE | | | |
| INTERSTAGE | | 12975. | 0. |
| FWD SKIRT | | 7187. | 5197. |
| FWD BULKHEAD | | 2474. | 2474. |
| FWD TANKWALL | | 24983. | 28726. |
| INT BULKHEAD | | 7852. | 4453. |
| CENTER SHELL SECTION | | 15384. | 0. |
| INT AFT BULKHEAD | | 2474. | 0. |
| AFT TANKWALL | | 12283. | 2481. |
| AFT BULKHEAD | | 7690. | 11296. |
| AFT SKIRT | | 7142. | 5973. |
| THRUST STRUCTURE | | 55913. | 7709. |
| ENGINES | | 112546. | 20203. |
| PROP SYS | | 33376. | 7850. |
| ULLAGE SYS | | 0. | 0. |
| SEP SYS | | 3169. | 100. |
| TVC SYS | | 10636. | 1247. |
| FIXED EQPT | | 7486. | 6874. |
| RES PROP | | 73223. | 13208. |
| CONT | | 0. | 3792. |
| | BURNOUT | 396792. | 121583. |
| PROPELLANT | | 4950839. | 1285434. |
| | GROSS | 5347631. | 1407016. |
| PAYLOAD | | 1852369. | 445352. |
| | VEHICLE | 720 0000. | 1852369. |

Table 17. Computer Weight Performance Data Saturn Class Vehicle Two-Stage 1985 Isp (445,000 lb Orbital Payload)

PERFORMANCE DATA

| | |
|---|---|
| STAGE | 1 |
| VEHICLE GROSS | 7200000. |
| STAGE GROSS | 5347631. |
| PROPELLANT | 4950839. |
| PAYLOAD | 1852369. |
| STAGE MASS FRACTION | 0.9258 |
| PERFORMANCE RATIO | 0.6876 |
| WEIGHT PARTIAL | 0.00812944 |
| MASS FRACTION PARTIAL | 0.00000019 |
| STAGE VELOCITY | 12476.00 |
| VEL. INCREMENT | 100.00 |
| ALLOWABLE VEL. | 1500.00 |
| STAGE | 2 |
| VEHICLE GROSS | 1852369. |
| STAGE GROSS | 1407016. |
| PROPELLANT | 1285434. |
| PAYLOAD | 445352. |
| STAGE MASS FRACTION | 0.9136 |
| PERFORMANCE RATIO | 0.6939 |
| WEIGHT PARTIAL | 0.02621951 |
| MASS FRACTION PARTIAL | 0.00000071 |
| STAGE VELOCITY | 19062.00 |
| VEL. INCREMENT | 100.00 |
| ALLOWABLE VEL. | 1500.00 |

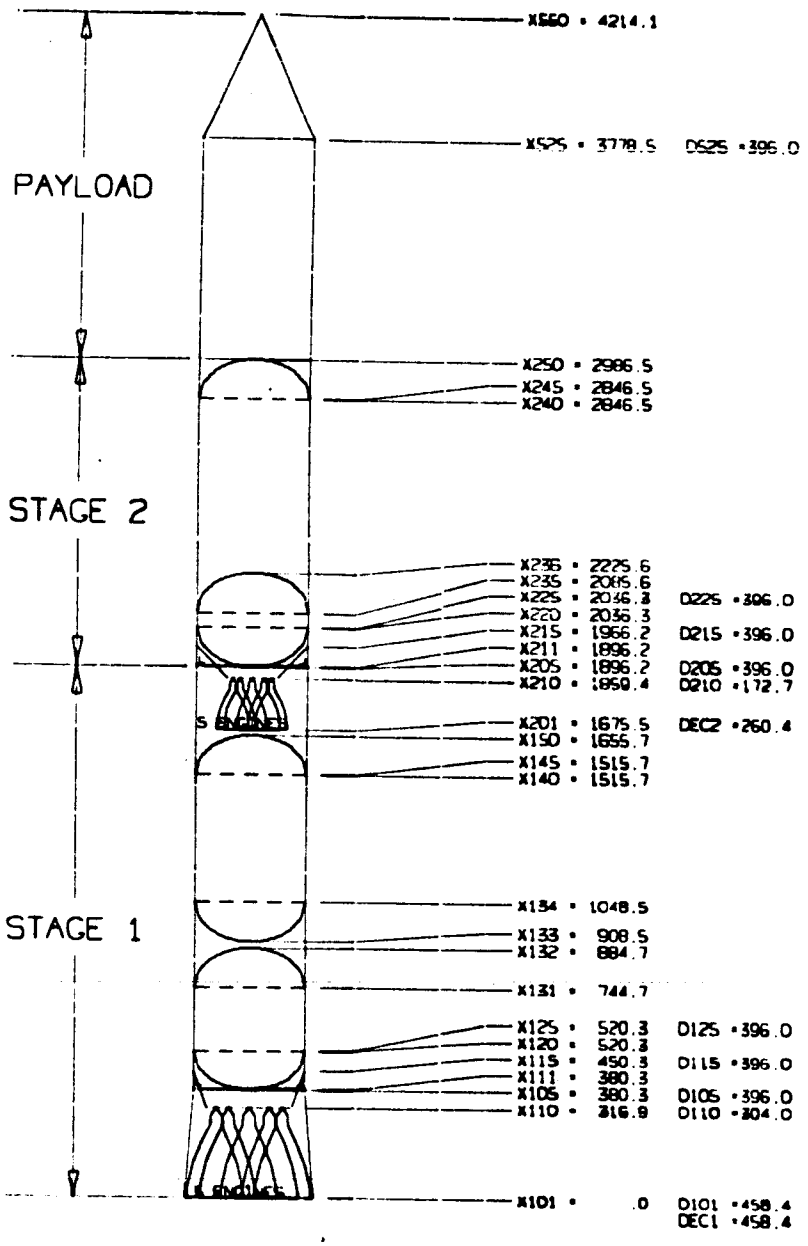



Figure 30. Inboard Profile Saturn Class Vehicle Two-Stage 1975 Isp 330,000 lb Orbital Payload

Table 18. Computer Weight Statement - Saturn Class Vehicle Two-Stage 1975 Isp
(330,000 lb Orbital Payload)

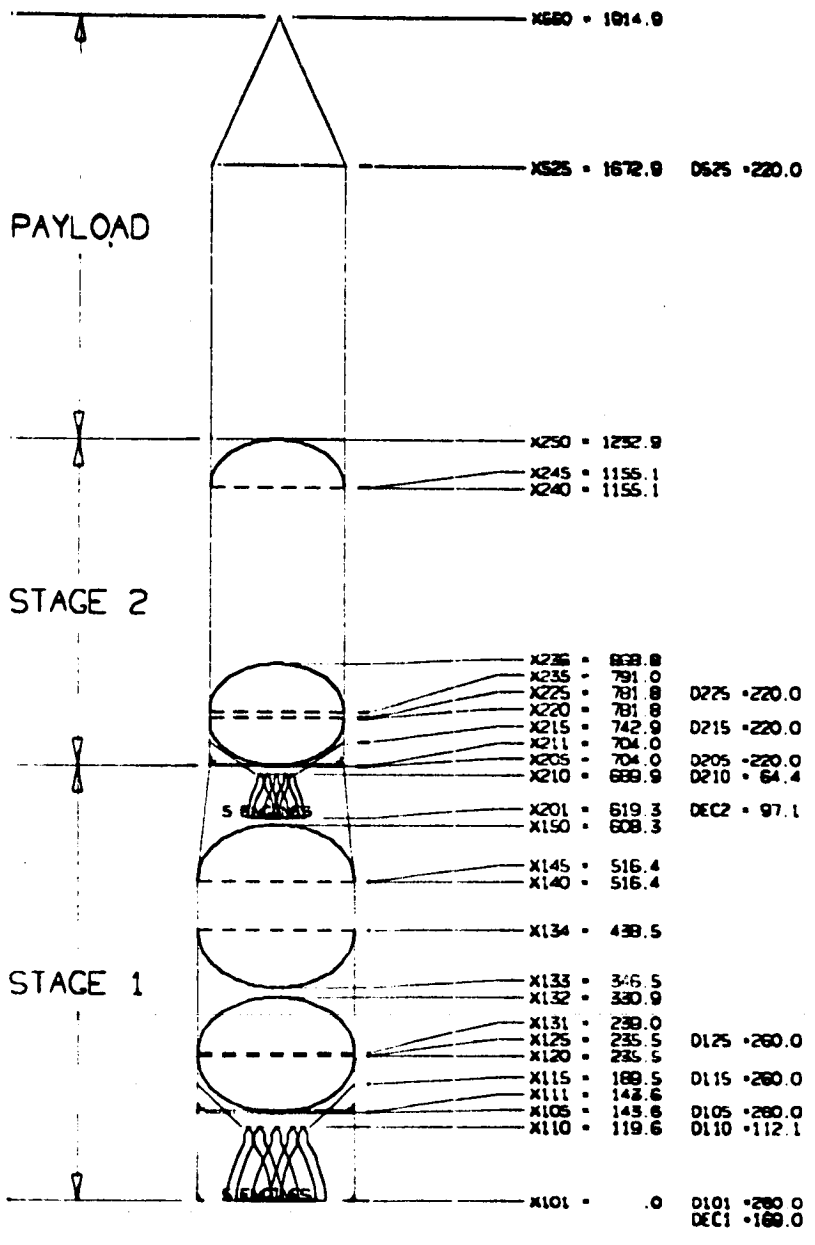
WEIGHT STATEMENT

| ITEM | | STAGE 1 WEIGHT (LB) | STAGE 2 WEIGHT (LB) |
|---|---|---|---|
| STRUCTURE | | | |
| INTERSTAGE | | 11856. | 0. |
| FWD SKIRT | | 6903. | 5100. |
| FWD BULKHEAD | | 2474. | 2474. |
| FWD TANKWALL | | 22061. | 27289. |
| INT BULKHEAD | | 7634. | 4453. |
| CENTER SHELL SECTION | | 14879. | 0. |
| INT AFT BULKHEAD | | 2474. | 0. |
| AFT TANKWALL | | 10502. | 1987. |
| AFT BULKHEAD | | 7497. | 11140. |
| AFT SKIRT | | 6896. | 5845. |
| THRUST STRUCTURE | | 51441. | 7128. |
| ENGINES | | 103545. | 18678. |
| PROP SYS | | 32042. | 7659. |
| ULLAGE SYS | | 0. | 0. |
| SEP SYS | | 2920. | 95. |
| TVC SYS | | 10005. | 1201. |
| FIXED EQPT | | 7106. | 5921. |
| RES PROP | | 67487. | 12573. |
| CONT | | 0. | 3610. |
| | BURNOUT | 367723. | 115153. |
| PROPELLANT | | 4562990. | 1223637. |
| | GROSS | 4930713. | 1338790. |
| PAYLOAD | | 1669287. | 330497. |
| | VEHICLE | 6600000. | 1669287. |

Table 19. Computer Weight Performance Data
Saturn Class Vehicle Two Stage 1975 Isp
(330,000 lb Orbital Payload)

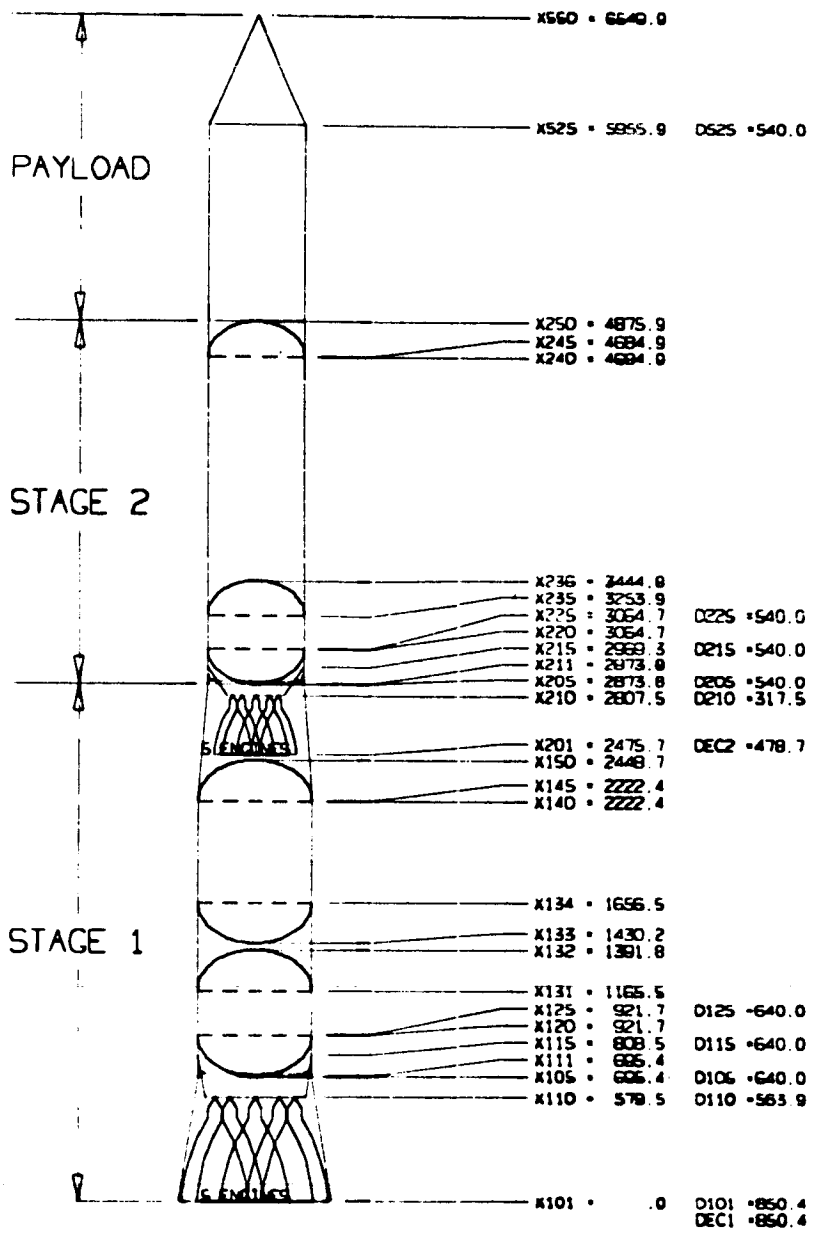
PERFORMANCE DATA

| | |
|---|---|
| STAGE | 1 |
| VEHICLE GROSS | 6600000. |
| STAGE GROSS | 4930713. |
| PROPELLANT | 4562990. |
| PAYLOAD | 1669287. |
| STAGE MASS FRACTION | 0.9254 |
| PERFORMANCE RATIO | 0.6914 |
| WEIGHT PARTIAL | 0.00770736 |
| MASS FRACTION PARTIAL | 0.00000020 |
| STAGE VELOCITY | 11659.00 |
| VEL. INCREMENT | 100.00 |
| ALLOWABLE VEL. | 1400.00 |
| STAGE | 2 |
| VEHICLE GROSS | 1669287. |
| STAGE GROSS | 1338790. |
| PROPELLANT | 1223637. |
| PAYLOAD | 330497. |
| STAGE MASS FRACTION | 0.9140 |
| PERFORMANCE RATIO | 0.7330 |
| WEIGHT PARTIAL | 0.02583931 |
| MASS FRACTION PARTIAL | 0.00000075 |
| STAGE VELOCITY | 19561.00 |
| VEL. INCREMENT | 100.00 |
| ALLOWABLE VEL. | 1400.00 |




30000 LB PAYLOAD 2 STAGES CURRENT ISP

Figure 31. Inboard Profile Medium Range Payload Class Vehicle Two Stage Current Isp (30,000 lb Orbital Payload)




1000000 LB PAYLOAD 2 STAGE CURRENT ISP

Figure 32. Inboard Profile—Post Saturn Class Vehicle Two Stage Current Isp (1,000,000 lb Orbital Payload)

Table 20. Computer Weight Statement—Medium Range Payload Vehicle
Two Stage Current Isp (30,000 lb Orbital Payload)

WEIGHT STATEMENT

| ITEM | | STAGE 1 WEIGHT (LB) | STAGE 2 WEIGHT (LB) |
|---|---|---|---|
| STRUCTURE | | | |
| INTERSTAGE | | 1505. | 0. |
| FWD SKIRT | | 1458. | 752. |
| FWD BULKHEAD | | 700. | 424. |
| FWD TANKWALL | | 1395. | 3882. |
| INT BULKHEAD | | 1595. | 764. |
| CENTER SHELL SECTION | | 3116. | 0. |
| INT AFT BULKHEAD | | 700. | 0. |
| AFT TANKWALL | | 63. | 103. |
| AFT BULKHEAD | | 1598. | 1315. |
| AFT SKIRT | | 1434. | 808. |
| THRUST STRUCTURE | | 7605. | 1610. |
| ENGINES | | 15309. | 4218. |
| PROP SYS | | 11648. | 2943. |
| ULLAGE SYS | | 0. | 0. |
| SEP SYS | | 386. | 14. |
| TVC SYS | | 2193. | 286. |
| FIXED EQPT | | 2649. | 1784. |
| RES PROP | | 8918. | 1857. |
| CONT | | 0. | 533. |
| | BURNOUT | 62273. | 21294. |
| PROPELLANT | | 602999. | 180698. |
| | GROSS | 665272. | 201992. |
| PAYLOAD | | 232010. | 30000. |
| | VEHICLE | 897282. | 231992. |

Table 21. Computer Weight Performance Data—Medium Range Payload Vehicle Two Stage Current Isp (30,000 lb Orbital Payload)

PERFORMANCE DATA

| | |
|---|---|
| STAGE | 1 |
| VEHICLE GROSS | 897282. |
| STAGE GROSS | 665272. |
| PROPELLANT | 602999. |
| PAYLOAD | 232010. |
| STAGE MASS FRACTION | 0.9064 |
| PERFORMANCE RATIO | 0.6720 |
| WEIGHT PARTIAL | 0.00261085 |
| MASS FRACTION PARTIAL | 0.00000150 |
| STAGE VELOCITY | 10402.00 |
| VEL. INCREMENT | 100.00 |
| ALLOWABLE VEL. | 1900.00 |
| STAGE | 2 |
| VEHICLE GROSS | 231992. |
| STAGE GROSS | 201992. |
| PROPELLANT | 180698. |
| PAYLOAD | 30000. |
| STAGE MASS FRACTION | 0.8946 |
| PERFORMANCE RATIO | 0.7788 |
| WEIGHT PARTIAL | 0.02382022 |
| MASS FRACTION PARTIAL | 0.00000495 |
| STAGE VELOCITY | 20600.00 |
| VEL. INCREMENT | 100.00 |
| ALLOWABLE VEL. | 1300.00 |

Table 22. Computer Weight Statement—Post Saturn Class Vehicle
Two Stage Current Isp (1,000,000 lb Orbital Payload)

WEIGHT STATEMENT

| ITEM | | STAGE 1 WEIGHT (LB) | STAGE 2 WEIGHT (LB) |
|---|---|---|---|
| STRUCTURE | | | |
| INTERSTAGE | | 67608. | 0. |
| FWD SKIRT | | 33230. | 15286. |
| FWD BULKHEAD | | 10444. | 6274. |
| FWD TANKWALL | | 74156. | 102531. |
| INT BULKHEAD | | 36978. | 11292. |
| CENTER SHELL SECTION | | 71023. | 0. |
| INT AFT BULKHEAD | | 10444. | 0. |
| AFT TANKWALL | | 31714. | 16703. |
| AFT BULKHEAD | | 36396. | 40930. |
| AFT SKIRT | | 33555. | 19979. |
| THRUST STRUCTURE | | 168054. | 17852. |
| ENGINES | | 338272. | 46782. |
| PROP SYS | | 59652. | 14323. |
| ULLAGE SYS | | 0. | 0. |
| SEP SYS | | 10122. | 332. |
| TVC SYS | | 25415. | 3072. |
| FIXED EQPT | | 13063. | 10300. |
| RES PROP | | 233903. | 43966. |
| CONT | | 0. | 12623. |
| | BURNOUT | 1254028. | 362246. |
| PROPELLANT | | 15814960. | 4278968. |
| | GROSS | 17068988. | 4641214. |
| PAYLOAD | | 5641232. | 1000000. |
| | VEHICLE | 22710220. | 5641214. |



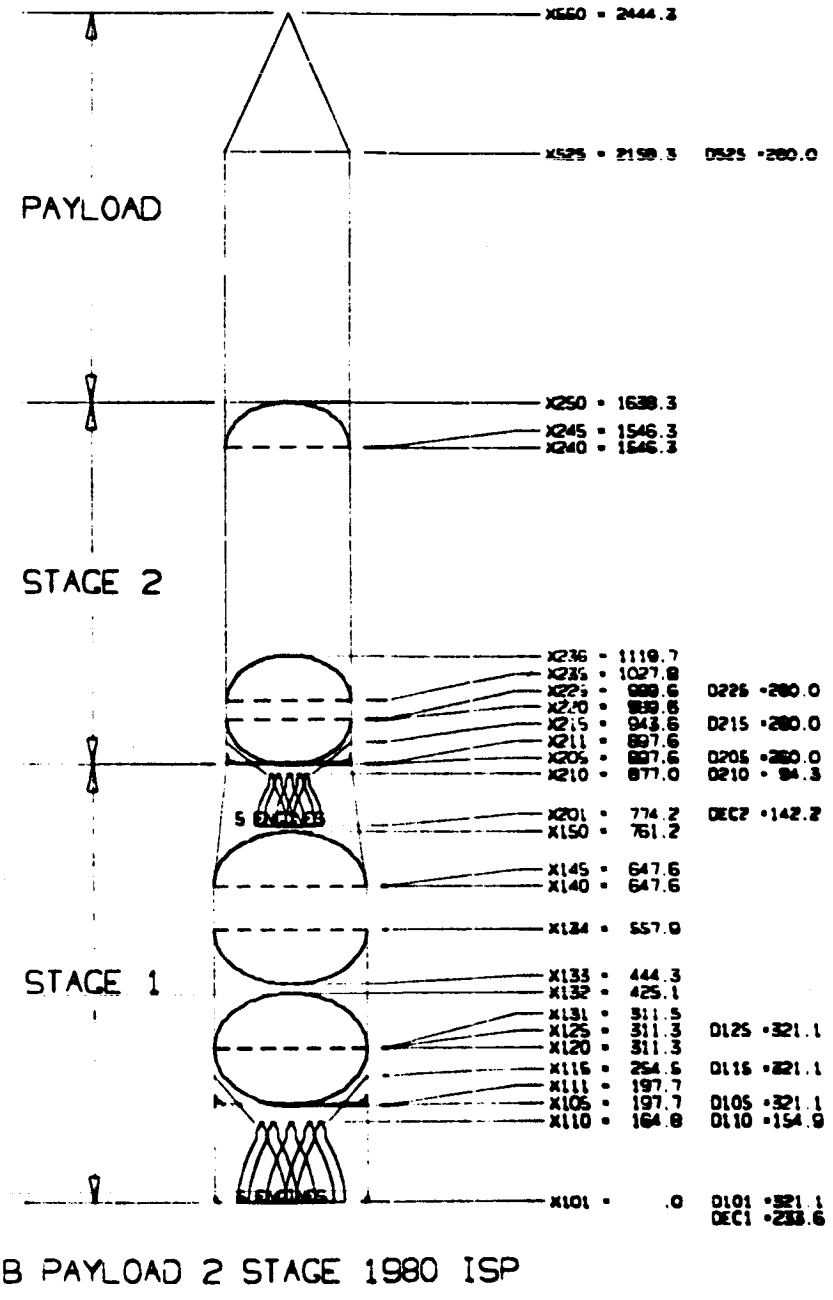


NORTH AMERICAN AVIATION, INC.
SPACE and INFORMATION SYSTEMS DIVISION

Table 23. Computer Weight Performance Data—
Post Saturn Class Vehicle Two Stage
Current Isp (1,000,000 lb Orbital Payload)

PERFORMANCE DATA

| | |
|---|---|
| STAGE | 1 |
| VEHICLE GROSS | 22710220. |
| STAGE GROSS | 17068988. |
| PROPELLANT | 15814960. |
| PAYLOAD | 5641232. |
| STAGE MASS FRACTION | 0.9265 |
| PERFORMANCE RATIO | 0.6964 |
| WEIGHT PARTIAL | 0.00722981 |
| MASS FRACTION PARTIAL | 0.00000006 |
| STAGE VELOCITY | 11123.00 |
| VEL. INCREMENT | 100.00 |
| ALLOWABLE VEL. | 1600.00 |
| STAGE | 2 |
| VEHICLE GROSS | 5641214. |
| STAGE GROSS | 4641214. |
| PROPELLANT | 4278968. |
| PAYLOAD | 1000000. |
| STAGE MASS FRACTION | 0.9220 |
| PERFORMANCE RATIO | 0.7585 |
| WEIGHT PARTIAL | 0.03009427 |
| MASS FRACTION PARTIAL | 0.00000022 |
| STAGE VELOCITY | 19400.00 |
| VEL. INCREMENT | 100.00 |
| ALLOWABLE VEL. | 1100.00 |



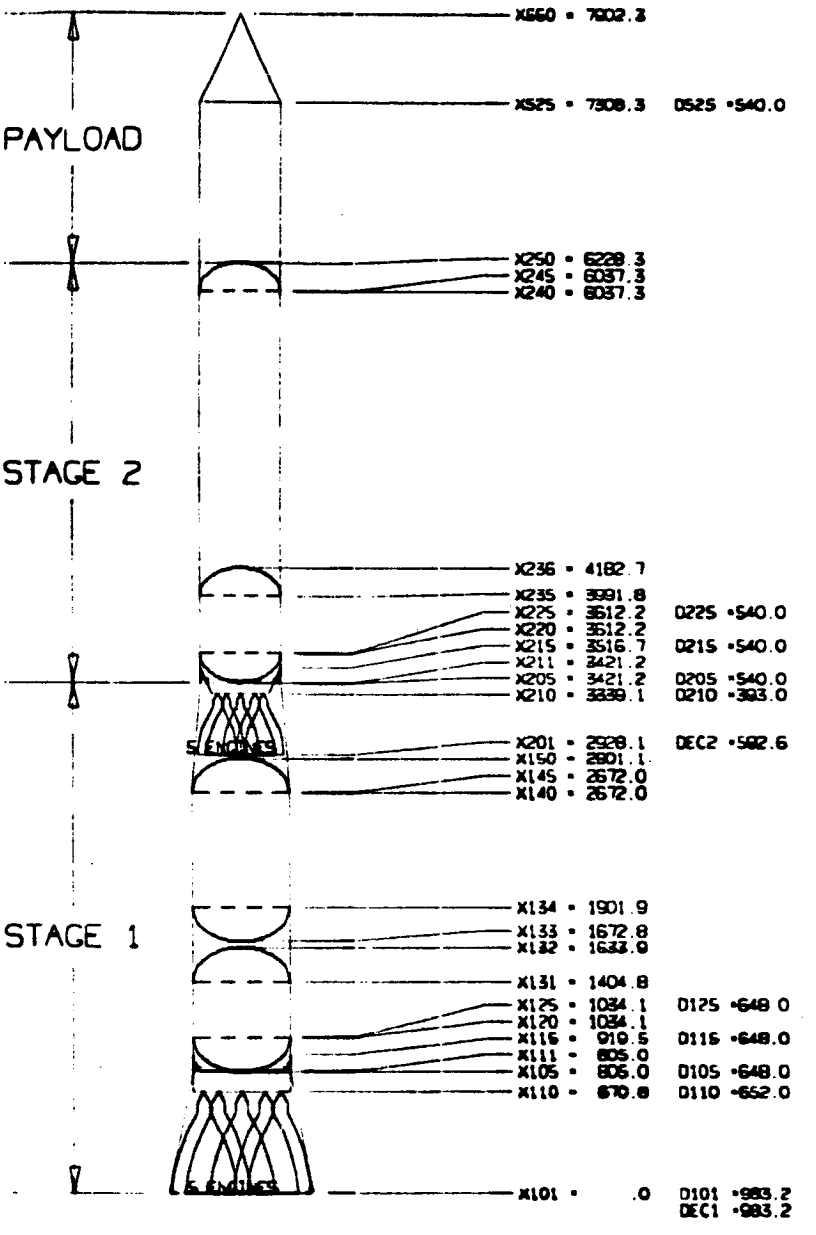

:00000 LB PAYLOAD 2 STAGE 1980 ISP

Figure 33. Inboard Profile Medium Payload Range Vehicle
Two Stage 1985 Isp (100,000 lb Orbital Payload)

Table 24. Computer Weight Statement—Medium Range Payload Vehicle
Two Stage 1985 Isp (100,000 lb Orbital Payload)

WEIGHT STATEMENT

| ITEM | | STAGE 1 WEIGHT (LB) | STAGE 2 WEIGHT (LB) |
|---|---|---|---|
| STRUCTURE | | | |
| INTERSTAGE | | 3431. | 0. |
| FWD SKIRT | | 2840. | 1302. |
| FWD BULKHEAD | | 1319. | 700. |
| FWD TANKWALL | | 2476. | 7793. |
| INT BULKHEAD | | 3109. | 1260. |
| CENTER SHELL SECTION | | 6079. | 0. |
| INT AFT BULKHEAD | | 1319. | 0. |
| AFT TANKWALL | | 6. | 618. |
| AFT BULKHEAD | | 3119. | 2387. |
| AFT SKIRT | | 2810. | 1427. |
| THRUST STRUCTURE | | 14133. | 2863. |
| ENGINES | | 28448. | 7503. |
| PROP SYS | | 15776. | 4151. |
| ULLAGE SYS | | 0. | 0. |
| SEP SYS | | 708. | 28. |
| TVC SYS | | 3457. | 479. |
| FIXED EQPT | | 3881. | 3257. |
| RES PROP | | 16361. | 3693. |
| CONT | | 0. | 1060. |
| | BURNOUT | 109273. | 38522. |
| PROPELLANT | | 1106198. | 359441. |
| | GROSS | 1215471. | 397963. |
| PAYLOAD | | 497961. | 100000. |
| | VEHICLE | 1713432. | 497963. |




2000000 LB PAYLOAD 2 STAGE 1980 ISP

Figure 34. Inboard Profile—Post Saturn Payload Class Vehicle Two-Stage 1985 Isp (2,000,000 lb Orbital Payload)

Table 25. Computer Weight Performance Data—Medium Range Payload Vehicle Two Stage 1985 Isp (100,000 lb Orbital Payload)

PERFORMANCE DATA

| | |
|---|---|
| STAGE | 1 |
| VEHICLE GROSS | 1713432. |
| STAGE GROSS | 1215471. |
| PROPELLANT | 1106198. |
| PAYLOAD | 497961. |
| STAGE MASS FRACTION | 0.9101 |
| PERFORMANCE RATIO | 0.6456 |
| WEIGHT PARTIAL | 0.00242393 |
| MASS FRACTION PARTIAL | 0.00000082 |
| STAGE VELOCITY | 11123.00 |
| VEL. INCREMENT | 100.00 |
| ALLOWABLE VEL. | 2200.00 |
| STAGE | 2 |
| VEHICLE GROSS | 497963. |
| STAGE GROSS | 397963. |
| PROPELLANT | 359441. |
| PAYLOAD | 100000. |
| STAGE MASS FRACTION | 0.9032 |
| PERFORMANCE RATIO | 0.7218 |
| WEIGHT PARTIAL | 0.02527332 |
| MASS FRACTION PARTIAL | 0.00000251 |
| STAGE VELOCITY | 20600.00 |
| VEL. INCREMENT | 100.00 |
| ALLOWABLE VEL. | 1300.00 |

Table 26. Computer Weight Statement—Post Saturn Vehicle
Two Stage 1985 Isp (2,000,000 lb Orbital Payload)

WEIGHT STATEMENT

| ITEM | | STAGE 1 WEIGHT (LB) | STAGE 2 WEIGHT (LB) |
|---|---|---|---|
| STRUCTURE | | | |
| INTERSTAGE | | 100241. | 0. |
| FWD SKIRT | | 40906. | 16604. |
| FWD BULKHEAD | | 10841. | 6274. |
| FWD TANKWALL | | 107677. | 176547. |
| INT BULKHEAD | | 41586. | 11292. |
| CENTER SHELL SECTION | | 83816. | 0. |
| INT AFT BULKHEAD | | 10841. | 0. |
| AFT TANKWALL | | 51158. | 39380. |
| AFT BULKHEAD | | 40607. | 46729. |
| AFT SKIRT | | 39350. | 23750. |
| THRUST STRUCTURE | | 221946. | 24627. |
| ENGINES | | 446751. | 64536. |
| PROP SYS | | 67246. | 17124. |
| ULLAGE SYS | | 0. | 0. |
| SEP SYS | | 12863. | 475. |
| TVC SYS | | 30419. | 4016. |
| FIXED EQPT | | 16170. | 14566. |
| RES PROP | | 297252. | 62846. |
| CONT | | 0. | 18043. |
| | BURNOUT | 1619671. | 526809. |
| PROPELLANT | | 20098176. | 6116427. |
| | GROSS | 21717847. | 6643236. |
| PAYLOAD | | 8643258. | 2000000. |
| | VEHICLE | 30361105. | 8643236. |





NORTH AMERICAN AVIATION, INC.
SPACE and INFORMATION SYSTEMS DIVISION

Table 27. Computer Weight Performance Data—Post Saturn Class Vehicle Two Stage 1985 Isp (2,000,000 lb Orbital Payload)

PERFORMANCE DATA

| | |
|---|---|
| STAGE | 1 |
| VEHICLE GROSS | 30361105. |
| STAGE GROSS | 21717847. |
| PROPELLANT | 20098176. |
| PAYLOAD | 8643258. |
| STAGE MASS FRACTION | 0.9254 |
| PERFORMANCE RATIO | 0.6620 |
| | |
| WEIGHT PARTIAL | 0.00853521 |
| MASS FRACTION PARTIAL | 0.00000005 |
| STAGE VELOCITY | 11630.00 |
| VEL. INCREMENT | 100.00 |
| ALLOWABLE VEL. | 1700.00 |
| | |
| STAGE | 2 |
| VEHICLE GROSS | 8643236. |
| STAGE GROSS | 6643236. |
| PROPELLANT | 6116427. |
| PAYLOAD | 2000000. |
| STAGE MASS FRACTION | 0.9207 |
| PERFORMANCE RATIO | 0.7077 |
| | |
| WEIGHT PARTIAL | 0.03812706 |
| MASS FRACTION PARTIAL | 0.00000015 |
| STAGE VELOCITY | 19800.00 |
| VEL. INCREMENT | 100.00 |
| ALLOWABLE VEL. | 1100.00 |

## PAYLOAD EXCHANGE RATIOS

Figure 35 summarizes the logic used to evolve generalized payload exchange ratios for the test case vehicles. The analytical approach is discussed in detail in Appendix A. The subroutine will accept inputs for unit changes in weight, thrust, and specific impulse or for specific changes in the same parameters. Since the weight and cost assessment ratio subroutine operates on unit changes, the computer printouts of payload exchange ratios in Tables 28 through 30 are for unit changes in the basic parameters. Table 28 covers exchange ratios for the Saturn payload class vehicles, Table 29 presents the medium range payload class vehicle ratios, and Table 30 presents printouts for the post-Saturn payload class vehicles. These tables illustrate the change in payload weight achieved for a one-unit position change in the particular parameter, with WO representing stage gross weight, WP(F) representing propellant weight for a fixed propellant tank where the tankage is off-loaded or on-loaded without changing tankage weight, and WP(NF) representing propellant weight for a tank that is resized to accommodate the on-loaded propellant. It can be readily seen from these tables that a significant advantage exists in changing specific impulse or thrust.

Although significant improvements are obtained with changes in specific impulse, these changes can be extremely expensive and might interact with other subsystem parameters. For example, specific impulse might be improved by changing engine expansion ratio; this would probably result in increases in engine weight, engine length, and associated changes in structural weight due to increased interstage-skirt lengths. Therefore, payload improvements due to specific impulse are subsequently reduced by interactions with propulsion-structural systems. With a change in stage gross weight (WO) both the propellant quantity and tankage are altered proportionately. This results in payload gain with increased propellant but payload loss with the associated tankage weight gain.

The intent of this study is to measure structural changes in terms of effectiveness and cost. Attempts to assess costs of propulsion propellant advancements are beyond the scope of this study; however, the evaluation tool developed for this study could be used, with modifications, to measure areas of propulsion and propellant improvements in similar base point vehicles. The payload exchange ratios were used as direct inputs to the weight and cost assessment subroutine discussed later in the Assessment section of this report.

## LOADING ENVIRONMENTS

The preliminary design synthesis step involves substituting materials and construction types in the base point vehicles and assessing their weight and cost influence. The loading environment for each shell component was

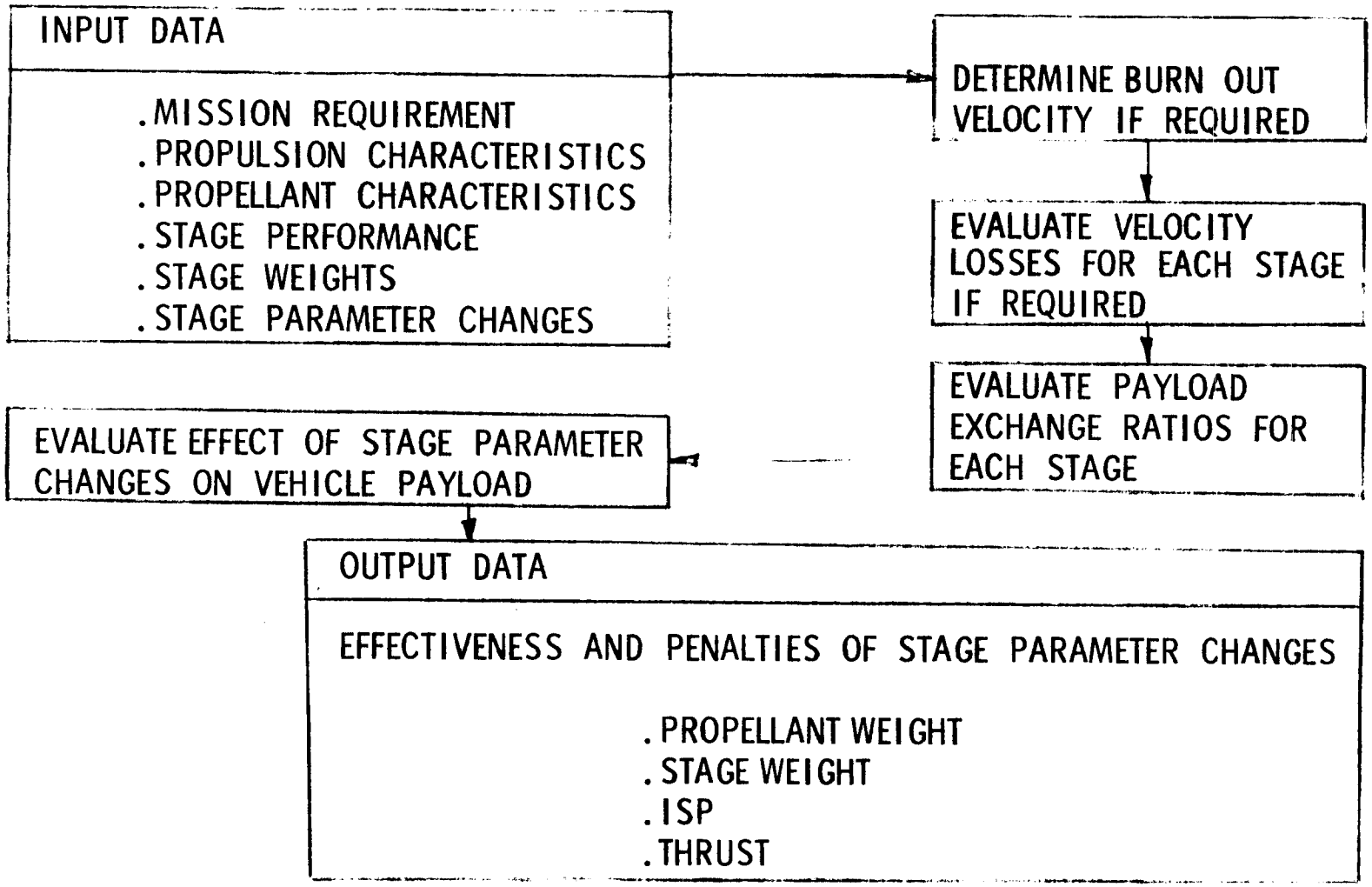



Figure 35. Generalized Payload Exchange Ratios

Table 28. Generalized Payload Exchange Ratios
Medium Range Payload Vehicles

2 Stage Current Isp (Payload 30, 000 lb)

| PARAMETER | VALUE | PAYLOAD EXCHANGE RATIO |
|---|---|---|
| PROPULSION | | |
| STAGE 1 | | |
| THRUST | 1197242.50 | 0.02 |
| ISP | 302.00 | 97.87 |
| STAGE 2 | | |
| THRUST | 180396.00 | 0.03 |
| ISP | 424.00 | 216.11 |
| WEIGHTS | | |
| STAGE 1 | | |
| WO | 957794.00 | 0.01 |
| WST | 78101.00 | -0.09 |
| WP(F) | 629143.00 | 0.02 |
| WP(NF) | 629143.00 | 0.01 |
| STAGE 2 | | |
| WO | 250550.00 | 0.01 |
| WST | 24801.00 | -1.00 |
| WP(F) | 195749.00 | 0.14 |
| WP(NF) | 195749.00 | 0.01 |

2 Stage 1985 + Isp (Payload 100, 000 lb)

| | | |
|---|---|---|
| PROPULSION | | |
| STAGE 1 | | |
| THRUST | 2120193.75 | 0.02 |
| ISP | 350.00 | 206.27 |
| STAGE 2 | | |
| THRUST | 369201.60 | 0.05 |
| ISP | 500.00 | 409.12 |
| WEIGHTS | | |
| STAGE 1 | | |
| WO | 1696155.00 | 0.01 |
| WST | 119398.00 | -0.12 |
| WP(F) | 1063977.00 | 0.03 |
| WP(NF) | 1063977.00 | 0.01 |
| STAGE 2 | | |
| WO | 512780.00 | 0.05 |
| WST | 41291.00 | -1.00 |
| WP(F) | 371489.00 | 0.17 |
| WP(NF) | 371489.00 | 0.06 |

Table 29. Generalized Payload Exchange Ratio
Saturn Class Vehicle

2 Stage Current Isp (Payload 240,000 lb)

| PARAMETER | VALUE | PAYLOAD EXCHANGE RATIO |
|---|---|---|
| PROPULSION | | |
| STAGE 1 | | |
| THRUST | 7500000.00 | 0.02 |
| ISP | 302.00 | 717.67 |
| STAGE 2 | | |
| THRUST | 1087199.98 | 0.02 |
| ISP | 424.00 | 1359.56 |
| WEIGHTS | | |
| STAGE 1 | | |
| WO | 6000000.00 | 0.01 |
| WST | 335300.00 | -0.11 |
| WP(F) | 4154000.00 | 0.02 |
| STAGE 2 | | |
| WO | 1510000.00 | 0.05 |
| WST | 98900.00 | -1.00 |
| WP(F) | 1149200.00 | 0.14 |

2 Stage 1985 + Isp (Payload 445,000 lb)

| | | |
|---|---|---|
| PROPULSION | | |
| STAGE 1 | | |
| THRUST | 9000000.00 | 0.02 |
| ISP | 350.00 | 1022.28 |
| STAGE 2 | | |
| THRUST | 1427039.98 | 0.03 |
| ISP | 500.00 | 1660.73 |
| WEIGHTS | | |
| STAGE 1 | | |
| WO | 7200000.00 | 0.01 |
| WST | 386116.00 | -0.15 |
| WP(F) | 4832000.00 | 0.03 |
| STAGE 2 | | |
| WO | 1982000.00 | 0.09 |
| WST | 114063.00 | -1.00 |
| WP(F) | 1380495.00 | 0.19 |

Table 30. Generalized Payload Exchange Ratios
Post Saturn Class Vehicle

2 Stage Current Isp (Payload 1 x $10^6$ lb)

| PARAMETER | VALUE | PAYLOAD EXCHANGE RATIO |
|---|---|---|
| PROPULSION | | |
| STAGE 1 | | |
| THRUST | 29492638.75 | 0.02 |
| ISP | 302.00 | 3038.74 |
| STAGE 2 | | |
| THRUST | 4405044.19 | 0.03 |
| ISP | 424.00 | 5500.14 |
| WEIGHTS | | |
| STAGE 1 | | |
| WO | 23594111.00 | 0.01 |
| WST | 1398661.00 | -0.11 |
| WP(F) | 16077333.00 | 0.02 |
| WP(NF) | 16077333.00 | 0.01 |
| STAGE 2 | | |
| WO | 6118117.00 | 0.04 |
| WST | 461627.00 | -1.00 |
| WP(F) | 4656491.00 | 0.14 |
| WP(NF) | 4656491.00 | 0.05 |

2 Stage 1985 + Isp (Payload 2 x $10^6$ lb)

| | | |
|---|---|---|
| PROPULSION | | |
| STAGE 1 | | |
| THRUST | 37949445.00 | 0.02 |
| ISP | 350.00 | 4212.97 |
| STAGE 2 | | |
| THRUST | 6564576.94 | 0.04 |
| ISP | 500.00 | 7436.39 |
| WEIGHTS | | |
| STAGE 1 | | |
| WO | 30359556.00 | 0.02 |
| WST | 1700080.00 | -0.13 |
| WP(F) | 19542009.00 | 0.03 |
| WP(NF) | 19542009.00 | 0.02 |
| STAGE 2 | | |
| WO | 9117468.00 | 0.07 |
| WST | 640795.00 | -1.00 |
| WP(F) | 6476673.00 | 0.18 |
| WP(NF) | 6476673.00 | 0.08 |

identified in terms of applied load and temperature. For the design synthesis and parametric synthesis vehicle sizing, loading safety factors of 1.10 for limit loads and 1.4 for ultimate loads were used. The initial parametric synthesis empirical loads assessment included these factors and investigated the maximum dynamic pressure ($q\alpha$) and maximum vehicle acceleration loading conditions.

The base point vehicles and the four alternatives were input to S&ID's preliminary design synthesis program to check their loads for prelaunch, liftoff, and maximum skin temperature conditions, as well as those conditions mentioned above. These data are shown in more detail in Appendix B. Figure 36 is a diagram of the maximum $q\alpha$ bending moments, axial loads, and shears for the Saturn class vehicle sized to current Isp and thrust. Figure 37 summarizes the actual ultimate design applied load for this vehicle and also for the vehicle sized to the 1985 Isp. Figure 38 presents similar applied loads for the medium range payload vehicle alternative cases and Figure 39 illustrates design applied loads for the post-Saturn payload vehicles. Figures 37 through 39 represent a summary of all pertinent design conditions, and Table 31 summarizes the parametric design applied loads for each component.

In the post-Saturn vehicle, the design load for the stage diameters considered are extremely large in magnitude. However, the diameters of these stages are somewhat large. It is obvious that program techniques such as those used in this study could be a useful preliminary design tool in investigation of fineness ratios and diameters for such future vehicle systems to determine effects of loading intensities and structural systems.

To simplify the initial checkout cases, a decision was made to establish a somewhat arbitrary design temperature regime based upon the Saturn V vehicle. In place of running a series of complicated temperature matrixes through the program, the structural data was run for unpressurized structures using room temperature properties and 300 F properties, this being the maximum skin temperature condition for most of the vehicles studied.

During the course of the parametric synthesis, tank pressures were calculated for all stage tanks which were based upon a minimum tank pressure of 7.5 psi and a required inflight ullage pressure of 30 psi. The mass fraction subroutine assesses hydraulic head-acceleration effects upon design pressures. In most of the vehicles the maximum design pressure range was from 45 to 60 psi;, therefore, again to reduce the test cases, it was decided to generalize the tankage design synthesis data to reflect a maximum burst pressure of 50 psi and a minimum relieving pressure of 7.5 with a generalized cryogenic temperature of -300 F. When considering a unique vehicle in the program, such generalized assumptions cannot be made; however, when comparing one vehicle to another, as is the case in the tradeoffs contained in this report, these generalized criteria do not greatly affect the

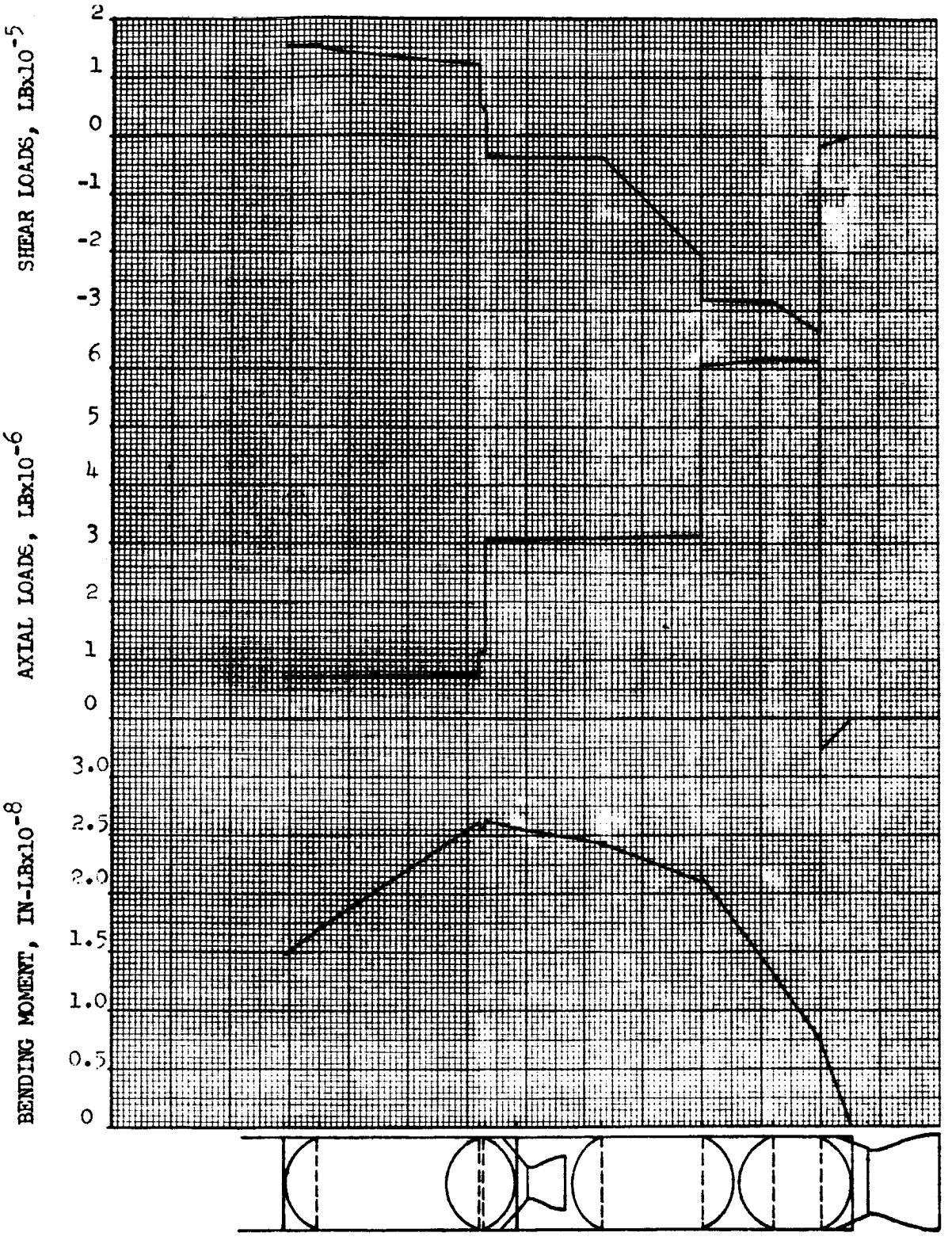



Figure 36. Limit Loads—Max qα Condition
Current Saturn Class Vehicle (240,000 lb Payload)

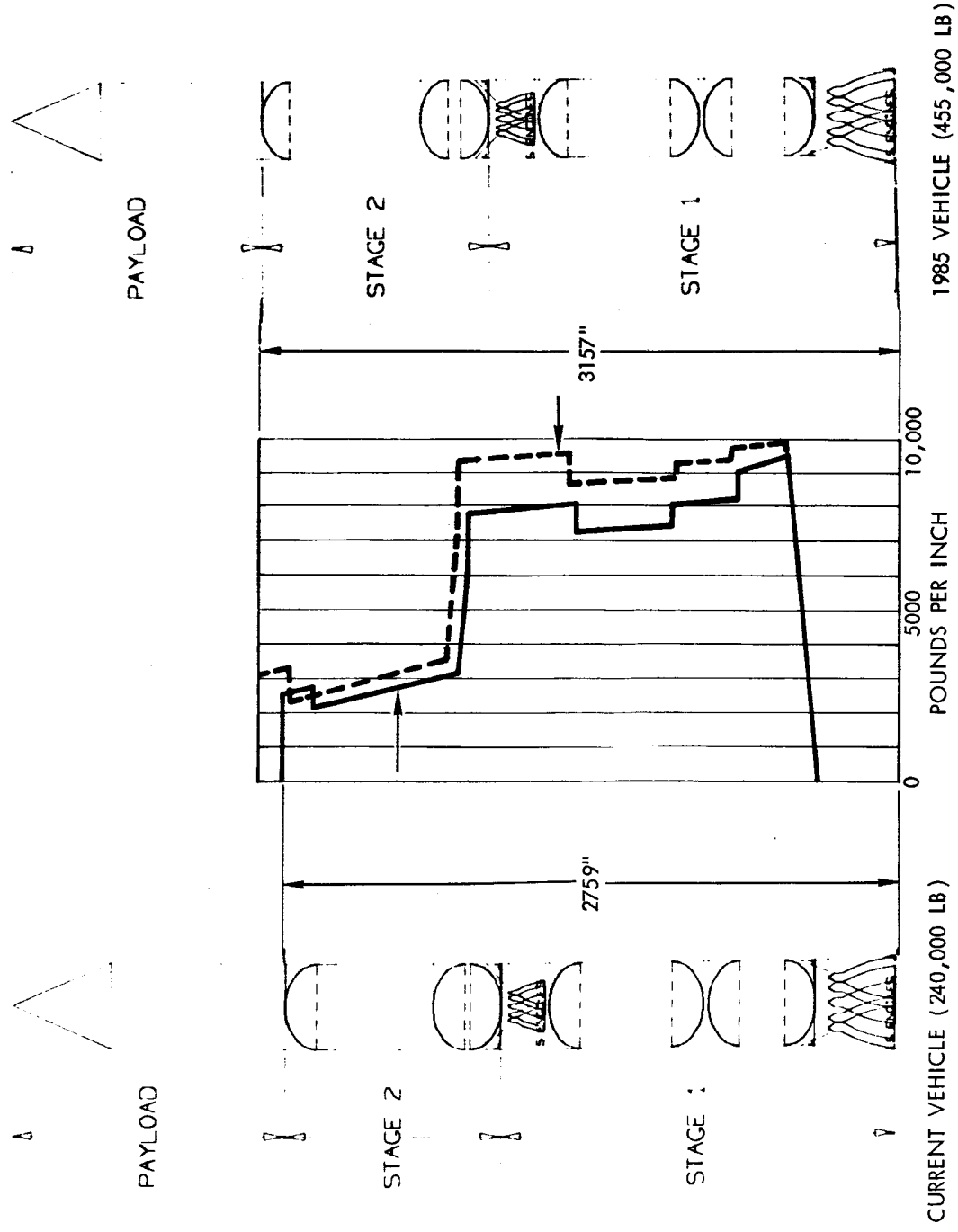



Figure 37. Ultimate Applied Loads - Saturn Payload Class Vehicles

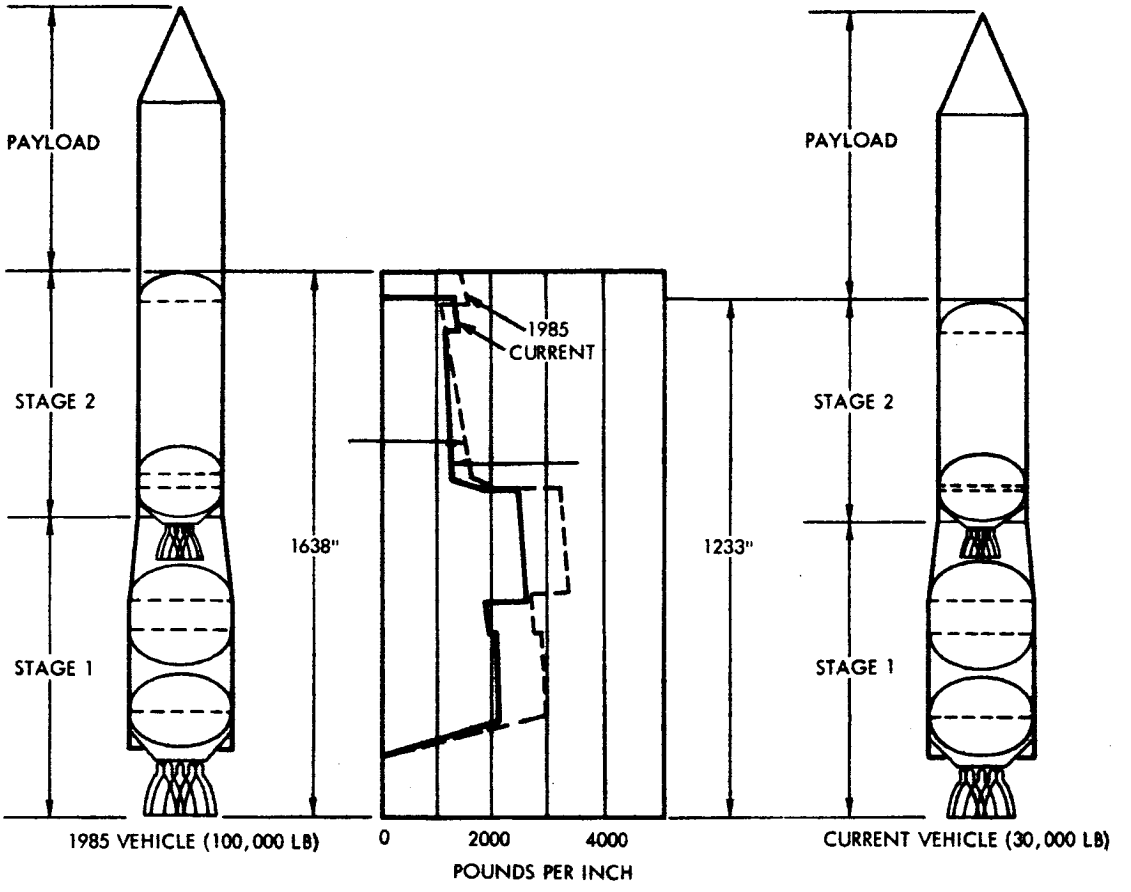



Figure 38. Ultimate Applied Loads Medium Payload Range Vehicle

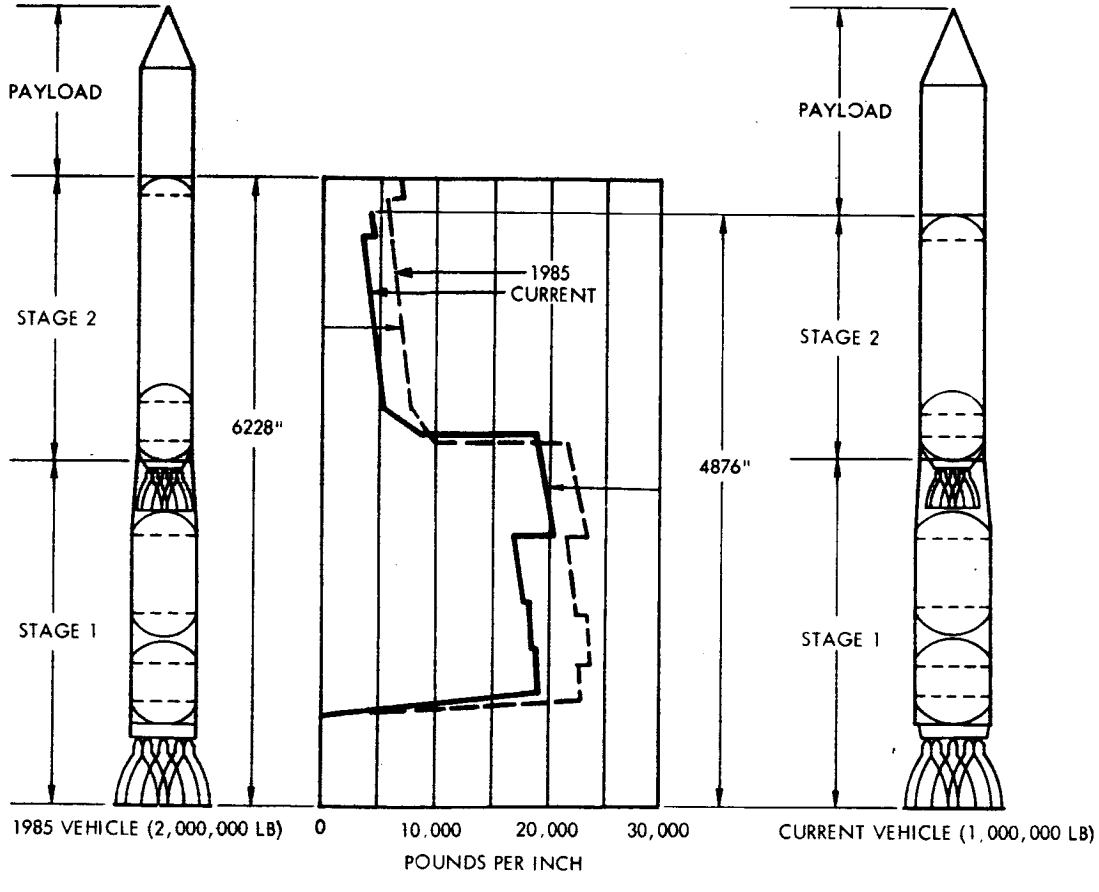



Figure 39. Ultimate Applied Loads Post Saturn Class Vehicles

Table 31. Structural Components and Their Design Applied
(Nx in pounds per inch)

| Vehicle Payload Class | Medium Range | | Saturn | | Post-Saturn | |
|---|---|---|---|---|---|---|
| Sizing Parameters (Isp, thrust) | Current | 1985 | Current | 1985 | Current | 1985 |
| DESIGN LOAD (Nx - pounds per inch) | | | | | | |
| Stage 1 | | | | | | |
| Interstage | 2,885 | 3,273 | 7,965 | 8,685 | 20,120 | 23,100 |
| Forward Skirt | 2,905 | 3,340 | 8,005 | 8,730 | 20,210 | 26,000 |
| Forward Tank Wall | 1,950 | 2,700 | 7,400 | 8,100 | 17,180 | 22,160 |
| Center Section | 2,100 | 2,950 | 8,365 | 9,115 | 17,500 | 23,500 |
| Aft Tank Wall | ——— | ——— | 9,700 | 9,745 | 18,500 | 22,500 |
| Aft Skirt | 1,800 | 2,285 | 6,965 | 7,535 | 9,300 | 17,500 |
| Stage 2 | | | | | | |
| Forward Skirt | 1,245 | 1,530 | 2,750 | 2,895 | 4,355 | 6,510 |
| Forward Tank Wall | 1,295 | 1,650 | 3,070 | 3,255 | 5,535 | 7,240 |
| Aft Tank Wall | 1,650 | 1,950 | 6,300 | 6,780 | 8,640 | 9,635 |
| Aft Skirt | 2,180 | 3,170 | 6,765 | 8,650 | 18,150 | 22,800 |

relative comparison and are worthwhile in reducing computer and evaluation time. Again, the basic objective, as previously stated, was to synthesize typical base point vehicles for the materials and structure tradeoff studies rather than design specific vehicles.

The curves in Figures 37, 38 and 39 summarize all critical ultimate design loading intensities and represent the maximum design envelope from the various flight conditions studied. The decreased loading intensities illustrated for tankage areas result from consideration of pressure relief.

## STRUCTURAL DESIGN SYNTHESIS

The portion of the program that describes structural components has been separated from the parametric synthesis section. This approach was adopted so that the structural components could be analyzed individually without associating any of the structural components with a particular launch vehicle system for this phase of the study. This approach allows independent exercise of the design synthesis for any given structural component to assess the effects on the structural component of the various advances in different types of material by material substitution, construction substitution, manufacturing limitation restrictions, and analysis method. The structural components considered by the program are essentially defined by a range of various diameters and lengths which, together with the associated load and the thermal environment complete the description. This permits the structure to be subjected to a design analysis to ascertain the unit weight of the various components for a range of typical loading and size parameters.

Unit shell weights are finally translated and associated with various components for specific vehicles in the final assessment portion of the program. Each of these structural components is subjected to various design loading conditions resulting from various portions of the vehicle trajectory flight path. The design analysis considers the tensile and compressive loading intensity with its associated thermal environment for these different portions of the flight trajectory. For example, the unpressurized shell experiences temperatures varying from room temperature during prelaunch conditions up to a maximum thermal environment of approximately 300 to 400 degrees F. Various components of the vehicle stages are subjected to the maximum compressive or tensile loading intensities at prelaunch, at the max $q\alpha$ flight regime, or at end boost. In order to consider all of these different loading and thermal environment factors, the structural design synthesis was conducted for ranges of loading intensities, cylindrical diameters, and thermal environments. The thermal regimes considered were room temperature (prelaunch), cryogenic temperature, and maximum external temperature associated with the end boost condition.

The tensile loading intensity to which a structural component is subjected results from a combination of criteria. In the case of propellant tanks, the maximum burst pressure resulting from the ullage requirement for the engine system and its associated bending moment from particular flight conditions determines the maximum tensile intensity for some portions

of the shell. This pressure essentially sets the required skin thickness for the structural component. Stability requirements for the structural components are dictated by the compressive loading intensity. In the case of the unpressurized shell, the axial acceleration coupled with the maximum bending moment is the compressive design. In the case of a pressure vessel, this compression intensity is relieved somewhat by a nominal relief pressure. The relief pressure is the ground atmospheric pressure plus a nominal pressure differential which is sufficient to preclude boiloff of the propellant.

All of these loading intensities are subjected to various safety factors for the design loading criteria. These factors are considered external to the design synthesis portion of the computer program. Therefore, the design synthesis considers only an ultimate tensile or an ultimate compressive load intensity. The magnitude of these ultimate intensities is controlled by the design flight loads from the various components modified by appropriate safety factors. In this study the limit factor is 1.1 and the ultimate is 1.4. Various types of analysis for the different construction configurations have been evaluated with the assumption that failure of the structural component will be precluded up to and including the ultimate loading intensity. For skin stringer construction, an alternative has been provided whereby an allowance can be made for the skin panels, between the various stiffener elements, to buckle before the ultimate loading condition is reached. This prebuckling load of the skin can be initially fixed with the input data to meet the specific choices of the user. After skin buckling, the remainder of the structure is considered as an effective sectional property and still must not collapse before the ultimate loading condition is reached.

Various types of improvements to the structural design of a component should be considered in assessing the effectiveness of advances. Considerations include changes of material by improving material allowables; for example, by increasing the compressive strength and the ultimate tensile properties of the various basic materials. Substitution of different types of construction and/or material in a particular basepoint configuration will result in substantial weight savings from the basepoint construction/material. The various types of construction that are used at present suffer from weight penalties associated with manufacturing restrictions. Removal of these restrictions result in a weight reduction for various types of structural components.

Another area of improvement is in the method of structural analysis that is used in the design synthesis of the various components. At present, the stability analysis for various types of construction utilizes theoretical buckling stress values resulting from either small deflection theory or large deflection theory. These values are corrected with experimental results which reduces the classical buckling load. An improvement in magnitude of

experimental correction factor will result in improved structural design and weight reduction of the various components.

Although all of the results discussed in this design synthesis section are for a generally loaded structural component for a large range of ultimate compressive loading intensities ($N_x$ from 0 to 20,000 pounds per inch) pertinent results can be translated and applied to specific vehicle systems for the merit assessment studies. This approach was adopted in order to embrace the complete spectrum of design parameters. For later studies, when specific vehicle systems are to be considered in detail, the exact loading environment unique to the vehicle system for each component would be used for these preliminary design studies instead of the broad loading spectrum presently considered.

Many of the present minimum weight design analysis studies tend to consider absolute minimum weight for single, simple loading conditions. These studies do not take into account restrictions and limitations that can be imposed upon the design philosophy to obtain realistic design concepts. Also, for practical component design, various load conditions make up the overall design load environmental envelope. Whereas one flight regime loading will help formulate the design criteria for a specific element of the structure, other flight regimes might dictate design of the remaining elements.

If consideration is given to absolute minimum weight concepts, the resulting configurations may not be realistic because of overlapping stiffeners, too thin material for skin and stiffener elements, impractical height-to-thickness relationships, etc. Also, to obtain explicit solutions for the minimum weight, simplifying assumptions are included and only a few of the stability criteria are considered. Figure 40 shows the results of a parametric minimum weight study in which design restrictions and limitations have not been considered. Other examples of this approach are given in References 20 through 24 where overall efficiency factors for the various types of constructions are parametrically developed and are then considered to apply to the complete range of loading spectrum and design parameters.

To obtain realistic optimum design concepts, the automated computer program for the design synthesis studies must consider the stiffness and stability criteria in depth. These design synthesis subroutines are capable of considering several different types of stability analysis with design sections in both elastic and plastic regimes. Classical buckling analysis for both small and large deflections can be considered for the theoretical minimum weights, but these buckling conditions have to be adjusted by selection of appropriate correction factors which are based on experimental data. The design concepts attained in this study were not results obtained from

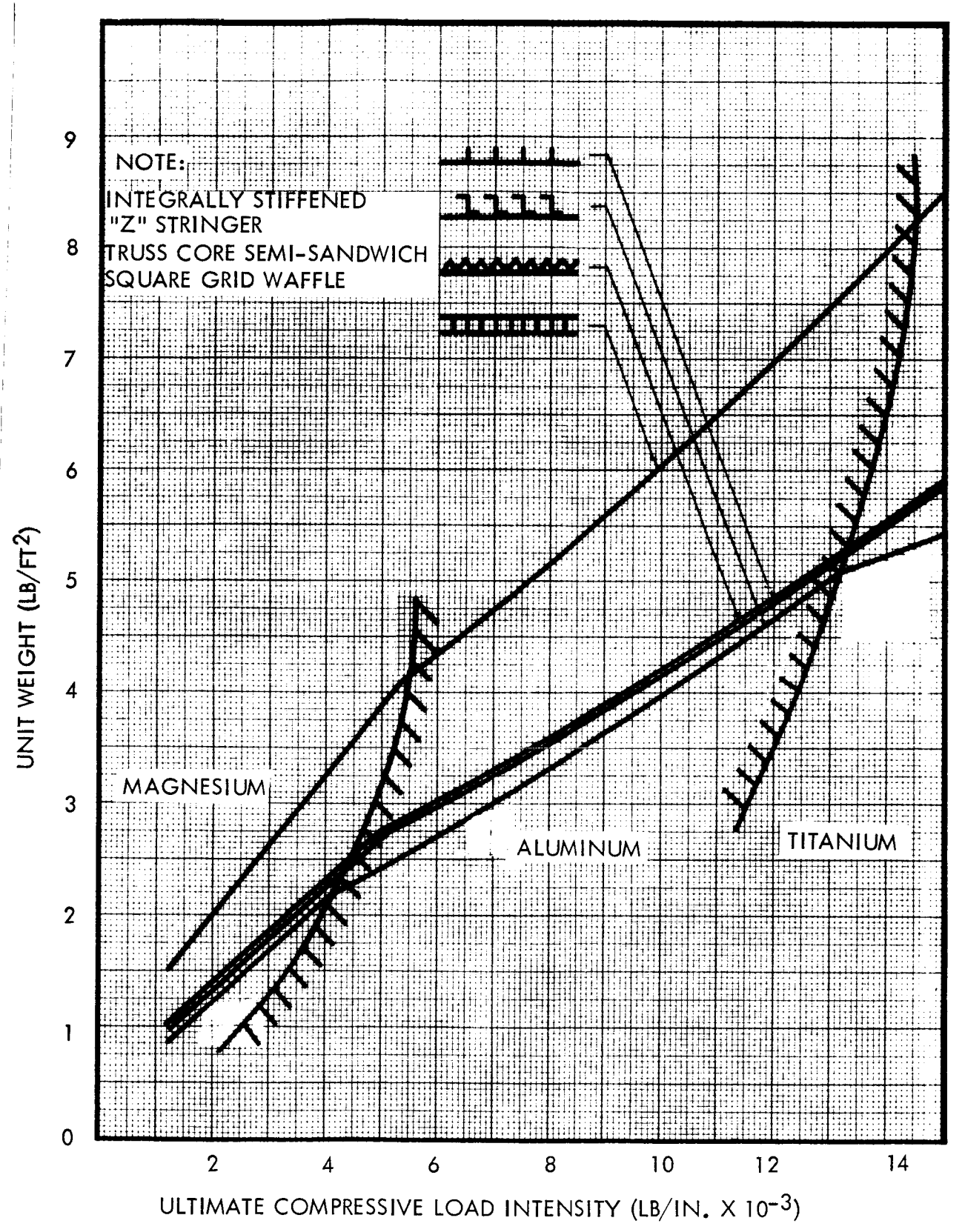



Figure 40. Minimum Weight Construction Comparisons

completely theoretical stability analysis: instead, these results reflect experience gained from experimental and test development programs.

The various design synthesis subroutines which have been developed for this program, have been partly exercised for various types and magnitudes of improvements for material and construction, types of analysis, etc. The results of all these different improvements have been summarized in this section to provide a description of the pertinent data obtained from the synthesis study. These advances and their associated unit shell weight reductions are discussed for the various vehicle systems in the Assessment section of this report. Each type of advance and improvement is evaluated and treated separately for the range of construction and materials under consideration in Phase I of this study.

The four design synthesis subroutines presently developed have been linked together by a main program together with an in-house CRT plotting subroutine. The four types of construction are waffle, honeycomb sandwich, skin-stringer, and monocoque. The continuous linking of the subroutines permits an extensive parametric study using all types of construction simultaneously and the resulting convenient displays of data. Tables 32 and 33 are copies of the IBM computer printouts of the design data for the four types of construction. These samples are for a component with a 198-inch radius, typical of the Saturn vehicle, and show a complete range of loading intensities from 2,000 to 18,000 pounds per inch. The compressive load was due to an axial load with no associated bending moment. The non-dimensional load and weight parameters for this aluminum design component are illustrated in Figure 41, which is a copy of the actual CRT plot generated by the digital program. A detailed description of the pertinent data in these design printouts has been included in Appendix B.

The material properties considered for the design synthesis study are shown in Tables 34 and 35. Table 34 shows these properties for a range of temperatures for current materials such as aluminum, titanium, and beryllium. These values formed the basis for the design evaluation of current materials from which a series of material properties improvements were considered. This series of upgraded values was based on the material predictions discussed in the Parametric Synthesis section. Table 35 shows the current material properties (material A) and two steps of upgrading designated material B and material C. These improvements were approximately 10 percent and 20 percent for aluminum, 5 percent and 10 percent for titanium, and optimistically, 15 and 25 percent for beryllium. These percentage improvements in material properties were used to exercise the preliminary design synthesis routines and the range of improvements covering the predicted material advances discussed in the Parametric Synthesis Section.

# Table 32. Monocoque and Waffle Printouts

CONSTRUCTION = MONOCOQUE

MATERIAL = ALUMINUM A

| | | | | | |
|---|---|---|---|---|---|
| MIN SKIN THICKNESS = | 0.0100 INS | YIELD STRESS = | 50000. PSI | LIMIT LOAD FACTOR = | 1.1 |
| BURST PRESSURE = | 0.0000 PSI | ULTIMATE STRESS = | 55000. PSI | ULTIMATE LOAD FACTOR = | 1.4 |
| RELIEF PRESSURE = | 0.0000 PSI | YOUNGS MODULUS = | 10000000. PSI | | |
| MATERIAL DENSITY = | 0.1000 PCI | TEMPERATURE = | 300. DEGF | | |

| COMPONENT RADIUS INS | AXIAL LOAD LBS | BENDING MOMENT IN-LBS | COMP. LOAD INTENSITY LB/IN | UNIT WEIGHT LB/FT2 | SKIN THICKNESS INS | NX/R PSI | WT/R PCI |
|---|---|---|---|---|---|---|---|
| 198. | 1774080. | 0. | 1996. | 6.66 | 0.4625 | 10.083 | 0.0002336 |
| 198. | 3548160. | 0. | 3993. | 9.06 | 0.6295 | 20.166 | 0.0003179 |
| 198. | 4515840. | 0. | 5082. | 10.11 | 0.7022 | 25.666 | 0.0003547 |
| 198. | 7096320. | 0. | 7986. | 12.44 | 0.8642 | 40.332 | 0.0004365 |
| 198. | 8870400. | 0. | 9982. | 13.80 | 0.9586 | 50.415 | 0.0004841 |
| 198. | 10644480. | 0. | 11979. | 15.03 | 1.0439 | 60.498 | 0.0005272 |
| 198. | 12418560. | 0. | 13975. | 16.16 | 1.1223 | 70.581 | 0.0005668 |
| 198. | 14192640. | 0. | 15972. | 17.22 | 1.1959 | 80.664 | 0.0006040 |
| 198. | 15966720. | 0. | 17968. | 18.21 | 1.2643 | 90.747 | 0.0006385 |

CONSTRUCTION = WAFFLE

MATERIAL = ALUMINUM A

| | | | | | |
|---|---|---|---|---|---|
| MIN SKIN THICKNESS = | 0.0150 INS | YIELD STRESS = | 50000. PSI | LIMIT LOAD FACTOR = | 1.1 |
| MIN WEB THICKNESS = | 0.0150 INS | ULTIMATE STRESS = | 55000. PSI | ULTIMATE LOAD FACTOR = | 1.4 |
| MAX HEIGHT/SKIN = | 15.0000 | YOUNGS MODULUS = | 10000000. PSI | RM RELIEF FACTOR = | 0.714 |
| BURST PRESSURE = | 0.0000 PSI | TEMPERATURE = | 300. DEGF | STABILITY FACTOR = | 0.330 |
| RELIEF PRESSURE = | 0.0000 PSI | MATERIAL DENSITY = | 0.1000 PCI | | |

| COMPONENT RADIUS INS | AXIAL LOAD LBS | BENDING MOMENT IN-LBS | COMP. LOAD INTENSITY LB/IN | UNIT WEIGHT LB/FT2 | SKIN THICKNESS INS | TOTAL HEIGHT INS | WEB THICKNESS INS | CELL PITCH INS | AVERAGE STRESS PSI | NX/R PSI | WT/R PCI |
|---|---|---|---|---|---|---|---|---|---|---|---|
| 198. | 1774080. | 0. | 1996. | 2.49 | 0.1271 | 1.91 | 0.0820 | 6.33 | 14400. | 10.083 | 0.0000879 |
| 198. | 3548160. | 0. | 3993. | 3.54 | 0.1741 | 2.61 | 0.1060 | 7.21 | 20800. | 20.166 | 0.0001241 |
| 198. | 4515840. | 0. | 5082. | 4.02 | 0.1994 | 2.84 | 0.1234 | 7.30 | 24000. | 25.666 | 0.0001409 |
| 198. | 7096320. | 0. | 7986. | 5.14 | 0.2244 | 3.35 | 0.1616 | 7.62 | 31000. | 40.332 | 0.0001804 |
| 198. | 8870400. | 0. | 9982. | 5.88 | 0.2463 | 3.66 | 0.1870 | 7.88 | 34800. | 50.415 | 0.0002062 |
| 198. | 10644480. | 0. | 11979. | 6.62 | 0.2856 | 4.01 | 0.2087 | 8.93 | 36400. | 60.498 | 0.0002322 |
| 198. | 12418560. | 0. | 13975. | 7.35 | 0.3280 | 4.36 | 0.2290 | 10.10 | 37400. | 70.581 | 0.0002575 |
| 198. | 14192640. | 0. | 15972. | 8.07 | 0.3736 | 4.69 | 0.2469 | 11.41 | 38000. | 80.664 | 0.0002830 |
| 198. | 15966720. | 0. | 17968. | 8.77 | 0.4176 | 5.00 | 0.2642 | 12.64 | 38600. | 90.747 | 0.0003076 |

# Table 33. Skin-Stringer and Honeycomb Sandwich Printouts

CONSTRUCTION - SKIN STRINGER

MATERIAL - ALUMINUM A
STRINGER SHAPE - HAT SECTION

| | | | | | | | |
|---|---|---|---|---|---|---|---|
| MIN SKIN THICKNESS | = 0.0100 INS | YIELD STRESS | = 50000. | PSI | STABILITY FACTOR | = 1.000 |
| MIN STRINGER PITCH | = 5.0000 INS | ULTIMATE STRESS | = 55000. | PSI | LIMIT LOAD FACTOR | = 1.100 |
| MIN FRAME PITCH | = 0.0000 INS | YOUNGS MODULUS | = 10000000. | PSI | ULTIMATE LOAD FACTOR | = 1.400 |
| BURST PRESSURE | = 0.0000 PSI | TEMPERATURE | = 300. | DEGF | BM RELIEF FACTOR | = 0.714 |
| RELIEF PRESSURE | = 0.0000 PSI | MATERIAL DENSITY | = 0.1000 | PCI | FRAME SHAPE FACTOR | = 0.000 |
| | | MAX FRAME STRESS | = 25000. | PSI | | |

| COMP. RADIUS INS | AXIAL LOAD LB | BENDING MOMENT IN-LBS | COMP. LOAD INTENSITY LBS/IN | UNIT WEIGHT LB/FT2 | | THICK OR AREA | PITCH INS | STRESS PSI | | STGR THICK | STGR ELEMENT LENGTH | NX/R PSI | WT/R PCI |
|---|---|---|---|---|---|---|---|---|---|---|---|---|---|
| 198. | 1774080. | 0. | 1996. | 2.17 | SK | 0.062 | | 15500. | UP | 0.050 | 1.77 | 10.083 | 0.0000761 |
| | | | | | ST | 0.33 | 5.0 | 15500. | BL | 0.050 | 0.71 | | |
| | | | | | FR | 1.17 | 53.2 | | BE | 0.050 | 1.77 | | |
| 198. | 3548160. | 0. | 3993. | 3.28 | SK | 0.078 | | 24501. | UP | 0.062 | 1.79 | 20.166 | 0.0001152 |
| | | | | | ST | 0.42 | 5.0 | 24501. | BL | 0.062 | 0.72 | | |
| | | | | | FR | 2.11 | 32.4 | | BE | 0.062 | 1.79 | | |
| 198. | 4515840. | 0. | 5082. | 3.81 | SK | 0.080 | | 25503. | UP | 0.065 | 2.43 | 25.666 | 0.0001335 |
| | | | | | ST | 0.60 | 5.0 | 25503. | BL | 0.065 | 0.97 | | |
| | | | | | FR | 2.29 | 35.7 | | BE | 0.065 | 2.43 | | |
| 198. | 7096320. | 0. | 7986. | 4.77 | SK | 0.091 | | 33151. | UP | 0.077 | 2.54 | 40.332 | 0.0001673 |
| | | | | | ST | 0.75 | 5.0 | 33151. | BL | 0.077 | 1.07 | | |
| | | | | | FR | 2.97 | 32.9 | | BE | 0.077 | 2.54 | | |
| 198. | 8870400. | 0. | 9982. | 5.31 | SK | 0.101 | | 37671. | UP | 0.085 | 2.52 | 50.415 | 0.0001861 |
| | | | | | ST | 0.81 | 5.0 | 37671. | BL | 0.085 | 1.01 | | |
| | | | | | FR | 3.36 | 32.0 | | BE | 0.085 | 2.52 | | |
| 198. | 10644480. | 0. | 11979. | 5.80 | SK | 0.109 | | 40593. | UP | 0.094 | 2.57 | 60.498 | 0.0002036 |
| | | | | | ST | 0.92 | 5.0 | 40593. | BL | 0.094 | 1.03 | | |
| | | | | | FR | 3.63 | 33.0 | | BE | 0.094 | 2.57 | | |
| 198. | 12418560. | 0. | 13975. | 6.27 | SK | 0.107 | | 40068. | UP | 0.106 | 3.18 | 70.581 | 0.0002196 |
| | | | | | ST | 1.21 | 5.0 | 40068. | BL | 0.106 | 1.11 | | |
| | | | | | FR | 3.53 | 40.7 | | BE | 0.106 | 2.78 | | |
| 198. | 14192640. | 0. | 15972. | 6.73 | SK | 0.116 | | 42706. | UP | 0.114 | 3.15 | 80.664 | 0.0002361 |
| | | | | | ST | 1.29 | 5.0 | 42706. | BL | 0.114 | 1.11 | | |
| | | | | | FR | 3.79 | 40.5 | | BE | 0.114 | 2.78 | | |
| 198. | 15966720. | 0. | 17968. | 7.20 | SK | 0.119 | | 43714. | UP | 0.124 | 3.43 | 90.747 | 0.0002529 |
| | | | | | ST | 1.46 | 5.0 | 43714. | BL | 0.124 | 1.11 | | |
| | | | | | FR | 3.97 | 43.5 | | BE | 0.124 | 2.78 | | |

CONSTRUCTION - HONEYCOMB SANDWICH

MATERIAL FACE SHEETS ALUMINUM A
SANDWICH CORE ALUMINUM

| | | | | | | | |
|---|---|---|---|---|---|---|---|
| MIN SKIN THICKNESS | = 0.0100 INS | YIELD STRESS | = 50000. | PSI | LIMIT LOAD FACTOR | = 1.1 |
| MIN CORE DENSITY | = 2.0000 PCF | ULTIMATE STRESS | = 55000. | PSI | ULTIMATE LOAD FACTOR | = 1.4 |
| MAX SAND HEIGHT | = 7.0000 INS | YOUNGS MODULUS | = 10000000. | PSI | BM RELIEF FACTOR | = 0.714 |
| BURST PRESSURE | = 0.0000 PSI | TEMPERATURE | = 300. | DEGF | | |
| RELIEF PRESSURE | = 0.0000 PSI | MATERIAL DENSITY | = 0.1000 | PCI | | |

| COMPONENT RADIUS INS | AXIAL LOAD LBS | BENDING MOMENT IN-LBS | COMP. LOAD INTENSITY LB/IN | UNIT WEIGHT LB/FT2 | SKIN THICKNESS INS | SAND HEIGHT INS | CORE DENSITY LB/FT3 | AVERAGE STRESS PSI | NX/R PSI | WT/R PCI |
|---|---|---|---|---|---|---|---|---|---|---|
| 198. | 1774080. | 0. | 1996. | 1.13 | 0.0255 | 2.32 | 2.00000 | 39087. | 10.083 | 0.0000397 |
| 198. | 3548160. | 0. | 3993. | 1.73 | 0.0463 | 2.38 | 2.00000 | 43094. | 20.166 | 0.0000608 |
| 198. | 4515840. | 0. | 5082. | 2.12 | 0.0562 | 3.03 | 2.00000 | 45249. | 25.666 | 0.0000744 |
| 198. | 7096320. | 0. | 7986. | 3.32 | 0.0882 | 4.76 | 2.00000 | 45245. | 40.332 | 0.0001165 |
| 198. | 8870400. | 0. | 9982. | 3.93 | 0.1051 | 4.90 | 2.26909 | 47511. | 50.415 | 0.0001378 |
| 198. | 10644480. | 0. | 11979. | 4.71 | 0.1261 | 5.87 | 2.26909 | 47511. | 60.498 | 0.0001652 |
| 198. | 12418560. | 0. | 13975. | 5.49 | 0.1471 | 6.85 | 2.26909 | 47511. | 70.581 | 0.0001927 |
| 198. | 14192640. | 0. | 15972. | 6.28 | 0.1681 | 6.83 | 2.26909 | 47511. | 80.664 | 0.0002201 |
| 198. | 15966720. | 0. | 17968. | 6.65 | 0.1801 | 6.86 | 2.67017 | 49887. | 90.747 | 0.0002332 |

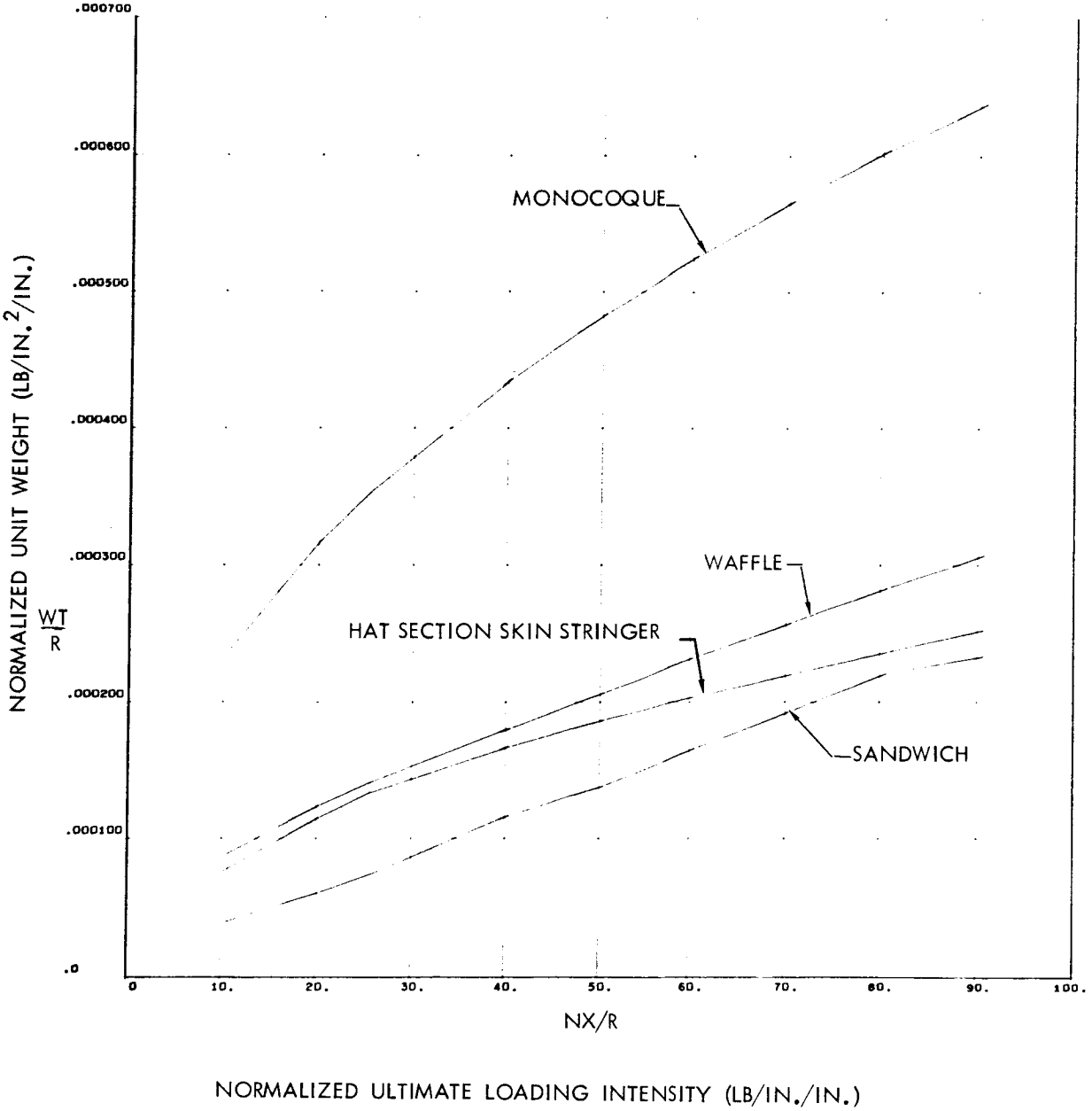



Figure 41. CRT Printout-Unit Weight Versus Loading Index

Table 34. Current Material Properties - Aluminum, Titanium, and Beryllium

| Temperature (Degrees F) | Aluminum 2014-T6 | | | | Aluminum 7075 | | | | Titanium 5A1-2.5 (ELI) | | | |
|---|---|---|---|---|---|---|---|---|---|---|---|---|
| | Fcy ($psix10^{-3}$) | Ftu ($psix10^{-3}$) | Fty ($psix10^{-3}$) | E ($psix10^{-6}$) | Fcy ($psix10^{-3}$) | Ftu ($psix10^{-3}$) | Fty ($psix10^{-3}$) | E ($psix10^{-6}$) | Fcy ($psix10^{-3}$) | Ftu ($psix10^{-3}$) | Fty ($psix10^{-3}$) | E ($psix10^{-6}$) |
| -423 | 75.3 | 90.4 | 73.7 | 11.90 | | | | | 190 | 210 | 190 | 17.05 |
| -300 | 68.2 | 76.5 | 65.6 | 11.45 | 89 | 87 | 75 | 11.1 | 149 | 166 | 149 | 16.88 |
| -100 | 62.7 | 69.1 | 60.0 | 10.95 | 76 | 80 | 70 | 10.7 | 113 | 125 | 113 | 16.30 |
| 78 | 60.4 | 66.6 | 59.0 | 10.60 | 71 | 77 | 66 | 10.5 | 94 | 104 | 94 | 15.52 |
| 200 | 57.2 | 62.5 | 56.0 | 10.40 | 67 | 72 | 62 | 9.9 | 84 | 93 | 84 | 15.26 |
| 400 | 33.5 | 37.1 | 29.3 | 9.56 | 38 | 34 | 31 | 8.6 | 72 | 80 | 72 | 15.12 |

| Temperature (Degrees F) | Titanium 6AL-4V | | | | Beryllium | | | |
|---|---|---|---|---|---|---|---|---|
| | Fcy ($psix10^{-3}$) | Ftu ($psix10^{-3}$) | Fty ($psix10^{-3}$) | E ($psix10^{-6}$) | Fcy ($psix10^{-3}$) | Ftu ($psix10^{-3}$) | Fty ($psix10^{-3}$) | E ($psix10^{-6}$) |
| -423 | 210 | 223 | 210 | 19.4 | | | | |
| -300 | 190 | 195 | 190 | 16.7 | | | | |
| -100 | 140 | 152 | 140 | 15.9 | | | | |
| 78 | 126 | 130 | 120 | 15.8 | 50 | 70 | 55 | 42 |
| 200 | 113 | 117 | 107 | 15.1 | 49 | 67 | 54 | 42 |
| 400 | 97 | 104 | 89 | 13.9 | 47 | 62 | 53 | 41 |

Table 35. Representative Material Properties and Advancements

| Temperature (Degrees F) | Aluminum A | | | Aluminum B | | | Aluminum C | | |
|---|---|---|---|---|---|---|---|---|---|
| | Fcy ($psix10^{-3}$) | Ftu ($psix10^{-3}$) | E ($psix10^{-6}$) | Fcy ($psix10^{-3}$) | Ftu ($psix10^{-3}$) | E ($psix10^{-6}$) | Fcy ($psix10^{-3}$) | Ftu ($psix10^{-3}$) | E ($psix10^{-6}$) |
| -300 | 65 | 75 | 10.6 | 75 | 80 | 10.6 | 75 | 85 | 10.6 |
| 300 | 50 | 55 | 10.0 | 55 | 60 | 10.0 | 60 | 65 | 10.0 |
| | Titanium A | | | Titanium B | | | Titanium C | | |
| -300 | 120 | 135 | 15.8 | 125 | 140 | 15.8 | 145 | 150 | 15.8 |
| 300 | 100 | 115 | 14.0 | 105 | 120 | 14.0 | 110 | 125 | 14.0 |
| | Beryllium A | | | Beryllium B | | | Beryllium C | | |
| -300 | 48 | 63 | 43 | 55 | 70 | 43 | 60 | 75 | 43 |
| 300 | 48 | 63 | 43 | 55 | 70 | 43 | 60 | 75 | 43 |

The material property improvements considered that the magnitude of both the compressive yield and tensile ultimate stress levels were correspondingly increased, but the shape of the stress strain curve was invariant and only shifted in its magnitude. Since no detailed knowledge of these advanced materials is obtainable and, at best, most of these advances are hypothetically postulated, the plasticity factor is assumed to be identical to the parent material. When these new materials have been developed and their properties are properly defined in detail, they can again be exercised through the design synthesis programs to obtain further detailed information for design concepts that utilize all the additional more exact values of the new material properties.

# EFFECTS OF IMPROVEMENT IN MATERIAL PROPERTIES

One way in which to obtain weight reductions for structural design purposes is to improve material properties by alloying the current materials. Present day alloy systems which have performed well in space structures are expected to continue in use with some improvements in their properties for the next 15 years or more. The types of materials that are considered for this study are aluminum, titanium, magnesium, beryllium, and high-strength stainless steels. The design synthesis for the magnesium and stainless steels was considered for a very limited number of cases and did not appear to be sufficiently attractive to pursue any further. The refractory alloys and superalloys were not included in Phase I of this study because the structural components under consideration are not subjected to any high thermal environment during their boost condition. For the design synthesis portion of this report, only improvements in the physical strength and stiffness properties of the material are considered. The effect of the manufacturing difficulties, fabrication limitations, cost considerations, etc., are considered and discussed in other sections of this report where the various structural components and types of materials are associated with specific vehicles in the assessment evaluation. The design synthesis assumes that any of the materials discussed and used in the structural evaluation will be readily attainable and have the desired and required fabrication properties from which to produce the components. Also, it is assumed that these materials can be welded and joined together to form the structural components under discussion. Manufacturing difficulties are discussed in the assessment portion of this study where the relative manufacturing complexity factors are covered.

The material improvements are expressed as a percentage increase of a nominal compression yield and tensile ultimate strength of current materials. The shape of the stress-strain diagram for the plasticity considerations for advanced alloy materials is assumed to be identical to that of the current material. The plasticity curve of the material is expressed mathematically for inclusion in the computer subroutines to provide access to the plasticity correction factors for the various materials. Design synthesis analyses to evaluate minimum weight for the structural components must consider materials in the elastic range and plastic range.

The first type of construction considered was honeycomb sandwich using light density aluminum core with thin facing sheets of various materials. Figure 42 indicates the effects of percentage improvements

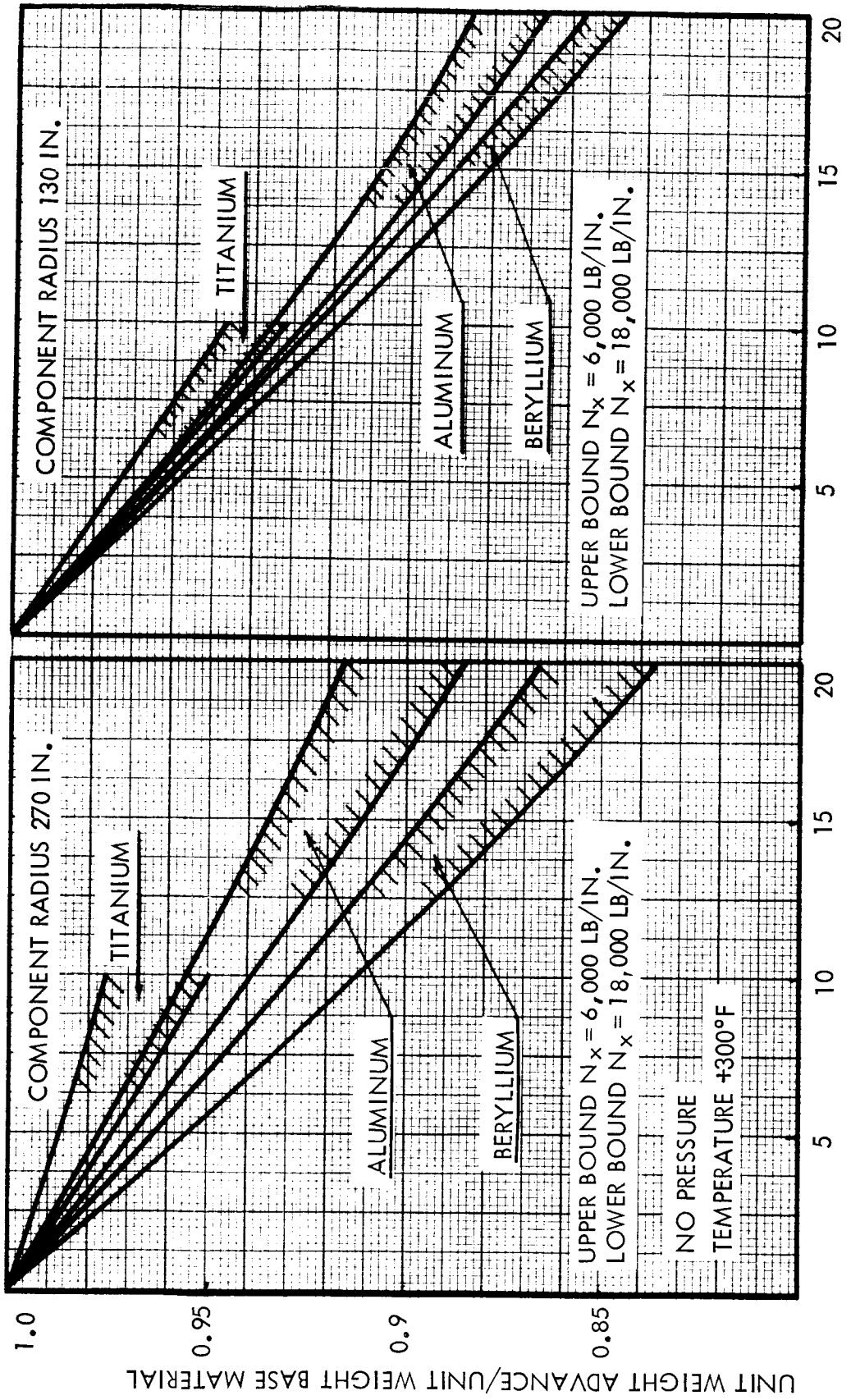



Figure 42. Unit Weight Reductions Resulting From Material Improvements — — Honeycomb Sandwich

in the compressive yield strengths for titanium, aluminum, and beryllium when applied to construction components which are typical for the diameter of post-Saturn vehicles. This diameter is approximately 540 inches. A typical printout of the computer program is shown in Table 33. This printout is for aluminum face sheet with a 2#-cubic-foot core density. The manufacturing restrictions imposed on this design were a skin thickness of 0.01 inch and a maximum sandwich height restriction of 7 inches. The input data in Table 33 is for an aluminum material with a compressive yield strength of 50,000 psi, an ultimate tensile stress level to 55,000 psi, and Young's modulus of elasticity $10^7$ psi. These values are typical of present day aluminum alloy when considered in the 300-degree temperature regime, which is the maximum external skin temperature for a typical manned booster vehicle system.

Three radii were investigated which are associated with the medium range payload class (130 inches), the Saturn class (198 inches), and finally, the post-Saturn class (270 inches) vehicles. The compressive loading intensities for these diameters ranged from 2,000 to 20,000 pounds per inch. In none of the cases did the honeycomb sandwich skin thickness approach the minimum allowable of 0.01 inch. The sandwich height for these minimum weights ranged from 1-1/2 inches for the small diameter component with the load intensity of around 2,000 pounds per inch up to a sandwich height of approximately 5-1/2 inches. The average stress level experienced by the facing sheet of the honeycomb sandwich was about 41,000 to 47,000 psi. These values were below the yield stress of the material under consideration.

It was considered possible that for the period under consideration the compressive yield stress would increase from the present value of 50,000 psi at 300 F up to 60,000 psi for typical 1980 and post-1980 materials. The results of these compressive yield improvements were referenced to the basic current material unit shell weight and these results are indicated in Figure 42. The current titanium value for compressive stress is 110,000 psi increasing up to 120,000 psi. Beryllium increased by 20 percent of the existing compressive yield value. The large diameter unpressurized components unit weight reduction resulting from compressive yield improvement is also shown in Figure 42 and indicates that there is still a potential weight reduction to be obtained from aluminum and beryllium for a 10-to-20-percent improvement in their compressive yield properties. The greatest weight saving is associated with improved beryllium properties. Any increase in the compression yield level will result in reducing the facing sheets thickness and a potential weight saving. Figure 42 also shows the 130-inch radius medium range payload class.

For stiffened sections, such as top-hat stringers either spot welded or mechanically fastened to a skin, the design analysis indicated that the minimum weight reduction for the low-load intensities is very difficult to obtain even with any material improvements. An optimum design results in closely spaced stringers to allow for thin unbuckled skin panels. To obtain manufacturable and realistic-looking configurations the design synthesis approach considered stringer spacing ranging from 4 to 8 inches. These stringer spacings are typical for a Saturn class vehicle where the 5-inch pitch is closely allied to a second stage vehicle and the large 8-inch pitch is closely allied to the first stage. The analysis included square top-hat sections of uniform thickness, "Z" section, and integrally stiffened stringers. Figure 43 indicates that for a top-hat section the unit weight reduction for a 20-percent improvement in the material compressive yield will result in less than a 1-percent reduction in the unit weight of the shell at an applied load less than or equal to 5000 pounds per inch. This indicates that the optimum design stress level is sufficiently removed from the compressive yield that any material improvement does not alter the unit shell weight appreciably.

In the advanced Saturn payload class and post-Saturn payload class vehicles where the loading intensity is somewhat larger (ranging between 10,000 to 16,000 pounds per inch), a unit weight reduction of 15 percent can be obtained with a 20-percent improvement in compressive yield. Figure 43 includes top-hat stiffened tank wall sections subjected to a 50-pound per square inch burst pressure. A top-hat section might present fabrication difficulties for a pressure vessel whose design requires it to be cleaned of metal chips and debris, etc. after fabrication; however, the resultant argument for weight reduction is still valid if the stringers are external. An additional weight saving can be achieved for the pressurized vessel at a high loading intensity of approximately 16,000 pounds per inch with improvement in the compressive yield of the material.

The effect of "Z" stringer sections is shown in Figure 44. This figure illustrates the effect of the material improvement on minimum unit weight for a range of component radii and loading intensities. It can be seen that for the highly loaded components ($N_x \geq 10,000$ pounds per inch) at least a 10-percent weight improvement can be obtained if the compressive yield of the beryllium could be increased by 25-percent. For a 10-percent improvement of compressive yield stress, only a 5-percent weight improvement is obtained. In the lightly loaded structure ($N_x \sim 5000$ pounds per inch), the 130-inch radius components benefit from property improvement in beryllium, while for the 200-inch and upward radii the beryllium design weight is insensitive to material improvements.

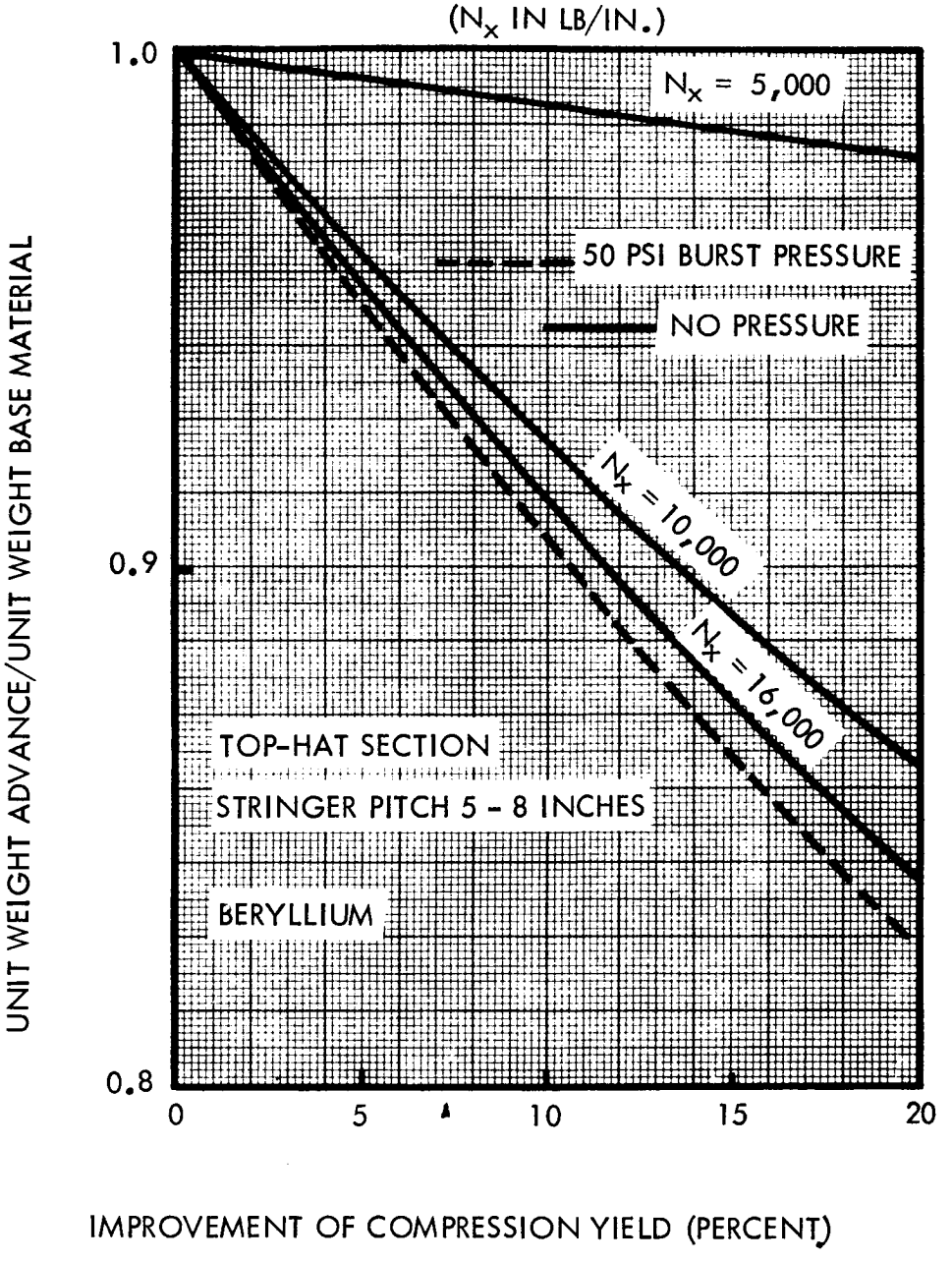



Figure 43. Unit Weights Resulting From Material Improvements - Skin Stringer (Top Hat Section - Beryllium)

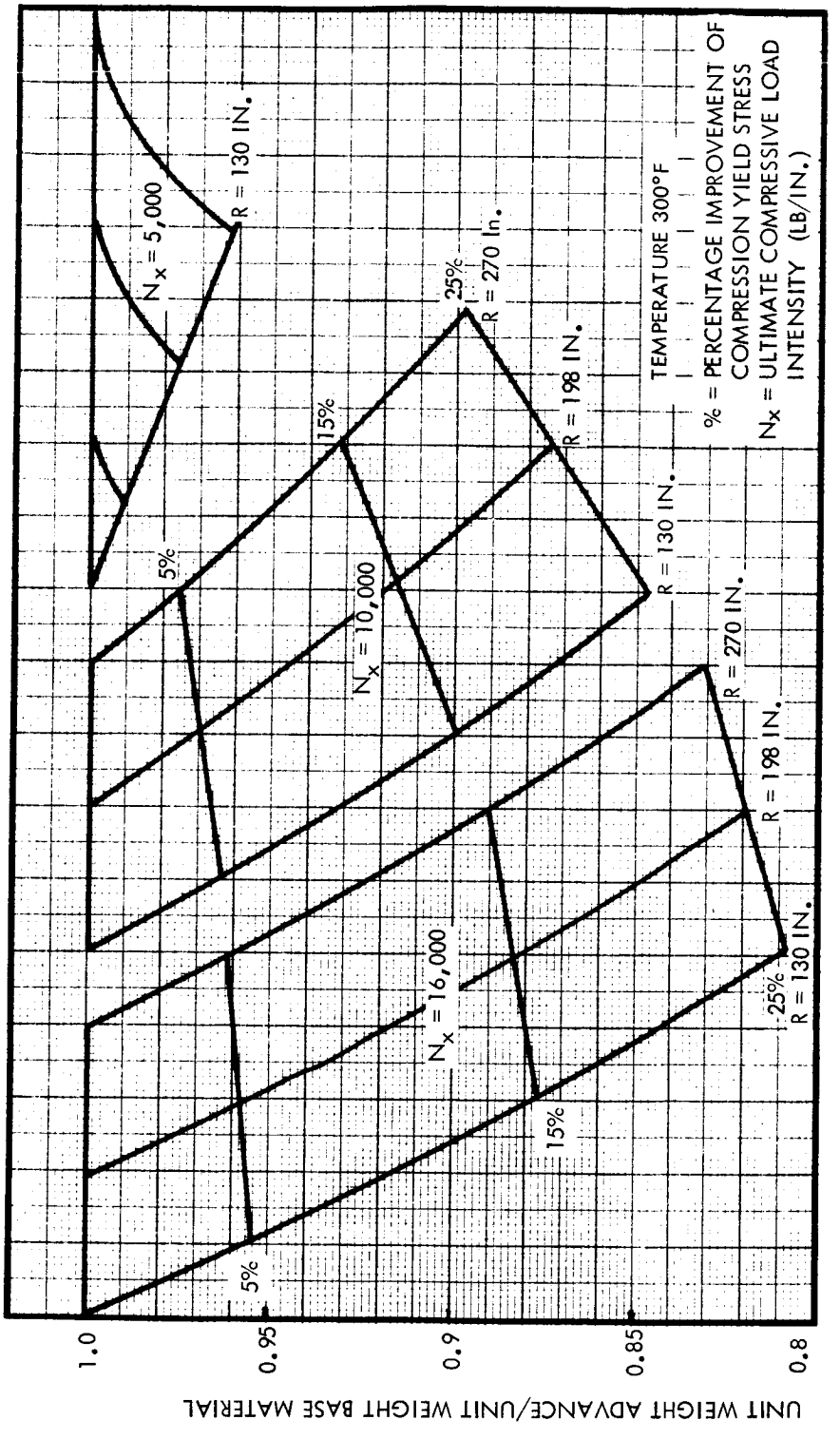



Figure 44. Effect of Compression Yield Improvement on Unit Weight - "Z" Section Skin-Stringer (Beryllium)

Figure 45 shows weight savings that can be obtained with material improvement for two types of skin-stiffened sections ("Z" and top-hat) for the 198-inch diameter Saturn payload class vehicle. The values were for an unpressurized beryllium component where the thermal environment was considered to be 300 F. The top-hat stringer design will benefit more in weight reduction from these material improvements than the "Z" stiffener design for all ranges of loading intensity.

The foregoing figures considered unpressurized components. In the design of propellant tanks, the internal burst pressure requirements dictate that the skin thickness and any material improvements will assist in reducing minimum weight design. Because of the hoop stress levels, the resulting overall design concept will not necessarily be as light and efficient as the unpressurized configuration. This implies that the thicker the minimum skin requirements arising from pressure considerations, the heavier the design weight will be. Therefore, improved ultimate tensile stress decreases the skin thickness requirements for pressure considerations and results in a weight reduction. This applies not only to beryllium but to the other two materials, titanium and aluminum.

Figure 46 demonstrates this effect for the three materials and for a range of size and loading environments. The reductions for the beryllium pressure design components are similar to the unpressurized design. It is not anticipated that beryllium will soon be used for pressure vessels unless there are improvements in its ductility, crack sensitivity, and joining. The beryllium improvements indicated in Figure 46 are applicable for all loading intensities up to 20,000 pounds per inch and all radii. This argument does not apply completely for the other two types of material. These reductions are applicable for a limited range of load intensities as shown in Figure 46. Aluminum achieves weight improvements for all radii but the magnitude of improvement is a function of the radii. The benefits obtained from the 270-inch radius design with aluminum are appreciable since the shell skins are completely determined by the large hoop stress design criteria. The values quoted in Figure 46 are the maximum compressive loading intensities where any material improvement will produce a weight reduction. For load intensities above these values, improvements result in a smaller weight reduction due to the design being primarily dictated by the compression criteria. In highly loaded components the skin thickness associated with minimum weight for both the pressurized and unpressurized design is similar. No reduction in design weight can be obtained with the smaller radii for titanium. In the 270-inch diameter post-Saturn payload class vehicle, there is a slight improvement for components where the loading intensity is $N_x$ of 8,000 pounds per inch.

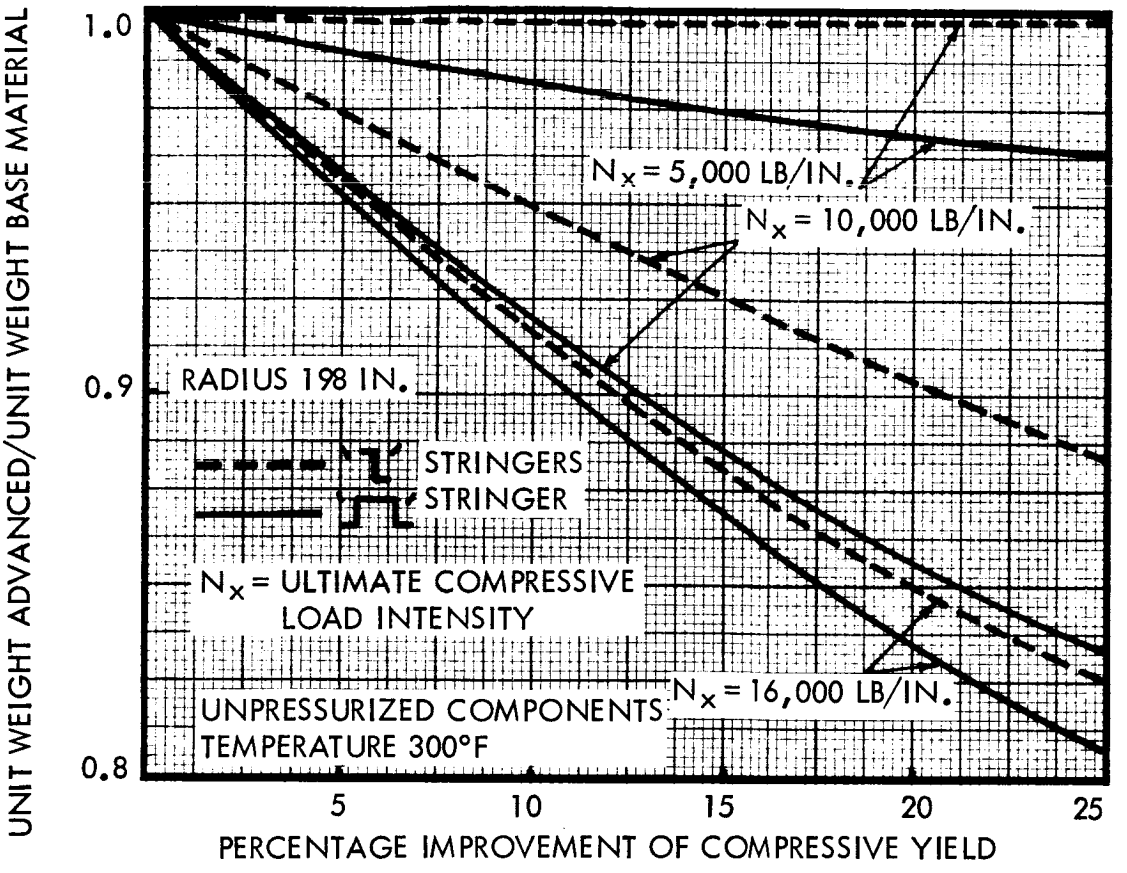
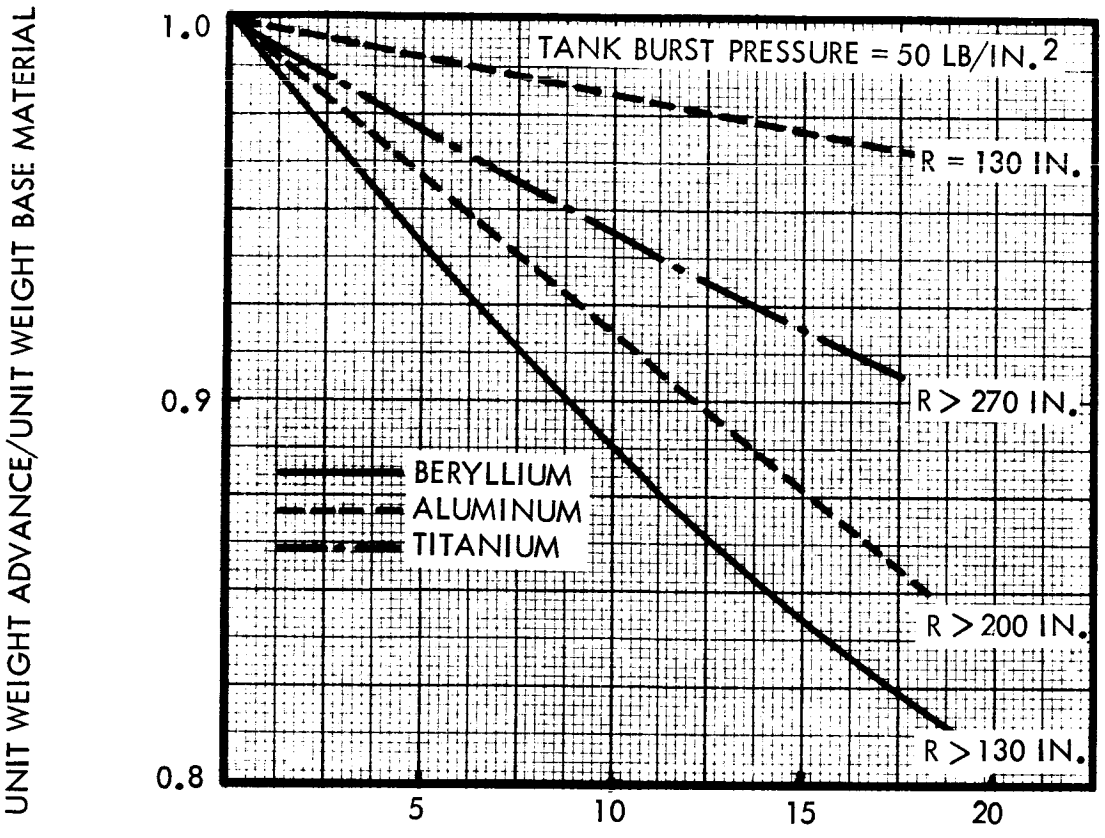



Figure 45. Effect of Material Improvements - Beryllium Constructions

For some of the waffle design concepts, material improvements can bring about an associated weight reduction. Because the stress levels associated with minimum weight design are lower than those for honeycomb sandwich, the waffle stress levels are further away from the yield limitations and improvements in yield properties produce a less noticeable effect on the design configuration.

Figure 47 shows material improvements for waffle construction for two radii (130 and 270 inches) for unpressurized components where the thermal environment is 300 F. This figure indicates that no improvement can be obtained with titanium throughout the complete loading spectrum for both of the radii considered. A slight weight reduction is obtained from aluminum waffle with the small radius but the effect is invariant with the 270-inch design. There is a 10-percent improvement in compressive yield properties between the two aluminum materials, A and B, and the maximum weight reduction resulting from this improvement is less than 8 percent in the highly loaded components. Any improvement in beryllium will bring about an associated weight reduction for all radii throughout the entire loading spectrum. The two curves (Figure 47) are for a 20-percent improvement of material properties from the base beryllium material.




| MATERIAL | STRINGER SECTION | RADIUS IN. | LOAD INTENSITY $N_x$* (LB/IN.) |
|---|---|---|---|
| ALUMINUM | 'Z' | 130<br>200<br>270 | 5,000<br>12,000<br>20,000 |
| TITANIUM | 'Z' | 130<br>200<br>270 | 0<br>0<br>8,000 |
| BERYLLIUM |  | 130<br>200<br>270 | 20,000<br>20,000<br>20,000 |

$N_x$* MAXIMUM LOAD INTENSITY WHERE MATERIAL IMPROVEMENT REDUCES UNIT WEIGHT

Figure 46. Effect of Material Improvements in Pressure Tanks

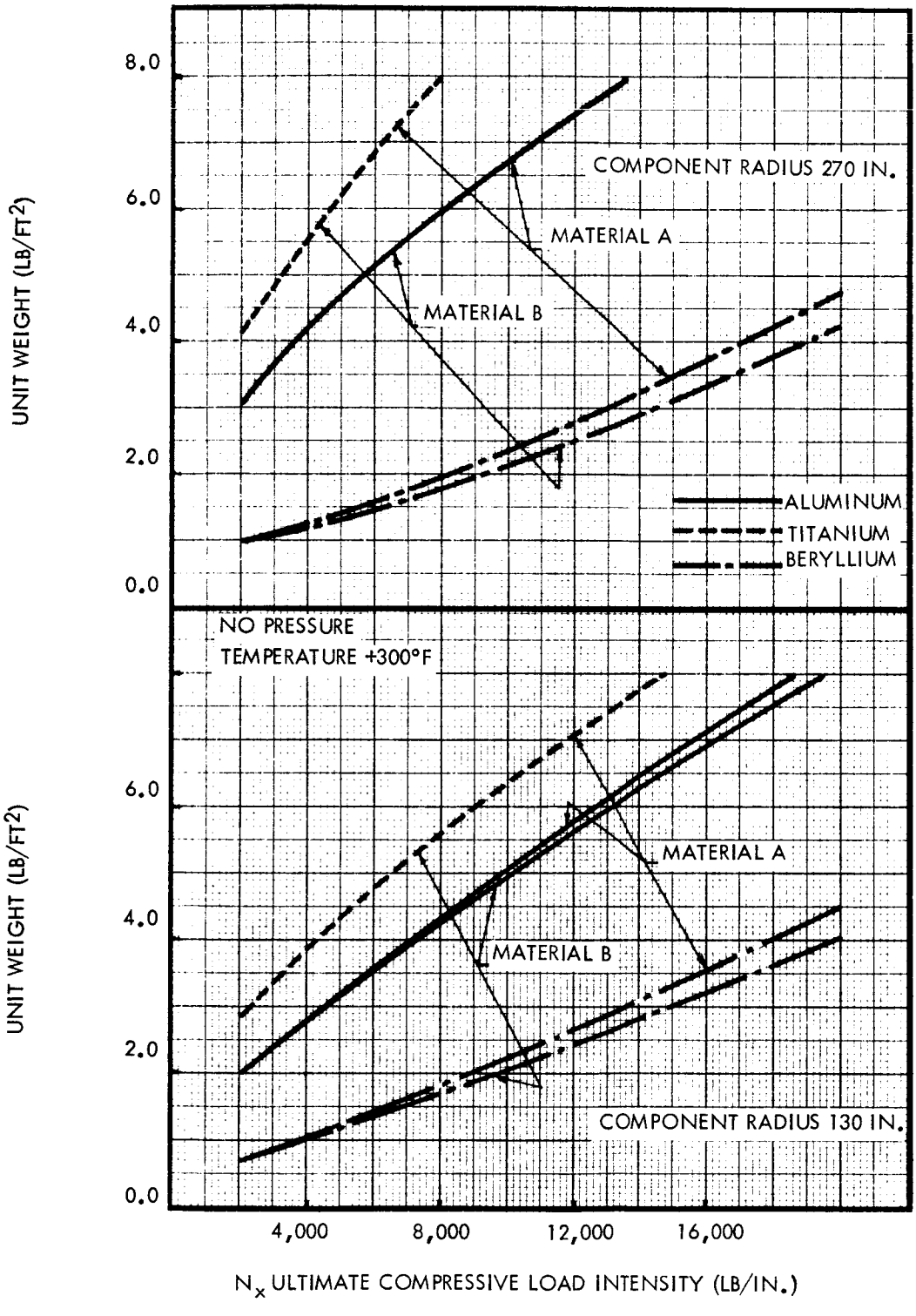



Figure 47. Material Improvements Applied to Waffle Construction

## EFFECT OF CHOICE OF BASIC CONSTRUCTION

For a given loading and its thermal regime, there is a material for use in the various design concepts that produces a minimum weight configuration for the loading spectrum. Examples are shown in Figures 48 through 50 in which, for the range of loading intensities, the optimum selection of beryllium, titanium, or aluminum is indicated.

Figure 48 presents data for the honeycomb sandwich construction. Three materials are shown for a range of loading intensities from 2,000 to 20,000 pounds per inch and for two basic component radii of 130 and 270 inches. The radius effect on the unit weight has a small penalty in aluminum and titanium, and produces identical results in beryllium. The titanium honeycomb sandwich is more efficient than aluminum for the higher loading intensities. These results are based upon the analysis discussed in Appendix C and are usable where deep-core sandwich sections are permissible and desirable for minimum weight constructions. For honeycomb sections with height restrictions, the results shown in Figure 48 are not applicable. Results in Figure 48 are for minimum weight design. The effect of height restrictions is discussed later. With $N_x = 6,000$ pounds per inch, the aluminum is more efficient than titanium, since titanium design concepts run into minimum gauge limitations.

If it is possible to fabricate beryllium sandwich honeycomb with beryllium face sheets and aluminum core, the result will be a lighter weight design throughout the complete range of loading intensities. When beryllium honeycomb is used for the design component, the lighter weight is not the only important consideration; other considerations such as additional cost, fabrication complexities, and currently inherent brittleness are additional influences that must be considered in determining its relative merit. In this design synthesis section, all materials are considered possible and practical and are treated for minimum weight considerations. The effects of cost, fabrication, etc., on the relative merits of these materials is considered in the cost assessment section of this study.

A similar material minimum weight boundary map was generated for the skin-stringer design concepts. Figure 49 represents "Z" section stringers; similar results are obtainable for top-hat and integrally stiffened sections. The radius effect is quite pronounced in the unit weight description for both aluminum and titanium. In the skin-stringer concept, the radius effect can be seen clearly for the aluminum design

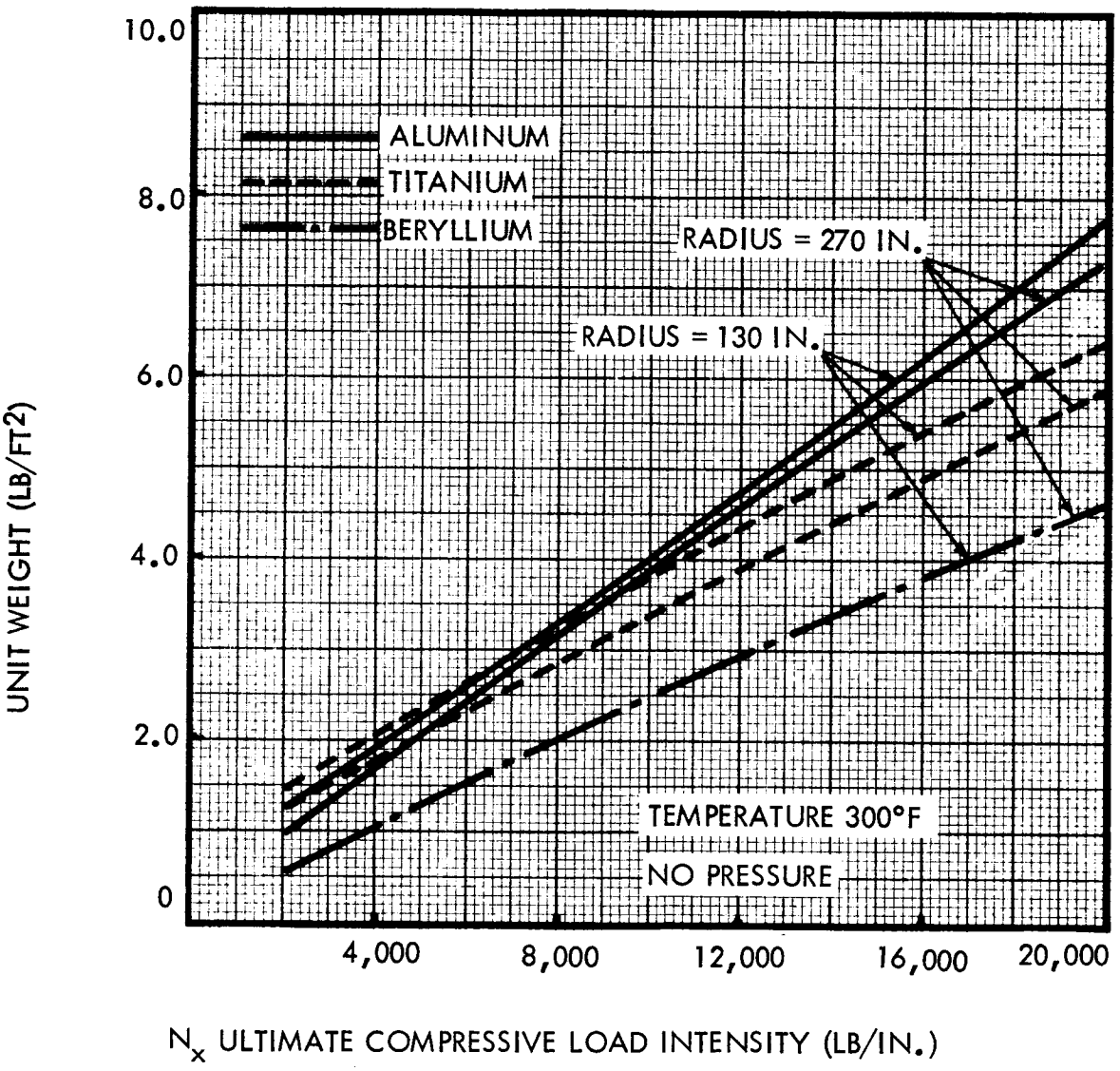



Figure 48. Effect of Material Change on Honeycomb Sandwich Construction

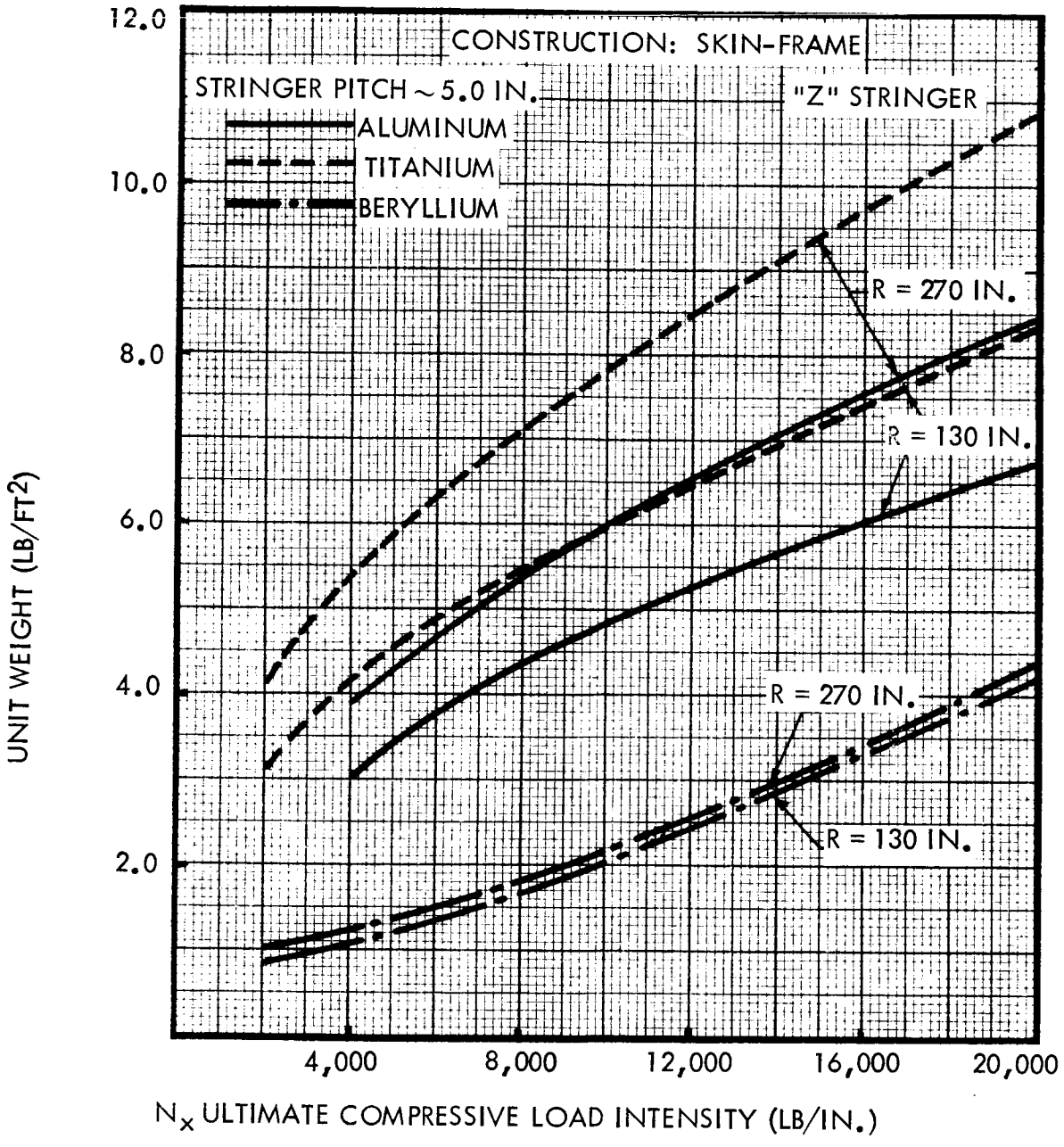



Figure 49. Material Substitution - Unit Weight (Skin-Stringer)

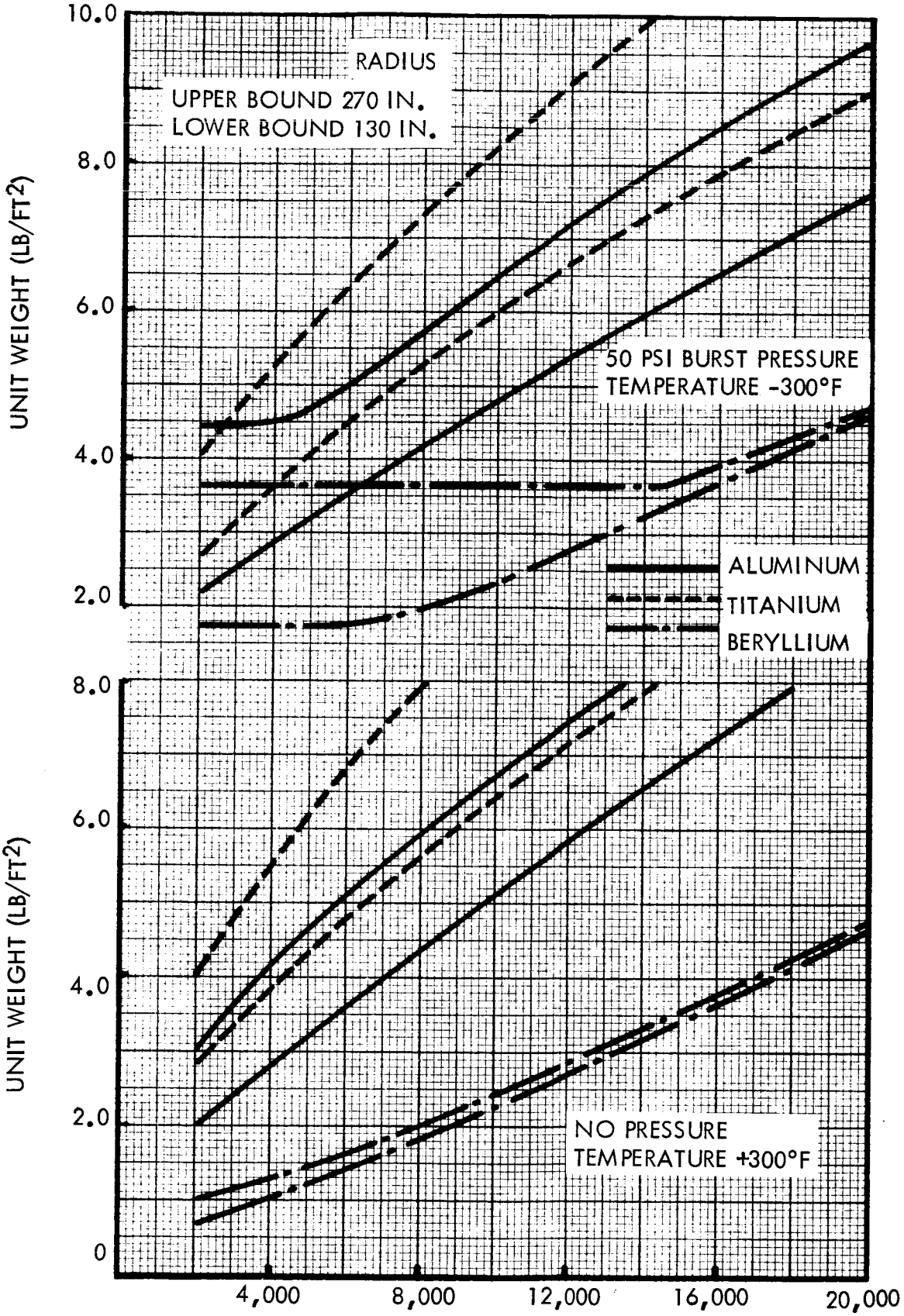



Figure 50. Effect of Material Change on Waffle

configuration for all radii and all loading intensities. The results of Figure 49 were based on values obtained using a stringer pitch of five inches with an unbuckled skin design philosophy for minimum weight considerations. This pitch is extremely close to the optimum design value; variation in nonoptimum stringer pitch is discussed later. The resulting designs obtained for the "Z" section stringers were realistic, with no overlapping or closely spaced stringers that would present difficult manufacturing problems. The design criteria and methods of analysis used for the skin-stringer are discussed in Appendix C. All beryllium designs will produce lower weights than the other two materials for the complete loading spectrum.

Figure 50 shows the weight effects of material changes in a square grid waffle-type construction. These curves are for pressurized and unpressurized components. The unpressurized design curves are similar to those of the skin stringer with an overall weight increase for the larger radius for titanium and aluminum. This radius effect is not so noticeable for beryllium. The order of preference for minimum weight material with waffle construction is beryllium, aluminum, and the heaviest, titanium. This order of preference will change slightly for the pressurized component. With a burst pressure of 50 pounds per square inch for the propellant tanks, the design of the skin thickness is governed by hoop tension and will result in optimum designs heavier than the unpressurized component. A marked example of this is with beryllium, radius 270 inches, where the weight is invariant for loading intensities less than 14,000 pounds per inch. This is due to the relatively low yield stress of beryllium and the high hoop tensile strength associated with the 270 inch radius. Even for the 130 inch radius, this pressure design criteria is felt for load intensities less than 7,000 pounds per inch. A small pressure design restraint is felt for the aluminum material with the large 270 radius and for extremely low loading intensities. No effect on the titanium can be seen for burst pressures up to and including 50 psi. It is assumed that titanium is compatible with the propellants that are stored in these tanks and here is considered only on its relative weight merit.

## EFFECTS OF DIFFERENT TYPES OF CONSTRUCTION

There is not only a minimum weight material boundary for design, but there also exists a minimum weight construction boundary map. This boundary map determines what type of construction should be used for a given vehicle size and associated load environment to obtain a minimum weight design concept. There are other considerations such as cost, manufacturing, etc., that must be considered in the final design selection, but these are not included in this section which considers minimum weight per se.

Figure 51 indicates minimum weight construction boundaries for aluminum unpressurized components for the following:

1. Monocoque, no rings for stability
2. Square grid waffle
3. Skin stringer - top hat-section
4. Honeycomb sandwich

For this portion of the study, the monocoque construction is considered to be a pure monocoque with no stability frames attached. If rings are included, the unit weights shown in the following figures can be reduced. The curves for the various types of construction show the large radius effect on the unit design weight for the monocoque, waffle, and skin stringer configurations. This is not so pronounced with the honeycomb sandwich design if it is permissible to use the deep core sections to obtain minimum weight. The top-hat stiffened skin is lighter than the waffle design for all radii throughout the entire loading spectrum, and it is obvious that waffle will be significantly lighter than the monocoque. The honeycomb sandwich concept for the large radii is more efficient than all the other constructions. For the small 130 inch radii component and with extremely large compressive load intensities (14,000 to 20,000), the honeycomb configuration is heavier than the skin stringer concept. This optimum construction boundary map has been developed for both titanium (Figure 52) and beryllium (Figure 53). These figures show similar effects for the four types of construction. The titanium monocoque is still heaviest, and the waffle configuration is heavier than the "Z" section skin stringers except for the low load regime with small component radii. Titanium honeycomb is considerably lighter than the other

PRECEDING PAGE BLANK NOT FILMED.

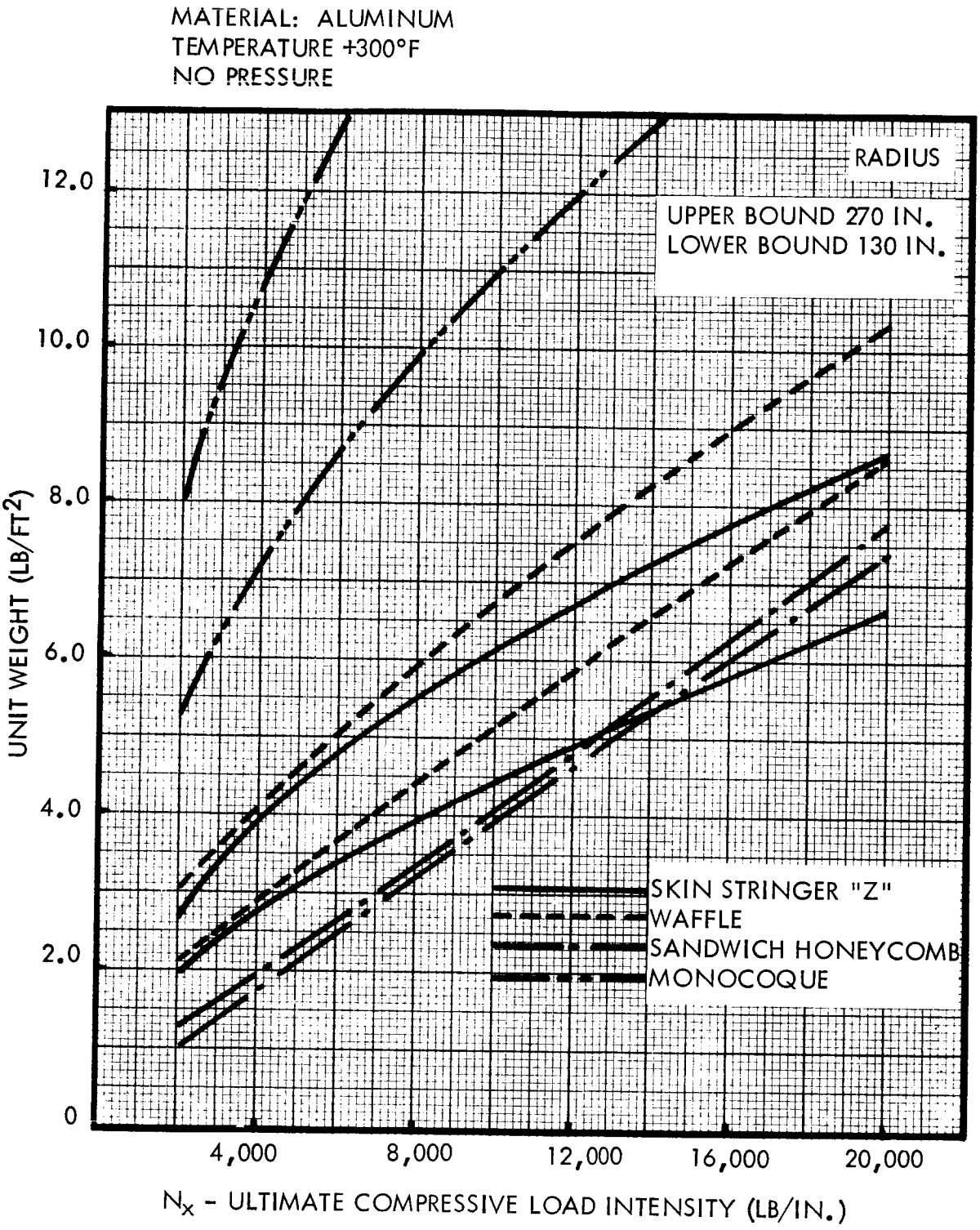



Figure 51. Unit Weight for Different Types of Construction (Aluminum)

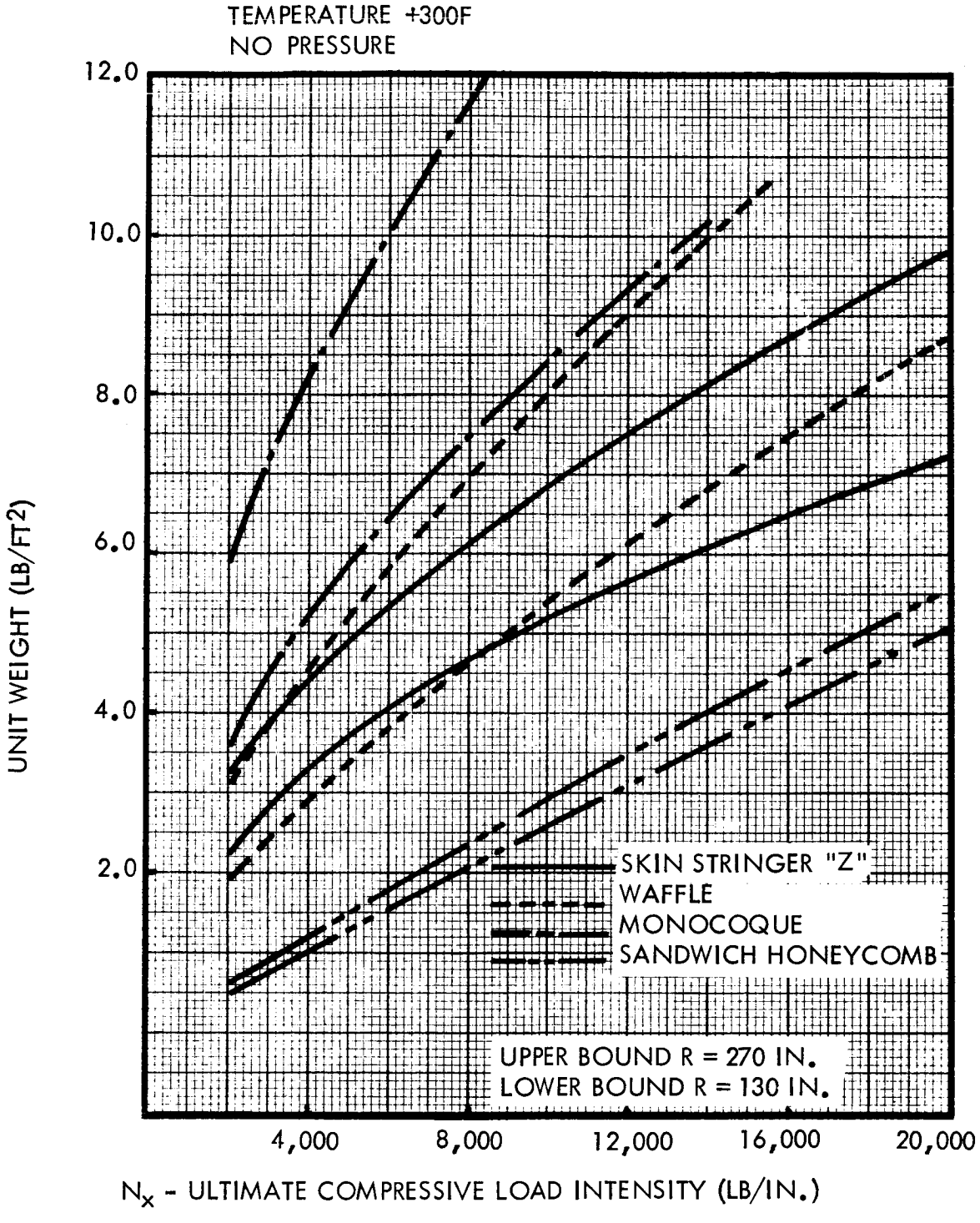



Figure 52. Unit Weights for Different Types of Construction (Titanium)

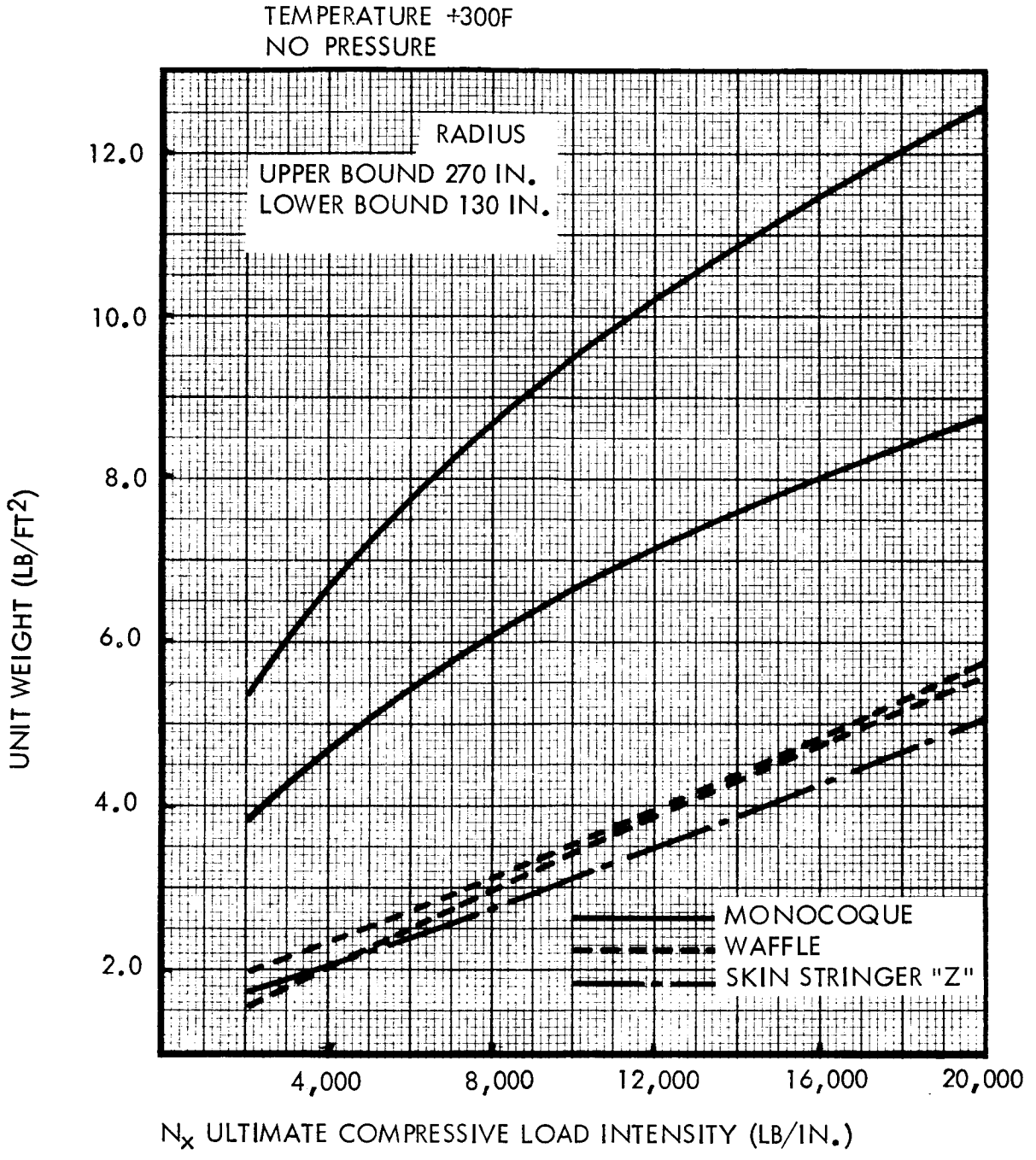



Figure 53. Unit Weights for Different Types of Construction (Beryllium)

three types of construction, throughout the entire design spectrum, this being somewhat different than for the aluminum design. With beryllium, there is hardly any noticeable radius effect for waffle, skin stringer or honeycomb sandwich. In Figure 53, the waffle type construction is only slightly heavier than the "Z" section stringer. "Z" section stringers are more efficient than the honeycomb section when beryllium is used. The honeycomb sandwich configuration is not shown on this figure because it is entirely hidden by the waffle values.

There are not only large variations in design concepts, but small perturbations of design exist in the skin stiffened concepts. Three types of longitudinal stiffeners were considered for this study—"Z", top-hat, and integral stiffeners. The minimum weight design for each of these three types of stiffeners was considered in defining where each particular design could be used most efficiently. Results for both a pressurized and unpressurized component are shown in Figure 54. In the unpressurized component, the top-hat stiffeners are more efficient than the "Z" sections for the small radii throughout the whole loading regime. These results are applicable to aluminum where the stringer pitch considered is five inches, which is close to the optimum pitch for minimum weight. The integral and "Z" section stiffeners produced minimum weight designs of identical magnitudes. For the larger radii, the "Z" stringers are more efficient than the top-hat stringers, with integral stiffeners slightly inferior by at least 10 percent. For the pressurized components, the minimum weight design for the three types of stringers is not radically changed from the unpressurized configuration for the 130-inch radius. In fact, in some cases, the pressurized component weights are slightly less, due to the improved material properties at the lower thermal environment associated with the cryogenic tanks. The optimum pitch for the 130-inch component is fairly close to five inches. For the larger diameter, the top-hat sections are superior to the other two sections because the skin is fairly thick, due to the pressure design criteria. It can, therefore, be worked to a much higher stress level, together with the basic elements of the top-hat stringer. The curves drawn for the 270-inch radius in Figure 54 are for an eight-inch pitch, these minimum weight values being less than those for the five-inch pitch. With the larger radii and typical internal pressure, it can be seen that it is advantageous to increase the stiffener pitch for aluminum material to obtain a lower minimum weight. For the low loading intensities, the integrally stiffened design is competitive with that of a "Z" stiffened section.

This portion of the design synthesis study used five-inch and eight-inch pitch stiffeners for the skin stringer configuration. These values approximate the minimum weight design and are closely related to the structural

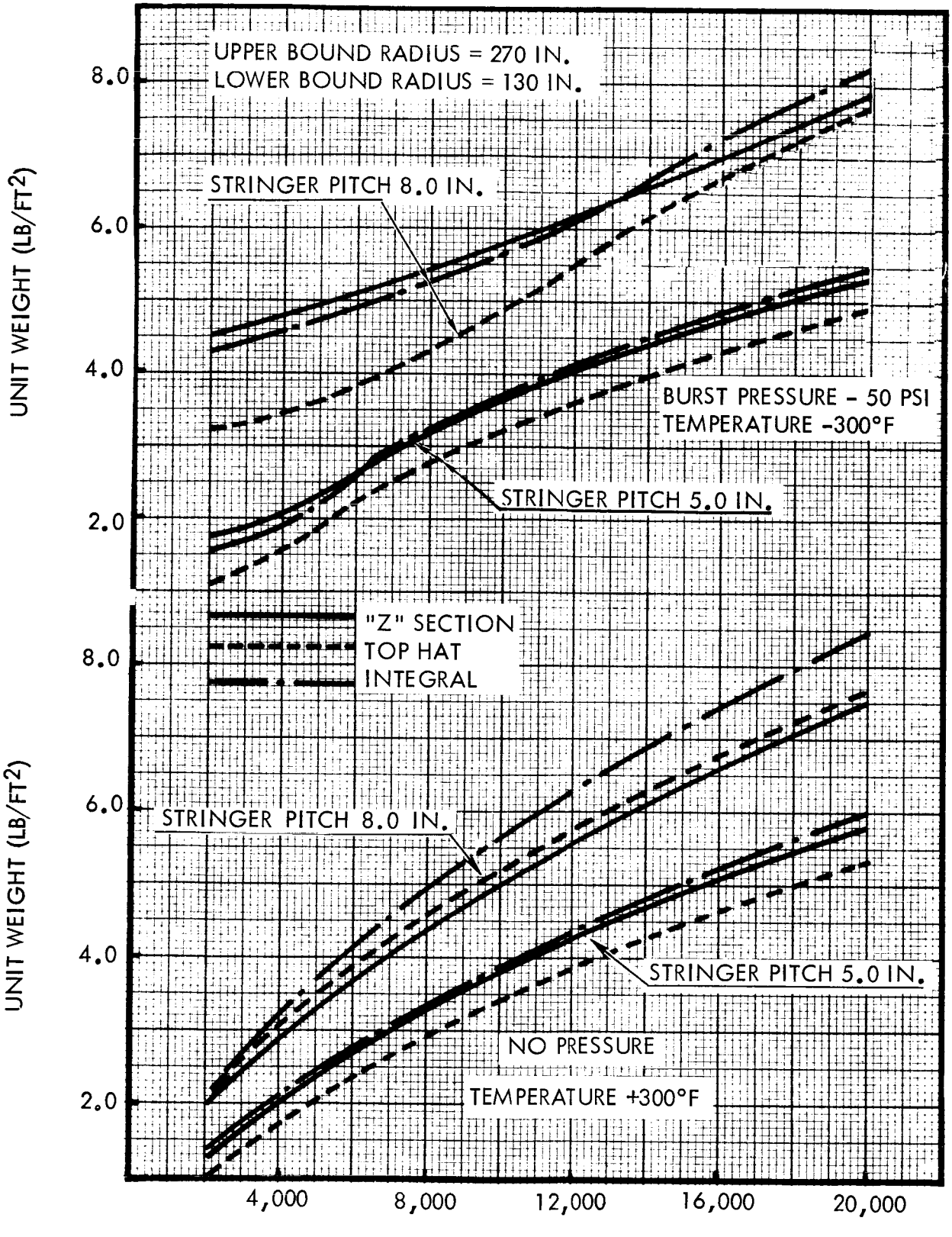



Figure 54. Effect of Change of Stringer Geometry

design of the first and second stages of the current Saturn V vehicle. An additional study using the design synthesis program would define the most efficient stringer pitch for minimum weight.

One way to obtain structural weight reductions could be in a more sophisticated analysis or a different analytical approach. Examples of this are the large or small deflection theories or types of analysis between these two for the design considerations of sandwich honeycomb. The widely used analysis of Reference 25 uses correction factors to account for the difference between theoretical and experimental test results. Figure 55 shows the effect of three different types of analysis on the shell unit weight. For minimum weight designs, sandwich construction concepts result in facing sheet stresses approaching material yield stress and the analysis requires the use of plasticity correction factors to obtain an acceptable design. If plasticity factors are ignored, the facing sheets should be kept below 80 percent of yield stress to ensure structural integrity. The deep core sandwich honeycomb is considered an equivalent height based on correction factors obtained from test results to evaluate its stiffness characteristics. Figure 56 shows the same effect of analytical methods when the radius is increased to 198 inches (Saturn vehicle) for the pressurized components. Figure 56 also shows that the unit weight change for two values of the buckling coefficient ($C_c = 1$ and 1.25) will result in a very small weight penalty. This buckling coefficient is used in the Forest Products Laboratory (FPL 1830) analytical approach (Reference 26). The effects of these various analytical methods for the other two materials, titanium and beryllium, are shown in Figures 57 and 58. There is a relatively small weight penalty in titanium honeycomb with the small radius but a very marked difference with the large radius components.

The design loading conditions for the structural components can radically alter the shell unit weight and design, e.g., in the design of the pressurized components for the propellant tanks. If these tanks are formed from honeycomb sandwich using aluminum with a tank pressure ranging from 40 to 60 psi, the pressure will dictate the design weight for a large range of loading intensities. Figure 59 illustrates pressure effects for loading intensities less than 6000 pounds per inch for the 130-inch radius and for loads of less than 14,000 pounds per inch for the post-Saturn designs of 270-inch radii. Figure 60 shows a similar effect for beryllium honeycomb sandwich for the pressure tank if this type of material should be considered. This curve indicates the maximum compressive load intensities where the design weight is fixed by the pressure requirements for a range of component radii and pressure.

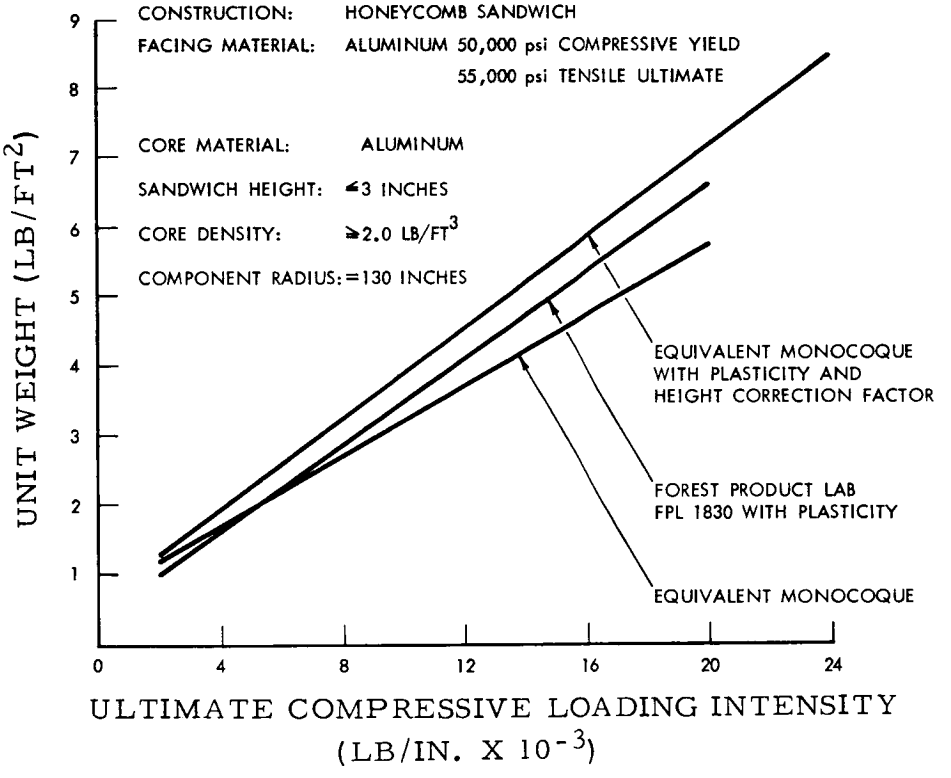



Figure 55. Effect of Analytical Methods

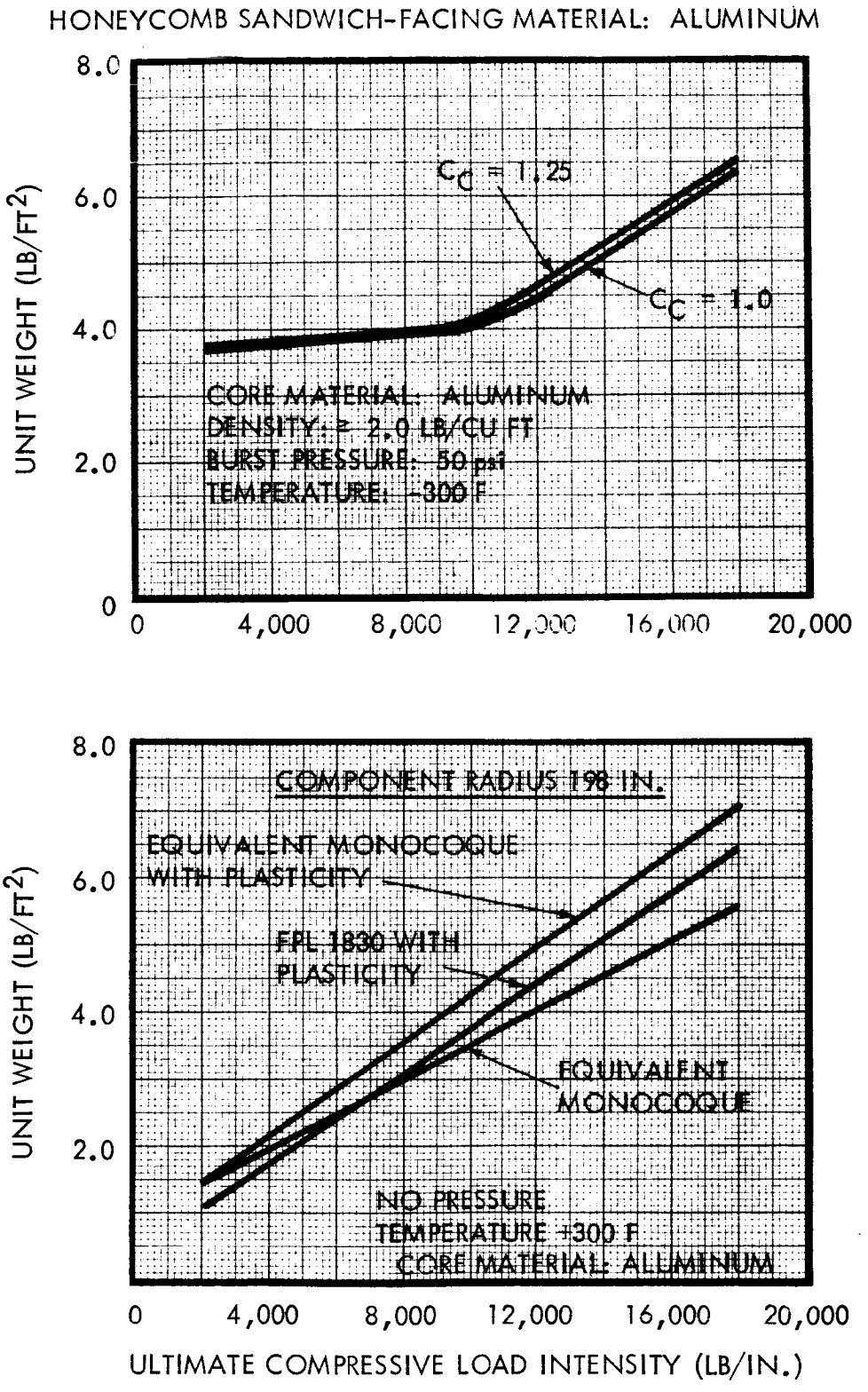



Figure 56. Effect of Analytical Methods (Aluminum - 198 In. Radius)

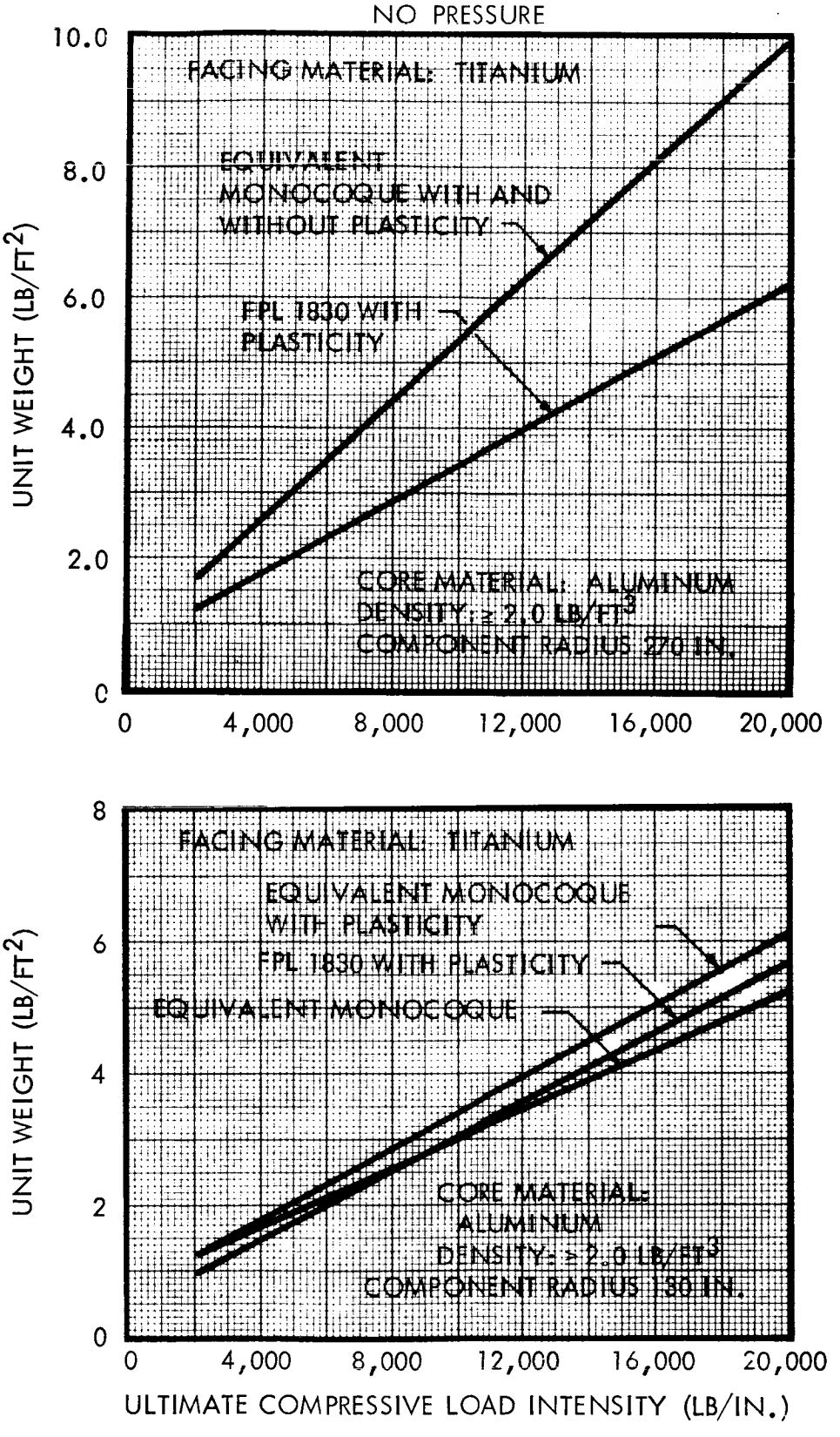



Figure 57. Effect of Analytical Methods - Honeycomb Sandwich

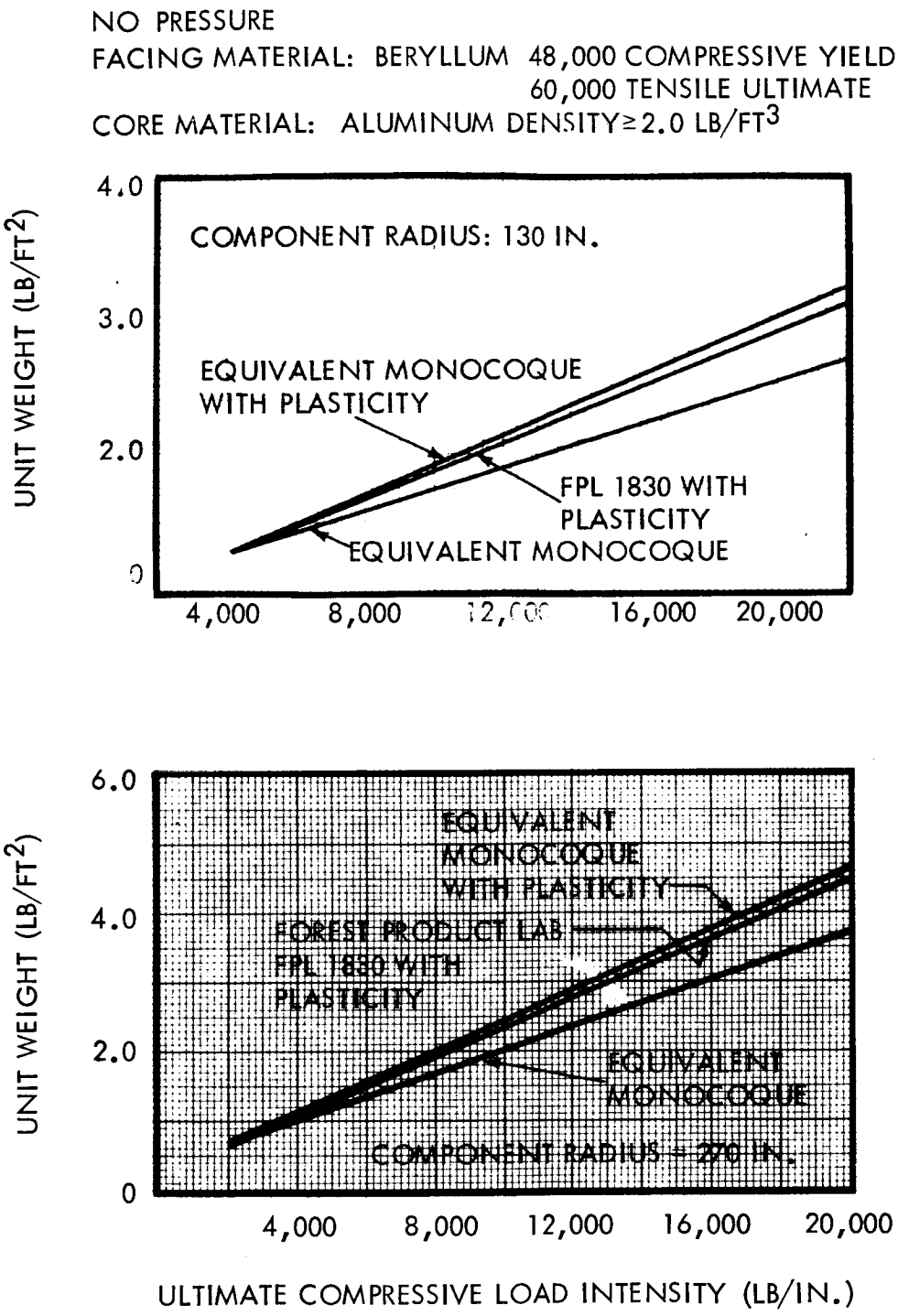



Figure 58. Effect of Analytical Methods - Honeycomb Sandwich - Beryllium

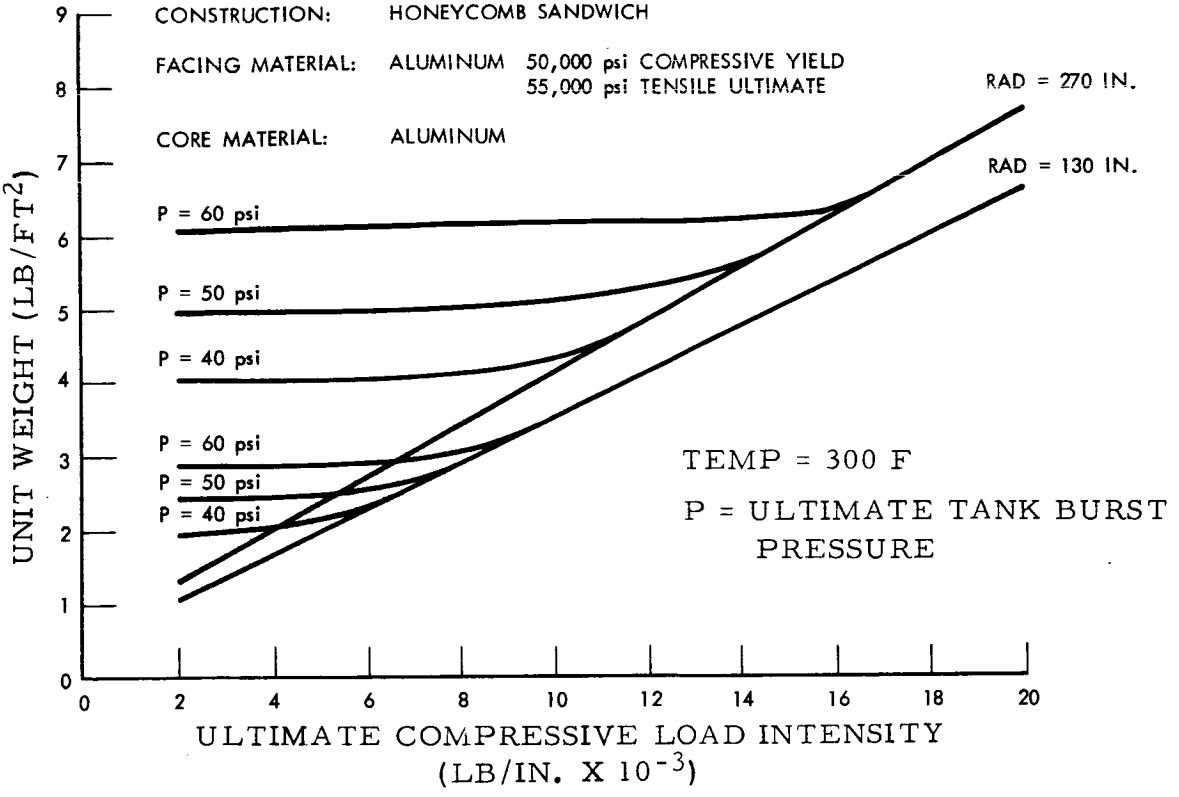



Figure 59. Effect of Tank Pressure on Minimum Weight Design

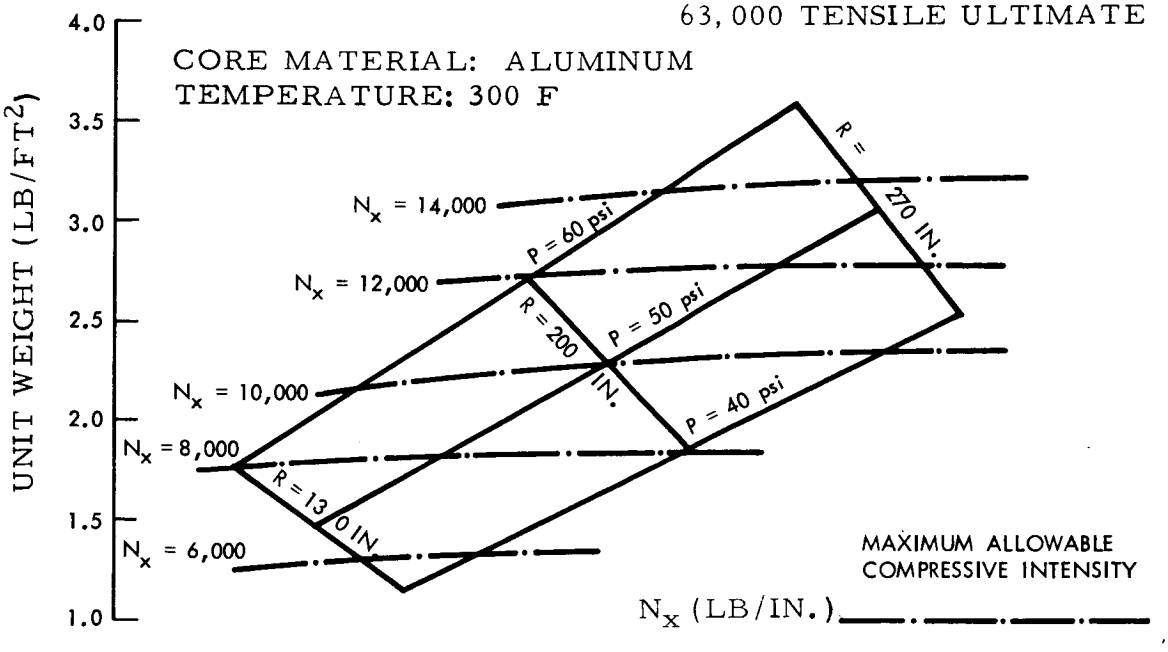



Figure 60. Effect of Radius and Internal Pressure on Minimum Weight Design

## EFFECT OF MANUFACTURING RESTRICTIONS

Weight penalties are not only imposed by the selection of materials or construction, but also by various restrictions and limitations on various types of construction. Some of these restrictions are arbitrary and are applied because of insufficient preliminary definition of the optimum configuration. Other restrictions considered result from the expediency required to ease manufacturing problems, reduce fabrication time, and take advantage of existing components and currently available material sections. Although these decision limitations are justifiable in terms of design, time, and/or fabrication costs, the weight penalties incurred by the restrictions should be fully assessed to determine their influence on the total vehicle system. Imposing these restrictions might be false economy or poor design practice; therefore, they should be considered an important figure of merit in the design evaluation of a minimum weight structure. Not only must these associated weight penalties be considered per se, but the effect of these penalties on the overall vehicle system performance and its cost effectiveness to perform its required mission must be investigated.

A good example of such design limitations is in the current honeycomb sandwich concept with limited height sections (less than 1-1/2 inches). Figure 61 indicates the effect of the shell unit weight for height restrictions imposed upon titanium honeycomb sandwich. The component has a 270-inch radius, is unpressurized, with a design thermal environment of 300 F. This size component can be closely aligned to a post-Saturn class vehicle. For the lightly loaded components ($N_x < 4000$ pounds per inch), the associated weight penalty is not too severe when the sandwich height is restricted to a maximum of 1-1/2 inches. When future vehicle systems are considered with large stage radii, the first stage of such a system will experience maximum compressive load intensities considerably greater than 10,000 pounds per inch. For these components, any imposed height restrictions will incur severe weight penalties — as much as 100 percent penalty, if height is restricted to 1-1/2 inches instead of the optimum. The design analysis for the honeycomb sandwich is expressed in detail in Appendix C. Included in this analysis are correction factors for deep core configurations based upon a limited amount of experimental data. Only a limited amount of design and fabrication of these deep core concepts has been attempted, and any results presented in this report will require extensive testing to verify the magnitude of the correction to be applied. Another factor that should be considered with these heavily loaded sections ($N_x > 10,000$ pounds per inch), is that the facing sheets will be extremely thick when the sandwich core height is

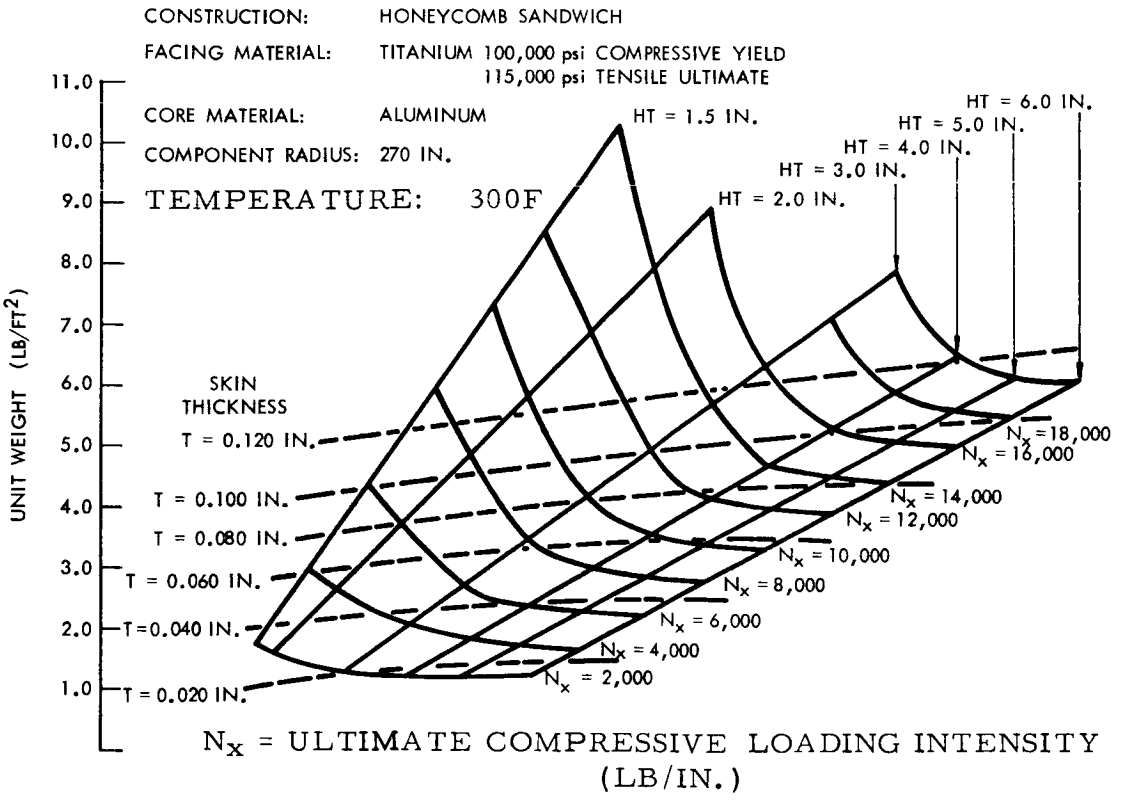



Figure 61. Effect of Sandwich Height Restriction

restricted to 1-1/2 inches (Figure 61). These thick skins could possibly result in bond voids between the core and facing sheet during the fabrication process if the core surface is uneven and/or incompatible with the surface contour of the facing sheets. With these relatively thick skins, high bonding pressures are required to attain a good bonded sandwich. This is especially true of the titanium sandwich, where the facing material exhibits a very springy characteristic and will require high pressures to contour the facing sheets. In aluminum and beryllium sandwich construction, with the facing sheet material of lighter densities than titanium, these facing sheets will become extremely thick and, in fact, resemble stiff plates. Therefore, with the height restrictions removed the increased core depth will effectively reduce the required skin thickness. Figure 61 indicates the required facing sheet thickness associated with the minimum weight design for the complete range of load intensities and sandwich heights considered.

Since these penalties are extremely pronounced for the titanium honeycomb sandwich for the large radius components, they will be reduced with decreased radii. This is clearly shown in Figure 62 for two loading intensities (Nx = 2000 and 10,000 and for a range of radii from 130 to 270 inches). The lower range of the radius parameter is applicable to the Saturn S-IVB stage

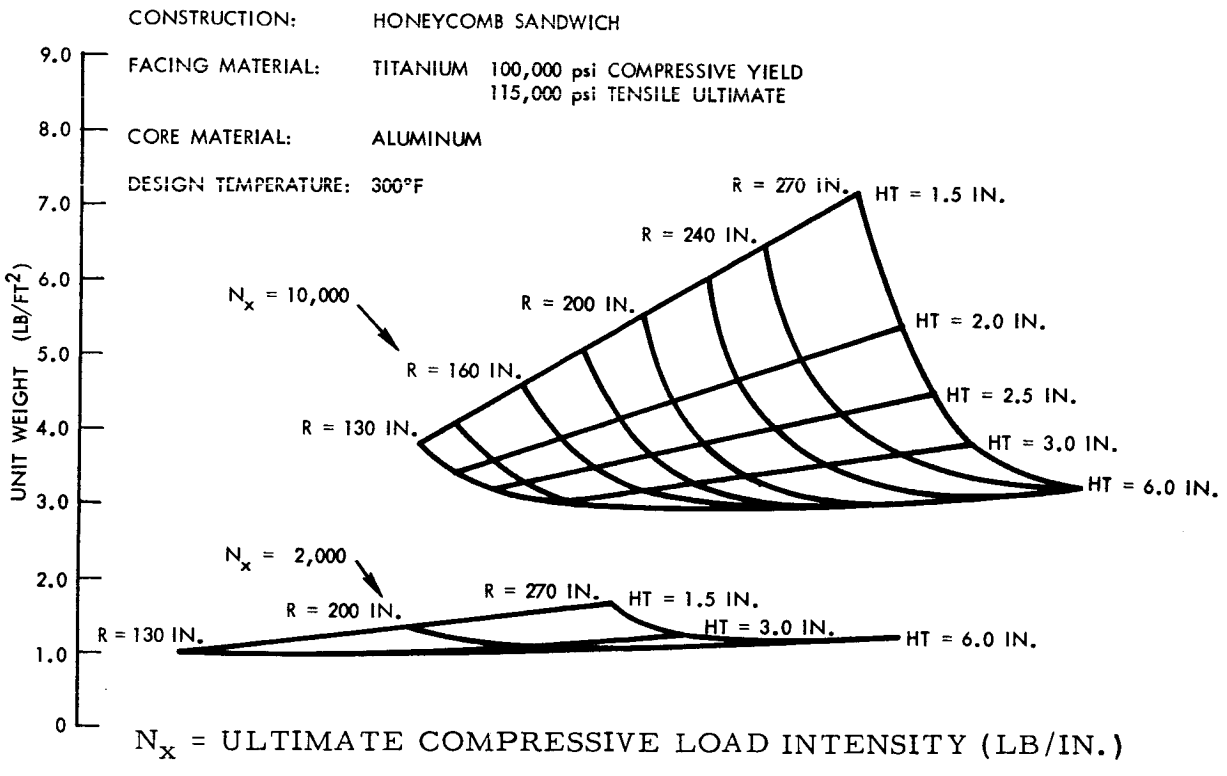



Figure 62. Radius and Height Restriction

and the medium range of 200-inch radius represents the remaining stages of the Saturn V vehicle, S-II and S-IC stages. The compressive loading intensities at 10,000 pounds per inch are somewhat greater than those experienced by the S-II stage, but are well within the range of the structure components of the S-IC. Figure 62 shows the penalties for existing vehicle systems if a component design considers the use of titanium sandwich with a limited depth. For the 200-inch radius component, the associated weight penalty is still greater than 75 percent if the core height is restricted to 1-1/2 inches instead of an optimum height of approximately 3 inches. For an Nx of 2000 pounds per inch, the effect of this height restriction is negligible throughout the entire range of component radii considered. These weight penalties are true for titanium honeycomb only. There are also weight penalties, lesser in magnitude, for aluminum honeycomb sandwich. Figures 63 and 64 show these weight penalties with height restriction for three materials and two component radii of 270 and 198 inches. These figures clearly indicate that titanium honeycomb is by far most influenced weightwise by these height restrictions. Honeycomb sandwich designs using aluminum face sheets also suffer weightwise when the sandwich height is restricted. For example, with a 270-inch radius component and a load intensity of 10,000 pounds per inch, the weight penalty is still 100 percent when the height is changed from 3 inches to 1-1/2 inches. For beryllium honeycomb sandwich, there are no weight penalties

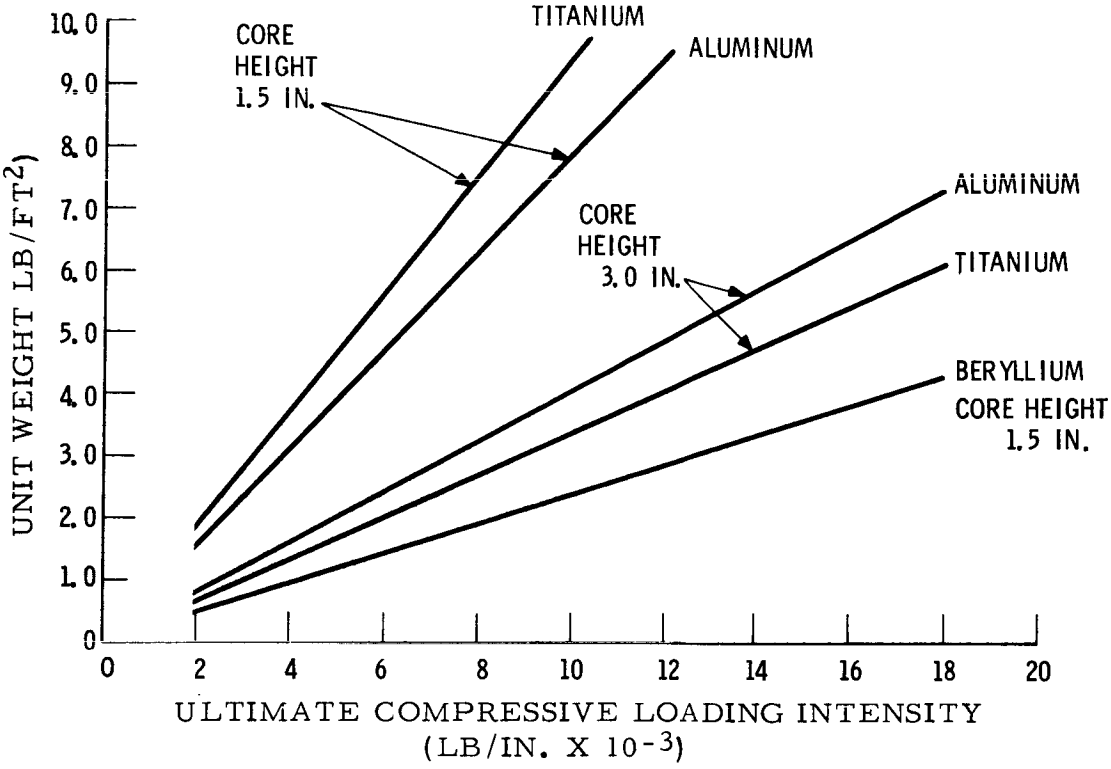



Figure 63. Honeycomb Sandwich - Effect of Material With Height Restriction (Radius 270 In.)

associated with height restrictions because of the relative low density of the facing sheets which result in an optimum design with a sandwich height less than 1-1/2 inches. All of these design concepts were considered with a minimum core density of 2 pounds per cubic foot, with the synthesis analysis selecting the optimum density compatible with the design height.

For the smaller radius component, the weight penalties are still present with these height restrictions, (Figures 64 and 65) but are considerably reduced in magnitude. For example, with a 130-inch radius and a loading intensity of 10,000 pounds per inch, the weight penalties are 30 percent for titanium and 12 percent for aluminum with still no penalty results with a beryllium honeycomb.

Various restrictions can be imposed on the skin stringer configurations to ease fabrication. These include stringer pitch, frame pitch, stringer height, and whether the concept is allowed to buckle or not. For a minimum weight design, there is an optimum stringer pitch for the various types of stringer sections. With the aluminum skin stringer unpressurized components, a range of these stringer pitches were evaluated, and the results are shown in Figure 66. This curve shows the effect of the minimum weight variation for a range of stringer pitch.

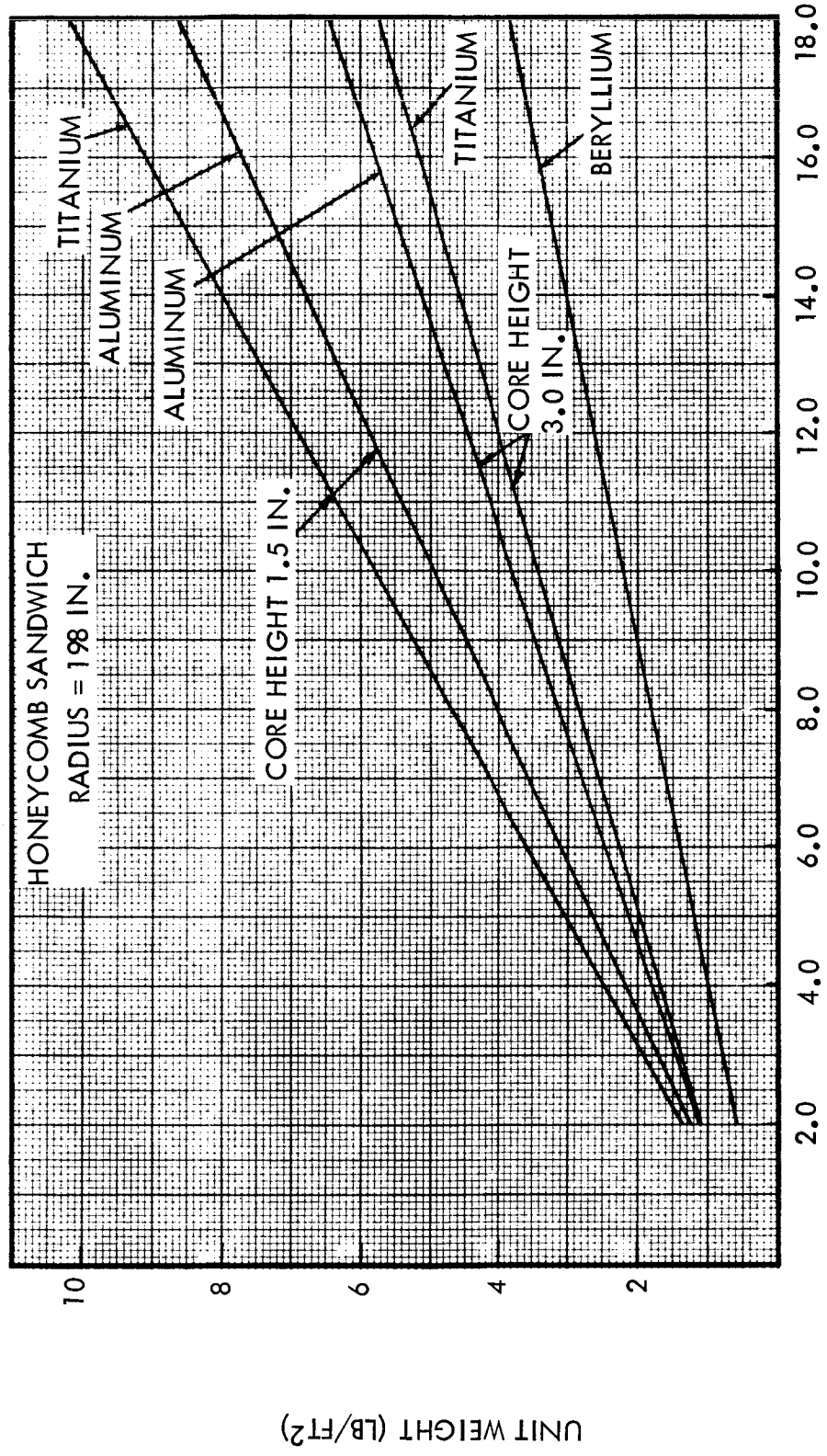



Figure 64. Various Materials With Height Restriction (Radius 198 In.)

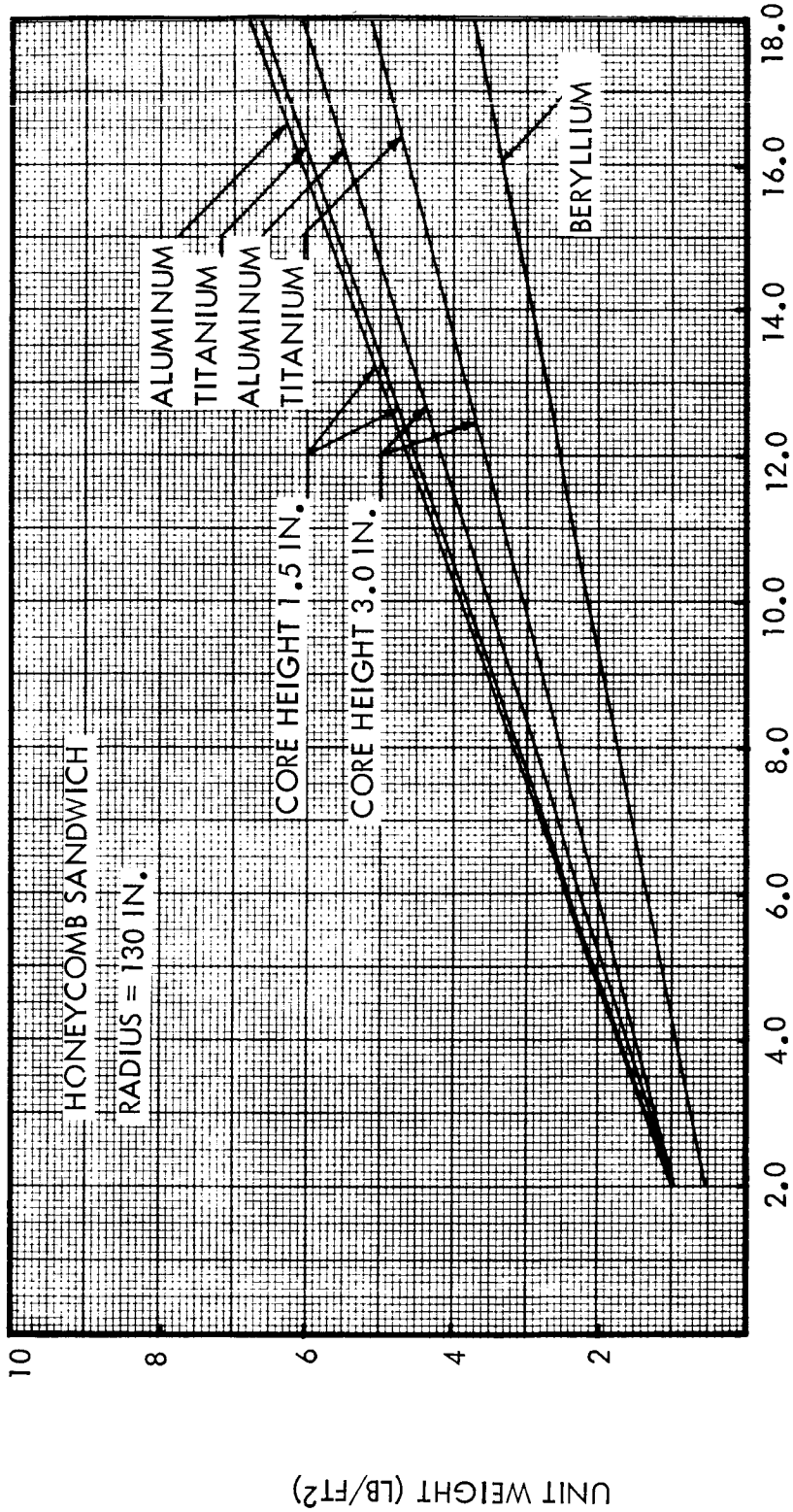



Figure 65. Various Materials With Height Restrictions (Radius 130 In.)

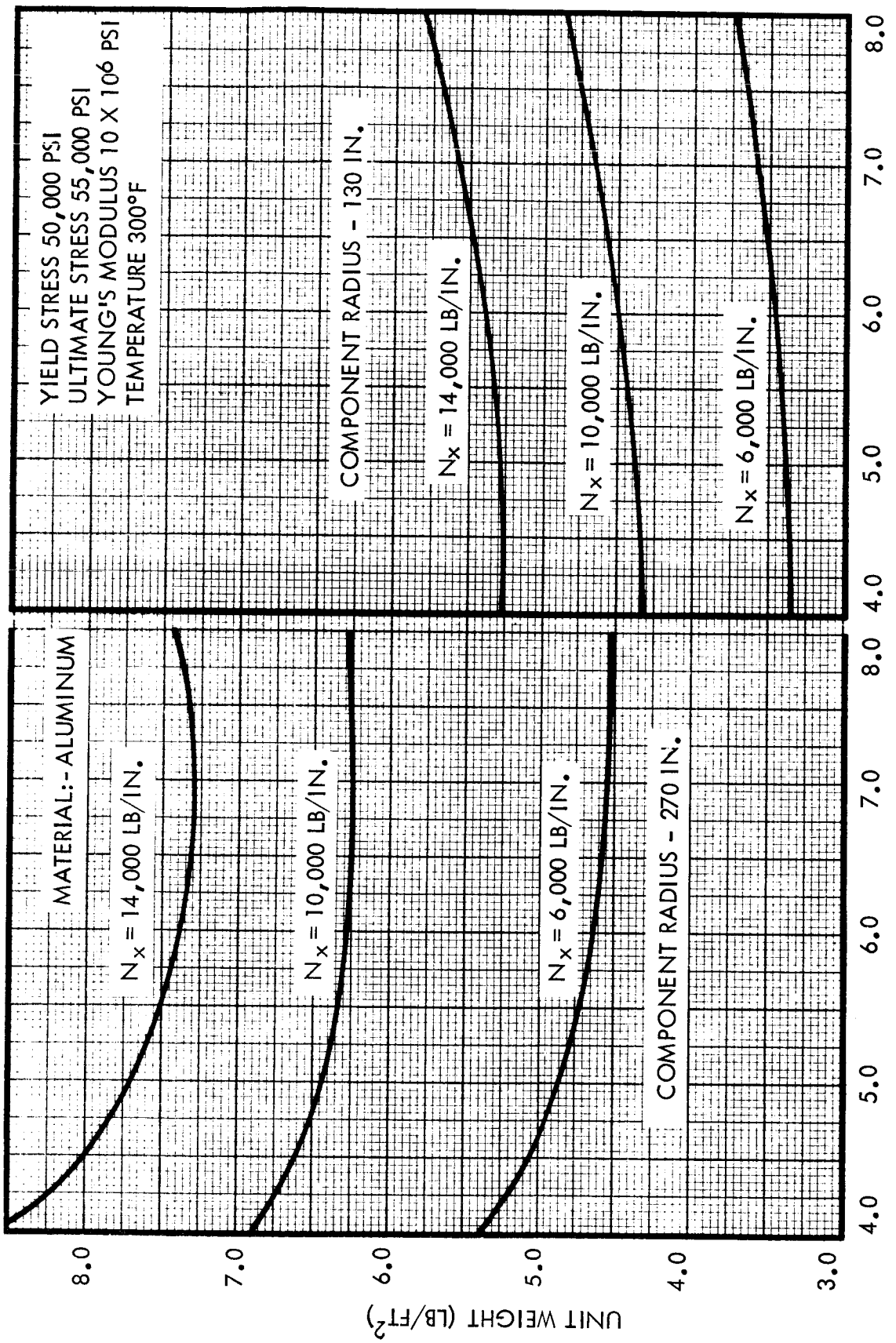



Figure 66. Effect of Pitch Restriction on Unit Weight

In the large diameter component the optimum pitch appears to be about 7 inches for loading intensities greater than 10,000 pounds per inch, increasing to 8 inches pitch for loads less than 6000 pounds per inch. It appears that quite a weight penalty can be incurred if the pitch is allowed to go below these optimum values. With the130-inch radius shell, the optimum pitch is less than 5 inches. Any further reduction in stringer pitch will result in increased fabrication time with negligible weight reduction. The slope of the weight curve for the two different diameter components appears to be totally different (Figure 66). A weight penalty of approximately 12 percent is incurred if the stringer pitch is 8 inches instead of 5 inches for most of the loaded 130-inch radius components. The Saturn class vehicle, at 198-inch radius, will lie between these two values of stringer pitch. These weight penalties for nonoptimum pitches will alter with the type of material considered and the stringer cross sections. Table 36 considers both "Z" sections and top-hat stringers for the two pitches (5 and 8 inches) for present day aluminum and titanium, and future advanced beryllium.

Consideration was given to aluminum and titanium top-hat stringer sections where the skin covering was allowed to buckle below the ultimate load. The synthesis subroutines have the ability to preselect the minimum buckling load for the skin to buckle at 50 percent of ultimate load. These results are shown in Figure 67. With aluminum construction for the 130-inch radius component, a 10 percent weight difference is incurred with the buckled configuration. The unbuckled concept produces a lighter weight design for all of the design loading spectrum and component sizes both for titanium and aluminum. Other restrictions that can be incurred with the skin stringer construction are the frame pitch, which will also have an effect on the minimum weight design configuration. Where an existing type of construction is being subjected to an uprating of the vehicle system, it is required to modify the existing construction to withstand the increased load environment. Therefore, a minimum amount of design modification is required, and it is desirable to determine the best approach to adopt for this modification and its asociated weight penalties.

The waffle design concept also has manufacturing limitations which can impose severe weight penalties. These include minimum cell size practical with mechanical and/or chemical milling and flux process, and easily produced height to depth relationships of web stiffeners. These design sections cannot be too deeply machined out, producing very thin skins, since the tolerances arising from the initial imperfections are magnified. With chemical milling, the etch rate is not uniform throughout the entire material matrix. This helps magnify the tolerance of the final skin thickness.

Table 36. Effect of Pitch Restriction on Unit Weight

| Material | Radius (in.) | Load Intensity (lb/in.) | "Z" Section | | Top-Hat Section | |
|---|---|---|---|---|---|---|
| | | | 5-inch Pitch | 8-inch Pitch | 5-inch Pitch | 8-inch Pitch |
| | 130 | 6,000 | 3.83 | 4.34 | 3.48 | 3.75 |
| | 130 | 10,000 | 4.76 | 5.60 | 4.37 | 5.00 |
| Aluminum | 130 | 14,000 | 5.59 | 6.44 | 5.18 | 5.80 |
| $f_{cy}$ = 50,000 | 198 | 5,000 | 4.00 | 4.36 | 4.08 | 3.83 |
| $f_{tu}$ = 55,000 | 198 | 10,000 | 5.36 | 6.16 | 5.34 | 5.69 |
| | 198 | 14,000 | 6.25 | 7.10 | 6.28 | 6.60 |
| | 270 | 6,000 | 4.74 | 5.09 | 4.80 | 4.55 |
| | 270 | 10,000 | 6.03 | 6.68 | 6.17 | 6.33 |
| | 270 | 14,000 | 7.08 | 7.72 | 7.27 | 7.43 |
| | 130 | 6,000 | 4.92 | 6.00 | 4.25 | 5.19 |
| | 130 | 10,000 | 6.04 | 7.28 | 5.33 | 6.30 |
| Titanium | 130 | 14,000 | 7.00 | 8.31 | 6.30 | 7.22 |
| $f_{cy}$ = 110,000 | 198 | 5,000 | 5.27 | 6.09 | 4.49 | 5.27 |
| $f_{tu}$ = 125,000 | 198 | 10,000 | 6.94 | 7.91 | 6.21 | 6.97 |
| | 198 | 14,000 | 7.97 | 9.04 | 7.70 | 8.06 |
| | 270 | 6,000 | 6.33 | 7.07 | 5.41 | 6.15 |
| | 270 | 10,000 | 7.84 | 8.67 | 7.15 | 7.63 |
| | 270 | 14,000 | 9.04 | 9.93 | 8.69 | 8.87 |

Table 36. Effect of Pitch Restriction on Unit Weight (Cont)

| Material | Radius (in.) | Load Intensity (lb/in.) | "Z" Section | | Top-Hat Section | |
|---|---|---|---|---|---|---|
| | | | 5-inch Pitch | 8-inch Pitch | 5-inch Pitch | 8-inch Pitch |
| | 130 | 6,000 | 1.35 | 1.61 | 1.21 | 1.43 |
| | 130 | 10,000 | 1.85 | 2.06 | 1.83 | 1.90 |
| Beryllium | 130 | 14,000 | 2.53 | 2.56 | 2.52 | 2.53 |
| | 198 | 5,000 | 1.37 | 1.59 | 1.22 | 1.39 |
| $f_{cy}$ = 55,000 | 198 | 10,000 | 1.94 | 2.18 | 1.89 | 1.99 |
| | 198 | 14,000 | 2.59 | 2.66 | 2.51 | 2.58 |
| $f_{tu}$ = 70,000 | 270 | 6,000 | 1.58 | 1.81 | 1.44 | 1.60 |
| | 270 | 10,000 | 2.07 | 2.31 | 1.99 | 2.12 |
| | 270 | 14,000 | 2.67 | 2.77 | 2.63 | 2.65 |

Unpressurized components $f_{cy}$ and $f_{tu}$ in psi

Design temperature 300 F

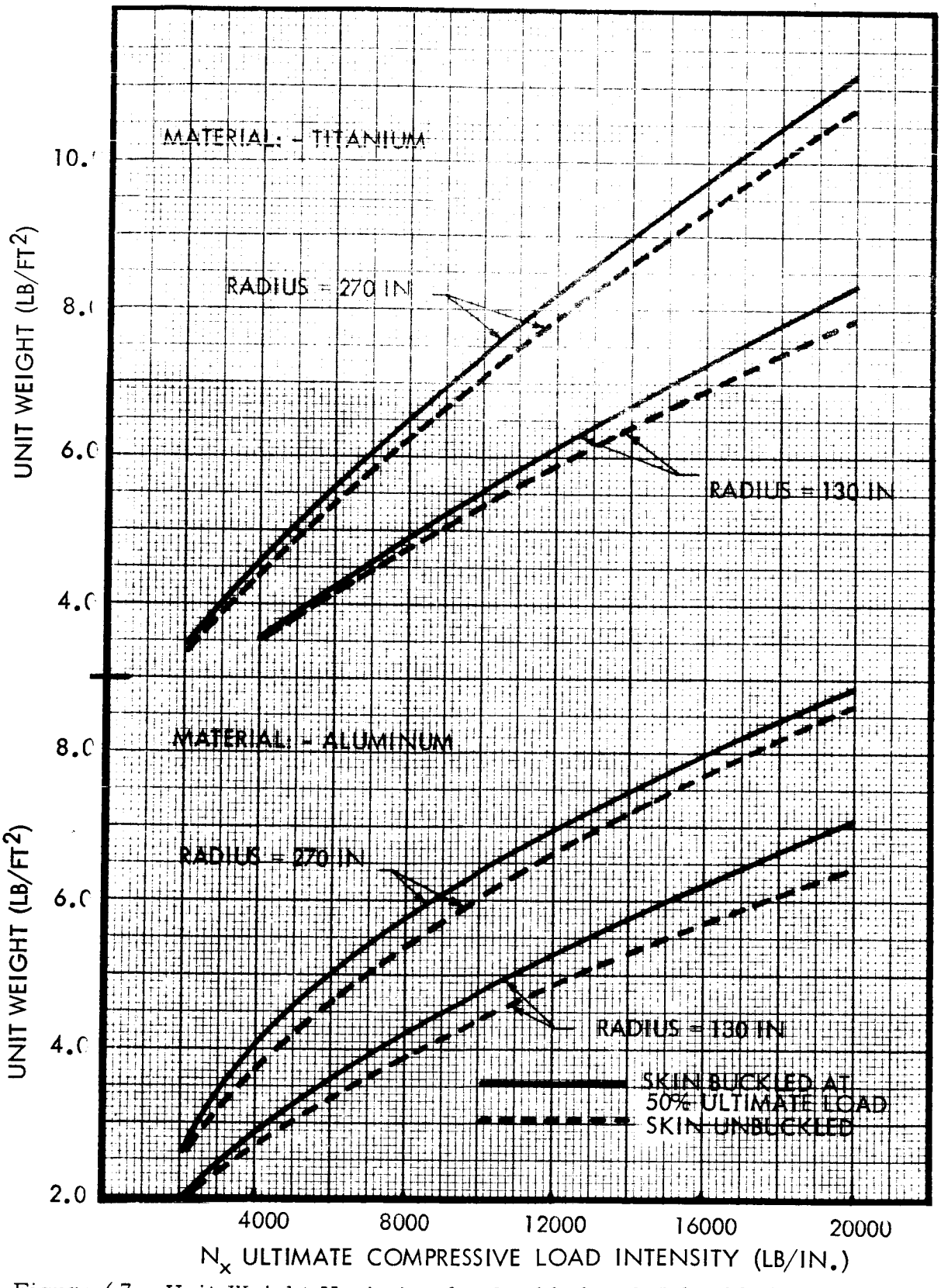



Figure 67. Unit Weight Variation for Buckled and Unbuckled Design

# ASSESSMENT

In order to obtain conclusive evidence as to where and when it is advantageous to achieve material property or construction type improvements, it is necessary to assess the effects of these improvements on specific structural components in particular vehicle systems. General conclusions cannot be drawn without citing ground rules and criteria for each case in question. To define an effective approach requires a clear definition of the merit functions upon which decisions are to be based. Three merit functions have been indicated in this report. The most obvious of these is the weight reduction which arises from a structures and materials advancement for each of the structural components in a particular vehicle system. This merit function gives a clear indication of the weight (poundwise) savings that can be directly obtained from a structural improvement.

Sometimes, the only merit function used, weight reduction per se, does not result in a true indication of the significance of the reduction. Its effect on overall system performance should be considered in terms of payload improvements resulting from the structural component weight decrease. These payload gains provide useful information for making management decisions but still do not present a complete picture. A measurement must also be included which translates the component pounds saved and the payload pounds gained into a cost index which demonstrates whether or not the advancement is economically justifiable from structures/materials standpoint.

It is true, depending upon the circumstances, that management decisions can be based on each of these merit functions by themselves; however, the objective of this study is to indicate and demonstrate a method wherein these decisions will be less limited and misleading. (Weight reduction, payload gain, and cost index are considered as a set of indexes unique to a component change in a particular vehicle base point.) Typical results are indicated, which are restricted to six vehicles selected for demonstration of the approach.

# WEIGHT MERIT FUNCTION

If the objective is only to remove a maximum number of pounds from a particular stage, weight changes from base point designs that result from material and structures improvements may give a clue as to where research effort shall be concentrated. Isolating weight as the only merit function simplifies the process. The various delta weights can then be placed in a matrix for visual comparison. In Table 37, a comparison of alternative constructions is illustrated for the current Saturn payload class vehicles using Aluminum A with various construction concepts. Basepoint weights are shown in Table 14. If the less expensive monocoque construction is employed a severe weight penalty must be paid in each shell component. Waffle construction does not appreciably change the weight picture but results in fairly severe weight penalties in the second stage forward tank wall area. Top-hat section skin-stringer appears to be favorable in the unpressurized areas, whereas in pressurized components external stringer-insulation-combinations might result in undesired complexity. The aluminum honeycomb sandwich construction appears to be superior weightwise to other aluminum constructions for all components. If, however, mere weight reduction is desired, then beryllium offers a distinct advantage if brittleness and other inherent drawbacks are ignored. From these data relative weight reductions for the same material for various construction concepts can be identified. Table 38 orders the weight changes in the same vehicle components for a honeycomb sandwich construction and for two material improvements over Aluminum A. Less percentage weight change occurs in the lightly loaded structures. Here again, weight reductions are obtained across the board with material improvement. Tables 39 and 40 illustrate the same type of weight data from the 1985 Saturn payload class vehicle. Basepoint weights are shown in Table 18. Tables 41 and 42 illustrate basic component weight changes for the alternative 30,000- to 100,000-pound payload and 1,000,000-to-2,000,000-pound payload vehicles while basepoint weights for these vehicles are illustrated in Tables 20, 22, 24, and 26, respectively. These weight data merely indicate what type and where weight reduction may be anticipated. Decisions as to their worth, with this limited data, must be made by management using additional criteria upon which to base judgments. From strictly a weight reduction standpoint, and within the limitations of the Phase I study, any material improvements are justified as are developments in bonding aluminum, titanium, and beryllium facing sheets to aluminum cores.

PAGE OF RECOMMENDATIONS IS NOT FILMED

Table 37. Component Weight Changes with Material and Construction Types (Current Saturn Payload Class Two-Stage Vehicle)—240,000-Pounds Orbital Payload

| Vehicle Stage | Weight Change from Aluminum A Integral Skin Stringer Component (lb) | | | | | |
|---|---|---|---|---|---|---|
| | Aluminum A | | | | Titanium A | Beryllium A |
| | Monocoque | Waffle | Top-Hat Skin Stringer | Honeycomb Sandwich | Honeycomb Sandwich | Honeycomb Sandwich |
| Stage 1 | | | | | | |
| Interstage | 14012 | 128 | -1243 | -4608 | -5358 | -7153 |
| Forward Skirt | 8657 | 57 | -793 | -2848 | -3233 | -4433 |
| Forward Tank Wall | 24785 | 135 | -2205 | -8775 | -10085 | -13405 |
| Center Section | 18431 | 106 | -1654 | -6089 | -6929 | -9474 |
| Aft Tank Wall | 10886 | 252 | -954 | -3514 | -4284 | -5784 |
| Aft Skirt | 8612 | -63 | -773 | -2978 | -3473 | -4588 |
| Stage 2 | | | | | | |
| Forward Skirt | 8028 | 443 | -672 | -2717 | -2852 | -3662 |
| Forward Tank Wall | 38004 | 2294 | -2996 | -12591 | -13171 | -17761 |
| Aft Tank Wall | 1266 | 66 | -74 | -394 | -434 | -589 |
| Aft Skirt | 8152 | 322 | -684 | -2278 | -2823 | -3853 |

Table 38. Component Weight Changes with Material Types (Current Saturn Payload Class Two-Stage Vehicle) — 240,000-Pound Orbital Payload — Aluminum Honeycomb Sandwich Construction

| Vehicle Stage | Weight Change from Aluminum A Integral Skin Stringer Component (lb) | | |
|---|---|---|---|
| | Aluminum A | Aluminum B | Aluminum C |
| Stage 1 | | | |
| Interstage | -4608 | -4933 | -5183 |
| Forward Skirt | -2848 | -3028 | -3188 |
| Forward Tank Wall | -8775 | -9325 | -9807 |
| Center Section | -6089 | -6484 | -6929 |
| Aft Tank Wall | -3514 | -3849 | -4149 |
| Aft Skirt | -2978 | -3233 | -3413 |
| Stage 2 | | | |
| Forward Skirt | -2717 | -2767 | -2803 |
| Forward Tank Wall | -12591 | -12881 | -12936 |
| Aft Tank Wall | -394 | -401 | -424 |
| Aft Skirt | -2278 | -2593 | -2753 |

Table 39. Component Weight Changes with Material and Construction Types 1985-Saturn Payload Class Two-Stage Vehicles—445,000 Pound Orbital Payload

| Vehicle Stage | Weight Change From Aluminum A Integral Skin Stringer Component (lb) | | | | | |
|---|---|---|---|---|---|---|
| | Aluminum A | | | | Titanium A | Beryllium A |
| | Monocoque | Waffle | Top-Hat Skin Stringer | Honeycomb Sandwich | Honeycomb Sandwich | Honeycomb Sandwich |
| Stage 1 | | | | | | |
| Interstage | 16510 | 195 | -1400 | -5220 | -6335 | -8430 |
| Forward Skirt | 9368 | 218 | -712 | -2857 | -3437 | -4607 |
| Forward Tank Wall | 32022 | -408 | -2488 | -10033 | -12018 | -16263 |
| Center Section | 19871 | 446 | -1524 | -5909 | -7299 | -9844 |
| Aft Tank Wall | 15877 | 362 | -1228 | -4638 | -5803 | -7823 |
| Aft Skirt | 9373 | 143 | -812 | -3027 | -3597 | -4757 |
| Stage 2 | | | | | | |
| Forward Skirt | 8273 | 478 | -622 | -2742 | -2922 | -3842 |
| Forward Tank Wall | 44409 | 2214 | -3036 | -14911 | -15881 | -21266 |
| Aft Tank Wall | 3539 | 159 | -206 | -1031 | -1201 | -1641 |
| Aft Skirt | 8597 | 467 | -453 | -2353 | -2838 | -3878 |

Table 40. Component Weight Changes with Material Types 1985 Saturn Payload Class Two-Stage Vehicle—445,000-Pound Orbital Payload (Aluminum Honeycomb Sandwich Construction)

| Vehicle Stage | Weight Change From Aluminum A Integral Skin Stringer Component (lb) | | |
|---|---|---|---|
| | Aluminum A | Aluminum B | Aluminum C |
| Stage 1 | | | |
| Interstage | -5220 | -5595 | -6050 |
| Forward Skirt | -2857 | -3072 | -3292 |
| Forward Tank Wall | -10033 | -11068 | -11748 |
| Center Section | -5909 | -6509 | -6904 |
| Aft Tank Wall | -4638 | -5173 | -5378 |
| Aft Skirt | -3027 | -3267 | -3462 |
| Stage 2 | | | |
| Forward Skirt | -2742 | -2827 | -2872 |
| Forward Tank Wall | -14911 | -15121 | -15811 |
| Aft Tank Wall | -1031 | -1081 | -1171 |
| Aft Skirt | -2353 | -2558 | -2718 |

Table 41. Component Weight Changes with Material and Construction Types—Weight Change from Aluminum A Integral Skin-Stringer Component (Pounds)—Medium Range Payload Class Vehicles

| Vehicle Stage | Current - 30,000-Pound Payload | | | | 1985 - 100,000-Pound Payload | | | |
|---|---|---|---|---|---|---|---|---|
| | Top-Hat Skin Stringer | Honeycomb Sandwich | | | Top-Hat Skin Stringer | Honeycomb Sandwich | | |
| | Al A | Al A | Ti A | Be A | Al A | Al A | Ti A | Be A |
| Stage 1 | | | | | | | | |
| Interstage | -12 | -865 | -918 | -1185 | -359 | -1869 | -2078 | -2598 |
| Forward Skirt | -23 | -818 | -876 | -1144 | -244 | -1611 | -1718 | -2199 |
| Forward Tank Wall | -96 | -268 | -428 | -616 | -354 | -573 | -780 | -1145 |
| Center Section | -65 | -1847 | -1923 | -2467 | -506 | -2966 | -3709 | -4774 |
| Aft Tank Wall | -5 | -23 | -27 | -36 | —— | —— | —— | —— |
| Aft Skirt | -48 | -824 | -880 | -1120 | -248 | -1557 | -2440 | -2778 |
| Stage 2 | | | | | | | | |
| Forward Skirt | -47 | -420 | -444 | -620 | -138 | -7 | -735 | -1062 |
| Forward Tank Wall | -121 | -580 | -1129 | -1597 | -1440 | -1648 | -2243 | -2337 |
| Aft Tank Wall | -2 | -17 | -30 | -43 | -95 | -105 | -178 | -191 |
| Aft Skirt | -76 | -406 | -438 | -603 | -221 | -670 | -798 | -846 |

Table 42. Component Weight Changes with Material and Construction Types—Weight Change from Aluminum A Integral Skin-Stringer Component (Pounds)—Post-Saturn Payload Class Vehicles

| Vehicle Stage | Current - 1,000,000-Pound Payload | | | | 1985 - 2,000,000-Pound Payload | | | |
|---|---|---|---|---|---|---|---|---|
| | Top-Hat Skin Stringer | Honeycomb Sandwich | | | Top-Hat Skin Stringer | Honeycomb Sandwich | | |
| | Al A | Al A | Ti A | Be A | Al A | Al A | Ti A | Be A |
| Stage 1 | | | | | | | | |
| Interstage | -11142 | -20354 | -28973 | -40266 | -14586 | -26054 | -41306 | -57793 |
| Forward Skirt | -5911 | -10964 | -15111 | -20487 | -5951 | -10616 | -16830 | -23445 |
| Forward Tank Wall | -15377 | -35709 | -34064 | - | -21452 | -45186 | -45534 | - |
| Center Section | -12747 | -24128 | -33178 | -44634 | -11779 | -21056 | -33264 | -47805 |
| Aft Tank Wall | -4550 | -15068 | -13666 | -19630 | -10278 | -21704 | -21698 | -28732 |
| Aft Skirt | -5084 | -15164 | -18163 | -23538 | -6312 | -9896 | -16515 | -22345 |
| Stage 2 | | | | | | | | |
| Forward Skirt | -1471 | -8018 | -8558 | -11360 | -1754 | -7919 | -8859 | -11748 |
| Forward Tank Wall | -35601 | -49257 | -49274 | -76256 | -58226 | -77267 | -88300 | -131090 |
| Aft Tank Wall | -5603 | -6516 | -8543 | -10578 | -12235 | -18317 | -20276 | -25240 |
| Aft Skirt | -1290 | -4978 | -6780 | -10686 | -2645 | -4962 | -7080 | -11627 |

Stress analysis results in a definition of the basic shell requirements while the weight of the component must include complexity factors to assess weight resulting from material tolerances, section closeouts, joining, fabrication techniques, etc. In most standard construction types, where enough historical data is available, these weight factors can be assessed as a percentage increment in component weight. For example, in the advanced titanium tankage parametric study (Reference 1), weight complexity factors of 10 percent were assessed to aluminum and titanium honeycomb sandwich shells for the upper stages of the vehicle system. This percentage was verified by the final full-scale stage design. In the lower stage this factor was increased to 12 percent. Aluminum skin-stringer factors were 8 percent for upper stages and 10 percent for lower stages while the titanium skin-stringer structure was similar to the sandwich. A survey of the Saturn V launch vehicle weight data confirms these assumptions. Because detail design points for beryllium structures are not available an estimate was included in the parametric synthesis phase of this study for all designs.

Cost also influences the weight complexity factor; for example, the cost of selecting particular sheet stock to meet minimum gage tolerances, or the cost of obtaining larger stock sizes to lessen joint weight penalties. In this study a medium complexity factor was selected for all structures typical of current Saturn V technology.

The estimated cylindrical shell weight complexity factors included in the parametric synthesis step of this study are as follows:

| Construction Type | Weight Complexity Factor (%) | |
|---|---|---|
| | Stage 1 | Upper Stages |
| Monocoque: | | |
| Aluminum | 8 | 7 |
| Titanium | 10 | 10 |
| Beryllium | 10 | 10 |
| Steel | 8 | 7 |
| Skin Stringer: | | |
| Aluminum | 10 | 8 |
| Titanium | 12 | 10 |
| Beryllium | 12 | 10 |
| Steel | 10 | 8 |

| Construction Type | Weight Complexity Factor (%) | |
|---|---|---|
| | Stage 1 | Upper Stages |
| Waffle: | | |
| Aluminum | 10 | 8 |
| Titanium | 12 | 10 |
| Beryllium | 12 | 10 |
| Steel | 10 | 8 |
| Honeycomb Sandwich: | | |
| Aluminum | 12 | 10 |
| Titanium | 12 | 10 |
| Beryllium | 14 | 12 |
| Steel | 12 | 10 |

These factors were not introduced in the structural design synthesis study and are not reflected in the basic shell data incorporated in that section; however, they were included in the assessment and mass fraction operations in this study. These factors were used in a study where conclusions are drawn from relative weight comparisons. Many unknowns can creep into the weight picture, during the hardware design phases, which result in increased weight complexity. However, in this study, it is assumed that these unknowns will influence each construction type to the same relative degree and therefore not change the basic comparative conclusions.

## PAYLOAD WEIGHT CHANGES

The second merit function is the equivalent payload gained from a structural component weight reduction. Weight savings in the uppermost stage in a launch vehicle system, though smaller in magnitude than in the lower stages, potentially result in a larger payload improvement. In most systems, a pound saved in upper stage structural weight is a pound gain in payload weight. In a typical three-stage system such as the Saturn V the lower stage has an exchange ratio ranging near 1/12 to 1. For every 12 pounds in structural weight saved the payload can be increased by 1 pound. The middle stage is in the range of 1/2 to 1/4 to 1.

Table 43 shows the equivalent payload gains for the current Saturn payload class vehicle (240,000-pound payload) with some component changes in material and construction. Stage two parameters are a direct reflection of the weight changes shown in Table 37. The waffle constructions show little merit Again, in the upper stages, honeycomb sandwich constructions demonstrate significant gains; however, honeycomb sandwich in pressurized structures, especially in cryogenic tankages, present leakage and purging problems as well as insulation installation effects upon tankage fabrication. The weights of hardware sandwich components (e.g., the aluminum honeycomb sandwich instrumentation unit of the Saturn V) have been appreciably increased due to the inability to perfect methods of closeout and attachments, without resorting to large masses of potting material within the core. Also, in some lightly loaded configurations the two bond lines can outweigh the facing sheets. In this study, a nominal value for material tolerances, closeouts, potting, joining, and secondary structure was fixed at about 10 percent for aluminum honeycomb sandwich with a core thickness of from 1-1/2 to 3 inches. In deeper core honeycomb, the maintenance of this tolerance would require good design practices.

The current stable of launch vehicles will probably be utilized for some time into the future, and, in the case of earth orbital support operations, significant research into solving the structural complexity problems (bonding, joinings, etc.) of honeycomb sandwich appear desirable from a weight and payload performance standpoint. However, these merit functions must be compared with a cost index before a logical decision can be reached.

PRECEDING PAGE BLANK NOT FILMED

Table 43. Payload Merit Functions for Current Two-Stage Saturn Class Vehicles (240,000-Pound Payload)

| Vehicle Stage | Change in Payload Weight (pounds) | | | | | | |
|---|---|---|---|---|---|---|---|
| | Top-Hat | Honeycomb | Waffle | Honeycomb | Honeycomb | Honeycomb | Honeycomb |
| | Al A | Al A | Al A | Al B | Al C | Ti A | Be A |
| Stage 1 | | | | | | | |
| Aft Skirt | 70 | 271 | 6 | 294 | 310 | 316 | 417 |
| Aft Tank Wall | 87 | 319 | -23 | 350 | 377 | 389 | 526 |
| Center Section | 150 | 554 | -10 | 589 | 630 | 630 | 861 |
| Forward Tank Wall | 200 | 798 | -12 | 848 | 892 | 917 | 1219 |
| Forward Skirt | 72 | 259 | -5 | 275 | 290 | 294 | 403 |
| Interstage | 113 | 419 | -12 | 448 | 471 | 487 | 650 |
| Stage 2 | | | | | | | |
| Aft Skirt | 648 | 2278 | -322 | 2593 | 2753 | 2823 | 3853 |
| Aft Tank Wall | 74 | 394 | -66 | 401 | 424 | 434 | 589 |
| Forward Tank Wall | 2996 | 12591 | -2294 | 12881 | 12936 | 13171 | 17761 |
| Forward Skirt | 672 | 2717 | -443 | 2767 | 2803 | 2852 | 3662 |

## COST MERIT FUNCTION

Another merit function that is a good indicator of any subsystem performance is its cost index. The total cost of a structural component is composed of several contributing factors: development, production (fabrication, tooling and equipment) and testing (static and flight vehicles). For this study, where all components were compared to a base point design, it was assumed that the development and testing costs were identical for both the improved component and the base point design; therefore, the only cost differences considered between the two structural components were production costs. The cost figure of merit is the cost difference between the improved and base point designs and the relative payload gained, and uses an index of dollars per pound in orbit for the ordering effectiveness

$$CR = \frac{(\$_{PRODUCTION})_{ADVANCE} - (\$_{PRODUCTION})_{BASEPOINT}}{(W_{PAYLOAD})_{ADVANCE} - (W_{PAYLOAD})_{BASEPOINT}}$$

An approach to the cost estimating for the structural components is given in Reference 27 and used in Reference 1. One of the basic principles in the aerospace industry of cost estimating for the structural components is that the cost of an item to be built can be determined by an analysis of the costs of analogous items that have been built. For cost estimating of advanced launch vehicle systems, available data from current systems is used. However, when the systems proposed for these future vehicles differ greatly in basic vehicle characteristics, such as vehicle size, weight, type of construction, and material, difficulties arise because of lack of identical historical background data. Estimating relationships must be established which go beyond the limits of the data available.

In the aircraft industry airframe weight has been used as the basis for cost estimating, but various other vehicle characteristics could readily be used. Examples of these characteristcs include vehicle total liftoff weight, propellant volume of weight, stage size, stage burnout weight, or a combination of these parameters in order to include additional stage criteria with the costing weights.

The approach adopted in this study was to use a cost-per-pound, or hours-per-pound, as the relationship between cost and the stage structural weight. Values of cost-per-pound used are not constant for all vehicle systems and have a scaling factor introduced to account for the relative weights and sizes of the components (Reference 28). Even with such an

adjustment for the weight difference, use of only component weight could be erroneous. Allowances have to include the effects of fabrication complexity due to the various types of construction and material. An array of complexity factors for fabrication, tooling and equipment was discussed in the Parametric Synthesis section of this report. The basic empirical relationship for costing the structural component is per Reference 16. A review of the complexity factors contained in the cost effectvity report (Reference 16) indicated that those presented by S&ID in the Parametric Synthesis section of this report were in fair agreement except in the area of titanium structures. Table 44 presents a comparison of these two sets of manufacturing complexity factors. These relationships were derived from costing data for the Saturn V stages by applying a best-fit curve to their normalized costs.

$$Y = CF\,(4619(X)^{-0.322})$$

where

Y = First unit airframe cost in dollars per pound of weight adjusted for complexity

CF = Total complexity factor of structural component

X = Component weight

Added to this fabrication cost is the material cost which, in the case of beryllium, is significant. Figure 68 illustrates the first unit component cost as a function of component weight for several construction concepts and material costs. Costs for titanium were assumed to be 30 dollars per pound and beryllium costs were 200 dollars per pound for currently procured material. This cost is assumed to decrease to 20 dollars per pound for beryllium during the 1985 period as shown in Figure 69. This projected material cost was assumed in order to investigate its effect on the overall fabrication cost of the components. Figure 70 shows that the predominant factor in defining the cost of beryllium structures is the complexity factor associated with its fabrication, and material cost is a second order effect using the cost approach discussed above. The future cost assumed for beryllium was extremely optimistic and was used only to investigate a large cost spectrum.

One of the most influential factors on production cost is the effect of experience gained from quantity production. In fabrication of components for large boost vehicles, the production quantities remain in that portion of the learning experience curve when the improvement rate per unit is relatively high. Reference 28 defines the experience curve by

Table 44. Manufacturing Complexity Factors — S&ID and Lockheed

| S&ID* | | | | | | | | | |
|---|---|---|---|---|---|---|---|---|---|
| Material | AL | TI | BE | AL | TI | BE | AL | TI | BE |
| Construction | Fabrication | | | Tooling | | | Equipment | | |
| Internal Stiffeners | 1.05 | 1.73 | 3.50 | 1.00 | 1.70 | 2.50 | 1.00 | 1.50 | 3.50 |
| Attached Stiffeners | 0.90 | 1.40 | 3.50 | 0.95 | 1.20 | 2.50 | 0.85 | 1.20 | 3.50 |
| Waffle | 1.15 | 1.75 | 3.70 | 1.00 | 1.70 | 2.50 | 1.10 | 1.50 | 3.50 |
| Bonded Honeycomb | 1.50 | 1.80 | 4.00 | 1.50 | 1.70 | 2.50 | 1.20 | 1.50 | 3.50 |

| LOCKHEED | | | | | |
|---|---|---|---|---|---|
| Material | Aluminum | Magnesium and Stainless Steel | Titanium | GFW René 41 INCO 718 | Lockalloy |
| Construction | Fabrication | | | | |
| Monocoque | 0.6 | 1.0 | 1.6 | 1.6 | 1.8 |
| Skin-Ring Stringer | 1.0 | 1.7 | 2.6 | 2.7 | 3.0 |
| Integrally or Corrugation Stiffened | 1.3 | 2.2 | 3.4 | 3.5 | 3.9 |
| Honeycomb Sandwich | 1.6 | 2.7 | 4.2 | 4.3 | 4.8 |
| Truss Core Sandwich | 1.8 | 3.1 | 4.7 | 4.9 | 5.4 |

*The base factor 1.0 is an aluminum skin-stringer construction typical of the Saturn S-II manufacturing program as discussed in the parametric synthesis section of this report.

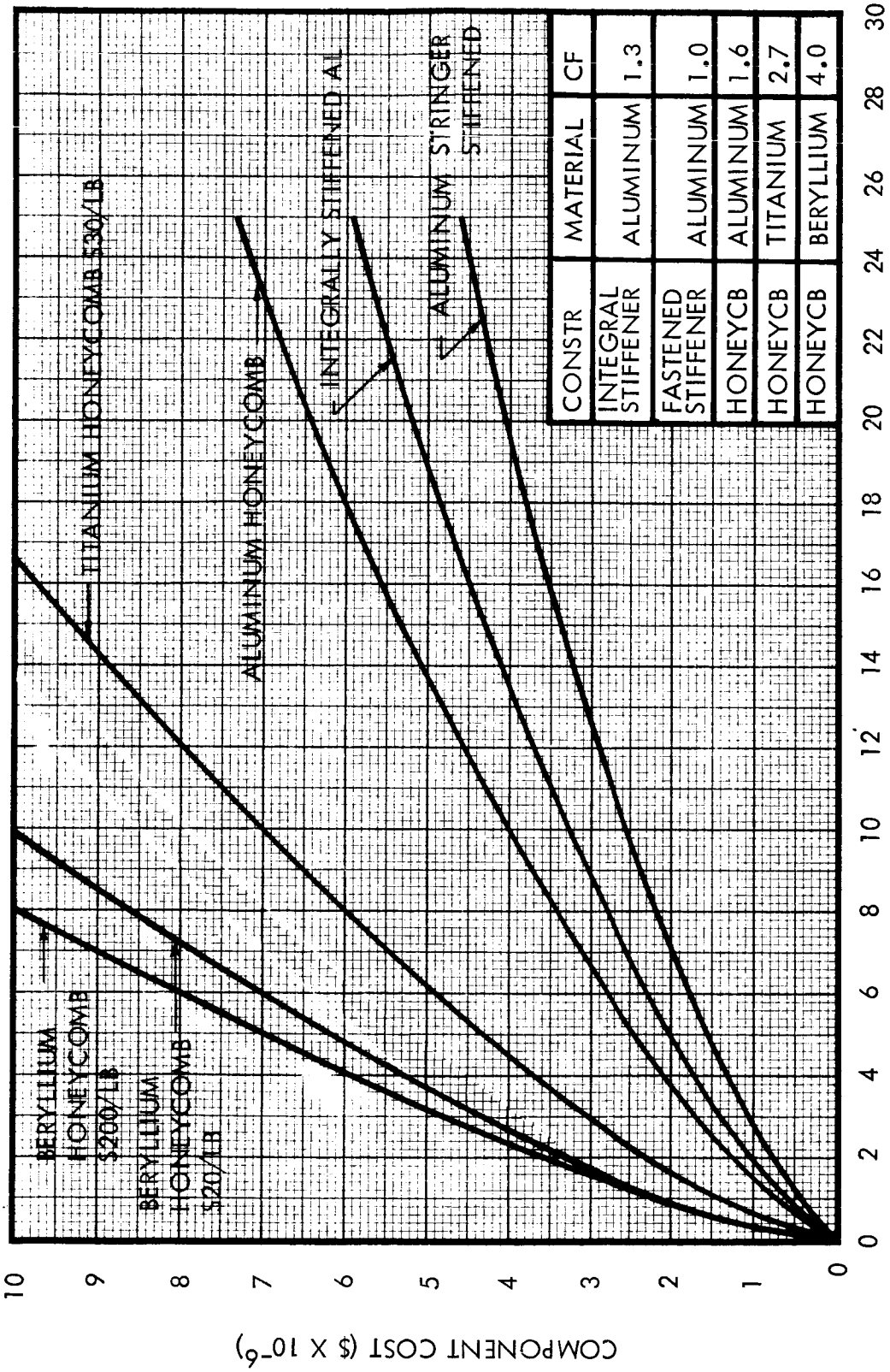



Figure 68. Component Cost Variation With Weight

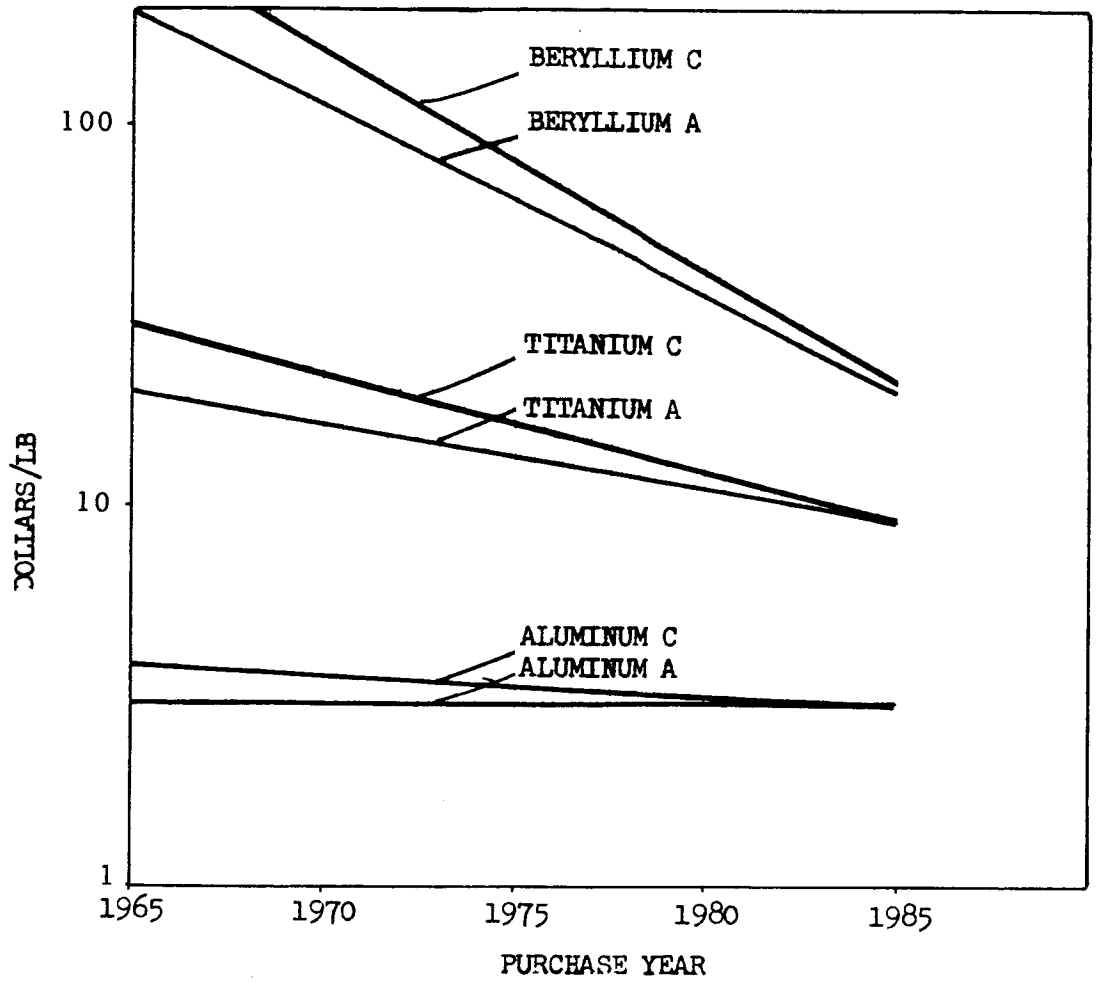



Figure 69. Estimated Material Cost with Year

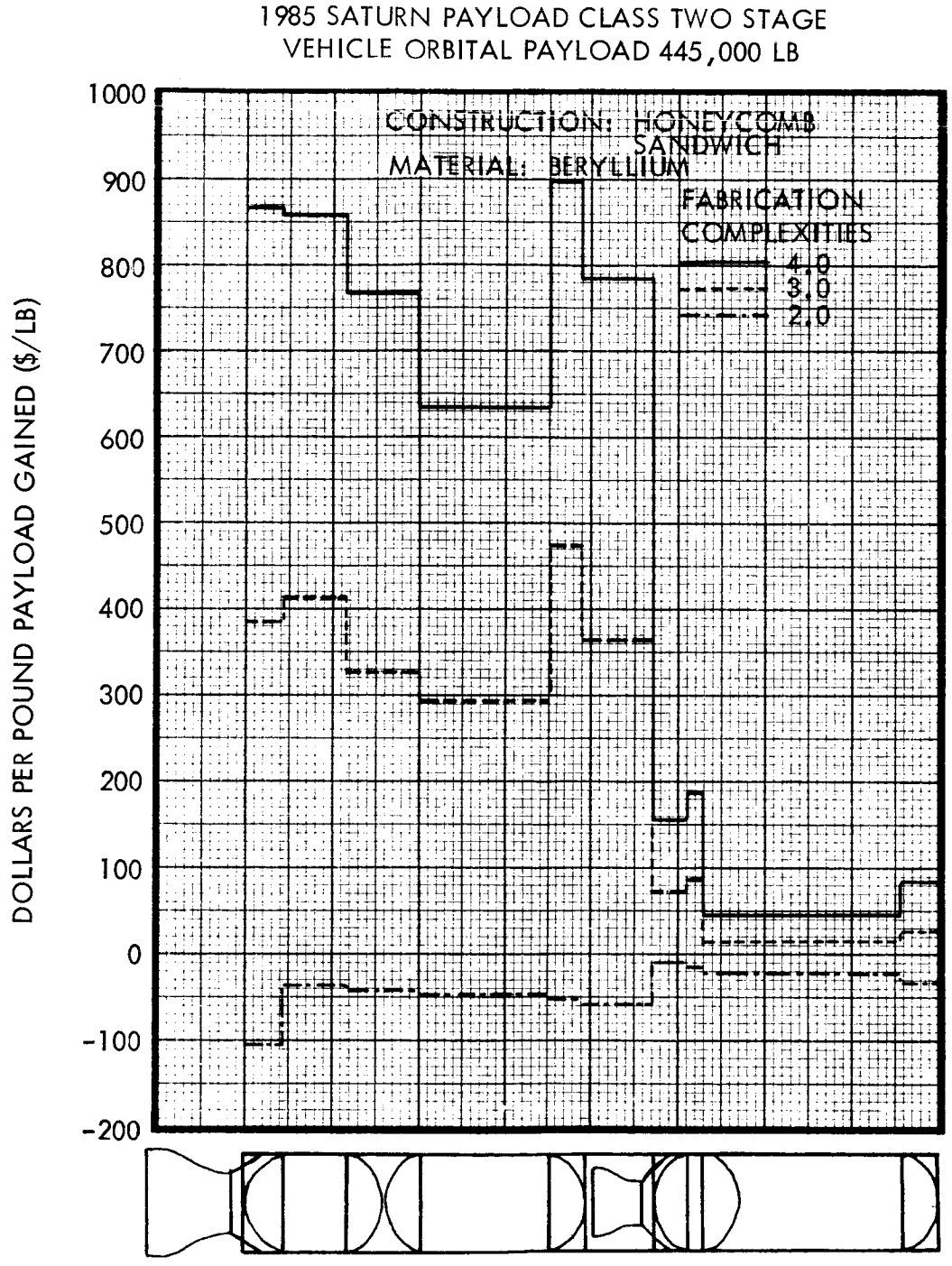



Figure 70. Comparison of Construction Complexity Factors

$$K_{exp} = A X^{-B}$$

where

A, B = Constants, values of which are selected to express appropriately the relation for a specific situation

$K_{exp.}$ = Adjustment factor based on experience

X = Consecutive number of a specific production unit

It has been found that the unit cost decreases for the experience curve by a constant factor as the number of consecutive production units is doubled. This constant factor is referred to as the "percent learning," (P); which for this study was 85 percent. The relationship between learning, (P), and the constant B of the experience curve is

$$P = 2^{-B}(100).$$

Total structural cost for the structural component is defined as

$$\text{Cost} = YX K_{exp} + X \$_{MAT}$$

where

$\$_{MAT}$ = dollars per pound for material stock

A digital program for the costing was developed using the preceding approach which systematically considered the effects of numerous construction and material improvements on each and every structural component for the family of base point vehicles. The cost merit functions are identified for the individual components. Each material and structural change from the base point design was considered to apply to the total vehicle simultaneously for reasons of computer time economy; however, this change could have reflected a single component. The costing approach discussed was finally adopted after several preliminary techniques were considered and their results examined and found to be unrealistic.

An attempt was made to break down the costing into recurring costs (fabrication and material) and nonrecurring costs (tooling, equipment, etc.). This method did not account for the weight scaling factor in the cost-per-pound of airframe and it could not be included since the required individual adjustment factors associated with fabrication, tooling, and equipment were not readily available. With the costs broken into these areas, a learning

curve was applied to the fabrication cost and a progressive maintenance curve was considered for the tooling and equipment. Also, the unit production rate can be assessed by including the number of sets of tools required to meet a specific number of units. It appears that this method would be an improvement from the one included in this phase of the study.

Figure 71 presents an engineering FORTRAN logic working sketch for this subroutine where the following input nomenclature is used:

ST = Number of Stages

WPAY = Payload Weight (lb)

FAB = Hours/Pound Fabrication for Aluminum Skin-Stringer

TOL = Hours/Pound Tooling for Aluminum Skin-Stringer

HEE = Hours/Pound Equipment for Aluminum Skin-Stringer

ENNU = Number of Sets of Units to be Investigated

YSTOP = Year Production Stops

YSTART = Year Production Starts

PFAB = Slope of Fabrication Learning Curve

PTOL = Slope of Tooling Sustaining Curve

PE = Slope of Equipment Sustaining Curve

COSTH = Dollar Cost Per Manhour

C = Number of Components Per Stage

TEST = Number of Test Vehicles

W(i, j) = Component Weight for $i^{th}$ Stage and $j^{th}$ Component

HR(i, j) = RDT/E Hours for $i^{th}$ Stage and $j^{th}$ Component

PER(i) = Payload Exchange Ratio for $i^{th}$ Stage

CFFAB = Complexity Factor Fabrication

CFTOL = Complexity Factor Tooling

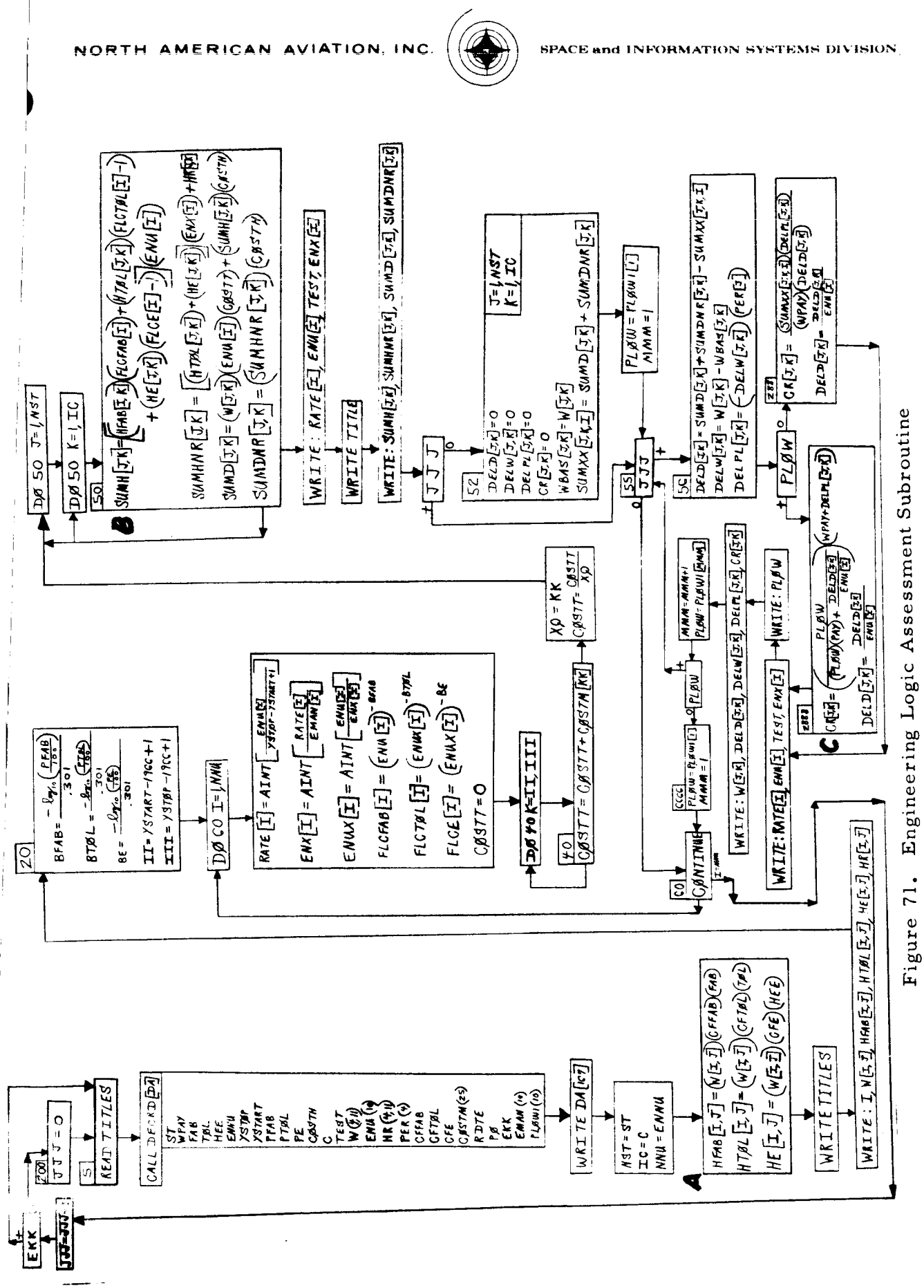



Figure 71. Engineering Logic Assessment Subroutine

CFE = Complexity Factor Equipment

COSTM(KK) = Material Costs as a Function of Year KK = 1, 25

RDTE = RDT/E Indicator

PO = Printing Indicator

EKK = Data Read Indicator

EMAN(i) = Maximum Manufacturing Rate/Year for a Tool/Equip Set

PLOW(i) = Payload Worth in Dollars Per Pound, if Desired

DELD is the component delta dollars over the base point, DELW is component delta weight, DELPL is payload delta weight, and CR is the resultant cost ratio.

The method finally used in this study eliminated the hours for fabrication, tooling and equipment in block A (Figure 71) and substituted the learning coefficients from Reference 12 adjusted to the best-fit data previously discussed in this section. This resulted in calculating only dollar sums in block B of Figure 71 as affected by the fabrication learning curve. The final cost merit function (CR) was then computed (instead of block C, Figure 71) by dividing delta dollars per component by delta pounds of payload per component. Figure 71 is presented here to generally illustrate the attempted approaches. Scaling factors to account for component size, per Reference 22, are required for fabrication, tooling and equipment to permit use of the initial cost model per Figure 71.

An examination of the cost ratios developed for the base point vehicles clearly indicated that further study should be devoted to the development of a more realistic cost model and the pertinent costing factors that are involved in this model. (See Reference 29.) In order to fully understand the fundamental significance of the relative cost ratios and deduce a meaningful interpretation of the results, the basic assumptions that are inherent in the cost model have to be known. If only the cost changes involved with the fabrication of the structural component are considered, and these costs are translated into dollars per pound of payload in orbit, the resulting magnitude of the cost ratios could be misleading. This is due to several significant factors that have not been considered, such as costs of research, development, testing, flight vehicles, etc. The true value of these ratios can be derived by comparing the cost ratios and obtaining a relative ordering of significance. Even with an ordering of cost ratios, a misunderstanding is present if a cost ratio associated with a small vehicle system is compared in magnitude to that obtained from a large vehicle system. A series of cost

ratios unique to a specific vehicle system can be compared to define the relative significance of the various structures and materials improvements when applied to that vehicle system.

The output of the computer program displays a listing of all three types of merit functions to allow assessment of the beneficial changes in the vehicle system parameters resulting from the various types of structures and materials improvements. Weight and cost data for the base point vehicles are shown in Tables 45 through 50. Examples of the merit functions for the base point vehicles and various improvements are given in Tables 51 through 56. Tables 51 through 56 show that major increases in payload capability are obtained by improvements in the upper stage of the two stage vehicles for a given material improvement considered throughout the vehicle. The structural weight reduction of the components is far greater in the lower stage. The payload benefits are derived more from the upper stages and the study cost ratio of dollars per pound of payload are most significant for the upper stages.

Selections of cost ratios for a future Saturn payload class two-stage vehicle with 445,000-pound payload capability are illustrated in Figures 70 and 72 for changes in construction, material, compressive yield, and complexity factors. Variations of these cost ratios for the different components throughout the vehicle length are illustrated in Figure 72, which shows that improvements of 10 percent and 20 percent in the compressive yield stress of aluminum honeycomb sandwich decrease the magnitude of the cost ratio, which is beneficial. There are large variations of the cost ratios for all components of the first stage with material improvement, while the upper stage is insensitive. The negative cost ratio obtained is due to the top-hat skin stringer component costing less than the base point concept of integral stiffeners. Their complexity factors are 0.90 and 1.05, respectively. It was assumed that the fabrication complexity did not alter with material property improvement. There was, however, a slight increase in the material cost which is insignificant. Figure 72 also indicates that top-hat stiffeners have a better cost ratio than honeycomb sandwich. This latter concept is identical in cost to the integral stiffeners but has a large payload improvement. The largest payload improvements were obtained from beryllium honeycomb which also produced the most adverse cost ratio.

The difference in total component cost for the titanium and aluminum honeycomb sandwich is significant when compared with the payload improvements. Cost ratios for the beryllium, based upon the fabrication complexity of 4.0, are appreciably higher than the other two materials. If the complexity factor is progressively reduced, per Figure 70, the cost ratio is drastically changed and is competitive with the base point for a factor of 2.0. Most of the cost ratios obtained indicated that the values associated with the first stage

## Table 45. Component Weights and Costs, Current Saturn Payload Class Vehicle (240,000 lbs Orbital Payload)

| STAGE | COMPONENT | ALUMINUM A INTEGRAL SKIN STRINGER WEIGHT PER UNIT | ALUMINUM A INTEGRAL SKIN STRINGER DOLLARS PER UNIT | BERYLLIUM A HONEYCOMB SANDWICH WEIGHT PER UNIT | BERYLLIUM A HONEYCOMB SANDWICH DOLLARS PER UNIT |
|---|---|---|---|---|---|
| 1 | INTERSTAGE | 0.19615E 05 | 0.10009E 07 | 0.35350E 04 | 0.18008E 07 |
| | FWD SKIRT | 0.56302E 04 | 0.72464E 06 | 0.22050E 04 | 0.13076E 07 |
| | FWD TANKWALL | 0.19629E 05 | 0.10111E 07 | 0.62200E 04 | 0.26614E 07 |
| | CENTER SECTION | 0.14364E 05 | 0.12241E 07 | 0.49100E 04 | 0.22501E 07 |
| | AFT TANKWALL | 0.39290E 04 | 0.82270E 06 | 0.32450E 04 | 0.16392E 07 |
| | AFT SKIRT | 0.65862E 04 | 0.72585E 06 | 0.20800E 04 | 0.12569E 07 |
| 2 | FWD SKIRT | 0.50170E 04 | 0.59935E 06 | 0.13550E 04 | 0.93925E 06 |
| | FWD TANKWALL | 0.24041E 05 | 0.17341E 07 | 0.62800E 04 | 0.26587E 07 |
| | AFT TANKWALL | 0.87400E 03 | 0.18323E 06 | 0.28500E 03 | 0.32662E 06 |
| | AFT SKIRT | 0.57030E 04 | 0.65376E 06 | 0.18500E 04 | 0.11609E 07 |

| STAGE | COMPONENT | ALUMINUM A TOP HAT SKIN STRINGER WEIGHT PER UNIT | ALUMINUM A TOP HAT SKIN STRINGER DOLLARS PER UNIT | ALUMINUM B HONEYCOMB SANDWICH WEIGHT PER UNIT | ALUMINUM B HONEYCOMB SANDWICH DOLLARS PER UNIT |
|---|---|---|---|---|---|
| 1 | INTERSTAGE | 0.94450E 04 | 0.78890E 06 | 0.57550E 04 | 0.93971E 06 |
| | FWD SKIRT | 0.58450E 04 | 0.56979E 06 | 0.36100E 04 | 0.68497E 06 |
| | FWD TANKWALL | 0.17420E 05 | 0.11947E 07 | 0.10300E 05 | 0.13944E 07 |
| | CENTER SECTION | 0.12730E 05 | 0.96585E 06 | 0.78000E 04 | 0.11449E 07 |
| | AFT TANKWALL | 0.80750E 04 | 0.70938E 06 | 0.51800E 04 | 0.87498E 06 |
| | AFT SKIRT | 0.58950E 04 | 0.57309E 06 | 0.34350E 04 | 0.66228E 06 |
| 2 | FWD SKIRT | 0.43450E 04 | 0.44601E 06 | 0.22500E 04 | 0.49712E 06 |
| | FWD TANKWALL | 0.21045E 05 | 0.13581E 07 | 0.11160E 05 | 0.14723E 07 |
| | AFT TANKWALL | 0.80000E 03 | 0.14795E 06 | 0.47300E 03 | 0.17268E 06 |
| | AFT SKIRT | 0.50550E 04 | 0.51637E 06 | 0.31100E 04 | 0.61912E 06 |

| STAGE | COMPONENT | ALUMINUM A HONEYCOMB SANDWICH WEIGHT PER UNIT | ALUMINUM A HONEYCOMB SANDWICH DOLLARS PER UNIT | ALUMINUM C HONEYCOMB SANDWICH WEIGHT PER UNIT | ALUMINUM C HONEYCOMB SANDWICH DOLLARS PER UNIT |
|---|---|---|---|---|---|
| 1 | INTERSTAGE | 0.60800E 04 | 0.97537E 06 | 0.55050E 04 | 0.91184E 06 |
| | FWD SKIRT | 0.37900E 04 | 0.70795E 06 | 0.34500E 04 | 0.66424E 06 |
| | FWD TANKWALL | 0.10850E 05 | 0.14445E 07 | 0.98180E 04 | 0.13408E 07 |
| | CENTER SECTION | 0.82950E 04 | 0.12040E 07 | 0.74550E 04 | 0.11200E 07 |
| | AFT TANKWALL | 0.55150E 04 | 0.91296E 06 | 0.48800E 04 | 0.84029E 06 |
| | AFT SKIRT | 0.36900E 04 | 0.69523E 06 | 0.32550E 04 | 0.63855E 06 |
| 2 | FWD SKIRT | 0.23000E 04 | 0.50459E 06 | 0.22140E 04 | 0.49171E 06 |
| | FWD TANKWALL | 0.11450E 05 | 0.14981E 07 | 0.11105E 05 | 0.14674E 07 |
| | AFT TANKWALL | 0.48000E 03 | 0.17441E 06 | 0.45000E 03 | 0.16694E 06 |
| | AFT SKIRT | 0.34250E 04 | 0.66097E 06 | 0.29500E 04 | 0.59734E 06 |

| STAGE | COMPONENT | TITANIUM A HONEYCOMB SANDWICH WEIGHT PER UNIT | TITANIUM A HONEYCOMB SANDWICH DOLLARS PER UNIT | ALUMINUM A WAFFLE WEIGHT PER UNIT | ALUMINUM A WAFFLE DOLLARS PER UNIT |
|---|---|---|---|---|---|
| 1 | INTERSTAGE | 0.53300E 04 | 0.10705E 07 | 0.10560E 05 | 0.10873E 07 |
| | FWD SKIRT | 0.34050E 04 | 0.79002E 06 | 0.66950E 04 | 0.79827E 06 |
| | FWD TANKWALL | 0.95400E 04 | 0.15885E 07 | 0.19490E 05 | 0.16473E 07 |
| | CENTER SECTION | 0.74550E 04 | 0.13440E 07 | 0.14490E 05 | 0.13474E 07 |
| | AFT TANKWALL | 0.47450E 04 | 0.98936E 06 | 0.92850E 04 | 0.90643E 06 |
| | AFT SKIRT | 0.31950E 04 | 0.75665E 06 | 0.66050E 04 | 0.79098E 06 |
| 2 | FWD SKIRT | 0.21650E 04 | 0.58117E 06 | 0.54600E 04 | 0.69519E 06 |
| | FWD TANKWALL | 0.10870E 05 | 0.17355E 07 | 0.26335E 05 | 0.20203E 07 |
| | AFT TANKWALL | 0.44000E 03 | 0.19730E 06 | 0.94000E 03 | 0.21090E 06 |
| | AFT SKIRT | 0.28800E 04 | 0.70523E 06 | 0.60250E 04 | 0.74319E 06 |

## Table 46. Component Weights and Costs, 1985 Saturn Payload Class Vehicle (445,000 lbs Orbital Payload)

| STAGE | COMPONENT | WEIGHT PER UNIT | DOLLARS PER UNIT | WEIGHT PER UNIT | DOLLARS PER UNIT |
|---|---|---|---|---|---|
| | | ALUMINUM A INTEGRAL SKIN STRINGER | | BERYLLIUM A HONEYCOMB SANDWICH | |
| 1 | INTERSTAGE | 0.12975E 05 | 0.11415E 07 | 0.45450E 04 | 0.21353E 07 |
| | FWD SKIRT | 0.71870E 04 | 0.76475E 06 | 0.25800E 04 | 0.14546E 07 |
| | FWD TANKWALL | 0.24093E 05 | 0.17799E 07 | 0.87200E 04 | 0.33214E 07 |
| | CENTER SECTION | 0.15304E 05 | 0.12812E 07 | 0.55420E 04 | 0.24420E 07 |
| | AFT TANKWALL | 0.12293E 05 | 0.10998E 07 | 0.44630E 04 | 0.21091E 07 |
| | AFT SKIRT | 0.71420E 04 | 0.76150E 06 | 0.23850E 04 | 0.13721E 07 |
| 2 | FWD SKIRT | 0.51970E 04 | 0.61385E 06 | 0.13550E 04 | 0.93335E 06 |
| | FWD TANKWALL | 0.28726E 05 | 0.19566E 07 | 0.74600E 04 | 0.32879E 07 |
| | AFT TANKWALL | 0.24810E 04 | 0.37182E 06 | 0.84000E 03 | 0.67260E 06 |
| | AFT SKIRT | 0.59730E 04 | 0.67459E 06 | 0.20950E 04 | 0.12430E 07 |
| | | ALUMINUM A TOP HAT SKIN STRINGER | | ALUMINUM B HONEYCOMB SANDWICH | |
| 1 | INTERSTAGE | 0.11575E 05 | 0.90553E 06 | 0.73800E 04 | 0.11123E 07 |
| | FWD SKIRT | 0.64750E 04 | 0.61074E 06 | 0.41150E 04 | 0.74956E 06 |
| | FWD TANKWALL | 0.22495E 05 | 0.14209E 07 | 0.13915E 05 | 0.17209E 07 |
| | CENTER SECTION | 0.13863E 05 | 0.10232E 07 | 0.98750E 04 | 0.12605E 07 |
| | AFT TANKWALL | 0.11055E 05 | 0.87774E 06 | 0.71100E 04 | 0.10846E 07 |
| | AFT SKIRT | 0.63300E 04 | 0.60143E 06 | 0.38750E 04 | 0.71967E 06 |
| 2 | FWD SKIRT | 0.45750E 04 | 0.48259E 06 | 0.23700E 04 | 0.51495E 06 |
| | FWD TANKWALL | 0.25690E 05 | 0.15547E 07 | 0.13605E 05 | 0.16840E 07 |
| | AFT TANKWALL | 0.22750E 04 | 0.30052E 06 | 0.14000E 04 | 0.36338E 06 |
| | AFT SKIRT | 0.55200E 04 | 0.54811E 06 | 0.34150E 04 | 0.65966E 06 |
| | | ALUMINUM A HONEYCOMB SANDWICH | | ALUMINUM C HONEYCOMB SANDWICH | |
| 1 | INTERSTAGE | 0.77550E 04 | 0.11503E 07 | 0.59250E 04 | 0.12653E 07 |
| | FWD SKIRT | 0.43300E 04 | 0.77486E 06 | 0.38950E 04 | 0.72110E 06 |
| | FWD TANKWALL | 0.14950E 05 | 0.17951E 07 | 0.13235E 05 | 0.16529E 07 |
| | CENTER SECTION | 0.94750E 04 | 0.13177E 07 | 0.84800E 04 | 0.12222E 07 |
| | AFT TANKWALL | 0.76450E 04 | 0.11392E 07 | 0.69050E 04 | 0.10633E 07 |
| | AFT SKIRT | 0.41150E 04 | 0.74856E 06 | 0.36830E 04 | 0.69395E 06 |
| 2 | FWD SKIRT | 0.24550E 04 | 0.52740E 06 | 0.23250E 04 | 0.50830E 06 |
| | FWD TANKWALL | 0.13815E 05 | 0.17015E 07 | 0.12915E 05 | 0.16256E 07 |
| | AFT TANKWALL | 0.14550E 04 | 0.36905E 06 | 0.13100E 04 | 0.34450E 06 |
| | AFT SKIRT | 0.36200E 04 | 0.68626E 06 | 0.32550E 04 | 0.63855E 06 |
| | | TITANIUM A HONEYCOMB SANDWICH | | ALUMINUM A WAFFLE | |
| 1 | INTERSTAGE | 0.66400E 04 | 0.12425E 07 | 0.13170E 05 | 0.12629E 07 |
| | FWD SKIRT | 0.37500E 04 | 0.84345E 06 | 0.74050E 04 | 0.85473E 06 |
| | FWD TANKWALL | 0.12965E 05 | 0.19558E 07 | 0.24575E 05 | 0.13277E 07 |
| | CENTER SECTION | 0.80850E 04 | 0.14109E 07 | 0.15830E 05 | 0.14307E 07 |
| | AFT TANKWALL | 0.64830E 04 | 0.12221E 07 | 0.12645E 05 | 0.12285E 07 |
| | AFT SKIRT | 0.35450E 04 | 0.81100E 06 | 0.72850E 04 | 0.84531E 06 |
| 2 | FWD SKIRT | 0.22750E 04 | 0.60103E 06 | 0.56750E 04 | 0.71364E 06 |
| | FWD TANKWALL | 0.12945E 05 | 0.19435E 07 | 0.30940E 05 | 0.22535E 07 |
| | AFT TANKWALL | 0.12800E 04 | 0.40696E 06 | 0.26400E 04 | 0.42475E 06 |
| | AFT SKIRT | 0.31350E 04 | 0.74699E 06 | 0.64400E 04 | 0.77753E 06 |

Table 47. Component Weights and Costs, Current Medium Range Payload Vehicle (30,000 lb Orbital Payload)

| STAGE | COMPONENT | ALUMINUM A INTEGRAL SKIN STRINGER WEIGHT PER UNIT | ALUMINUM A INTEGRAL SKIN STRINGER DOLLARS PER UNIT | TITANIUM A HONEYCOMB SANDWICH WEIGHT PER UNIT | TITANIUM A HONEYCOMB SANDWICH DOLLARS PER UNIT |
|---|---|---|---|---|---|
| 1 | INTERSTAGE | 0.15050E 04 | 0.25494E 06 | 0.58700E 03 | 0.23358E 06 |
| | FWD SKIRT | 0.14560E 04 | 0.25930E 06 | 0.58200E 03 | 0.23850E 06 |
| | FWD TANKWALL | 0.13950E 04 | 0.25165E 06 | 0.56700E 03 | 0.33650E 06 |
| | CENTER SECTION | 0.31160E 04 | 0.43396E 06 | 0.11930E 04 | 0.38860E 06 |
| | AFT TANKWALL | 0.63000E 02 | 0.30813E 05 | 0.36000E 02 | 0.35144E 05 |
| | AFT SKIRT | 0.14340E 04 | 0.25640E 06 | 0.55400E 03 | 0.23066E 06 |
| 2 | FWD SKIRT | 0.75200E 03 | 0.16552E 06 | 0.30600E 03 | 0.15492E 06 |
| | FWD TANKWALL | 0.38820E 04 | 0.50359E 06 | 0.27530E 04 | 0.68399E 06 |
| | AFT TANKWALL | 0.10300E 03 | 0.43002E 05 | 0.73000E 02 | 0.58371E 05 |
| | AFT SKIRT | 0.80800E 03 | 0.17378E 06 | 0.37000E 03 | 0.17543E 06 |

| STAGE | COMPONENT | ALUMINUM A TOP HAT SKIN STRINGER WEIGHT PER UNIT | ALUMINUM A TOP HAT SKIN STRINGER DOLLARS PER UNIT | BERYLLIUM A HONEYCOMB SANDWICH WEIGHT PER UNIT | BERYLLIUM A HONEYCOMB SANDWICH DOLLARS PER UNIT |
|---|---|---|---|---|---|
| 1 | INTERSTAGE | 0.14930E 04 | 0.22586E 06 | 0.32000E 03 | 0.35330E 06 |
| | FWD SKIRT | 0.14810E 04 | 0.22453E 06 | 0.31400E 03 | 0.34879E 06 |
| | FWD TANKWALL | 0.12990E 04 | 0.20552E 06 | 0.77900E 03 | 0.64582E 06 |
| | CENTER SECTION | 0.31810E 04 | 0.37720E 06 | 0.64900E 03 | 0.57063E 06 |
| | AFT TANKWALL | 0.58000E 02 | 0.24971E 05 | 0.27000E 02 | 0.66087E 05 |
| | AFT SKIRT | 0.13860E 04 | 0.21476E 06 | 0.31400E 03 | 0.34879E 06 |
| 2 | FWD SKIRT | 0.70500E 03 | 0.13580E 06 | 0.13200E 03 | 0.19382E 06 |
| | FWD TANKWALL | 0.26730E 04 | 0.33523E 06 | 0.22850E 04 | 0.13396E 07 |
| | AFT TANKWALL | 0.79000E 02 | 0.30791E 05 | 0.60000E 02 | 0.11356E 06 |
| | AFT SKIRT | 0.73200E 03 | 0.13931E 06 | 0.20500E 03 | 0.26123E 06 |

| STAGE | COMPONENT | ALUMINUM A HONEYCOMB SANDWICH WEIGHT PER UNIT | ALUMINUM A HONEYCOMB SANDWICH DOLLARS PER UNIT | ALUMINUM C HONEYCOMB SANDWICH WEIGHT PER UNIT | ALUMINUM C HONEYCOMB SANDWICH DOLLARS PER UNIT |
|---|---|---|---|---|---|
| 1 | INTERSTAGE | 0.64000E 03 | 0.21197E 06 | 0.58100E 03 | 0.19852E 06 |
| | FWD SKIRT | 0.64000E 03 | 0.21197E 06 | 0.57600E 03 | 0.19736E 06 |
| | FWD TANKWALL | 0.11270E 04 | 0.31109E 06 | 0.10740E 04 | 0.30110E 06 |
| | CENTER SECTION | 0.12690E 04 | 0.33716E 06 | 0.11670E 04 | 0.31853E 06 |
| | AFT TANKWALL | 0.40000E 02 | 0.32350E 05 | 0.38000E 02 | 0.31245E 05 |
| | AFT SKIRT | 0.61000E 03 | 0.20518E 06 | 0.56900E 03 | 0.19573E 06 |
| 2 | FWD SKIRT | 0.33200E 03 | 0.13584E 06 | 0.30800E 03 | 0.12910E 06 |
| | FWD TANKWALL | 0.33020E 04 | 0.64478E 06 | 0.31520E 04 | 0.62478E 06 |
| | AFT TANKWALL | 0.86000E 02 | 0.54359E 05 | 0.82000E 02 | 0.52632E 05 |
| | AFT SKIRT | 0.40200E 03 | 0.15465E 06 | 0.36600E 03 | 0.14512E 06 |

Table 48. Component Weights and Costs, 1985 Medium Range Payload Vehicle (100,000 lb Orbital Payload)

| STAGE | COMPONENT | ALUMINUM A INTEGRAL SKIN STRINGER WEIGHT PER UNIT | ALUMINUM A INTEGRAL SKIN STRINGER DOLLARS PER UNIT | TITANIUM A HONEYCOMB SANDWICH WEIGHT PER UNIT | TITANIUM A HONEYCOMB SANDWICH DOLLARS PER UNIT |
|---|---|---|---|---|---|
| 1 | INTERSTAGE | 0.34310E 04 | 0.46323E 06 | 0.13530E 04 | 0.42256E 04 |
| | FWD SKIRT | 0.38400E 04 | 0.40750E 06 | 0.21220E 04 | 0.57332E 04 |
| | FWD TANKWALL | 0.24760E 04 | 0.37132E 06 | 0.16960E 04 | 0.49251E 04 |
| | CENTER SECTION | 0.60790E 04 | 0.68268E 06 | 0.33700E 04 | 0.61734E 04 |
| | AFT TANKWALL | 0.60000E 01 | 0.62570E 04 | 0.30030E 01 | 0.67043E 04 |
| | AFT SKIRT | 0.28100E 04 | 0.40458E 06 | 0.37000E 03 | 0.17543E 06 |
| 2 | FWD SKIRT | 0.13020E 04 | 0.24015E 06 | 0.56700E 03 | 0.23431E 06 |
| | FWD TANKWALL | 0.77930E 04 | 0.80790E 06 | 0.55500E 04 | 0.11033E 07 |
| | AFT TANKWALL | 0.61800E 03 | 0.14490E 06 | 0.44000E 03 | 0.19730E 06 |
| | AFT SKIRT | 0.14270E 04 | 0.25555E 06 | 0.62900E 03 | 0.25139E 06 |

| STAGE | COMPONENT | ALUMINUM A TEE HAT SKIN STRINGER WEIGHT PER UNIT | ALUMINUM A TEE HAT SKIN STRINGER DOLLARS PER UNIT | BERYLLIUM A HONEYCOMB SANDWICH WEIGHT PER UNIT | BERYLLIUM A HONEYCOMB SANDWICH DOLLARS PER UNIT |
|---|---|---|---|---|---|
| 1 | INTERSTAGE | 0.30720E 04 | 0.36839E 06 | 0.83300E 03 | 0.67595E 06 |
| | FWD SKIRT | 0.25960E 04 | 0.32965E 06 | 0.64100E 03 | 0.56595E 06 |
| | FWD TANKWALL | 0.21220E 04 | 0.28666E 06 | 0.13310E 04 | 0.92863E 06 |
| | CENTER SECTION | 0.55730E 04 | 0.55167E 06 | 0.13050E 04 | 0.91630E 06 |
| | AFT TANKWALL | 0.50000E 01 | 0.47305E 04 | 0.94500E 03 | 0.73620E 06 |
| | AFT SKIRT | 0.25620E 04 | 0.32572E 06 | 0.63200E 03 | 0.56045E 06 |
| 2 | FWD SKIRT | 0.11640E 04 | 0.19079E 06 | 0.24030E 03 | 0.29059E 06 |
| | FWD TANKWALL | 0.63530E 04 | 0.60291E 06 | 0.54560E 04 | 0.24169E 07 |
| | AFT TANKWALL | 0.52300E 03 | 0.11091E 06 | 0.42700E 03 | 0.42962E 06 |
| | AFT SKIRT | 0.12060E 04 | 0.19543E 06 | 0.98100E 03 | 0.70201E 06 |

| STAGE | COMPONENT | ALUMINUM A HONEYCOMB SANDWICH WEIGHT PER UNIT | ALUMINUM A HONEYCOMB SANDWICH DOLLARS PER UNIT | ALUMINUM C HONEYCOMB SANDWICH* WEIGHT PER UNIT | ALUMINUM C HONEYCOMB SANDWICH* DOLLARS PER UNIT |
|---|---|---|---|---|---|
| 1 | INTERSTAGE | 0.15620E 04 | 0.38815E 06 | 0.14570E 04 | 0.37026E 06 |
| | FWD SKIRT | 0.12290E 04 | 0.32991E 06 | 0.11790E 04 | 0.32075E 06 |
| | FWD TANKWALL | 0.19030E 04 | 0.44375E 06 | | |
| | CENTER SECTION | 0.31130E 04 | 0.61952E 06 | 0.29140E 04 | 0.59239E 06 |
| | AFT TANKWALL | 0.40000E 01 | 0.67902E 04 | 0.40000E 01 | 0.67902E 04 |
| | AFT SKIRT | 0.12530E 04 | 0.33427E 06 | 0.12190E 04 | 0.32791E 06 |
| 2 | FWD SKIRT | 0.12950E 04 | 0.34182E 06 | 0.11970E 04 | 0.32406E 06 |
| | FWD TANKWALL | 0.84410E 04 | 0.12184E 07 | | |
| | AFT TANKWALL | 0.51300E 03 | 0.18245E 06 | 0.48900E 03 | 0.17662E 06 |
| | AFT SKIRT | 0.75700E 03 | 0.23753E 06 | 0.70500E 03 | 0.22634E 06 |

Table 49. Component Weights and Costs, Current Post-Saturn Payload Class Vehicle (1,000,000 lb Orbital Payload)

| STAGE | COMPONENT | ALUMINUM A INTEGRAL SKIN STRINGER WEIGHT PER UNIT | ALUMINUM A INTEGRAL SKIN STRINGER DOLLARS PER UNIT | TITANIUM A HONEYCOMB SANDWICH WEIGHT PER UNIT | TITANIUM A HONEYCOMB SANDWICH DOLLARS PER UNIT |
|---|---|---|---|---|---|
| 1 | INTERSTAGE | 0.67608E 05 | 0.34956E 07 | 0.38635E 05 | 0.41005E 07 |
| | FWD SKIRT | 0.33230E 05 | 0.21596E 07 | 0.18119E 05 | 0.24540E 07 |
| | FWD TANKWALL | 0.74156E 05 | 0.37217E 07 | 0.40092E 05 | 0.42047E 07 |
| | CENTER SECTION | 0.71023E 05 | 0.36143E 07 | 0.37845E 05 | 0.40435E 07 |
| | AFT TANKWALL | 0.31714E 05 | 0.20923E 07 | 0.18048E 05 | 0.24475E 07 |
| | AFT SKIRT | 0.33555E 05 | 0.21739E 07 | 0.15392E 05 | 0.21971E 07 |
| 2 | FWD SKIRT | 0.15286E 05 | 0.12757E 07 | 0.67280E 04 | 0.12534E 07 |
| | FWD TANKWALL | 0.10253E 06 | 0.46360E 07 | 0.53257E 05 | 0.50974E 07 |
| | AFT TANKWALL | 0.16703E 05 | 0.13547E 07 | 0.81600E 04 | 0.14289E 07 |
| | AFT SKIRT | 0.19979E 05 | 0.15296E 07 | 0.12139E 05 | 0.19797E 07 |

| STAGE | COMPONENT | ALUMINUM A TOP HAT SKIN STRINGER WEIGHT PER UNIT | ALUMINUM A TOP HAT SKIN STRINGER DOLLARS PER UNIT | BERYLLIUM A HONEYCOMB SANDWICH * WEIGHT PER UNIT | BERYLLIUM A HONEYCOMB SANDWICH * DOLLARS PER UNIT |
|---|---|---|---|---|---|
| 1 | INTERSTAGE | 0.56466E 05 | 0.26518E 07 | 0.27342E 05 | 0.72081E 07 |
| | FWD SKIRT | 0.27319E 05 | 0.16209E 07 | 0.12743E 05 | 0.42056E 07 |
| | FWD TANKWALL | 0.58779E 05 | 0.27250E 07 | 0.26389E 05 | 0.70368E 07 |
| | CENTER SECTION | 0.58276E 05 | 0.27092E 07 | 0.12084E 05 | 0.41437E 07 |
| | AFT TANKWALL | 0.27164E 05 | 0.16147E 07 | 0.10017E 05 | 0.35488E 07 |
| | AFT SKIRT | 0.28471E 05 | 0.16669E 07 | | |
| 2 | FWD SKIRT | 0.13815E 05 | 0.10209E 07 | 0.39260E 04 | 0.19335E 07 |
| | FWD TANKWALL | 0.66930E 05 | 0.29758E 07 | | |
| | AFT TANKWALL | 0.11100E 05 | 0.88016E 06 | 0.61250E 04 | 0.26140E 07 |
| | AFT SKIRT | 0.18689E 05 | 0.12531E 07 | 0.92930E 04 | 0.34679E 07 |

| STAGE | COMPONENT | ALUMINUM A HONEYCOMB SANDWICH WEIGHT PER UNIT | ALUMINUM A HONEYCOMB SANDWICH DOLLARS PER UNIT | ALUMINUM C HONEYCOMB SANDWICH WEIGHT PER UNIT | ALUMINUM C HONEYCOMB SANDWICH DOLLARS PER UNIT |
|---|---|---|---|---|---|
| 1 | INTERSTAGE | 0.47254E 05 | 0.39170E 07 | 0.40418E 05 | 0.35232E 07 |
| | FWD SKIRT | 0.22266E 05 | 0.23517E 07 | 0.19808E 05 | 0.21724E 07 |
| | FWD TANKWALL | 0.38447E 05 | 0.34058E 07 | 0.36386E 05 | 0.32809E 07 |
| | CENTER SECTION | 0.46895E 05 | 0.38968E 07 | 0.43542E 05 | 0.37056E 07 |
| | AFT TANKWALL | 0.16646E 05 | 0.19308E 07 | 0.16162E 05 | 0.18925E 07 |
| | AFT SKIRT | 0.18391E 05 | 0.20658E 07 | 0.17459E 05 | 0.19942E 07 |
| 2 | FWD SKIRT | 0.72680E 04 | 0.11008E 07 | 0.67280E 04 | 0.10447E 07 |
| | FWD TANKWALL | 0.53274E 05 | 0.42487E 07 | 0.51218E 05 | 0.41369E 07 |
| | AFT TANKWALL | 0.10187E 05 | 0.13840E 07 | 0.96670E 04 | 0.13357E 07 |
| | AFT SKIRT | 0.15001E 05 | 0.17993E 07 | 0.14360E 05 | 0.17468E 07 |

Table 50. Component Weights and Costs, 1985 Post-Saturn Payload Class Vehicle (2,000,000 lb Orbital Payload)

| STAGE | COMPONENT | WEIGHT PER UNIT | DOLLARS PER UNIT | WEIGHT PER UNIT | DOLLARS PER UNIT |
|---|---|---|---|---|---|
| | | ALUMINUM A INTEGRAL SKIN STRINGER | | TITANIUM A HONEYCOMB SANDWICH | |
| 1 | INTERSTAGE | 0.10024E 06 | 0.45655E 07 | 0.58935E 05 | 0.54598E 07 |
| | FWD SKIRT | 0.40906E 05 | 0.24864E 07 | 0.24076E 05 | 0.29756E 07 |
| | FWD TANKWALL | 0.10768E 06 | 0.47925E 07 | 0.62143E 05 | 0.56596E 07 |
| | CENTER SECTION | 0.83816E 05 | 0.40439E 07 | 0.50552E 05 | 0.49204E 07 |
| | AFT TANKWALL | 0.51158E 05 | 0.28935E 07 | 0.29460E 05 | 0.34120E 07 |
| | AFT SKIRT | 0.39350E 05 | 0.24219E 07 | 0.22835E 05 | 0.28708E 07 |
| 2 | FWD SKIRT | 0.16604E 05 | 0.13492E 07 | 0.77450E 04 | 0.13792E 07 |
| | FWD TANKWALL | 0.17655E 06 | 0.67012E 07 | 0.88247E 05 | 0.71787E 07 |
| | AFT TANKWALL | 0.39380E 05 | 0.24231E 07 | 0.19104E 05 | 0.25437E 07 |
| | AFT SKIRT | 0.23750E 05 | 0.17198E 07 | 0.16670E 05 | 0.23192E 07 |
| | | ALUMINUM A TOP HAT SKIN STRINGER | | BERYLLIUM A HONEYCOMB SANDWICH * | |
| 1 | INTERSTAGE | 0.85655E 05 | 0.35176E 07 | 0.42448E 05 | 0.97127E 07 |
| | FWD SKIRT | 0.34955E 05 | 0.19157E 07 | 0.17461E 05 | 0.53183E 07 |
| | FWD TANKWALL | 0.86225E 05 | 0.35334E 07 | | |
| | CENTER SECTION | 0.72037E 05 | 0.31279E 07 | 0.36011E 05 | 0.86879E 07 |
| | AFT TANKWALL | 0.40880E 05 | 0.21303E 07 | 0.22426E 05 | 0.63018E 07 |
| | AFT SKIRT | 0.33038E 05 | 0.18438E 07 | 0.17005E 05 | 0.52238E 07 |
| 2 | FWD SKIRT | 0.14850E 05 | 0.10722E 07 | 0.48560E 04 | 0.22333E 07 |
| | FWD TANKWALL | 0.11832E 06 | 0.43790E 07 | | |
| | AFT TANKWALL | 0.27145E 05 | 0.16139E 07 | 0.14140E 05 | 0.46095E 07 |
| | AFT SKIRT | 0.21105E 05 | 0.13607E 07 | 0.12123E 05 | 0.41528E 07 |
| | | ALUMINUM A HONEYCOMB SANDWICH | | ALUMINUM C HONEYCOMB SANDWICH | |
| 1 | INTERSTAGE | 0.74187E 05 | 0.53182E 07 | 0.63470E 05 | 0.47844E 07 |
| | FWD SKIRT | 0.30290E 05 | 0.28974E 07 | 0.25788E 05 | 0.25979E 07 |
| | FWD TANKWALL | 0.62491E 05 | 0.47342E 07 | 0.60447E 05 | 0.46287E 07 |
| | CENTER SECTION | 0.62760E 05 | 0.47480E 07 | 0.54186E 05 | 0.42979E 07 |
| | AFT TANKWALL | 0.29454E 05 | 0.28429E 07 | 0.28584E 05 | 0.27857E 07 |
| | AFT SKIRT | 0.29454E 05 | 0.28429E 07 | 0.24908E 05 | 0.25375E 07 |
| 2 | FWD SKIRT | 0.86850E 04 | 0.12421E 07 | 0.84400E 04 | 0.12183E 07 |
| | FWD TANKWALL | 0.99280E 05 | 0.64797E 07 | 0.94705E 05 | 0.62757E 07 |
| | AFT TANKWALL | 0.21063E 05 | 0.22648E 07 | 0.20039E 05 | 0.21896E 07 |
| | AFT SKIRT | 0.18788E 05 | 0.20959E 07 | 0.18160E 05 | 0.20482E 07 |

are more sensitive than the upper stages to any change or improvement. It can be seen that the values assigned to the cost ratios can be somewhat misleading. If we consider, for example, the aft skirt of a second stage and the forward skirt of a first stage to be identical in material, construction, size and weight due to similar loading intensities, their unit costs will be identical with payload gains of 1000 pounds for the second stage and 100 pounds for the first stage. Their relative cost ratio variations are indicated in the following table.

| Case | Stage | Payload Gain (pounds) | Unit Cost (dollars) | Cost Ratio | Material | Cost Ratio Magnitude | Cost Ratio Assessment |
|---|---|---|---|---|---|---|---|
| 1 | 1 | 100 | $-10^6$ | $-10^4$ | A | 2 | 3 |
| 2 | 2 | 1000 | $-10^6$ | $-10^3$ | A | 3 | 1 |
| 3 | 1 | 100 | $-2\times10^6$ | $-2\times10^4$ | B | 1 | 2 |
| 4 | 1 | 100 | $10^6$ | $10^4$ | C | 5 | 4 |
| 5 | 2 | 1000 | $10^6$ | $10^4$ | C | 4 | 5 |
| 6 | 1 | 100 | $2\times10^6$ | $2\times10^4$ | D | 6 | 6 |

Material A results in a cost reduction from the base point concept and material B shows an even greater cost reduction. Materials C and D result in a change of fabrication complexity producing additional costs for the component. Shown also in the table is an ordering in ascending magnitude of the cost ratios by case numbers together with an assessment ordering of importance. Examination shows the most effective merit function to be in case number 2 which is third in the cost ratio magnitude ordering. Also, it is obvious that case number 3 is more effective than case number 2. This simple example demonstrates the difficulty involved in ordering these cost ratios to obtain a coherent picture of their figure of merit; therefore, it is obvious further study should be devoted to defining a useful cost index to identify the economic aspect of projected research areas, understanding of the effects of component size and weight on the component costs, and further justification of the complexity factors from historical data. The cost data presented here for the different types of constructions and materials can be extremely useful if caution is exercised when comparing two different cost ratios. Consideration must be given to both the payload gain and the component cost simultaneously.

| STAGE | COMPONENT | WEIGHT PER UNIT | DELTA DOLLARS PER UNIT | DELTA WEIGHT PER UNIT | DELTA PAYLOAD PER UNIT |
|---|---|---|---|---|---|
| | | ALUMINUM A<br>INTEGRAL SKIN STRINGER | | | |
| 1 | INTERSTAGE | C.94450E 04 | | | |
| | FWD SKIRT | 0.58450E 04 | | | |
| | FWD TANKWALL | 0.17420E 05 | | | |
| | CENTER SECTION | 0.12730E 05 | | | |
| | AFT TANKWALL | 0.80750E 04 | | | |
| | AFT SKIRT | 0.58950E 04 | | BASE POINT | |
| 2 | FWD SKIRT | 0.43450E 04 | | | |
| | FWD TANKWALL | 0.21045E 05 | | | |
| | AFT TANKWALL | C.80000E 03 | | | |
| | AFT SKIRT | 0.50550E 04 | | | |
| | | ALUMINUM A<br>TOP HAT SKIN STRINGER | | | |
| 1 | INTERSTAGE | 0.94450E 04 | 0.21196E 06 | 0.12430E 04 | 0.13673E 03 |
| | FWD SKIRT | 0.58450E 04 | 0.15485E 06 | 0.79300E 03 | 0.87230E 02 |
| | FWD TANKWALL | 0.17420E 05 | 0.31643E 06 | 0.22050E 04 | 0.24255E 03 |
| | CENTER SECTION | 0.12730E 05 | 0.25827E 06 | 0.16540E 04 | 0.18194E 03 |
| | AFT TANKWALL | 0.80750E 04 | 0.18332E 06 | 0.95400E 03 | 0.10494E 03 |
| | AFT SKIRT | 0.58950E 04 | 0.15377E 06 | 0.77300E 03 | 0.85030E 02 |
| 2 | FWD SKIRT | 0.43450E 04 | 0.13335E 06 | 0.67200E 03 | 0.67200E 03 |
| | FWD TANKWALL | 0.21045E 05 | 0.37598E 06 | 0.29960E 04 | 0.29960E 04 |
| | AFT TANKWALL | 0.80000E 03 | 0.35330E 05 | 0.74000E 02 | 0.74000E 02 |
| | AFT SKIRT | 0.50550E 04 | 0.13740E 06 | 0.64800E 03 | 0.64800E 03 |
| | | ALUMINUM A<br>HONEYCOMB SANDWICH | | | |
| 1 | INTERSTAGE | 0.60800E 04 | 0.25488E 05 | 0.46080E 04 | 0.50688E 03 |
| | FWD SKIRT | 0.37900E 04 | 0.16694E 05 | 0.28480E 04 | 0.31328E 03 |
| | FWD TANKWALL | 0.10850E 05 | 0.66688E 05 | 0.87750E 04 | 0.96525E 03 |
| | CENTER SECTION | 0.82950E 04 | 0.20080E 05 | 0.60890E 04 | 0.66979E 03 |
| | AFT TANKWALL | 0.55150E 04 | 0.20260E 05 | 0.35140E 04 | 0.38654E 03 |
| | AFT SKIRT | 0.36900E 04 | 0.31631E 05 | 0.29780E 04 | 0.32758E 03 |
| 2 | FWD SKIRT | 0.23000E 04 | 0.94767E 05 | 0.27170E 04 | 0.27170E 04 |
| | FWD TANKWALL | 0.11450E 05 | 0.23593E 06 | 0.12591E 05 | 0.12591E 05 |
| | AFT TANKWALL | 0.48000E 03 | 0.88773E 04 | 0.39400E 03 | 0.39400E 03 |
| | AFT SKIRT | 0.34250E 04 | 0.72105E 04 | 0.22780E 04 | 0.22780E 04 |
| | | TITANIUM A<br>HONEYCOMB SANDWICH | | | |
| 1 | INTERSTAGE | 0.53300E 04 | 0.69638E 05 | 0.53580E 04 | 0.58938E 03 |
| | FWD SKIRT | 0.34050E 04 | 0.65383E 05 | 0.32330E 04 | 0.35563E 03 |
| | FWD TANKWALL | 0.95400E 04 | 0.77395E 05 | 0.10085E 05 | 0.11093E 04 |
| | CENTER SECTION | 0.74550E 04 | 0.11983E 06 | 0.69290E 04 | 0.76219E 03 |
| | AFT TANKWALL | 0.47450E 04 | 0.96657E 05 | 0.42840E 04 | 0.47124E 03 |
| | AFT SKIRT | 0.31950E 04 | 0.29792E 05 | 0.34730E 04 | 0.38203E 03 |
| 2 | FWD SKIRT | 0.21650E 04 | 0.18180E 05 | 0.28520E 04 | 0.28520E 04 |
| | FWD TANKWALL | 0.10870E 05 | 0.14420E 04 | 0.13171E 05 | 0.13171E 05 |
| | AFT TANKWALL | 0.44000E 03 | 0.14015E 05 | 0.43400E 03 | 0.43400E 03 |
| | AFT SKIRT | 0.28800E 0 | 0.51471E 05 | 0.28230E 04 | 0.28230E 04 |

## Table 51. Study Merit Functions, Current Saturn Payload Class Vehicle (240,000 lb Orbital Payload)

| COST RATIO | WEIGHT PER UNIT | DELTA DOLLARS PER UNIT | DELTA WEIGHT PER UNIT | DELTA PAYLOAD PER UNIT | COST RATIO |
|---|---|---|---|---|---|
| | **BERYLLIUM A HONEYCOMB SANDWICH** | | | | |
| | 0.35350E 04 | 0.79992E 06 | -0.71530E 04 | 0.78683E 03 | 0.1016633E 04 |
| | 0.22050E 04 | 0.58298E 06 | -0.44330E 04 | 0.48763E 03 | 0.1195545E 04 |
| | 0.62200E 04 | 0.11303E 07 | -0.13405E 05 | 0.14746E 04 | 0.7665394E 03 |
| | 0.49100E 04 | 0.10260E 07 | -0.94740E 04 | 0.10421E 04 | 0.9845106E 03 |
| | 0.32450E 04 | 0.80654E 06 | -0.57840E 04 | 0.63624E 03 | 0.1267672E 04 |
| | 0.20800E 04 | 0.53004E 06 | -0.45880E 04 | 0.50468E 03 | 0.1050240E 04 |
| | 0.13550E 04 | 0.34060E 06 | -0.36620E 04 | 0.36620E 04 | 0.9300974E 02 |
| | 0.62800E 04 | 0.92462E 06 | -0.17761E 05 | 0.17761E 05 | 0.5205918E 02 |
| | 0.28500E 03 | 0.14333E 06 | -0.58900E 03 | 0.58900E 03 | 0.2433460E 03 |
| | 0.18500E 04 | 0.50714E 06 | -0.38530E 04 | 0.38530E 04 | 0.1316213E 03 |
| | **ALUMINUM B HONEYCOMB SANDWICH** | | | | |
| .1550210E 04 | 0.57550E 04 | -0.61149E 05 | -0.49330E 04 | 0.54263E 03 | -0.1126902E 03 |
| .1775202E 04 | 0.36100E 04 | -0.39668E 05 | -0.30280E 04 | 0.33308E 03 | -0.1190942E 03 |
| .1304588E 04 | 0.10300E 05 | -0.11675E 06 | -0.93250E 04 | 0.10257E 04 | -0.1138160E 03 |
| .1419547E 04 | 0.79000E 04 | -0.59257E 05 | -0.64840E 04 | 0.71324E 03 | -0.8308191E 02 |
| .1746919E 04 | 0.51800E 04 | -0.17717E 05 | -0.38490E 04 | 0.42339E 03 | -0.4184665E 02 |
| .1808415E 04 | 0.34350E 04 | -0.64579E 05 | -0.32330E 04 | 0.35563E 03 | -0.1815912E 03 |
| .1984322E 03 | 0.22500E 04 | -0.10223E 06 | -0.27670E 04 | 0.27670E 04 | -0.3694633E 02 |
| .1254936E 03 | 0.11160E 05 | -0.26176E 06 | -0.12881E 05 | 0.12881E 05 | -0.2032145E 02 |
| .4774277E 03 | 0.47300E 03 | -0.10606E 05 | -0.40100E 03 | 0.40100E 03 | -0.2644836E 02 |
| .2120304E 03 | 0.31100E 04 | -0.34642E 05 | -0.25930E 04 | 0.25930E 04 | -0.1335966E 02 |
| | **ALUMINUM C HONEYCOMB SANDWICH** | | | | |
| .5028466E 02 | 0.55050E 04 | -0.89023E 05 | -0.51830E 04 | 0.57013E 03 | -0.1561458E 03 |
| .5328642E 02 | 0.34500E 04 | -0.60401E 05 | -0.31880E 04 | 0.35068E 03 | -0.1722397E 03 |
| .6908918E 02 | 0.98180E 04 | -0.16133E 06 | -0.98070E 04 | 0.10788E 04 | -0.1495484E 03 |
| .2997896E 02 | 0.74550E 04 | -0.10416E 06 | -0.69290E 04 | 0.76219E 03 | -0.1366569E 03 |
| .5241312E 02 | 0.48800E 04 | -0.52404E 05 | -0.41490E 04 | 0.45639E 03 | -0.1148220E 03 |
| .9656088E 02 | 0.32550E 04 | -0.88312E 05 | -0.34130E 04 | 0.37543E 03 | -0.2352296E 03 |
| .3487930E 02 | 0.22140E 04 | -0.10764E 06 | -0.28030E 04 | 0.28030E 04 | -0.3840074E 02 |
| .1873786E 02 | 0.11105E 05 | -0.26668E 06 | -0.12936E 05 | 0.12936E 05 | -0.2061566E 02 |
| .2253114E 02 | 0.45000E 03 | -0.16344E 06 | -0.42400E 03 | 0.42400E 03 | -0.3854779E 02 |
| .3165297E 01 | 0.29500E 04 | -0.56420E 05 | -0.27530E 04 | 0.27530E 04 | -0.2049406E 02 |
| | **ALUMINUM A WAFFLE** | | | | |
| .1181542E 03 | 0.10560E 05 | 0.86402E 05 | -0.12800E 03 | 0.14080E 02 | 0.6136501E 04 |
| .1838508E 03 | 0.66950E 04 | 0.73628E 05 | 0.57000E 02 | -0.62700E 01 | -0.1174283E 05 |
| .6976621E 02 | 0.19490E 05 | 0.13619E 06 | -0.13500E 03 | 0.14850E 02 | 0.9171098E 04 |
| .1572225E 03 | 0.14490E 05 | 0.12327E 06 | 0.10600E 03 | -0.11660E 02 | -0.1057233E 05 |
| .2051124E 03 | 0.92850E 04 | 0.10373E 06 | 0.25600E 03 | -0.28160E 02 | -0.3683564E 04 |
| .7799336E 02 | 0.66050E 04 | 0.64117E 05 | -0.63000E 02 | 0.69300E 01 | 0.9252131E 04 |
| .6374551E 01 | 0.54600E 04 | 0.95842E 05 | 0.44300E 03 | -0.44300E 03 | -0.2163477E 03 |
| .1094865E 00 | 0.26335E 05 | 0.28621E 06 | 0.22940E 04 | -0.22940E 04 | -0.1247634E 03 |
| .3229170E 02 | 0.94000E 03 | 0.27612E 05 | 0.66000E 02 | -0.66000E 02 | -0.4183697E 03 |
| .1823286E 02 | 0.60250E 04 | 0.89430E 05 | 0.32200E 03 | -0.32200E 03 | -0.2777325E 03 |

Table

| STAGE | COMPONENT | WEIGHT PER UNIT | DELTA DOLLARS PER UNIT | DELTA WEIGHT PER UNIT | DELTA PAYLOAD PER UNIT | CO RA |
|---|---|---|---|---|---|---|
| | ALUMINUM A INTEGRAL SKIN STRINGER | | | | | |
| 1 | INTERSTAGE | 0.12975E 05 | | | | |
| | FWD SKIRT | 0.71870E 04 | | | | |
| | FWD TANKWALL | 0.24983E 05 | | | | |
| | CENTER SECTION | 0.15384E 05 | | | | |
| | AFT TANKWALL | 0.12283E 05 | | | | |
| | AFT SKIRT | 0.71420E 04 | | | BASE POINT | |
| 2 | FWD SKIRT | 0.51970E 04 | | | | |
| | FWD TANKWALL | 0.28726E 05 | | | | |
| | AFT TANKWALL | 0.24810E 04 | | | | |
| | AFT SKIRT | 0.59730E 04 | | | | |
| | ALUMINUM A TOP HAT SKIN STRINGER | | | | | |
| 1 | INTERSTAGE | 0.11575E 05 | 0.23595E 06 | 0.14000E 04 | 0.21000E 03 | 0.112 |
| | FWD SKIRT | 0.64750E 04 | 0.15401E 06 | 0.71200E 03 | 0.10680E 03 | 0.144 |
| | FWD TANKWALL | 0.22495E 05 | 0.35900E 06 | 0.24880E 04 | 0.37320E 03 | 0.961 |
| | CENTER SECTION | 0.13860E 05 | 0.25802E 06 | 0.15240E 04 | 0.22860E 03 | 0.112 |
| | AFT TANKWALL | 0.11055E 05 | 0.22210E 06 | 0.12280E 04 | 0.18420E 03 | 0.120 |
| | AFT SKIRT | 0.63300E 04 | 0.16007E 06 | 0.81200E 03 | 0.12180E 03 | 0.131 |
| 2 | FWD SKIRT | 0.45750E 04 | 0.13126E 06 | 0.62200E 03 | 0.62200E 03 | 0.211 |
| | FWD TANKWALL | 0.25690E 05 | 0.40183E 06 | 0.30360E 04 | 0.30360E 04 | 0.132 |
| | AFT TANKWALL | 0.22750E 04 | 0.71308E 05 | 0.20600E 03 | 0.20600E 03 | 0.346 |
| | AFT SKIRT | 0.55200E 04 | 0.12648E 06 | 0.45300E 03 | 0.45300E 03 | 0.279 |
| | ALUMINUM A HONEYCOMB SANDWICH | | | | | |
| 1 | INTERSTAGE | 0.77550E 04 | 0.88434E 04 | 0.52200E 04 | 0.78300E 03 | 0.112 |
| | FWD SKIRT | 0.43300E 04 | 0.10106E 05 | 0.28570E 04 | 0.42855E 03 | 0.235 |
| | FWD TANKWALL | 0.14950E 05 | 0.15252E 05 | 0.10033E 05 | 0.15049E 04 | 0.101 |
| | CENTER SECTION | 0.94750E 04 | 0.36470E 05 | 0.59090E 04 | 0.88635E 03 | 0.411 |
| | AFT TANKWALL | 0.76450E 04 | 0.39394E 05 | 0.46380E 04 | 0.69570E 03 | 0.566 |
| | AFT SKIRT | 0.41150E 04 | 0.12943E 05 | 0.30270E 04 | 0.45405E 03 | 0.285 |
| 2 | FWD SKIRT | 0.24550E 04 | 0.86451E 05 | 0.27420E 04 | 0.27420E 04 | 0.315 |
| | FWD TANKWALL | 0.13815E 05 | 0.25502E 06 | 0.14911E 05 | 0.14911E 05 | 0.171 |
| | AFT TANKWALL | 0.14500E 04 | 0.27700E 04 | 0.10310E 04 | 0.10310E 04 | 0.268 |
| | AFT SKIRT | 0.36200E 04 | 0.11668E 05 | 0.23530E 04 | 0.23530E 04 | 0.495 |
| | TITANIUM A HONEYCOMB SANDWICH | | | | | |
| 1 | INTERSTAGE | 0.66400E 04 | 0.10101E 06 | 0.63350E 04 | 0.95025E 03 | 0.106 |
| | FWD SKIRT | 0.37500E 04 | 0.78695E 05 | 0.34370E 04 | 0.51555E 03 | 0.152 |
| | FWD TANKWALL | 0.12965E 05 | 0.17595E 06 | 0.12018E 05 | 0.18027E 04 | 0.976 |
| | CENTER SECTION | 0.80850E 04 | 0.13875E 06 | 0.72990E 04 | 0.10948E 04 | 0.126 |
| | AFT TANKWALL | 0.64800E 04 | 0.12228E 06 | 0.58030E 04 | 0.87045E 03 | 0.140 |
| | AFT SKIRT | 0.35450E 04 | 0.50401E 05 | 0.35970E 04 | 0.53955E 03 | 0.934 |
| 2 | FWD SKIRT | 0.22750E 04 | 0.12817E 05 | 0.29220E 04 | 0.29220E 04 | 0.438 |
| | FWD TANKWALL | 0.12845E 05 | 0.13047E 06 | 0.15881E 05 | 0.15881E 05 | 0.821 |
| | AFT TANKWALL | 0.12800E 04 | 0.35136E 05 | 0.12010E 04 | 0.12010E 04 | 0.292 |
| | AFT SKIRT | 0.31350E 04 | 0.72398E 05 | 0.28380E 04 | 0.28380E 04 | 0.255 |

52. Stu[redacted] Merit Functions, 1985 Saturn Payload Class Vehicle
(445, 000 lb Orbital Payload)

| WEIGHT PER UNIT | DELTA DOLLARS PER UNIT | DELTA WEIGHT PER UNIT | DELTA PAYLOAD PER UNIT | COST RATIO |
|---|---|---|---|---|
| **BERYLLIUM A HONEYCOMB SANDWICH** | | | | |
| 0.45450E 04 | 0.99383E 06 | -0.84300E 04 | 0.12645E 04 | 0.7859431E 03 |
| 0.25800E 04 | 0.68980E 06 | -0.46070E 04 | 0.69105E 03 | 0.9981948E 03 |
| 0.87200E 04 | 0.15416E 07 | -0.16263E 05 | 0.24394E 04 | 0.6319263E 03 |
| 0.55400E 04 | 0.11608E 07 | -0.98440E 04 | 0.14766E 04 | 0.7861578E 03 |
| 0.44600E 04 | 0.10083E 07 | -0.78230E 04 | 0.11734E 04 | 0.8592666E 03 |
| 0.23850E 04 | 0.61758E 06 | -0.47570E 04 | 0.71355E 03 | 0.8654983E 03 |
| 0.13550E 04 | 0.32611E 06 | -0.38420E 04 | 0.38420E 04 | 0.8487900E 02 |
| 0.74600E 04 | 0.10314E 07 | -0.21266E 05 | 0.21266E 05 | 0.4849830E 02 |
| 0.84000E 03 | 0.30787E 06 | -0.16410E 04 | 0.16410E 04 | 0.1876105E 03 |
| 0.20950E 04 | 0.58844E 06 | -0.38780E 04 | 0.38780E 04 | 0.1517388E 03 |
| **ALUMINUM B HONEYCOMB SANDWICH** | | | | |
| 0.73800E 04 | -0.29170E 05 | -0.55950E 04 | 0.83925E 03 | -0.3475763E 02 |
| 0.41150E 04 | -0.16193E 05 | -0.30720E 04 | 0.46080E 03 | -0.3514108E 02 |
| 0.13915E 05 | -0.62977E 05 | -0.11068E 05 | 0.16602E 04 | -0.4214955E 02 |
| 0.88750E 04 | -0.20696E 05 | -0.65090E 04 | 0.97635E 03 | -0.2119762E 02 |
| 0.71100E 04 | -0.15287E 05 | -0.51730E 04 | 0.77595E 03 | -0.1970141E 02 |
| 0.36750E 04 | -0.42829E 05 | -0.32670E 04 | 0.49005E 03 | -0.8739701E 02 |
| 0.23700E 04 | -0.98902E 05 | -0.28270E 04 | 0.28270E 04 | -0.3498476E 02 |
| 0.13605E 05 | -0.27260E 06 | -0.15121E 05 | 0.15121E 05 | -0.1802773E 02 |
| 0.14000E 04 | -0.11447E 05 | -0.10810E 04 | 0.10810E 04 | -0.1058914E 02 |
| 0.34150E 04 | -0.14927E 05 | -0.25580E 04 | 0.25580E 04 | -0.5835351E 01 |
| **ALUMINUM C HONEYCOMB SANDWICH** | | | | |
| 0.69250E 04 | -0.76140E 05 | -0.60500E 04 | 0.90750E 03 | -0.8390114E 02 |
| 0.38950E 04 | -0.43566E 05 | -0.32920E 04 | 0.49380E 03 | -0.8322583E 02 |
| 0.13235E 05 | -0.12708E 06 | -0.11748E 05 | 0.17622E 04 | -0.7211718E 02 |
| 0.84800E 04 | -0.59011E 05 | -0.69040E 04 | 0.10356E 04 | -0.5698215E 02 |
| 0.69050E 04 | -0.36588E 05 | -0.53780E 04 | 0.80670E 03 | -0.4535567E 02 |
| 0.36800E 04 | -0.67552E 05 | -0.34620E 04 | 0.51930E 03 | -0.1300834E 03 |
| 0.23250E 04 | -0.10555E 06 | -0.28720E 04 | 0.28720E 04 | -0.3675191E 02 |
| 0.12915E 05 | -0.33099E 06 | -0.15811E 05 | 0.15811E 05 | -0.2093387E 02 |
| 0.13100E 04 | -0.27322E 05 | -0.11710E 04 | 0.11710E 04 | -0.2333179E 02 |
| 0.32550E 04 | -0.36043E 05 | -0.27180E 04 | 0.27180E 04 | -0.1326083E 02 |
| **ALUMINUM A WAFFLE** | | | | |
| 0.13170E 05 | 0.12142E 06 | 0.19500E 03 | -0.29250E 02 | -0.4151131E 04 |
| 0.74050E 04 | 0.89376E 05 | 0.21800E 03 | -0.32700E 02 | -0.2751553E 04 |
| 0.24575E 05 | 0.14787E 06 | -0.40800E 03 | 0.61200E 02 | 0.2416149E 04 |
| 0.15830E 05 | 0.14947E 06 | 0.44600E 03 | -0.66900E 02 | -0.2234269E 04 |
| 0.12645E 05 | 0.12370E 06 | 0.36200E 03 | -0.54300E 02 | -0.2370233E 04 |
| 0.72850E 04 | 0.83310E 05 | 0.14300E 03 | -0.21450E 02 | -0.3907218E 04 |
| 0.56750E 04 | 0.99790E 05 | 0.47800E 03 | -0.47800E 03 | -0.2087657E 03 |
| 0.30940E 05 | 0.29697E 06 | 0.22140E 04 | -0.22140E 04 | -0.1341337E 03 |
| 0.26400E 04 | 0.52929E 05 | 0.15900E 03 | -0.15900E 03 | -0.3328874E 03 |
| 0.64400E 04 | 0.10394E 06 | 0.46700E 03 | -0.46700E 03 | -0.2204180E 03 |

| STAGE | COMPONENT | WEIGHT PER UNIT | DELTA DOLLARS PER UNIT | DELTA WEIGHT PER UNIT | DELTA PAYLOAD PER UNIT |
|---|---|---|---|---|---|
| | **ALUMINUM A INTEGRAL SKIN STRINGER** | | | | |
| 1 | INTERSTAGE | 0.15050E 04 | | | |
| | FWD SKIRT | 0.14580E 04 | | | |
| | FWD TANKWALL | 0.13950E 04 | | | |
| | CENTER SECTION | 0.31160E 04 | | | |
| | AFT TANKWALL | 0.63000E 02 | | | |
| | AFT SKIRT | 0.14340E 04 | | | BASE POINT |
| 2 | FWD SKIRT | 0.75200E 03 | | | |
| | FWD TANKWALL | 0.38820E 04 | | | |
| | AFT TANKWALL | 0.10300E 03 | | | |
| | AFT SKIRT | 0.80800E 03 | | | |
| | **ALUMINUM A TOP HAT SKIN STRINGER** | | | | |
| 1 | INTERSTAGE | 0.14930E 04 | 0.39078E 05 | 0.12000E 02 | 0.10800E 0 |
| | FWD SKIRT | 0.14810E 04 | 0.34672E 05 | 0.23000E 02 | 0.20700E 0 |
| | FWD TANKWALL | 0.12990E 04 | 0.46130E 05 | 0.96000E 02 | 0.86400E 0 |
| | CENTER SECTION | 0.31810E 04 | 0.56750E 05 | 0.65000E 02 | 0.58500E 0 |
| | AFT TANKWALL | 0.58000E 02 | 0.58419E 04 | 0.50000E 01 | 0.45000E 0 |
| | AFT SKIRT | 0.13860E 04 | 0.41644E 05 | 0.48000E 02 | 0.43200E 0 |
| 2 | FWD SKIRT | 0.70500E 03 | 0.29720E 05 | 0.47000E 02 | 0.47000E 0 |
| | FWD TANKWALL | 0.26730E 04 | 0.16846E 06 | 0.12090E 04 | 0.12090E 0 |
| | AFT TANKWALL | 0.79000E 02 | 0.12210E 05 | 0.24000E 02 | 0.24000E 0 |
| | AFT SKIRT | 0.73200E 03 | 0.34476E 05 | 0.76000E 02 | 0.76000E 0 |
| | **ALUMINUM A HONEYCOMB SANDWICH** | | | | |
| 1 | INTERSTAGE | 0.64000E 03 | 0.52973E 05 | 0.86500E 03 | 0.77850E 02 |
| | FWD SKIRT | 0.64000E 03 | 0.47334E 05 | 0.81800E 03 | 0.73620E 02 |
| | FWD TANKWALL | 0.11270E 04 | 0.59438E 05 | 0.26800E 03 | 0.24120E 02 |
| | CENTER SECTION | 0.12690E 04 | 0.96795E 05 | 0.18470E 04 | 0.16623E 03 |
| | AFT TANKWALL | 0.40000E 02 | 0.15374E 04 | 0.23000E 02 | 0.20700E 01 |
| | AFT SKIRT | 0.61000E 03 | 0.51221E 05 | 0.82400E 03 | 0.74160E 02 |
| 2 | FWD SKIRT | 0.33200E 03 | 0.29686E 05 | 0.42000E 03 | 0.42000E 03 |
| | FWD TANKWALL | 0.33020E 04 | 0.14110E 06 | 0.58000E 03 | 0.58000E 03 |
| | AFT TANKWALL | 0.86000E 02 | 0.11358E 05 | 0.17000E 02 | 0.17000E 02 |
| | AFT SKIRT | 0.40200E 03 | 0.19133E 05 | 0.40600E 03 | 0.40600E 03 |

Table 53. Study Merit Functions, Current Medium Range Payload Vehicle
(30,000 lb Orbital Payload)

| WEIGHT PER UNIT | DELTA DOLLARS PER UNIT | DELTA WEIGHT PER UNIT | DELTA PAYLOAD PER UNIT | COST RATIO |
|---|---|---|---|---|
| | | TITANIUM A HONEYCOMB SANDWICH | | |
| 0.58700E 03 | -0.25058E 05 | -0.91800E 03 | 0.82620E 02 | -0.3032946E 03 |
| 0.58200E 03 | -0.20807E 05 | -0.87600E 03 | 0.78840E 02 | -0.2639160E 03 |
| 0.96700E 03 | 0.84846E 05 | -0.42800E 03 | 0.38520E 02 | 0.2202636E 04 |
| 0.11930E 04 | -0.45955E 05 | -0.19230E 04 | 0.17307E 03 | -0.2655290E 03 |
| 0.36000E 02 | 0.53311E 04 | -0.27000E 02 | 0.24300E 01 | 0.2193866E 04 |
| 0.55400E 03 | -0.25746E 05 | -0.88000E 03 | 0.79200E 02 | -0.3250813E 03 |
| 0.30800E 03 | -0.10604E 05 | -0.44400E 03 | 0.44400E 03 | -0.2388394E 02 |
| 0.27530E 04 | 0.18031E 06 | -0.11290E 04 | 0.11290E 04 | 0.1597059E 03 |
| 0.73000E 02 | 0.15369E 05 | -0.30000E 02 | 0.30000E 02 | 0.5123131E 03 |
| 0.37000E 03 | 0.16480E 04 | -0.43800E 03 | 0.43800E 03 | 0.3762553E 01 |
| | | BERYLLIUM A HONEYCOMB SANDWICH | | |
| 0.32000E 03 | 0.88358E 05 | -0.11850E 04 | 0.10665E 03 | 0.8284841E 03 |
| 0.31400E 03 | 0.89491E 05 | -0.11440E 04 | 0.10296E 03 | 0.8691838E 03 |
| 0.77900E 03 | 0.39417E 06 | -0.61600E 03 | 0.55440E 02 | 0.7109862E 04 |
| 0.64900E 03 | 0.13668E 06 | -0.24670E 04 | 0.22203E 03 | 0.6155849E 03 |
| 0.27000E 02 | 0.35274E 05 | -0.36000E 02 | 0.32400E 01 | 0.1088705E 05 |
| 0.31400E 03 | 0.92393E 05 | -0.11200E 04 | 0.10080E 03 | 0.9165957E 03 |
| 0.13200E 03 | 0.28299E 05 | -0.62000E 03 | 0.62000E 03 | 0.4564295E 02 |
| 0.22850E 04 | 0.83592E 06 | -0.15970E 04 | 0.15970E 04 | 0.5234298E 03 |
| 0.60000E 02 | 0.70562E 05 | -0.43000E 02 | 0.43000E 02 | 0.1640971E 04 |
| 0.20500E 03 | 0.87446E 05 | -0.60300E 03 | 0.60300E 03 | 0.1450166E 03 |
| | | ALUMINUM C HONEYCOMB SANDWICH | | |
| 0.58100E 03 | -0.66426E 05 | -0.92400E 03 | 0.83160E 02 | -0.7987792E 0 |
| 0.57600E 03 | -0.61948E 05 | -0.88200E 03 | 0.79380E 02 | -0.7803987E 03 |
| 0.10740E 04 | 0.49442E 05 | -0.32100E 03 | 0.28890E 02 | 0.1711342E 04 |
| 0.11670E 04 | -0.11542E 06 | -0.19490E 04 | 0.17541E 03 | -0.6574755E 03 |
| 0.38000E 02 | 0.43170E 03 | -0.25000E 02 | 0.22500E 01 | 0.1912256E 03 |
| 0.56900E 03 | -0.60676E 05 | -0.86500E 03 | 0.77850E 02 | -0.7793923E 03 |
| 0.30800E 03 | -0.36424E 05 | -0.44400E 03 | 0.44400E 03 | -0.8203629E 02 |
| 0.31520E 04 | 0.12109E 06 | -0.73000E 03 | 0.73000E 03 | 0.1658756E 03 |
| 0.82000E 02 | 0.96303E 04 | -0.21000E 02 | 0.21000E 02 | 0.4585839E 03 |
| 0.36600E 03 | -0.28664E 05 | -0.44200E 03 | 0.44200E 03 | -0.6485029E 02 |

| STAGE | COMPONENT | WEIGHT PER UNIT | DELTA DOLLARS PER UNIT | DELTA WEIGHT PER UNIT | DELTA PAYLOAD PER UNI |
|---|---|---|---|---|---|
| | ALUMINUM A INTEGRAL SKIN STRINGER | | | | |
| 1 | INTERSTAGE | 0.34310E 04 | | | |
| | FWD SKIRT | 0.28400E 04 | | | |
| | FWD TANKWALL | 0.24760E 04 | | | |
| | CENTER SECTION | 0.60790E 04 | | | |
| | AFT TANKWALL | 0.60000E 01 | | | |
| | AFT SKIRT | 0.28100E 04 | BASE POINT | | |
| 2 | FWD SKIRT | 0.13020E 04 | | | |
| | FWD TANKWALL | 0.77930E 04 | | | |
| | AFT TANKWALL | 0.61800E 03 | | | |
| | AFT SKIRT | 0.14270E 04 | | | |
| | ALUMINUM A TOP HAT SKIN STRINGER | | | | |
| 1 | INTERSTAGE | 0.30720E 04 | -0.94841E 05 | -0.35900E 03 | 0.43080E |
| | FWD SKIRT | 0.25960E 04 | -0.78854E 05 | -0.24400E 03 | 0.29280E |
| | FWD TANKWALL | 0.21220E 04 | -0.84656E 05 | -0.35400E 03 | 0.42480E |
| | CENTER SECTION | 0.55730E 04 | -0.13101E 06 | -0.50600E 03 | 0.60720E |
| | AFT TANKWALL | 0.50000E 01 | -0.15175E 04 | -0.10000E 01 | 0.12000E |
| | AFT SKIRT | 0.25620E 04 | -0.78855E 05 | -0.24800E 03 | 0.29760E |
| 2 | FWD SKIRT | 0.11640E 04 | -0.49365E 05 | -0.13800E 03 | 0.13800E |
| | FWD TANKWALL | 0.63530E 04 | -0.20499E 06 | -0.14400E 04 | 0.14400E |
| | AFT TANKWALL | 0.52300E 03 | -0.33989E 05 | -0.95000E 02 | 0.95000E |
| | AFT SKIRT | 0.12060E 04 | -0.60124E 05 | -0.22100E 03 | 0.22100E |
| | ALUMINUM A HONEYCOMB SANDWICH | | | | |
| 1 | INTERSTAGE | 0.15620E 04 | -0.75080E 05 | -0.18690E 04 | 0.22428E |
| | FWD SKIRT | 0.12290E 04 | -0.77590E 05 | -0.16110E 04 | 0.19332E |
| | FWD TANKWALL | 0.19030E 04 | 0.72438E 05 | -0.57300E 03 | 0.68760E |
| | CENTER SECTION | 0.31130E 04 | -0.63159E 05 | -0.29660E 04 | 0.35592E |
| | AFT TANKWALL | 0.40000E 01 | 0.53313E 03 | -0.20000E 01 | 0.24000E |
| | AFT SKIRT | 0.12530E 04 | -0.70312E 05 | -0.15570E 04 | 0.18684E |
| 2 | FWD SKIRT | 0.12950E 04 | 0.10167E 06 | -0.70000E 01 | 0.70000E |
| | FWD TANKWALL | 0.84410E 04 | 0.41047E 06 | 0.64800E 03 | -0.64800E |
| | AFT TANKWALL | 0.51300E 03 | 0.37549E 05 | -0.10500E 03 | 0.10500E |
| | AFT SKIRT | 0.75700E 03 | -0.18027E 05 | -0.67000E 03 | 0.67000E |

Table 54. Study Merit Functions, 1985 Medium Range Payload Vehicle
(100,000 lb Orbital Payload)

| WEIGHT PER UNIT | DELTA DOLLARS PER UNIT | DELTA WEIGHT PER UNIT | DELTA PAYLOAD PER UNIT | COST RATIO |
|---|---|---|---|---|
| | | TITANIUM A HONEYCOMB SANDWICH | | |
| 0.13530E 04 | -0.40674E 05 | -0.20780E 04 | 0.24936E 03 | -0.1631123E 03 |
| 0.21220E 04 | 0.16582E 06 | -0.71800E 03 | 0.86160E 02 | 0.1924531E 04 |
| 0.16960E 04 | 0.12119E 06 | -0.78000E 03 | 0.93600E 02 | 0.1294804E 04 |
| 0.23700E 04 | -0.64747E 05 | -0.37090E 04 | 0.44508E 03 | -0.1454728E 03 |
| 0.30000E 01 | 0.44726E 03 | -0.30000E 01 | 0.36000E 00 | 0.1242400E 04 |
| 0.37000E 03 | -0.22915E 06 | -0.24400E 04 | 0.29280E 03 | -0.7826129E 03 |
| | | | | |
| 0.56700E 03 | -0.58411E 04 | -0.73500E 03 | 0.73500E 03 | -0.7347[illegible]E 01 |
| 0.55500E 04 | 0.29236E 06 | -0.22430E 04 | 0.22430E 04 | 0.1303434E 03 |
| 0.44000E 03 | 0.52398E 05 | -0.17800E 03 | 0.17800E 03 | 0.2943717E 03 |
| 0.62900E 03 | -0.41619E 04 | -0.79800E 03 | 0.79800E 03 | -0.5215426E 01 |
| | | BERYLLIUM A HONEYCOMB SANDWICH | | |
| 0.83300E 03 | 0.21262E 06 | -0.25980E 04 | 0.31176E 03 | 0.6819939E 03 |
| 0.64100E 03 | 0.15835E 06 | -0.21990E 04 | 0.26388E 03 | 0.6000725E 03 |
| 0.13310E 04 | 0.55732E 06 | -0.11450E 04 | 0.13740E 03 | 0.4056168E 04 |
| 0.13050E 04 | 0.23361E 06 | -0.47740E 04 | 0.57288E 03 | 0.4077861E 03 |
| 0.94500E 03 | 0.72994E 06 | 0.93900E 03 | -0.11268E 03 | -0.6477997E 04 |
| 0.63200E 03 | 0.15587E 06 | -0.21780E 04 | 0.26136E 03 | 0.5963873E 03 |
| | | | | |
| 0.24000E 03 | 0.50541E 05 | -0.10620E 04 | 0.10620E 04 | 0.4759007E 02 |
| 0.54560E 04 | 0.16090E 07 | -0.23370E 04 | 0.23370E 04 | 0.6884755E 03 |
| 0.42700E 03 | 0.28472E 06 | -0.19100E 03 | 0.19100E 03 | 0.1490662E 04 |
| 0.88100E 03 | 0.44646E 06 | -0.54600E 03 | 0.54600E 03 | 0.8176935E 03 |
| | | ALUMINUM C HONEYCOMB SANDWICH | | |
| 0.14570E 04 | -0.92968E 05 | -0.19740E 04 | 0.23688E 03 | -0.3924690E 03 |
| 0.11790E 04 | -0.86751E 05 | -0.16610E 04 | 0.19932E 03 | -0.4352351E 03 |
| | | | | |
| 0.29140E 04 | -0.90294E 05 | -0.31690E 04 | 0.37980E 03 | -0.2377417E 03 |
| 0.40000E 01 | 0.53313E 03 | -0.2[illegible]E 01 | 0.24000E 00 | 0.2221392E 04 |
| 0.12180E 04 | -0.76672E [illegible] | [illegible] 04 | 0.19104E 03 | -0.4013382E 03 |
| | | | | |
| 0.11970E 04 | 0.83911[illegible] | [illegible]500E 03 | 0.10500E 03 | 0.7991564E 03 |
| | | | | |
| 0.48900E 03 | 0.31717E 06 | -0.12900E 03 | 0.12900E 03 | 0.2458669E 03 |
| 0.70500E 03 | -0.29216E 06 | -0.72200E 03 | 0.72200E 03 | -0.4046520E 02 |

| STAGE | COMPONENT | WEIGHT PER UNIT | DELTA DOLLARS PER UNIT | DELTA WEIGHT PER UNIT | DELTA PAYLOAD PER UNI |
|---|---|---|---|---|---|
| | ALUMINUM A<br>INTEGRAL SKIN STRINGER | | | | |
| 1 | INTERSTAGE | 0.67608E 05 | | | |
| | FWD SKIRT | 0.33230E 05 | | | |
| | FWD TANKWALL | 0.74156E 05 | | | |
| | CENTER SECTION | 0.71023E 05 | | | |
| | AFT TANKWALL | 0.31714E 05 | | | |
| | AFT SKIRT | 0.33555E 05 | BASE POINT | | |
| 2 | FWD SKIRT | 0.15286E 05 | | | |
| | FWD TANKWALL | 0.10253E 06 | | | |
| | AFT TANKWALL | 0.16703E 05 | | | |
| | AFT SKIRT | 0.19979E 05 | | | |
| | ALUMINUM A<br>TOP HAT SKIN STRINGER | | | | |
| 1 | INTERSTAGE | 0.56466E 05 | -0.84375E 06 | -0.11142E 05 | 0.12256E |
| | FWD SKIRT | 0.27319E 05 | -0.53872E 06 | -0.59110E 04 | 0.65021E |
| | FWD TANKWALL | 0.58779E 05 | -0.99669E 06 | -0.15377E 05 | 0.16915E |
| | CENTER SECTION | 0.58276E 05 | -0.90517E 06 | -0.12747E 05 | 0.14022E |
| | AFT TANKWALL | 0.27164E 05 | -0.47766E 06 | -0.45500E 04 | 0.50050E |
| | AFT SKIRT | 0.28471E 05 | -0.50699E 06 | -0.50840E 04 | 0.55924E |
| 2 | FWD SKIRT | 0.13815E 05 | -0.25473E 06 | -0.14710E 04 | 0.14710E |
| | FWD TANKWALL | 0.66930E 05 | -0.16602E 07 | -0.35601E 05 | 0.35601E |
| | AFT TANKWALL | 0.11100E 05 | -0.47451E 06 | -0.56030E 04 | 0.56030E |
| | AFT SKIRT | 0.18689E 05 | -0.27652E 06 | -0.12900E 04 | 0.12900E |
| | ALUMINUM A<br>HONEYCOMB SANDWICH | | | | |
| 1 | INTERSTAGE | 0.47254E 05 | 0.42140E 06 | -0.20354E 05 | 0.22389E |
| | FWD SKIRT | 0.22266E 05 | 0.19209E 06 | -0.10964E 05 | 0.12060E |
| | FWD TANKWALL | 0.38447E 05 | -0.31589E 06 | -0.35709E 05 | 0.39280E |
| | CENTER SECTION | 0.46895E 05 | 0.28244E 06 | -0.24128E 05 | 0.26541E |
| | AFT TANKWALL | 0.16646E 05 | -0.16155E 06 | -0.15068E 05 | 0.16575E |
| | AFT SKIRT | 0.18391E 05 | -0.10814E 06 | -0.15164E 05 | 0.16680E |
| 2 | FWD SKIRT | 0.72680E 04 | -0.17482E 06 | -0.80180E 04 | 0.80180E |
| | FWD TANKWALL | 0.53274E 05 | -0.38723E 06 | -0.49257E 05 | 0.49257E |
| | AFT TANKWALL | 0.10187E 05 | 0.29330E 05 | -0.65160E 04 | 0.65160E |
| | AFT SKIRT | 0.15001E 05 | 0.26968E 06 | -0.49780E 04 | 0.49780E |

Table 55. Study Merit Functions, Current Post Saturn Payload Class Vehicles (1,000,000 lb Orbital Payload)

| WEIGHT PER UNIT | DELTA DOLLARS PER UNIT | DELTA WEIGHT PER UNIT | DELTA PAYLOAD PER UNIT | COST RATIO |
|---|---|---|---|---|
| **TITANIUM A HONEYCOMB SANDWICH** | | | | |
| 0.38635E 05 | 0.60492E 06 | -0.28973E 05 | 0.31870E 04 | 0.1898070E 03 |
| 0.18119E 05 | 0.29440E 06 | -0.15111E 05 | 0.16622E 04 | 0.1771137E 03 |
| 0.40092E 05 | 0.48303E 06 | -0.34064E 05 | 0.37470E 04 | 0.1289105E 03 |
| 0.37845E 05 | 0.42912E 06 | -0.33178E 05 | 0.36496E 04 | 0.1175815E 03 |
| 0.18048E 05 | 0.35518E 06 | -0.13666E 05 | 0.15033E 04 | 0.2362712E 03 |
| 0.15392E 05 | 0.23178E 05 | -0.18163E 05 | 0.19979E 04 | 0.1160102E 02 |
| 0.67280E 04 | -0.22018E 05 | -0.85580E 04 | 0.85580E 04 | -0.2572752E 01 |
| 0.53257E 05 | 0.46141E 06 | -0.49274E 05 | 0.49274E 05 | 0.9364268E 01 |
| 0.81600E 04 | 0.74185E 05 | -0.85430E 04 | 0.85430E 04 | 0.8683690E 01 |
| 0.13199E 05 | 0.45009E 06 | -0.67800E 04 | 0.67800E 04 | 0.6638490E 02 |
| **BERYLLIUM A HONEYCOMB SANDWICH** | | | | |
| 0.27342E 05 | 0.37125E 07 | -0.40266E 05 | 0.44293E 04 | 0.8381867E 03 |
| 0.12743E 05 | 0.21360E 07 | -0.20487E 05 | 0.22536E 04 | 0.9478270E 03 |
| 0.26389E 05 | 0.34225E 07 | -0.44634E 05 | 0.49097E 04 | 0.6970787E 03 |
| 0.12084E 05 | 0.20514E 07 | -0.19630E 05 | 0.21593E 04 | 0.9500283E 03 |
| 0.10017E 05 | 0.14749E 07 | -0.23538E 05 | 0.25892E 04 | 0.5696362E 03 |
| 0.39260E 04 | 0.65787E 06 | -0.11360E 05 | 0.11360E 05 | 0.5791143E 02 |
| 0.61250E 04 | 0.12593E 07 | -0.10578E 05 | 0.10578E 05 | 0.1190535E 03 |
| 0.92930E 04 | 0.19383E 07 | -0.10686E 05 | 0.10686E 05 | 0.1813856E 03 |
| **ALUMINUM C HONEYCOMB SANDWICH** | | | | |
| 0.40418E 05 | 0.27644E 05 | -0.27190E 05 | 0.29909E 04 | 0.9242692E 01 |
| 0.19808E 05 | 0.12779E 05 | -0.13422E 05 | 0.14764E 04 | 0.8655735E 01 |
| 0.36386E 05 | -0.44076E 06 | -0.37770E 05 | 0.41547E 04 | -0.1060880E 03 |
| 0.43542E 05 | 0.91292E 05 | -0.27481E 05 | 0.30229E 04 | 0.3020015E 02 |
| 0.16162E 05 | -0.19980E 06 | -0.15552E 05 | 0.17107E 04 | -0.1167905E 03 |
| 0.17459E 05 | -0.17971E 06 | -0.16096E 05 | 0.17706E 04 | -0.1014982E 03 |
| 0.67280E 04 | -0.23096E 06 | -0.85580E 04 | 0.85580E 04 | -0.2698722E 02 |
| 0.51218E 05 | -0.49911E 06 | -0.51313E 05 | 0.51313E 05 | -0.9726686E 01 |
| 0.96670E 04 | -0.18971E 05 | -0.70360E 04 | 0.70360E 04 | -0.2696290E 01 |
| 0.14360E 05 | 0.21719E 06 | -0.56190E 04 | 0.56190E 04 | 0.3865269E 02 |

| STAGE | COMPONENT | WEIGHT PER UNIT | DELTA DOLLARS PER UNIT | DELTA WEIGHT PER UNIT | DELTA PAYLOAD PER UNIT |
|---|---|---|---|---|---|
| | ALUMINUM A<br>INTEGRAL SKIN STRINGER | | | | |
| 1 | INTERSTAGE | 0.10024E 06 | | | |
| | FWD SKIRT | 0.40906E 05 | | | |
| | FWD TANKWALL | 0.10768E 06 | | | |
| | CENTER SECTION | 0.83816E 05 | | | |
| | AFT TANKWALL | 0.51158E 05 | | | |
| | AFT SKIRT | 0.39350E 05 | BASE POINT | | |
| 2 | FWD SKIRT | 0.16604E 05 | | | |
| | FWD TANKWALL | 0.17655E 06 | | | |
| | AFT TANKWALL | 0.39380E 05 | | | |
| | AFT SKIRT | 0.23750E 05 | | | |
| | ALUMINUM A<br>TOP HAT SKIN STRINGER | | | | |
| 1 | INTERSTAGE | 0.85655E 05 | -0.10480E 07 | -0.14586E 05 | 0.18962E 0 |
| | FWD SKIRT | 0.34955E 05 | -0.57068E 06 | -0.59510E 04 | 0.77363E 0 |
| | FWD TANKWALL | 0.86225E 05 | -0.12591E 07 | -0.21452E 05 | 0.27888E 0 |
| | CENTER SECTION | 0.72037E 05 | -0.91594E 06 | -0.11779E 05 | 0.15313E 0 |
| | AFT TANKWALL | 0.40880E 05 | -0.76322E 06 | -0.10278E 05 | 0.13361E 0 |
| | AFT SKIRT | 0.33038E 05 | -0.57804E 06 | -0.63120E 04 | 0.82056E 0 |
| 2 | FWD SKIRT | 0.14850E 05 | -0.27705E 06 | -0.17540E 04 | 0.17540E 0 |
| | FWD TANKWALL | 0.11832E 06 | -0.23222E 07 | -0.58226E 05 | 0.58226E 0 |
| | AFT TANKWALL | 0.27145E 05 | -0.80924E 06 | -0.12235E 05 | 0.12235E 0 |
| | AFT SKIRT | 0.21105E 05 | -0.35910E 06 | -0.26450E 04 | 0.26450E 0 |
| | ALUMINUM A<br>HONEYCOMB SANDWICH | | | | |
| 1 | INTERSTAGE | 0.74187E 05 | 0.75269E 06 | -0.26054E 05 | 0.33870E 0 |
| | FWD SKIRT | 0.30290E 05 | 0.41096E 06 | -0.10616E 05 | 0.13801E 0 |
| | FWD TANKWALL | 0.62491E 05 | -0.58274E 05 | -0.45186E 05 | 0.58742E 0 |
| | CENTER SECTION | 0.62760E 05 | 0.70415E 06 | -0.21056E 05 | 0.27373E 0 |
| | AFT TANKWALL | 0.29454E 05 | -0.50598E 05 | -0.21704E 05 | 0.28215E 0 |
| | AFT SKIRT | 0.29454E 05 | 0.42102E 06 | -0.98960E 04 | 0.12865E 0 |
| 2 | FWD SKIRT | 0.86850E 04 | -0.10709E 06 | -0.79190E 04 | 0.79190E 0 |
| | FWD TANKWALL | 0.99280E 05 | -0.22149E 06 | -0.77267E 05 | 0.77267E 0 |
| | AFT TANKWALL | 0.21063E 05 | -0.15834E 06 | -0.18317E 05 | 0.18317E 0 |
| | AFT SKIRT | 0.18788E 05 | 0.37610E 06 | -0.49620E 04 | 0.49620E 0 |

Table 56. Study Merit Functions, 1985 Post Saturn Payload Class Vehicle (2,000,000 lb Orbital Payload)

| WEIGHT PER UNIT | DELTA DOLLARS PER UNIT | DELTA WEIGHT PER UNIT | DELTA PAYLOAD PER UNIT | COST RATIO |
|---|---|---|---|---|
| **TITANIUM A HONEYCOMB SANDWICH** | | | | |
| 0.58935E 05 | 0.89429E 06 | -0.41306E 05 | 0.53698E 04 | 0.1665417E 03 |
| 0.24076E 05 | 0.48922E 06 | -0.16830E 05 | 0.21879E 04 | 0.2236012E 03 |
| 0.62143E 05 | 0.86710E 06 | -0.45534E 05 | 0.59194E 04 | 0.1464837E 03 |
| 0.50552E 05 | 0.87652E 06 | -0.33264E 05 | 0.43243E 04 | 0.2026947E 03 |
| 0.29460E 05 | 0.51845E 06 | -0.21698E 05 | 0.28207E 04 | 0.1838009E 03 |
| 0.22835E 05 | 0.44887E 06 | -0.16515E 05 | 0.21470E 04 | 0.2090720E 03 |
| 0.77450E 04 | 0.29952E 05 | -0.88590E 04 | 0.88590E 04 | 0.3380939E 01 |
| 0.88247E 05 | 0.47755E 06 | -0.88300E 05 | 0.88300E 05 | 0.5408306E 01 |
| 0.19104E 05 | 0.12057E 06 | -0.20276E 05 | 0.20276E 05 | 0.5946273E 01 |
| 0.16670E 05 | 0.59938E 06 | -0.70800E 04 | 0.70800E 04 | 0.8465809E 02 |
| **BERYLLIUM A HONEYCOMB SANDWICH** | | | | |
| 0.42448E 05 | 0.51472E 07 | -0.57793E 05 | 0.75131E 04 | 0.6850924E 03 |
| 0.17461E 05 | 0.28319E 07 | -0.23445E 05 | 0.30479E 04 | 0.9291507E 03 |
| 0.36011E 05 | 0.46440E 07 | -0.47805E 05 | 0.62147E 04 | 0.7472719E 03 |
| 0.22426E 05 | 0.34082E 07 | -0.28732E 05 | 0.37352E 04 | 0.9124770E 03 |
| 0.17005E 05 | 0.28019E 07 | -0.22345E 05 | 0.29049E 04 | 0.9645483E 03 |
| 0.48560E 04 | 0.88408E 06 | -0.11748E 05 | 0.11748E 05 | 0.7525370E 02 |
| 0.14140E 05 | 0.21864E 07 | -0.25240E 05 | 0.25240E 05 | 0.8662402E 02 |
| 0.12123E 05 | 0.24330E 07 | -0.11627E 05 | 0.11627E 05 | 0.2092519E 03 |
| **ALUMINUM C HONEYCOMB SANDWICH** | | | | |
| 0.63470E 05 | 0.21885E 06 | -0.36771E 05 | 0.47802E 04 | 0.4578254E 02 |
| 0.25788E 05 | 0.11150E 06 | -0.15118E 05 | 0.19653E 04 | 0.5673371E 02 |
| 0.60447E 05 | -0.16382E 06 | -0.47230E 05 | 0.61399E 04 | -0.2668175E 02 |
| 0.54186E 05 | 0.25406E 06 | -0.29630E 05 | 0.38519E 04 | 0.6595594E 02 |
| 0.28584E 05 | -0.10781E 06 | -0.22574E 05 | 0.29346E 04 | -0.3673589E 02 |
| 0.24908E 05 | 0.11558E 06 | -0.14442E 05 | 0.18775E 04 | 0.6156388E 02 |
| 0.84400E 04 | -0.13096E 06 | -0.81640E 04 | 0.81640E 04 | -0.1604100E 02 |
| 0.94705E 05 | -0.42547E 06 | -0.81842E 05 | 0.81842E 05 | -0.5198702E 01 |
| 0.20039E 05 | -0.23359E 06 | -0.19341E 05 | 0.19341E 05 | -0.1207727E 02 |
| 0.18160E 05 | 0.32835E 06 | -0.55900E 04 | 0.55900E 04 | 0.5873818E 02 |

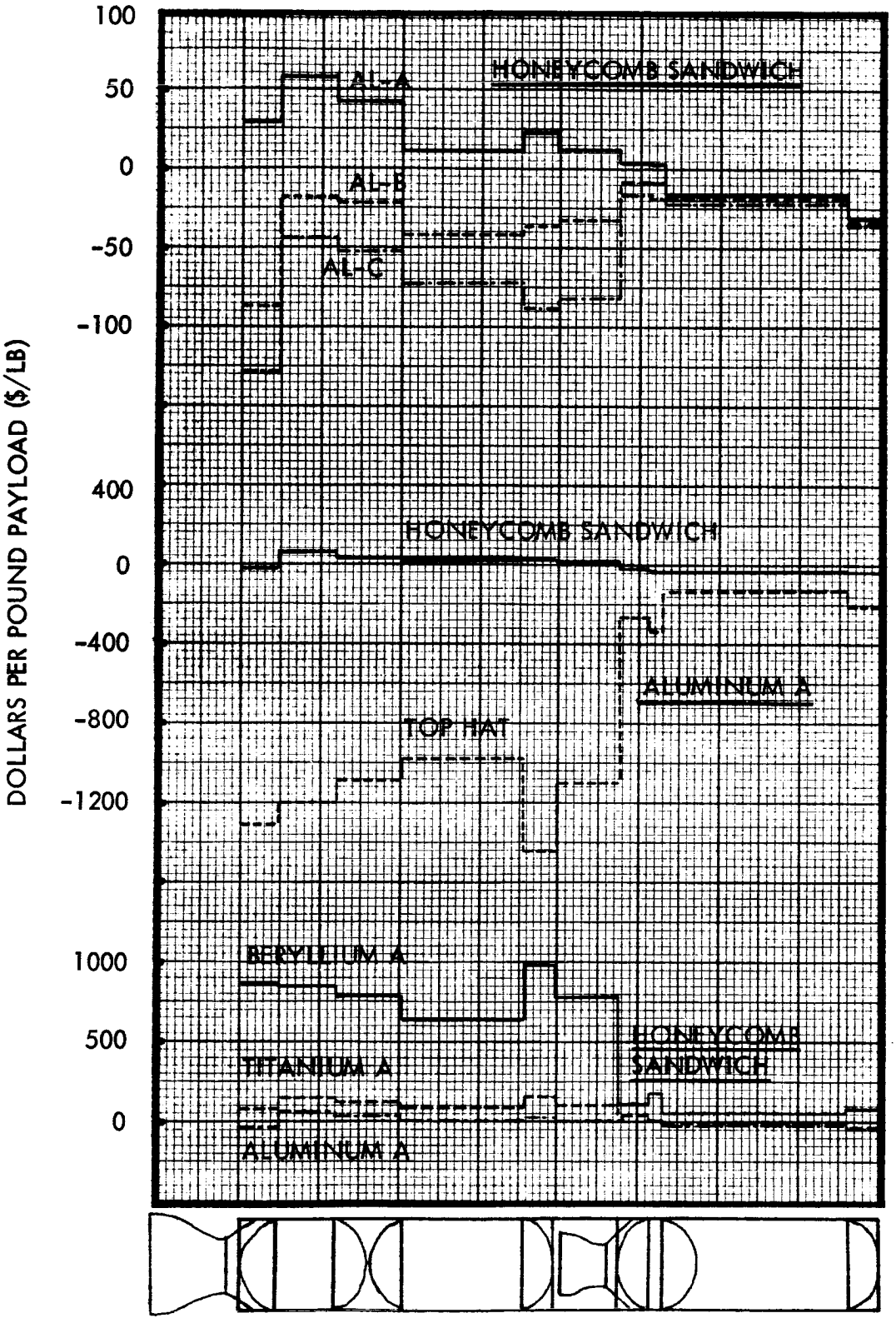



Figure 72. Cost Ratios for 1985 Saturn Payload Class Two Stage Vehicle

# CONCLUSIONS

Phase I of the study contract illustrates the areas of structural design in launch vehicle systems where structural and material improvements are most beneficial with respect to component weight reduced, equivalent payload gained, and economic justification. Several types of improvements selected for study have not produced favorable benefits in any vehicle system, whereas others have had their gains limited to a particular family of vehicle systems.

The following preliminary conclusions can be made from the materials, types of construction, and vehicle loadings considered to date:

1. Improvements in materials obtained by increasing their compressive yield or ultimate tensile stress resulted in noticeable decreases in structural weight for (a) honeycomb sandwich concepts, (b) highly loaded components (future vehicle systems), (c) internal pressure designed components (propellant tanks), and (d) components with small radii. Percentage increases in the material properties does not correspond to an identical percentage weight reduction. At best the effect of a 10-percent compressive yield increase results in a 7-percent weight reduction if the designs considered are both optimum concepts (minimum weight).

2. Material advances in fabricability, forming, welding, etc., although not considered in this report, will contribute to significant improvements in component design and costs by the removal of certain design restrictions and reduction of the fabrication complexity factors and hence component cost. Various protective linings, coatings, and treatments are required for some classes of materials if they are subject to incompatible elements. The study design analysis of such components and materials investigates weight reduction effects and does not consider the incompatibility aspect.

3. For the four different types of construction concepts investigated, results indicated that honeycomb sandwich offered the best returns in unit weight reduction with property improvements. Highly efficient honeycomb sandwich designs were obtained for the ranges of component radii and loading intensities considered, if deep core sandwich designs are permissible. Benefits from deep core honeycomb sandwich designs are more significant with larger component radii and higher load intensities associated with the



PRECEDING PAGE BLANK NOT FILMED.

1 to 2 million pound payload vehicles. Core height restrictions of 1.5 inches in titanium and aluminum for future vehicle systems (radii greater than 270 inches) will produce weight penalties of 100 percent from minimum designs. Continued research is required to permit exploitation of the potentials of deep core honeycomb sandwich. Minimum weight analysis for the deep core considered adjusted core properties and height, per Appendix C. These correction factors were based upon a limited amount of test data and require further test verification.

Associated with these deep cores are closeout, attachment, and joining problems. Densified cores to solve these problems will severely penalize design weights. Attaching internal equipment and substructure to both facing sheets of deep core sandwich imposes weight problems. For thick face sheet sandwich in the 20,000-pound-per-inch compressive load intensity class, attachments to a single facing merit serious consideration. Even with height restricted, sandwich fabrication problems are present for the highly loaded designs. Facing sheets for these concepts are extremely thick and stiff and require excessive pressures to obtain complete bonding. Experimental and manufacturing effort is required to develop methods for circumferential joining of facing sheets and to solve bonding adhesive problems in the transference of high loading intensities between facing sheets. Circumferential joining of the facing sheets with loading intensities in the range of 20,000 pound-per-inch presents formidable problems in joining a facing sheet after it has been bonded to the core. Splice and lap joints will require stronger bonding adhesives than those currently used to transfer the high loading intensities between panels.

4. Skin stringer construction conventionally uses stringers equal to or one gage larger than the skin gage. This design practice permits the assumption that panel buckling occurs between adjacent stringers. For the minimum weight concepts in the preliminary design synthesis study, the stringers were permitted to be thinner than the skin. The resulting designs were theoretically checked to determine if the stringer members were sufficiently rigid to restrict panel buckling to individual panels and not allow the buckles to jump between panels across the stringers. Further experimental investigation is required to justify this procedure, and additional design synthesis for the skin stringer concept will indicate the weight penalties, if any, associated with having the stringers thicker than the skin.

5. Although the waffle designs considered were not competitive weight-wise with skin-stringer and honeycomb sandwich, these penalties could be imposed by the height-to-thickness restrictions and the conservative general stability correction coefficients applied to the analysis. Easing of these restrictions could reduce the shell weights and make the construction weight competitive. Waffle designs, although slightly heavier, could be used effectively when considerations are based upon cost or internal height restriction imposed upon the stiffener elements.

6. Structural concepts for future vehicle classes with large radii and highly loaded components require experimental verification. Most of the stability analysis relies upon correction factors to adjust the classical theory to agree with test results. Unfortunately these tests were confined to small radii and lightly loaded specimens and results are assumed to be applicable to future concepts which are an order of magnitude different in size and loading. A preliminary investigation of methods of analysis for general instability has been included in this study and shows significant weight penalties to be incurred with different analytical approaches. Typical analyses of waffle and skin-stringer concepts do not consider the torsional, shearing, or transverse stretching and bending stiffnesses. This is primarily due to the lack of experimental data to make a realistic estimate of the transverse and shear effectiveness coefficients present in the stiffness expressions $\alpha$, $\alpha'$, $\beta$, $\beta'$. (See Appendix C, Reference 19.)

7. A preliminary attempt at detailing cost estimates for the various structural components illustrated relative costs arising from concept and material changes for the study vehicle spectrum. The principal conclusion from these results indicates the cost sensitivity to the complexity factors associated with fabrication. Before research direction decisions are based upon the cost ratios developed here, a better understanding is required of the derivation of component structural cost and its influence in the overall vehicle cost effectiveness. The cost ratio values shown in Tables 51 through 56 were developed for fabrication and manufacturing costs only. Additional cost factors should be considered to develop a more comprehensive cost ratio; these include design (drafting and analysis), research, testing, and development of both the structural and material improvement and its application applied to a specific vehicle system.

In conclusion, the study results illustrate that structural benefits are obtainable from material improvements and construction concept selection. Also, research and experimental verification in other areas will produce significant improvements; e.g., methods of analysis, stability correction

factors, manufacturing restrictions and limitations. Additional investigation, verification, and application (and their effect on structural design) are required in the following areas:

1. Methods of stability analysis
2. Stability correction factors to allow for experimental data
3. Manufacturing restrictions and limitations
4. Cost ratio definition
5. Costing approach
6. Manufacturing complexity factor determination

# APPENDIXES

## APPENDIX A —STAGE PROPORTIONING

One problem arising from rocket vehicle design concerns the minimizing of system expenditure whether it is propellant mass, vehicle cost, etc., and the maximizing of the overall performance returns. To achieve either of these effects, it is desirable to determine the optimum number of stages required and their optimal size relationships. This will help to maximize the performance returns such as decreased liftoff weight, larger payloads in orbit and/or lower cost per pound in orbit. With the large booster systems envisaged for further missions, the cost of building, launching, propellants, ground support equipment, etc., become expensive items; therefore, badly designed and conceived rocket launch systems will incur expensive cost penalties which could far outweigh the time and effort spent in initiating an optimally designed vehicle system.

Initial design studies for launch vehicle concepts require analytical techniques for optimally sizing the vehicle (ascertaining type and arrangement of vehicle stages, and determining propulsion systems, propellant combinations, types of structures and materials and their interaction effects) to determine the most efficient vehicle combination to undertake a specific type of operation. A basic requirement is to design and develop the best cost effective system to fulfill the mission requirements. For the smaller rocket vehicles the approach was to minimize the fuel used and design the lightest structure components. Although, with the large launch systems, fuel and structure weight are of prime importance, additional factors are involved which will influence the design decisions by reason of their cost and implifications. The final merit function that should be considered, therefore, is the cost effectiveness of the overall vehicle system. This could be a measure of the dollar-per-pound payload in orbit when considering the expenditures due to design and development, manufacturing, propellant requirements, cost per launch, launch complex and ground support equipment, and the number of vehicle systems required to fulfill the overall mission requirements.

The main objective of this study is to determine the significance of structures/material research for launch vehicle structural design on the overall vehicle system. Consideration has to be given to the most efficient types of construction, material, fabrication, etc., for the various structural components of the vehicle system. Therefore, in order to investigate these structural and material effects, suitable and realistic base point vehicles are required for the study in addition to the associated design environment for the components and the overall performance indices of the vehicle systems.

There are several techniques for optimally proportioning vehicle systems to maximize the performance. These include calculus of variations and Lagrange multipliers, but most of these techniques suffer from various imposed limitations in order to obtain explicit solutions. The limitations include constant performance characteristic for each stage, constant and identical mass fractions for all stages and, for a large number of stages, the amount of computation required is greatly increased.

Although many of these weight and cost estimates can be expressed as continuous functions dependent on launch weights, there are others that can only be expressed as stepwise, discontinuous functions dependent on the number of items used and the type of material, propellants, etc.

An alternative approach is outlined herein which allows the evaluation of vehicle systems without the previously discussed imposed limitations on the system characteristic performance. Using a dynamic programming technique (Reference A1, A2), these various step functions can be easily considered in the evaluation of the optimal proportioning for the best performance vehicle system. Dynamic programming also helps the operator to investigate the relative flatness of the optima, which is valuable information of the performance of the rocket stages if they must be designed away from the "ideal optimum." The dynamic programming approach is an extension of that developed in Reference A-3 but has been extensively modified to allow consideration of varying velocity losses as functions of the vehicle size and performance. This will allow a realistic evaluation of the vehicle system to fulfill specified mission requirements.

## VELOCITY LOSSES

Procedures for estimating the liftoff weight of future vehicle systems and for efficiently proportioning the stages of any "N" stage vehicle, involve determining the ideal characteristic velocity to fulfill a given mission requirement ($\Delta V_t$). This value of $\Delta V_t$ must be apportioned between the N stages and corrected for gravity, atmospheric, and drag velocity losses. The presentation of material in this section will be concentrated on the problem of allocating the total required velocity increments into the individual requirement of the stages, correcting these increment velocities, and then sizing the vehicle.

Since the vehicle sizing is strongly dependent upon the magnitude of the assumed velocity losses, three basic estimation techniques were assessed during this study and test cases evaluated using basic Saturn class vehicle combinations with payloads of 30,000- to 60,000-pound payload (Reference A-4). These vehicle test cases use the upper two stages of the Saturn vehicle (S-II and S-IVB) with stretched propellant tanks and modified engine systems. The results obtained using the empirical velocity loss

techniques were compared to the results obtained from a sophisticated flight trajectory-mass fraction computer program. The three types of loss estimation techniques are as follows:

1. Constant velocity loss, irrespective of stage size

2. Velocity loss as a function of altitude and vehicle burning time

3. Velocity loss as a function of stage performance characteristics and trajectory flight path

These three techniques were tried for a basepoint vehicle to determine their relative effectiveness in assessing the magnitude of the velocity losses. The initial technique assumes the velocity loss to be a constant value of 6000 feet per second and the propellant allotted between the two stages to optimize the payload but with the restriction that the initial $T/W = 1.25$ for the engine systems considered. Resultant payload capability is shown in Figure A-1 for this constant velocity loss assumption. The estimated payload variation with the first-stage propellant loading does not resemble the payloads evaluated using the flight trajectory program. Using this constant velocity loss, irrespective of the stage proportion, will result in erroneous propellant apportioning between the vehicle stages, although the maximum payload in the above case was comparable. The effect of assumed variations of velocity losses for a first stage having 566,000 pounds of propellant is indicated in Figure A-2. Resulting large variations in payload capability for a typical range of velocity loss estimates is clearly shown. Therefore, it is required to obtain realistic estimates for the velocity loss to obtain any sensible vehicle stage proportioning.

The next technique was to allow the velocity losses to be a function of the burnout altitude and the duration of the burning time of the vehicle stages. (Reference A-5). These results shown in Figure A-3 exhibit the characteristics of the payload decrease either side of an optimum propellant loading at 590,000 pounds. Although the payload variations are similar to those obtained from the flight trajectory program, their payload magnitudes are quite different.

The third technique considered the velocity losses, broken into first stage and upper stage losses, as a function of stage performance characteristics (Reference A-6). The first-stage losses can be subdivided into drag, gravity, and thrust atmospheric losses. The results obtained with these techniques are shown in Figure A-4, where the burnout angle of the first stage is assumed to be 65 degrees. This approach closely agreed with the exact solution obtained from the flight trajectory program which exhibited the maximum payload characteristic trend and the resultant magnitude. The effect of selecting various burnout angles is indicated in Figure A-5 for a

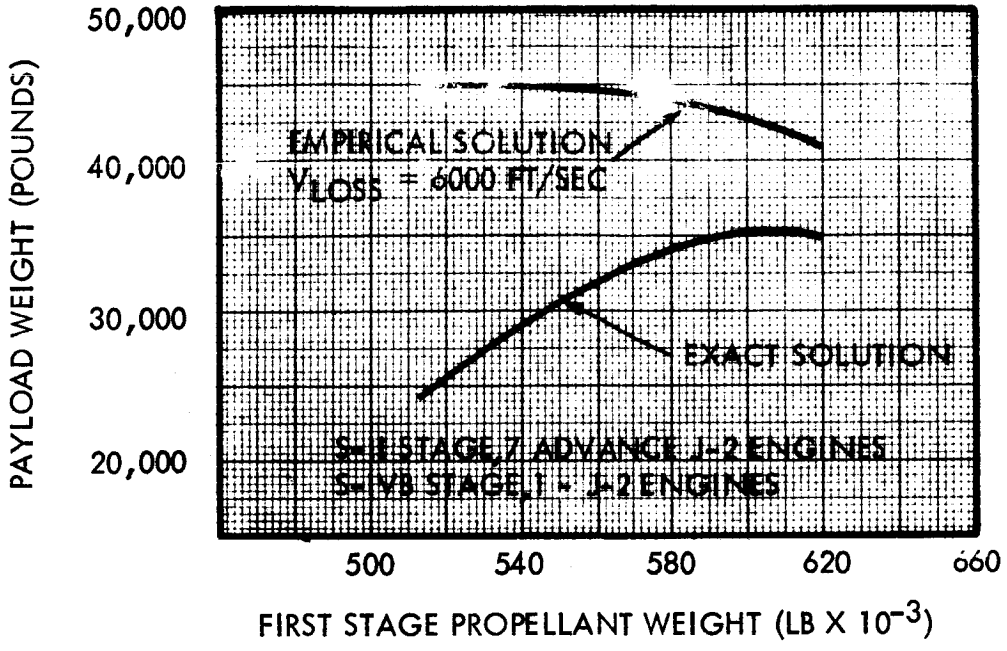



Figure A-1. Payload Variation With Constant Velocity Losses

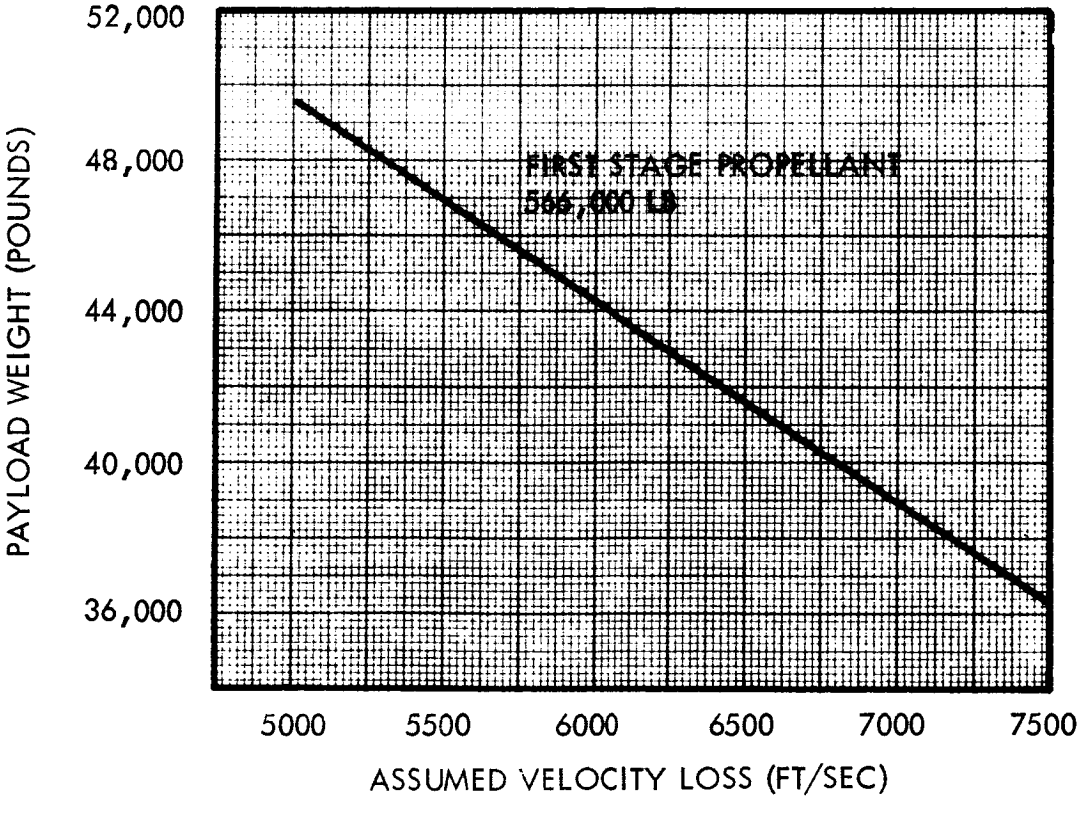



Figure A-2. Payload Variation With Velocity Loss Estimation

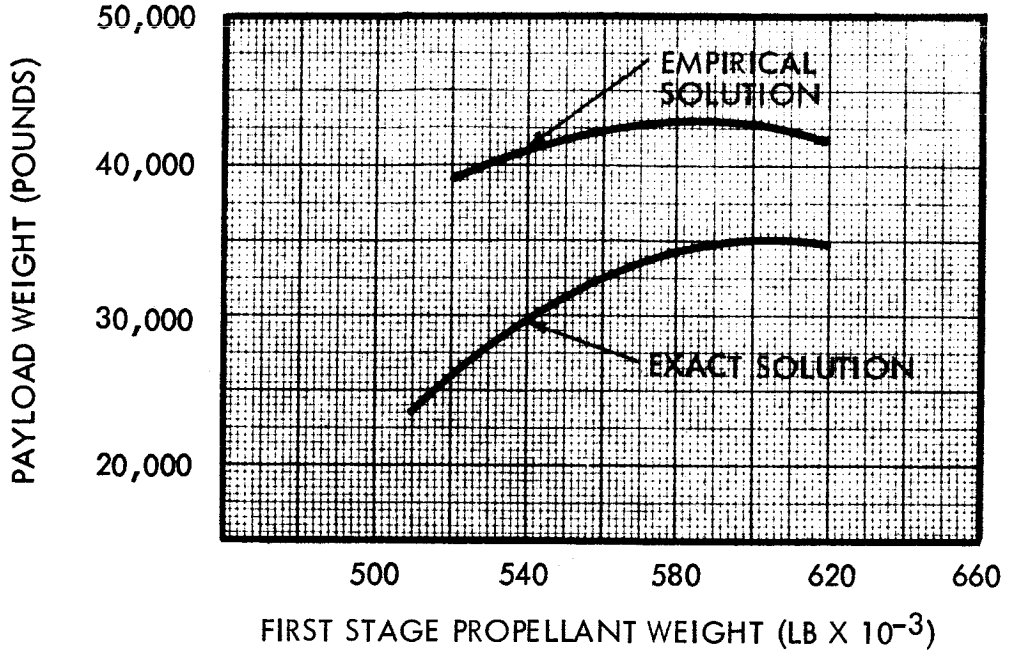



Figure A-3. Payload Variation - Velocity Loss Size Dependent

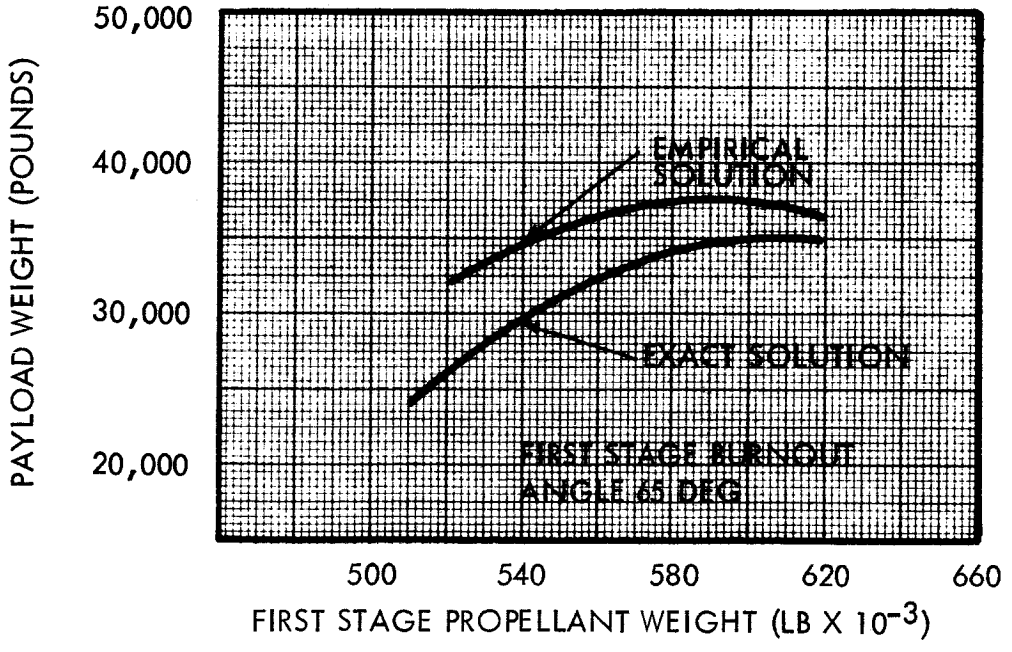



Figure A-4. Payload Variation - Velocity Loss Performance Dependent

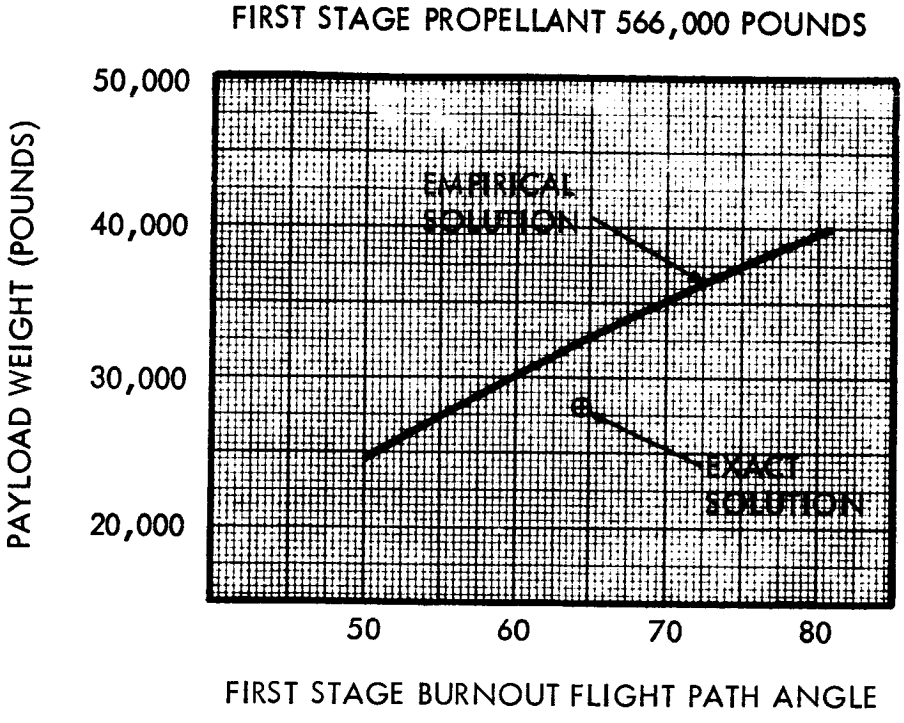



Figure A-5. Payload Variation With Burnout Angle

range of angles from 50 to 80 degrees. This range should more than amply cover any typical burnout angles of manned system first stages.

Although all the methods discussed, with experienced estimates for the various parameters involved in the velocity losses, produce realistic maximum payload magnitudes, some of them produce the maximum capability with an adverse apportioning of propellant between the various stages. The method of losses based upon altitude and burning time produce meaningful results with only a minimum of knowledge of the flight trajectory of the vehicle. If these results can then be referred to the payload capability of a known basepoint design, an adjustment factor can be incorporated to correct the other vehicles' payload performance. This technique is possible when a vehicle design is being perturbed with a series of modifications about an existing basepoint for which trajectory data is available. Final method requires information about the flight paths and burnout angle of the first stage of the vehicle. Existing empirical relationships are available for obtaining an estimate of the burnout angle. Also, one should consider a change of burnout angle of the first stage dependent on the size of the stage. This is discussed later in this section.

These various techniques for estimating velocity loss were incorporated in the stage proportioning program for the vehicle synthesis. A detailed description of the latter two techniques and their empirical relationships is subsequently discussed.

## VELOCITY LOSS–ALTITUDE TIME

In some mathematical developments that have been presented, attempts are made to estimate the velocity losses for families of launch trajectories. These methods provide a feel for the significant source of the losses; however, they do not generally provide the most accurate data. For this reason an empirical approach based on Reference A-5 for estimating the total loss due to gravity and aerodynamic forces was used. This technique consists of correlating velocity loss data obtained from numerical integration of trajectories for a range of typical burning time, burnout angle, velocities, and flight path angle. Most of the missions considered were for a circular orbit and a final stage burnout angle of 90 degrees. It is assumed that all missions other than ascent to circular orbits very closely approximate ascent to a circular orbit, with a subsequent burning period at zero flight path. Therefore, since the velocity loss due to gravity varies as the sine of the flight path angle and since at these altitudes atmospheric losses are negligible, the velocity loss of these trajectories will thus be a function of the time spent below orbital velocity. The data, therefore, are correlated as functions of time below orbital speed and the altitude of burnout (Figure A-6). For the synthesis program, Figure A-6 was expressed mathematically to reduce the storage requirements of the subroutine. This mathematical presentation is as follows:

$$V_{Loss} = 2350 + 5.6t + (8.33 - 3.5 \times 10^{-3} t)\, h + (0.0166 - 5 \times 10^{6} t)\, h^2 \qquad (1)$$

where

t = burning time below orbital speed (secs)

h = burnout altitude (naut mi)

## VELOCITY LOSS - PERFORMANCE CHARACTERISTICS

This technique is based on the method developed in Reference A-6 and slightly modified for this study synthesis program. To obtain an exact solution for the velocity losses, an analysis of the equations of motion of a vehicle system thrusting in the atmosphere will indicate a complicated set of differential equations requiring solutions by a digital computer. However, investigation of each term of the equation will indicate the effects of gravity, drag, and atmospheric losses on the overall vehicle performance. This

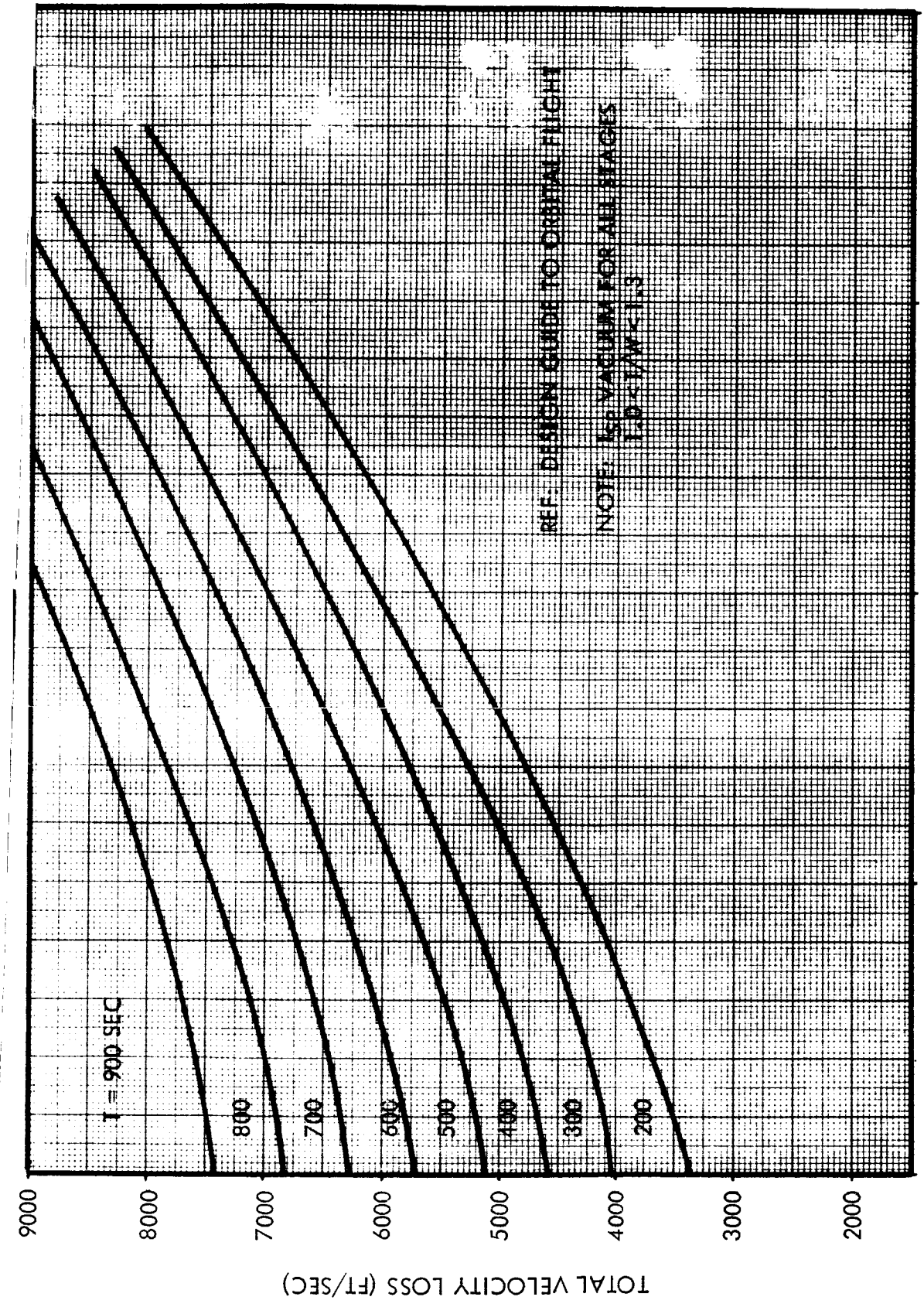



Figure A-6. Velocity Loss - Altitude, Time Dependent

mination leads to expressions representing empirical data generated in t studies. The equations of motion of a vehicle thrusting in the earth's iosphere are

$$m\dot{V} = T_{vac}\left[1-\frac{P_h}{P_{sl}}(1-\lambda)\right] - (W_o-\dot{W}t)\left(\frac{r_e}{r_h}\right)^2\cos\beta - C_D\,1/2\,\rho_h V^2 A \qquad (2)$$

$$mV\dot{\beta} = (W_o-\dot{W}t)\left(\frac{r_e}{r_h}\right)^2\sin\beta - \frac{mV^2\sin\beta}{r_h}$$

s assumed that the first stage will have a pitch program that follows a ivity turn (zero angle of attack). Rewriting and integrating Equation 2 sults in an expression for the velocity at burnout:

$$\frac{V_{bo}}{g_e} = Isp_{vac}\ln\frac{W_o}{W_{bo}} - \int_o^{t_B}\frac{\frac{T}{W_o}(1/\lambda-1)\frac{P_h}{P_{sl}}}{\left[1-\frac{T/W_o}{Isp_{sl}}t\right]}dt - \int_o^{t_B}\left(\frac{r_e}{r}\right)^2\cos\beta\,dt - \int_o^{t_B}\frac{1/2\rho_h V^2 C_D A\,dt}{W_o\left[1-\frac{T/W_o}{Isp_{sl}}t\right]} \qquad (3)$$

his equation clearly indicates the form that the various losses due to gravity, rag, and thrust atmospheric effects take in the overall velocity equation. hese velocity losses can be defined respectively for the following integrals:

$$V_{loss\ gravity} = g_e\int_o^{t_B}\left(\frac{r_e}{r}\right)^2\cos\beta\,dt$$

$$V_{loss\ drag} = g_e\int_o^{t_B}\frac{1/2\rho_h V^2 C_D A\,dt}{W_o\left[1-\frac{T/W_o}{Isp_{sl}}t\right]} \qquad (4)$$

$$V_{loss\ atmos} = \int_o^{t_B} \frac{T\,(1/\lambda - 1)P_h/P_{sl}}{W_o\left[1 - \frac{T/W_o}{I_{sp_{sl}}}t\right]}\,dt$$

The ideal velocity of the vehicle system for any particular stage is given by

$$V_I = g_e\, Isp_{vac}\ \ln\frac{W_o}{W_{bo}} \tag{5}$$

so that the burnout velocity of the stage operated in the atmosphere is

$$V_{bo} = V_I - V_{loss\,gravity} - V_{loss\,drag} - V_{loss\,atmos} \tag{6}$$

The exact values of these various components of the velocity loss would require numerical integration for a solution. Thus, the results of numerous trajectory calculations generated in various studies, (Reference A-6), were combined into empirical relationships for vehicles with a large range of typical design parameters. The gravitational losses for the first stage of the vehicle synthesis can be empirically expressed by

$$V_{loss\ gravity} = (g_e\, t_b - K_{gg})\left[1 - K_g\,(1 - 1/r)\left(\frac{\beta_{bo}}{90}\right)^2\right] \tag{7}$$

indicating that the gravitational losses are functions of the vehicle design parameters, the burnout angle, and two empirical constants $K_{gg}$ and $K_g$. The expression $g_e t_b$ in this expression is the gravitational loss exptected from vertical flight in a constant gravitational field. However, due to an inverse square gravitation field, the constant, $K_{gg}$ is required to correct the overestimated loss determined by the vertical flight. The value of $K_{gg}$ is shown in Figure A-7 and is a function specifically of the vacuum specific impulse of the vehicle system. An expression for $K_{gg}$ is

$$K_{gg} \approx 103 - 0.7695\ Isp + 1.655 \times 10^{-3}\ Isp^2 \tag{8}$$

The constant, $K_g$, is a function of the initial thrust-to-weight ratio, vacuum specific impulse, and mass ratio. This constant is shown in Figure A-8 for a typical mass ratio of 2.5 for the first stage. The expression for these curves is given by

$$K_g \approx -0.606 + 1.256\,\frac{T}{W_o} - 0.239\left(\frac{T}{W_o}\right)^2 + 0.0107\left(2.4 - \frac{T}{W_o}\right)\left(\frac{T}{W_o}\right)\left(\frac{Isp - 400}{100}\right) \tag{9}$$

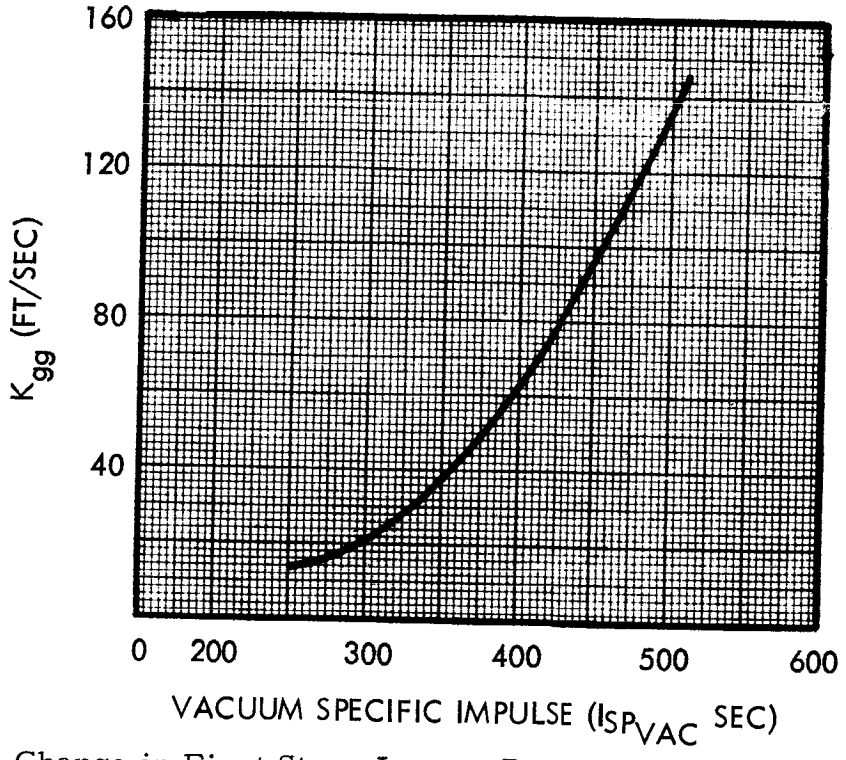



Figure A-7. Change in First Stage Losses Due to Altitude Variation of Gravity

If the first stage has a mass ratio other than 2.5, an additional multiplying factor, $\Delta K_g$, is required and varies as shown in Figure A-9 with an appropriate mathematical representations given by

$$\Delta K_g = 1 + \left(\frac{1}{r} - \frac{1}{2.5}\right)\left(1.14\left(\frac{T}{W_o}\right)^2 - 2.62\left(\frac{T}{W_o}\right) + 1.515\right)\left(\frac{T}{W_o} - 1.15\right);$$

$$1.25 \leq \frac{W_o}{W_{bo}} \leq 2.5$$

$$\Delta K_g = 1 + \left[-0.16\left(\frac{W_o}{W_{bo}}\right)^2 + 1.6\left(\frac{W_o}{W_{bo}}\right) - 3.0\right] \left[0.0467\,\frac{T}{W_o} + 0.04\right]; \quad \frac{W_o}{W_{bo}} > 2.5, \quad \frac{T}{W} > 1.5 \tag{10}$$

$$\Delta K_g = 1 + \left[-0.16\left(\frac{W_o}{W_{bo}}\right)^2 + 1.6\left(\frac{W_o}{W_{bo}}\right) - 3.0\right] \left[0.2\left(\frac{T}{W_o}\right) - 0.19\right]; \quad \frac{W_o}{W_{bo}} > 2.5, \quad \frac{T}{W} < 1.5$$

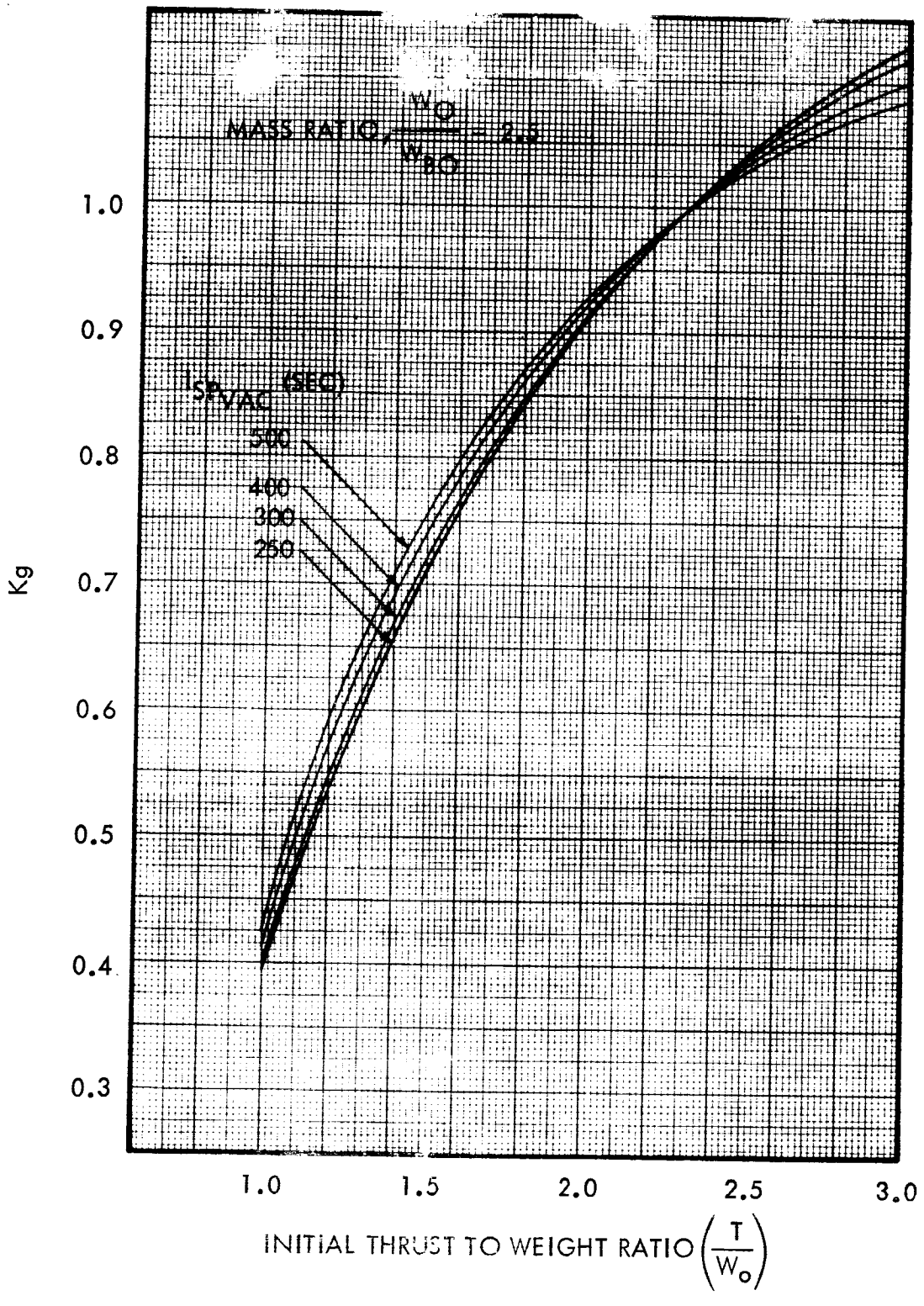



Figure A-8. First-Stage Gravity Loss Constant

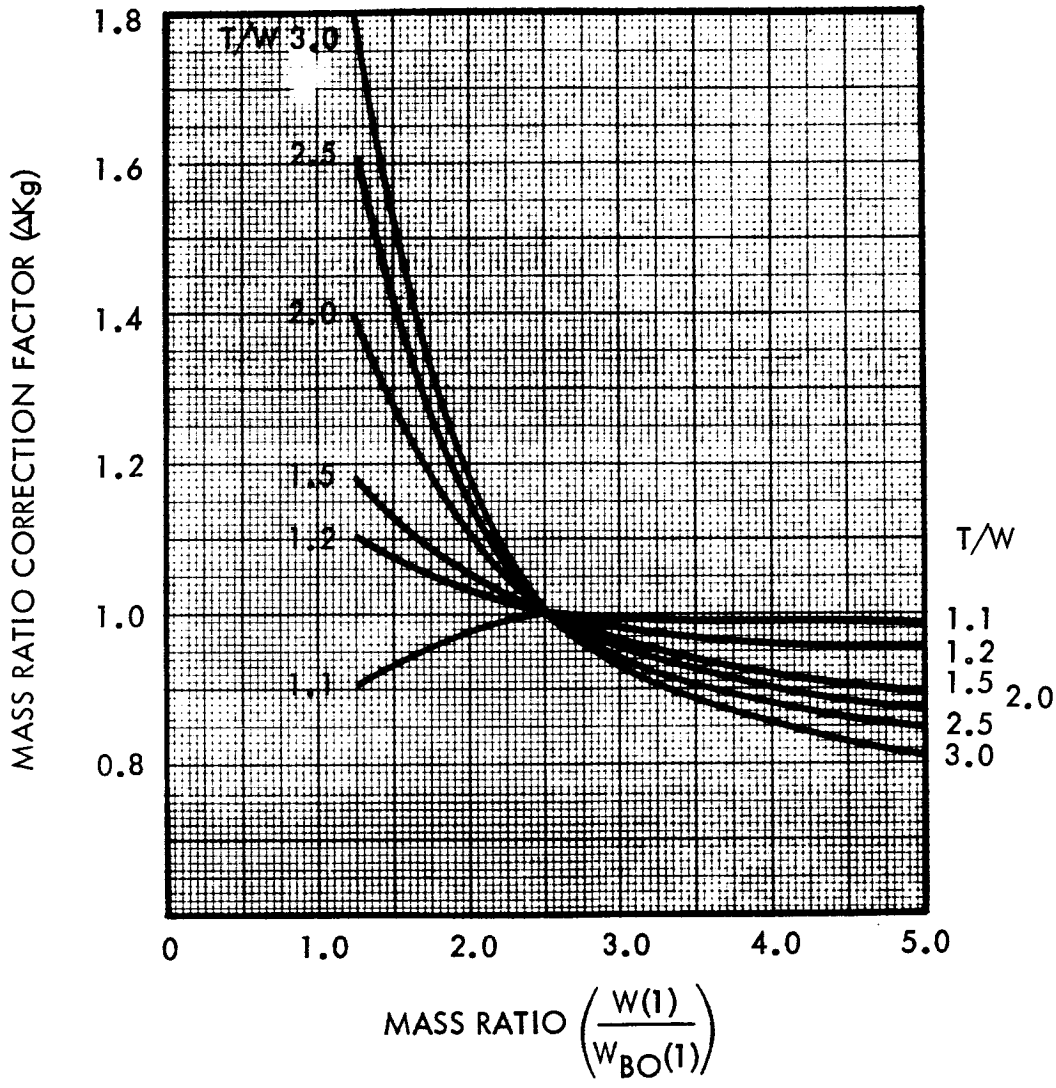



Figure A-9. First-Stage Mass Ratio Correction Factor

An examination of the drag velocity integral indicates that the losses are functions of the ballistic parameter $W_o/C_DA$ which is also a time-varying function. It has been found that these losses can be represented by the relationship

$$V_{\text{loss drag}} = K_D \frac{C_{D_{PD}}}{W_o} \tag{11}$$

The empirical constant, $K_D$, is a function of the specific impulse, thrust-to-weight ratio, and burnout angle. This is shown in Figure A-10 and is expressed by

$$K_D = 10^6 \left(\frac{21.2}{\chi - 2.68} - 0.536\right) - \left[1 - \left(60 - \beta_{bo}\right)\left(1 + \left(\frac{18-\chi}{7}\right)^{1.5}\right)\left(7.5 \times 10^{-5}\ \beta_{bo} + 0.003\right)\right] \tag{12}$$

where

$$\chi = \frac{\left(Isp_{vac}\right)^{1/2}}{T/W_o}$$

The applicable drag coefficient at maximum drag forces during the trajectory requires knowledge of the mach number at maximum drag in order to use the correct value for this drag coefficient, a typical range is $(0.6 < C_D < 0.77)$ .

There are losses associated with the atmosphere thrust. Isp changes are caused by the reduction of the vacuum thrust level by atmospheric pressure during the early portion of the flight through the atmosphere. Thus, the ratio of sea level to the vacuum specific impulse is the important parameter in determining these losses. This variation is shown in Figure A-11 and is represented by

$$V_{\text{loss atmos}} = Ka$$

$$Ka = 340\left(\frac{T}{W_o} - 1.5\right)\left(1 - \frac{Isp_{sl}}{Isp_{vac}}\right) + 4250\left(\frac{Isp_{sl}}{Isp_{vac}}\right)^2 - 10800\left(\frac{Isp_{sl}}{Isp_{vac}}\right) + 6550 \tag{13}$$

The remaining velocity losses occur in the vehicle upper stages and are due primarily to gravity and angle of attack. Since the gravity loss is larger the upper stage losses can be expressed as

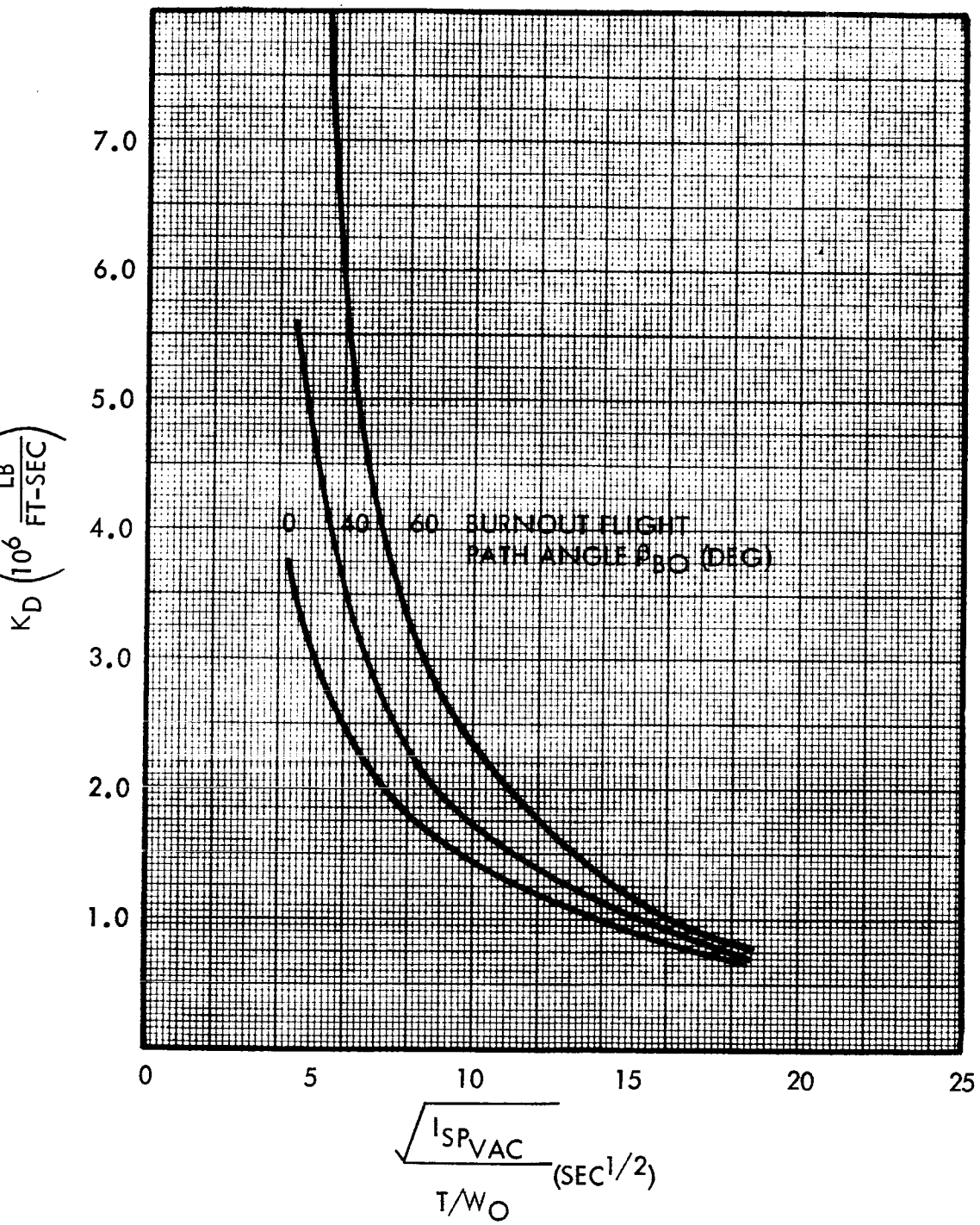



Figure A-10. First Stage Drag - Loss Constant

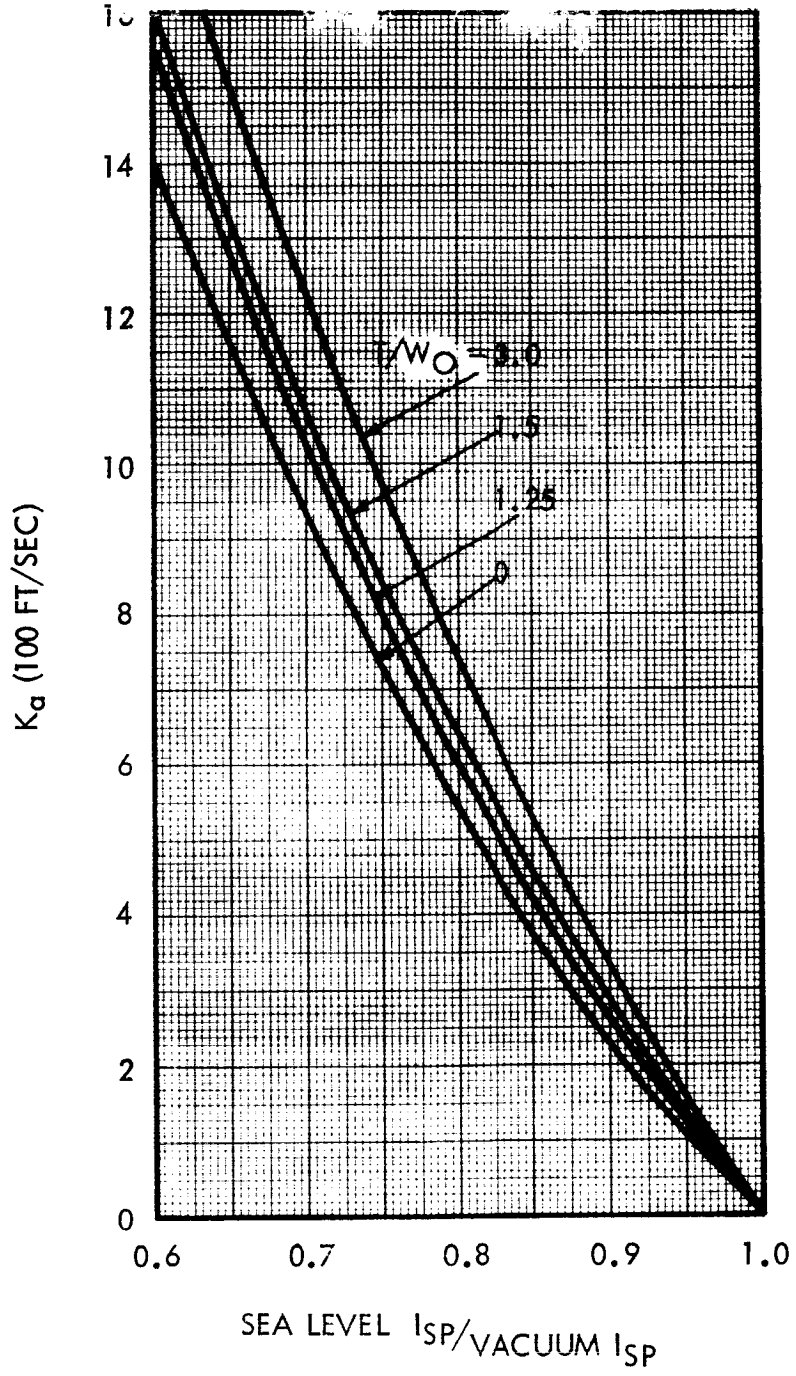



Figure A-11. First-Stage Thrust Atmospheric Losses

$$V_{loss\ upper} = g_e\, t_B^{(2)} \cos\bar{\beta} \qquad (14)$$

where

$t_B^{(2)}$ = burning time of upper stages below orbital velocity

and $\bar{\beta}$ is an average flight path angle selected between the initial values of the upper stage flight path angle and the final burnout angle. The average angle, $\bar{\beta}$, is dependent upon the thrust pitch program for the upper stages. Typical value for these flight path angles is shown in Figure A-12 and can be expressed by

$$\cos\beta = 5 \times 10^{-5}\ \beta_{bo}^{2} - 1.217 \times 10^{-2}\ \beta_{bo} + 0.6901 \qquad (15)$$

$\beta_{bo}$ = burnout angle of first stage

The nomograph in Figure A-13 indicates an approach for evaluating the appropriate first stage burnout angle for inclusion in the velocity loss estimation. For the vehicle systems used in the Phase I of this study, where the thrust-to-weight ratio for the first stage was 1.25 and for Isp ranging from 260 to 350, this nomograph was sensitive to predicting this burnout angle. Therefore, a relationship based on additional vehicle system studies was utilized and is represented by

$$\beta_{bo} = \beta_o + \frac{\dot{\beta}_o}{W_o/W_{bo}} \left( \frac{1}{r_o} - \frac{1}{W_o/W_{bo}} \right) \qquad (16)$$

The values used in the relationship for the particular vehicle considered were

$\beta_o = 63°$

$\dot{\beta}_o = 425$

$r_o = 2.5$

This empirical relationship allowed for change of burnout angle dependent upon the relative stage sizing, and gave close agreement to the two-stage Saturn class vehicles.

## MINIMUM LIFTOFF MODE

The basic dynamic programming technique will be discussed initially where the total mission ideal velocity has been defined to demonstrate the step-wise computational procedures, which are ideally suited for digital computers. Later discussions will indicate how this technique was modified

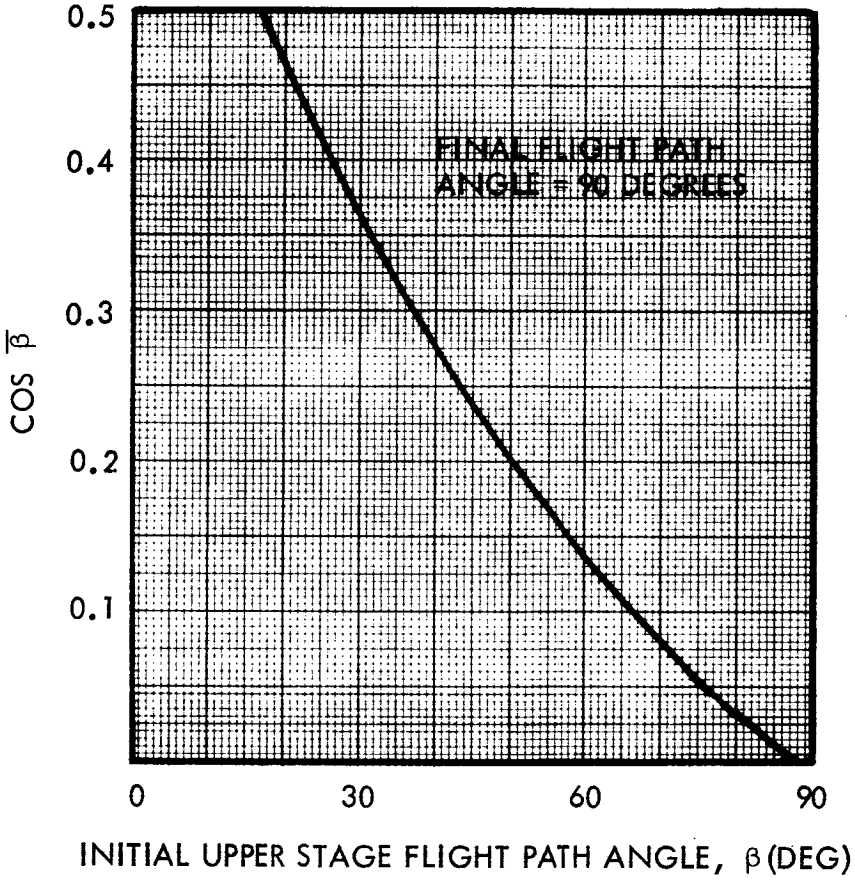



Figure A-12. Average Upper-Stage Flight-Path Angle

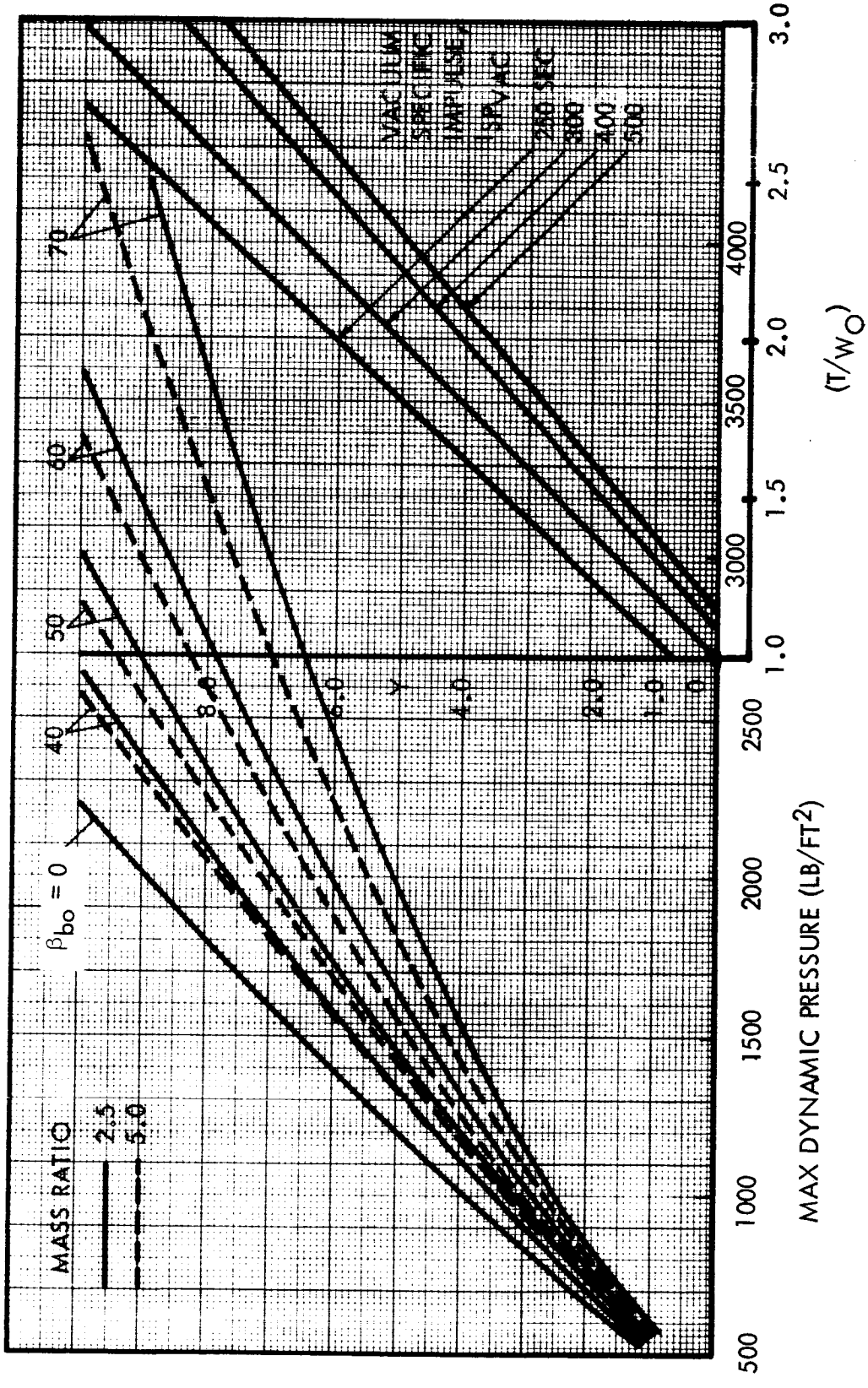



Figure A-13. First Stage Burnout Angle Nomograph

o include the effects of size varying, performance characteristics, and llowances for realistic velocity loss evaluation.

The problem of an N-stage rocket required to inject a given weight into rbit can be considered as a vertical launched vehicle required to obtain an deal velocity of

$$V = \sum_{n=1}^{N} V_n \tag{17}$$

where

$V_n$ = the velocity gained by the $n^{th}$ stage.

The expression for velocity gained by a rocket stage is given by

$$V_n = Isp_n \; g \ln \mu_n \tag{18}$$

where

$Isp_n$ = specific impulse of the $n^{th}$ stage

$\mu_n$ = burnout mass ratio $W_n/W_{n+1} + w_n \zeta_n$

$W_n$ = initial gross weight of rocket n

$w_n$ = initial gross weight of stage n

$\zeta_n$ = proportion of the nth stage that is jettisonable

Employing dynamic programming, the initial gross weight is minimized by maximizing performance during the $n^{th}$ stage by the state variable (the $n^{th}$ stage velocity increment $v_n$) given the initial condition of the $(n+1)^{th}$ stage. This will obtain a recursive relationship for the $n^{th}$ stage dependent on the $(n+1)^{th}$ stage. Using the principle of optimality,

$f_n[V] \triangleq$ minimum weight of the n stage rocket with burnout velocity V and a given payload $W_{pl}$ for optimum staging.

$$f_n[V] = \text{Minimum} \left[ w(v_n, f_{n+1}) + f_{n+1} (V - v_n) \right] \tag{19}$$

$$0 \leq v_n \leq V$$

$$n = 1, 2, \ldots\ldots N-1$$

and

$$f_N[V] = \left[ V\left(V,\ W_{PL}\right) + W_{PL} \right]$$

where

$w(v_n,\ f_{n+1}) \triangleq$ is the weight of the $n^{th}$ stage of an N stage vehicle with the $n^{th}$ stage velocity increment ($v_n$) and a weight of the remaining n+1 stage rocket, $f_{n+1}$.

The percentage of the $n^{th}$ stage weight that is jettisonable, $\zeta_n w_n$, can be considered initially to consist of three separate proportions:

$$\zeta_n w_n = w_{x_n} + \beta_n N'_n W_n + \alpha_n w_n \tag{20}$$

where

$w_{x_n}$ = constant jettison weight of stage n

$\beta_n$ = proportion of $n^{th}$ stage jettison weight dependent on thrust

$\alpha_n$ = proportion of $n^{th}$ stage jettison weight dependent on stage weight

$N'$ = stage thrust to weight ratio

The total velocity of the entire rocket is the sum of the individual stage velocities

$$V = \sum_{n=1}^{N} v_n = \sum_{n=1}^{N} Isp_n\, g \ln r_n \tag{21}$$

From Equations (18) and (21) and the definitions, the weight of the $n^{th}$ stage can be expressed as a function of the $(n+1)^{th}$ stage and the velocity increment from the definitions

$$W_n = W_{n+1} + w_n \tag{22}$$

Rearranging Equation (1) and combining with (5)

$$\exp \frac{v_n}{Isp_n g} = \mu_n = \frac{W_n}{W_{n+1} + \zeta_n w_n} \tag{23}$$

and therefore

$$\exp \frac{v_n}{Isp_n g} = \frac{W_n}{W_{n+1}(1 - \alpha_n) + W_n(\alpha_n + \beta_n N_n) + w_{x_n}} \tag{24}$$

which upon rearranging yields

$$W_n = \frac{W_{n+1}(1 - \alpha_n) + w_{x_n}}{\exp\left[\frac{-v_n}{Isp_n g}\right] - \beta_n N_n - \alpha_n} \tag{25}$$

Using dynamic programming and defining,

$f_n[V] \triangleq$ minimum weight of an n stage rocket with burnout velocity of V and a given payload $W_{PL}$ using optimally proportioned staging deployment.

Therefore,

$$f_n[V] = \text{Minimum } [W_n]$$

$$0 \le v_n \le V \tag{26}$$

$$= \text{Minimum}_{0 \le v_n \le V} \left\{ \frac{W_{n+1}(1 - \alpha_n) + w_{x_n}}{\exp\left[\frac{-V_n}{Isp_n g}\right] - \beta_n N'_n - \alpha_n} \right\}$$

but

$$W_{n+1} = f_{n+1}\left[V - v_n\right]$$

Rearranging the basic equations, the optimum staging of the $n^{th}$ stage can be written in terms of the $(n + 1)^{th}$ stage to obtain recursive relationships from the vehicle stages.

$$f_n[V] = \underset{0 \le v_n \le V}{\text{Minimum}} \left\{ \frac{f_{n+1}\left[V - v_n\right](1 - \alpha_n) + w_{x_n}}{\exp\left[\frac{-v_n}{Isp_n g}\right] - \beta_n N'_n - \alpha_n} \right\} \qquad (27)$$

$$n = 1, 2, \ldots\ldots N-1$$

and for the final stage the expression is

$$f_N[V] = \left\{ \frac{W_{PL}(1 - \alpha_N) + w_{x_N}}{\exp\left[\frac{-V}{Isp_N g}\right] - \beta_N N'_N - \alpha_N} \right\} \qquad (28)$$

Although optimization techniques were based on the dynamic program approach, the program includes several major modifications to allow evaluation of realistic proportioned vehicles. Major alterations resulted from the effect of including varying velocity losses as a function of the vehicle system characteristics. These losses will therefore alter the total ideal velocity requirements to fulfill a specified mission. Also, iteration loops are incorporated in the program to obtain consistent stage mass fraction estimates with the required propellant loadings.

The developed program has the capability of optimally, proportioning vehicle systems up to and including four stage vehicles both for operation in near earth orbits and for earth escape missions. For vehicles with more than two stages, the top stage is evaluated for a range of velocity increments as shown in Figure A-14. Each stage is initially sized with a preliminary estimate for its mass fraction; its size and performance is evaluated; and then the stage is recycled through the mass fraction subroutine to check the previous estimate for the stage mass fraction. This procedure is repeated until convergence is assured between the previously estimated mass fraction with that of the calculated value. When a constant stage size and performance has been obtained, the velocity increment is increased and the process repeated. The initializing estimate for the mass fraction can now be the value calculated for the previous velocity step. This value will produce extremely good agreement with the actual evaluated one. Therefore, with this realistic estimate for the initial value of the mass fraction, the number of required iterations is considerably reduced to essentially one or two times through each velocity step evaluated. The burning time below circular orbital velocity for the top stage for each velocity increment evaluated is now determined for the velocity loss estimation involved with the lower stage optimization.

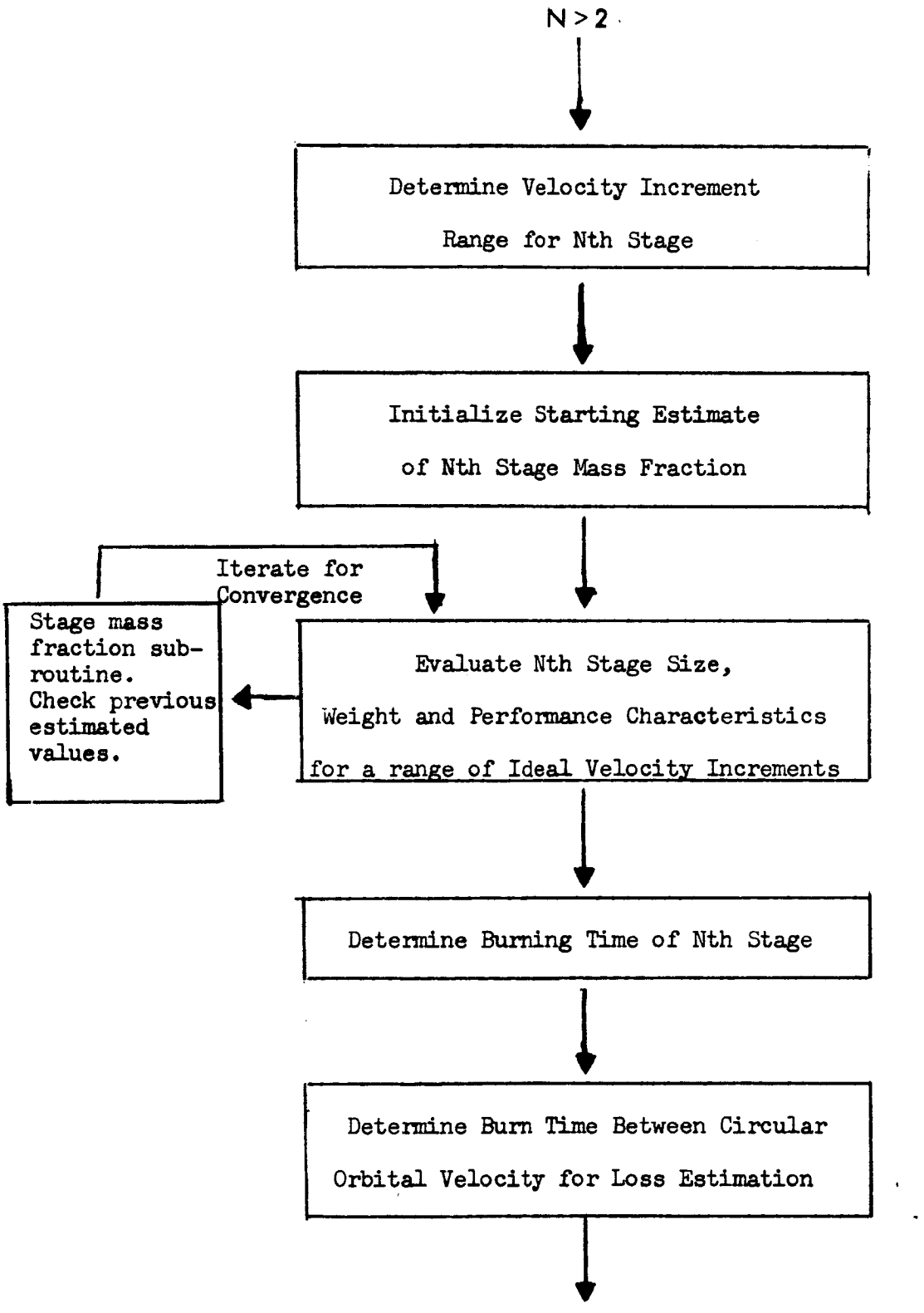



Figure A-14. Flow Logic for Top Stage Evaluation

For vehicle systems with more than three stages, the next step is to optimally combine the stages above the second stage by the dynamic programming technique. This procedure is indicated in Figure A-15 for staging $N - 1 > n > 2$ where for a given total ideal velocity increment ($V_{ideal}$) for stages n through N, the $n^{th}$ stage is considered as a range of $n^{th}$ stages velocity increments ($v_n$) combined with ($V_{ideal} - v_n$) for the remaining upper stages. This process is repeated until the optimally proportioning stages are achieved. This mathematical representation was discussed at the beginning of this section.

The remaining two stages of the vehicle must be considered simultaneously due to the inclusion of the velocity losses and the total mission velocity requirements. For two stage vehicles the previous steps are not considered, and the vehicle stages are evaluated only as shown in Figure A-16. The previous dynamic program technique is still applied by combining the second stage with stages above. This technique also includes an estimate for the first stage size and velocity loss. Since this will involve additional iteration loops for the mass fraction and the total vehicle burning time below orbital velocity, it will also involve velocity loss estimates. The optimally proportioned stages are now considered for a range of actual burnout velocities rather than the previously used ideal velocities for the upper stages. These incremental steps are considered to obtain a minimum weight relationship for a range of first stage burnout velocities. The initial estimates for the mass fraction of the first stage can therefore be selected from the values obtained from the previous velocity increment steps.

The results from this program are obtained rapidly, approximately less than 2 seconds for a 2- and 3-stage vehicle. Each stage is proportioned optimally with a series of consistent mass fraction values that are realistic for both the stage size and its associated loading environment.

Representative minimum liftoff stage proportioning printouts for two stage vehicles are presented in Tables 9, 10, and 11 of the text. Table 12 is a typical printout for a three-stage vehicle. The engineering program logic for the proportioning mode is shown in Figure A-17 and FORTRAN symbols for input data is given in Table A-1.

Table A-1. Minimum Liftoff Input Nomenclature

| | |
|---|---|
| ST | Number of stages |
| WPL | Payload weight |
| VCIRO | Velocity at Orbit |
| VBOF | Final velocity |

Table A-1. Minimum Liftoff Input Nomenclature (Cont)

| | |
|---|---|
| XMRO | Basepoint mass ratio |
| ANGELO | Assumed burnout angle of first stage vehicle with mass ratio XMRO |
| ERROR | Tolerance in velocity loss iteration |
| XISL | Sea level impulse of stage 1 |
| CDMAX | Drag coefficient |
| DIA | Diameter of stage 1 for drag loss calculation |
| XISP | Specific impulse in vacuum |
| TOW | Thrust to weight ratio |
| XKV | Reserve propellant factor |
| DV | Velocity increment |
| VBOMN | Minimum velocity including velocity loss initial guess |
| VBOMX | Maximum velocity |

MAXIMUM PAYLOAD MODE

Besides the minimum gross takeoff weight, another requirement is to maximize the payload capability for a given initial gross vehicle weight and a final burnout velocity requirement. This can be achieved by a similar technique of off-loading the propellant between existing stages of a vehicle system to obtain an optimal staging policy to maximize the overall performance. This maximization of the payload capability will allow association of the capabilities of existing vehicle systems which are being uprated by changes of propellant characteristics, (Isp), change of engine thrust, etc., where the basic structural and subsystem weight definition of the existing stages are known for the various basepoint designs. These estimations can be used for the preliminary definition of the stage mass fractions. An approach for this problem is the reverse of the previous technique. It is required to obtain a recursive formulation for the payload of the $n^{th}$ stage as a function of the payload from the previous stage (n - 1) and thus for an N stage vehicle this is given by

$$f_n[V] = \underset{0 < v_n < V}{\text{Maximum}} \left[ W(v_n, f_{n-1}(V - v_n)) - \zeta w_n \right] \qquad (29)$$

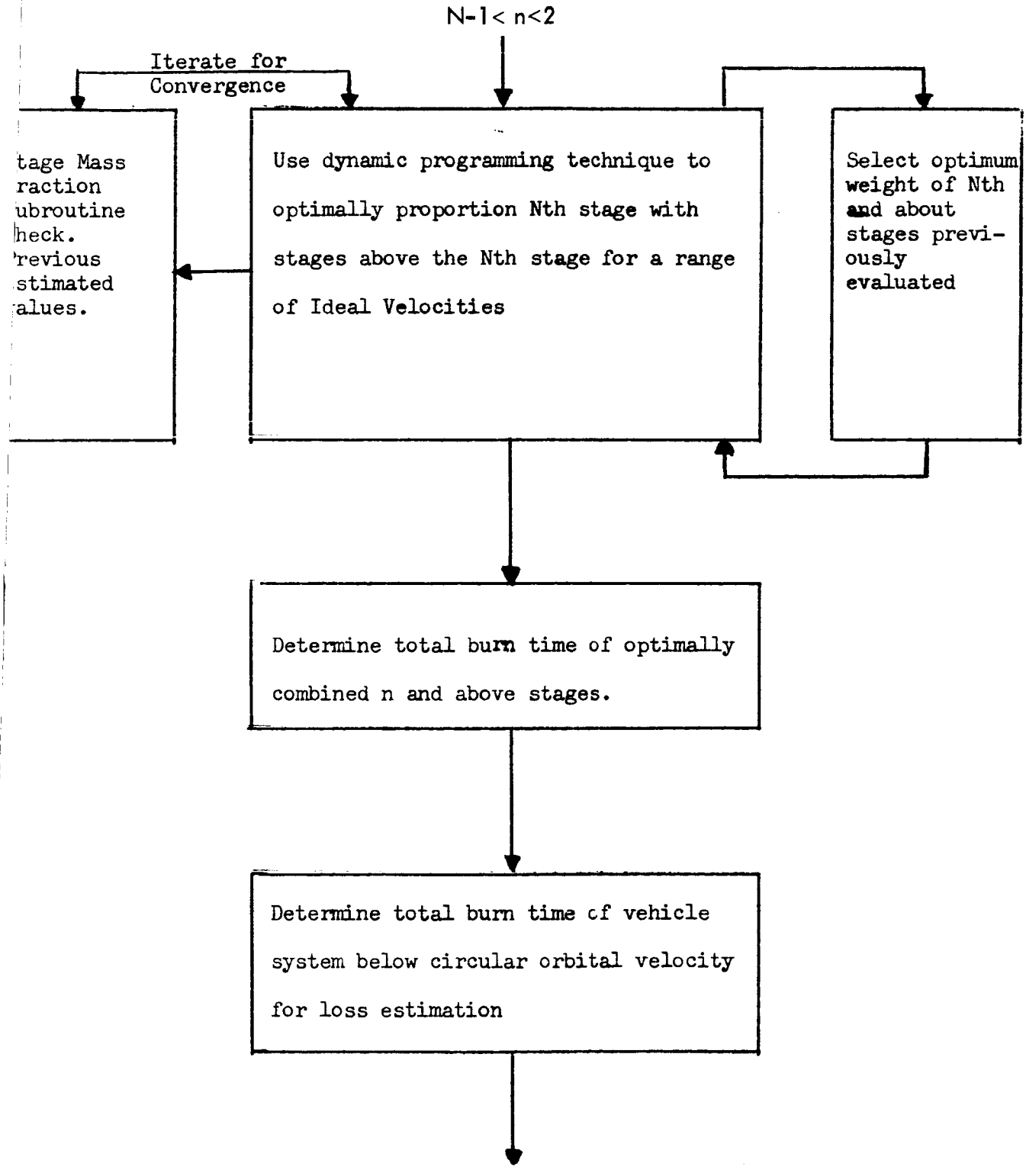



Figure A-15. Flow Logic of Other Stage Evaluation

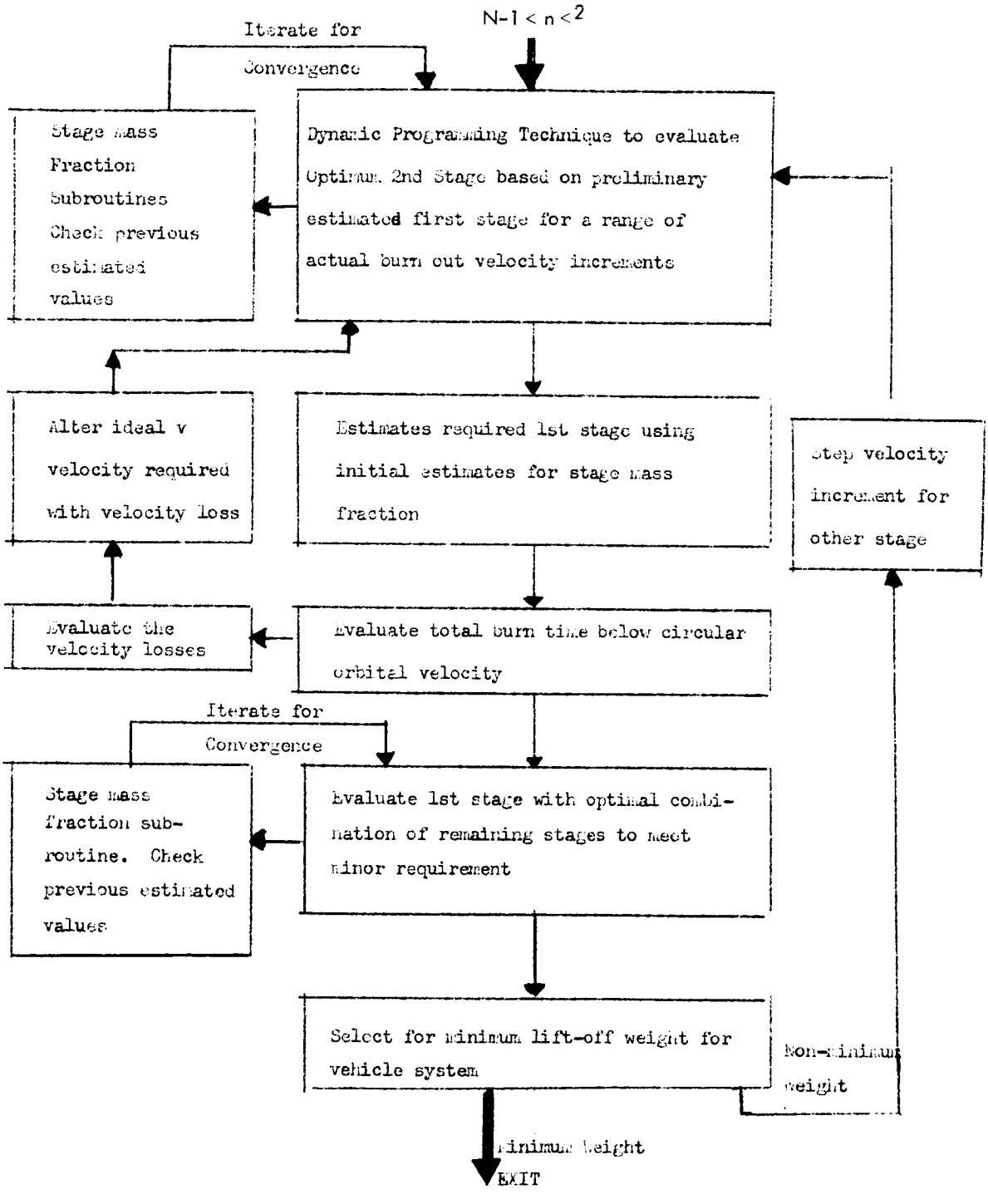



Figure A-16. Flow Logic for 2nd and 1st Stages

for

$$n = 2, 3, \ldots N$$

$$f_1[V] = \left[W(V, W_{O_1}) - \zeta w_1\right] \tag{30}$$

$f_n[V] \triangleq$ the payload and remaining stages of an N stage rocket attaining an $n^{th}$ stage burnout velocity $V_{ft}$ per second with the first n stages being proportioned by an optimal policy.

$W\left(v_n, f_{n-1}(V - v_n)\right) \triangleq$ the burnout weight of the $n^{th}$ stage for a velocity increment $v_n$ and with an initial weight of the $n^{th}$ stage of $f_{n-1}(V - v_n)$.

For this proportioning mode, the burnout weight of the rocket is expressed as a function of the initial gross weight:

$$W_{n+1} = \frac{1}{1 - \alpha_n}\left[W_n\left\{\exp\left[\frac{-v_n}{Isp_n g}\right] - \beta_n N'_n - \alpha_n\right\} - w_{x_n}\right] \tag{31}$$

Therefore, from the previous definition

$$f_n[V] = \underset{0 \le v_n < V}{\text{Maximum}}\left[W_{n+1}\right]$$

$$n = 1, 2, \ldots N-1 \tag{32}$$

$$f_N[V] = \left[W_{PL}\right]$$

Using the expression for the launch weight as a function of the structural weight, thrust level, and stage size, the resulting optimal equations are given by

$$f_n[V] = \underset{0 \le v_n < V}{\text{Maximum}}\left[\frac{1}{1 - \alpha_n}\left\{f_{n-1}(V - v_n)\left\{\exp\left[\frac{-v_n}{Isp_n g}\right] - \beta_n N'_n - \alpha_n\right\} - w_{x_n}\right\}\right] \tag{33}$$

PRECEDING PAGE BLANK NOT FILMED.

for

$$n = 2, 3, \ldots N$$

$$f_1[V] = \frac{1}{1 - \alpha_1}\left[W_{O_1}\left\{\exp\left[\frac{-V}{Isp_1 g}\right] - \beta_1 N'_1 - \alpha_1\right\} - w_{x_1}\right] \qquad (34)$$

This is subject to the restriction that the final velocity after N stages is the desired burnout mission velocity $V_N$. Although this is the simple mathematical formulation of the problem, its integration into a computer synthesis subroutine required extensive modification to include the variational effects of velocity losses, mass fraction, fixed stage size, etc. The approach adopted was similar to the technique that was implemented for the minimum takeoff subroutine, but uses reverse procedure by describing the lower stages first and gradually progressing up the vehicle. With this approach, the velocity losses can be simultaneously included with the stages. The stage is then defined for a range of actual burnout velocities. This velocity is composed of the ideal velocity together with the effects of the vehicle losses.

The program has the ability to consider an existing fixed stage size to determine its effect on the overall performance on the vehicle system. This staging mode can be operated in three fashions: (1) fixed tankage, (2) stretch tankage, and (3) rubberized tankage.

The first mode considered the burnout weight of the stage to be invariant, but the stage propellant can be off-loaded for optimum performance. This considers the existing stage without any structural modifications. With the second mode the tanks are allowed to be stretched to accommodate additional propellant if required. Any off-loading to produce an optimum performance can be evaluated, but the resulting stage burnout weight is considered to be the existing basepoint weight for the tank. Stretching and additional tankage weight are consistent with the increased propellant volume. Rubberized tanks used in the third mode allow the tanks to be both stretched and decreased in length, if required to accommodate the propellant volume.

The overall program logic for the maximum payload mode is indicated in Figure A-18 and the FORTRAN language input data is given in Table A-2. The output data for the maximum payload mode indicates a range of stage combinations together with the optimum for sensitivity studies. Allowances have been included in the program to obtain a large range of burnout velocities for the various nonoptimum design combinations. Examples are shown in Table A-3.

Table A-2. Maximum Payload Input Nomenclature

| | |
|---|---|
| XNS | Number of stages |
| TSL | Sea-level thrust of stage I |
| XISPSL | Sea-level specific impulse of stage I |
| CDMAX | Drag coefficient |
| WO | Total weight at liftoff |
| SO | Strap-on indicator |
| VINCLS | Minimum velocity increment of last stage |
| ERROR | Tolerance in velocity loss iteration |
| V STEP | Velocity increment |
| XKO | Number of retroactive computational steps to initialize next velocity increment to decrease computer running time. |
| XISPVC | Specific impulse in vacuum |
| TVACO | Thrust in vacuum |
| WEO | Weight at burnout |
| RUB | Rubberization indicator |
| WP | Propellant weight (not including residuals) |
| XMR | Mixture ratio |
| DO | Density of oxidizer |
| DF | Density of fuel |
| R | Radius of tank |
| DELW | Pounds per inch for increase or decrease in tank length |



PRECEDING PAGES BLANK NOT FILMED

Table A-2. Maximum Payload Input Nomenclature (Cont)

| | |
|---|---|
| WSO | Weight of strap-ons |
| TSLSO | Sea-level thrust of strap-ons |
| TVACSO | Vacuum thrust of strap-ons |
| XISOSL | Sea-level specific impulse of strap-ons |
| XISOVC | Vacuum specific impulse of strap-on |
| TIMESCO | Burning time of strap-ons |
| ASO | Area of strap-ons |
| VBOMX | Maximum burnout velocity (actual) |
| VBOMN | Minimum burnout velocity (actual) |
| RPF | Reserve propellant factor |
| READ | Read indicator |
| XMRO | Basepoint mass ratio |
| ANGELO | Assumed burnout angle of first stage vehicle with mass ratio XMRO |
| ABOS | Preselected rate of change of burnout angle with mass ratio |

# Table A-3. Two-Stage Vehicle Maximum Payload Printout

## Stage Two (Optimum)

| | | | VBO | WBO | TIMEBO | WPROP | VLOSF | WSTR | WSTAGE | WPL | ANGBO |
|---|---|---|---|---|---|---|---|---|---|---|---|
| 1 | 15 | 0 | 6500. | 7879314. | 141. | 16120888. | 4282. | 1286857. | 17407543. | 6592457. | 73.00 |
| 1 | 16 | 0 | 6600. | 7791473. | 142. | 16208527. | 4291. | 1291496. | 17500023. | 6499977. | 73.40 |
| 1 | 17 | 0 | 6700. | 7711166. | 143. | 16288834. | 4291. | 1295738. | 17584572. | 6415428. | 73.75 |
| 1 | 18 | 0 | 6800. | 7625277. | 143. | 16374723. | 4299. | 1300274. | 17674994. | 6325004. | 74.11 |
| 1 | 19 | 0 | 6900. | 7546683. | 144. | 16453317. | 4299. | 1304424. | 17757741. | 6242259. | 74.43 |
| 1 | 20 | 0 | 7000. | 7462767. | 145. | 16537233. | 4307. | 1308856. | 17846089. | 6153911. | 74.77 |
| 1 | 21 | 0 | 7100. | 7385848. | 146. | 16614152. | 4307. | 1312918. | 17927070. | 6072930. | 75.07 |
| 1 | 22 | 0 | 7200. | 7303805. | 146. | 16696195. | 4315. | 1317251. | 18013446. | 5986554. | 75.37 |

## Stage Two (Nonoptimum)

| | | | VBO | WBO | TIMEBO | WPROP | VLOSS | WSTR | WSTAGE | WPL |
|---|---|---|---|---|---|---|---|---|---|---|
| 2 | 0 | 11 | 25500. | 1515714. | 511. | 5439368. | 5525. | 381888. | 5821237. | 1133826. |
| 2 | 0 | 12 | 25500. | 1512759. | 502. | 5349149. | 5473. | 375835. | 5724984. | 1136924. |
| 2 | 0 | 13 | 25500. | 1509430. | 494. | 5260435. | 5423. | 369880. | 5630315. | 1139550. |
| 2 | 0 | 14 | 25500. | 1505736. | 486. | 5173112. | 5377. | 364831. | 5537943. | 1140905. |
| 2 | 0 | 15 | 25500. | 1502211. | 478. | 5090246. | 5332. | 360144. | 5450389. | 1142067. |
| 2 | 0 | 16 | 25500. | 1497359. | 470. | 5002617. | 5293. | 355187. | 5357804. | 1142172. |
| 2 | 0 | 17 | 25500. | 1493235. | 462. | 4922194. | 5252. | 350702. | 5272896. | 1142532. |
| 2 | 0 | 18 | 25500. | 1487659. | 454. | 4837344. | 5218. | 345973. | 5183317. | 1141687. |
| 2 | 0 | 19 | 25500. | 1483091. | 447. | 4759168. | 5181. | 341615. | 5100782. | 1141476. |
| 2 | 0 | 20 | 25500. | 1476991. | 439. | 4676921. | 5152. | 337520. | 5014441. | 1139471. |
| 2 | 0 | 21 | 25500. | 1471927. | 432. | 4601003. | 5119. | 333797. | 4934800. | 1138130. |
| 2 | 0 | 22 | 25500. | 1465349. | 425. | 4521205. | 5093. | 329884. | 4851089. | 1135465. |
| 2 | 0 | 23 | 25500. | 1459842. | 418. | 4447456. | 5063. | 326447. | 4773902. | 1133395. |
| 2 | 0 | 24 | 25500. | 1452829. | 410. | 4369967. | 5041. | 322911. | 4692878. | 1129918. |

## Stage One (Optimum)

| | | | VBO | WBO | TIMEBO | WPROP | VLOSS | WSTR | WSTAGE | WPL |
|---|---|---|---|---|---|---|---|---|---|---|
| 2 | 1 | 17 | 24700. | 1586287. | 494. | 4829141. | 5233. | 345515. | 5174656. | 1240772. |
| 2 | 2 | 17 | 24900. | 1562513. | 496. | 4852915. | 5238. | 346841. | 5199756. | 1215673. |
| 2 | 3 | 17 | 25100. | 1539103. | 498. | 4876325. | 5242. | 348145. | 5224471. | 1190958. |
| 2 | 4 | 17 | 25300. | 1516052. | 460. | 4899376. | 5247. | 349430. | 5248807. | 1166622. |
| 2 | 5 | 17 | 25500. | 1493353. | 462. | 4922075. | 5251. | 350696. | 5272771. | 1142658. |
| 2 | 6 | 17 | 25700. | 1471002. | 464. | 4944427. | 5256. | 351941. | 5296368. | 1119060. |
| 2 | 7 | 17 | 25900. | 1448992. | 467. | 4966436. | 5260. | 353168. | 5319605. | 1095824. |
| 2 | 8 | 19 | 26100. | 1417688. | 453. | 4824571. | 5193. | 345261. | 5169831. | 1072428. |
| 2 | 9 | 19 | 26300. | 1396514. | 455. | 4845745. | 5197. | 346441. | 5192186. | 1050073. |
| 2 | 10 | 19 | 26500. | 1375663. | 457. | 4866596. | 5200. | 347603. | 5214199. | 1028060. |

Note: See Table 9 for detailed description of printout.

## GENERALIZED PAYLOAD EXCHANGE RATIO

This section presents the generalized payload exchange ratios used in the preliminary design synthesis phase of the computer program. These exchange ratios provide an expedient and relatively accurate tool for predicting the effects of and assessing the effectiveness of any design structural/material/construction changes to a preliminary basepoint vehicle configuration. Also, they indicate the relative merits or penalties in terms of payload performance and thus, cost assessment of structural design decisions, nonoptimum designs, and limitations imposed by manufacturing and fabrication, etc.

Analytical expression for the exchange ratios is based on the total velocity requirements of the vehicle system, assuming constant burn-out velocity and vehicle gravitational losses are linearly proportional to the vehicle burn time (Reference A-7). The ratios considered include the payload variation with respect to (1) thrust, (2) specific impulse, (3) initial vehicle weight at start of stage burning, (4) stage structural weight, (5) propellant loading fixed tank weight, and (6) propellant loading with rubberized tanks.

Analytical expressions are derived which relate the change of the vehicle payload capability to any perturbation of the booster performance parameters. These parameters include specific impulse, structural weight, initial stage gross weight, propellant weight, and stage thrust levels. For these payload exchange derivations, it is assumed that the vehicle burnout velocity remains constant with the vehicle velocity losses attributed to atmospheric effects and the engine thrust components not acting along the flight path angle. The only velocity loss variations considered are those due to gravity, and they are approximated by

$$V_{loss}(i)_{gravity} \approx g t_b(i) \cos \bar{\beta}(i) \tag{35}$$

where $\bar{\beta}(i)$ is the average flight path angle of the $i^{th}$ stage, and $t_b(i)$ is the burn time of the $i^{th}$ stage.

The total actual velocity gained by the vehicle at burnout can be expressed as:

$$V = \sum_{i=1}^{N} \left[ g Isp_{i(i)} \ln \left( \frac{W_o}{W_{bo}} \right)_i - g t_b(i) \cos \bar{\beta}(i) \right] = \sum_{i=1}^{N} \Delta V_i \tag{36}$$

Since the burnout velocity is assumed constant to fulfill a given mission with all the vehicle systems under consideration, the total differential of the velocity is zero and is, therefore, given by

$$\sum_{i=1}^{N} \left[\frac{\partial(\Delta V)}{\partial I_{sp}}\right]_i dI_{sp_i} + \left[\frac{\partial(\Delta V)}{\partial W_o}\right]_i dW_{o_i} + \left[\frac{\partial(\Delta V)}{\partial W_{bo}}\right]_i dW_{bo_i} + \left[\frac{\partial(\Delta V)}{dt_{b_i}}\right] = dV = 0 \tag{37}$$

The partials of equation 37 can be evaluated from the terms in equation 2 and, upon substitution into equation 37, result in

$$\sum_{i=1}^{N} \left\{ g \ln\left(\frac{W_o}{W_{bo}}\right)_i dIsp_i + \left(\frac{gIsp}{W_o}\right)_i dW_{o_i} - \left(\frac{gIsp}{W_{bo}}\right)_i dW_{bo_i} - g \cos\beta(i)\, dt_{b_i} \right\} = 0 \tag{38}$$

An indication of the development of the sensitivity ratios is shown for the first sensitivity ratio; the other ratios are simply quoted, with their development being similar

$$\left(\frac{\partial W_{pl}}{\partial I_{sp}}\right)_n$$

This sensitivity ratio represents a change in vacuum $I_{sp}$ for a particular stage and is assumed to correspond to a change in propellant mass flow ratio for that stage. No change in either the structural weight or propellant weight of the stage is considered with this sensitivity ratio. Therefore, evaluating the change of parameters for all the stages we obtain

$$\begin{aligned} dIsp_i &= dIsp_n, \quad (i=n) \\ dIsp_i &= 0, \quad (i \neq n) \\ dWo_i &= dW_{pl}, \quad (1 \leq i \leq N) \\ dW_{bo_i} &= dW_{pl}, \quad (1 \leq i \leq N) \end{aligned} \tag{39}$$

$$dt_{b_i} = \left(1 - \frac{1}{r_n}\right)\frac{\lambda_n \, dIsp_n}{(T/W_o)_n}, \quad (i=n)$$

$$dt_{b_i} = 0, (i \neq n)$$

$$r_n = \left(\frac{W_o}{W_{bo}}\right)_n \qquad \text{(39 Cont)}$$

$$\lambda_n = \left(\frac{Isp_{sl}}{Isp_{VAC}}\right)_n$$

Rearranging the preceding differentials and substituting into equation 38, gives the required sensitivity ratio

$$\left(\frac{dW_{pl}}{dIsp}\right)_n = - \frac{g \ln r_n - \dfrac{\lambda_n \, g \cos \beta(n) \left(1 - \frac{1}{r_n}\right)}{(T/W_o)n}}{\sum_{i=1}^{n}\left[\left(\frac{gIsp}{W_o}\right)_i - \left(\frac{gIsp}{W_{bo}}\right)_i\right]} \qquad (40)$$

The remaining sensitivity ratios can be developed along similar lines. These partials are listed as follows:

Payload to specific impulse of $n^{th}$ stage:

$$\left(\frac{dW_{pl}}{dIsp}\right)_n = \frac{\ln r_n - \theta_n \left(1 - \frac{1}{r_n}\right)}{A_n} \qquad (41)$$

Payload to structural weight of $n^{th}$ stage

$$\left(\frac{dW_{pl}}{dW_{st}}\right)_n = -\frac{A_n}{A_N} \qquad (42)$$

It is assumed that with a structural weight change in any stage, the propellant weight and specific impulse of all the vehicle stages remains constant.

Payload change to initial gross weight variation of $n^{th}$ stage

$$\left(\frac{dW_{pl}}{dW_o}\right)_n = \frac{B_n - A_n}{B_n + (A_N - A_n)} \tag{43}$$

It is assumed that both the propellant and structural weight are perturbed, corresponding with an additional structural weight to accommodate the propellant weight change. The specific impulse of the propellant system is assumed to be constant throughout.

Payload to propellant loading of $n^{th}$ stage

$$\left(\frac{dW_{pl}}{dW_p}\right)_{n_{W_{stn}}} = \left[\left(\frac{Isp}{W_o}\right)_n (1 - \theta_n) - A_{n-1}\right] \frac{1}{A_N} \tag{44}$$

It is assumed that the structural weight is unaffected by the changes of propellant weight. This case is similar to an off-loading or topping-up of the propellant within a fixed volume tankage.

Payload to propellant weight, allowing for appropriate structural weight to accommodate the difference in propellant weight (rubber staging)

$$\left(\frac{dW_{pl}}{dW_p}\right)_n = \frac{B_n - A_n}{A_N(1 - \zeta n)} \tag{45}$$

Payload to initial thrust (percentage change of nominal thrust)

$$\left(\frac{dW_{pl}}{dT}\right)_n = \frac{\theta_n \, Isp_n \left(1 - \frac{1}{r_n}\right)}{100 \, A_N} \tag{46}$$

Specific impulse is assumed to be constant, and, therefore, a thrust perturbation results in variations of both propellant mass flow rate and burn time.

The terms expressed in the preceding sensitivity ratio are given by

$$r_n = \text{stage n mass ratio} = \left(\frac{W_o}{W_{bo}}\right)_n$$

$$A_n = \sum_{i=1}^{n}\left[\frac{Isp}{W_o}\right]_i (r_i - 1)$$

$$B_n = (1 - \zeta_n)\left(\frac{Isp}{W_o}\right)_n (r_n - \theta_n)$$

$$\theta_r = \lambda_n \cos \beta n/(T/W_o)_n \qquad (47)$$

$$\zeta_n = \left(Wo_n - Wo_{n+1}\right)/Wst_n$$

$Wst_n$ = structure weight of the $n^{th}$ stage

$\lambda_n$ = Ratio of sea-level specific impulse to vacuum specific impulse

Figure A-19 is an engineer-oriented flow diagram. Representative generalized exchange ratio printouts for two-stage vehicles are presented in Tables 28, 29, and 30. Table A-4 shows the input nomenclature for generalized payload exchange ratios.

Table A-4. Input Nomenclature for Generalized Payload Exchange Ratios

| | |
|---|---|
| ST | Number of stages |
| WPL | Payload weight (pounds) |
| VLOSS | Velocity loss (feet per second) |
| TIME | Burn time (seconds) |
| SPSL | Sea level specific impulse |

Table A-4. Input Nomenclature for Generalized Payload Exchange Ratios (Cont)

| | |
|---|---|
| XISP | Vacuum specific impulse |
| TOW | Thrust-to-weight ratio |
| WO | Liftoff weight |
| WSTR | Stage burnout weight |
| DSP | Perturbation in specific impulse |
| DWSTR | Perturbation in structure weight |
| DWO | Perturbation in liftoff weight |
| DPFIX | Perturbation in propellant weight with fixed tanks |
| DPRUB | Perturbation in propellant weight with rubberized tanks |
| DTHRST | Perturbation in thrust level |

## EMPIRICAL EVALUATION OF MAXIMUM DYNAMIC PRESSURE CONDITIONS

To fully develop the proportioning subroutines, a realistic stage mass fraction routine was utilized. The subroutine sizes the vehicle structure based on propellant loading of the stage and estimates for the external load environments. Such a routine has to be empirical in nature since no flight trajectories have been developed for this parametric evaluation. The loading environments being considered are prelaunch; max $q\alpha$; and maximum acceleration, assuming the vehicle to be a simple beam analogy.

The analysis presented here yields preliminary design loads and parameters to a reasonable degree of accuracy so that design criteria can be formulated. Relationships for these load environments were based on Reference A-6.

The axial acceleration at first stage burnout is a function of the vacuum thrust-to-weight ratio and the mass ratio of the vehicle system

$$a_{bo} = \left\{ \left[ 1 - (1-\lambda)\frac{P_{bo}}{P_o} \right] \frac{T_{vac}}{W_o} - \frac{q_{bo}}{W_o/C_D A} \right\} r \qquad (48)$$

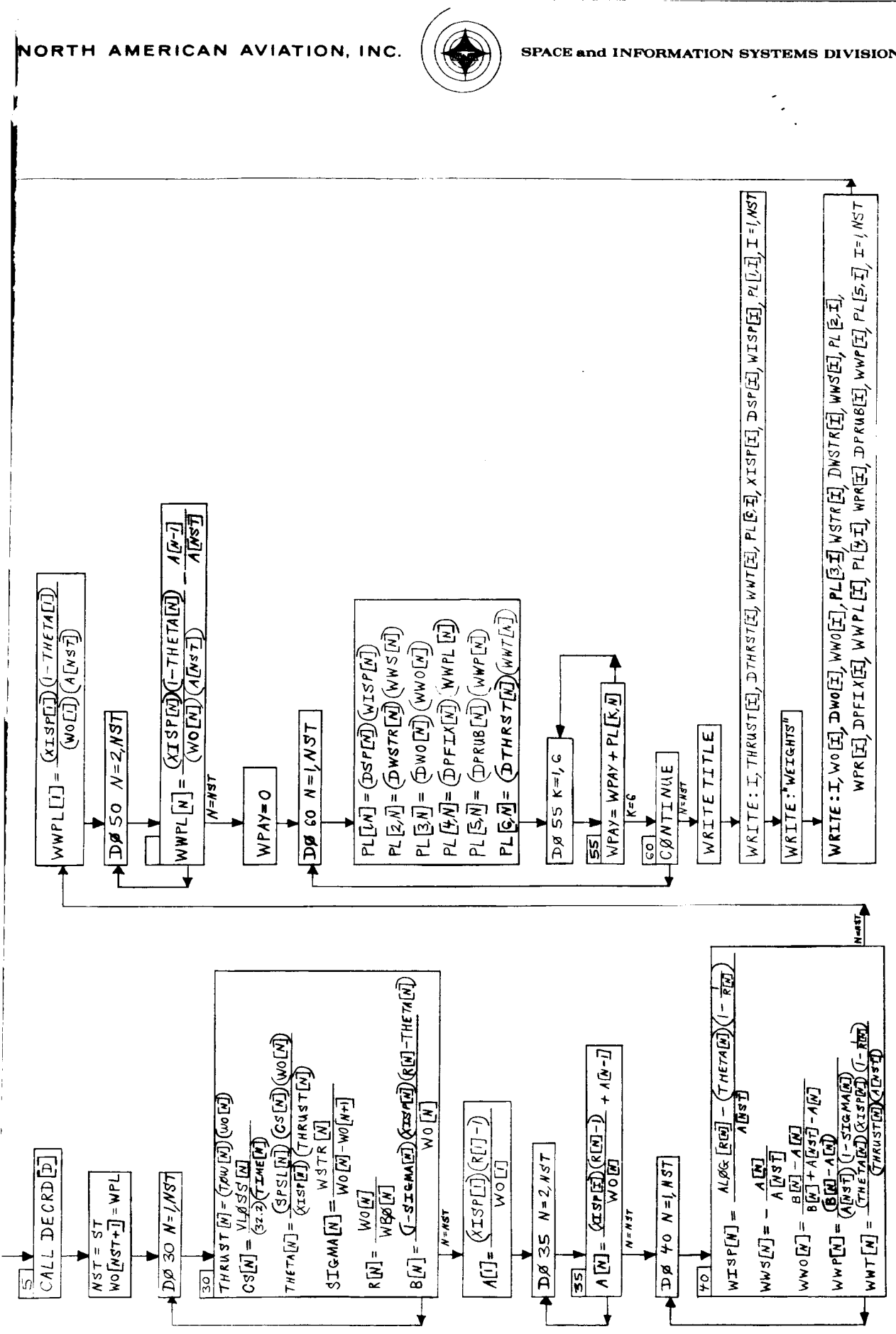



Figure A-19. Generalized Payload Exchange Ratio Program Logic

The staging of the first stage after burnout is usually accomplished at extremely low dynamic pressure regions (i.e., $q_{bo} \approx 0$) such that the final term in equation 48 can be neglected. For most of the vehicle systems considered, the burnout attitude is sufficiently high that the pressure ratio term is also negligible, therefore, the axial acceleration at first stage end boost can be approximated by

$$a_{bo} \approx \left(\frac{T_{vac}}{W_o}\right) r \tag{49}$$

Another major design flight condition is the maximum dynamic pressure region which usually occurs at altitudes between 30,000 and 35,000 feet. For space shots, maximum dynamic pressure usually occurs near the upper altitude limit; vehicle-sounding rockets and highly lofted shots occur nearer the lower limit. The nomograph in Figure A-13 is used to estimate the maximum dynamic pressure for the various vehicle systems. This curve was derived empirically and is based on vehicle parameters representative of presently conceived vehicles. In construction of this nomograph, a rectilinear thrust-time variation was assumed; for other thrust-time variations, an initial thrust-to-weight ratio based on a mean thrust value will give reasonably accurate results.

To incorporate this nomograph into the machine program and minimize the storage requirements, it was represented by two simple mathematical models with the dummy parameter (Y) connecting the two models. With the vehicle propulsion and propellant characteristics fixed, this dummy parameter can be evaluated.

$$Y = \frac{T_{vac}}{W_o}\left[4.2 + 4.64\left(\frac{500 - Isp_{vac}}{500}\right)^2\right] - 4.8 \tag{50}$$

Maximum dynamic pressure is given as a function of the first stage burnout flight path angle, which is dependent on the flight trajectory and mass ratio of the first stage. If the burnout angle is not known, it is suggested that a typical value be assumed.

$$q_{max} = \left[\frac{117500}{21.7 - Y} - 5050\right]\left[1 - 15.48 \times 10^{-5} Y^{1/2} \left(70 - \beta_{bo}\right)^{1/2} \left(\beta_{bo} + 128\right)\right]$$
$$- 9 \times 10^{-7} Y (\beta_{bo})^4 (r - 2.5) \ \text{lb/ft}^2 \tag{51}$$

The axial acceleration experienced by the vehicle is associated with this dynamic pressure.

An estimate for this can be expressed by

$$a_{q_{max}} = \left\{ a \left[ 1 - (1 - \lambda) \frac{P_{q_{max}}}{P_o} \right] - \frac{q_{max}}{\frac{T_{vac}}{W_o} \frac{W_o}{C_D A}} \right\} \tag{52}$$

The acceleration term (a) in equation 52 is shown in Figure A-20, and was represented by

$$a = \frac{T_{vac}/W_o}{1 - \left(\frac{T_{vac}}{W_o}\right)\left(\frac{t_{q_{max}}}{Isp_{vac}}\right)} \tag{53}$$

This expression depended on the stage burn time associated with maximum dynamic pressure region ($t_{q_{max}}$). This burn time for a range of thrust-to-weight and burnout flight path angle is shown in Figure A-21, and can be represented by

$$t_{q_{max}} \approx \left[ 17.45 \left(\frac{T_{sl}}{W_o}\right)^2 - 95.25 \left(\frac{T_{sl}}{W_o}\right) + 165.2 \right] - 1/2 \left(60 - \beta_{bo}\right)^{1/2} \left(\frac{T_{sl}}{W_o} - 1\right) \tag{54}$$

The burn time is taken for a typical proportional vehicle during the proportioning subroutine and due to the short time, variation with burnout angles of the other proportion vehicles has been neglected.

Since the altitude pressure ratio term in equation 52 depends on the altitude of max q (i.e., 30,000 to 35,000 feet) and its contribution to equation 52 is insignificant. An average value is assumed to be

$$\frac{P_{q_{max}}}{P_o} \approx 0.27 \tag{55}$$

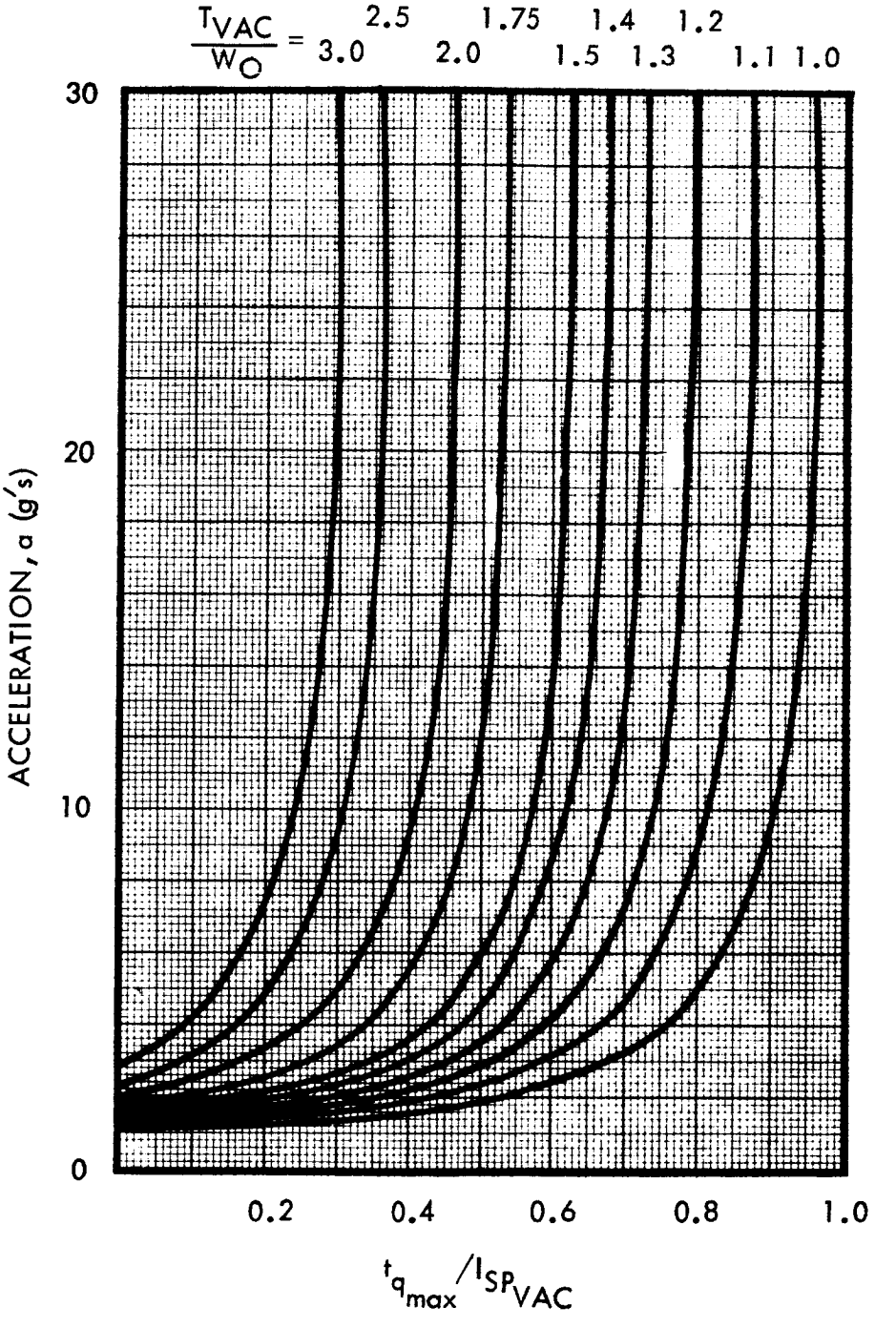



Figure A-20. Axial Acceleration During Stage Operation (Vacuum Atmosphere)

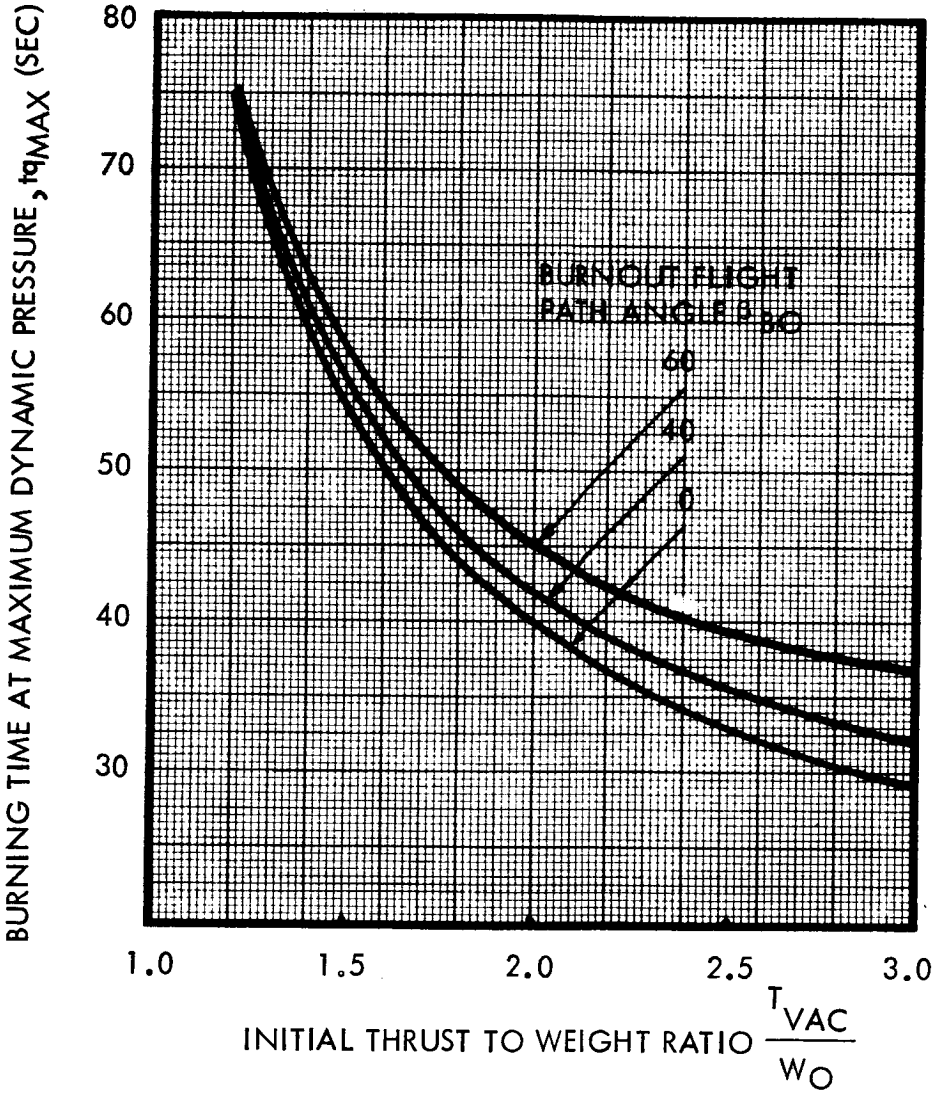



Figure A-21. Time at Maximum Dynamic Pressure

# APPENDIX B - STAGE MASS FRACTION SUBROUTINE

Stage mass fraction ($\nu_B$) is used as the principal stage efficiency parameter in measuring vehicle performance. This mass fraction is defined as the stage usable propellant weight ($W_P$), divided by the sum of the stage usable propellant weight plus the stage burnout weight ($W_{BO}$). Stage burnout weight includes all structure and subsystems plus residual and reserve propellants and gases. The effect of the stage mass fraction is illustrated by

$$\frac{W_{PL_i}}{W_{O_i}} = \left(1 - \frac{\nu_i}{\nu_{B_i}}\right)$$

where

$i$ = the stage in question

$W_{PL_i}$ = the stage payload weight

$W_{O_i}$ = the vehicle gross weight at ignition of the particular stage in question

$\nu_i$ = the stage performance ratio which has the following derivations:

$$\nu_i = \frac{W_{P_i}}{W_{Oi}}$$

and

$$\nu_i = 1 - \frac{1}{\exp\left(\frac{\Delta V_i + \Delta V_{L_i}}{Isp_i\, g}\right)}$$

where

$\Delta V_i$ = the stage performance velocity

$\Delta V_{L_i}$ = the stage velocity loss

$Isp_i$ = the delivered specific impulse of the stage

$g$ = the gravity constant

$W_{P_i}$ = stage propellant weight

From the previous expressions, it can be seen that stage mass fraction is a usable efficiency factor in measuring stage performance. However, in many studies, estimation of the stage mass fraction has been over-simplified. For example, mass fraction curves have been estimated as functions of propellant weight changes for a rubberized stage using the loading indexes from a basepoint design which include only one set of applied loads and internal pressures. Use of these curves can easily result in significant error because as the stage size changes within the vehicle stack, the design environment also changes.

The stage mass fraction subroutine was developed to provide a parametric assessment which includes the changes in design environment for each design point investigated and provides quick-response calculations of stage efficiency considering the total vehicle effects of the trajectory and loading environment upon the particular stage or stages in question. Changes in parameters above and below the particular stages are considered, such as the stage payload effect upon bending moment and the lower stage axial load influence. Also, various design conditions in the vehicle trajectory must be considered to select flight conditions which actually design components.

However, an effective subroutine must be handled in a parametric fashion and must contain many empirical relationships. The decision must be made to determine the particular system to which the more detailed assessment must be assigned. In the subroutine described, the structural subsystem has been assigned preference with other subsystem being treated in a more empirical fashion. At present, due to the requirements of this study, major emphasis has been placed on fairly accurate assessments of delta changes in shell structures.

## OPERATIONAL MODES

The subroutine may be operated in the following two sizing modes similar to those described in the stage proportioning operation: (1) minimum liftoff weight; (2) maximum payload weight. Subroutine internal routing and printout is also handled in two primary modes. For the first mode a complete, thorough route is conducted through the subroutine, and automated output is provided of stage geometries, mass properties, axial loads and bending moments for various flight conditions, ultimate applied load definitions, design pressures, and stage weight statements. Geometry nomenclature is similar to that included in S&ID's Computer Aided Design Preliminary Design Synthesis Program. In this study, the Computer Aided Design program was used, by transferring the output data array between it and the mass fraction subroutine, to provide automated inboard profile drawings of the test case vehicles. Automated techniques from the S&ID program were also used to provide cathode-ray-tube curves of stage mass fraction trends. Subroutine operation is controlled by a fairly simple initialization of control

indicators. This mode of operation for a four-stage vehicle requires approximately 20 seconds of computer time.

The second operational mode provides a minimum output of stage performance data that defines stage propellant weight, stage payload weight, vehicle gross weight, stage gross weight ($W_{ST}$), stage mass fraction ($\nu_B$) and stage velocity ($\Delta V$). Execution time required in this mode is approximately 1 second for a four-stage vehicle.

The subroutine also contains logic to parametrically assess how far the stage tankage can be "stretched" and onloaded with propellant without exceeding an input tolerance on the applied load. Results from this calculation are stage weight partials and mass fraction partials which can be added to stage weight and stage mass fraction for unit changes in propellant weight. This logic is controlled by inputting a stage velocity increment and a loads tolerance. The program conducts a stepwise measurement, adding the velocity increment to the stage velocity until the cutoff point of the loads has been reached and then prints out the resulting partials, the allowed velocity increment, and the total additional velocity. These data are valuable in measuring the sensitivity of the mass fraction curves and also in measuring small weight changes in a configuration.

Provisions are also included in the subroutine to input a fixed stage, a fixed diameter, or a fixed fineness ratio of a stage. In the case of the fixed stage input, an indicator controls the subroutine operation to permit cycling through the parametric loads assessment even though output is limited to the stage performance mode previously indicated. Detailed parametric data is printed out for all new stages in a fixed-nonfixed combination of stages along with the calculated loads.

In a parametric assessment where thousands of cases may be investigated, other limitations must be built into a program operation. Typical of these is a maximum acceleration cutoff. In the subroutine, whether operating in the minimum liftoff or maximum payload mode, maximum acceleration allowables can be input for the prime flight conditions. If accelerations, in a particular case, exceed these values the subroutine will stop and printout where and what limit was exceeded. This operation assists the screening process, especially in the case of manned systems.

## SUBROUTINE LOGIC

The launch vehicle may have from one to four liquid bipropellant booster stages as illustrated in Figure B-1. For this study, two basic stage models were utilized for analysis and are illustrated in Figures B-2 and B-3. The subroutine consists of four basic phases as follows:

1. Vehicle sizing

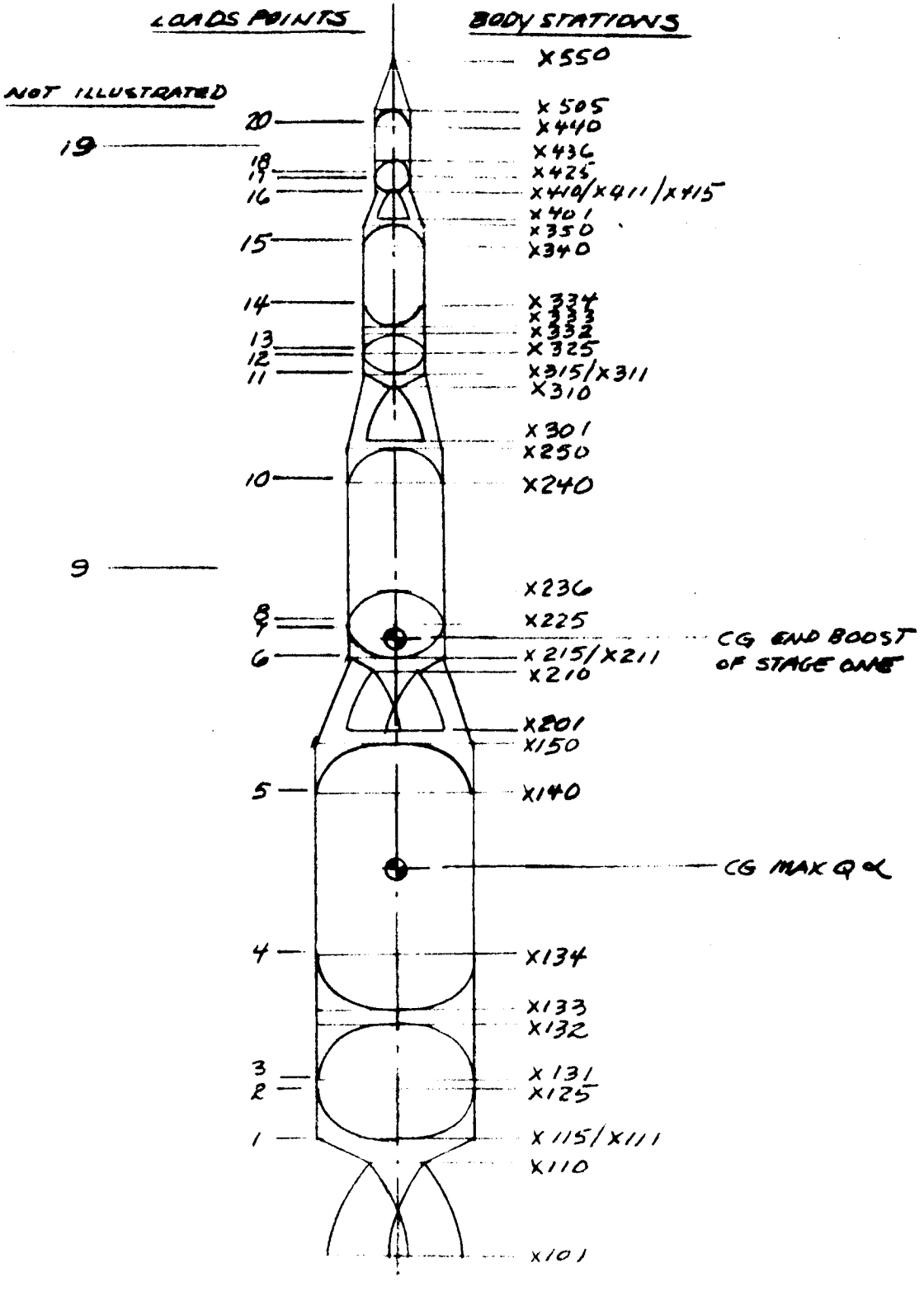



Figure B-1. Tandem Tankage Multistage Vehicle

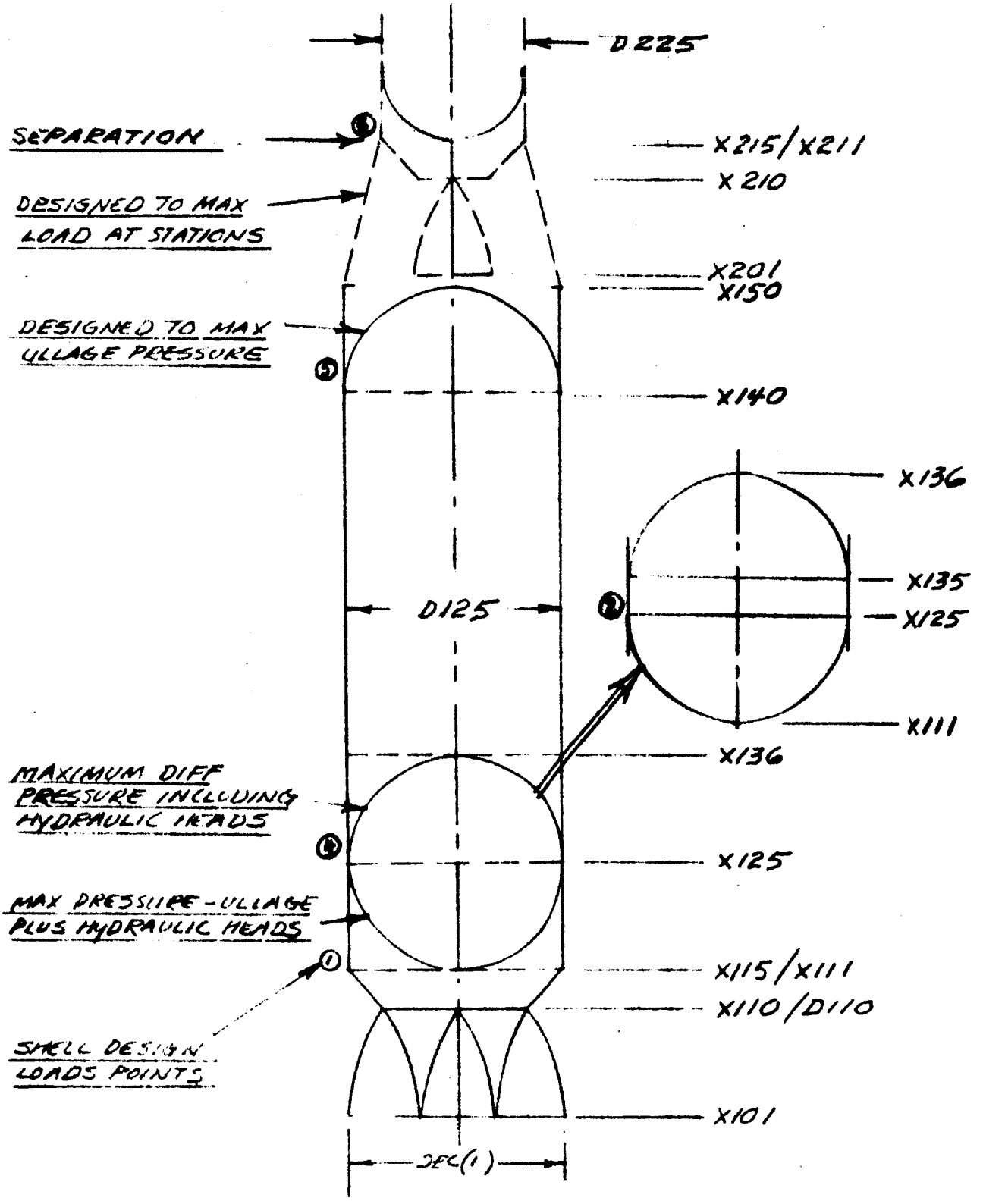



Figure B-2. Stage Geometry—Indicator = 0

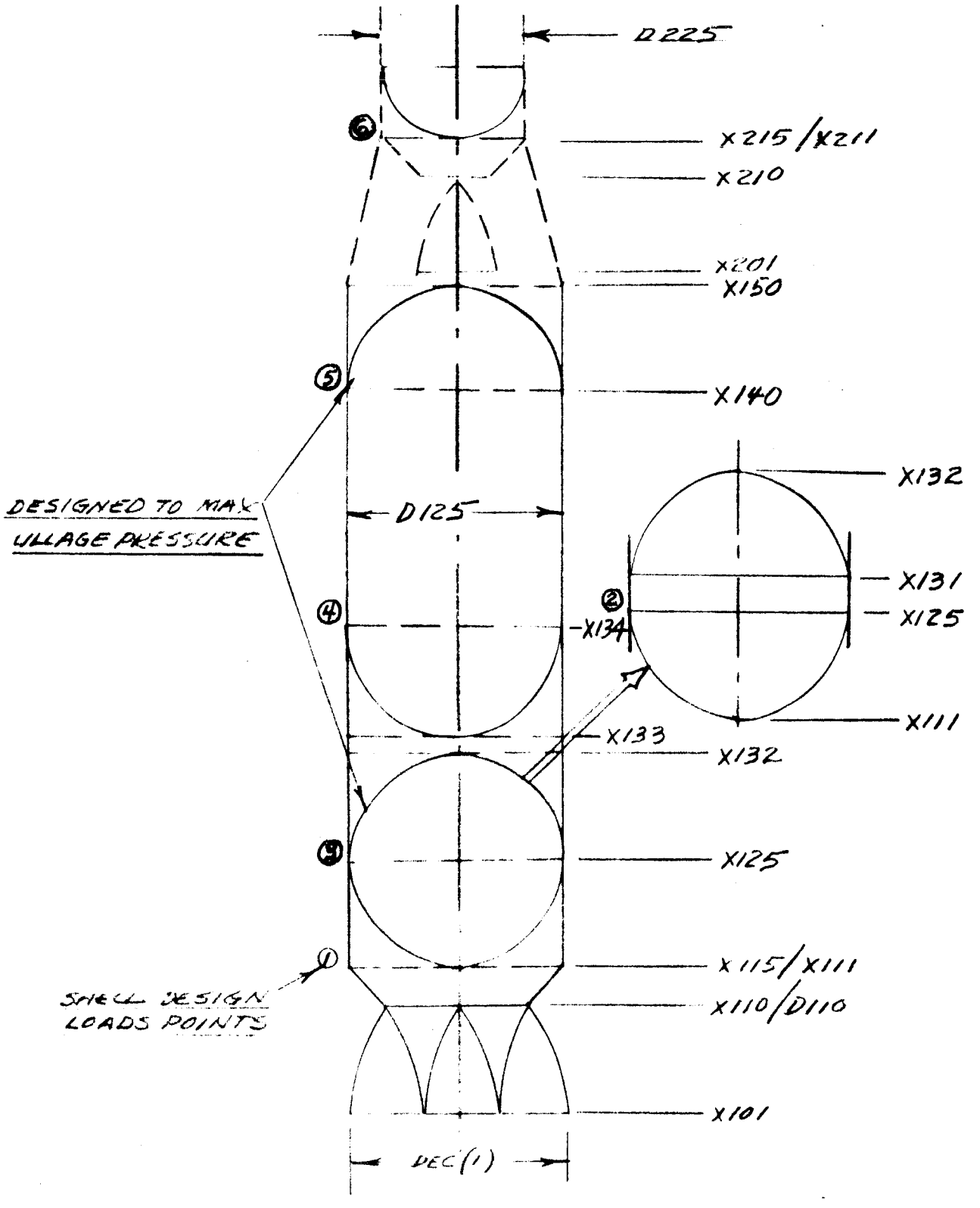



Figure B-3. Stage Geometry—Indicator = 1

2. Loads estimation

3. Weight estimation and mass fraction summation

4. Detailed geometry definition.

Operational modes and subroutine routes are controlled by input indicators to permit cycling through selected portions of the program. The subroutine utilizes stored arrays of the structural shell data as functions of applied load. These data are stored for both pressurized and unpressurized shells considering relief pressures and thermal environment. The subroutine, as previously indicated in this report, accepts performance input from the stage proportioning operation. Also, as previously mentioned, two sizing methods are available: (1) starting with final vehicle payload, the vehicle is sized for minimum liftoff weight; (2) starting with vehicle liftoff weight (or thrust and thrust-to-weight ratio), the vehicle is sized to achieve maximum payload. These sizing modes are used in conjunction with those described in Appendix A.

The vehicle sizing operation is controlled by the stage geometry indicators, the input stage propellant properties, stage performance requirements, and either input payload weight or total vehicle thrust. Basic stage sizing is as follows:

1. If payload ($W_{PL_n}$) is input:

$$W_{O_i} = \frac{W_{PL_i}}{1 - \left(\frac{\nu_i}{\nu_{B_i}}\right)} \quad ; i = n, 1$$

2. If total thrust ($T_1$) is input:

$$W_{O_i} = T_1 \times T/W_1$$

$$W_{PL_i} = W_{O_i}\left(1 - \frac{\nu_i}{\nu_{B_i}}\right) \quad ; i = 1, n$$

$$W_{O_{i+1}} = W_{PL_i}$$

Stage velocity values can be retained from previous runs, or if an initial run is being made and only one stage is known then

$$\Delta V_i = \text{input}$$

$$\Delta V_T = \text{input}$$

$$\Delta V_{n-1} = \frac{\Delta V_T - \Delta V_i}{n-1}$$

The stage mass fraction ($\nu_{B_i}$) can be handled in the same manner; if no previous data is available it will be initialized as 0.900.

Stage diameters are initially set by the denser propellant, which, if not specified, is considered to be in the aft tank as follows:

$$D_i = 2\left(\frac{VO_i}{2(C1_i)}\right)^{1/3}$$

($C1_i$ is a volume coefficient for ellipsoidal bulkhead shapes and is input for the particular bulkhead aspect ratio being considered. These coefficients are illustrated in Figure B-4.) This diameter is altered by the required engine cluster exit diameter or by input controls restricting stage fineness ratio or stage diameters. Engine cluster diameter is estimated as follows from Reference B-1:

$$AT_i = \frac{T_i}{EN_i} (PC_i) (C2_i)$$

$$AE_i = AT_i (E_i)$$

$$DE_i = 1.127 (AE_i)^{1/2}$$

$$LE_i = 0.1 (AT_i)^{1/3} (SP_i)^{1/2} + (1.38 (AE_i)^{1/2})$$

and

$$DEC_i = C3_i (DE_i)$$

Geometry of the ith stage is estimated using some of the logic contained in Reference B-2. If diameter or fineness ratio controls are input, the same basic logic is used. The total vehicle length is then determined and the mass properties at stage midboost (or max $q\alpha$) and endboost are estimated. Loads at these center of gravity points are estimated as follows:

$$BM = \frac{W (CG) (L-CG)}{L} (a) (\sin\alpha) + 0.076 (W(CG-CP) - 0.5T (L-CG)$$

$$AL = T - 0.001 (W)(CG) + 0.7854 (D_1)^2 (Q) (K2)$$

Bending moment and axial load are then multiplied by an input ultimate safety factor and distributed along the vehicle length, assuming that moment is zero at the aft and forward end of the vehicle and the total thrust load is taken in the aft skirt of the first stage.

Pressures are determined for the same loading conditions at the aft end of the tank wall, the crown of the aft bulkhead, and across the common bulkhead by using an input minimum ullage pressure and the acceleration hydraulic heads. Hoop tension, axial compression, and axial tension applied loads are then computed and the maximum value from these data are found for each design point on the shell as shown in Figure B-1. A search is then made to weigh the structural shell from the stored data.

Bulkhead weights are estimated for forward bulkheads using input weight and area coefficients shown in Figures B-5 and B-6.

$$WFB_i = \frac{\rho P_i \, (C10_i) \, \pi R_i^3 \, (C8_i)}{F_{tu_i}}$$

aft bulkhead weights are estimated as follows:

$$WAB_i = \frac{P_i \, R_i^2}{2h_i} \quad \frac{1.5}{F_{tu_i}} \, \rho(C11_i) \, R^2 \, (C8_i)$$

Stage engine weights are estimated as indicated in References B-1 and B-3 using unique equations for a specific input propellant type

$$WENG_i = K4 \, (T_i)^{K5} \quad (C12_i)$$

Upper-stage engines are designed to vacuum thrust conditions, while the first-stage engines assume both sea level and vacuum thrust. Other systems are estimated from equations presented in Reference B-1 through B-7. An iteration loop is contained in the program to close in the stage mass fraction. Experience indicates that only these iterations are required.

## COEFFICIENTS

The subroutine utilizes stored arrays of coefficients to operate on the basic sizing and weight equations. These coefficients are organized into two classes. The first class includes those values that assist in bulkhead geometric sizing and forward bulkhead weight deviations. The subroutine nomenclature for these coefficients is as follows:

| Name | Description |
|---|---|
| $C1_i$ | Bulkhead volume (Figure B-4) |
| $C4_i$ | Bulkhead aspect ratio (Bulkhead height-to-radius ratio) |

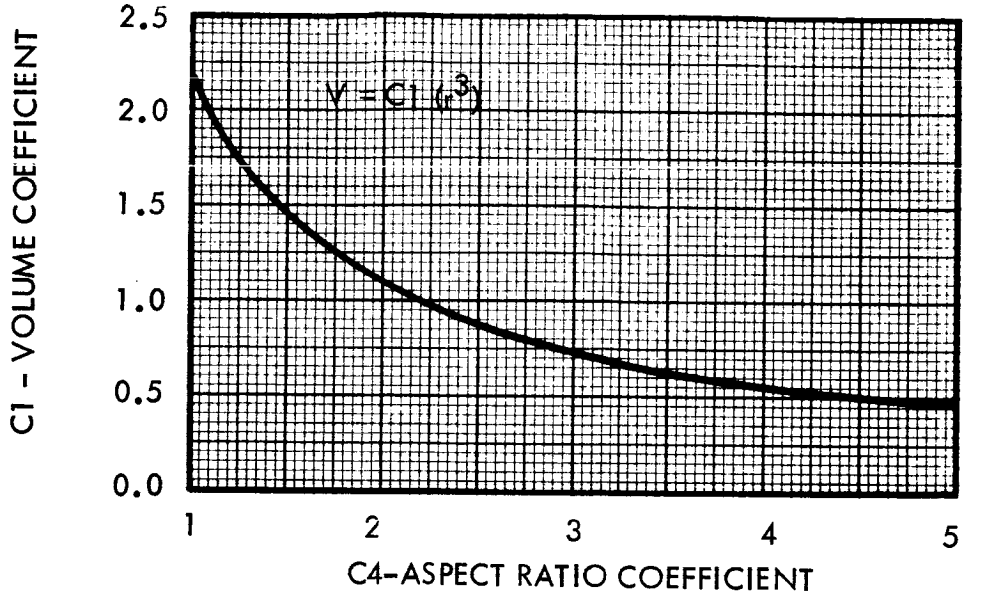



Figure B-4. Bulkhead Volume Coefficients

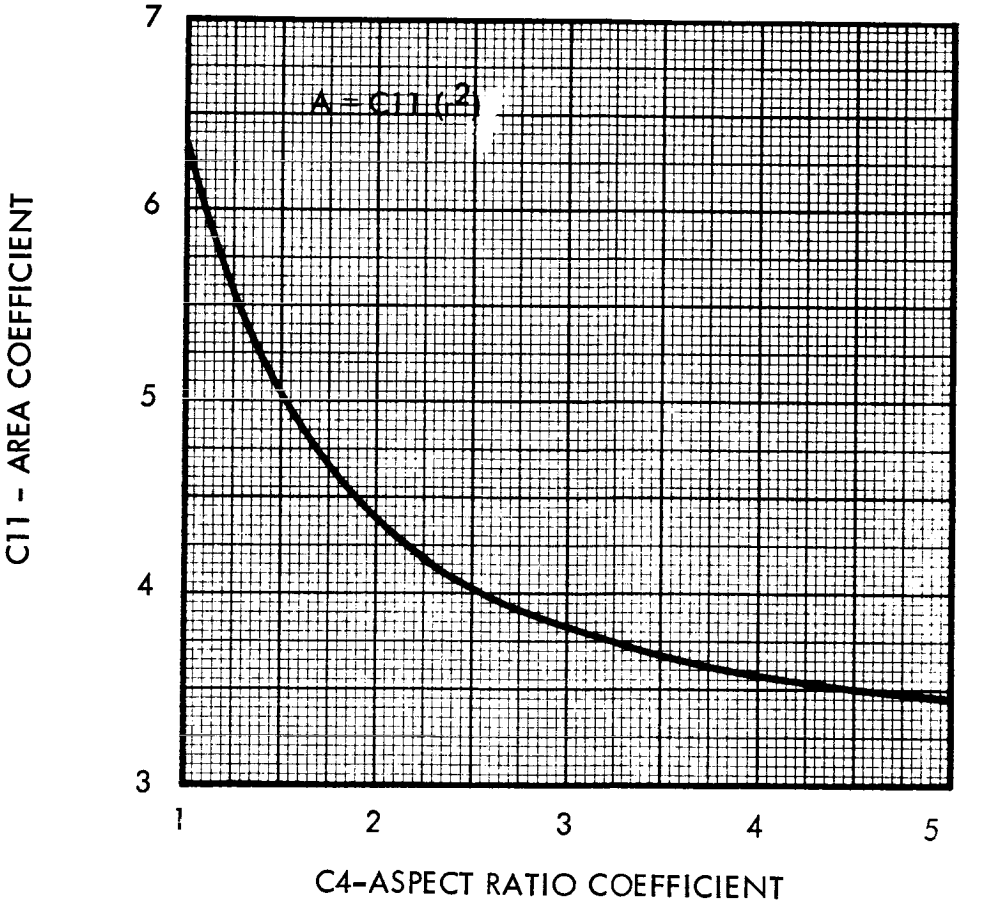



Figure B-5. Bulkhead Area Coefficients

| Name | Description |
|---|---|
| $C10_i$ | Forward bulkhead weight (Figure B-6) |
| $C11_i$ | Bulkhead area (Figure B-5) |

The coefficients C1, C10, and C11 are all handled in terms of the aspect ratio coefficient (C4).

The other class of coefficients (C2, C3, C5-C9, and C12 through C20) provide the mechanics of including experience and adjustment factors in all basic elements of the stage. In these arrays, correction factors can be included for assessing the weight effects of manufacturing tolerances, increased contingencies, and altered subsystems. These coefficients are invaluable in providing internal weight adjustments after initial trail runs have been made. As in the case in any launch vehicle program, careful consideration must be given to these weight factors, and they must be formulated only from experience and from hardware or test case data. One of the benefits of the subroutine is that a measurement can be made of the overall effect of reducing a particular manufacturing weight tolerance in a particular component. Also, the effect of substituting one piece of equipment for another can be parametrically assessed.

Table B-1 presents the nomenclature used in the subroutine for basic sizing inputs. The control indicators are as follows:

| Name | Description |
|---|---|
| DIN (i) | Fixed stage diameter (in) |
| DVI (i) | Velocity increment (fps) |
| DST (i) | Fixed stage indicator |
| EOD (i) | Fineness ratio |
| EMOD (i) | Stage geometric model indicator |
| REED | Indicator that controls next case data read |
| PRIND | Indicator that controls print mode |
| CRT | Indicator that organizes data for NAA, S&ID computer aided design drawing subroutines |

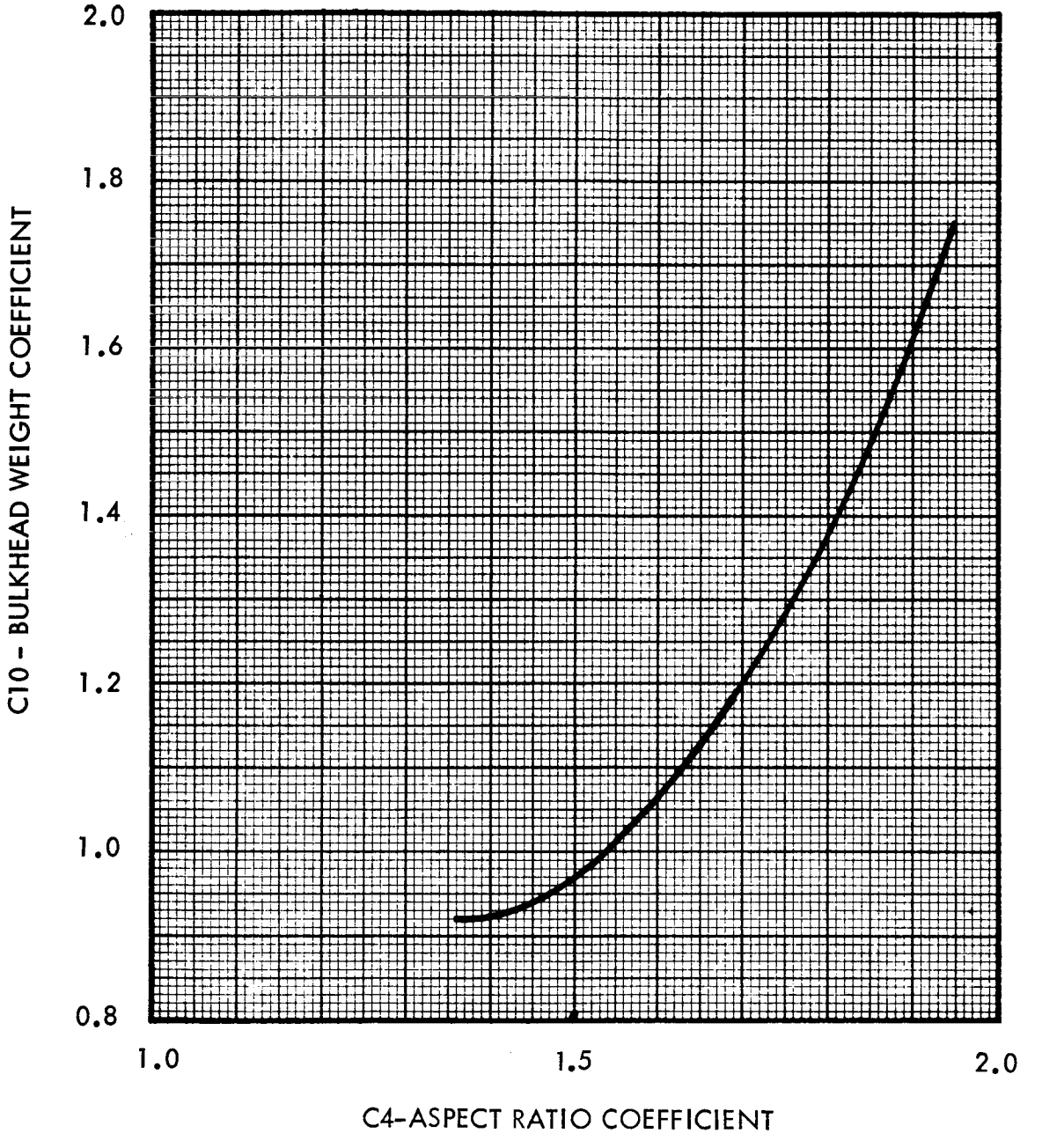



Figure B-6. Bulkhead Weight Coefficients

Table B-1. Stage Mass Fraction Subroutine Input Nomenclature

| Input Type | Name | Description |
|---|---|---|
| Generalized shell | WTU | Structural shell unit weight curve (unpressurized) |
| Curves (PSI/R) | ELU | Structural shell load curve (unpressurized) |
| | WTP | Structural shell unit weight curve (pressurized) |
| | ELP | Structural shell load curve (pressurized) |
| Sizing | ST | Number of stages |
| | PAY | Desired payload weight |
| | FSTO | First stage thrust |
| | TOW | Thrust-to-weight ratio (initial) |
| | BRO (i) | Stage mass fraction (if known) |
| | RM (i) | Propellant mixture ratios |
| | DF (i) | Fuel densities (lb, cu in.) |
| | DO (i) | Oxidizer-Densities (lb, cu in.) |
| | UF (i) | Ullage factors (percent) |
| | EN (i) | Number of engines |

Table B-1. Stage Mass Fraction Subroutine Input Nomenclature (Cont)

| Input Type | Name | Description |
|---|---|---|
| Sizing | PC (i) | Chamber pressures (psi) |
| | E (i) | Engine expansion ratios |
| | SP (i) | Stage specific impulse (SGC) |
| | AQF 1 | Maximum q $\alpha$ (degrees) |
| | Q | Dynamic pressure at max q $\alpha$ (psi) |
| | SF | Ultimate safety factor |
| | ACCO | Maximum allowable acceleration at max q |
| | ACC10 | Maximum allowable acceleration at end boost Stage 1 |
| | DENS (i) | Material density (lb cu in.) |
| | EFTU (i) | Material ultimate strength (psi) |
| | DELV (i) | Stage velocity (fps) |

The aforementioned FORTRAN names can be located in the flow diagram (Figure B-7). S&ID's experience in subroutine documentation has resulted in similar diagrams. Since no subroutine actually remains static, a working diagram results in the best logic record for explanation. These diagrams can be studied by the engineers to familiarize themselves with the logic and to indicate where and how changes should be made to this logic.

## TEST CASES

During this study, more than 330 basic vehicles were run through this subroutine. Detailed parametric printouts were obtained for 20 percent of these cases. Table B-2 presents a summary of the weight performance printouts for the three-stage vehicles shown in Figure 8 in the main text of this report. Table B-3 presents a similar summary for the two-stage vehicles itemized in Table 7 in the main text of this report.

The amount of data derived in this study was so extensive that to present individual data pieces would involve volumes of printouts. However, these results have been summarized in the main report. The enclosed computer printouts are presented to show the depth of the investigation. Figure B-8 shows an inboard profile sketch for the Case 9 three-stage vehicle with a 400,000-pound payload listed in Table 8 in the main report. Table B-4 presents the tabular form of geometry printout that gives rise to the profile drawing. Figure B-9 presents a CRT plot of stage mass fractions derived from the minimum liftoff mode proportioning. These data were subsequently used to maximize the payload for this vehicle. Tables B-5 and B-6 illustrate parametric design loads that were used in the subroutine to weigh structural shells while Table B-7 presents a weight statement for this three-stage vehicle.

The minimum liftoff weight two-stage vehicle profiles and mass fraction data are illustrated in Figures B-10 through B-15 for Cases 12, 15, and 18 per Table 7 in the main text of this report. The primary candidate vehicle selected for weight and cost assessment in this study consisted of a two-stage configuration sized to the current Isp appearing similar in size and performance to the first two stages of the Saturn V vehicle. Similar vehicles resulting from the maximum payload proportioning, using the already illustrated mass fraction curves (Figures B-11, B-13, and B-15) are identified in this study as Case 20 (240,000-pound payload), Case 21 (333,000-pound payload) and Case 22 (445,000-pound payload). The vehicles are illustrated in Figures B-16, B-17, and B-18. Case 20 was selected to demonstrate the loads check of the parametric synthesis subroutine with S&ID's Computer Aided Design Program. (See Reference 2 in the main text.)

Table B-8 presents a vehicle geometry table for Case 20, while B-9 and B-10 illustrate parametric loads. Table B-11 presents the parametric weight statement for the two-stage 240,000-pound payload vehicle.

## PRELIMINARY DESIGN SYNTHESIS LOADS CHECK

In all cases subjected to weight and cost assessment in this study, the design loads of the parametrically sized vehicles were checked against those computed by the sizing and loads subroutines of S&ID's Computer Aided Design Program. Figure B-19 illustrates the stations at which loads are computed in this program. The mass properties for Case 20, per Table B-12, were used to compute loads for the various flight conditions shown in Table B-13. It should be noted that, in measuring body stations, the stage mass fraction subroutine initializes the aft end of the first-stage engine as station zero and works forward to the top of the payload whereas the preliminary design loads subroutine initializes the forward point on the payload as station zero and works aft. Centers-of-gravity in Table B-13 are listed in these stations, while the mass property centers-of-gravity in Table B-12 are in stage mass fraction subroutine terms. Load results summarized from all loading conditions for Cases 20, 22, 11, 17, 13, and 19 are present in tabular and curve form in the Parametric Synthesis section of this report. These vehicles were subjected to the same degree of analysis as was Case 20.

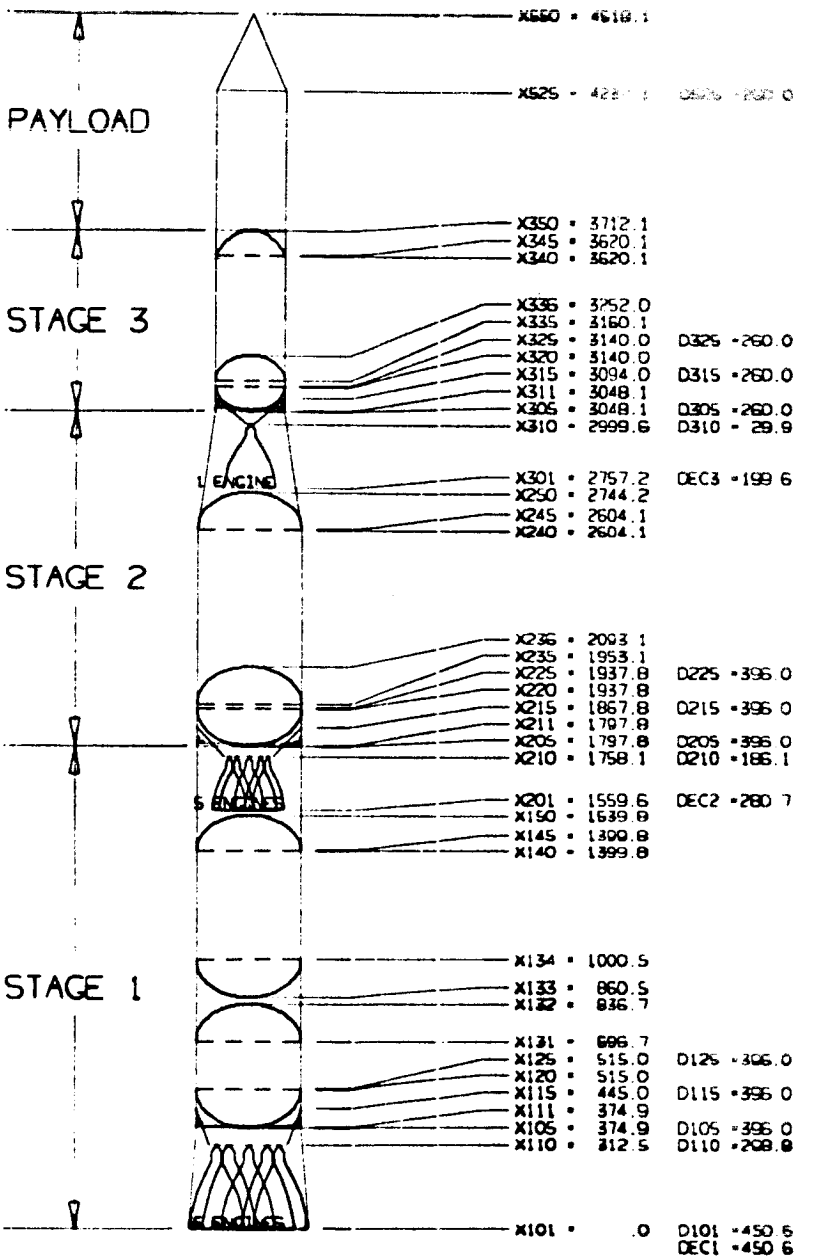
Table B-2. Weight Performance Printout Summary Three Stage Vehicles - Minimum Liftoff Mode

| CASE | 2 | 3 | 4 | 5 | 6 | 7 | 8 | 9 | 10 |
|---|---|---|---|---|---|---|---|---|---|
| TIME PERIOD | CURRENT | CURRENT | CURRENT | 1975 | 1975 | 1975 | 1985 | 1985 | 1985 |
| STAGE | 3 | 3 | 3 | 3 | 3 | 3 | 3 | 3 | 3 |
| VEHICLE GROSS | 142016. | 526870. | 2254611. | 234094. | 611641. | 3017512. | 312783. | 755993. | 3805200. |
| STAGE GROSS | 112016. | 301870. | 1254611. | 174094. | 311641. | 1517512. | 212753. | 365993. | 1805300. |
| PROPELLANT | 95380. | 258303. | 1088383. | 149065. | 264739. | 1306088. | 183288. | 311395. | 1546902. |
| PAYLOAD | 30000. | 225000. | 1000000. | 60000. | 300000. | 1500000. | 100000. | 400000. | 2000000. |
| STAGE MASS FRACTION | 0.8515 | 0.8557 | 0.8675 | 0.8562 | 0.8495 | 0.8607 | 0.8615 | 0.8508 | 0.8569 |
| PERFORMANCE RATIO | 0.6715 | 0.4903 | 0.4827 | 0.6328 | 0.4328 | 0.4328 | 0.5860 | 0.4065 | 0.4065 |
| STAGE | 2 | 2 | 2 | 2 | 2 | 2 | 2 | 2 | 2 |
| VEHICLE GROSS | 273157. | 1552120. | 6729967. | 417616. | 1758681. | 8857319. | 546619. | 1939069. | 9819211. |
| STAGE GROSS | 131124. | 1025250. | 4475362. | 183317. | 1147043. | 5841811. | 233862. | 1172978. | 6013910. |
| PROPELLANT | 109583. | 917018. | 4055677. | 153671. | 1027516. | 5176038. | 197106. | 1046932. | 5385179. |
| PAYLOAD | 142033. | 526870. | 2254605. | 234099. | 611637. | 3017509. | 312757. | 765991. | 3805301. |
| STAGE MASS FRACTION | 0.8357 | 0.8944 | 0.9062 | 0.8383 | 0.8958 | 0.8860 | 0.8428 | 0.8925 | 0.8955 |
| PERFORMANCE RATIO | 0.4011 | 0.5908 | 0.6026 | 0.3681 | 0.5842 | 0.5842 | 0.3506 | 0.5399 | 0.5484 |
| STAGE | 1 | 1 | 1 | 1 | 1 | 1 | 1 | 1 | 1 |
| VEHICLE GROSS | 939172. | 5382799. | 23404467. | 1410714. | 6223064. | 29582711. | 1815087. | 6370744. | 33190308. |
| STAGE GROSS | 665989. | 3830178. | 15674505. | 993290. | 4163366. | 20723398. | 1268462. | 4436764. | 23371595. |
| PROPELLANT | 602288. | 3528251. | 14506845. | 905066. | 3836422. | 19095622. | 1159655. | 4089286. | 20580743. |
| PAYLOAD | 273183. | 1552121. | 6729962. | 417425. | 1758698. | 8859314. | 546625. | 1938980. | 9819213. |
| STAGE MASS FRACTION | 0.9044 | 0.9212 | 0.9255 | 0.9112 | 0.9215 | 0.9215 | 0.9144 | 0.9216 | 0.9196 |
| PERFORMANCE RATIO | 0.6512 | 0.6555 | 0.6475 | 0.6415 | 0.6478 | 0.6455 | 0.6330 | 0.6413 | 0.6383 |

PRECEDING PAGE BLANK NOT FILMED.

## Table B-3. Weight Performance Printout Summary Two Stage Vehicles - Minimum Liftoff Mode

| CASE | 11 | 12 | 13 | 14 | 15 | 16 | 17 | 18 | 19 |
|---|---|---|---|---|---|---|---|---|---|
| TIME PERIOD | CURRENT | CURRENT | CURRENT | 1975 | 1975 | 1975 | 1985 | 1985 | 1985 |
| STAGE | 2 | 2 | 2 | 2 | 2 | 2 | 2 | 2 | 2 |
| VEHICLE GROSS | 231992. | 1394810. | 5641214. | 372927. | 1556499. | 7488787. | 497963. | 1797854. | 9643236. |
| STAGE GROSS | 201992. | 1169810. | 4641214. | 312927. | 1256499. | 5988787. | 397963. | 1397854. | 6643236. |
| PROPELLANT | 180698. | 1067693. | 4278968. | 281358. | 1147603. | 5521505. | 359441. | 1278741. | 6116427. |
| PAYLOAD | 30000. | 225000. | 1000000. | 60000. | 300000. | 1500000. | 100000. | 400000. | 2000000. |
| STAGE MASS FRACTION | 0.8946 | 0.9127 | 0.9220 | 0.8991 | 0.9133 | 0.9220 | 0.9032 | 0.9148 | 0.9207 |
| PERFORMANCE RATIO | 0.7788 | 0.7655 | 0.7585 | 0.7545 | 0.7373 | 0.7373 | 0.7218 | 0.7113 | 0.7077 |
| STAGE | 1 | 1 | 1 | 1 | 1 | 1 | 1 | 1 | 1 |
| VEHICLE GROSS | 897282. | 5461697. | 22710220. | 1320200. | 5852068. | 27637091. | 1713432. | 6287698. | 30361105. |
| STAGE GROSS | 665272. | 4066911. | 17068988. | 947270. | 4295580. | 20148304. | 1215471. | 4489850. | 21717847. |
| PROPELLANT | 602999. | 3756156. | 15814960. | 863288. | 3967175. | 18658030. | 1106198. | 4143349. | 20098176. |
| PAYLOAD | 232010. | 1394786. | 5641232. | 372929. | 1556488. | 7488786. | 497961. | 1797848. | 9643258. |
| STAGE MASS FRACTION | 0.9064 | 0.9236 | 0.9265 | 0.9113 | 0.9235 | 0.9260 | 0.9101 | 0.9228 | 0.9254 |
| PERFORMANCE RATIO | 0.6720 | 0.6877 | 0.6964 | 0.6539 | 0.6779 | 0.6751 | 0.6456 | 0.6590 | 0.6620 |




CASE 9 400000 LB PAYLOAD 1980 ISP

Figure B-8. Case 9 Inboard Profile—Three-Stage Vehicle

Table B-4. Case 9 Vehicle Geometry—Three-Stage Vehicle

| PAYLOAD | | STAGE 4 | | STAGE 3 | | STAGE 2 | | STAGE1 | |
|---|---|---|---|---|---|---|---|---|---|
| DIAMETERS (INCHES) | | | | | | | | | |
| D505 | 260. | D505 | 0. | D405 | 260. | D305 | 260. | D205 | 396. |
| D520 | 0. | D425 | 0. | D325 | 260. | D225 | 396. | D125 | 396. |
| D525 | 260. | D415 | 0. | D315 | 260. | D215 | 396. | D115 | 396. |
| | | D410 | 0. | D310 | 30. | D210 | 186. | D110 | 299. |
| | | D405 | 0. | D305 | 260. | D205 | 396. | D105 | 396. |
| | | D401 | 0. | D301 | 396. | D201 | 396. | D101 | 451. |
| | | DEC4 | 0. | DEC3 | 200. | DEC2 | 281. | DEC1 | 451. |
| BODY STATIONS (INCHES FROM X101) | | | | | | | | | |
| X550 | 4518.1 | X505 | 0.0 | X405 | 3712.1 | X305 | 3048.1 | X205 | 1797.8 |
| X525 | 4232.1 | X450 | 0.0 | X350 | 3712.1 | X250 | 2744.2 | X150 | 1539.8 |
| X505 | 3712.1 | X445 | 0.0 | X345 | 3620.1 | X245 | 2604.1 | X145 | 1399.8 |
| | | X440 | 0.0 | X340 | 3620.1 | X240 | 2604.1 | X140 | 1399.8 |
| | | | | X339 | 0.0 | X239 | 0.0 | X139 | 0.0 |
| | | | | X338 | 0.0 | X238 | 0.0 | X138 | 0.0 |
| | | X436 | 0.0 | X336 | 3252.0 | X236 | 2093.1 | X136 | 0.0 |
| | | X435 | 0.0 | X335 | 3160.1 | X235 | 1953.1 | X135 | 0.0 |
| | | X434 | 0.0 | X334 | 0.0 | X234 | 0.0 | X134 | 1000.5 |
| | | X433 | 0.0 | X333 | 0.0 | X233 | 0.0 | X133 | 860.5 |
| | | X432 | 0.0 | X332 | 0.0 | X232 | 0.0 | X132 | 836.7 |
| | | X431 | 0.0 | X331 | 0.0 | X231 | 0.0 | X131 | 696.7 |
| | | X430 | 0.0 | X330 | 0.0 | X230 | 0.0 | X130 | 0.0 |
| | | X426 | 0.0 | X326 | 0.0 | X226 | 0.0 | X126 | 0.0 |
| | | X425 | 0.0 | X325 | 3140.0 | X225 | 1937.8 | X125 | 515.0 |
| | | X420 | 0.0 | X320 | 3140.0 | X220 | 1937.8 | X120 | 515.0 |
| | | X415 | 0.0 | X315 | 3094.0 | X215 | 1867.8 | X115 | 445.0 |
| | | X411 | 0.0 | X311 | 3048.1 | X211 | 1797.8 | X111 | 374.9 |
| | | X410 | 0.0 | X310 | 2999.6 | X210 | 1758.1 | X110 | 312.5 |
| | | X405 | 0.0 | X305 | 3048.1 | X205 | 2744.2 | X105 | 374.9 |
| | | X401 | 0.0 | X301 | 2757.2 | X201 | 1559.6 | X101 | 0.0 |

Table B-5. Case 9 Parametric Loads—Three-Stage Vehicle

| STATION | MAX Q LOADS MOMENT | MAX Q LOADS AXIAL | END BOOST LOADS MOMENT | END BOOST LOADS AXIAL |
|---|---|---|---|---|
| 374.9 | 0.9947E 08 | 0.7810E 07 | 0.2592E 08 | 0.7810E 07 |
| 515.0 | 0.1366E 09 | 0.7071E 07 | 0.3560E 08 | 0.7653E 07 |
| 696.7 | 0.1848E 09 | 0.6810E 07 | 0.4816E 08 | 0.7598E 07 |
| 1000.5 | 0.2654E 09 | 0.6374E 07 | 0.6917E 08 | 0.7505E 07 |
| 1399.8 | 0.3713E 09 | 0.5801E 07 | 0.9677E 08 | 0.7383E 07 |
| 1797.8 | 0.3658E 09 | 0.5107E 07 | 0.1243E 09 | 0.7262E 07 |
| 1937.8 | 0.3470E 09 | 0.4844E 07 | 0.1340E 09 | 0.7219E 07 |
| 1953.1 | 0.3450E 09 | 0.4816E 07 | 0.1350E 09 | 0.7215E 07 |
| 2093.1 | 0.3261E 09 | 0.4553E 07 | 0.1447E 09 | 0.7172E 07 |
| 2604.1 | 0.2574E 09 | 0.3593E 07 | 0.1407E 09 | 0.6206E 07 |
| 3048.1 | 0.4766E 07 | 0.1977E 09 | 0.1080E 09 | 0.4864E 07 |
| 3140.0 | 0.4468E 07 | 0.1853E 09 | 0.1013E 09 | 0.4559E 07 |
| 3160.1 | 0.4403E 07 | 0.1826E 09 | 0.9981E 08 | 0.4493E 07 |
| 3252.0 | 0.4105E 07 | 0.1703E 09 | 0.9306E 08 | 0.4189E 07 |
| 3620.1 | 0.2911E 07 | 0.1208E 09 | 0.6600E 08 | 0.2971E 07 |

PRESSURES MAX Q

| STAGE | FWD TANK | AFT TANK |
|---|---|---|
| 1 | 47.5 | 46.8 |
| 2 | 33.4 | 47.5 |
| 3 | 32.4 | 42.1 |

PRESSURES END BOOST

| STAGE | FWD TANK | AFT TANK |
|---|---|---|
| 1 | 30.0 | 30.0 |
| 2 | 36.5 | 63.2 |
| 3 | 34.5 | 52.9 |

Table B-6. Case 9 Parametric Applied and Design Loads — Three-Stage Vehicle

APPLIED LOADS

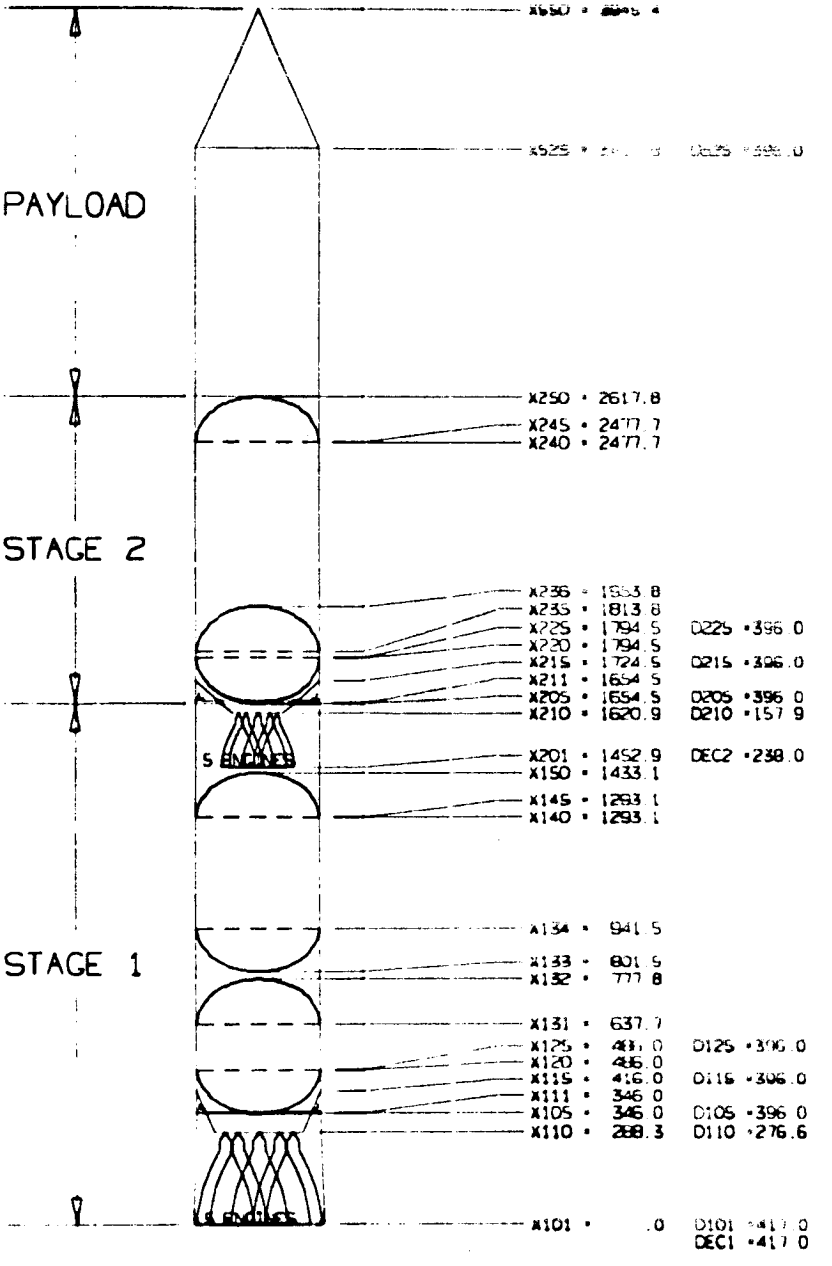
| STATION | MAX Q NX | END BOOST NX |
|---|---|---|
| 374.9 | 7085.6 | 6488.5 |
| 515.0 | 9275.1 | 5940.0 |
| 696.7 | 6974.9 | 6498.3 |
| 1000.5 | 9409.0 | 5940.0 |
| 1399.8 | 7678.2 | 6720.5 |
| 1797.8 | 7075.7 | 6946.4 |
| 1937.8 | 9405.7 | 6890.6 |
| 1953.1 | 6671.8 | 6895.4 |
| 2093.1 | 6618.8 | 7225.8 |
| 2604.1 | 4978.3 | 6130.4 |
| 3048.1 | 9558.8 | 7989.3 |
| 3140.0 | 6225.1 | 6877.1 |
| 3160.1 | 8830.3 | 7386.4 |
| 3252.0 | 6127.0 | 4636.3 |
| 3620.1 | 5838.9 | 4880.2 |

| TOTAL VEHICLE LENGTH | MAX Q CG | END BOOST CG |
|---|---|---|
| 4518. | 1520. | 2328. |

| STATION | DESIGN LOAD | UNIT WEIGHT |
|---|---|---|
| 374.9 | 35.8 | 0.0001461 |
| 515.0 | 46.8 | 0.0001378 |
| 696.7 | 35.2 | 0.0001505 |
| 1000.5 | 47.5 | 0.0001385 |
| 1399.8 | 38.8 | 0.0001393 |
| 1797.8 | 35.7 | 0.0001460 |
| 1937.8 | 47.5 | 0.0001385 |
| 1953.1 | 34.8 | 0.0001448 |
| 2093.1 | 36.5 | 0.0001245 |
| 2604.1 | 31.0 | 0.0001393 |
| 3048.1 | 73.5 | 0.0002049 |
| 3140.0 | 52.9 | 0.0001455 |
| 3160.1 | 67.9 | 0.0001965 |
| 3252.0 | 47.1 | 0.0001380 |
| 3620.1 | 44.9 | 0.0001613 |

Table B-7. Case 9 Parametric Weight Statement—Three-Stage Vehicle

| ITEM | WEIGHT STATEMENT | STAGE 3 WEIGHT (LB) | STAGE 2 WEIGHT (LB) | STAGE 1 WEIGHT (LB) |
|---|---|---|---|---|
| STRUCTURE | | | | |
| INTERSTAGE | | 0. | 14613. | 12895. |
| FWD SKIRT | | 2520. | 5527. | 6998. |
| FWD BULKHEAD | | 700. | 2474. | 2474. |
| FWD TANKWALL | | 10785. | 22961. | 18393. |
| INT BULKHEAD | | 1751. | 4453. | 7255. |
| CENTER SHELL SECTION | | 0. | 0. | 14682. |
| INT AFT BULKHEAD | | 0. | 0. | 2474. |
| AFT TANKWALL | | 497. | 598. | 8313. |
| AFT BULKHEAD | | 2286. | 9641. | 7151. |
| AFT SKIRT | | 3201. | 5793. | 6803. |
| THRUST STRUCTURE | | 1348. | 7980. | 49766. |
| ENGINES | | 6454. | 20911. | 100172. |
| PROP SYS | | 2263. | 7085. | 30332. |
| ULLAGE SYS | | 236. | 0. | 0. |
| SEP SYS | | 110. | 81. | 2617. |
| TVC SYS | | 484. | 1069. | 9215. |
| FIXED EQPT | | 12984. | 9015. | 7659. |
| RES PROP | | 3199. | 10757. | 60478. |
| CONT | | 5792. | 3088. | 0. |
| | BURNOUT | 54608. | 126046. | 347678. |
| PROPELLANT | | 311385. | 1046932. | 4089086. |
| | GROSS | 365993. | 1172978. | 4436764. |
| PAYLOAD | | 400000. | 765991. | 1938980. |
| | VEHICLE | 765993. | 1938969. | 6375744. |




CASE 12 225000 LB PAYLOAD 2 STAGE CURRENT ISP

Figure B-10. Case 12 Inboard Profile

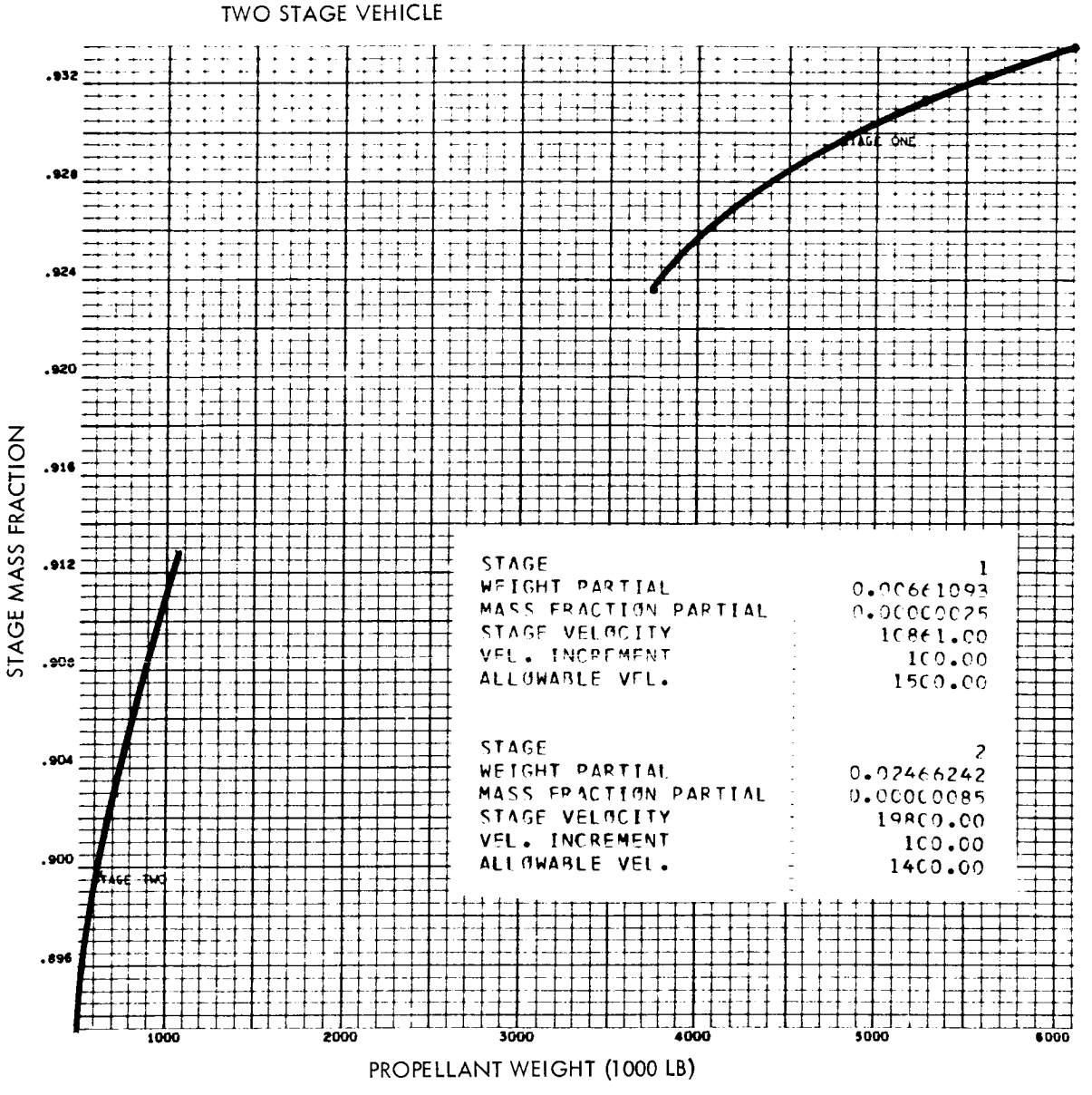
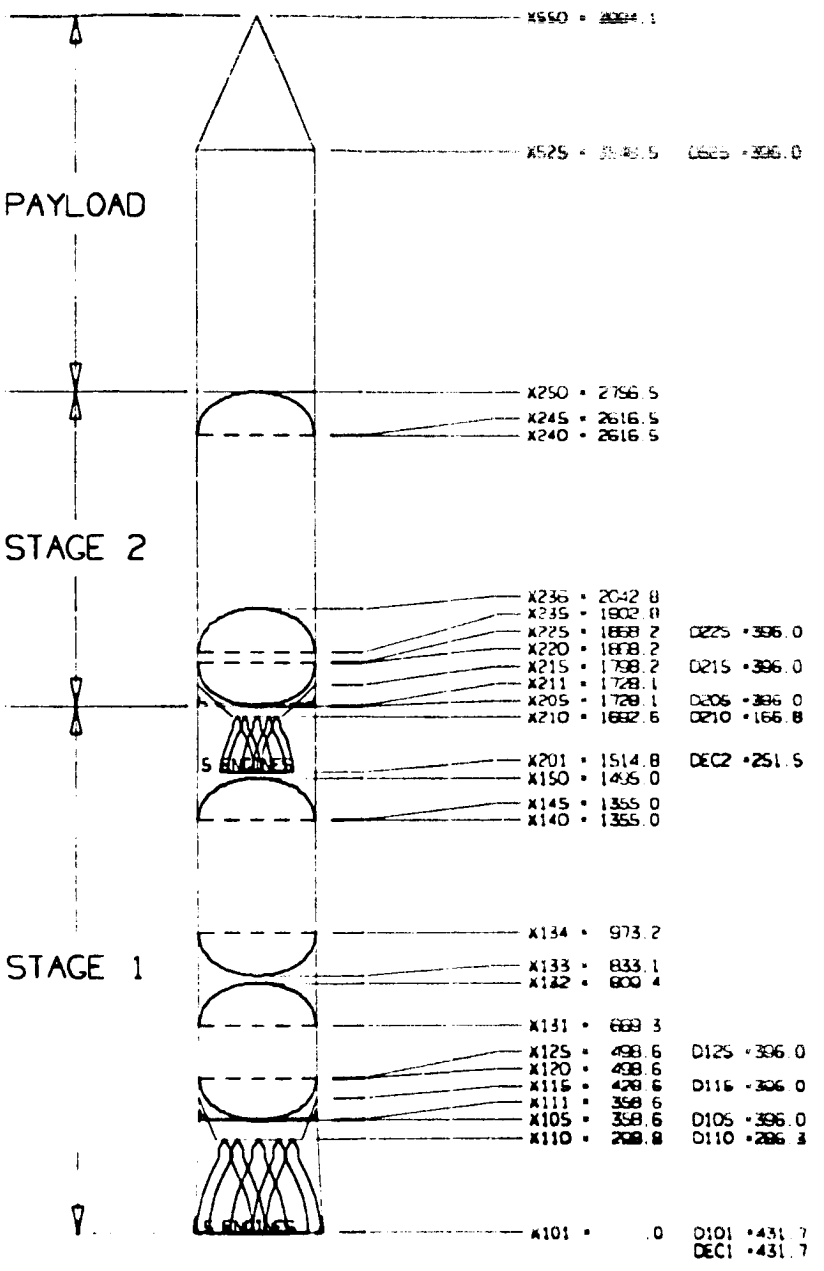



Figure B-11. Case 12 Stage Mass Fractions and Partials




CASE 15 300000 LB PAYLOAD 2 STAGE FUTURE ISP

Figure B-12. Case 15 Inboard Profile

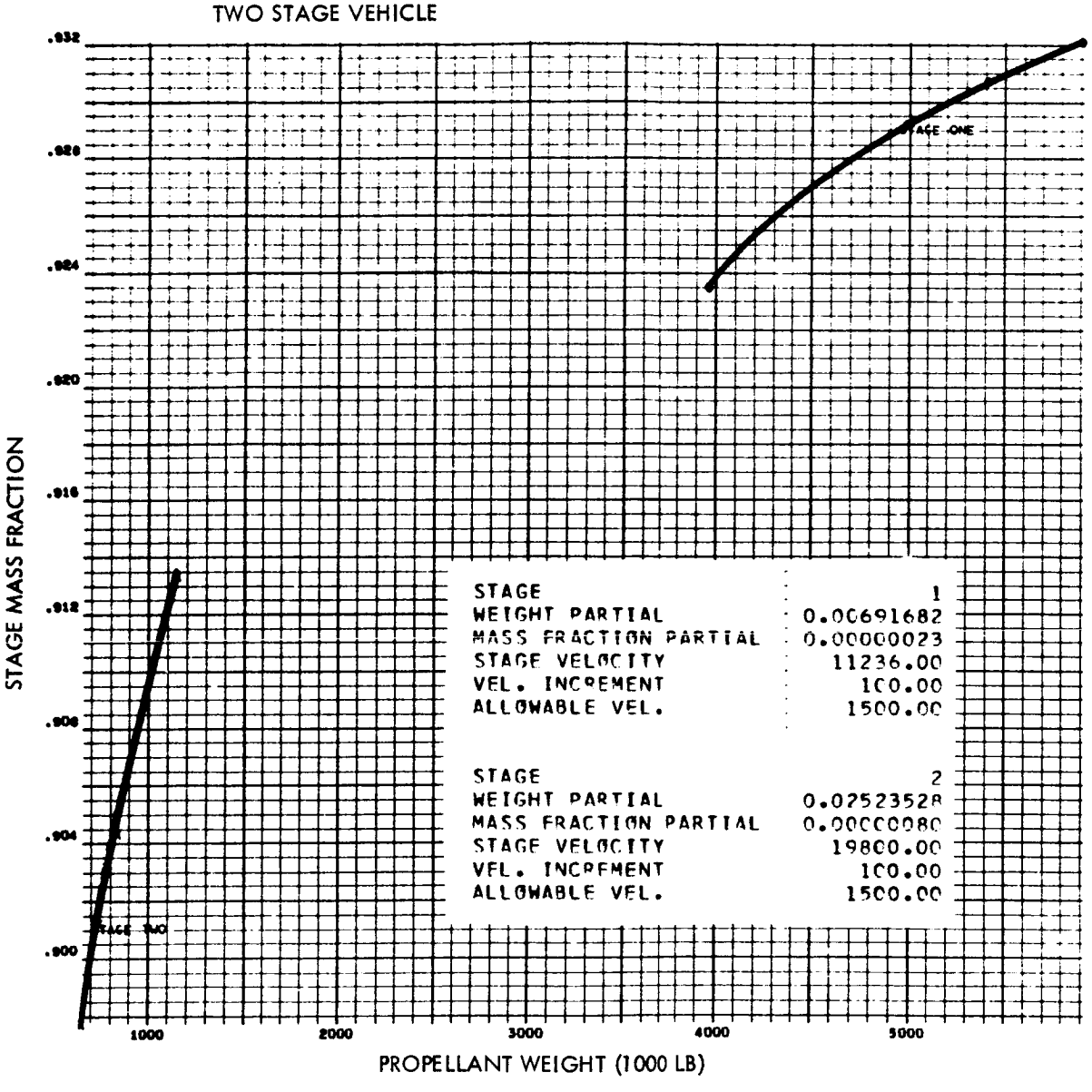
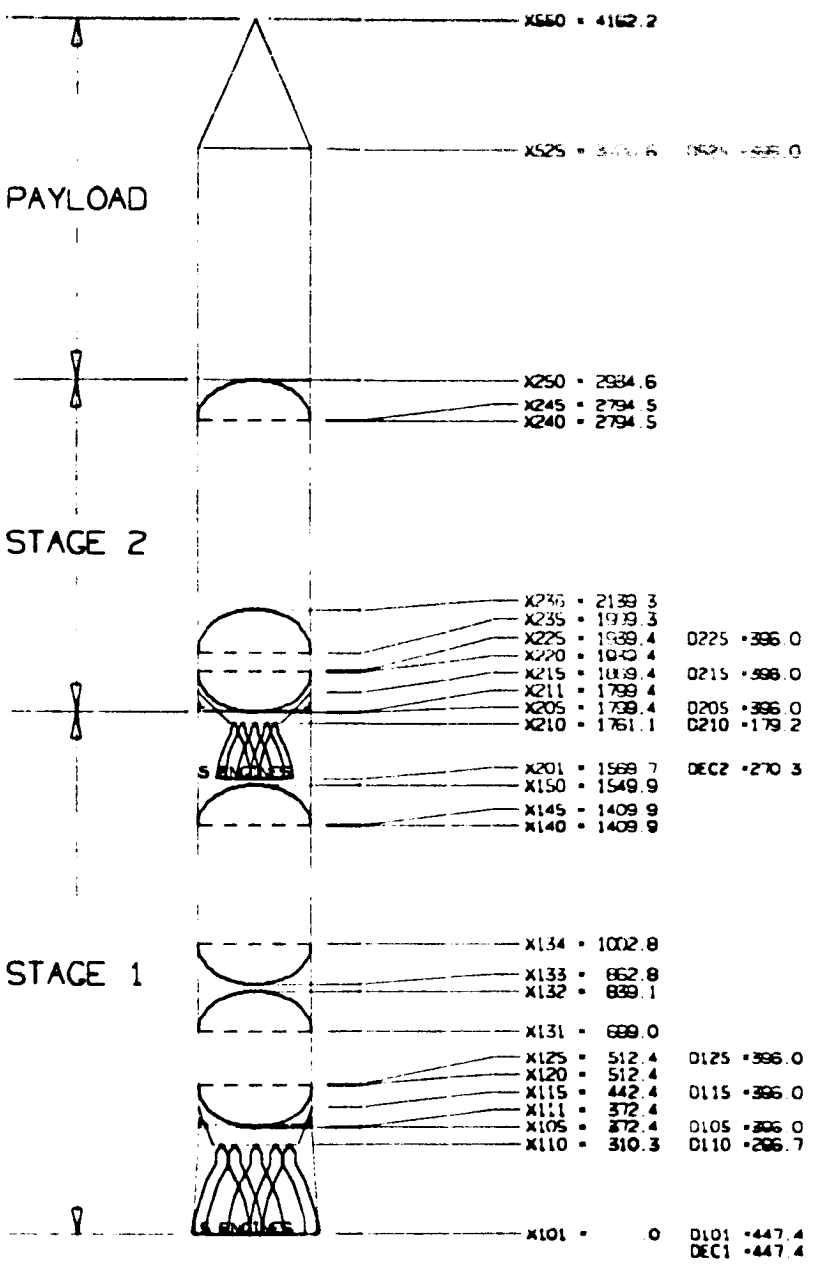



Figure B-13. Case 15 Stage Mass Fractions and Partials




CASE 18 400000 LB PAYLOAD 2 STAGE 1980 ISP

Figure B-14. Case 18 Inboard Profile—Two-Stage Vehicle

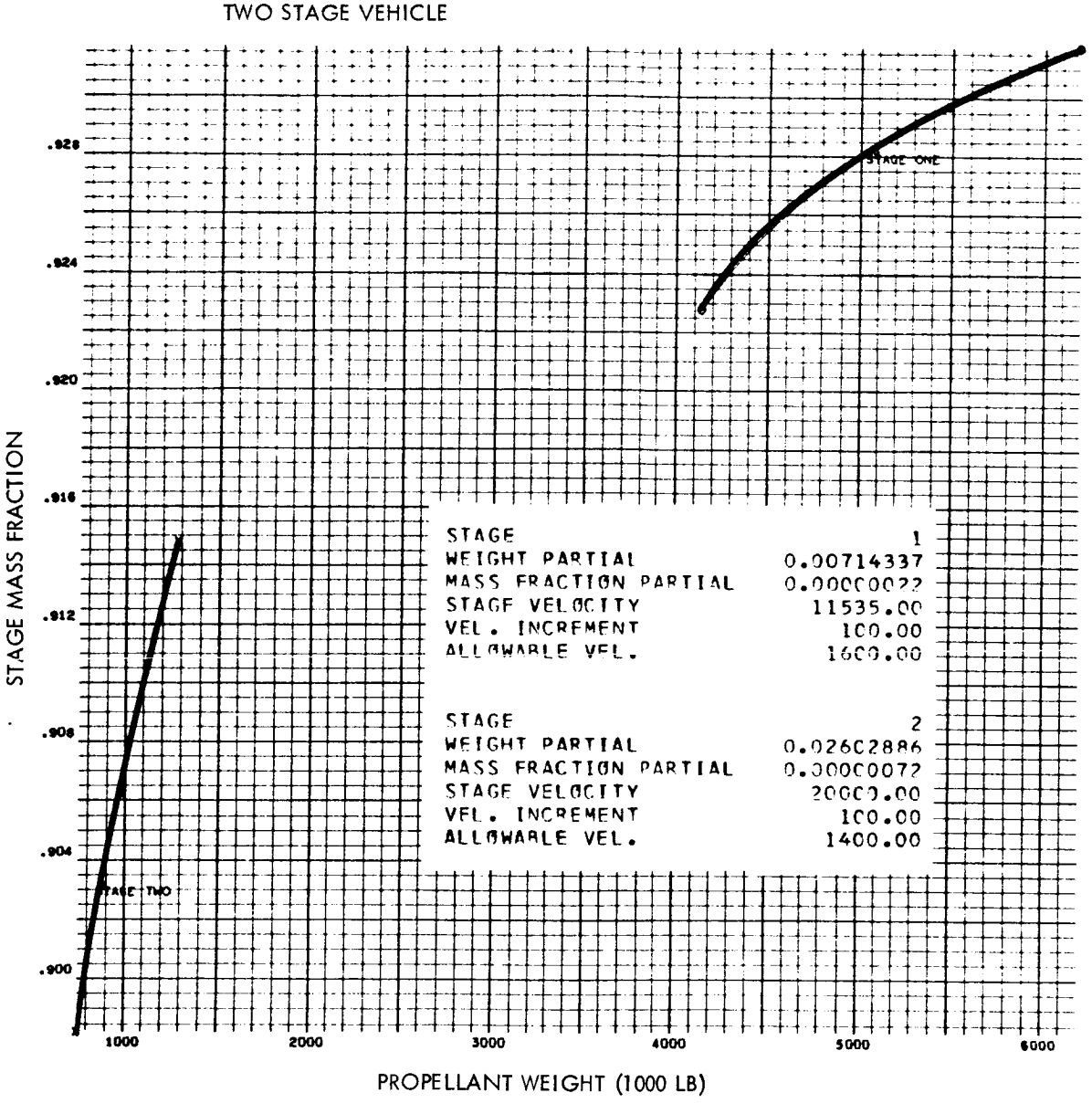
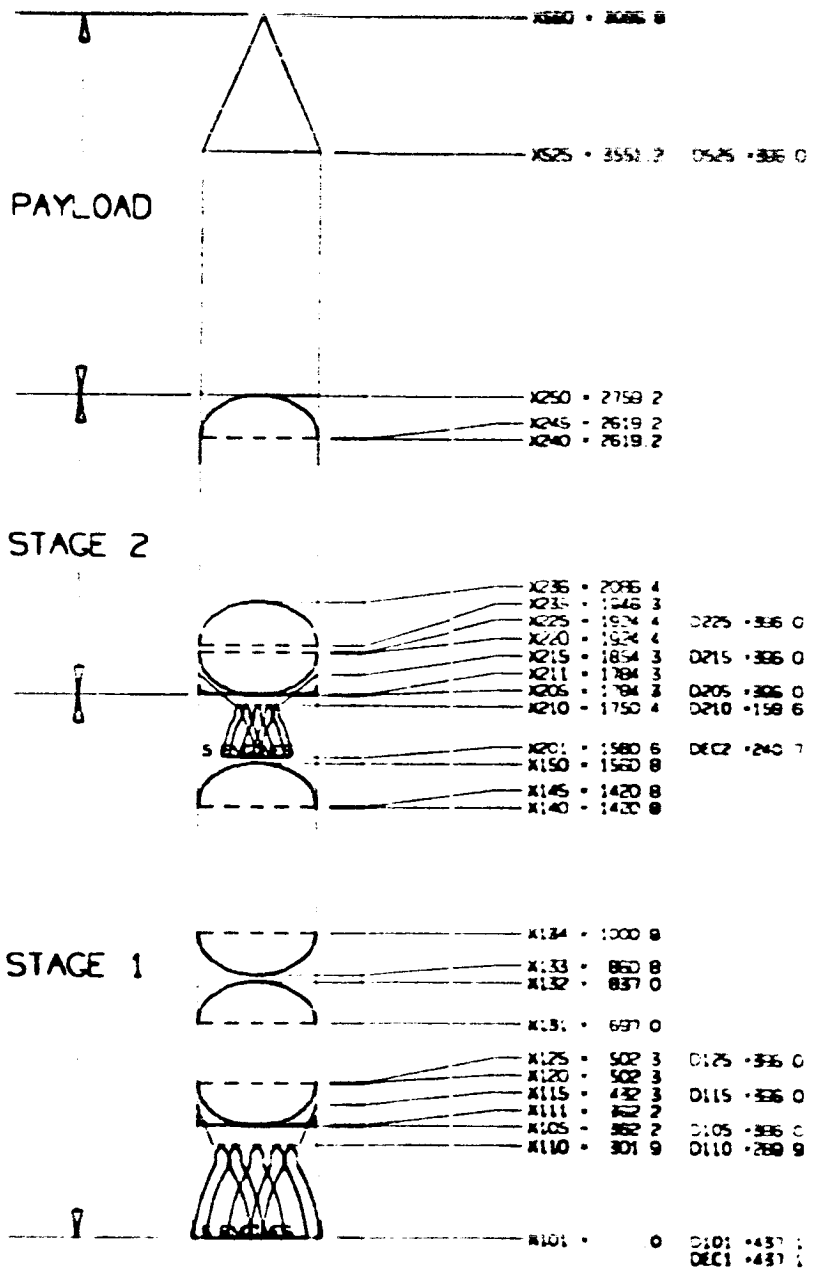
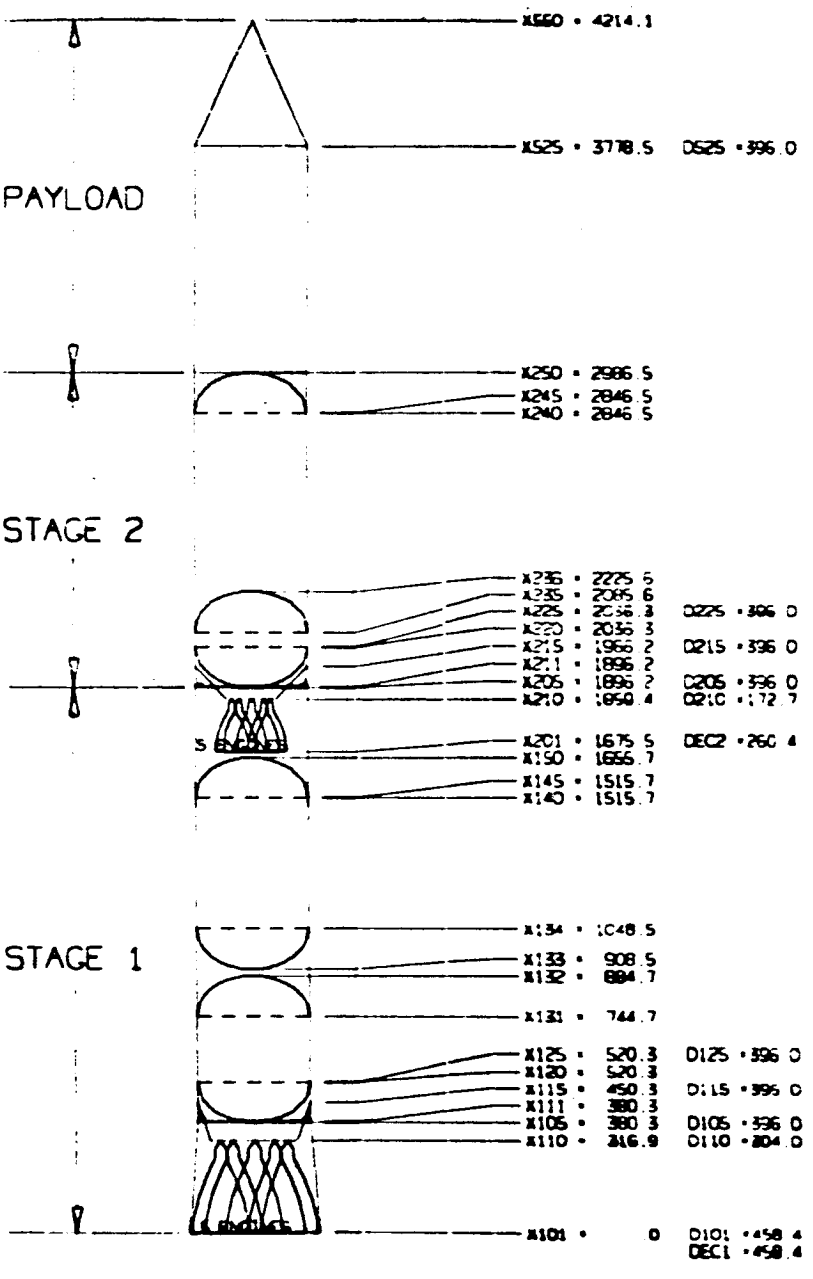



Figure B-15. Case 18 Stage Mass Fractions and Partials




CASE 20 2 STAGE SATURN TYPE PRESENT

Figure B-16. Case 20 Inboard Profile 240,000 lb Payload Two-Stage Current Isp




CASE 21 2 STAGE SATURN TYPE 1975

Figure B-17. Case 21 Inboard Profile 333,000 lb Payload Two-Stage Vehicle 1975 Isp

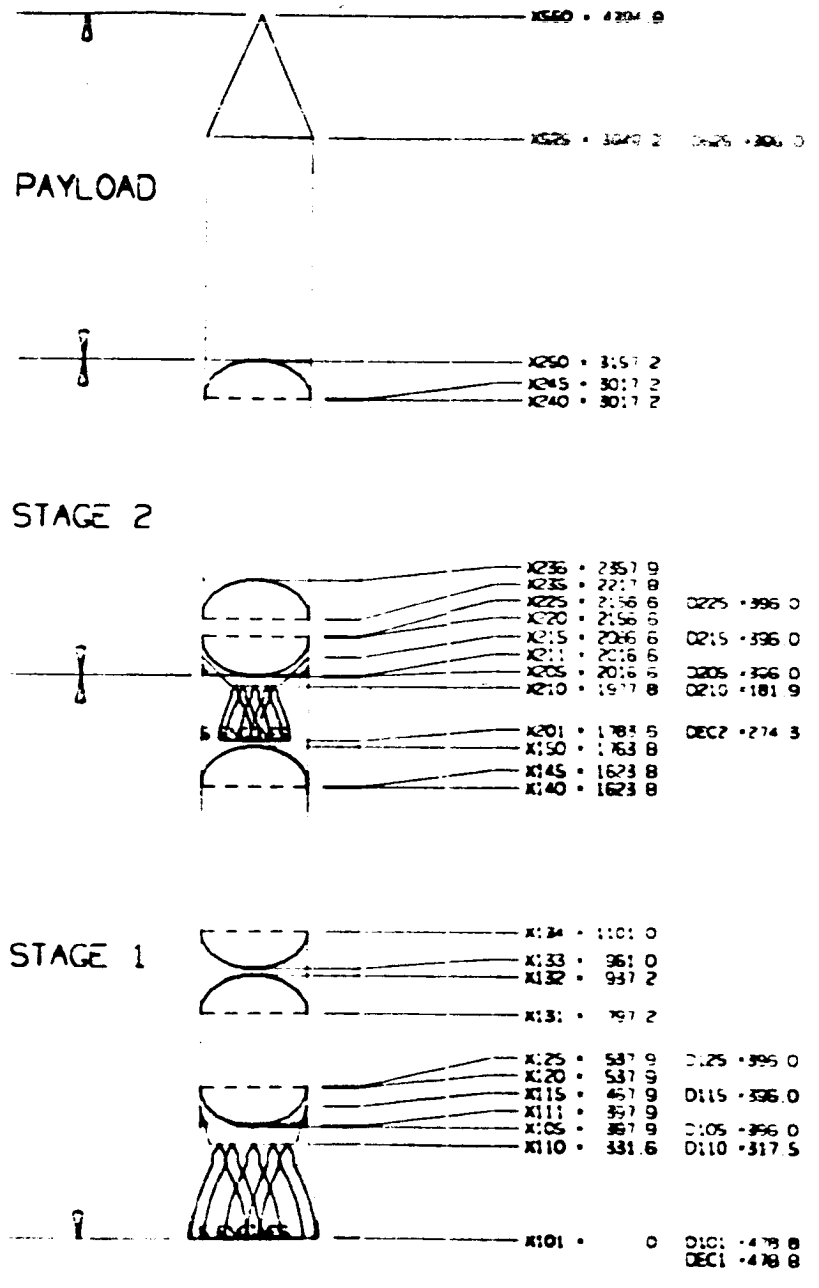



Figure B-18. Case 22 Inboard Profile 445,000 lb Payload Two-Stage Vehicle 1985 Isp

Table B-8. Case 20 Vehicle Geometry

| PAYLOAD | | STAGE 4 | | STAGE 3 | | STAGE 2 | | STAGE1 | |
|---|---|---|---|---|---|---|---|---|---|
| DIAMETERS (INCHES) | | | | | | | | | |
| D5C5 | 396. | D505 | 0. | D405 | 0. | D305 | 396. | D205 | 396. |
| D520 | 0. | D425 | 0. | D325 | 0. | D225 | 396. | D125 | 396. |
| D525 | 396. | D415 | 0. | D315 | 0. | D215 | 396. | D115 | 396. |
| | | D410 | 0. | D310 | 0. | D210 | 160. | D110 | 290. |
| | | D405 | 0. | D305 | 0. | D205 | 396. | D105 | 396. |
| | | D401 | 0. | D301 | 0. | D201 | 396. | D101 | 437. |
| | | DEC4 | 0. | DEC3 | 0. | DEC2 | 241. | DEC1 | 437. |
| BODY STATIONS (INCHES FROM X101) | | | | | | | | | |
| X550 | 3986.8 | X505 | 0.0 | X405 | 0.0 | X305 | 2759.2 | X205 | 1784.3 |
| X525 | 3551.2 | X450 | 0.0 | X350 | 0.0 | X250 | 2759.2 | X150 | 1560.8 |
| X505 | 2759.2 | X445 | 0.0 | X345 | 0.0 | X245 | 2619.2 | X145 | 1420.8 |
| | | X440 | 0.0 | X340 | 0.0 | X240 | 2619.2 | X140 | 1420.8 |
| | | | | X339 | 0.0 | X239 | 0.0 | X139 | 0.0 |
| | | | | X338 | 0.0 | X238 | 0.0 | X138 | 0.0 |
| | | X436 | 0.0 | X336 | 0.0 | X236 | 2086.4 | X136 | 0.0 |
| | | X435 | 0.0 | X335 | 0.0 | X235 | 1946.3 | X135 | 0.0 |
| | | X434 | 0.0 | X334 | 0.0 | X234 | 0.0 | X134 | 1000.8 |
| | | X433 | 0.0 | X333 | 0.0 | X233 | 0.0 | X133 | 860.8 |
| | | X432 | 0.0 | X332 | 0.0 | X232 | 0.0 | X132 | 837.0 |
| | | X431 | 0.0 | X331 | 0.0 | X231 | 0.0 | X131 | 697.0 |
| | | X430 | 0.0 | X330 | 0.0 | X230 | 0.0 | X130 | 0.0 |
| | | X426 | 0.0 | X326 | 0.0 | X226 | 0.0 | X126 | 0.0 |
| | | X425 | 0.0 | X325 | 0.0 | X225 | 1924.4 | X125 | 502.3 |
| | | X420 | 0.0 | X320 | 0.0 | X220 | 1924.4 | X120 | 502.3 |
| | | X415 | 0.0 | X315 | 0.0 | X215 | 1854.3 | X115 | 432.3 |
| | | X411 | 0.0 | X311 | 0.0 | X211 | 1784.3 | X111 | 362.2 |
| | | X410 | 0.0 | X310 | 0.0 | X210 | 1750.4 | X110 | 301.9 |
| | | X405 | 0.0 | X305 | 0.0 | X205 | 1784.3 | X105 | 362.2 |
| | | X401 | 0.0 | X301 | 0.0 | X201 | 1580.6 | X101 | 0.0 |

Table B-9. Case 20 Parametric Loads

| STATION | END BOOST LOADS MOMENT | END BOOST LOADS AXIAL | MAX Q LOADS MOMENT | MAX Q LOADS AXIAL |
|---|---|---|---|---|
| 362.2 | 0.2505E 08 | 0.7350E 07 | 0.9458E 08 | 0.7350E 07 |
| 502.3 | 0.3474E 08 | 0.7296E 07 | 0.1311E 09 | 0.6609E 07 |
| 697.0 | 0.4821E 08 | 0.7275E 07 | 0.1820E 09 | 0.6321E 07 |
| 1000.9 | 0.6922E 08 | 0.7243E 07 | 0.2613E 09 | 0.5873E 07 |
| 1420.8 | 0.9826E 08 | 0.7198E 07 | 0.2934E 09 | 0.5144E 07 |
| 1784.3 | 0.1234E 09 | 0.7159E 07 | 0.2518E 09 | 0.4415E 07 |
| 1924.4 | 0.1326E 09 | 0.7131E 07 | 0.2358E 09 | 0.4134E 07 |
| 1946.3 | 0.1312E 09 | 0.7055E 07 | 0.2333E 09 | 0.4090E 07 |
| 2086.4 | 0.1222E 09 | 0.6571E 07 | 0.2173E 09 | 0.3809E 07 |
| 2619.2 | 0.8703E 08 | 0.4729E 07 | 0.1563E 09 | 0.2741E 07 |

PRESSURES MAX Q

| STAGE | FWD TANK | AFT TANK |
|---|---|---|
| 1 | 48.9 | 48.2 |
| 2 | 33.7 | 48.8 |

PRESSURES END BOOST

| STAGE | FWD TANK | AFT TANK |
|---|---|---|
| 1 | 30.0 | 30.0 |
| 2 | 38.1 | 71.3 |

Table B-10. Case 20 Parametric Applied and Design Loads Stage Partials

APPLIED LOADS

| STATION | MAX Q NX | END BOOST NX |
|---|---|---|
| 362.2 | 6676.0 | 6111.4 |
| 502.3 | 9539.1 | 5940.0 |
| 697.0 | 6558.6 | 6239.4 |
| 1000.8 | 9692.0 | 5940.0 |
| 1420.8 | 6516.3 | 6583.5 |
| 1784.3 | 5593.1 | 6756.3 |
| 1924.4 | 9660.9 | 6808.9 |
| 1946.3 | 5181.6 | 6736.3 |
| 2086.4 | 6672.1 | 7549.4 |
| 2619.2 | 3472.9 | 4514.9 |

| TOTAL VEHICLE LENGTH | MAX Q CG | END BOOST CG |
|---|---|---|
| 3987. | 1214. | 1921. |

| STATION | DESIGN LOAD | UNIT WEIGHT |
|---|---|---|
| 362.2 | 33.7 | 0.0001432 |
| 502.3 | 48.2 | 0.0001394 |
| 697.0 | 33.1 | 0.0001424 |
| 1000.8 | 48.9 | 0.0001405 |
| 1420.8 | 33.2 | 0.0001425 |
| 1784.3 | 34.1 | 0.0001438 |
| 1924.4 | 48.8 | 0.0001403 |
| 1946.3 | 34.0 | 0.0001436 |
| 2086.4 | 38.1 | 0.0001261 |
| 2619.2 | 22.8 | 0.0001265 |

| STAGE | 1 | 2 |
|---|---|---|
| WEIGHT PARTIAL | 0.00731002 | 0.02486917 |
| MASS FRACTION PARTIAL | 0.00000022 | 0.00000084 |
| STAGE VELOCITY | 11410.00 | 19412.00 |
| VEL. INCREMENT | 100.00 | 100.00 |
| ALLOWABLE VEL. | 1400.00 | 1500.00 |

Table B-11. Case 20 Parametric Weight Statement

WEIGHT STATEMENT

| ITEM | | STAGE 2 WEIGHT (LB) | STAGE 1 WEIGHT (LB) |
|---|---|---|---|
| STRUCTURE | | | |
| INTERSTAGE | | 0. | 10688. |
| FWD SKIRT | | 5017. | 6638. |
| FWD BULKHEAD | | 2474. | 2474. |
| FWD TANKWALL | | 24041. | 19625. |
| INT BULKHEAD | | 4453. | 7473. |
| CENTER SHELL SECTION | | 0. | 14384. |
| INT AFT BULKHEAD | | 0. | 2474. |
| AFT TANKWALL | | 874. | 9029. |
| AFT BULKHEAD | | 10887. | 7355. |
| AFT SKIRT | | 5703. | 6668. |
| THRUST STRUCTURE | | 6330. | 46952. |
| ENGINES | | 16587. | 94509. |
| PROP SYS | | 7202. | 30863. |
| ULLAGE SYS | | 0. | 0. |
| SEP SYS | | 84. | 2709. |
| TVC SYS | | 1095. | 9458. |
| FIXED EQPT | | 5046. | 6568. |
| RES PROP | | 11118. | 62613. |
| CONT | | 3192. | 0. |
| | BURNOUT | 104103. | 340481. |
| PROPELLANT | | 1081997. | 4233452. |
| | GROSS | 1186100. | 4573934. |
| PAYLOAD | | 239966. | 1426066. |
| | VEHICLE | 1426066. | 6000000. |

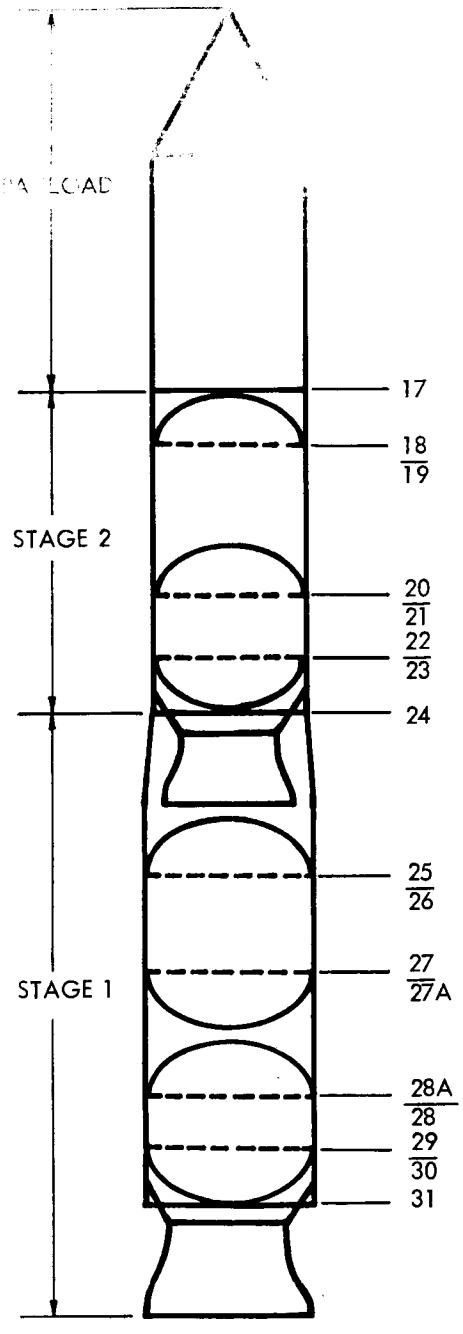



Figure B-19. Loads Stations Preliminary Design Snythesis

Table B-12. Case 20 Preliminary Design Synthesis—Weight and Balance Summary

PRELIMINARY DESIGN SYNTHESIS PROGRAM

BOOSTER WEIGHT AND BALANCE SUMMARY

| | WEIGHT(LB) | C.G.(STA) | INERTIA(LB/IN.SQ) |
|---|---|---|---|
| PAYLOAD | 239977. | 3302. | 2.77700E 10 |
| END BOOST STAGE 2 | 344118. | 2904. | 1.66131E 11 |
| MID BOOST STAGE 2 | 885110. | 2285. | 3.92018E 11 |
| BEGIN BOOST STAGE 2 | 1426102. | 2209. | 4.33172E 11 |
| END BOOST STAGE 1 | 1766400. | 1866. | 1.34401E 12 |
| MID BOOST STAGE 1 | 3883200. | 1328. | 2.45355E 12 |
| BEGIN BOOST STAGE 1 | 6000000. | 1266. | 2.71904E 12 |

Table B-13. Case 20 Preliminary Design Synthesis Loads Check

| STATION NUMBER | LOADS---PRE-LAUNCH SHEAR | BENDING MOMENT | AXIAL LOAD |
|---|---|---|---|
| 17 | 3.3989867E 04 | 1.7427604E 07 | 2.3997662E 05 |
| 18 | 3.8870095E 04 | 2.2709441E 07 | 2.4482379E 05 |
| 19 | 3.8870095E 04 | 2.2709441E 07 | 2.5019584E 05 |
| 20 | 6.1561099E 04 | 5.6560965E 07 | 2.7273310E 05 |
| 21 | 6.1561099E 04 | 5.6560965E 07 | 4.5843661E 05 |
| 22 | 6.2289651E 04 | 5.7901306E 07 | 4.5916022E 05 |
| 23 | 6.2289651E 04 | 5.7901306E 07 | 1.4168615E 06 |
| 24 | 6.8260800E 04 | 6.9480869E 07 | 1.4261019E 06 |
| 25 | 7.8836425E 04 | 9.2589086E 07 | 1.4369940E 06 |
| 26 | 7.8836425E 04 | 9.2589086E 07 | 1.4425645E 06 |
| 27 | 9.2978545E 04 | 1.2868279E 08 | 1.4571297E 06 |
| 28 | 1.0287509E 05 | 1.5747474E 08 | 4.4094180E 06 |
| 29 | 1.0944660E 05 | 1.7820073E 08 | 4.4161861E 06 |
| 30 | 1.0944660E 05 | 1.7820073E 08 | 5.9779391E 06 |
| 31 | 1.1654314E 05 | 2.0152716E 08 | 5.9999994E 06 |
| 20A | 0.0000000E-39 | 0.0000000E-39 | 0.0000000E-39 |
| 21A | 0.0000000E-39 | 0.0000000E-39 | 0.0000000E-39 |
| 27A | 9.2978545E 04 | 1.2868279E 08 | 4.3936549E 06 |
| 28A | 1.0287509E 05 | 1.5747474E 08 | 4.4038475E 06 |

Table B-13. Case 20 Preliminary Design Synthesis Loads Check (Cont)

LOADS--BEGIN BOOST STAGE 1

| STATION NUMBER | SHEAR | BENDING MOMENT | AXIAL LOAD |
|---|---|---|---|
| 17 | 1.1796216E 05 | 7.1134353E 07 | 2.9997081E 05 |
| 18 | 1.2378753E 05 | 8.8685626E 07 | 3.0602976E 05 |
| 19 | 1.2955783E 05 | 8.9080786E 07 | 3.1274483E 05 |
| 20 | 1.7075124E 05 | 1.9261953E 08 | 3.4091640E 05 |
| 21 | 1.8093902E 05 | 1.9394780E 08 | 5.7304580E 05 |
| 22 | 1.8251388E 05 | 1.9812644E 08 | 5.7395033E 05 |
| 23 | 1.7846716E 05 | 1.9962660E 08 | 1.7710770E 06 |
| 24 | 1.8422325E 05 | 2.3184905E 08 | 1.7826276E 06 |
| 25 | 1.9397287E 05 | 2.9134349E 08 | 1.7962426E 06 |
| 26 | 1.4806934E 05 | 2.8972852E 08 | 1.8032058E 06 |
| 27 | -1.7740639E 05 | 2.9549396E 08 | 1.8214124E 06 |
| 28 | -3.6473424E 05 | 2.1581281E 08 | 5.5117730E 06 |
| 29 | -5.6955180E 05 | 1.2730994E 08 | 5.5202331E 06 |
| 30 | 1.6926953E 03 | -1.6512400E 06 | -2.7575500E 04 |
| 31 | 3.9062500E-02 | 2.0625000E 00 | -1.2500000E-01 |
| 20A | -0.0000000E-39 | -0.0000000E-39 | 0.0000000E-39 |
| 21A | -0.0000000E-39 | -0.0000000E-39 | 0.0000000E-39 |
| 27A | -2.8293291E 05 | 3.0205719E 08 | 5.4920691E 06 |
| 28A | -2.7562227E 05 | 2.2001249E 08 | 5.5048099E 06 |

TOTAL WEIGHT = 5.9999993E 06 LB
NORMAL ACCELERATION = 1.5008445E-01 G
AXIAL ACCELERATION = -1.2500001E 00 G

MOMENT OF INERTIA = 7.0441477E 09 LB*IN*SEC**2
CG = 1.2664562E 03 IN
ROTATIONAL ACCELERATION = -9.4797244E-02 RAD/SEC**2
THRUST = 7.5000000E 06 LB

Table B-13. Case 20 Preliminary Design Synthesis Loads Check (Cont)

LOADS--MID BOOST STAGE 1

| STATION NUMBER | SHEAR | BENDING MOMENT | AXIAL LOAD |
|---|---|---|---|
| 17 | 1.5513650E 05 | 1.4848388E 08 | 7.0343292E 05 |
| 18 | 1.5435108E 05 | 1.7091956E 08 | 7.1314287E 05 |
| 19 | 1.4945822E 05 | 1.7064241E 08 | 7.2390429E 05 |
| 20 | 1.2660847E 05 | 2.6055394E 08 | 7.6905145E 05 |
| 21 | 5.4272727E 04 | 2.5697287E 08 | 1.1410570E 06 |
| 22 | 3.8984398E 04 | 2.5790212E 08 | 1.1425066E 06 |
| 23 | -3.5562641E 04 | 2.6256808E 08 | 3.0609958E 06 |
| 24 | -3.7059937E 04 | 2.5617417E 08 | 3.0795065E 06 |
| 25 | -3.8824855E 04 | 2.4425306E 08 | 3.1013257E 06 |
| 26 | -3.9727438E 04 | 2.4418989E 08 | 3.1124847E 06 |
| 27 | -2.0638248E 05 | 2.0977349E 08 | 3.1416621E 06 |
| 28 | -2.8300638E 05 | 1.3100783E 08 | 6.1200771E 06 |
| 29 | -3.3794318E 05 | 7.3030152E 07 | 6.1336352E 06 |
| 30 | -1.6738812E 04 | 1.3960010E 06 | -5.4896700E 05 |
| 31 | 1.1718750E-02 | 1.1812500E 01 | -1.8750000E-01 |
| 20A | 0.0000000E-39 | 0.0000000E-39 | 0.0000000E-39 |
| 21A | 0.0000000E-39 | 0.0000000E-39 | 0.0000000E-39 |
| 27A | -2.8045716E 05 | 2.1377094E 08 | 6.0884999E 06 |
| 28A | -2.8210375E 05 | 1.3107101E 08 | 6.1089181E 06 |

TOTAL WEIGHT = 3.9831996E 06 LB
NORMAL ACCELERATION = 1.6203722E-01 G
AXIAL ACCELERATION = -2.0032231E 00 G
BASE DRAG = 5.0458712E 05 LB
SIN GIMBAL ANGLE = 4.8773626E-02
AMBIENT PRESSURE = 3.0000000E 00 PSIA
MOMENT OF INERTIA = 6.3563456E 09 LB*IN*SEC**2
CG = 1.3282681E 03 IN
ROTATIONAL ACCELERATION = 0.0000000E-39 RAD/SEC**2
THRUST = 8.5063966E 06 LB
TOTAL ANGLE OF ATTACK = 1.8000000E-01 RAD
DYNAMIC PRESSURE = 5.2800000E 00 PSIG
AERODYNAMIC CENTER = 3.3150960E 03 IN





NORTH AMERICAN AVIATION, INC.
SPACE and INFORMATION SYSTEMS DIVISION

Table B-13. Case 20 Preliminary Design Synthesis Loads Check (Cont)

LOADS--END BOOST STAGE 1

| STATION NUMBER | SHEAR | BENDING MOMENT | AXIAL LOAD |
|---|---|---|---|
| 17 | 5.2855701E 03 | 5.3217110E 06 | 1.2065190E 06 |
| 18 | 5.2421622E 03 | 6.0848978E 06 | 1.2302968E 06 |
| 19 | 4.9717484E 03 | 6.0695806E 06 | 1.2566493E 06 |
| 20 | 3.3773065E 03 | 8.8219592E 06 | 1.3672058E 06 |
| 21 | -2.8887610E 02 | 8.6240439E 06 | 2.2781737E 06 |
| 22 | -1.1338173E 03 | 8.6086471E 06 | 2.2817233E 06 |
| 23 | -5.2538143E 03 | 8.8620997E 06 | 6.9797234E 06 |
| 24 | -5.3365656E 03 | 7.9253832E 06 | 7.0250524E 06 |
| 25 | -5.4341074E 03 | 6.2333662E 06 | 7.0784833E 06 |
| 26 | -5.4839933E 03 | 6.2298746E 06 | 7.1058096E 06 |
| 27 | -5.6144298E 03 | 3.8983945E 06 | 7.1772593E 06 |
| 28 | -5.8054882E 03 | 2.2195820E 06 | 7.2819162E 06 |
| 29 | -5.8660989E 03 | 1.0802485E 06 | 7.3151172E 06 |
| 30 | -5.8082434E 02 | 3.8527391E 04 | -1.7466000E 05 |
| 31 | 1.2207031E-04 | 2.2216797E-01 | -1.8359375E-01 |
| 20A | -0.0000000E-39 | -0.0000000E-39 | 0.0000000E-39 |
| 21A | -0.0000000E-39 | -0.0000000E-39 | 0.0000000E-39 |
| 27A | -5.6643237E 03 | 3.9018877E 06 | 7.2045899E 06 |
| 28A | -5.7556023E 03 | 2.2230735E 06 | 7.2545899E 06 |

TOTAL WEIGHT = 1.7663998E 06 LB
NORMAL ACCELERATION = 8.9553236E-03 G
AXIAL ACCELERATION = -4.9054965E 00 G
BASE DRAG = 6.6418191E 04 LB
SIN GIMBAL ANGLE = 8.6814441E-04
AMBIENT PRESSURE = 4.2100000E-02 PSIA
MOMENT OF INERTIA = 3.4818927E 09 LB*IN*SEC**2
CG = 1.8662971E 03 IN
ROTATIONAL ACCELERATION = 0.0000000E-39 RAD/SEC**2
THRUST = 8.7608257E 06 LB
TOTAL ANGLE OF ATTACK = 5.2400000E-02 RAD
DYNAMIC PRESSURE = 6.9500000E-01 PSIG
AERODYNAMIC CENTER = 3.3150060E 03 IN

Table B-13. Case 20 Preliminary Design Synthesis Loads Check (Cont)

LOADS--BEGIN BOOST STAGE 2

| STATION NUMBER | SHEAR | BENDING MOMENT | AXIAL LOAD |
|---|---|---|---|
| 17 | 1.4368864E 04 | 1.2041690E 07 | 1.7241713E 05 |
| 18 | 1.4757421E 04 | 1.4203708E 07 | 1.7530759E 05 |
| 19 | 1.3998733E 04 | 1.4198188E 07 | 1.7851104E 05 |
| 20 | 1.0148281E 03 | 1.9632566E 07 | 1.9195044E 05 |
| 21 | -4.6580947E 04 | 1.7489905E 07 | 3.0268894E 05 |
| 22 | -5.8373678E 04 | 1.6488548E 07 | 3.0312044E 05 |
| 23 | 1.3183193E 03 | -1.8388175E 05 | -1.2419645E 05 |
| 24 | 3.9062500E-03 | -1.3203125E 00 | -1.9531250E-02 |
| 20A | -0.0000000E-39 | -0.0000000E-39 | 0.0000000E-39 |
| 21A | -0.0000000E-39 | -0.0000000E-39 | 0.0000000E-39 |

MOMENT OF INERTIA = 1.1222081E 09 LB*IN*SEC**2
CG = 2.2086768E 03 IN
ROTATIONAL ACCELERATION = -5.1978899E-02 RAD/SEC**2
THRUST = 9.9841220E 05 LB
TOTAL ANGLE OF ATTACK = 0.0000000E-39 RAD
DYNAMIC PRESSURE = 6.9500000E-01 PSIG
AERODYNAMIC CENTER = 3.6212329E 03 IN

TOTAL WEIGHT = 1.4261019E 06 LB
NORMAL ACCELERATION = 8.5320580E-02 G
AXIAL ACCELERATION = -5.9631886E-01 G
BASE DRAG = 1.1868618E 05 LB
SIN GIMBAL ANGLE = 1.2186935E-01
AMBIENT PRESSURE = 4.2100000E-02 PSIA





NORTH AMERICAN AVIATION, INC.
SPACE and INFORMATION SYSTEMS DIVISION

Table B-13. Case 20 Preliminary Design Synthesis Loads Check (Cont)

LOADS--MID BOOST STAGE 2

| STATION NUMBER | SHEAR | BENDING MOMENT | AXIAL LOAD |
|---|---|---|---|
| 17 | 9.1237866E 03 | 9.8884497E 06 | 2.7112627E 05 |
| 18 | 8.7801792E 03 | 1.1204719E 07 | 2.7660261E 05 |
| 19 | 8.3970439E 03 | 1.1193053E 07 | 2.8267197E 05 |
| 20 | -1.0641963E 04 | 1.4259387E 07 | 3.0813463E 05 |
| 21 | -1.1650430E 04 | 1.4203933E 07 | 4.1607398E 05 |
| 22 | -2.1279967E 04 | 1.3983369E 07 | 4.1689152E 05 |
| 23 | 2.0727793E 03 | -2.8184150E 05 | -1.0439906E 04 |
| 24 | 5.8593750E-03 | -3.1796875E 00 | -1.5625000E-02 |
| 20A | -0.0000000E-39 | -0.0000000E-39 | 0.0000000E-39 |
| 21A | -0.0000000E-39 | -0.0000000E-39 | 0.0000000E-39 |

TOTAL WEIGHT = 8.8511016E 05 LB
NORMAL ACCELERATION = 1.3768834E-01 G
AXIAL ACCELERATION = -1.1298029E 00 G
MOMENT OF INERTIA = 1.0155921E 09 LB*IN*SEC**2
CG = 2.2345988E 03 IN
ROTATIONAL ACCELERATION = -6.6637465E-02 RAD/SEC**2
THRUST = 1.0000000E 06 LB

Table B-13. Case 20 Preliminary Design Synthesis Loads Check (Cont.)

LOADS--END BOOST STAGE 2

| STATION NUMBER | SHEAR | BENDING MOMENT | AXIAL LOAD |
|---|---|---|---|
| 17 | -2.6476262E 03 | 2.2459261E 07 | 6.9736642E 05 |
| 18 | -5.3371719E 03 | 2.1972065E 07 | 7.1145216E 05 |
| 19 | -8.3293134E 03 | 2.1838285E 07 | 7.2706322E 05 |
| 20 | -2.8720106E 04 | 1.0443262E 07 | 7.9255596E 05 |
| 21 | -3.4904815E 04 | 1.0096806E 07 | 8.0816955E 05 |
| 22 | -3.5778755E 04 | 9.3381040E 06 | 8.1027235E 05 |
| 23 | 1.2205857E 04 | -1.6308720E 06 | -2.6852562E 04 |
| 24 | 1.2695313E-02 | -1.7968750E-01 | -7.8125000E-03 |
| 20A | -0.0000000E-39 | -0.0000000E-39 | 0.0000000E-39 |
| 21A | -0.0000000E-39 | -0.0000000E-39 | 0.0000000E-39 |

TOTAL WEIGHT = 3.4411841E 05 LB
NORMAL ACCELERATION = 3.5414945E-01 G
AXIAL ACCELERATION = -2.9059765E 00 G

MOMENT OF INERTIA = 4.3039078E 08 LB*IN*SEC**2
CG = 2.9043467E 03 IN
ROTATIONAL ACCELERATION = -3.3273192E-01 RAD/SEC**2
THRUST = 1.0000000E 06 LB

## SUBROUTINE NOMENCLATURE

| | |
|---|---|
| $W_{O_i}$ | ith stage gross weight-includes payload above ith stage |
| $W_{PL_i}$ | ith stage payload weight |
| $\nu_i$ | ith stage performance mass ratio |
| $\nu_{B_i}$ | ith stage mass fraction |
| $T_1$ | Initial vehicle thrust |
| $T/W_i$ | Thrust to weight ratio of ith stage |
| $(SP_i)$, $I_i$ | Specific impulse of ith stage |
| g | Gravity constant |
| $K1_i$ | Velocity loss factor for ith stage |
| $\Delta V_i$ | Characteristic stage velocity |
| $\Delta V_T$ | Total vehicle velocity |
| N, M | Number of stages |
| $D_i$ | Stage diameter of ith stage |
| $VO_i$ | Volume of aft tank |
| $AT_i$ | Nozzle thrust area |
| $T_i$ | Stage design thrust |
| $EN_i$ | Number of engines |
| $PC_i$ | Chamber pressure |
| $C2_i$ | Thrust coefficient |
| $AE_i$ | Exit area |

| | |
|---|---|
| $E_i$ | Expansion ratio |
| $DE_i$ | Nozzle exit diameter |
| $LE_i$ | Engine length-gimbal point to exit |
| $DEC_i$ | Engine cluster diameter |
| $C3_i$ | Cluster coefficient |
| W | Weight |
| CG | Distances reference point to center of gravity |
| L | Total vehicle length |
| a | Acceleration |
| $\alpha$ | Angle of attack |
| K2 | Drag coefficient |
| $WFB_i$ | Forward bulkhead weight |
| $\rho$ | Material density |
| $P_i$ | Design pressure |
| $C10_i$ | Weight coefficient |
| $R_i$ | Stage radius |
| $C8_i$ | Bulkhead correction coefficients |
| $F_{tu_i}$ | Tensile ultimate stress |
| $h_i$ | Bulkhead height |
| $C11_i$ | Bulkhead area coefficient |
| $K4_i$ | Engine propellant coefficient |
| $K5_i$ | Engine weight coefficient |
| $C12_i$ | Engine correction coefficient |

# APPENDIX C. STRESS ANALYSIS

The structural components generated in the design synthesis subroutine are based on a range of vehicle diameters, loading intensities, and thermal environments representative of the medium, Saturn, and post-Saturn range payload class vehicles. The procedures used to define the principal structural parameters and to evaluate the structural integrity of the resulting components are presented in this appendix.

## OPTIMIZATION PROCEDURE

Optimum design problems are integrally related to stress analysis problems. However, the objective of optimum design is to determine the final form of the structure, while that of stress analysis is to determine stresses and strains associated with a given structural form. The final form of the structure may be determined by one or more criteria. For instance, the merit function used to evaluate the candidate design may be based on minimum weight, uniform strength, or minimum strain energy. Regardless of the criteria selected to evaluate the designs, the results obtained are integrally related with the stress analysis procedure. For this section of the study, the merit function selected is based on the minimum weight concept.

The selection of the minimum weight criteria does not eliminate the problems of defining procedures to determine the final form of the optimum configuration. One method of definition generally used is to differentiate the merit function with respect to the significant parameters (References C-1 and C-2). However, the differentiation is generally tedious for complicated merit functions. In addition, the optimum structural parameter obtained in this manner may not be feasible because of manufacturing or other constraints. Hence, the optimized structural form obtained in this manner may vary significantly from the optimized form based on a procedure that correctly incorporates the influences of external constraints such as fabrication problems.

The optimization procedure used in this study considers the combination of structural parameters that results in a configuration, satisfying the given design conditions, to be a point in an n-dimensional configuration space. Each of the coordinates of this space represents one of the structural parameters in the final configuration. For example, the coordinates of configuration space associated with a skin-stringer cylinder may consist of the skin gauge, the area of the stringers, the stringer pitch,

or the frame spacing. With this nomenclature, the objective of the optimum design is to locate the point or points in configuration space that result in the minimum numerical value of the merit function that satisfies the design loading conditions, without violating the external constraints (manufacturing limitations, etc.).

The first task performed in the optimization procedure is the selection of a configuration which satisfies the specified design conditions and criteria. Having established an initial form for the structure, the optimization procedure varies one of the structural parameters associated with this design to access its influence on the merit function. The selected parameter is continuously varied until the numerical value of the merit function finally increases or until a design constraint is reached. Then, the process is repeated for the remaining parameters until the minimum value of the merit function is obtained.

The objective of this procedure is to replace the intuitive formulation of the principal structural dimensions and subsequent verification of the assumed dimensions by direct calculations with analytical methods consistent with the external constraints placed on the final design.

Having established the merit function that will be used to evaluate the alternate designs and the procedure for determining the minimum value of the merit function, the next step is to select the analytical methods that will be used to verify the structural integrity. If the analytical methods used in the stress analysis are complex, the number of structural parameters is generally increased, and the results obtained are generally more complicated. If the analytical methods are simple, then the number of structural parameters is generally reduced, and the corresponding difficulties associated with defining an optimum design are reduced (References C-3, C-4, and C-5).

For this reason, many investigations of minimum weight designs have been based on limit analysis (References C-6, C-7, and C-8). These investigators assume that the materials used in the structure are ductile. Therefore, they assert that a more realistic estimate of the strength of the structure can be obtained by using the plastic hinge concept than by using the general theory of elasticity. In addition, the form of the governing equations is considerably simpler for limit analysis than for elastic analysis. However, in spite of the simplicity afforded by limit analysis, the structural integrity of missile and space components is usually verified by conventional elastic analysis. In addition, the materials used in many applications have limited ductility; therefore, the results obtained by limit analysis are not necessarily valid. Consequently, for this study, the structural integrity is based on conventional elastic analysis with suitable plasticity factors to account for the ductility of the materials.

The following sections presents a concise review of the methods used to define the optimum configuration for each construction and loading condition. Each construction is analyzed in sufficient detail to permit assessment of the influences of the following:

Manufacturing constraints, such as minimum skin gauge or minimum core density for a honeycomb sandwich cylinder

Changes in base materials and/or the improvement of base material properties, such as 10-percent increase in the compressive yield stress

The analytical methods used to verify the structural integrity of the designs

Plasticity effects

## STRUCTURAL ANALYSIS CRITERIA

The primary failure modes considered in the stress analysis of the shell structures are material failure, general instability, and local instability.

### Material Failure

The classes of loads used for design are defined as follows:

AL, BM, P--limit inertia loads, limit pressures

FSYAL, FSYBM, FSYP--yield inertial loads, yield pressures

FSUAL, FSUBM, FSUP--ultimate inertia loads, ultimate pressures

FSY = yield factor of safety

FSU = ultimate factor of safety

The following criteria were used to analyze the shell structures for material failure:

1. A tensile stress resulting from ultimate pressure loads and/or inertia loads will not exceed the tensile ultimate stress of the material. If the inertia loads are added to the tensile stresses, ultimate inertia loads are used. Limit inertia loads are used if the inertia loads are subtracted from the tensile stresses.

2. A tensile stress caused by yield pressure and/or limit inertia loads will not exceed the tensile yield stress of the material. If the inertia loads are added to the tensile stresses, yield inertia loads are used. Limit inertia loads are used when the inertia loads are subtracted from the tensile stress.

3. A compressive stress resulting from ultimate inertia loads and pressure will not exceed the allowable compressive strength of the material. If the pressure is added to the compressive stresses, ultimate pressure is used. Minimum pressure is used when the pressure is subtracted from the compressive stresses.

4. A compressive stress resulting from yield inertia loads and pressure will not exceed the yield compressive strength of the material. If the pressure is added to the compressive stresses, yield pressure is used. Minimum pressure is used when the pressure is subtracted from the compressive stresses.

General Instability

The second primary mode of structural failure considered in this program is general instability. A compressive stress resulting from ultimate inertia loads and/or pressure will not exceed the critical general instability stress of the structure. If the pressure is added to the compressive stresses, ultimate pressure is used. Minimum pressure is used when the pressure subtracts from the compressive stress. If the shell structure is stabilized by internal pressure, the minimum internal pressure is used in the analysis.

Local Instability

The third primary mode of structural failure considered in this program is local instability. A compressive stress resulting from ultimate inertia loads and/or pressure will not exceed the critical local stability stress of the structural component. If the pressure is added to the compressive stresses, ultimate pressure is used. If the pressure is subtracted from the compressive stresses, minimum pressure is used.

MONOCOQUE

The monocoque cylindrical shell (Figure C-1) is a homogeneous isotropic cylinder without ring frames. The procedure used to analyze this structure is presented in this section. The failure modes considered for this construction are material failure and general instability.

Material Failure

The minimum material gauges and the material failure criteria presented in Section are used to determine the minimum skin thickness. The general form of the governing equations are

$$t_1 = \frac{1}{F_{cy}}\left[\left(\frac{AL}{2\pi R} + \frac{BM}{\pi R^2}\right) FSY - \frac{P_{min} R}{2}\right]$$

$$t_2 = \frac{1}{F_{tu}}\left[\left(\frac{BM}{\pi R^2} + \frac{Pull\ R}{2}\right) FSU - \frac{AL}{2\pi R}\right]$$

$$t = \text{maximum}\left[t_1, t_2, t_3, t_4, t_5, t_{min}\right]$$

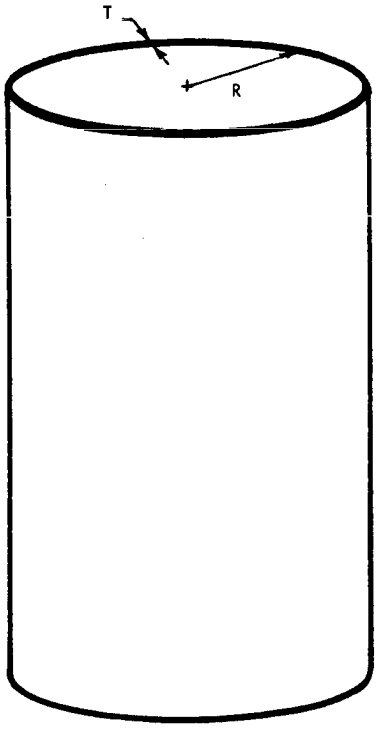



Figure C-1. Monocoque Cylinder

where

AL = the applied axial load

BM = the bending moment,

Pull = the ullage pressure,

R = the radius,

$F_{cy}$ = the compressive yield stress,

$F_{tu}$ = the ultimate tensile stress,

FSY = the yield factor, and

FSU = the ultimate safety factors.

General Instability

The critical general instability stress for an homogeneous isotropic cylindrical shell is given by

$$F = C_c E \frac{t}{R}$$

The increase in the critical buckling stress due to the stabilizing influence of internal pressure is

$$\Delta F = \Delta C_c E \frac{t}{R}$$

The recommended design values for these coefficients are given in Figures C-2 and C-3 (Reference C-9).

Mathematical approximation of these curves is given by

$$C_c = 0.07 + 0.178 \exp\left(-7.24 \times 10^{-4} (R/t)^{1.06}\right)$$

and

$$\Delta C_c = 0.24\left(1 - \exp\left(-2.135\left[\frac{P}{E}\left(\frac{R}{t}\right)^2\right]^{0.685}\right)\right)$$

Therefore, in combining these equations with the combined longitudinal applied stress expression, the solution for the monocoque construction is given by

$$\frac{\left(AL + \frac{2BM}{KR}\right)\frac{1}{2\pi Rt} - \frac{PR}{2t}}{E\,(C_c + \Delta C_c)\frac{t}{R}} = 1$$

where

p = the internal pressure,

E = the modulus of elasticity, and

K = the bending moment correction factor $\approx$ 1.3.

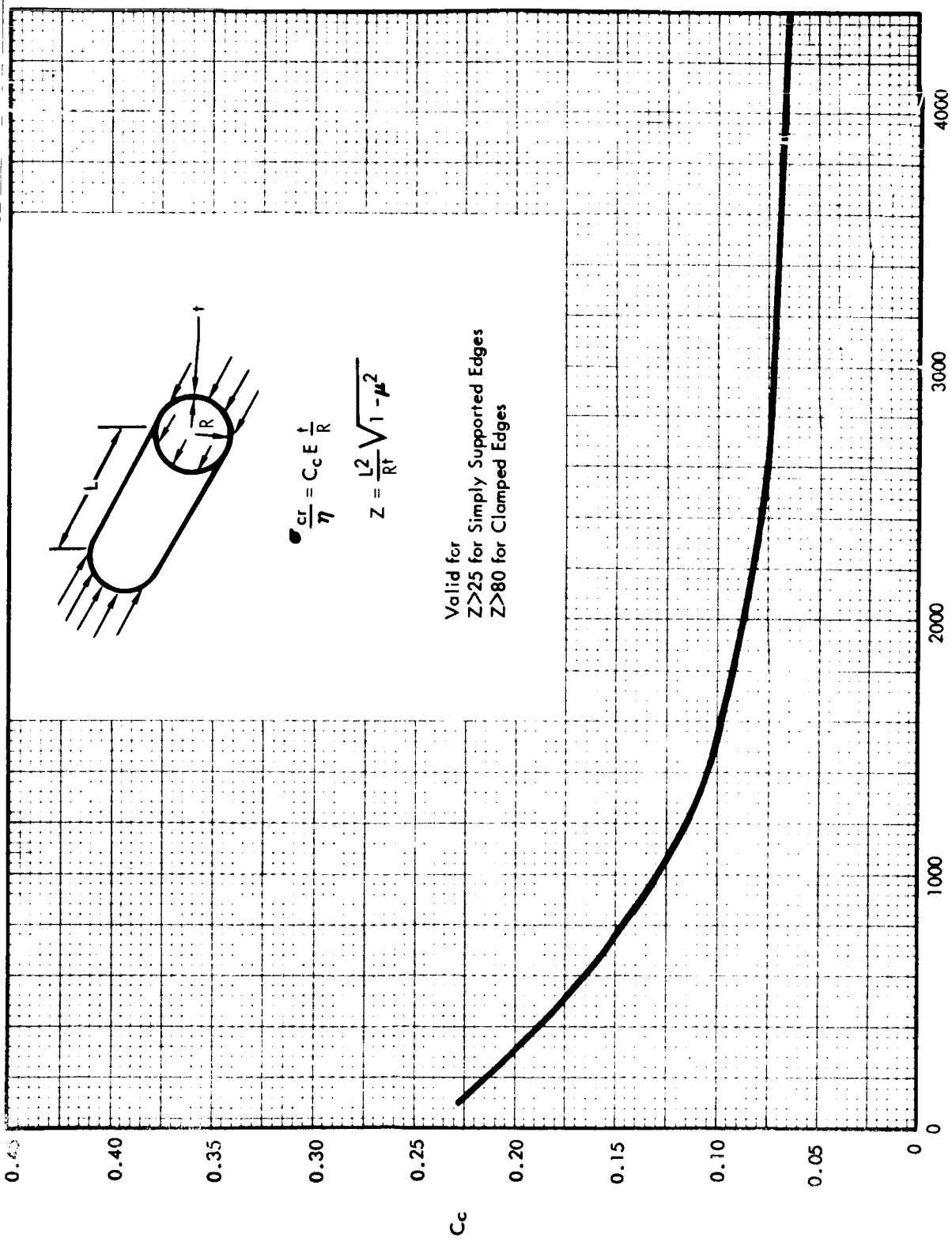



Figure C-2. Buckling-Stress Coefficient, $C_c$, For Unstiffened Unpressurized Circular Cylinders in Axial Compression

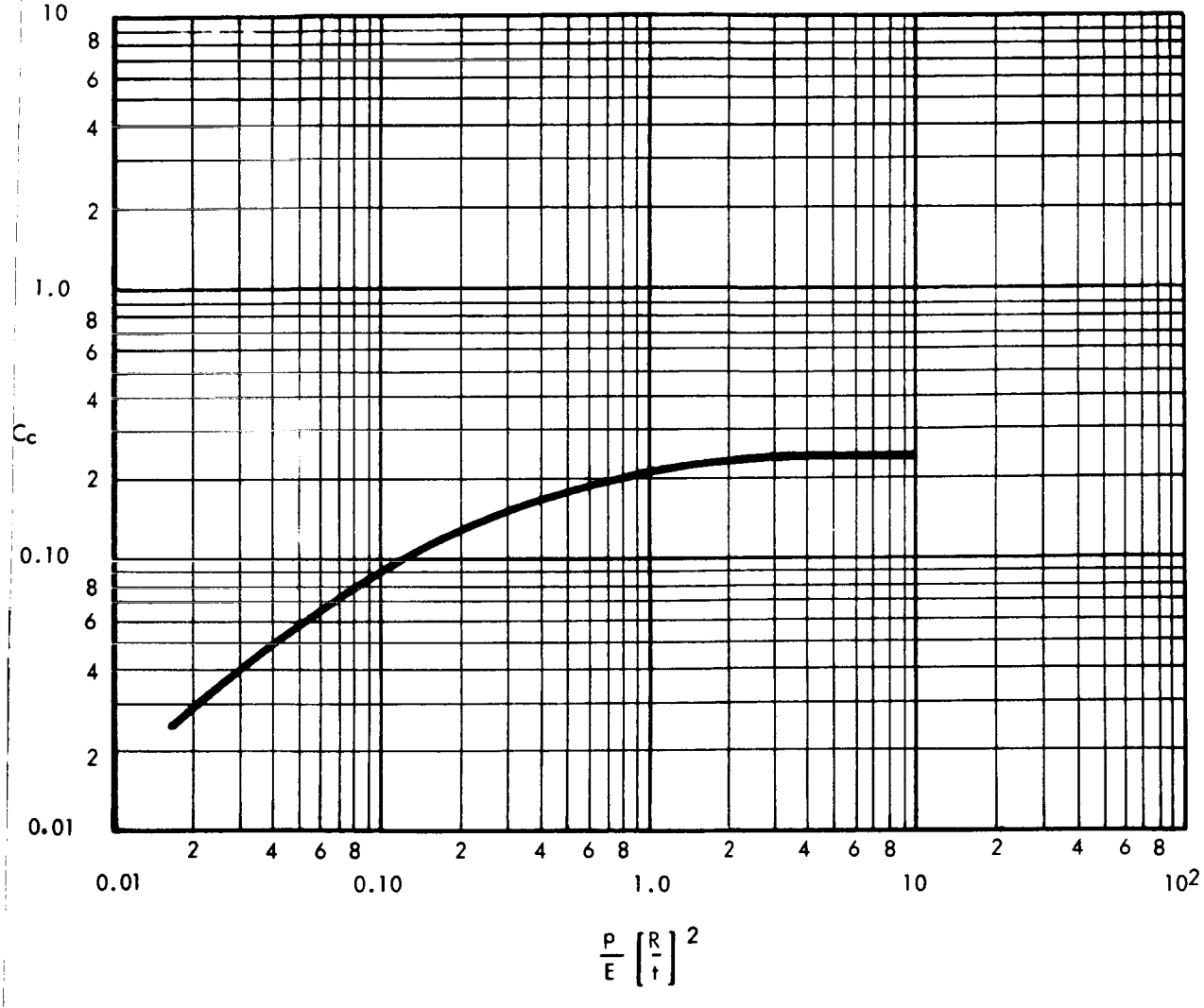



Figure C-3. Increase in Axial-Compressive Buckling-Stress Coefficient of Cylinders Due to Internal Pressure

## SKIN-STRINGER

The skin-stringer cylinder (Figure C-4) is a composite structure consisting of a thin face sheet stiffened by longitudinal stringers and transverse ring frames. The stringer configurations analyzed are integral, "z," and hat section. The primary failure modes considered are material failure of the face skins and/or stringer, general instability of the composite structure, and local instability of the face skins and stringer elements.

### Material Failure

The failure criteria presented in Section is used to determine the minimum equivalent thickness required to prevent material failure. The general form of the equations is

$$\bar{t} = t_{skin} + \frac{Astr}{b} = \max \left| \frac{f\ (loads)}{f_1\ (matl\ allowables)},\ \text{min gauges} \right|$$

$$t_{skin} = \max \left| \frac{f\ (pressure)}{f_1\ (matl\ allowables)},\ \text{min gauges} \right|$$

where

f and $f_1$ are loads and material allowable functions

$\bar{t}$ = the equivalent skin thickness,

t = the skin thickness,

Astr = the area of the stringer, and

b = the stringer spacing.

### Local Instability

The local instability modes considered in this study are panel instability of the face sheets and crippling of the stringer.

#### Panel Instability

If the stiffened-skin structure has sufficiently stiff ring frames, the first failure mode generally encountered is panel instability. In this failure mode, the ring frames and stringers effectively divide the shell into small panels, whose principal dimensions are the spacings of the rings frame and stringers.

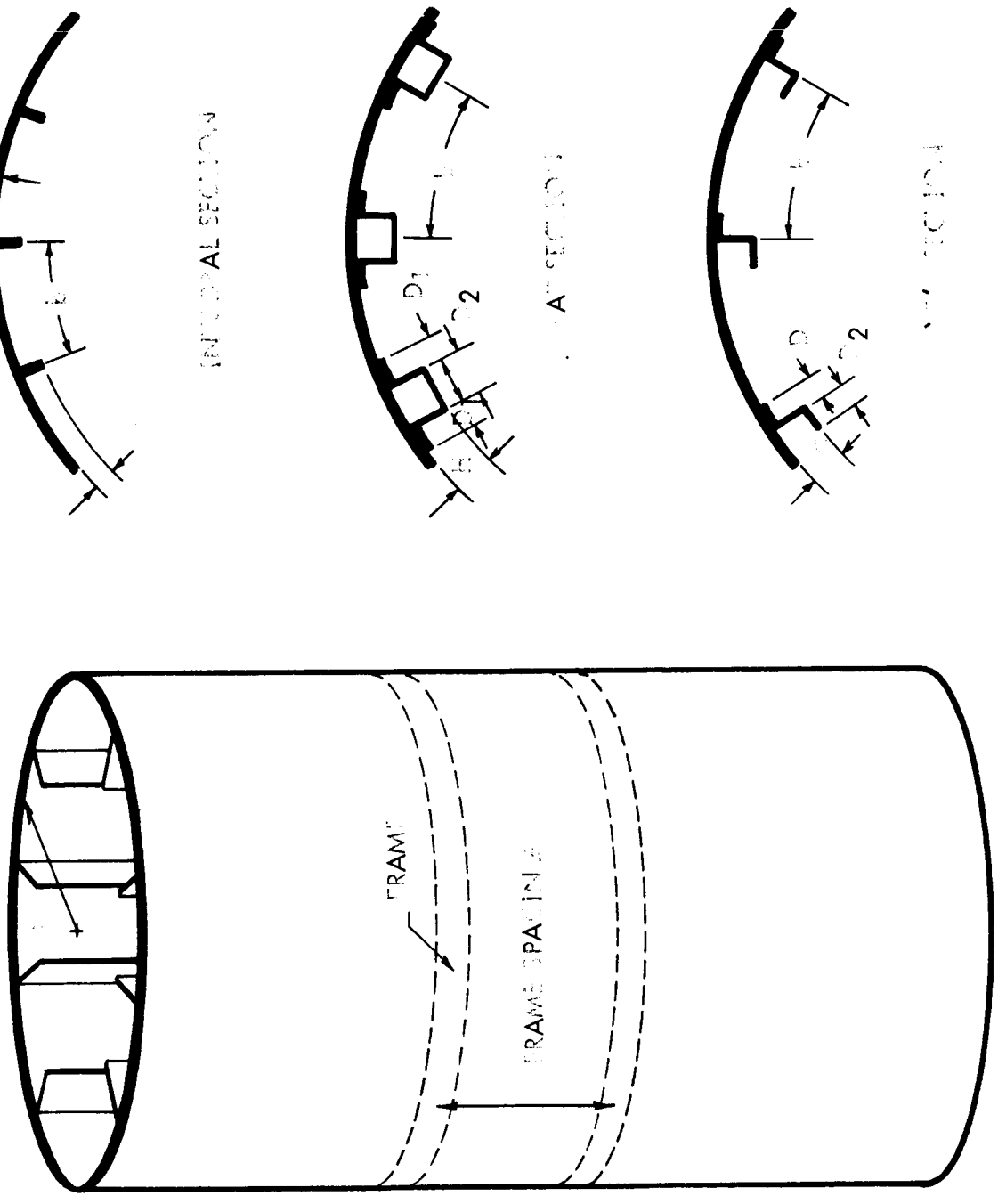


Figure C-4. Skin-Stringer Cylinder

In general, the structure does not fail because of panel instability. Instead, the load is redistributed, and the composite structure is able to carry additional loads before failure. However, if the design criteria specify that the skin panels shall not buckle, panel instability is a primary failure mode.

The critical buckling stress for the plate element (Reference C-10) is

$$\frac{F_{CR}}{\eta} = KE \left(\frac{t}{b}\right)^2$$

where

K = a coefficient which includes the effects of end fixity,

b = the stringer spacing,

$\eta$ = a plasticity correction factor

Stringer Instability

The crippling stress for the stringer is determined by

$$Fcc = \sum_{i=1}^{N} \frac{Ai\ Cei\ \sqrt{Fcyi\ Ei}\ \left(\frac{t}{b}\right)_i^{3/4}}{\Sigma Ai} \qquad \text{(Reference C-9)}$$

where

Ai = the area of the ith element,

Cei = the material and shape constant for the ith element,

Fcyi = the compressive yield stress of the ith element,

Ei = the compressive modulus of elasticity of the ith element,

t = the material gauge, and

b = the length of the element.

The critical buckling stress for stringer column instability is given by the Euler equation (Reference C-9).

$$Fc = \frac{\pi^2 E}{\left(L'/\rho\right)^2}$$

where $L'$ is the effective length of the stringer and $\rho$ is the radius of gyration of the section. When the critical stress obtained from the Euler equation is greater than approximately 50 percent of the crippling stress, the stringer column instability stress is determined by the Johnson - Euler equation (Reference C-9).

$$Fc = Fcrip - \frac{Fcrip^2}{4\pi^2 E}\left(L'/\rho\right)^2$$

where Fcrip is the crippling stress.

General Instability

General instability occurs when the ring frames are not stiff enough to force buckling modes to occur at the ring frame. Therefore, the deflected shape for this failure mode extends over several panels and ring frames. The general procedure for preventing this failure mode is by designing ring frames of sufficient stiffness. Shanley (Reference C-11) determines the required ring frame stiffness as

$$(EI)_f = \frac{MD^2}{16000L}$$

where

E = the elastic modulus of the frame material,

I = the moment of inertia of the ring frame,

D = the diameter of the cylinder,

L = the frame spacing, and

M = the bending moment on the shell.

The critical general instability stress for the stiffened cylinder is given by (Reference C-12).

$$F_{CR} = KE\sqrt{\frac{\rho_s^3 \rho_f^3}{bL}}$$

This equation is modified in Reference C-12 to include the effects of internal pressure. The resulting equation is

$$F_{CR} = EK_1\left[\frac{t}{b}\frac{t}{L}\frac{t}{R}\right]^{1/4} + \gamma K_2 E\left(\frac{p}{E}\right)^{\alpha}\left[\frac{t}{b}\frac{t}{L}\frac{t}{R}\right]^{\frac{1-2\alpha}{m}}$$

where

$$K_1 = C\left[\frac{\rho_f}{R}\frac{\rho_s}{t}\right]^{3/4}$$

$$K_2 = \left\{C/0.728\left[\frac{\rho_f}{R}\frac{\rho_s}{t}\right]^{3/4}\right\}^{\frac{1-2\alpha}{m}}$$

and

c, $\alpha$, m are coefficients determined from experimental data

$\rho_s$ = the radius of gyration of the stringer with effective skin, and

$\rho_f$ = the radius of gyration of the frame with all skin effective.

The optimum frame spacing is given by (Reference C-13).

$$L = \left[16\pi\,(6.84 \times 10^{-5})\right]^{2/5} \left(\frac{R}{\rho_{f_o}}\right) \left(M + \frac{K_3 F}{2\pi E R^2}\right)^{1/5} R$$

where $\rho_{f_o}$ is the radius of gyration of the frame.

WAFFLE

The waffle cylinder (Figure C-5) is a composite structure consisting of a face sheet stiffened by internal ribs. The ribs are oriented at angles of $\pm\theta$ degrees with respect to the axis of the cylinder.

In reference C-14, the influence of rib orientation on the strength of unpressurized, axially compressed cylinders is evaluated. For this loading condition, the optimum rib orientation is approximately ±15 degrees. However, the weight penalty associated with a ±45-degree orientation is small for the range of parameters considered. In this study, the influence of rib orientation on the weight of cylindrical shell subjected to combined loading conditions is assumed to be negligible. The 45-degree orientation is selected for all computations. Synthesis of symmetrical section waffle concepts is illustrated in Reference C-15.

The primary failure modes considered for the waffle cylinder are material failure, local instability of the face sheet and ribs, and general instability of the composite structure.

Material Failure

The failure criteria presented in this section is used to prevent material failure. The effective skin thickness is determined by equations of the general form

$$t = \max \left\{ \frac{f\,(\text{applied loads})}{f_1\,(\text{matl allowables})},\ \text{minimum gauge} \right\}$$

$$t_{skin} = \max \left\{ \frac{f\,(\text{pressure})}{f_1\,(\text{matl allowables})},\ \text{minimum gauge} \right\}$$

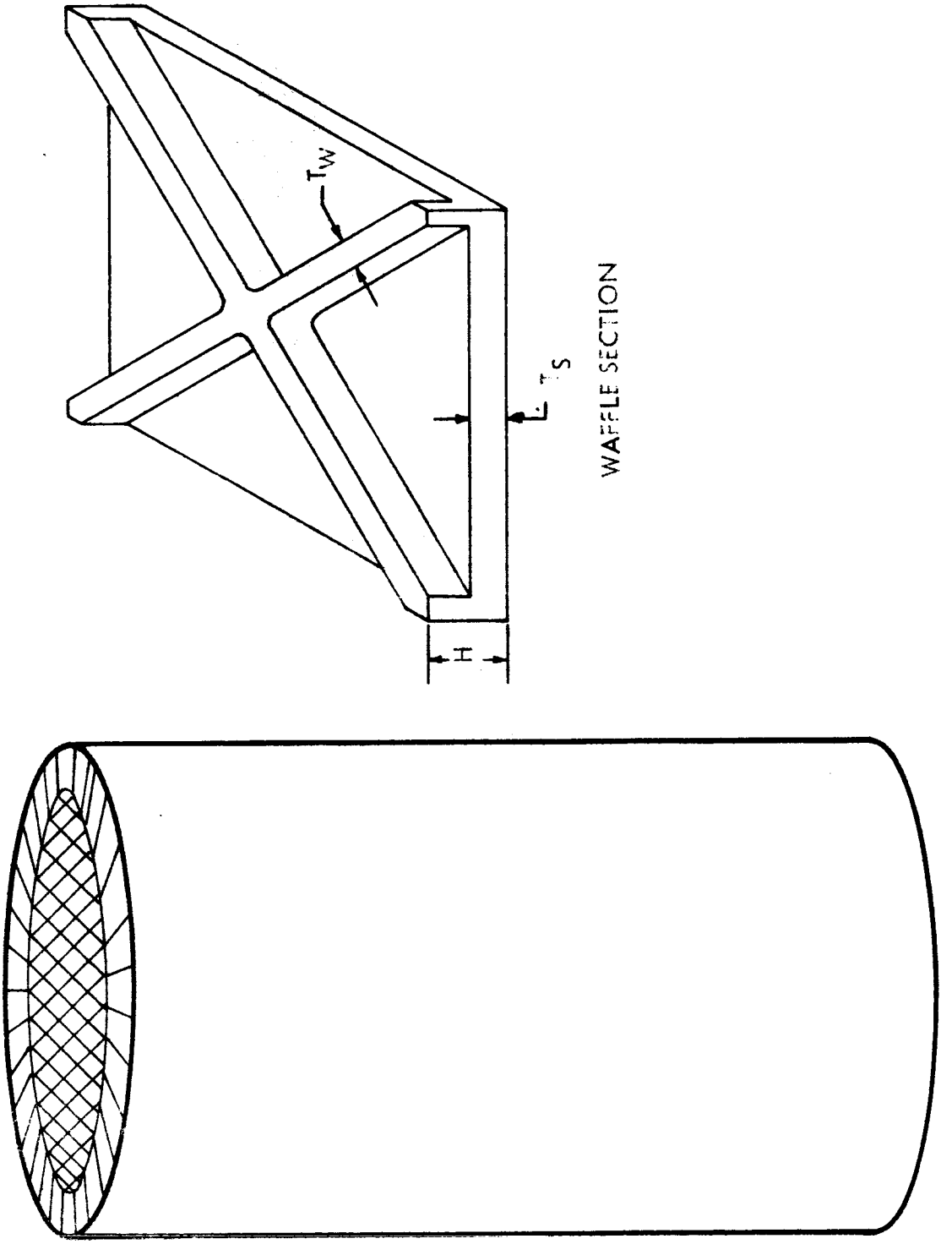



Figure C-5. Waffle Cylinder

Local Instability

When the ribs are sufficiently stiff to force buckling nodes to occur at the ribs, the critical buckling stress for the plate element is given by

$$F_{CR} = KE \left(\frac{t}{b}\right)^2$$

where

K = a plate shape factor, and

b = the rib spacing.

For ribs oriented at ±45 degrees, the plate element is subjected to uniform compression and shear stress equal to one-half the applied stress on the composite structure. For this loading condition and plate shape, the value of K is 3.87 (Reference C-9).

The crippling stress for the rib is given by

$$F_{CRIP} = Kr\,E \left(\frac{t_r}{L_r}\right)^2$$

where

$K_r$ = a shape factor

E = the modulus of elasticity

$t_r$ = the rib thickness

$L_r$ = the rib width.

The numerical value of the coefficient Kr is a function of the rotational constraint provided by the face sheets. For plates with one edge fixed, the approximate value of Kr is 0.43.

General Instability

The waffle cylinder, with sufficiently small rib spacing will respond similar to an orthotropic shell. However, a generally accepted procedure does not exist for determining the design buckling load for orthotropic shells. The theoretical buckling load predicted by classical small deflection theory is unconservative and the minimum postbuckling load predicated on large deflection theory is usually very conservative. Consequently, neither of the loads is generally acceptable for design analysis. The situation is further complicated by the absence of sufficient test data for waffle constructions.

For this study, the critical buckling load for the waffle cylinder is determined by a joint consideration of large and small deflection theory for an orthotropic shell.

The buckling load of an axially compressed orthotropic shell can be characterized by three primary parameters (Reference C-16). These parameters are:

1. H, the extensional stiffness parameter of the orthotropic shell

$$H = \frac{H_{12} + \frac{1}{2} H_{33}}{\sqrt{H_{11} H_{22}}}$$

2. D, the bending stiffness parameter

$$D = \frac{D_{12} + 2 D_{33}}{\sqrt{D_{11} D_{22}}}$$

3. $\gamma$, the principal stiffness parameter

$$\gamma = \frac{D_{11} H_{11}}{D_{22} H_{22}}$$

for the orthotropic shell. These three parameters provide an efficient method for evaluating the buckling and postbuckling behavior of orthotropic shells. The most important parameter for studying the buckling behavior is $\gamma$. For small $\gamma$ ($\gamma$ less than 1) the cylinder is assumed to be circumferentially stiffened. For $\gamma$ greater than unity, the cylinder is longitudinally stiffened. The ratio of the minimum postbuckling load to the classical buckling load is inversely proportional to $\gamma$ (i.e., when $\gamma$ is very small ($\gamma \ll 1$) the minimum theoretical postbuckling load is approximated equal to the classical buckling load. When $\gamma$ is large (i.e., $\gamma \geq 1$), the postbuckling load is approximately ten percent of the classical buckling load.

For waffle cylinders with ribs oriented at ±45 degrees, the value of $\gamma$ is unity. $\gamma$ is also equal to 1 for monocoque shells; therefore, it appears that a reasonable estimate, for the correction factor to be used with the classical buckling load, can be obtained by using test data for isotropic monocoque shells (Reference C-14).

When extrapolating the test data for isotropic cylinders to 45-degree waffle cylinders, it is necessary to remember that all of the orthotropic shell parameters are equal to unity for the isotropic shell, while two may not be equal to unity for the waffle. This is significant because the classical buckling loads are identical for axisymmetric and asymmetric buckling of isotropic shells, but may be different for orthotropic shells.

The unpressurized isotropic cylindrical shells generally buckle asymmetrically. Since the theoretical axisymmetric and asymmetric buckling loads for isotropic shells are identical, it is not important which theoretical buckling load is corrected to obtain a design load. However, for orthotropic shells, the correction factor should not be identical for both buckling modes. The observed postbuckling deformation patterns for longitudinal stiffened shells is generally asymmetric, and the corresponding buckling load is a small percentage of the theoretical load. The postbuckling deformation pattern changes as the cylinder is stiffened circumferentially and the ratio of the postbuckling load to the classical load increases. With sufficient circumferential stiffening, and/or with sufficient internal pressure, the axisymmetric buckling pattern is observed, and the classical buckling load obtained.

For these reasons, the isotropic correction factor is only applied to the asymmetric buckling load. No correction factor is used for axisymmetric buckling. The design buckling load is based on the minimum buckling load obtained by this procedure. For most cases, the design load for the 45-degree waffle cylinder will be based on asymmetric buckling.

The critical buckling stress for asymmetric buckling of a 45-degree waffle cylinder is given by (References C-14, C-17, and C-18).

$$\frac{N_c R}{E H^2} = 2\gamma \sqrt{\overline{D}_2 \overline{E}_1 \frac{1 + \mu_x + \dfrac{2\overline{D}_K}{\overline{D}_2}}{1 - \mu_1 + \dfrac{\overline{E}_1}{2\overline{G}_K}}}$$

/here the elastic constants (Reference C-19) are defined in the following omenclature list For symmetric buckling, the critical buckling load is Reference C-18)

$$\frac{N_c R}{E H^2} = 2.0\sqrt{\overline{D}_2 \overline{E}_1}$$

)efinition of Waffle Elastic Constants

$A_{W_S}$ Twice the cross-sectional area of the ribs

$b_s$ Spacing or ribs

$\overline{D}_k$ Twisting stiffness

$\overline{D}_2$ Bending stiffness

$\overline{E}_1$ Extensional stiffness

$\overline{G}_k$ Shear stiffness

H Total height of waffle

$Iw_s$ Twice the moment of inertia of the ribs

$Kw_s$ Dimensionless distance from middle surface of sheet to centroid of ribs

$N_c$ Critical axial stress per unit width

$t_s$ Skin thickness

$\mu_1$ Poisson's ratio associated with stretching

$\mu_x$ Poisson's ratio associated with bending

$$\overline{D}_2 = Iy - \frac{\overline{A}s^2 \, Ay}{\overline{A}s^2}\left(\overline{K}y - \overline{K}s\right)^2$$

$$\overline{E}_1 = \frac{\overline{A}s^2}{Ay}$$

$$\overline{D}_k = \frac{Ixy}{4}$$

$$\overline{G}_k = Axy$$

$$\mu_x = \frac{\overline{I}s^2}{\overline{A}s^2 \overline{D}_2}$$

$$K_1 = \frac{As}{Ay}$$

$$Ay = \frac{1}{1-\mu^2}\frac{t_s}{H} + \frac{A_{W_s}}{b_s H}\cos^4\theta$$

$$As = \frac{\mu}{1-\mu^2}\frac{t_s}{H} + \frac{A_{W_s}}{b_s H}\sin^2\theta\cos^2\theta$$

$$Axy = \frac{1}{2(1+\mu)}\frac{t_s}{H} + \frac{A_{W_s}}{b_s H}\sin^2\theta\cos^2\theta$$

$$\overline{As}^2 = Ay^2 - As^2$$

$$\overline{Ky} = \frac{A_{W_s}}{b_s H}\frac{Kw_s}{Ay}\cos^4\theta$$

$$\overline{Ks} = \frac{A_{W_s}}{b_s H}\frac{Kw_s}{As}\cos^2\theta\sin^2\theta$$

$$\overline{Kxy} = \frac{A_{W_s}}{b_s H}\frac{Kw_s}{Axy}\sin^2\theta\cos^2\theta$$

$$Iy = \frac{1}{12(1-\nu)^2}\left(\frac{t_s}{H}\right)^3 + \frac{Iw_s}{b_s H^3}\sin^4\theta + \frac{A_{W_s}}{b_s H}\left[(Kw_s - Rs)^2 \sin^4\theta\right]$$

$$+ \frac{1}{1-\nu^2}\left(\frac{t_s}{H}\right)\overline{K}y^2$$

$$Ixy = \frac{1}{6(1+\nu)}\left(\frac{t_s}{H}\right)^3 + \frac{2}{1+\nu}\left(\frac{t_s}{H}\right)\overline{K}xy^2 + 4\left[\frac{Iw_s}{b_s H^3} + \frac{A_{W_s}}{b_s H}(Kw_s - \overline{K}xy)^2\right]$$

$$\sin^2\theta \cos^2\theta$$

$$\overline{I}s^2 = Is\,\overline{A}s^2 + As\,Ay^2\,(\overline{K}y - \overline{K}s)^2$$

## SANDWICH CYLINDERS

The honeycomb sandwich cylinder (Figure C-20) is a composite construction consisting of relatively thin face sheets, a honeycomb core, and two layers of adhesive material. The face sheets are assumed to carry all of the applied pressures, axial loads, and bending moments. The core provides the required spacing of the face sheets for bending rigidity. The bonding material is assumed to have sufficient strength to allow the composite to operate as an efficient structural unit.

The failure modes considered for the sandwich cylinder are material failure of the face sheets, local instability of the face sheets, and general instability of the composite structure.

### Material Failure

The minimum face sheet thickness is determined by examining the manufacturing limitations for the candidate materials, the limit load design condition, and the ultimate load design condition. The maximum face sheet thickness obtained from these conditions is used as the minimum allowable face sheet thickness for all subsequent calculations.

### Local Instability

The local instability failure modes considered are wrinkling and dimpling of the face sheets. When wrinkling occurs, the face sheets buckle

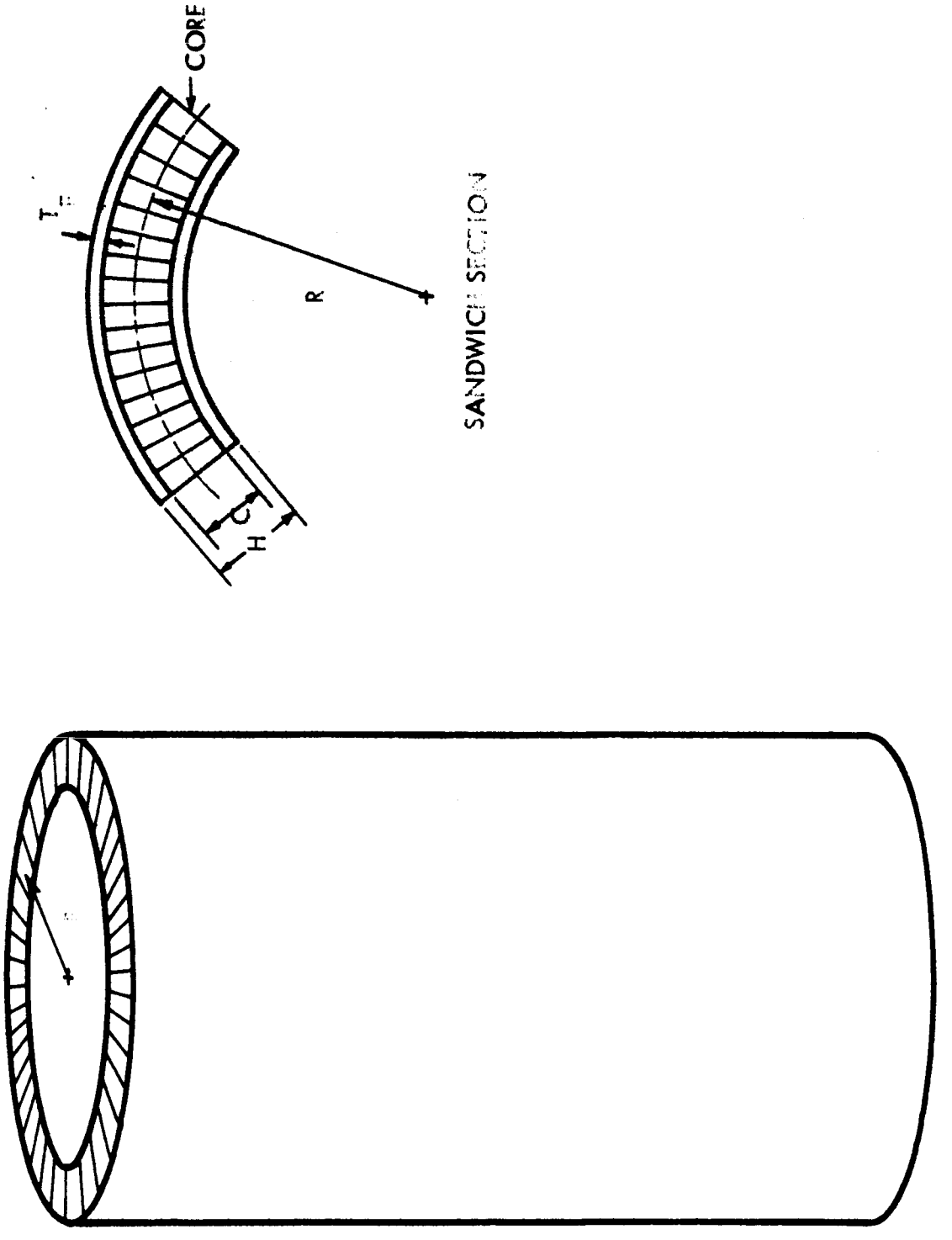



Figure C-6. Sandwich Cylinder

similar to a plate on an elastic foundation. If the core face sheet bond is strong, the wrinkling of the face sheets may cause tensile failure of the core. The critical wrinkling stress is given by (Reference C-9)

$$Fc = 0.5 (E_F' E_C' G_c')^{1/3}$$

where

$E_F'$ = the effective modulus of elasticity of the face sheet,

$E_C'$ = the effective elastic moduli of the core,

$G_c'$ = the shear moduli of the core.

The effective modulus of the face sheet is

$$E_F' = E_F \eta_2^3$$

where $\eta_2$ is the plasticity factor. The effective elastic moduli of the core for densities less than 16.7 pounds per cubic foot are (Reference C-9)

$$E_C' = 2.13 \left(\frac{\rho_c}{\rho}\right)^{1.415} E_C$$

and

$$G_c' = 2.43 \left(\frac{\rho_c}{\rho}\right)^{1.54} G_c$$

When intracell buckling occurs, the face sheets dimple into the cells of the honeycomb core. If the dimples encompass several cells, failure of the structure due to wrinkling may occur. The critical intracell buckling stress is given by (Reference C-9)

$$Fc = 2.28 \left(\frac{\eta E_F}{1 - \nu^2}\right) \left(\frac{t}{s}\right)^2$$

where

$E_F$ = the compressive elastic modulus of the face sheets,

t = the face sheet thickness,

s = the core cell size, and

$\eta$ = the plasticity factor.

General Instability

In the general instability analysis, the honeycomb sandwich cylinder is assumed to consist of equal face sheets and an orthotropic core. The critical buckling load is given by the large deflection equation of March and Kuenze (References C-21, C-22, and C-23)

$$\sigma = \frac{4}{5} \frac{N}{Q} \frac{EH}{R}$$

where

$$Q = \frac{3.3}{\sqrt{\left(\frac{c}{H}\right)^2 + \frac{c}{H} + 1}}$$

$$N = f(Sx)$$

$$Sx = \frac{16}{45} \frac{E t c}{R G_c H}$$

R = the radius of the cylinder,

E = the elastic modulus of the face sheets,

H = the total height of the sandwich,

c = the core depth, and

N = a sandwich shear rigidity factor.

The critical load obtained with this formula is the postbuckling load that the cylinder will carry. This load will be referred to as the base point load.

The critical buckling load for the sandwich cylinder is greater than the postbuckling load. However, a generally accepted criteria for determining this load is not available. Almroth (Reference C-1) suggests that the critical buckling load for orthotropic cylinders be taken as the minimum postbuckling load plus a percentage of the difference between the classical buckling load and the postbuckling load. The percentage to be taken is a function of an empirical factor based on the cylinder's geometry.

In the first alternate analysis, a more conservative approach is used to indicate the influence of analytical methods of the results obtained. If the core thickness in March and Kuenze's analysis is allowed to go to zero, the critical stress is given by 0.24 Et/R. A correction factor that is a function of the R/t of the shell is used to make the monocoque result agree with the recommended design curve for monocoque cylinders in Reference C-9. The correction factor obtained in this manner is applied to all sandwich cylinders in the alternate analysis method.

The anticipated optimum sandwich cylinder design will consist of deep honeycomb core between relatively thin face sheets. At present, there are not enough data to effectively evaluate the influence of sandwich depth on the elastic properties of the core and the subsequent performance of the composite structure. However, a reduction in core properties is known to occur with increasing depth. The reduction curve used in this analysis is obtained from limited test data available at S&ID. The analysis provides for inserting different correction factors as available. An upper limit is set on the total allowable depth of sandwich. If the structure is unable to carry the design loads with a core depth equal to or less than the maximum allowed, the face sheet gauges are increased until the sandwich depth is within the specified constraints.

Bending Moment

The influence of the applied bending moment on the stability of the composite structure is analyzed by converting the bending moment to an equivalent axial load. A linear distribution is assumed on the cross-section, and the maximum load is used as the predesign value. This value is reduced by the bending moment correction factor (BMC). The BMC factor is the ratio of the stability coefficients for isotropic cylindrical shell subjected to uniform axial loads and pure bending moments. The stability coefficients are obtained from Reference C-24. The approximate value of the equivalent axial load is $M/1.3\pi R^2$.

Internal Pressure

Internal pressure on the basepoint design is influenced by the reduction of the axial load. In the alternate analysis, the increase in the stability

coefficients for pressurized monocoque cylinder is used to evaluate the influence of internal pressure.

## COMPUTER PROGRAM

The procedures and equations presented in the preceding pages are used in the computer program to synthesize a minimum weight structural component. The synthesis process is generally facilitated by modifying the form of the equations, and employing various iteration and systematic search procedures.

The computer input data required to define the optimum structural component is presented in Table C-1. In general, this data consists of the radius, applied loads, material properties, and manufacturing constraints. A concise summary of the computer program is presented in the following paragraphs and in Figure 2.

### Monocoque

The computer input data required to define the minimum weight monocoque shell is presented in Table C-1. These data include axial load, bending moment, internal pressure, shell radius, material properties, safety factors, and minimum skin thickness.

The computer iterates with these data to obtain the skin thickness which results in the minimum weight structure consistent with the fabrication constraints. The flow diagram is presented in Figure C-7.

A representative computer printout is shown in Table C-2. The first portion of this printout consists of the invariant input data for this construction. The first column contains the minimum allowable skin thickness, the burst and relief pressures, and the material density. The second column consists of the yield and ultimate material stress, the elastic modulus, and the temperature corresponding to these properties. The third column consists of the limit and ultimate factors of safety.

The second part of the printout consists of the variable input data and the output results of the computer. The first three columns of the second segment consists of the components radius, axial load, and bending moment, respectively. The fourth column contains the resultant stress. The unit shell weight is presented in the fifth column. The last three columns consist of the resultant skin thickness, loading index, and the weight-to-radius ratio, respectively.

Table C-1. Input-Output Nomenclature

| Item | Monocoque | Stringer | Waffle | Sandwich |
|---|---|---|---|---|
| INPUT DATA | | | | |
| Applied Loads | | | | |
| Axial load | AL | AL | AL | AL |
| Bending moment | BM | BM | BM | BM |
| Maximum pressure | PMAX | PMAX | PMAX | PMAX |
| Minimum pressure | PMIN | PMIN | PMIN | PMIN |
| Ullage pressure | PULL | PULL | PULL | PULL |
| Safety Factors | | | | |
| Ultimate | FSU | FSU | FSU | FSU |
| Yield | FSY | FSY | FSY | FSY |
| Material Properties | | | | |
| Face sheet | | | | |
| Density | RHOF | RHOF | RHOF | RHOF |
| Elastic modulus | E | E | E | E |
| Poisson's ratio | NA* | EMU | EMU | EMU |
| Ultimate tensile stress | FTU | FTU | FTU | FTU |
| Yield tensile stress | FTY | FTY | FTY | FTY |
| Ultimate compressive stress | FCU | FCU | FCU | FCU |
| Yield compressive stress | FCY | FCY | FCY | FCY |
| Buckling stress | NA | BL | NA | NA |
| Minimum skin gauge | TMIN | TMINSK | TSMIN | TMIN |
| Support structure | | | | |
| Elastic modulus | NA | E | E | ECO |
| Elastic modulus (frame) | NA | EF | NA | NA |
| Poisson's ratio | NA | EMU | EMU | EMUC |
| Minimum skin gauge | NA | TMINST | TWMIN | NA |
| Minimum core density | NA | NA | NA | RHOMIN |
| Sandwich bond weight | NA | NA | NA | |
| Minimum frame stress | NA | STFRM | NA | NA |
| Core material density | NA | NA | NA | RHO |

*NA not applicable

Table C-1. Input-Output Nomenclature (Cont)

| Item | Monocoque | Stringer | Waffle | Sandwich |
|---|---|---|---|---|
| Geometry | | | | |
| Radius | R | R | R | R |
| Stringer height | NA* | HT | NA | NA |
| Total height | NA | NA | NA | H |
| Maximum height/skin thickness | NA | BO | HTS | NA |
| Stiffener spacing | NA | BO | NA | NA |
| Minimum stiffener spacing | NA | NA | BS | NA |
| Maximum frame spacing | NA | XLG | NA | NA |
| Minimum frame spacing | NA | XLM | NA | NA |
| Frame form factor | NA | FFORM | NA | NA |
| Stringer shape indicator | NA | XK | NA | NA |
| Stringer form indicator | NA | UNI | NA | NA |
| Stability factors | | | | |
| Stability indicator | NA | BUCK | IND | IND |
| Local stability coefficient crippling | NA | CE | NA | NA |
| Frame coefficient | NA | ALPHA | NA | NA |
| Frame coefficient | NA | EM | NA | NA |
| Frame coefficient | NA | CF | NA | NA |
| General stability coefficient | NA | SCF | STCOEF | CC |
| OUTPUT DATA | | | | |
| Unit Shell Weight | WT | WT | WT | WT |
| Unit Shell Weight/Radius | WTR | WTR | WTR | WTR |
| Total Shell Height | NA | NA | H | H |
| Skin Gauge | T | TSKIN | T | T |
| Support Structure | | | | |
| Skin gauge | NA | TD | TW | NA |
| Stringer height | NA | UP | NA | NA |
| Stringer leg length | NA | BL | NA | NA |
| Stringer outer element | NA | OE | NA | NA |

*NA not applicable

Table C-1. Input-Output Nomenclature (Cont)

| Item | Monocoque | Stringer | Waffle | Sandwich |
|---|---|---|---|---|
| Stringer area | NA | ASTR | NA | NA |
| Core density | NA | NA | NA | RHOP |
| Stiffener spacing | NA | BO | BS | NA |
| Frame spacing | NA | XL | NA | NA |
| Frame area | NA | AF | NA | NA |
| Frame form factor | NA | FFORM | NA | NA |
| Compressive Stress Resultant | ENXU | ENXU | ENXU | ENXU |
| Compressive Stress Resultant/Radius | ENXR | ENXR | ENXR | ENXR |
| Average Compressive Stress | NA | STSKIN | FC | FC |
| Average Stringer Stress | NA | ST | NA | NA |

Table C-2. Monocoque Printout

CONSTRUCTION - MONOCOQUE

MATERIAL - ALUMINUM A

MIN SKIN THICKNESS = 0.0100 INS  YIELD STRESS = 50000. PSI  LIMIT LOAD FACTOR = 1.1
BURST PRESSURE = 0.0000 PSI  ULTIMATE STRESS = 5500[illegible]. PSI  ULTIMATE LOAD FACTOR = 1.4
RELIEF PRESSURE = 0.0000 PSI  YOUNGS MODULUS = 10000000. PSI
MATERIAL DENSITY = 0.1000 PCI  TEMPERATURE = 300. DEGF

| COMPONENT RADIUS INS | AXIAL LOAD LBS | BENDING MOMENT IN-LBS | COMP. LOAD INTENSITY LB/IN | UNIT WEIGHT LB/FT2 | SKIN THICKNESS INS | NX/R PSI | WT/R PCI |
|---|---|---|---|---|---|---|---|
| 130. | 1164800. | 0. | 1994. | 5.27 | 0.3658 | 15.357 | 0.0002813 |
| 130. | 2329600. | 0. | 3993. | 7.21 | 0.5005 | 30.714 | 0.0003850 |
| 130. | 3494400. | 0. | 5986. | 8.69 | 0.6035 | 46.072 | 0.0004643 |
| 130. | 4659200. | 0. | 7984. | 9.94 | 0.6903 | 61.429 | 0.0005310 |
| 130. | 5824000. | 0. | 9983. | 11.04 | 0.7667 | 76.786 | 0.0005898 |
| 130. | 6988800. | 0. | 11976. | 12.04 | 0.8361 | 92.143 | 0.0006431 |
| 130. | 8153600. | 0. | 13976. | 12.95 | 0.8995 | 107.501 | 0.0006919 |
| 130. | 10483200. | 0. | 17969. | 14.60 | 1.0139 | 138.215 | 0.0007799 |
| 130. | 11648000. | 0. | 19964. | 15.36 | 1.0667 | 153.583 | 0.0008203 |
| 198. | 1774080. | 0. | 1994. | 6.64 | 0.4625 | 10.083 | 0.0002336 |
| 198. | 3548160. | 0. | 3987. | 9.39 | 0.6525 | 20.166 | 0.0003179 |
| 198. | 4515840. | 0. | 5982. | 11.11 | 0.7722 | 25.666 | 0.0003547 |
| 198. | 7096320. | 0. | 7984. | 12.44 | 0.8642 | 40.332 | 0.0004365 |
| 198. | 8872000. | 0. | 9982. | 13.40 | 0.9306 | 50.415 | 0.0004841 |
| 198. | 10644480. | 0. | 11976. | 14.23 | 1.0439 | 60.498 | 0.0005272 |
| 198. | 12416640. | 0. | 13975. | 16.16 | 1.1223 | 70.581 | 0.0005668 |
| 198. | 14192640. | 0. | 15972. | 17.22 | 1.1959 | 80.664 | 0.0006040 |
| 198. | 15966720. | 0. | 17969. | 18.21 | 1.2643 | 90.747 | 0.0006385 |
| 270. | 2419200. | 0. | 1994. | 7.95 | 0.5523 | 7.394 | 0.0002045 |
| 270. | 4838400. | 0. | 3993. | 10.76 | 0.7470 | 14.788 | 0.0002767 |
| 270. | 7257600. | 0. | 5986. | 12.91 | 0.8963 | 22.183 | 0.0003319 |
| 270. | 9676800. | 0. | 7984. | 14.71 | 1.0217 | 29.577 | 0.0003784 |
| 270. | 12096000. | 0. | 9982. | 16.30 | 1.1320 | 36.971 | 0.0004193 |
| 270. | 14515200. | 0. | 11976. | 17.74 | 1.2317 | 44.365 | 0.0004562 |
| 270. | 16934400. | 0. | 13975. | 19.06 | 1.3233 | 51.760 | 0.0004901 |
| 270. | 19353600. | 0. | 15972. | 20.28 | 1.4086 | 59.154 | 0.0005217 |
| 270. | 21772800. | 0. | 17969. | 22.53 | 1.5642 | 73.942 | 0.0005799 |

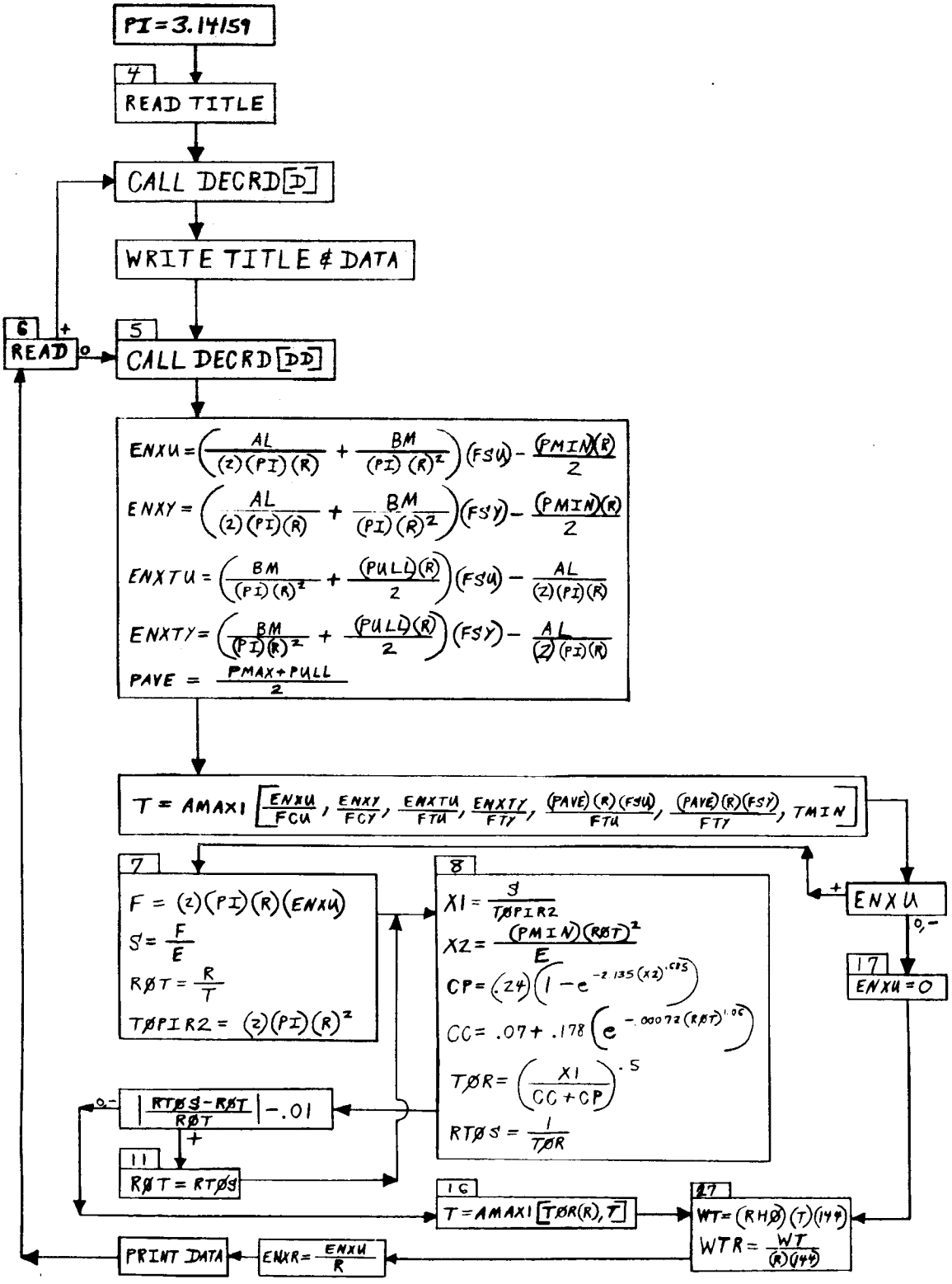



Figure C-7. Monocoque Program Logic

Skin Stringer

The computer input data required to define the optimum skin stringer cylinder are presented in Table C-1. These data include the axial load, bending moment, shell radius, safety factors, type of stringer (i.e., integral, zee, or hat section), and the stringer spacing. In addition, the material allowables and minimum skin gauges must be specified.

With these data, the computer iterates to define the optimum stress level for the shell components, the optimum distribution of material between the face sheets and stringers, and the required ring frame area and frame spacing. The resulting design is a minimum weight cylinder consistent with the input constraints.

A typical stringer printout for the skin stringer construction is presented in Table C-3. The title of the printout consists of the type of construction and material. The first segment consists of the invariant input data for this construction and material, and the second segment of the printout consists of the variable input data and the results of the computers computation.

The first column of the initial segment consists of the minimum allowable skin thickness, the minimum stringer and frame spacing, and the burst and relief pressures. The second column consists of the yield and ultimate allowable material stresses, the elastic modulus of the material, and the temperature corresponding to these properties. In addition, the material density and the maximum frame stress are presented in this column. The third column consists of the stability factor and the yield and ultimate factors of safety.

The first four columns of the second segment of the printout consist of the component radius, axial load, bending moment, and compressive load intensity. The unit weight of the shell is presented in the fifth column. The sixth column contains the skin thickness, the stringer thickness, and the frame area. The seventh column contains the stringer pitch and frame spacing. The stress level in the skin and stringer are presented in the eighth column. The ninth column contains the thicknesses of the upright segment, the base leg, and the outer edge segment of the stringer element. The corresponding lengths of these three stringer segments are presented in the tenth column. The last two columns contain the loading index and the weight-to-radius ratio of the configuration.

## Table C-3. Skin Stringer Printout

CONSTRUCTION - SKIN STRINGER

MATERIAL - ALUMINUM A
STRINGER SHAPE - HAT SECTION

| | | | | | |
|---|---|---|---|---|---|
| MIN SKIN THICKNESS = | 0.0130 INS | YIELD STRESS = | 50000. PSI | STABILITY FACTOR | = 1.000 |
| MIN STRINGER PITCH = | 4.000 INS | ULTIMATE STRESS = | 55000. PSI | LIMIT LOAD FACTOR | = 1.100 |
| MIN FRAME PITCH = | 0.000 INS | YOUNGS MODULUS = | 10000000. PSI | ULTIMATE LOAD FACTOR | = 1.400 |
| BURST PRESSURE = | 0.0000 PSI | TEMPERATURE = | 300. DEGF | BM RELIEF FACTOR | = 0.714 |
| RELIEF PRESSURE = | 0.0000 PSI | MATERIAL DENSITY = | 0.1000 PCI | FRAME SHAPE FACTOR | = 3.326 |
| | | MAX FRAME STRESS = | 25000. PSI | | |

| COMP. RADIUS INS | AXIAL LOAD LB | BENDING MOMENT IN-LBS | COMP. LOAD INTENSITY LBS/IN | UNIT WEIGHT LB/FT2 | | THICK OR AREA | PITCH INS | STRESS PSI | | STGR THICK | STGR ELEMENT LENGTH | NX/R PSI | MT/R PCI |
|---|---|---|---|---|---|---|---|---|---|---|---|---|---|
| 130. | 1164800. | 0. | 1996. | 2.48 | SK | 0.091 | | 12000. | UP | 0.073 | 2.18 | 15.357 | 0.0001324 |
| | | | | | ST | 0.40 | 8.0 | 12000. | BL | 0.073 | 0.87 | | |
| | | | | | FR | 0.43 | 74.0 | | BE | 0.073 | 2.18 | | |
| 130. | 2329600. | 0. | 3993. | 3.15 | SK | 0.116 | | 19500. | UP | 0.093 | 2.01 | 30.714 | 0.0001682 |
| | | | | | ST | 0.71 | 8.0 | 19500. | BL | 0.093 | 0.80 | | |
| | | | | | FR | 0.72 | 51.8 | | BE | 0.093 | 2.01 | | |
| 130. | 3494400. | 0. | 5989. | 3.72 | SK | 0.133 | | 25503. | UP | 0.106 | 2.02 | 46.072 | 0.0001987 |
| | | | | | ST | 0.82 | 8.0 | 25503. | BL | 0.106 | 0.81 | | |
| | | | | | FR | 0.98 | 41.9 | | BE | 0.106 | 2.02 | | |
| 130. | 4659200. | 0. | 7986. | 4.28 | SK | 0.146 | | 30545. | UP | 0.116 | 2.09 | 61.429 | 0.0002286 |
| | | | | | ST | 0.93 | 8.0 | 30545. | BL | 0.116 | 0.84 | | |
| | | | | | FR | 1.24 | 34.8 | | BE | 0.116 | 2.09 | | |
| 130. | 5824000. | 0. | 9982. | 4.86 | SK | 0.154 | | 33691. | UP | 0.123 | 2.43 | 76.786 | 0.0002595 |
| | | | | | ST | 1.14 | 8.0 | 33691. | BL | 0.123 | 0.97 | | |
| | | | | | FR | 1.41 | 33.9 | | BE | 0.123 | 2.43 | | |
| 130. | 6988800. | 0. | 11979. | 5.43 | SK | 0.163 | | 36576. | UP | 0.131 | 2.65 | 92.143 | 0.0002900 |
| | | | | | ST | 1.31 | 8.0 | 36576. | BL | 0.131 | 1.06 | | |
| | | | | | FR | 1.59 | 32.1 | | BE | 0.131 | 2.65 | | |

## Table C-4. Waffle Printout

CONSTRUCTION - WAFFLE

MATERIAL - ALUMINUM A

| | | | | | |
|---|---|---|---|---|---|
| MIN SKIN THICKNESS = | 0.0150 INS | YIELD STRESS = | 50000. PSI | LIMIT LOAD FACTOR | = 1.1 |
| MIN WEB THICKNESS = | 0.0150 INS | ULTIMATE STRESS = | 55000. PSI | ULTIMATE LOAD FACTOR | = 1.4 |
| MAX HEIGHT/SKIN = | 15.0000 | YOUNGS MODULUS = | 10000000. PSI | BM RELIEF FACTOR | = 0.714 |
| BURST PRESSURE = | 0.0000 PSI | TEMPERATURE = | 300. DEGF | STABILITY FACTOR | = 0.330 |
| RELIEF PRESSURE = | 0.0000 PSI | MATERIAL DENSITY = | 0.1000 PCI | | |

| COMPONENT RADIUS INS | AXIAL LOAD LBS | BENDING MOMENT IN-LBS | COMP. LOAD INTENSITY LB/IN | UNIT WEIGHT LB/FT2 | SKIN THICKNESS INS | TOTAL HEIGHT INS | WEB THICKNESS INS | CELL PITCH INS | AVERAGE STRESS PSI | NX/R PSI | MT/R PCI |
|---|---|---|---|---|---|---|---|---|---|---|---|
| 130. | 1164800. | 0. | 1996. | 2.02 | 0.1027 | 1.54 | 0.0602 | 4.60 | 17800. | 15.357 | 0.0001080 |
| 130. | 2329600. | 0. | 3993. | 2.90 | 0.1345 | 2.00 | 0.0890 | 4.95 | 26400. | 30.714 | 0.0001551 |
| 130. | 3494400. | 0. | 5989. | 3.66 | 0.1559 | 2.32 | 0.1157 | 5.11 | 33200. | 46.072 | 0.0001953 |
| 130. | 4659200. | 0. | 7986. | 4.39 | 0.1909 | 2.66 | 0.1380 | 5.97 | 36400. | 61.429 | 0.0002345 |
| 130. | 5824000. | 0. | 9982. | 5.12 | 0.2336 | 3.00 | 0.1577 | 7.16 | 37800. | 76.786 | 0.0002734 |
| 130. | 6988800. | 0. | 11979. | 5.82 | 0.2790 | 3.31 | 0.1747 | 8.45 | 38600. | 92.143 | 0.0003110 |
| 130. | 8153600. | 0. | 13975. | 6.52 | 0.3172 | 3.62 | 0.1936 | 9.43 | 39800. | 107.501 | 0.0003484 |
| 130. | 10483200. | 0. | 17968. | 7.90 | 0.4073 | 4.18 | 0.2233 | 11.96 | 40600. | 138.215 | 0.0004218 |
| 130. | 11648800. | 0. | 19966. | 8.58 | 0.4476 | 4.47 | 0.2395 | 13.02 | 41200. | 153.583 | 0.0004581 |
| 198. | 1774080. | 0. | 1996. | 2.49 | 0.1271 | 1.91 | 0.0820 | 6.33 | 14400. | 10.083 | 0.0000875 |
| 198. | 3548160. | 0. | 3993. | 3.54 | 0.1741 | 2.61 | 0.1060 | 7.21 | 20800. | 20.166 | 0.0001241 |
| 198. | 4515840. | 0. | 5082. | 4.02 | 0.1894 | 2.84 | 0.1234 | 7.30 | 24000. | 25.666 | 0.0001409 |
| 198. | 7096320. | 0. | 7986. | 5.14 | 0.2244 | 3.35 | 0.1616 | 7.62 | 31000. | 40.332 | 0.0001804 |
| 198. | 8870400. | 0. | 9982. | 5.88 | 0.2463 | 3.66 | 0.1870 | 7.88 | 34800. | 50.415 | 0.0002062 |
| 198. | 10644480. | 0. | 11979. | 6.62 | 0.2856 | 4.01 | 0.2087 | 8.93 | 36400. | 60.498 | 0.0002322 |
| 198. | 12418560. | 0. | 13975. | 7.35 | 0.3280 | 4.36 | 0.2290 | 10.10 | 37400. | 70.581 | 0.0002579 |
| 198. | 14192640. | 0. | 15972. | 8.07 | 0.3736 | 4.69 | 0.2469 | 11.41 | 38000. | 80.664 | 0.0002830 |
| 198. | 15966720. | 0. | 17968. | 8.77 | 0.4176 | 5.00 | 0.2642 | 12.64 | 38600. | 90.747 | 0.0003076 |
| 270. | 2419200. | 0. | 1996. | 2.91 | 0.1508 | 2.26 | 0.0994 | 8.16 | 12200. | 7.394 | 0.0000749 |
| 270. | 4838400. | 0. | 3993. | 4.12 | 0.2106 | 3.16 | 0.1222 | 9.54 | 17400. | 14.788 | 0.0001060 |
| 270. | 7257600. | 0. | 5989. | 5.07 | 0.2490 | 3.71 | 0.1500 | 10.08 | 21800. | 22.183 | 0.0001304 |
| 270. | 9676800. | 0. | 7986. | 5.90 | 0.2729 | 4.09 | 0.1815 | 10.11 | 26000. | 29.577 | 0.0001518 |
| 270. | 12096000. | 0. | 9982. | 6.68 | 0.2981 | 4.43 | 0.2083 | 10.39 | 29400. | 36.971 | 0.0001718 |
| 270. | 14515200. | 0. | 11979. | 7.42 | 0.3182 | 4.74 | 0.2344 | 10.53 | 32600. | 44.365 | 0.0001908 |
| 270. | 16934400. | 0. | 13975. | 8.16 | 0.3376 | 5.05 | 0.2602 | 10.71 | 35400. | 51.760 | 0.0002098 |
| 270. | 19353600. | 0. | 15972. | 8.89 | 0.3792 | 5.40 | 0.2814 | 11.85 | 36400. | 59.154 | 0.0002287 |
| 270. | 24192000. | 0. | 19964. | 10.36 | 0.4683 | 6.10 | 0.3205 | 14.38 | 37600. | 73.942 | 0.0002663 |

affle

The minimum weight waffle cylinder is defined as a function of the input ta presented in Table C-1. These data include the axial load, bending oment, internal pressure, and material allowables. In addition, manufac- ring constraints, such as the minimum skin and/or rib gauge and the aximum skin to thickness ratio of the waffle, may be prescribed.

The computer program iterates to determine the stress intensity for ie composite cylinder, the percentage of material in the face sheets and ibs, and the corresponding principal dimensions of the waffle cylinder. he resultant configuration is a minimum weight structure that satisfies ie design criteria without violating manufacturing constraints.

A representative computer printout for the waffle cylinder is shown in able C-4. The first part of the printout consists of the invariant input data or this construction and material. The second segment consists of the ariable input data and the results of the computer computation.

The minimum allowable skin and web thicknesses, the maximum waffle eight to skin thickness ratio, and the burst and relief pressures are pre- ented in the first column of the printout. The second column contains the ield and ultimate allowable material stresses, the material's elastic modu- us, and the temperature at which these properties are applicable. In ddition, the material density is presented in the second column. The third olumn contains the limit and ultimate safety factors, the bending moment elief factor, and the stability coefficient.

Honeycomb Sandwich Cylinder

The optimum sandwich cylinder is determined as a function of the input variables presented in Table C-1. These variables include the axial load, bending moment, internal pressure and material allowables. In addition, manufacturing constraints such as minimum skin gauges and/or maximum sandwich depth may be specified.

The computer iterates with the input variables, face sheet stress level, and core density and depth in order to define the minimum weight cylinder consistent with the design criteria and the designated manufacturing con- straints.

A representative honeycomb sandwich cylinder printout is shown in Table C-5. The first segment of this printout consists of the input data, and the second segment contains the computer results.

The first column of the printout contains the minimum allowable skin thickness, the minimum allowable core density, the maximum height of the composite section, and the burst and relief pressures. The yield and ultimate allowable material stresses, the elastic modulus of the material, and the design temperature of the structure are presented in the second column. In addition, the second column contains the density of the material. The third column contains the limit and ultimate safety factors and the bending moment relief factor.

The first five columns of the second segment of the printout are identical with the skin stringer and waffle printouts. The next three columns define the skin thickness, sandwich height, and the core density. The ninth column contains the face sheet stresses, and the last two columns contain the loading index and the weight-to-radius ratio for the honeycomb sandwich cylinder.

## PROGRAM OPTIONS

The optimum configurations obtained by the preceding methods are integrally related with the equations used to perform the structural analysis. Therefore the optimum structure form as defined by one analyst may not be the optimum structural form as defined by a second analyst. At the present time, an entirely satisfactory method for alleviating this difficulty does not exist. Precise documentation will show the ground rules used to evaluate the designs but will not necessarily allow the assessment of changes in the ground rules. Typical ground rules used to evaluate designs are the constraints associated with minimum material gauges available, welding or joining problem, etc. However, in addition to these factors, the procedure selected for determining the critical instability stresses plays a significant role in the definition of minimum weight orthotropic shells.

The equations used to determine the local instability stresses have been verified by test results, and the use of these equations to analyze structures is generally accepted. However, a generally accepted procedure for determining the general instability stress for orthotropic shells does not exist. Consequently, the optimum structural form will of necessity be a function of the inclinations and prejudices of the analyst. In order to minimize this effect, a literature survey on the stability of orthotropic shells was conducted. As a result of the survey, the following optional methods for computing the critical instability stresses were included in the stress analysis program.

### Skin Stringer Options

The program options for the skin stringer subroutine may be classified as face sheet options, stringer options, frame options, and general instability options.

Table C-5. Honeycomb Sandwich Printout

CONSTRUCTION = HONEYCOMB SANDWICH

MATERIAL FACE SHEETS ALUMINUM 5
SANDWICH CORE ALUMINUM

| | | | | | | | |
|---|---|---|---|---|---|---|---|
| MIN SKIN THICKNESS | = 0.0100 INS | YIELD STRESS | = 50000. PSI | LIMIT LOAD FACTOR | = 1.1 |
| MIN CORE DENSITY | = 2.5000 PCF | ULTIMATE STRESS | = 66000. PSI | ULTIMATE LOAD FACTOR | = 1.4 |
| MAX SAND HEIGHT | = 3.0000 INS | YOUNGS MODULUS | = 10000000. PSI | BM RELIEF FACTOR | = 0.714 |
| BURST PRESSURE | = 0.0000 PSI | TEMPERATURE | = 300. DEGF | | |
| RELIEF PRESSURE | = 0.0000 PSI | MATERIAL DENSITY | = 0.1000 PCI | | |

| COMPONENT RADIUS INS | AXIAL LOAD LBS | BENDING MOMENT IN-LBS | COMP. LOAD INTENSITY LB/IN | UNIT WEIGHT LB/FT2 | SKIN THICKNESS INS | SAND HEIGHT INS | CORE DENSITY LB/FT3 | AVERAGE STRESS PSI | NX/R PSI | WT/R LB/IN |
|---|---|---|---|---|---|---|---|---|---|---|
| 130. | 1144800. | 0. | 1996. | 1.03 | 0.0255 | 1.36 | 2.50000 | 39197. | 15.357 | 0.0000548 |
| 130. | 2234400. | 0. | 3993. | 1.72 | 0.0436 | 1.56 | 2.50000 | 41042. | 30.714 | 0.0000920 |
| 130. | 3494400. | 0. | 5989. | 2.39 | 0.0695 | 1.30 | 2.50000 | 43034. | 46.072 | 0.0001275 |
| 130. | 4658200. | 0. | 7986. | 3.04 | 0.0927 | 1.30 | 2.50000 | 43094. | 61.429 | 0.0001624 |
| 130. | 5824000. | 0. | 9982. | 3.69 | 0.1159 | 2.57 | 2.50000 | 45249. | 76.786 | 0.0001969 |
| 130. | 6988800. | 0. | 11979. | 4.31 | 0.1324 | 2.57 | 2.50000 | 45249. | 92.143 | 0.0002333 |
| 130. | 8153600. | 0. | 13975. | 4.94 | 0.1544 | 2.57 | 2.50000 | 45249. | 107.500 | 0.0002687 |
| 130. | 10443200. | 0. | 17969. | 6.19 | 0.1985 | 2.57 | 2.50000 | 45249. | 138.215 | 0.0003306 |
| 130. | 11649800. | 0. | 19965. | 6.82 | 0.2206 | 2.57 | 2.50000 | 45249. | 153.582 | 0.0003641 |
| 198. | 1774000. | 0. | 1996. | 1.17 | 0.0269 | 1.38 | 2.50000 | 37226. | 10.083 | 0.0000411 |
| 198. | 3464000. | 0. | 3993. | 1.49 | 0.0436 | 2.37 | 2.50000 | 41042. | 20.166 | 0.0000664 |
| 198. | 4515940. | 0. | 5092. | 2.27 | 0.0619 | 2.37 | 2.50000 | 41042. | 26.664 | 0.0000796 |
| 198. | 7096320. | 0. | 7986. | 3.25 | 0.0927 | 2.30 | 2.50000 | 43094. | 40.332 | 0.0001140 |
| 198. | 8870400. | 0. | 9982. | 3.91 | 0.1158 | 2.30 | 2.50000 | 43094. | 50.415 | 0.0001371 |
| 198. | 10644480. | 0. | 11979. | 4.57 | 0.1390 | 2.30 | 2.50000 | 43094. | 60.499 | 0.0001602 |
| 198. | 12413560. | 0. | 13975. | 5.22 | 0.1621 | 2.30 | 2.50000 | 43094. | 70.581 | 0.0001832 |
| 198. | 14182640. | 0. | 15971. | 5.88 | 0.1853 | 2.30 | 2.50000 | 43094. | 80.664 | 0.0002063 |
| 198. | 15966720. | 0. | 17968. | 6.54 | 0.2085 | 2.30 | 2.50000 | 43094. | 90.747 | 0.0002293 |
| 270. | 2419200. | 0. | 1996. | 1.32 | 0.0268 | 2.55 | 2.50000 | 37226. | 7.394 | 0.0000339 |
| 270. | 4338400. | 0. | 3993. | 2.06 | 0.0511 | 2.33 | 2.50000 | 39087. | 14.788 | 0.0000529 |
| 270. | 7257600. | 0. | 5989. | 2.79 | 0.0766 | 2.33 | 2.50000 | 39087. | 22.183 | 0.0000716 |
| 270. | 9476800. | 0. | 7986. | 3.51 | 0.1022 | 2.33 | 2.50000 | 39087. | 29.577 | 0.0000902 |
| 270. | 12096000. | 0. | 9982. | 4.23 | 0.1277 | 2.33 | 2.50000 | 39087. | 36.971 | 0.0001089 |
| 270. | 14515200. | 0. | 11979. | 4.96 | 0.1532 | 2.33 | 2.50000 | 39087. | 44.365 | 0.0001275 |
| 270. | 16934400. | 0. | 13975. | 5.68 | 0.1788 | 2.33 | 2.50000 | 39087. | 51.759 | 0.0001461 |
| 270. | 19353600. | 0. | 15971. | 6.41 | 0.2043 | 2.33 | 2.50000 | 39087. | 59.154 | 0.0001648 |
| 270. | 24192000. | 0. | 19964. | 7.86 | 0.2554 | 2.33 | 2.50000 | 39087. | 73.942 | 0.0002021 |

The face sheet options allow the analyst to specify that the face sheets will or will not buckle when subjected to ultimate loads. If the face sheet is allowed to buckle, the percentage of the ultimate load at which buckling occurs must be specified.

Table C-6 illustrates the influence of this option for one configuration. The optimum geometry for the unbuckled face sheet is presented in Table C-6a. The data presented in Table C-6b is for a face sheet that buckles at approximately fifty percent of the ultimate load. A comparison of the design unit weights indicates the best designs.

The stringer options permit the analyst to specify integral stringers, zee stringers, or hat section. The respective stringer cross sections may be of uniform or nonuniform dimensions. If nonuniform stringers are selected, the height of the stringer must be specified. In addition, the analyst can select the stringer pitch.

Tables C-7 and C-8 illustrate the influence of stringer options on the optimum skin stringer configuration. Table C-7 presents typical results for integral and "z" section stringers. Table C-8 shows the influence of varying the stringer pitch for top hat skin stringer configurations.

The frame options permit the analyst to specify the maximum frame spacing, the minimum frame stress, and the values of the empirical coefficient present in the frame analysis routine. The results presented in this section are based on frame coefficients recommended by Shanley (Reference C-11) and Becker (Reference C-13).

The stability option permits the analyst to specify the correction factor to be applied to the general instability equation. The coefficient used to obtain the results is based on NAA-S&ID data.

Sandwich Program Options

The program options for the honeycomb sandwich subroutine may be classified as core options and stability options. The core options permit the analyst to select the minimum core density and/or the maximum sandwich height for each configuration. Tables C-5 and C-9 illustrate the influence of this option on the unit shell weight for one configuration.

The stability option permits the analyst to select one of three general instability analyses. The first analysis is a large deflection analyses based on Reference C-21. This analysis includes the effects of initial imperfection and shear deformations. The second analysis applies a stability correction factor to the large deflection analysis. This correction factor adjusts the sandwich analysis to agree with the recommended monocoque cylinder data, (Reference C-9). The correction factor is correlated with an equivalent radius of gyration ratio. The third stability analysis allows the analyst to select the stability correction factor to be applied to the large deflection analysis.

Table C-10 illustrates the influence of this option on the unit shell weight.

Waffle Options

The program options of the waffle subroutine may be classified as geometric options and stability options. The geometric options allow the analyst to specify the minimum grid spacing and the maximum height to skin thickness ratio of the waffle. The stability option allows the selection of one of two general instability analysis based on Reference C-18. A stability correction factor based on NAA-S&ID stability coefficients for homogenous isotropic cylindrical shells is applied to the small deflection analysis. The second method permits the analyst to designate the value of the correction factor.

# Table C-6. Influence of Face Sheet Buckling on Unit Shell Weight

## a. Unbuckled Face Sheet

CONSTRUCTION - SKIN STRINGER

MATERIAL - ALUMINUM B
STRINGER SHAPE - HAT SECTION

| | | | | | | | |
|---|---|---|---|---|---|---|---|
| MIN SKIN THICKNESS | = 0.0000 INS | YIELD STRESS | = 55000. PSI | STABILITY FACTOR | = 1.000 |
| MIN STRINGER PITCH | = 5.0000 INS | ULTIMATE STRESS | = 60000. PSI | LIMIT LOAD FACTOR | = 1.100 |
| MIN FRAME PITCH | = 0.0000 INS | YOUNGS MODULUS | = 10000000. PSI | ULTIMATE LOAD FACTOR | = 1.400 |
| BURST PRESSURE | = 0.0000 PSI | TEMPERATURE | = 300. DEGF | BM RELIEF FACTOR | = 0.714 |
| RELIEF PRESSURE | = 0.0000 PSI | MATERIAL DENSITY | = 0.1000 PCI | FRAME SHAPE FACTOR | = 0.000 |
| | | MAX FRAME STRESS | = 25000. PSI | | |

| COMP. RADIUS INS | AXIAL LOAD LB | BENDING MOMENT IN-LBS | COMP. LOAD INTENSITY LBS/IN | UNIT WEIGHT LB/FT2 | | THICK OR AREA | PITCH INS | STRESS PSI | | STGR THICK | STGR ELEMENT LENGTH | NX/R PSI | WT/R PCI |
|---|---|---|---|---|---|---|---|---|---|---|---|---|---|
| 130. | 1164800. | 0. | 1996. | 1.94 | SK | 0.064 | | 16500. | UP | 0.051 | 1.46 | 15.357 | 0.0001035 |
| | | | | | ST | 0.28 | 5.0 | 16500. | BL | 0.051 | 0.58 | | |
| | | | | | FR | 0.57 | 41.9 | | OE | 0.051 | 1.46 | | |
| 130. | 2329600. | 0. | 3993. | 2.70 | SK | 0.078 | | 24500. | UP | 0.062 | 1.79 | 30.714 | 0.0001443 |
| | | | | | ST | 0.42 | 5.0 | 24500. | BL | 0.062 | 0.72 | | |
| | | | | | FR | 0.87 | 35.4 | | OE | 0.062 | 1.79 | | |
| 130. | 3494400. | 0. | 5989. | 3.48 | SK | 0.086 | | 29507. | UP | 0.069 | 2.25 | 46.072 | 0.0001858 |
| | | | | | ST | 0.59 | 5.0 | 29507. | BL | 0.069 | 0.90 | | |
| | | | | | FR | 1.16 | 30.0 | | OE | 0.069 | 2.25 | | |
| 130. | 4659200. | 0. | 7986. | 3.95 | SK | 0.094 | | 35095. | UP | 0.075 | 2.34 | 61.429 | 0.0002112 |
| | | | | | ST | 0.67 | 5.0 | 35095. | BL | 0.075 | 0.94 | | |
| | | | | | FR | 1.36 | 29.0 | | OE | 0.075 | 2.34 | | |
| 130. | 5824000. | 0. | 9982. | 4.37 | SK | 0.102 | | 40110. | UP | 0.082 | 2.35 | 76.786 | 0.0002336 |
| | | | | | ST | 0.73 | 5.0 | 40110. | BL | 0.082 | 0.94 | | |
| | | | | | FR | 1.55 | 28.2 | | OE | 0.082 | 2.35 | | |
| 130. | 6988800. | 0. | 11979. | 4.78 | SK | 0.111 | | 43527. | UP | 0.089 | 2.42 | 92.143 | 0.0002553 |
| | | | | | ST | 0.82 | 5.0 | 43527. | BL | 0.089 | 0.97 | | |
| | | | | | FR | 1.66 | 29.3 | | OE | 0.089 | 2.42 | | |

## b. Buckled Face Sheet

CONSTRUCTION - SKIN STRINGER

MATERIAL - ALUMINUM B
STRINGER SHAPE - HAT SECTION

| | | | | | | | |
|---|---|---|---|---|---|---|---|
| MIN SKIN THICKNESS | = 0.0100 INS | YIELD STRESS | = 55000. PSI | STABILITY FACTOR | = 1.000 |
| MIN STRINGER PITCH | = 5.0000 INS | ULTIMATE STRESS | = 60000. PSI | LIMIT LOAD FACTOR | = 1.100 |
| MIN FRAME PITCH | = 0.0000 INS | YOUNGS MODULUS | = 10000000. PSI | ULTIMATE LOAD FACTOR | = 1.400 |
| BURST PRESSURE | = 0.0000 PSI | TEMPERATURE | = 300. DEGF | BM RELIEF FACTOR | = 0.714 |
| RELIEF PRESSURE | = 0.0000 PSI | MATERIAL DENSITY | = 0.1000 PCI | FRAME SHAPE FACTOR | = 0.000 |
| | | MAX FRAME STRESS | = 25000. PSI | | |

| COMP. RADIUS INS | AXIAL LOAD LB | BENDING MOMENT IN-LBS | COMP. LOAD INTENSITY LBS/IN | UNIT WEIGHT LB/FT2 | | THICK OR AREA | PITCH INS | STRESS PSI | | STGR THICK | STGR ELEMENT LENGTH | NX/R PSI | WT/R PCI |
|---|---|---|---|---|---|---|---|---|---|---|---|---|---|
| 130. | 1164800. | 0. | 1996. | 1.72 | SK | 0.057 | | 13251. | UP | 0.046 | 1.71 | 15.357 | 0.0001028 |
| | | | | | ST | 0.24 | 5.0 | 26501. | BL | 0.046 | 0.68 | | |
| | | | | | FR | 0.50 | 37.4 | | OE | 0.046 | 1.71 | | |
| 130. | 2329600. | 0. | 3993. | 2.89 | SK | 0.074 | | 19751. | UP | 0.060 | 1.79 | 30.714 | 0.0001545 |
| | | | | | ST | 0.41 | 5.0 | 39502. | BL | 0.060 | 0.72 | | |
| | | | | | FR | 1.08 | 23.0 | | OE | 0.060 | 1.79 | | |
| 130. | 3494400. | 0. | 5989. | 3.55 | SK | 0.076 | | 21035. | UP | 0.076 | 2.13 | 46.072 | 0.0001896 |
| | | | | | ST | 0.61 | 5.0 | 42069. | BL | 0.076 | 0.85 | | |
| | | | | | FR | 1.25 | 25.8 | | OE | 0.076 | 2.13 | | |
| 130. | 4659200. | 0. | 7986. | 4.11 | SK | 0.082 | | 22575. | UP | 0.089 | 2.31 | 61.429 | 0.0002195 |
| | | | | | ST | 0.79 | 5.0 | 45149. | BL | 0.089 | 0.92 | | |
| | | | | | FR | 1.35 | 28.4 | | OE | 0.089 | 2.31 | | |
| 130. | 5824000. | 0. | 9982. | 4.65 | SK | 0.088 | | 23990. | UP | 0.101 | 2.42 | 76.786 | 0.0002486 |
| | | | | | ST | 0.92 | 5.0 | 47981. | BL | 0.101 | 0.97 | | |
| | | | | | FR | 1.50 | 29.9 | | OE | 0.101 | 2.42 | | |
| 130. | 6988800. | 0. | 11979. | 5.18 | SK | 0.094 | | 25099. | UP | 0.112 | 2.52 | 92.143 | 0.0002769 |
| | | | | | ST | 1.07 | 5.0 | 50199. | BL | 0.112 | 1.01 | | |
| | | | | | FR | 1.62 | 31.0 | | OE | 0.112 | 2.52 | | |

# Table C-7. Influence of Stringer Shape on Optimum Configuration

## Integral Stringer

CONSTRUCTION - SKIN STRINGER

MATERIAL - ALUMINUM A
STRINGER SHAPE - INTEGRAL

| | | | | | | | |
|---|---|---|---|---|---|---|---|
| MIN SKIN THICKNESS | = 0.0100 INS | YIELD STRESS | = 50000. PSI | STABILITY FACTOR | = 1.000 |
| MIN STRINGER PITCH | = 5.0000 INS | ULTIMATE STRESS | = 66000. PSI | LIMIT LOAD FACTOR | = 1.100 |
| MIN FRAME PITCH | = 0.0000 INS | YOUNGS MODULUS | = 10000000. PSI | ULTIMATE LOAD FACTOR | = 1.400 |
| BURST PRESSURE | = 0.0000 PSI | TEMPERATURE | = 300. DEGF | BM RELIEF FACTOR | = 0.714 |
| RELIEF PRESSURE | = 0.0000 PSI | MATERIAL DENSITY | = 0.1000 PCI | FRAME SHAPE FACTOR | = 0.000 |
| | | MAX FRAME STRESS | = 25000. PSI | | |

| COMP. RADIUS INS | AXIAL LOAD LB | BENDING MOMENT IN-LBS | COMP. LOAD INTENSITY LBS/IN | UNIT WEIGHT LB/FT2 | | THICK OR AREA | PITCH INS | STRESS PSI | | STGR THICK | STGR ELEMENT LENGTH | NX/R PSI | WT/R PCI |
|---|---|---|---|---|---|---|---|---|---|---|---|---|---|
| 130. | 1164800. | 0. | 1996. | 2.23 | SK | 0.102 | | 15000. | UP | 0.088 | 1.77 | 15.357 | 0.0001193 |
| | | | | | ST | 0.16 | 5.00 | 15000. | BL | 0.000 | 0.00 | | |
| | | | | | FR | 0.67 | 30.26 | | OE | 0.000 | 0.00 | | |
| 130. | 2329600. | 0. | 3993. | 3.02 | SK | 0.122 | | 22000. | UP | 0.133 | 2.19 | 30.714 | 0.0001613 |
| | | | | | ST | 0.29 | 5.00 | 22000. | BL | 0.000 | 0.00 | | |
| | | | | | FR | 0.91 | 32.40 | | OE | 0.000 | 0.00 | | |
| 130. | 3494400. | 0. | 5989. | 3.82 | SK | 0.137 | | 27007. | UP | 0.169 | 2.52 | 46.072 | 0.0002041 |
| | | | | | ST | 0.43 | 5.00 | 27007. | BL | 0.000 | 0.00 | | |
| | | | | | FR | 1.21 | 27.70 | | OE | 0.000 | 0.00 | | |
| 130. | 4659200. | 0. | 7986. | 4.36 | SK | 0.150 | | 32094. | UP | 0.191 | 2.60 | 61.429 | 0.0002323 |
| | | | | | ST | 0.50 | 5.00 | 32094. | BL | 0.000 | 0.00 | | |
| | | | | | FR | 1.42 | 26.73 | | OE | 0.000 | 0.00 | | |
| 130. | 5824000. | 0. | 9982. | 4.81 | SK | 0.163 | | 36576. | UP | 0.210 | 2.61 | 76.786 | 0.0002570 |
| | | | | | ST | 0.55 | 5.00 | 36576. | BL | 0.000 | 0.00 | | |
| | | | | | FR | 1.60 | 25.19 | | OE | 0.000 | 0.00 | | |
| 130. | 6988800. | 0. | 11979. | 5.26 | SK | 0.178 | | 40068. | UP | 0.230 | 2.63 | 92.143 | 0.0002803 |
| | | | | | ST | 0.60 | 5.00 | 40068. | BL | 0.000 | 0.00 | | |
| | | | | | FR | 1.75 | 26.47 | | OE | 0.000 | 0.00 | | |

## Zee Section

CONSTRUCTION - SKIN STRINGER

MATERIAL - ALUMINUM A
STRINGER SHAPE - ZEE SECTION

| | | | | | | | |
|---|---|---|---|---|---|---|---|
| MIN SKIN THICKNESS | = 0.0000 INS | YIELD STRESS | = 50000. PSI | STABILITY FACTOR | = 1.000 |
| MIN STRINGER PITCH | = 5.0000 INS | ULTIMATE STRESS | = 55000. PSI | LIMIT LOAD FACTOR | = 1.100 |
| MIN FRAME PITCH | = 0.0000 INS | YOUNGS MODULUS | = 10000000. PSI | ULTIMATE LOAD FACTOR | = 1.400 |
| BURST PRESSURE | = 0.0000 PSI | TEMPERATURE | = 300. DEGF | BM RELIEF FACTOR | = 0.714 |
| RELIEF PRESSURE | = 0.0000 PSI | MATERIAL DENSITY | = 0.1000 PCI | FRAME SHAPE FACTOR | = 0.000 |
| | | MAX FRAME STRESS | = 25000. PSI | | |

| COMP. RADIUS INS | AXIAL LOAD LB | BENDING MOMENT IN-LBS | COMP. LOAD INTENSITY LBS/IN | UNIT WEIGHT LB/FT2 | | THICK OR AREA | PITCH INS | STRESS PSI | | STGR THICK | STGR ELEMENT LENGTH | NX/R PSI | WT/R PCI |
|---|---|---|---|---|---|---|---|---|---|---|---|---|---|
| 130. | 1164800. | 0. | 1996. | 2.27 | SK | 0.100 | | 14500. | UP | 0.080 | 1.31 | 15.357 | 0.0001214 |
| | | | | | ST | 0.19 | 5.0 | 14500. | BL | 0.080 | 0.52 | | |
| | | | | | FR | 0.65 | 32.2 | | OE | 0.080 | 0.52 | | |
| 130. | 2329600. | 0. | 3993. | 3.09 | SK | 0.120 | | 21000. | UP | 0.096 | 2.01 | 30.714 | 0.0001649 |
| | | | | | ST | 0.35 | 5.0 | 21000. | BL | 0.096 | 0.80 | | |
| | | | | | FR | 0.87 | 35.8 | | OE | 0.096 | 0.80 | | |
| 130. | 3494400. | 0. | 5989. | 3.83 | SK | 0.133 | | 25503. | UP | 0.106 | 2.67 | 46.072 | 0.0002048 |
| | | | | | ST | 0.51 | 5.0 | 25503. | BL | 0.106 | 1.07 | | |
| | | | | | FR | 1.08 | 34.4 | | OE | 0.106 | 1.07 | | |
| 130. | 4659200. | 0. | 7986. | 4.32 | SK | 0.146 | | 30545. | UP | 0.116 | 2.76 | 61.429 | 0.0002310 |
| | | | | | ST | 0.58 | 5.0 | 30545. | BL | 0.116 | 1.11 | | |
| | | | | | FR | 1.28 | 32.9 | | OE | 0.116 | 1.11 | | |
| 130. | 5824000. | 0. | 9982. | 4.76 | SK | 0.157 | | 34801. | UP | 0.126 | 2.86 | 76.786 | 0.0002543 |
| | | | | | ST | 0.65 | 5.0 | 34801. | BL | 0.126 | 1.14 | | |
| | | | | | FR | 1.43 | 32.8 | | OE | 0.126 | 1.14 | | |
| 130. | 6988800. | 0. | 11979. | 5.17 | SK | 0.168 | | 37871. | UP | 0.135 | 3.06 | 92.143 | 0.0002764 |
| | | | | | ST | 0.74 | 5.0 | 37871. | BL | 0.135 | 1.22 | | |
| | | | | | FR | 1.51 | 35.2 | | OE | 0.135 | 1.22 | | |

# Table C-8. Influence of Stringer Pitch

## 4-Inch Stringer Pitch

CONSTRUCTION - SKIN STRINGER

MATERIAL - ALUMINUM A
STRINGER SHAPE - HAT SECTION

| | | | | | | | | |
|---|---|---|---|---|---|---|---|---|
| MIN SKIN THICKNESS | = | 0.0100 INS | YIELD STRESS | = | 50000. PSI | STABILITY FACTOR | = | 1.000 |
| MIN STRINGER PITCH | = | 4.0000 INS | ULTIMATE STRESS | = | 55000. PSI | LIMIT LOAD FACTOR | = | 1.100 |
| MIN FRAME PITCH | = | 0.0000 INS | YOUNGS MODULUS | = | 10000000. PSI | ULTIMATE LOAD FACTOR | = | 1.400 |
| BURST PRESSURE | = | 0.0000 PSI | TEMPERATURE | = | 300. DEGF | RM RELIEF FACTOR | = | 0.714 |
| RELIEF PRESSURE | = | 0.0000 PSI | MATERIAL DENSITY | = | 0.1000 PCI | FRAME SHAPE FACTOR | = | 3.326 |
| | | | MAX FRAME STRESS | = | 25000. PSI | | | |

| COMP. RADIUS INS | AXIAL LOAD LB | BENDING MOMENT IN-LBS | COMP. LOAD INTENSITY LBS/IN | UNIT WEIGHT LB/FT2 | | THICK OR AREA | PITCH INS | STRESS PSI | | STGR THICK | STGR ELEMENT LENGTH | NX/R PSI | WT/P PCI |
|---|---|---|---|---|---|---|---|---|---|---|---|---|---|
| 130. | 1164800. | 0. | 1996. | 1.80 | SK | 0.054 | | 18500. | UP | 0.043 | 1.30 | 15.357 | 0.0000963 |
| | | | | | ST | 0.21 | 4.0 | 18500. | BL | 0.043 | 0.52 | | |
| | | | | | FR | 0.62 | 35.5 | | OE | 0.043 | 1.30 | | |
| 130. | 2329600. | 0. | 3993. | 2.62 | SK | 0.067 | | 28515. | UP | 0.054 | 1.42 | 30.714 | 0.0001401 |
| | | | | | ST | 0.29 | 4.0 | 28515. | BL | 0.054 | 0.57 | | |
| | | | | | FR | 1.04 | 24.9 | | OE | 0.054 | 1.42 | | |
| 130. | 3494400. | 0. | 5989. | 3.35 | SK | 0.073 | | 33151. | UP | 0.059 | 1.93 | 46.072 | 0.0001787 |
| | | | | | ST | 0.43 | 4.0 | 33151. | BL | 0.059 | 0.77 | | |
| | | | | | FR | 1.28 | 24.7 | | OE | 0.059 | 1.93 | | |
| 130. | 4659200. | 0. | 7984. | 3.84 | SK | 0.092 | | 38564. | UP | 0.067 | 1.96 | 61.429 | 0.0002049 |
| | | | | | ST | 0.50 | 4.0 | 38564. | BL | 0.067 | 0.78 | | |
| | | | | | FR | 1.47 | 24.8 | | OE | 0.067 | 1.96 | | |
| 130. | 5824000. | 0. | 9982. | 4.31 | SK | 0.092 | | 42706. | UP | 0.076 | 1.97 | 76.786 | 0.0002301 |
| | | | | | ST | 0.57 | 4.0 | 42706. | BL | 0.076 | 0.79 | | |
| | | | | | FR | 1.64 | 25.0 | | OE | 0.076 | 1.97 | | |
| 130. | 6988800. | 0. | 11979. | 4.80 | SK | 0.103 | | 45962. | UP | 0.084 | 1.97 | 92.143 | 0.0002562 |
| | | | | | ST | 0.63 | 4.0 | 45962. | BL | 0.084 | 0.79 | | |
| | | | | | FR | 1.80 | 24.9 | | OE | 0.084 | 1.97 | | |

## 6-Inch Stringer Pitch

CONSTRUCTION - SKIN STRINGER

MATERIAL - ALUMINUM A
STRINGER SHAPE - HAT SECTION

| | | | | | | | | |
|---|---|---|---|---|---|---|---|---|
| MIN SKIN THICKNESS | = | 0.0100 INS | YIELD STRESS | = | 50000. PSI | STABILITY FACTOR | = | 1.000 |
| MIN STRINGER PITCH | = | 6.0000 INS | ULTIMATE STRESS | = | 55000. PSI | LIMIT LOAD FACTOR | = | 1.100 |
| MIN FRAME PITCH | = | 0.0000 INS | YOUNGS MODULUS | = | 10000000. PSI | ULTIMATE LOAD FACTOR | = | 1.400 |
| BURST PRESSURE | = | 0.0000 PSI | TEMPERATURE | = | 300. DEGF | RM RELIEF FACTOR | = | 0.714 |
| RELIEF PRESSURE | = | 0.0000 PSI | MATERIAL DENSITY | = | 0.1000 PCI | FRAME SHAPE FACTOR | = | 3.326 |
| | | | MAX FRAME STRESS | = | 25000. PSI | | | |

| COMP. RADIUS INS | AXIAL LOAD LB | BENDING MOMENT IN-LBS | COMP. LOAD INTENSITY LBS/IN | UNIT WEIGHT LB/FT2 | | THICK OR AREA | PITCH INS | STRESS PSI | | STGR THICK | STGR ELEMENT LENGTH | NX/R PSI | WT/R PCI |
|---|---|---|---|---|---|---|---|---|---|---|---|---|---|
| 130. | 1164800. | 0. | 1996. | 2.11 | SK | 0.072 | | 14500. | UP | 0.058 | 1.80 | 15.357 | 0.0001126 |
| | | | | | ST | 0.39 | 6.0 | 14500. | BL | 0.058 | 0.72 | | |
| | | | | | FR | 0.49 | 56.5 | | OE | 0.058 | 1.80 | | |
| 130. | 2329600. | 0. | 3993. | 2.78 | SK | 0.092 | | 23501. | UP | 0.073 | 1.68 | 30.714 | 0.0001484 |
| | | | | | ST | 0.47 | 6.0 | 23501. | BL | 0.073 | 0.67 | | |
| | | | | | FR | 0.85 | 37.1 | | OE | 0.073 | 1.68 | | |
| 130. | 3494400. | 0. | 5989. | 3.43 | SK | 0.101 | | 28515. | UP | 0.081 | 2.13 | 46.072 | 0.0001832 |
| | | | | | ST | 0.65 | 6.0 | 28515. | BL | 0.081 | 0.85 | | |
| | | | | | FR | 1.04 | 37.1 | | OE | 0.081 | 2.13 | | |
| 130. | 4659200. | 0. | 7984. | 4.12 | SK | 0.110 | | 33151. | UP | 0.088 | 2.36 | 61.429 | 0.0002207 |
| | | | | | ST | 0.79 | 6.0 | 33151. | BL | 0.088 | 0.94 | | |
| | | | | | FR | 1.35 | 29.7 | | OE | 0.088 | 2.36 | | |
| 130. | 5824000. | 0. | 9982. | 4.56 | SK | 0.119 | | 37210. | UP | 0.095 | 2.47 | 76.786 | 0.0002436 |
| | | | | | ST | 0.89 | 6.0 | 37210. | BL | 0.095 | 0.99 | | |
| | | | | | FR | 1.48 | 30.7 | | OE | 0.095 | 2.47 | | |
| 130. | 6988800. | 0. | 11979. | 4.99 | SK | 0.129 | | 40068. | UP | 0.103 | 2.63 | 92.143 | 0.0002665 |
| | | | | | ST | 1.02 | 6.0 | 40068. | BL | 0.103 | 1.05 | | |
| | | | | | FR | 1.56 | 33.0 | | OE | 0.103 | 2.63 | | |

## Table C-8. Influence of Stringer Pitch (Cont)

### 8-Inch Stringer Pitch

CONSTRUCTION - SKIN STRINGER

MATERIAL - ALUMINUM A
STRINGER SHAPE - HAT SECTION

| | | | | | | | |
|---|---|---|---|---|---|---|---|
| MIN SKIN THICKNESS | = 0.0100 INS | YIELD STRESS | = 50000. PSI | STABILITY FACTOR | = 1.000 |
| MIN STRINGER PITCH | = 8.0000 INS | ULTIMATE STRESS | = 55000. PSI | LIMIT LOAD FACTOR | = 1.100 |
| MIN FRAME PITCH | = 0.0000 INS | YOUNGS MODULUS | = 10000000. PSI | ULTIMATE LOAD FACTOR | = 1.400 |
| BURST PRESSURE | = 0.0000 PSI | TEMPERATURE | = 300. DEGF | RM RELIEF FACTOR | = 0.714 |
| RELIEF PRESSURE | = 0.0000 PSI | MATERIAL DENSITY | = 0.1000 PCI | FRAME SHAPE FACTOR | = 3.326 |
| | | MAX FRAME STRESS | = 25000. PSI | | |

| COMP. RADIUS INS | AXIAL LOAD LB | BENDING MOMENT IN-LBS | COMP. LOAD INTENSITY LBS/IN | UNIT WEIGHT LB/FT2 | | THICK OR AREA | PITCH INS | STRESS PSI | | STGR THICK | STGR ELEMENT LENGTH | NX/P PSI | WT/P PCI |
|---|---|---|---|---|---|---|---|---|---|---|---|---|---|
| 130. | 1164800. | 0. | 1996. | 2.48 | SK | 0.091 | | 12000. | UP | 0.073 | 2.18 | 15.357 | 0.0001324 |
| | | | | | ST | 0.66 | 8.0 | 12000. | RL | 0.073 | 0.87 | | |
| | | | | | FR | 0.43 | 74.0 | | AE | 0.073 | 2.18 | | |
| 130. | 2329600. | 0. | 3993. | 3.15 | SK | 0.116 | | 19500. | UP | 0.093 | 2.01 | 30.714 | 0.0001682 |
| | | | | | ST | 0.71 | 8.0 | 19500. | RL | 0.093 | 0.80 | | |
| | | | | | FR | 0.72 | 51.8 | | AE | 0.093 | 2.01 | | |
| 130. | 3494400. | 0. | 5989. | 3.72 | SK | 0.133 | | 25503. | UP | 0.104 | 2.02 | 46.072 | 0.0001987 |
| | | | | | ST | 0.82 | 8.0 | 25503. | RL | 0.104 | 0.81 | | |
| | | | | | FR | 0.98 | 41.9 | | AE | 0.104 | 2.07 | | |
| 130. | 4659200. | 0. | 7986. | 4.28 | SK | 0.146 | | 30545. | UP | 0.114 | 2.09 | 61.429 | 0.0002286 |
| | | | | | ST | 0.93 | 8.0 | 30545. | RL | 0.114 | 0.84 | | |
| | | | | | FR | 1.24 | 34.8 | | AE | 0.114 | 2.09 | | |
| 130. | 5824000. | 0. | 9982. | 4.86 | SK | 0.154 | | 33691. | UP | 0.123 | 2.43 | 76.786 | 0.0002595 |
| | | | | | ST | 1.14 | 8.0 | 33691. | RL | 0.123 | 0.97 | | |
| | | | | | FR | 1.41 | 33.9 | | AE | 0.123 | 2.43 | | |
| 130. | 6988800. | 0. | 11979. | 5.43 | SK | 0.163 | | 36574. | UP | 0.131 | 2.65 | 92.143 | 0.0002900 |
| | | | | | ST | 1.31 | 8.0 | 36574. | RL | 0.131 | 1.06 | | |
| | | | | | FR | 1.59 | 32.1 | | AE | 0.131 | 2.65 | | |

## Table C-9. Influence of Core Depth and Density on Unit Shell Weight

CONSTRUCTION - HONEYCOMB SANDWICH

MATERIAL FACE SHEETS ALUMINUM A
SANDWICH CORE ALUMINUM

| | | | | | | | |
|---|---|---|---|---|---|---|---|
| MIN SKIN THICKNESS | = 0.0100 INS | YIELD STRESS | = 50000. PSI | LIMIT LOAD FACTOR | = 1.1 |
| MIN CORE DENSITY | = 2.0000 PCF | ULTIMATE STRESS | = 55000. PSI | ULTIMATE LOAD FACTOR | = 1.4 |
| MAX SAND HEIGHT | = 4.0000 INS | YOUNGS MODULUS | = 10000000. PSI | RM RELIEF FACTOR | = 0.714 |
| BURST PRESSURE | = 50.0000 PSI | TEMPERATURE | = 300. DEGF | | |
| RELIEF PRESSURE | = 0.0000 PSI | MATERIAL DENSITY | = 0.1000 PCI | | |

| COMPONENT RADIUS INS | AXIAL LOAD LBS | BENDING MOMENT IN-LBS | COMP. LOAD INTENSITY LB/IN | UNIT WEIGHT LB/FT2 | SKIN THICKNESS INS | SAND HEIGHT INS | CORE DENSITY LB/FT3 | AVERAGE STRESS PSI | NX/P PSI | WT/P PCI |
|---|---|---|---|---|---|---|---|---|---|---|
| 130. | 1164800. | 0. | 1996. | 2.45 | 0.0827 | 0.47 | 2.00000 | 12066. | 15.357 | 0.0001309 |
| 130. | 2329600. | 0. | 3993. | 2.51 | 0.0827 | 0.84 | 2.00000 | 24133. | 30.714 | 0.0001342 |
| 130. | 3494400. | 0. | 5989. | 2.58 | 0.0827 | 1.24 | 2.00000 | 36199. | 46.072 | 0.0001378 |
| 130. | 4659200. | 0. | 7986. | 2.96 | 0.0912 | 2.11 | 2.00000 | 43778. | 61.429 | 0.0001584 |
| 130. | 5824000. | 0. | 9982. | 3.59 | 0.1103 | 2.61 | 2.00000 | 45249. | 76.786 | 0.0001919 |
| 130. | 6988800. | 0. | 11979. | 4.22 | 0.1324 | 2.64 | 2.00000 | 45249. | 92.143 | 0.0002257 |
| 130. | 8153600. | 0. | 13975. | 4.87 | 0.1471 | 3.07 | 2.00824 | 47511. | 107.500 | 0.0002600 |
| 130. | 10493200. | 0. | 17968. | 6.13 | 0.1491 | 4.01 | 2.36422 | 47511. | 138.215 | 0.0003301 |
| 130. | 11648800. | 0. | 19964. | 6.83 | 0.2101 | 4.04 | 2.53175 | 47511. | 153.592 | 0.0003649 |
| 198. | 1774080. | 0. | 1996. | 3.69 | 0.1260 | 0.54 | 2.00000 | 7922. | 10.083 | 0.0001295 |
| 198. | 3548160. | 0. | 3993. | 3.75 | 0.1260 | 0.99 | 2.00000 | 15845. | 20.166 | 0.0001316 |
| 198. | 4515840. | 0. | 5082. | 3.79 | 0.1260 | 1.09 | 2.00000 | 20164. | 25.666 | 0.0001329 |
| 198. | 7094320. | 0. | 7984. | 3.89 | 0.1260 | 1.64 | 2.00000 | 31689. | 40.332 | 0.0001360 |
| 198. | 8870400. | 0. | 9982. | 3.97 | 0.1260 | 2.21 | 2.00000 | 39612. | 50.415 | 0.0001393 |
| 198. | 10644480. | 0. | 11973. | 4.44 | 0.1323 | 3.96 | 2.00000 | 45271. | 60.498 | 0.0001559 |
| 198. | 12414560. | 0. | 13975. | 5.07 | 0.1544 | 3.97 | 2.00000 | 45249. | 70.581 | 0.0001760 |
| 198. | 14192640. | 0. | 15971. | 5.71 | 0.1765 | 3.99 | 2.00000 | 45249. | 80.664 | 0.0002001 |
| 198. | 15964720. | 0. | 17968. | 6.34 | 0.1985 | 4.01 | 2.00000 | 45249. | 90.747 | 0.0002223 |
| 270. | 2419200. | 0. | 1996. | 5.01 | 0.1718 | 0.61 | 2.00000 | 5810. | 7.394 | 0.0001289 |
| 270. | 4838400. | 0. | 3993. | 5.07 | 0.1718 | 0.95 | 2.00000 | 11419. | 14.788 | 0.0001303 |
| 270. | 7257600. | 0. | 5989. | 5.13 | 0.1718 | 1.31 | 2.00000 | 17429. | 22.183 | 0.0001319 |
| 270. | 9676800. | 0. | 7986. | 5.19 | 0.1718 | 1.68 | 2.00000 | 23239. | 29.577 | 0.0001335 |
| 270. | 12096000. | 0. | 9982. | 5.25 | 0.1718 | 2.06 | 2.00000 | 29049. | 36.971 | 0.0001351 |
| 270. | 14515200. | 0. | 11973. | 5.32 | 0.1718 | 2.47 | 2.00000 | 34858. | 44.365 | 0.0001369 |
| 270. | 16934400. | 0. | 13975. | 5.45 | 0.1718 | 3.23 | 2.00000 | 40668. | 51.759 | 0.0001401 |
| 270. | 19353600. | 0. | 15971. | 5.93 | 0.1804 | 4.65 | 2.00000 | 44265. | 59.154 | 0.0001525 |
| 270. | 24192000. | 0. | 19964. | 7.29 | 0.2206 | 5.42 | 2.00000 | 45249. | 73.942 | 0.0001852 |

# Table C-10. Influence of Analytical Methods on Honeycomb Sandwich Construction

## Large Deflection Analysis

CONSTRUCTION - HONEYCOMB SANDWICH

MATERIAL FACE SHEETS ALUMINUM A
SANDWICH CORE ALUMINUM

| | | | | | |
|---|---|---|---|---|---|
| MIN SKIN THICKNESS = | 0.0100 INS | YIELD STRESS = | 50000. PSI | LIMIT LOAD FACTOR = | 1.1 |
| MIN CORE DENSITY = | 2.0000 PCF | ULTIMATE STRESS = | 55000. PSI | ULTIMATE LOAD FACTOR = | 1.4 |
| MAX SAND HEIGHT = | 5.0000 INS | YOUNGS MODULUS = | 10000000. PSI | BM RELIEF FACTOR = | 0.714 |
| BURST PRESSURE = | 0.0000 PSI | TEMPERATURE = | 300. DEGF | | |
| RELIEF PRESSURE = | 0.0000 PSI | MATERIAL DENSITY = | 0.1000 PCI | | |

| COMPONENT RADIUS INS | AXIAL LOAD LBS | BENDING MOMENT IN-LBS | COMP. LOAD INTENSITY LB/IN | UNIT WEIGHT LB/FT2 | SKIN THICKNESS INS | SAND HEIGHT INS | CORE DENSITY LB/FT3 | AVERAGE STRESS PSI | NX/R PSI | WT/R LB/IN |
|---|---|---|---|---|---|---|---|---|---|---|
| 130. | 1164800. | 0. | 1996. | 0.97 | 0.0243 | 1.56 | 2.00000 | 41042. | 15.357 | 0.0000618 |
| 130. | 2329600. | 0. | 3993. | 1.65 | 0.0443 | 1.90 | 2.00000 | 43094. | 30.714 | 0.0000893 |
| 130. | 3494400. | 0. | 5989. | 2.31 | 0.0695 | 1.90 | 2.00000 | 43094. | 46.072 | 0.0001234 |
| 130. | 4659200. | 0. | 7986. | 2.96 | 0.0892 | 2.57 | 2.00000 | 45249. | 61.429 | 0.0001590 |
| 130. | 5824000. | 0. | 9982. | 3.59 | 0.1109 | 2.57 | 2.00000 | 45249. | 76.786 | 0.0001914 |
| 130. | 6988800. | 0. | 11979. | 4.21 | 0.1324 | 2.57 | 2.00000 | 45249. | 92.143 | 0.0002251 |
| 130. | 8153600. | 0. | 13975. | 4.84 | 0.1544 | 2.57 | 2.00000 | 45249. | 107.500 | 0.0002597 |
| 130. | 10483200. | 0. | 17968. | 6.06 | 0.1991 | 3.03 | 2.00000 | 47511. | 138.215 | 0.0003335 |
| 130. | 11648800. | 0. | 19966. | 6.65 | 0.2101 | 3.03 | 2.00000 | 47511. | 153.582 | 0.0003554 |
| 198. | 1774080. | 0. | 1996. | 1.09 | 0.0255 | 2.08 | 2.00000 | 33087. | 10.083 | 0.0000383 |
| 198. | 3548160. | 0. | 3993. | 1.80 | 0.0486 | 2.37 | 2.00000 | 41043. | 20.166 | 0.0000630 |
| 198. | 4515840. | 0. | 5082. | 2.18 | 0.0618 | 2.37 | 2.00000 | 41043. | 25.666 | 0.0000769 |
| 198. | 7096320. | 0. | 7986. | 3.14 | 0.0927 | 2.90 | 2.00000 | 43094. | 40.332 | 0.0001101 |
| 198. | 8870400. | 0. | 9982. | 3.80 | 0.1158 | 2.90 | 2.00000 | 43094. | 50.415 | 0.0001332 |
| 198. | 10644480. | 0. | 11979. | 4.44 | 0.1324 | 3.92 | 2.00000 | 45249. | 60.498 | 0.0001567 |
| 198. | 12418560. | 0. | 13975. | 5.07 | 0.1544 | 3.92 | 2.00000 | 45249. | 70.581 | 0.0001777 |
| 198. | 14192640. | 0. | 15971. | 5.69 | 0.1765 | 3.92 | 2.00000 | 45249. | 80.664 | 0.0001997 |
| 198. | 15966720. | 0. | 17968. | 6.32 | 0.1985 | 3.92 | 2.00000 | 45249. | 90.747 | 0.0002218 |
| 270. | 2419200. | 0. | 1996. | 1.21 | 0.0258 | 2.58 | 2.00000 | 37226. | 7.394 | 0.0000312 |
| 270. | 4838400. | 0. | 3993. | 1.94 | 0.0488 | 3.24 | 2.00000 | 41042. | 14.788 | 0.0000499 |
| 270. | 7257600. | 0. | 5989. | 2.63 | 0.0730 | 3.24 | 2.00000 | 41042. | 22.183 | 0.0000677 |
| 270. | 12096000. | 0. | 9982. | 3.97 | 0.1158 | 3.96 | 2.00000 | 43094. | 36.971 | 0.0001032 |
| 270. | 14515200. | 0. | 11979. | 4.63 | 0.1390 | 3.96 | 2.00000 | 43094. | 44.365 | 0.0001192 |
| 270. | 16934400. | 0. | 13975. | 5.29 | 0.1621 | 3.96 | 2.00000 | 43094. | 51.759 | 0.0001361 |
| 270. | 19353600. | 0. | 15971. | 5.95 | 0.1853 | 3.96 | 2.00000 | 43094. | 59.154 | 0.0001531 |
| 270. | 21772800. | 0. | 17968. | 6.61 | 0.2085 | 3.96 | 2.00000 | 43094. | 66.548 | 0.0001700 |
| 270. | 24192000. | 0. | 19966. | 7.27 | 0.2316 | 3.96 | 2.00000 | 43094. | 73.942 | 0.0001870 |

## Large Deflection Analysis Corrected to Monocoque Test Data

CONSTRUCTION - HONEYCOMB SANDWICH

MATERIAL FACE SHEETS ALUMINUM A
SANDWICH CORE ALUMINUM

| | | | | | |
|---|---|---|---|---|---|
| MIN SKIN THICKNESS = | 0.0100 INS | YIELD STRESS = | 50000. PSI | LIMIT LOAD FACTOR = | 1.1 |
| MIN CORE DENSITY = | 2.0000 PCF | ULTIMATE STRESS = | 55000. PSI | ULTIMATE LOAD FACTOR = | 1.4 |
| MAX SAND HEIGHT = | 5.0000 INS | YOUNGS MODULUS = | 10000000. PSI | BM RELIEF FACTOR = | 0.714 |
| BURST PRESSURE = | 0.0000 PSI | TEMPERATURE = | 300. DEGF | | |
| RELIEF PRESSURE = | 0.0000 PSI | MATERIAL DENSITY = | 0.1000 PCI | | |

| COMPONENT RADIUS INS | AXIAL LOAD LBS | BENDING MOMENT IN-LBS | COMP. LOAD INTENSITY LB/IN | UNIT WEIGHT LB/FT2 | SKIN THICKNESS INS | SAND HEIGHT INS | CORE DENSITY LB/FT3 | AVERAGE STRESS PSI | NX/R PSI | WT/R PCI |
|---|---|---|---|---|---|---|---|---|---|---|
| 130. | 1164800. | 0. | 1996. | 1.20 | 0.0268 | 2.50 | 2.00000 | 37226. | 15.357 | 0.0000639 |
| 130. | 2329600. | 0. | 3993. | 1.92 | 0.0486 | 3.13 | 2.00000 | 41042. | 30.714 | 0.0001028 |
| 130. | 3494400. | 0. | 5989. | 2.62 | 0.0730 | 3.16 | 2.00000 | 41042. | 46.072 | 0.0001400 |
| 130. | 4659200. | 0. | 7986. | 3.30 | 0.0927 | 3.85 | 2.00000 | 43094. | 61.429 | 0.0001761 |
| 130. | 5824000. | 0. | 9982. | 3.96 | 0.1158 | 3.88 | 2.00000 | 43094. | 76.786 | 0.0002116 |
| 130. | 6988800. | 0. | 11979. | 4.62 | 0.1390 | 3.90 | 2.00000 | 43094. | 92.143 | 0.0002470 |
| 130. | 8153600. | 0. | 13975. | 5.29 | 0.1621 | 3.92 | 2.00000 | 43094. | 107.500 | 0.0002824 |
| 130. | 10483200. | 0. | 17968. | 6.61 | 0.2085 | 3.97 | 2.00000 | 43094. | 138.215 | 0.0003533 |
| 130. | 11648800. | 0. | 19966. | 7.28 | 0.2317 | 4.00 | 2.00000 | 43094. | 153.582 | 0.0003888 |
| 198. | 1774080. | 0. | 1996. | 1.41 | 0.0282 | 3.54 | 2.00000 | 35453. | 10.083 | 0.0000494 |
| 198. | 3548160. | 0. | 3993. | 2.17 | 0.0511 | 4.17 | 2.00000 | 39087. | 20.166 | 0.0000760 |
| 198. | 4515840. | 0. | 5082. | 2.57 | 0.0650 | 4.19 | 2.00000 | 39087. | 25.666 | 0.0000900 |
| 198. | 7096320. | 0. | 7986. | 3.59 | 0.0973 | 4.80 | 2.00000 | 41042. | 40.332 | 0.0001258 |
| 198. | 8870400. | 0. | 9982. | 4.28 | 0.1216 | 4.82 | 2.00000 | 41042. | 50.415 | 0.0001502 |
| 198. | 10644480. | 0. | 11979. | 4.98 | 0.1459 | 4.85 | 2.00000 | 41042. | 60.498 | 0.0001746 |
| 198. | 12418560. | 0. | 13975. | 5.68 | 0.1703 | 4.87 | 2.00000 | 41042. | 70.581 | 0.0001991 |
| 198. | 14192640. | 0. | 15971. | 6.37 | 0.1946 | 4.90 | 2.00000 | 41042. | 80.664 | 0.0002235 |
| 198. | 15966720. | 0. | 17968. | 7.07 | 0.2189 | 4.92 | 2.00000 | 41042. | 90.747 | 0.0002479 |
| 270. | 2419200. | 0. | 1996. | 1.62 | 0.0296 | 4.55 | 2.00000 | 33765. | 7.394 | 0.0000416 |
| 270. | 4838400. | 0. | 3993. | 2.43 | 0.0563 | 4.84 | 2.00000 | 35453. | 14.788 | 0.0000624 |
| 270. | 7257600. | 0. | 5989. | 3.23 | 0.0845 | 4.87 | 2.00000 | 35453. | 22.183 | 0.0000832 |
| 270. | 12096000. | 0. | 9982. | 4.85 | 0.1408 | 4.93 | 2.00000 | 35453. | 36.971 | 0.0001247 |
| 270. | 14515200. | 0. | 11979. | 5.65 | 0.1689 | 4.96 | 2.00000 | 35453. | 44.365 | 0.0001456 |
| 270. | 16934400. | 0. | 13975. | 6.46 | 0.1971 | 4.99 | 2.00000 | 35453. | 51.759 | 0.0001661 |
| 270. | 19353600. | 0. | 15971. | 7.54 | 0.2365 | 4.76 | 2.00000 | 33765. | 59.154 | 0.0001940 |
| 270. | 21772800. | 0. | 17968. | 8.39 | 0.2661 | 4.79 | 2.00000 | 33765. | 66.548 | 0.0002158 |
| 270. | 24192000. | 0. | 19964. | 9.24 | 0.2956 | 4.83 | 2.00000 | 33765. | 73.942 | 0.0002376 |

## REFERENCES


1. Titanium Tankage Program Phase I - Final Report, Advanced Tankage Configuration Study. Technical Documentary Report No. SSD-TOR-63-1 (1 February 1963).

2. Harris, L.A., J.C. Mitchell, and G. W. Morgan. Computer Aided Design For Civil Engineering Structures, presented at the Technology Status and Trend Symposium, MSFC, NAA, S&ID (21 Apr. 1965).

3. A Study of High-Strength-to-Weight Ratio Structures as Applied to Dynamically Scaled Models of Second and Third Stages of the Saturn V Space Flight Vehicle. NAA S&ID, SID 64-1331 (10 Sept. 1964).

4. Design Study of MS-II Stage for Modified Launch Vehicle (MLV) Saturn V. NAA S&ID, SID 65-244-1 (29 Apr. 1965).

5. Deleted.

6. Deleted.

7. McLaughlin, J.F. "Sizing Nuclear Orbital Launch Vehicles for Interplanetary Mission," Astronautics and Aeronautics, (Feb. 1964), pp. 70-76.

8. Gillespie, R.W., R. V. Ragsac, and E. Ross. "Prospects For Early Manned Interplanetary Flight," Astronautics and Aeronautics, (Aug. 1963), pp. 16-21.

9. Greenlee, M. L. and R. G. Broadwell. Engineering Properties of High Temperature Super Alpha Titanium Alloys, Titanium Metals Corporation of America (1 July 1963).

10. Bomberger, H.B. and V.C. Petersen. Development of Manufacturing Process for Compound-Face Beta Titanium Alloy, AFML-TDR-64-328, (Oct. 1964).

11. Hallowell, J. B. and H.R. Ogden. An Introduction to Magnesium Alloys, DMIC Report 206 (Aug. 1964).

2. Masters, J.N., "Booster Case Materials Evaluation," Fourth Maraging Steel Project Review, ML-TDR-64-225, Vol. 1 (July 1964).

3. Fourth Progress Report by the Committee on Beryllium Metallurgy of the Materials Advisory Board, MAB-199-M(4), (Aug. 1965).

4. Rippel, J.M. Final Report on High Energy Rate Extrusion, ML-TDR-64-312 (Sept. 1964).

5. Air Force Materials Symposium, AFML-TR-65-29, (June 1965).

6. Launch Vehicle Component Costs Study, Lockheed Missiles and Space Co. LMSC-895424 (30 June 1965).

17. Bellman, R. Dynamic Programming New Jersey: Princeton University Press (1957).

18. Bellman, R. and S. Dreyfus. Applied Dynamic Programming, New Jersey: Princeton University Press (1962).

19. Ten-Dyke, R. P., "Computation of Rocket Step Weights to Minimize Initial Gross Weights," Jet Propulsion Vol. 28 (1958), pp. 338-340.

20. Design Investigation of Cylindrical Structures Other Than Honeycomb, NAA LAD NA-65-1026 (31 Dec. 1965).

21. Shanley, F.R. Weight-Strength Analysis of Aircraft Structures, New York: Dover Publications.

22. Burns, B.A. Structural Optimization of Axially Compressed Cylinders Stiffened Externally with Rings and/or Stringers of Rectangular Cross-section Lockheed Missiles and Space Company Technical Report 6-62-64-7 (May 1964).

23. Gallagher, R.H., I. Rattinger, and A. Krivetsky. "Minimum Weight Shells In Bending," Aerospace Engineering, (Feb. 1962).

24. Emero, D.H. and L. Spunt. "Optimization of Multirib and Multiweb Wing Box Structures Under Shear and Moment Loads," AIAA 6th Structures and Materials Conference, (5 Apr. 1965) pp. 330-353.

25. Gerard, G. "Elastic and Plastic Stability of Orthotropic Cylinders," Collected Papers on Stability of Shell Structures, NASA-TN-D1510 (Dec. 1962) pp. 277-295.

6. March, H.W. and E.W. Keunze. "Buckling of Cylinders of Sandwich Construction in Axial Compression," U.S. Forest Products Laboratory Report No. 1830 (1957).

7. Large, J.P. Concepts and Procedures of Cost Analysis, The Rand Corporation, Memorandum RM 3589PR (June 1963).

8. Koelle, H.H. Handbook of Astronautical Engineering, New York: McGraw-Hill Book Co. (1961) pp. 3-2 to 11-26.

9. Kazanowski, A.D. Cost Effectiveness Methodology and Limitations, NAA S&ID, SID 64-1829 (1 Oct. 1964).

PPENDIX A

A-1 Bellman, R. Dynamic Programming, Princeton University Press, Princeton, New Jersey (1953).

A-2 Bellman, R., and S. Dreyfus, Applied Dynamic Programming, Princeton University Press, Princeton, New Jersey (1962).

A-3 Ten Dyke, Richard P. "Computation of Rocket Step Weights to Minimize Initial Gross Weight," Jet Propulsion, Vol. 28 (1959), pp 338-340.

A-4 "Saturn S-II Launch Vehicle Derivatives," NAA S&ID, SID 64-1216 (June 1964).

A-5 Jensen, J., et al. "Orbital Flight Manual," The Martin Co. (1961).

A-6 White, J.F. "Flight Performance Handbook for Powered Flight Operations," Space Technology Laboratory, Inc. (March 1962).

APPENDIX B

B-1 NASA TM C-53053, Booster Parametric Design Method for Performance and Trajectory Analysis, Part II: Propulsion (June 2, 1964).

B-2 NASA TM X-53026, Booster Parametric Design Method for Performance and Trajectory Analysis, Part I: Configuration (March 18, 1964).

B-3 Garrocq, Carlos A., Optimum Solidity, Paper presented to Aviation and Space Division Conference, ASME (March 19, 1965).

B-4 RTD-TOR-63-1060 Vehicle Scaling and Performance Computer Program, (July 1963).

B-5 Shanley, F.R. Weight-Strength Analysis of Aircraft Structures, Dover, N.Y., N.Y. (1960).

B-6 Priest, H.M., Design Manual for High-Strength Steels, R&T U.S. Steel Corp. (1957).

B-7 Mitchell, J.C., J.A. Boddy, R.E. Lawrence, Computer-Aided Design Final Report, STR 137 NAA/S&ID (September 1965).

APPENDIX C

C-1. Gerard, George, "Optimum Structural Design Concepts for Aerospace Vehicles: Bibliography and Assessment," AFFDL-TR-65-9 (June 1965)

C-2. Gegard, G., "Minimum Weight Analysis of Compression Structures," New York University Press, New York (1956)

C-3. Crawford, R.F. and A.B. Burns, "Minimum Weight Potentials for Stiffened Plates and Shells." AIAA Journal Vol. 1, No. 4, pp. 879-886 (April 1963)

C-4. Crawford, R.F. and A.B. Burns, "Strength Efficiency and Design Data for Beryllium Structures." ASD TR 61-692 (February 1962)

C-5. Gellatly, R.A., R.H. Gallagher, and W.A. Luberacki, "Development of a Procedure for Automated Synthesis of Minimum Weight Structures" FDL-TDR-64-141 (October 1964)

C-6. Drucker, D.C. and R.T. Shields, Bounds on Minimum Weight Design, Quarterly Applied Mathematics, Vol. 15, No. 3, pp. 269-281 (1957)

C-7. Shields, R.T., "On the Optimum Design of Shells," Journal of Applied Mechanics, Vol. 27, TG 316-322 (1960)

C-8. Shields, R.T., Plate Design for Minimum Weight, Quarterly Applied Mathematics, Vol. 18, No. 2, pp. 131-144 (1960)

C-9. Structures Manual, NAA-S&ID

C-10. Becker, H., Handbook of Structural Stability Part II - Buckling of Composite Elements, MACA TN 3782 (July 1957)

C-11. Shanley, F.R., Weight-Strength Analysis of Aircraft Structures, McGraw-Hill Book Co., New York (1952)

C-12. Jones, T.B., "The Derivation of Statements of Weight, Enclosed Volume, and Geometry of Monocoque and Stiffened Cylindrical Tank Component, "NAA-S&ID Internal Letter

C-13. Becker, H., Handbook of Structural Stability, Part IV - Strength of Stiffened Curved Plates and Shells, NACA TN 3786 (July 1958)

C-14. Seide, P., "The Effectiveness of Integral Waffle-Like Stiffening for Long, Thin Circular Cylinders Under Axial Compression," Part I - Chemically Milled Sheet, RAMO-Wooldridge GM-TR-15 (April 1965)

C-15. Schmit, L.A. and T.P. Kicher, "Structural Synthesis of Symmetrical Waffle Plate," NASA Technical Note D-1691 (December 1962)

C-16. Thielemann, W., "New Developments in the Nonlinear Buckling Theory of Thin Cylindrical Shells," Proceedings of the Durand Conference, Stanford University, Stanford, Calif. (August 5-8, 1959)

C-17. Baker, H., Design Procedure for Integrally Stiffened Waffle Cylinders Under Axial Compression, NAA-S&ID STR 77 (May 1961)

C-18. Baker, E.H., General Instability of Waffle Cylinders Subjected to Combined Loads, NAA-S&ID STR-96 (September 1963)

C-19. Dow, N.F., C. Libove, and R.E. Hubka, Formulas for the Elastic Constants of Plates With Integral Waffle-Like Stiffening, NACA RM L63E13a (August 1953)

C-20. Becker, H., General Instability of Stiffened Cylinders, NACA TN 4237 (July 1958)

C-21. March, H.W. and E.W. Keunze, "Buckling of Cylinders of Sandwich Construction in Axial Compression," U.S. Forest Products Laboratory Report, No. 1820 (1957)

C-22. Peterson, James P. and J.K. Anderson, "Structural Behavior and Buckling Strength of Honeycomb Sandwich Cylinders Subjected to Buckling" NASA Technical Note D-2926 (August 1965)

C-23. Fulton, R.E., "Effects of Face-Sheet Stiffness on Buckling of Curved Plates and Cylindrical Shells of Sandwich Construction in Axial Compression," NASA Technical Note D-2783 (April 1965)

C-24. Gallagher, R.H., I. Rattinger, and A. Krivetsky, "Minimum Weight Shells in Bending," Aerospace Engineering, Vol. 21, No. 2, pp. 58-59, 64, 68, 72, 74-78 (February 1962)